UNIVERSAL
LIBRARY
OU_168043
UNIVERSAL
LIBRARY

OSMANIA UNIVERSITY LIBRARY

Call No. 542.68/T78L Accession No. 3172

Author Treybal. Robert E.

Title Liquid extraction. 1951

This book should be returned on or before the date last marked below.

CHEMICAL ENGINEERING SERIES

# LIQUID EXTRACTION

# McGRAW-HILL CHEMICAL ENGINEERING SERIES

*Texts and Reference Works Outlined by the Following Committee*


S. D. KIRKPATRICK, *Consulting Editor* · Editor, Chemical Engineering

H. C. PARMELEE · Editor Emeritus, Engineering and Mining Journal

HARRY A. CURTIS · Commissioner, Tennessee Valley Authority

J. V. N. DORR · Chairman, The Dorr Company

A. W. HIXSON Professor Emeritus of Chemical Engineering, Columbia University

H. FRASER JOHNSTONE · Professor of Chemical Engineering, University of Illinois

WEBSTER N. JONES · Director, College of Engineering and Science, Carnegie Institute of Technology

W. K. LEWIS · Professor Emeritus of Chemical Engineering, Massachusetts Institute of Technology

ALBERT E. MARSHALL · Vice President, Heyden Chemical Corporation

R. S. McBRIDE · Consulting Chemical Engineer

MOTT LOUDERS · Associate Director of Research, Shell Development Company

C. M. A. STINE · Director, E. I. du Pont de Nemours & Co.

E. R. WEIDLEIN · Director, Mellon Institute of Industrial Research

M. C. WHITAKER · Director, American Cyanamid Company

A. H. WHITE · Professor Emeritus of Chemical Engineering, University of Michigan

WALTER G. WHITMAN · Professor of Chemical Engineering, Massachusetts Institute of Technology


## THE SERIES

BADGER AND BAKER—*Inorganic Chemical Technology*

BADGER AND McCABE—*Elements of Chemical Engineering*

CLARKE—*Manual for Process Engineering Calculations*

DAVIS—*Chemical Engineering Nomographs*

DODGE—*Chemical Engineering Thermodynamics*

EDWARDS, FRARY, AND JEFFRIES—*The Aluminum Industry (in Two Volumes): Aluminum and Its Production; Aluminum Products and Their Fabrication*

GRISWOLD—*Fuels, Combustion, and Furnaces*

GROGGINS—*Unit Processes in Organic Synthesis*

HUNTINGTON—*Natural Gas and Natural Gasoline*

KIRKBRIDE—*Chemical Engineering Fundamentals*

LEWIS AND RADASCH—*Industrial Stoichiometry*

MANTELL—*Adsorption*

MANTELL—*Industrial Electrochemistry*

NELSON—*Petroleum Refinery Engineering*

PERRY (EDITOR)—*Chemical Engineers' Handbook*

PIERCE—*Chemical Engineering for Production Supervision*

RHODES, F. H.—*Technical Report Writing*

RHODES, T. J.—*Industrial Instruments for Measurement and Control*

ROBINSON AND GILLILAND—*Elements of Fractional Distillation*

SCHMIDT AND MARLIES—*Principles of High-polymer Theory and Practice*

SHERWOOD — *Absorption and Extraction*

SHERWOOD AND REED—*Applied Mathematics in Chemical Engineering*

SHREVE—*The Chemical Process Industries*

SMITH—*Introduction to Chemical Engineering Thermodynamics*

TREYBAL—*Liquid Extraction*

TYLER—*Chemical Engineering Economics*

VILBRANDT—*Chemical Engineering Plant Design*

WALKER, LEWIS, McADAMS, AND GILLILAND—*Principles of Chemical Engineering*

WILSON AND WELLS—*Coal, Coke, and Coal Chemicals*

WINDING AND HASCHE—*Plastics, Theory and Practice*

# LIQUID EXTRACTION

ROBERT E. TREYBAL
*Professor of Chemical Engineering*
*New York University*

FIRST EDITION

New York Toronto London
McGRAW-HILL BOOK COMPANY, INC.
1951

LIQUID EXTRACTION

Copyright, 1951, by the McGraw-Hill Book Company, Inc. Printed in the United States of America. All rights reserved This book, or parts thereof, may not be reproduced in any form without permission of the publishers.

# PREFACE

The unit operation, liquid extraction, has rapidly assumed major industrial significance as a means of separating the components of solutions. Whereas simple extraction procedures have been a common and familiar laboratory practice for many years, in the technical application to large-scale industrial processes a wide variety of complex flowsheets and equipment types has been developed, the usefulness of which has not been thoroughly explored. As so frequently happens, the needs of the chemical industry have advanced much more rapidly than the accumulation of design data necessary for adequate application of these techniques. Much of the resulting confusion and possible hesitancy in applying extraction to separation problems can be removed by outlining its potentialities and limitations in organized form. It is sincerely hoped that this book will be of service in this respect.

Relatively little instruction is given in liquid extraction in undergraduate chemical-engineering courses, and graduate courses have been developed only recently. As a consequence, many chemical engineers and chemists who must work with extraction have had little if any formal introduction to the subject. It is one of the purposes of this book to provide a text suitable not only for organized courses, but also for those who must study without benefit of guidance. To this end, the book contains many illustrative examples worked out in detail and a collection of problems for student practice. In addition, for those who may wish to investigate sources of original data, fairly complete bibliographies are appended to each chapter. In so far as it was possible a consistent notation was used throughout the book; the number of mathematical symbols required was so great, however, that duplicate meanings for a few could not be avoided. The table of notation at the end of each chapter provides adequate definition of these so that there should be no confusion.

It is the additional purpose of this book to set forth in logical order the known facts concerning liquid extraction and as far as possible to establish from them general principles which can be used as guides in evaluation. It would be presumptuous to suppose that, in the present early stages of technical development of the operation, this has been entirely successful; there is as yet too much that is contradictory. Indeed, in the preparation of this manuscript I have been singularly impressed by the wisdom of the observation of Sir Charles Singer, the medical historian: "If from the facts no laws emerge, the facts themselves become an obstacle, not an aid, to

scientific advance." On the other hand, if knowledge of the shortcomings of our available information leads to more logically organized research and investigation in the future, much will have been gained.

The contribution of many industrial firms, technical organizations and publications, and individuals to this book have been acknowledged at appropriate places throughout the text, but this cannot indicate the trouble to which many of them were put and the very considerable cooperation which they offered. This rather inadequate mention of their assistance is in no way indicative of my gratitude. In addition, I wish to thank J. C. Elgin, W. E. Lobo, V. S. Morello, and J. H. Rushton, who were helpful in many ways; and my colleagues at New York University, T. W. Davis, John Happel, Morris Newman, and J. E. Ricci, who read and criticized portions of the manuscript. Most of all my thanks are due my wife, Gertrude I. Treybal, who assisted so much in the preparation of the manuscript.

ROBERT E. TREYBAL

NEW YORK, N. Y.
*April*, 1951

# CONTENTS


Preface . . . . . v

1. Introduction . . . . . 1

2. Liquid Equilibria . . . . . 5

3. Prediction of Distribution . . . . . 38

4. Choice of Solvent . . . . . 86

5. Diffusion and Mass Transfer . . . . . 99

6. Methods of Calculation I. Stagewise Contact with a Single Solvent . . . . . 125

7. Methods of Calculation II. Stagewise Contact with Mixed and Double Solvents . . . . . 204

8. Methods of Calculation III. Continuous Countercurrent Contact . . . . . 241

9. Equipment for Stagewise Contact . . . . . 257

10. Equipment for Continuous Countercurrent Contact . . 290

11. Liquid-extraction Processes . . . . . 346

Problems . . . . . 399

Name Index . . . . . 409

Subject Index . . . . . 417

# CHAPTER 1

## INTRODUCTION

One of the most frequently occurring problems in the field of chemical engineering is the separation of the components of a liquid solution. Consider a dilute solution of two substances which it is desired to separate into its component parts with recovery of each in substantially pure form. There are available to the engineer several general techniques whereby this separation may be brought about, some of which may be inapplicable because of certain physical properties peculiar to the system at hand. Because of the requirement that the components be recovered in nearly pure form, these techniques are usually physical rather than chemical operations. Many depend upon the tendency of a substance, when distributed between two insoluble phases, to come to different concentrations in each of the phases at equilibrium.

*Fractional distillation*, whereby a portion of the solution is vaporized resulting in a vapor richer in one of the components than the original solution, may be used as a separating means. This is perhaps the operation most frequently resorted to when both components of the original solution are volatile. In certain instances, however, it is found that this technique is inconvenient. For example, in the case of some systems, the enrichment occurring on partial volatilization is relatively insignificant, requiring the use of large amounts of heat and cooling water for reflux, and large equipment. In other instances, substantially complete separation by ordinary fractional distillation is impossible because of the formation of an azeotrope, or constant boiling mixture. In still others, high boiling temperatures necessitate the use of low-pressure operation in order to reduce the likelihood of thermal decomposition of one of the components. If the solute of the solution is less volatile than the solvent, then the majority of the original solution will have to be vaporized, again with the expenditure of large quantities of heat and cooling water.

For separations potentially feasible by ordinary fractional distillation but rendered difficult by the presence of an azeotropic mixture or by low relative volatility of the components, *azeotropic distillation* or the newly developed techniques of *extractive distillation* may sometimes be employed. In the case of the former, a third component is added to the original mixture which will form with one of the components of the solution an azeotrope which may be separated easily from the solution. This azeotrope

must then be separated by another means. Extractive distillation involves the addition of a relatively nonvolatile third component which increases the degree of separability by distillation of the original components, and which itself may be separated from the mixture with ease.

If the solute in solution is nonvolatile, the solvent may be removed by *evaporation*, resulting in the deposition of crystals of the solute after the solubility limit has been reached. *Crystallization* can also be brought about by cooling such a solution or by a combination of evaporation and cooling. Obviously the application of these types of operations is limited to solutions containing one nonvolatile component.

In certain instances, it has been found that a solute may be preferentially *adsorbed* from a solution onto some activated substance such as carbon, alumina, silica, or certain clays. The adsorbed material may then be recoverable from the solid by leaching or evaporation. The number of successful applications of such a process has been increasing in recent years.

The removal of a volatile solute from a relatively nonvolatile solvent may be accomplished by the operation of *stripping*, whereby some chemically inert gas such as air is brought into intimate contact with the solution. The volatile material is then vaporized into the unsaturated gas and carried away, leaving behind the solute. The vaporized material must then be recovered from the gas phase by condensation (brought about by cooling and compressing), or adsorption.

The addition of an inorganic salt, such as sodium chloride, will frequently result in the precipitation of an organic solute from its aqueous solution, and this constitutes the operation of "salting out." Variants of this operation involving the use of liquid third components are known, where the added material may be either entirely or only partially miscible in the components of the original solution.

*Liquid extraction* as a means of separation may be carried out in several ways, all involving the distribution of a substance between two insoluble liquids. The original solution may be washed with a second liquid, immiscible with the solvent of the original solution, thereby preferentially dissolving the solute. The original solution may be cooled or heated so that it forms two liquid phases, whereupon the concentrations of solute in each phase will differ. The cooling or heating may be carried out after the addition of a third liquid. In the most complex of these operations, two mutually immiscible liquids are added to the original solution, each of which preferentially dissolves a different component of the original (*fractional extraction*). On infrequent occasions simultaneous chemical reaction and liquid extraction occur.

All of the operations described are applicable not only to the separation of two-component solutions such as that used as an example, but also, by proper manipulation, to the separation of multicomponent mixtures.

Before proceeding with the detailed discussion of extraction, several important factors influencing the choice of one of the various separative operations for particular circumstances should be emphasized. It will frequently happen that the nature of the original solution will prevent application of one or more of the processes, but usually at least a limited choice is possible.

1. Those operations such as azeotropic and extractive distillation, salting out, and liquid extraction which require the addition of extraneous material to the original mixture are usually considered less desirable in industrial practice than the others. The presence of a third component complicates the choice of materials of construction to ensure resistance to corrosion. Sometimes large inventories of a third component must be kept on hand, thus tying up relatively large amounts of capital. Plant equipment will practically always be larger for such processes, since storage and recovery facilities must be available, in addition to extra piping, pumps, etc. The processes always require solvent-recovery systems, in themselves consumers of heat and power. The opportunity for contamination of the ultimate product by a material not normally expected to be associated with it is always present. For these reasons, at least, such processes are to be avoided if possible.

2. In choosing between liquid extraction and other applicable processes as a means of separation, cost of the operation as a whole is of primary interest. Distillation processes which are most frequently considered are inherently expensive since part of the original mixture must be volatilized, necessitating the expenditure of heat. Distillation operations requiring high reflux ratios are especially expensive because of the large heat and cooling-water requirements and also because of the large plant equipment required to handle large volumes of vapor. Distillation of dilute solutions where large quantities of solvent must be volatilized are expensive, especially if the solvent is water which has a high latent heat of vaporization. Liquid extraction is frequently useful in these cases.

3. Liquid extraction is a means of separation based upon chemical characteristics rather than such physical properties as boiling point and relative volatility. Many industrial solutions are mixtures of substances of different chemical types of overlapping volatility or boiling points. In these cases, liquid extraction offers perhaps the only feasible method of separating the various chemical types short of direct chemical reaction.

4. Liquid-extraction operations must always be followed by solvent-recovery systems, and these are usually distillation processes. It follows that the combined extraction and recovery system must be more economical than any other single process or combination which might be applicable, and this is a distinct handicap operating against the choice of extraction.

There are other more subtle differences and even similarities between

liquid extraction and other separation operations which will be considered at the proper time. Despite obvious disadvantages, there are many situations where extraction seems to be the only method which will accomplish the purpose at hand. Its potentialities have not been fully realized, and there are many occasions where extraction might have been chosen rather than another operation, had more engineering information been available to assist in its evaluation.

Extraction is relatively new in chemical-engineering practice. Although the literature reveals several instances of the use of the operation dating back to before 1900, it was not until the 1930's that installations began to appear in appreciable numbers. Since that time, research in the subject has been limited, and data for design are somewhat scanty. There are nevertheless many basic principles which may be drawn upon to help the engineer in this field, and it is the purpose of this book to bring these together into one place.

Four major principles must be considered in a study of the factors which have a bearing upon the design of extraction processes:

1. Phase-equilibrium relationships which describe the concentrations of substances distributed between insoluble phases.
2. Rates of extraction and diffusion, which depend upon the departure from equilibrium which exists in the system as well as physical characteristics of the fluids.
3. Material balances, which describe the quantities of the various substances involved in the several parts of the process.
4. Capacities and performance characteristics of equipment.

In what follows, these principles are each considered in some detail.

# CHAPTER 2

## LIQUID EQUILIBRIA

There are two approaches to the study of phase equilibria, both of which are of importance in systematizing the large number of data which have been accumulated and in simplifying the gathering of new data. These are the phase rule (18) and the laws of distribution.

**Phase Rule.** For the present purposes, this may simply be stated:

$$F = N - P + 2 \tag{2.1}$$

where $F$ = the number of degrees of freedom, or the number of independent variables (limited to temperature, pressure, and concentration) which must be fixed to define completely a system at equilibrium

$N$ = the number of components, or the lowest number of independently variable constituents required to express the composition of each phase

$P$ = the number of phases. A phase is defined as any homogeneous part of a system, bounded by surfaces, and capable of mechanical separation from the rest of the system

The definition of these terms must be made most carefully for proper application of the rule. A complete discussion is beyond the scope of this book; for this and a derivation of the phase rule the reader is referred to the standard works of physical chemistry and others dealing specifically with the subject (16, 21, 53). It is important to emphasize here that the rule applies only to systems at equilibrium and that additional restrictions imposed on a system have the effect of reducing the value of $F$ by one for each restriction.

**Laws of Distribution.** These laws, frequently empirical, attempt to systematize the relationship among concentrations of various components in the various phases of a system at equilibrium. Unfortunately, there is no satisfactory rule which can be used to describe all situations, and what generalizations are available will be considered at the appropriate time.

### TWO-COMPONENT SYSTEMS

Two-component liquid systems may be classified according to whether the components are completely or only partially miscible. In liquid extraction, only those systems exhibiting limited solubility are of interest,

and these alone will be considered. From a practical viewpoint, it may be sometimes considered that complete immiscibility occurs, such as in the case of the system mercury–water, but it should be realized that actually all liquids dissolve in each other if only to a limited extent.

Consider two liquids $A$ and $B$, exhibiting only partial miscibility. If at first $A$ is added in only small amounts to $B$, complete solution will occur. Since $N$ = two components, $P$ = two phases, one liquid and one vapor, $F = 2 - 2 + 2 = 2$. The system is bivariant, and the variables temperature, pressure, and concentration may be independently varied within limits in pairs without changing the number of phases. Thus, temperature and concentration may both be independently varied without the appearance of a new phase, but the pressure will be fixed by the system as long as a liquid and vapor phase are present at equilibrium and is outside the control of the experimenter.

As more $A$ is added to the solution, eventually the limit of solubility of $A$ in $B$ at the prevailing temperature is reached, and further addition of $A$ results in the appearance of two liquid phases which are saturated solutions of $A$ in $B$, and of $B$ in $A$. The appearance of the additional liquid phase results in a univariant system, and only one of the principal variables is now under the control of the experimenter. For example, at constant temperature addition of still more $A$ will merely change the relative amounts of the phases present without affecting their composition or their vapor pressure. Sufficient additional $A$, however, will again bring the system to a condition of one liquid phase when all the $B$ present will dissolve. Thus, for a substantial range of compositions for the system as a whole, there exist at a fixed temperature two liquid phases of constant composition, the saturated solutions. The variation of the composition of these saturated solutions with temperature is conveniently shown graphically.

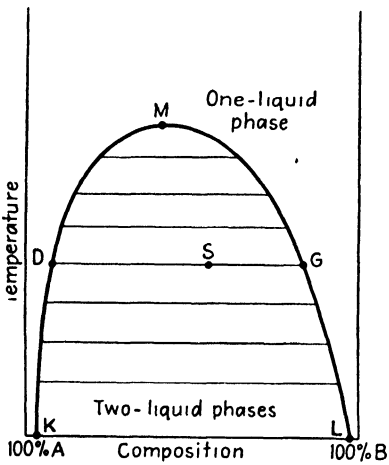



FIG. 2.1. Equilibrium compositions in a two-component system with an upper critical solution temperature.

Figure 2.1 is a plot of the compositions of the saturated liquid phases at equilibrium as a function of temperature for a system of the type just described. In this diagram, the pressure is not constant but rather is the equilibrium vapor pressure of the various liquids; the vapor composition is not shown. The curve *KDM* shows the composition of saturated solutions of $B$ in $A$ as a function of temperature, and *LGM* those of $A$ in $B$.

The area above the curves represents the mixtures which form a single liquid phase, while that below the curve represents mixtures which form two mutually saturating liquid solutions. Consider a mixture whose overall composition and temperature are given by the point $S$. The two saturated solutions formed by such a mixture, called conjugate solutions, are those at $D$ and $G$, and the horizontal line $DG$ which joins these is a tie line. It may be imagined that there are an infinite number of such horizontal tie lines in the area below the curve.

Let weight fraction of $A$ in the mixtures be $D$, $S$, and $G$, respectively, at these points. A material balance for the entire system is

$$\text{Weight of } S = \text{weight of } D + \text{weight of } G \tag{2.2}$$

A material balance for component $A$ is

$$S \text{ (weight of } S) = D \text{ (weight of } D) + G \text{ (weight of } G) \tag{2.3}$$

If the equations are solved simultaneously there results

$$\frac{\text{Weight of } D}{\text{Weight of } G} = \frac{G - S}{S - D} = \frac{\overline{GS}}{\overline{SD}} \tag{2.4}$$

or, as it is usually stated in words, the relative weights of the two saturated phases formed are inversely proportional to the lengths of the tie-line segments. This provides a convenient graphical method of obtaining material quantities. If the composition is plotted in terms of mole fraction and the quantities of the saturated solutions in moles, the same rule applies.

**Systems with an Upper Critical Solution Temperature.** In the case described in Fig. 2.1, which is typified by the system phenol–water, the solubilities of $A$ in $B$ and $B$ in $A$ increase with increase in temperature, so that at some elevated temperature the two conjugate solutions become identical and the interface between them consequently disappears. This temperature, termed the critical solution temperature (C.S.T.), or consolute temperature, occurs at the point $M$ in the figure and represents the temperature above which mixtures of $A$ and $B$ in any proportions form but one liquid phase. Point $M$ is the maximum on the continuous solubility curve but is not ordinarily at the midpoint of composition, nor are the solubility curves ordinarily symmetrical. The C.S.T. is the point where the two branches of the solubility curve merge, and the constant temperature ordinate is tangent to the curve at this temperature. The phase rule may be applied to this significant point:

$N = 2$ components
$P = 3$ phases (2 liquid, 1 vapor)
$F = 2 - 3 + 2 -$ restriction that the liquid phases be identical
$F = 1 -$ restriction

The restriction reduces the value of $F$ by one to bring $F = 0$, and the system is invariant at $M$. The C.S.T., therefore, is a function solely of the two substances comprising the system.

**Systems with a Lower Critical Solution Temperature.** Figure 2.2 is typical of the composition-temperature data for systems whose mutual solubility increases with decreasing temperature, as exemplified by the system triethylamine–water. The curve encloses an area where two conjugate liquid solutions form, while the area below the curve represents

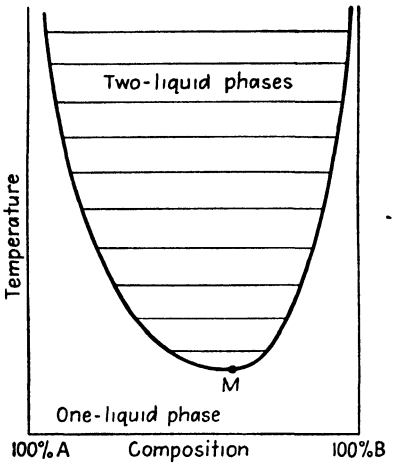



FIG. 2.2. Equilibrium compositions in a two-component system with a lower critical solution temperature.

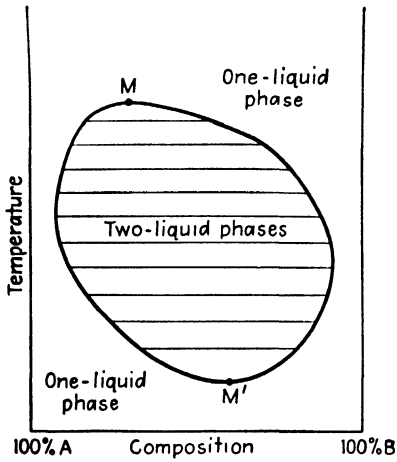



FIG. 2.3. Equilibrium compositions in a two-component system with both upper and lower critical solution temperatures.

mixtures forming a single liquid solution. As in the previous case, the area between the solubility curves may be imagined as filled with horizontal tie lines joining the conjugate solutions. The lowest point on the curve, $M$, is a C.S.T. for the system. Application of the phase rule to the various parts of the diagram leads to the same conclusions as in the previous case.

**Systems with Upper and Lower Critical Solution Temperature.** In the case of some liquids which are only partially miscible, complete solution is possible both above an upper C.S.T. and below a lower C.S.T., giving rise to solubility curves of the type indicated in Fig. 2.3. Despite the several examples which have been discovered where apparently the composition of both upper and lower critical points are nearly the same, there is no requirement that this be the case.

**Systems with No Critical Solution Temperature.** A large number of liquid pairs form systems without upper or lower critical points. In these cases, a solid phase forms before the appearance of a lower C.S.T. on cooling, and on heating, a vapor-liquid critical condition (vapor phase of the same composition and density as one of the liquid phases) occurs. Ether

and water form such a system, and quite probably all relatively insoluble pairs belong to this category.

Tables 2.1, 2.2, and 2.3 list a few typical systems of the type just described.

TABLE 2.1. SOME SYSTEMS WITH AN UPPER CRITICAL SOLUTION TEMPERATURE

| Components | | C.S.T., °C. | Weight per cent *B* at critical point |
|---|---|---|---|
| *A* | *B* | | |
| Water | Methyl acetate | 108 | 52.5 |
| Water | *n*-Butanol | 125.2 | 32.5 |
| Water | Furfural | 122.7 | 51 |
| Water | Phenol | 66.0 | 34.0 |
| Sulfur dioxide | Cyclohexane | 13.5 | 55.6 |
| Sulfur dioxide | *n*-Hexane | 10.1 | 71 |

TABLE 2.2. SOME SYSTEMS WITH A LOWER CRITICAL SOLUTION TEMPERATURE

| Components | | C.S.T., °C. | Weight per cent *B* at critical point |
|---|---|---|---|
| *A* | *B* | | |
| Water | Diethylamine | 143.5 | 37.5 |
| Water | Triethylamine | 18.7 | 50 |
| Water | 1-Methyl piperidine | 48.3 | 16.7 |
| Water | 4-Methyl piperidine | 189.5 | 36.2 |

TABLE 2.3. SOME SYSTEMS SHOWING UPPER AND LOWER CRITICAL SOLUTION TEMPERATURES

| Components | | C.S.T., °C. | Weight per cent *B* at critical point |
|---|---|---|---|
| *A* | *B* | | |
| Water | Ethylene glycol mono-*n*-butyl ether | 49.1<br>128 | 24.8<br>24.8 |
| Water | Ethylene glycol mono-isobutyl ether | 24.5<br>150.4 | 24.6<br>28 |
| Water | 1,2-Propylene glycol-2-propyl ether | 42.6<br>162 | 35<br>35 |
| Water | 2,6-Dimethyl pyridine | 45.3<br>164.9 | 27.2<br>33.8 |
| Water | Nicotine | 60.8<br>208 | 29<br>32 |
| Water | Methyl ethyl ketone | −6<br>150 | 31<br>45 |

**Effect of Pressure.** The temperature-composition diagrams discussed above were considered to be plotted at the pressure of the system, *i.e.*, at the equilibrium vapor pressure of the two-component mixture, which varies both with temperature and in the areas of one liquid phase with composition. However, it is an observed fact that the change in solubility

TABLE 2.4. VARIATION OF CRITICAL SOLUTION TEMPERATURE WITH PRESSURE*

| Components | | Temperature, °C. | Pressure range, kg/sq. cm. | $\frac{\Delta t}{\Delta p}$ |
|---|---|---|---|---|
| *A* | *B* | | | |
| Water | Nitromethane | 103.3 | 1–150 | −0.008 |
| Water | Propionitrile | 111.0 | 5–165 | −0.02 |
| Water | Methylal | 160.3 | 20–64 | −0.21 |
| Water | Succinonitrile | 52.3 | 10–160 | −0.003 |

* "International Critical Tables," Vol. III.

of the relatively immiscible liquids with externally applied pressure is very small and may be ignored in most situations. The nature of the effect may be predicted from the principle of Le Châtelier; if solution of the two components is accompanied by an increase in volume, it follows that an increased pressure will favor a decreased solubility, and vice versa. Table 2.4 indicates the small change that occurs at the critical solution point for several systems.

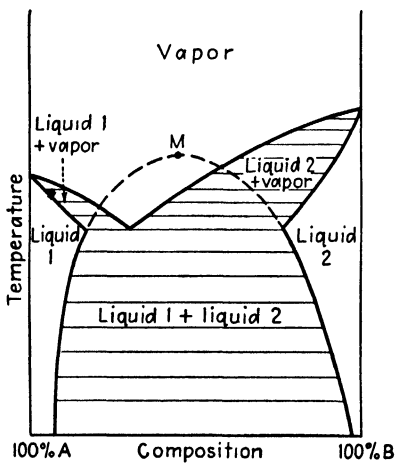



FIG. 2.4. Equilibrium compositions in a two-component system at a reduced pressure.

If the composition-temperature diagram for a system which has an upper C.S.T. is plotted at a constant pressure less than the equilibrium vapor pressure at the C.S.T., then it must be remembered that the upper C.S.T. will not be reached. As the temperature increases, when the vapor pressure of the system reaches that of the plot vaporization occurs, and the vapor-liquid equilibria of the system must be considered. Thus, Fig. 2.4 is the composition-temperature diagram for a system of the type aniline–water which has an upper C.S.T. plotted at 745 mm. Hg pressure. The liquid-solubility curves, normally merging at *M* (167.5°C.), are interrupted at 99°C. by the vapor-liquid equilibria. This is the type of diagram obtained for systems where the vapor pres-

sure of the liquid phases at equilibrium is greater than that of either pure component. For cases where the two-liquid-phase vapor pressure is intermediate between the vapor pressures of the pure liquids, a different type of vapor-liquid equilibria results, but the liquid-solubility curve is again interrupted.

**Effect of Impurities on the Critical Solution Temperature.** The addition of even a small amount of a third component to a two-liquid system will ordinarily alter the C.S.T. considerably. Thus, for example, the addition of 0.2 per cent of water to glacial acetic acid raises the C.S.T. with cyclohexane from 4.2 to approximately 8.2°C. Useful methods of analysis have been devised based on such observations. For example, the amount of deuterium oxide in water can be estimated by measuring the C.S.T. with phenol and the aromatic hydrocarbon content of petroleum fractions by the C.S.T. with aniline. In general, the C.S.T. will be raised if the added component is highly soluble in only one of the original components (salting out) and lowered if it is highly soluble in both. Such systems properly must be considered as three-component mixtures, however.

**Experimental Determination of the Solubility Curve.** There are two general methods in common use for the determination of the solubility curve, based on experiments at constant composition or at constant temperature. In the case of the former, a known mixture of the two components is weighed out in a thick-walled test tube in such proportions that two liquid layers form. The tube is then sealed, allowing a vapor space for subsequent expansion of the liquid. The sealed tube is then shaken in a bath while the temperature is slowly raised or lowered, until the two liquid phases are replaced by a single liquid solution. The temperature at which this occurs is noted, and the experiment provides one point on the solubility curve. A check on the observed temperature can be obtained by reversing the temperature effect, allowing the homogeneous solution again to form two conjugate solutions. The temperature can ordinarily be determined to within 0.1 to 0.01°C. without difficulty. For the constant-temperature procedure, one component may be titrated into a known quantity of the other until on shaking a slight turbidity is observed, the entire measurement being made at constant temperature. If analysis in the system is convenient, a mixture forming two liquid layers may be analyzed for one of the components. Ordinarily, the constant-temperature methods are most convenient for those portions of the solubility curve relatively far removed from the C.S.T. or where the solubility curve is reasonably parallel to the temperature axis. The constant-composition method is superior for portions of the curve near the C.S.T., where the curve is more nearly parallel to the composition axis. Both methods may be used for a single system and the data combined, since the effect of pressure in the ordinary ranges is so insignificant.

## THREE-COMPONENT SYSTEMS

As in the case of binary systems, the pressure effect on the liquid equilibria is relatively insignificant. Consequently we may exclude consideration of the vapor phase as unimportant for the present purposes, confine discussion to condensed systems, and study only temperature and concentration variables. A graphical representation which is most useful involves plotting compositions on triangular coordinates and temperature at right angles to the plane of the composition triangle. This produces a prismatic figure, and it will be convenient to consider isothermal sections of the space diagrams.

**Triangular Coordinates.** An equilateral triangle is used for representing compositions, use being made of the fact that the sum of the perpendiculars from any point within the triangle to the three sides equals the altitude (19). The length of the altitude is then allowed to represent 100 per cent composition, and the length of the perpendiculars from any point the percentages of the three components. Refer to Fig. 2.5. The apexes of the triangle represent the pure components $A$, $B$, and $C$, respectively.

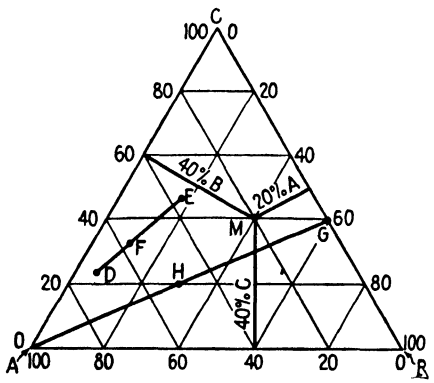



FIG. 2.5. Triangular coordinates.

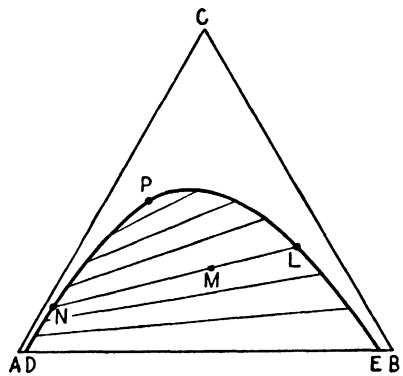



FIG. 2.6. Type 1 ternary liquid equilibria.

Any point on the side of the triangle represents a binary mixture of the two components marked at the ends of the side: thus, point $M$ is a mixture of 20 per cent $A$, 40 per cent $B$, and 40 per cent $C$. Points outside the triangle represent imaginary mixtures and have constructional significance only.

Several other characteristics of such plots are significant. A mixture at $D$, when added to one at $E$, will form a third mixture $F$ on the straight line $DFE$ (45). Furthermore, the relative weights of $D$ and $E$ mixed will cause the point $F$ to be so located that

$$\frac{\text{Weight of } E}{\text{Weight of } D} = \frac{\overline{DF}}{\overline{FE}} \tag{2.5}$$

Similarly, if $E$ is removed from $F$, the point $D$ representing the residue is on the straight line $EF$ extended through $F$, and the above relationship of weights and line-segments again applies. Geometrical measurements of this sort may be used for quantitative calculations, or the weights may be calculated from the compositions arithmetically by material balances. It is clear from what has been described that all points on the line $AG$ represent mixtures with constant ratios of $C$ to $B$ with varying amounts of $A$, and that if all of the $A$ is removed from mixture $H$, the mixture at $G$ will result.

**Ternary Systems of Interest in Liquid Extraction.** If all three components mix in all proportions to form homogeneous solutions, the system is of no importance in liquid extraction. Those where immiscibility occurs, and of consequent interest here, can be classified in the following manner:

| | | |
|---|---|---|
| Type 1. | Formation of one pair of partially miscible liquids | All three components liquid at the prevailing temperature |
| Type 2. | Formation of two pairs of partially miscible liquids | |
| Type 3. | Formation of three pairs of partially miscible liquids | |
| Type 4. | Formation of solid phases | |

**Type 1. Formation of One Pair of Partially Miscible Liquids.** This most frequently occurring combination is typified by the isotherm shown in Fig. 2.6. In a system of this sort, the liquid pairs $A$–$C$ and $B$–$C$ are miscible in all proportions at the prevailing temperature; $A$ and $B$ are partially miscible, and points $D$ and $E$ represent the saturated solutions in the binary system. A typical example is available in the system benzene ($A$)–water ($B$)–ethanol ($C$). All mixtures of the components represented by points in the area outside the curve $DNPLE$ are homogeneous single-liquid-phase solutions, while mixtures within the area bounded by the curve and the line $DE$ form two insoluble liquid layers. The curve $DNPLE$ represents the saturated solutions and is called the solubility or binodal curve. It is ordinarily concave throughout, as shown in Fig. 2.6, but several cases exhibiting a change in curvature have been recorded, such as the system water–ethylene glycol–amyl alcohol (30). A mixture of over-all composition $M$ will form the two immiscible liquid solutions of compositions $L$ and $N$, respectively, and the point $M$ is therefore on the straight line $LN$, which is a tie line. All mixtures represented on the line $LN$ form conjugate layers of the same composition, while the relative weights of the two layers can be calculated analytically from the compositions or graphically from the tie-line segments as indicated above.

The area of heterogeneity is to be imagined as filled with an infinite number of tie lines, only a few of which are shown in Fig. 2.6. These are

not parallel and ordinarily change their slope slowly in one direction with changing concentration. In a few systems there is a reversal of the slope, as in the case of water–ethyl acetate–ethanol at 0°C. (3) and ethanol–ethyl ether–water (33). In the case of the system of Fig. 2.6, it is clear that component $C$, when added to a heterogeneous liquid mixture of $A$ and $B$, distributes itself unequally between the two conjugate layers, with a greater concentration in the $B$-rich solutions. As more $C$ is added to such a mixture, the mutual solubility of $A$ and $B$ increases. At point $P$, the plait point, the two branches of the solubility curve merge, not ordinarily at the maximum value of $C$ on the curve. The tie lines shrink in length at higher concentrations of $C$ until at the plait point they vanish. Since at the plait point two liquid layers of identical composition and density form, the point is a true critical condition.

**Application of the Phase Rule.** For three components, $F = 5 - P$, and at constant temperature and pressure, $F = 3 - P$. For mixtures of one liquid phase, $F = 2$, and two compositions must be stated in order to determine the system. In the area of heterogeneity with two liquid phases, the system is univariant; at the plait point, with the restriction that the two liquid phases be identical, the system is invariant. It is noteworthy that, while for binary systems the critical-solution point is defined if the pressure is fixed, in ternary systems the critical or plait point is defined only at fixed temperature and pressure.

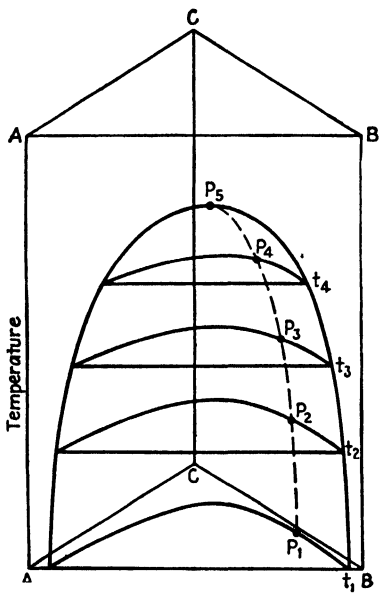



FIG. 2.7. Ternary system with no ternary critical solution temperature.

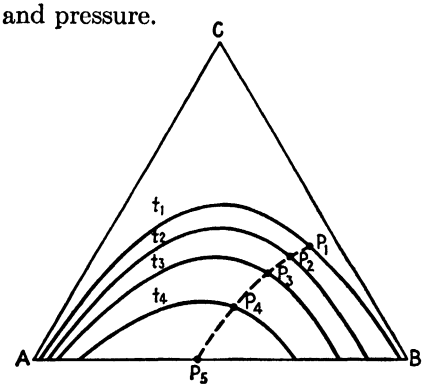



FIG. 2.8. Isotherms for a ternary system with no ternary critical solution temperature.

**Effect of Temperature.** A constant-pressure representation which includes temperature as well as composition variables will be a triangular prism. For systems of the type just considered, two cases are of interest.

1. Systems with no ternary C.S.T., as indicated in Fig. 2.7. The curve

in the plane $AB$–$AB$ is the binary solubility-temperature relationship for mixtures of $A$ and $B$, with a binary upper C.S.T. at $P_5$. Points $P_1$, $P_2$, $P_3$, and $P_4$ are plait points of the various isothermals at the corresponding temperatures, and the curve through these points passes up to the binary C.S.T. at $P_5$. This curve does not have a maximum within the space figure but reaches its highest point only in the absence of component $C$. There is therefore no ternary C.S.T. Figure 2.8 shows the isotherms projected onto the base of the prism. An excellent example of this type of system is that of diphenylhexane–docosane–furfural (9).

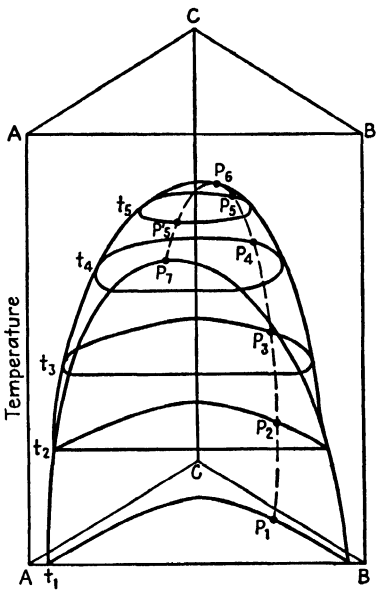



FIG. 2.9. Ternary system with a ternary critical solution temperature.

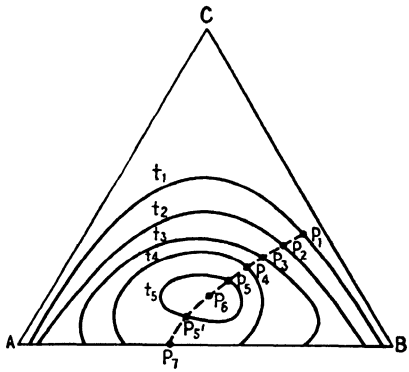



FIG. 2.10. Isotherms for a ternary system with a ternary critical solution temperature.

2. Systems which have a ternary C.S.T. Refer to Fig. 2.9. In this case, the curve through the plait points $P_1$, $P_2$, $P_3$, $P_4$, and $P_5$ reaches a ternary maximum at $P_6$, which then becomes a true ternary C.S.T. The curve continues through $P_5'$ to $P_7$, the binary C.S.T. Projections of the isotherms onto the base of the figure are indicated in Fig. 2.10. It is clear that for temperatures between that at $P_7$ and $P_6$, such as that at $t_5$, there will be closed, isothermal solubility curves, with two plait points, $P_5$ and $P_5'$, while the binary pairs show individually complete miscibility. An example of this type of system is that of water–phenol–acetone with a ternary C.S.T. at 92°C., and a binary C.S.T. (water–phenol) at 66°C. (42).

For ternary systems containing an incompletely miscible binary pair showing a lower C.S.T., or both upper and lower C.S.T.'s, it is simple to imagine the nature of the various space diagrams possible.

In general, not only do the areas of heterogeneity change with changing temperature, as indicated in Figs. 2.7 to 2.10, but the slopes of the tie lines, or the distribution of component $C$ between the insoluble layers, change as

well. The latter effect is relatively small with moderate temperature changes but in most cases cannot be ignored.

**Type 2. Formation of Two Pairs of Partially Miscible Liquids.** Refer to the isotherm, Fig. 2.11. In this case, at the temperature of the plot, both the liquid pairs *A*–*B* and *A*–*C* are partially miscible, while *B* dissolves in any proportion in *C*. The area within the band lying across the triangle represents mixtures which form two liquid layers, the compositions of which are at the ends of the tie lines through the points representing the mixtures as a whole. On this type of diagram there can be no plait point. Typical examples are the systems aniline (*A*)–*n*-heptane (*B*)–methyl cyclohexane (*C*) (58), and water (*A*)–chlorobenzene (*B*)–methyl ethyl ketone (*C*) (35).

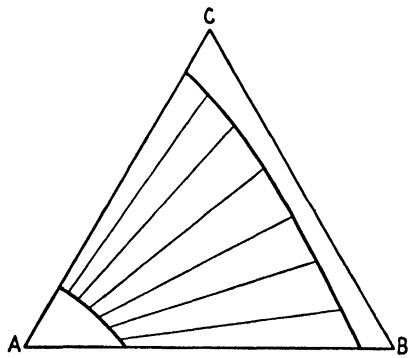



FIG. 2.11. Type 2 ternary liquid equilibria.

This type of solubility diagram can be considered as having evolved from a simpler situation by a change in temperature, as shown in Fig. 2.12. At $t_1$, the solubility diagram appears like a combination of two systems of Type 1, with plait points at $P_1$ and $P_2$. As the temperature is changed to $t_2$, the area of mutual solubility changes, the plait points moving in such a manner that they meet. At $t_3$, the common plait point has changed to a tie line, and at still further change in temperature, the type of diagram shown in Fig. 2.11 results. The system water–phenol–aniline exhibits this behavior (43). If, however, the two plait points do not meet as the area of mutual solubility grows smaller, then a system exhibiting three equilibrium liquid layers develops, as indicated in Fig. 2.13 at $t_2$. Here, any ternary mixture whose over-all composition lies within the area *DEF* will form the three liquid phases at *D*, *E*, and *F*, and the system becomes invariant at constant temperature and pressure. As examples, the systems silver perchlorate–water–benzene and silver perchlorate–water–toluene may be cited (25, 26). On further temperature change, this three-liquid area would ordinarily be expected to get smaller and eventually disappear, giving rise again to the band-type diagram of Fig. 2.11. In some cases, the banded

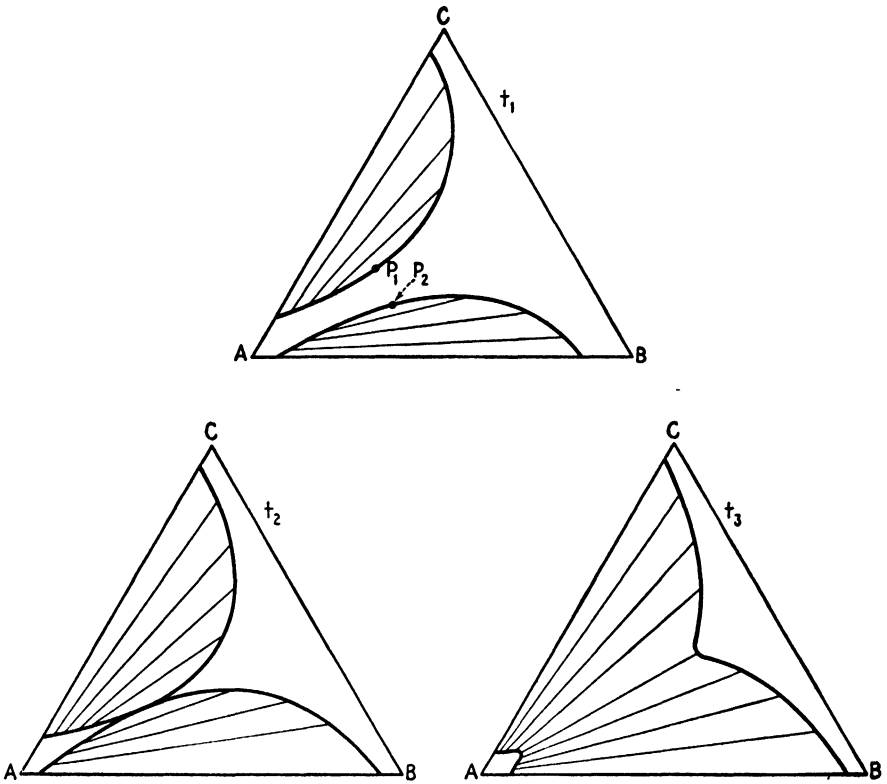



FIG. 2.12. Formation of Type 2 system from two Type 1 systems with changing temperature.

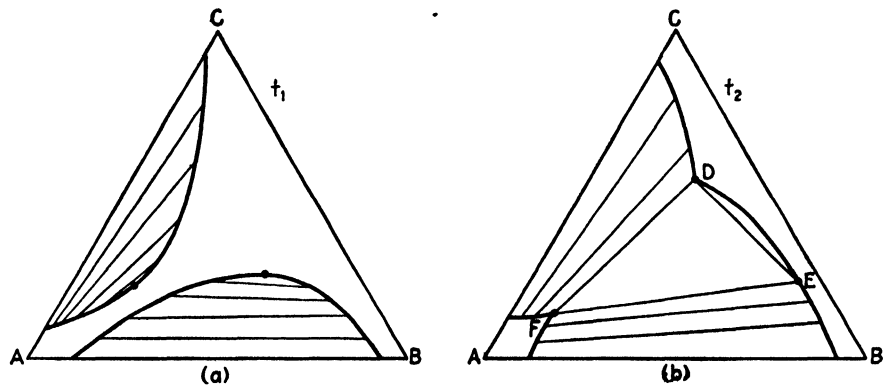



FIG. 2.13. Formation of three liquid phases in equilibrium.

type of diagram results from an expansion of the heterogeneous area of a Type 1 system, as indicated in Fig. 2.14 (13, 27).

As in the case of Type 1 systems, either upper, lower, or both types of ternary C.S.T.'s may form, or there may be none.

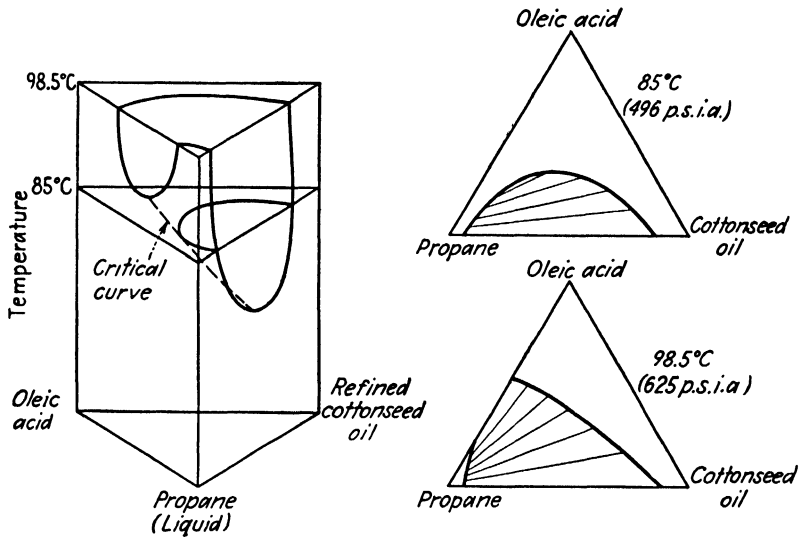



FIG. 2.14. The system propane–oleic acid–refined cottonseed oil. [*Hixson and Bockelman, Trans. Am. Inst. Chem. Engrs.* **38,** 891 (1942)]

**Type 3. Formation of Three Pairs of Partially Miscible Liquids.** If the three binary pairs are mutually only partially miscible, then at some temperature three separate solubility curves might appear such as at $t_1$ in Fig. 2.15. If changing the temperature will cause the separate binodal curves to meet as at $t_2$, Fig. 2.15, then a three-liquid area *DEF*, invariant at constant temperature and pressure, will result. At some intermediate temperature, two of the binodal curves might meet to give a configuration

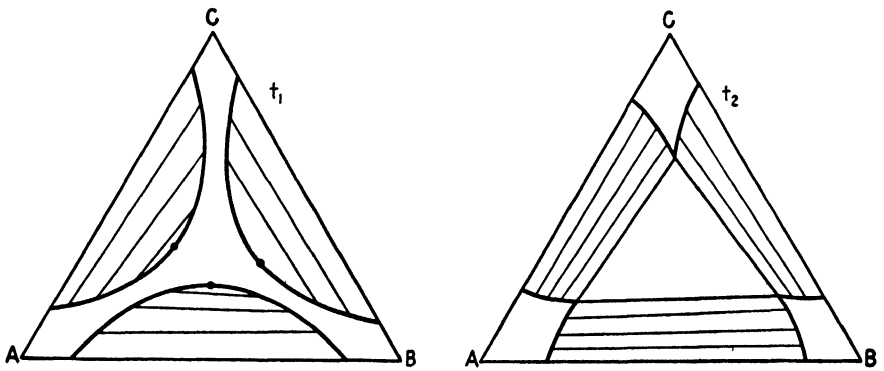



FIG. 2.15. Formation of three liquid phases in equilibrium.

like that of Fig. 2.13 at $t_2$, but with an additional binodal curve. These types of diagrams have been relatively little investigated, but examples are available in the systems iron–zinc–lead (54) and succinic nitrile–ether–water (42).

**Type 4. Formation of Solid Phases.** These systems may be very complex in the number of equilibria which may exist, and for a complete description of the possibilities reference must be made to any of the standard works on the phase rule. A few of the more simple situations are of interest in liquid extraction, and they will be described.

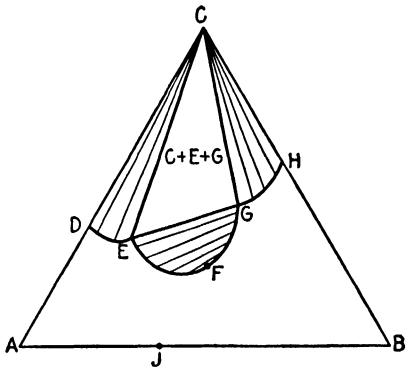



FIG. 2.16. Equilibria in a ternary system containing a solid component.

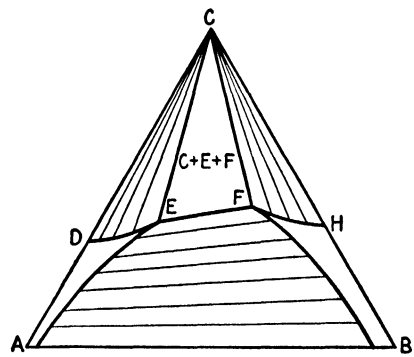



FIG. 2.17. Distribution of a solid between two insoluble liquids.

Refer to Fig. 2.16. In this system, $C$ is a solid at the temperature of the diagram, while $A$ and $B$ are mutually soluble liquids. As an example, the system ethanol ($A$)–water ($B$)–potassium fluoride ($C$) may be cited. $D$ is the solubility of $C$ in liquid $A$, and $H$ that of $C$ in liquid $B$. The area $DABHGFED$ represents single-liquid-phase solutions. A solution of composition such as that at $J$, to which $C$ is added, will eventually form two liquid layers where the line $CJ$ (not shown) passes through the area $EFGE$. In this area, compositions of the equilibrium liquid layers are given by the tie lines which culminate in the plait point at $F$, and the process just described is the familiar one of salting out. The curve $DE$ is the solubility of $C$ in $A$-rich ternary solutions, and the tie lines therefore converge to the $C$ apex, indicating that the solid phase $C$ may be in equilibrium with any of the solutions along $DE$. The significance of the area $CGHC$ is the same, except that it applies to $B$-rich solutions. In the area $CEGC$, three condensed phases will form, always the same irrespective of the overall composition of the mixture: solid $C$, and saturated liquids at $E$ and $G$.

Simple extensions to cases where liquids $A$ and $B$ are only partially soluble and where solid $C$ is distributed between the equilibrium layers are readily visualized. For example, in the configuration shown in Fig. 2.17, the situation is fundamentally similar to that in Fig. 2.16, except that the

two-liquid-phase area is so large that it reaches to the $B$–$A$ axis. The various areas need no additional explanation. In some instances, the solubility of the solid $C$ is extremely small in an organic liquid $B$, so that the diagram appears to be considerably distorted, as in the case of sodium hydroxide–acetone–water (20), sodium hydroxide–isobutanol–water (17), and calcium chloride–methyl ethyl ketone–water (32), but the interpretation is nevertheless the same. On the other hand, in the case of certain soap systems, despite the fact that the soap may be fairly insoluble in the pure immiscible liquids, single-phase ternary liquids containing appreciable quantities of all three components may exist, as shown in Fig. 2.18 (39).

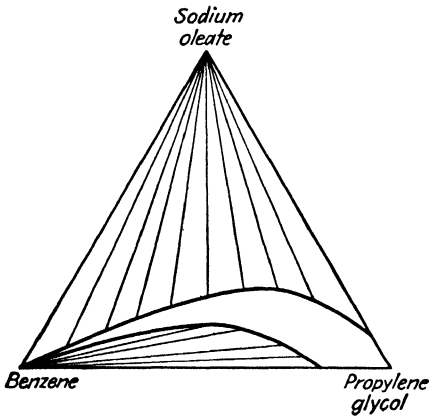



FIG. 2.18. The system sodium oleate–benzene–propylene glycol at 20°C. [*Palit and McBain, Ind. Eng. Chem.* **38**, 741 (1946).]

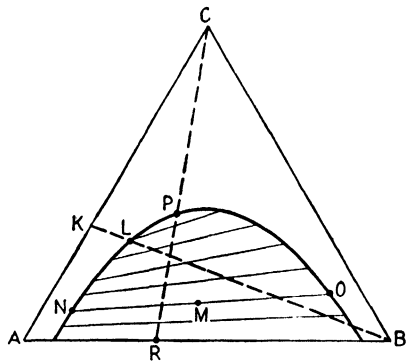



FIG. 2.19. Determination of the ternary-liquid equilibria.

Much more complex equilibria may arise, as in the case of the system succinic nitrile–ether–water at 2°C. (42), where, while the binary pairs behave as do $A$, $B$, and $C$ of Fig. 2.17, three separate, isothermally invariant ternary areas exist. Compound formation will further complicate the equilibria.

**Experimental Determination of the Ternary-equilibrium Data.** If chemical analysis for two of the three components in the system is readily carried out, both tie lines and binodal curve may be determined simultaneously. Refer to Fig. 2.19. If a mixture of composition at $M$ is shaken in a thermostat at the temperature corresponding to that of the diagram, then on standing, two layers at $N$ and $O$ will form. These may be withdrawn, most conveniently if the original mixture is prepared in a separatory funnel and each analyzed for two components. Repetition of this procedure at different over-all mixture compositions will result in knowledge of the complete diagram.

Ordinarily, it is difficult to make the analyses for two of the components, and for such cases it is necessary to determine the binodal curves separately

from the tie lines. If a mixture of known weight and composition $K$ is prepared and titrated with pure $B$ while held in a thermostat, then when sufficient $B$ is added to produce a solution on the solubility curve at $L$, a turbidity will be observed. The composition at $L$ can be calculated from the amounts of the liquids used. In this manner, points along the $A$-rich portion of the solubility curve can be determined satisfactorily up to the maximum per cent $C$ on the curve. For the $B$-rich portions, it is necessary to titrate known mixtures of $C$ and $B$ with $A$. These data do not give the tie lines, however, which must be determined separately. If one component of the three can be analytically determined easily, then equilibrium layers such as those at $N$ and $O$ can be prepared from a mixture such as $M$, the layers analyzed for the component, and the position of $N$ and $O$ determined since they must be on the solubility curve. For experimental details the work of McDonald (31), Bogin (5), and Hand (22) may be consulted.

If analysis of all three components is difficult, it is usually possible to determine a physical property of mixtures along the binodal curve which will vary sufficiently with concentration so that it can be used for analytical purposes. Specific gravity, or refractive index, is frequently chosen, since these are simple to measure. Thus, determination of the specific gravity of the layers $N$ and $O$ and reference to a plot of specific gravity vs. per cent $C$ along the solubility curve will fix the position of $N$ and $O$. Modification of these methods can be made as necessary for other types of diagrams.

In all of the above methods, an independent material-balance check is provided by the fact that the over-all composition of an equilibrium mixture such as $M$ must lie on the straight line $ON$ joining the equilibrium layers. On the other hand, for very rapid but perhaps less accurate work, the principle that the weights of the layers are inversely proportional to the lengths of the tie-line segments may be utilized to determine the composition of the conjugate layers if the binodal curve is known. If the mixture of known composition at $M$ is prepared in a graduated cylinder, the volumes of the two equilibrium layers which form may be read directly. Their specific gravities may be readily determined without removal by a Westphal balance, and hence their relative weights calculated. Points $N$ and $O$ on the phase diagram are then so located that

$$\frac{\overline{NM}}{\overline{MO}} = \frac{\text{weight of } O}{\text{weight of } N} \tag{2.6}$$

A simple method of doing this has been described by Othmer and Tobias (37).

The position of the plait point may be established experimentally by first locating a two-phase mixture $R$ by trial (24). If $C$ is added to such a mixture, the two liquid phases will change to a single liquid phase at the plait point $P$, with the interface between the liquid layers located near the

center of the containing vessel until miscibility is reached. If any mixture other than $R$ is used, the interface will move to the bottom or top of the mixture as $C$ is added. Ordinarily, it is more convenient to locate the plait point by empirical treatment of the tie-line data, as explained below.

An accurately determined ternary-phase diagram is not only essential to the complete understanding of liquid-extraction operations but is also useful in assisting in the analysis of binary and ternary mixtures where chemical analysis is difficult or impossible. A. S. Smith (46) has presented the details of this type of work.

**Rectangular Coordinates for Ternary Data.** For some purposes, a plot of the ternary-equilibrium data on rectangular coordinates is preferable to the triangular plots described above. Several methods have been described, perhaps the most useful of which was first proposed by Janecke (29). For a system of the type shown in Fig. 2.6, $\%B/(\%A + \%C)$ is plotted as ordinate against $\%C/(\%A + \%C)$ as abscissa, to give a diagram of the type shown in Fig. 2.20*a*. In the case of systems of the type shown in Fig. 2.11, $\%A/(\%B + \%C)$ is the ordinate, $\%B/(\%B + \%C)$ the abscissa (Fig. 2.20*b*). The special usefulness of these coordinates will be shown later. A. S. Smith (47) avoids the use of the triangular diagram by plotting, for a system of the type of Fig. 2.6, $\%C$ as ordinate against $[\%C + 2(\%B)]\sqrt{3}$ as abscissa. In this manner, the appearance of the binodal curve is retained, and several other useful results follow.

## TIE-LINE CORRELATIONS FOR TERNARY SYSTEMS

**Interpolation and Extrapolation of Tie-line Data. Type 1 Systems.** In the case of many systems described in the literature, only a few tie lines have been experimentally determined. Direct interpolation of such data on the triangular diagram, and particularly extrapolation, ordinarily leads to highly inaccurate results and should not be attempted. Several methods of dealing with the problem have been devised, however, and these will be found exceedingly useful in all liquid-extraction work.

**Graphical Interpolation on the Triangular Plot.** In Fig. 2.21, if $DE$ is a tie line, line $DG$ may be drawn parallel to $CB$, and $EF$ parallel to $AC$, the two constructed lines intersecting at $H$. A tie-line correlation curve or conjugation curve $PHJ$ is then drawn through several such intersections obtained from corresponding known tie lines. From any point on the tie-line correlation curve, two constructed lines parallel, respectively, to $AC$ and $BC$ will intersect the solubility curve at concentrations corresponding to conjugate solutions. The curve $PHJ$ is not straight, although the curvature is ordinarily small, and it necessarily passes through the plait point. The method is excellent for interpolation in cases where at least three or four tie lines are known but is not very precise for extrapolating any considerable distance because of the curvature of the correlation curve. The

position of the plait point can be found by extrapolation only when tie lines very close to the plait point are known. The method is used extensively in the "International Critical Tables" (28).

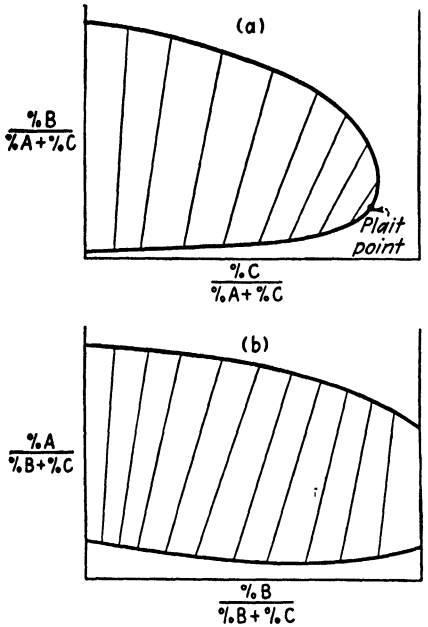



FIG. 2.20. Rectangular coordinates for (*a*) Type 1, and (*b*) Type 2 ternary systems.

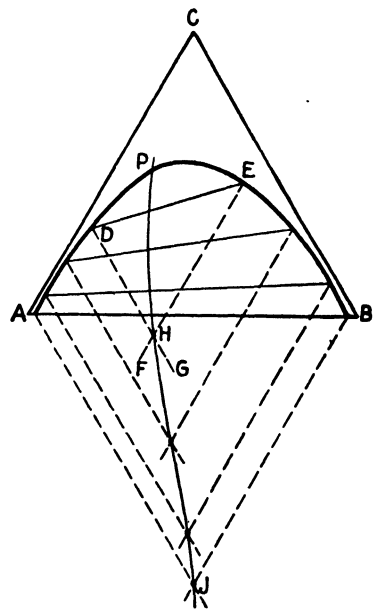



FIG. 2.21. Graphical interpolation of tie lines.

Since the method of Fig. 2.21 requires extension of the plot below the base of the triangle and since this cannot be done conveniently on the triangular graph paper ordinarily available, Sherwood (44) has devised a modification which is useful. Refer to Fig. 2.22. The construction is similar to that previously described, except that the lines *EH* and *DH* are drawn parallel to sides *AC* and *AB*, respectively, intersecting at *H*. The tie line correlation curve *JHP* may be drawn through several such intersections and passes through the plait point *P*. The correlation curve now falls wholly within the triangle but has greater curvature than previously, thereby somewhat lessening its usefulness.

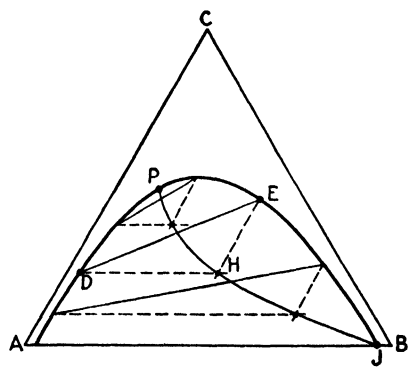



FIG. 2.22. Graphical interpolation of tie lines.

Hand (22) presented an interesting method of plotting the ternary data

in such a manner as to make the tie lines parallel to the base of the triangle, thus simplifying interpolation and extrapolation. The plait point is then at the maximum of the binodal curve. The method has not been investigated thoroughly to determine the extent of its applicability, however.

In some cases, the tie lines when produced beyond the binodal curve all intersect at a single point on the extended base of the triangle (50, 51, 52), but the principle is not sufficiently general to be of great practical value. In a few isolated instances, the extended tie lines appear to be tangents of a curve (41).

**Distribution Curves.** Many methods of plotting the concentrations of conjugate solutions, one against the other, have been devised for the purpose of correlating data and to facilitate interpolation and extrapolation. Preferably, such plots should be rectilinear for all systems, since then not only is extrapolation facilitated, but in addition two accurately determined tie lines can be used to predict the position of all other tie lines with considerable confidence. In order to describe these readily and to systematize them, the following notation will be used:

$X$ = weight fraction of component.
Subscripts: $A$, $B$, and $C$ refer to components $A$, $B$, and $C$, respectively. The first subscript refers to the component whose concentration is indicated, and the second to the predominant component of the solution. Thus,

$X_{CA}$ = weight fraction of $C$ in an $A$-rich phase,

$X_{BB}$ = weight fraction of $B$ in a $B$-rich phase, etc.
In Type 1 systems, $C$ is the component distributed between the partially miscible components $A$ and $B$ (Fig. 2.6)

1. The simplest distribution curve consists of a plot of the concentrations of $C$ in the $A$-rich phase ($X_{CA}$) against equilibrium concentrations of $C$ in the $B$-rich phase ($X_{CB}$), on arithmetic coordinates. Figure 2.23*b* is typical for the ternary systems of the type shown in Fig. 2.23*a*. It will be noted that the resulting curve lies wholly above the 45° line, drawn in for reference, indicating that in this case component $C$, on distribution between the phases, favors the $B$-rich layers. The curve is ordinarily reasonably straight near the origin but necessarily terminates at the plait point on the 45° line. If the plait point is not on the maximum of the triangular binodal curve, the distribution curve will rise through a maximum, as shown. The ratio $X_{CB}/X_{CA}$ at any point on the curve is called the distribution coefficient, or ratio. Nernst (34) proposed that, provided the concentrations referred only to those molecules which are in the same condition in both phases, the distribution coefficient will be constant, irrespective of the total concentration of distributed substance present. This requires that, if component $C$ is represented by the same molecular species in both phases, the curve of Fig. 2.23*b* be a straight line. If ordinary

concentrations are used for plotting, without regard to any association, dissociation, or compound formation which may occur, the curve is ordinarily straight for a short distance from the origin but cannot be so for its entire length as long as a plait point exists in the system. The simple distribution law

$$\frac{X_{CB}}{X_{CA}} = \text{const.} = m \tag{2.7}$$

therefore will apply, if at all, to very dilute solutions only. In the case of a solid distributed between immiscible liquids, as in Fig. 2.17, the absolute adherence to such a law requires that the ratio of concentrations of distributed substance equal the ratio of the respective solubilities of the substance in the two solvents. This never occurs except perhaps at very low concentrations. Nernst provided corrections for the total concentrations where association or dissociation occur, indicated in Table 2.5.

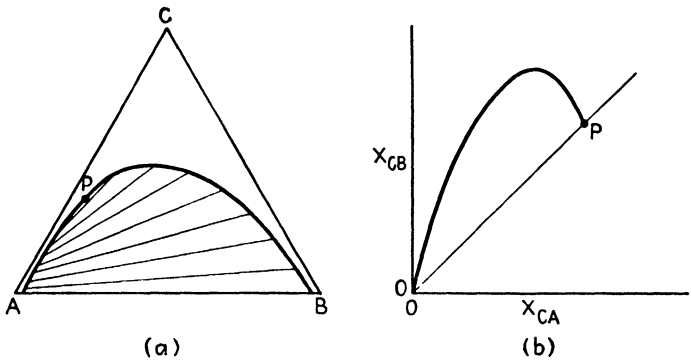



FIG. 2.23. Distribution of $C$ between $A$ and $B$, in a Type 1 system.

In some instances, association to polymolecules is nearly complete, so that $\alpha'$ is negligible. For a case 3 combination, the distribution ratio would then become

$$m = \frac{X_{CB}}{\sqrt[n]{X_{CA}}} \tag{2.8}$$

Plotting the concentrations on logarithmic paper would therefore yield a line whose slope indicates the number of simple molecules in the polymer [see, for example, the work of Hendrixson (23)]. Campbell (11) proposed the general use of logarithmic coordinates in this manner for various distributions, but, as has been shown (30), the method cannot be relied upon to describe data near the plait point. The simple distribution curve itself is useful for interpolating data when a relatively large number of tie lines are available but should not be used for extrapolation.

2. Brancker, Hunter, and Nash (6), in the case of the system toluene ($A$)–water ($B$)–acetic acid ($C$), plotted $X_{AA}$ against equilibrium concentra-

tions of $X_{BB}$ on arithmetic coordinates and found that the resulting tie-line correlation had a pronounced curvature. However, by adjusting the scale of the $X_{AA}$ axis, the curve could be made a straight line. Thirty-three other systems plotted on the adjusted coordinates also gave straight lines. The method is similar to that of Cox (12) in the case of vapor pressures and requires the coordinates to be set up with a system which has been very completely and accurately determined. A few systems did not give straight lines, but in these cases the tie lines on the original triangular diagram changed their direction of slope, which occurs only in a relatively few systems.

TABLE 2.5. NERNST CORRECTIONS FOR THE SIMPLE DISTRIBUTION LAW

| Case | Condition of $C$ in | | Distribution law |
|---|---|---|---|
| | Phase 1 ($B$-rich) | Phase 2 ($A$-rich) | |
| 1 | No molecular change | No molecular change | $\frac{X_{CB}}{X_{CA}} = m$ |
| 2 | Dissociation | No molecular change | $\frac{X_{CB}(1-\alpha)}{X_{CA}} = m$ |
| 3 | No molecular change | Association $nM \rightleftarrows M_n$ | $\frac{X_{CB}}{\sqrt[n]{X_{CA}(1-\alpha')}} = m$ |
| 4 | Dissociation | Association $nM \rightleftarrows M_n$ | $\frac{X_{CB}(1-\alpha)}{\sqrt[n]{X_{CA}(1-\alpha')}} = m$ |

$X_{CB}$ and $X_{CA}$ represent total concentrations of $C$ in the phases.
$\alpha$ = degree of dissociation of simple molecules.
$\alpha'$ = degree of dissociation of polymolecules.

3. Bachman (1) found that the equations of the lines on the Brancker, Hunter, and Nash coordinates are

$$X_{AA}X_{BB} = aX_{AA} + bX_{BB} \tag{2.9}$$

where $a$ and $b$ are constants. Rewriting the equation to read

$$X_{BB} = a + b\left(\frac{X_{BB}}{X_{AA}}\right) \tag{2.10}$$

indicates that plotting $X_{BB}$ against $X_{BB}/X_{AA}$ on arithmetic coordinates will give a straight line for the tie-line data, and this eliminates the necessity for having the unusual coordinate system first described.

4. Othmer and Tobias (38) have found that a plot of conjugate values of $(1 - X_{AA})/X_{AA}$ against $(1 - X_{BB})/X_{BB}$ on double logarithmic coordinates produced straight lines. These of course are useful for interpolation and extrapolation.

5. Methods 2, 3, and 4 just described suffer principally from the fact that the concentration of $C$, the distributed component, is not indicated in the coordinates. Hand (22) showed that a double logarithmic graph of $X_{CA}/X_{AA}$ against $X_{CB}/X_{BB}$ at equilibrium, which includes the concentration of $C$ in the coordinates, is ordinarily rectilinear. This method of plotting was first proposed by Bancroft (2). As in previous cases, those systems which are not represented by straight lines are those relatively rare cases where the direction of the tie-line slope changes with concentration. The straight lines can be represented by equations of the form

$$\frac{X_{CB}}{X_{BB}} = k\left(\frac{X_{CA}}{X_{AA}}\right)^n \qquad (2.11)$$

The significance of the constants $k$ and $n$ in these equations has been pointed out (54) and will be considered later (Chap. 3). Furthermore, a simple method of locating the plait point based on this method has been devised (57). If on the same graph as the tie-line data the binodal curve is plotted as $X_C/X_B$ against $X_C/X_A$, where $X_A$, $X_B$, and $X_C$ are concentrations of the components at any point on the binodal curve, a single curve of two branches is obtained, one branch representing the $A$-rich layer, and the other the $B$-rich layer (Fig. 2.24). At the plait point, the distinction between the $A$-rich and $B$-rich phases disappears. Therefore,

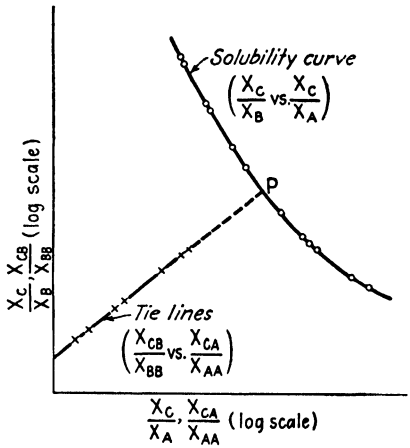



FIG. 2.24. Estimation of the plait point.

$$\left(\frac{X_{CB}}{X_{BB}}\right)_p = \left(\frac{X_{CA}}{X_{BA}}\right)_p = \left(\frac{X_C}{X_B}\right)_p \qquad (2.12)$$

and

$$\left(\frac{X_{CA}}{X_{AA}}\right)_p = \left(\frac{X_{CB}}{X_{AB}}\right)_p = \left(\frac{X_C}{X_A}\right)_p \qquad (2.13)$$

where the subscript $p$ represents the plait point. Since the plait point represents a limiting tie line, the coordinates $(X_{CA}/X_{AA})_p$ and $(X_{CB}/X_{BB})_p$ must fall simultaneously on the tie-line correlation and on the binodal curve. Consequently, extrapolating the straight-line tie-line correlation to intersection with the solubility curve will locate the plait point.

Figures 2.25, 2.26, 2.27, and 2.28 have been prepared to illustrate the appearance of distribution data on the various types of coordinates. For purposes of comparison, the same systems are shown on each. In the case of two, ethanol–*n*-butanol–water and 1,4-dioxane–benzene–water, the measurements have been carried up to the plait points. The first of these

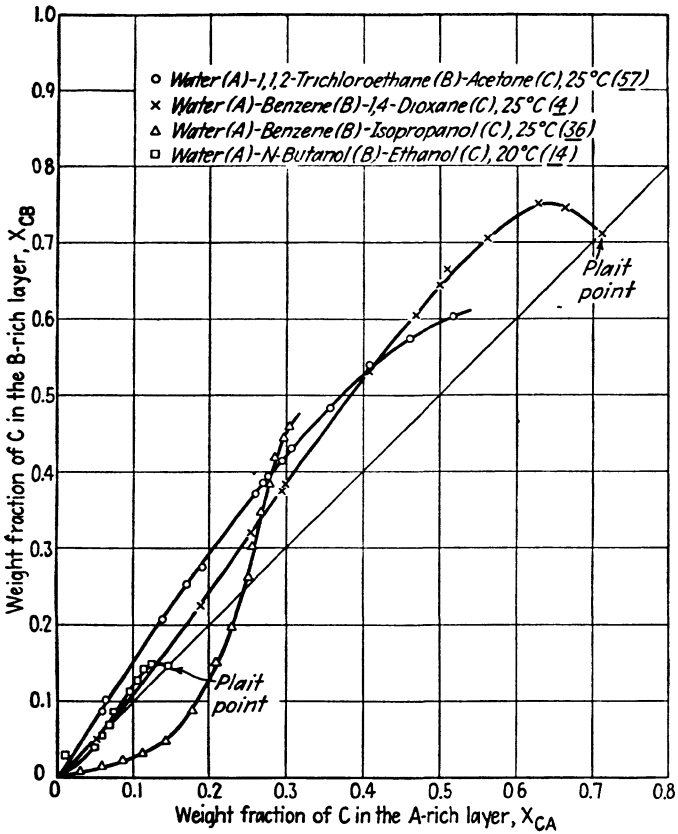



FIG. 2.25. Distribution curves, Type 1 systems.

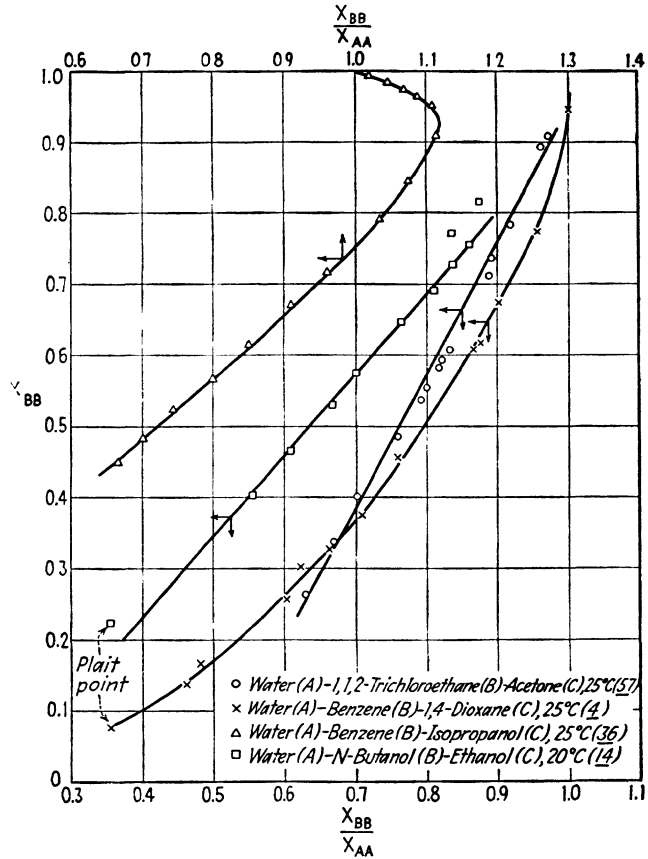



FIG. 2.26 Bachman coordinates (1).

is characterized by unusually high mutual solubility of the nonconsolute components, resulting in only 14.9 per cent as the maximum concentration of the distributed component. The system isopropanol–benzene–water is unusual in that it shows a marked reversal of the distribution ratio. Of the four, the systems 1,4-dioxane–benzene–water and acetone–1,1,2-trichloroethane–water offer data which are perhaps most representative of Type 1 systems.

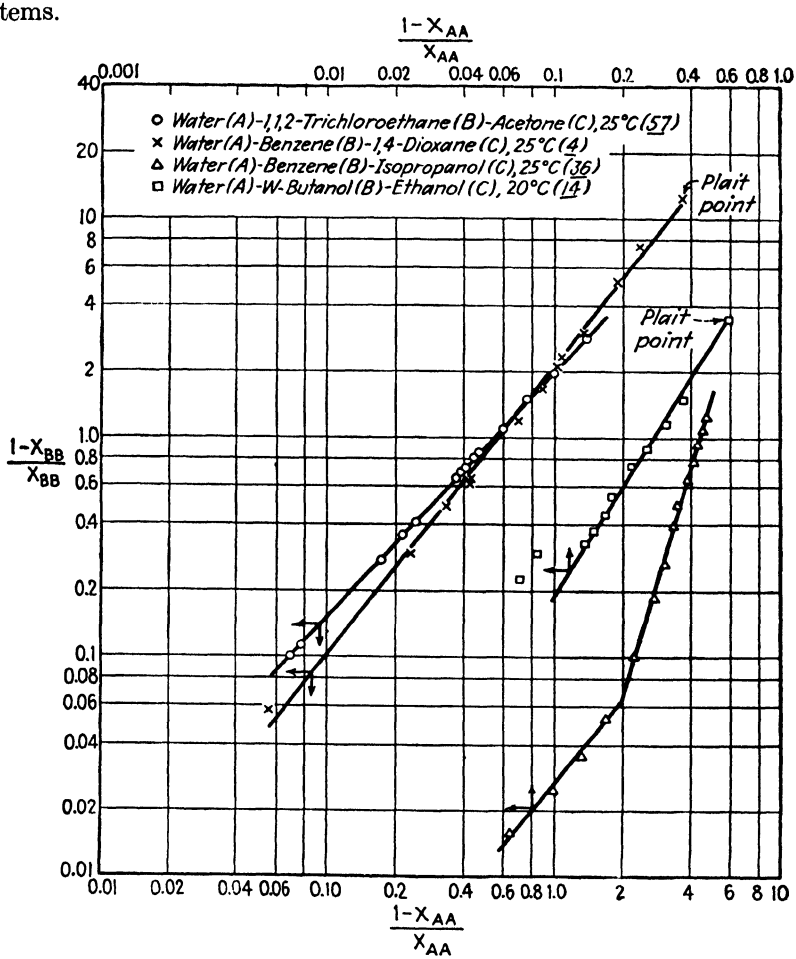



FIG. 2.27. Othmer-Tobias coordinates (38).

On Fig. 2.25, a simple distribution plot, the reversal of distribution for isopropanol–benzene–water is clearly evident. A careful study of the data for ethanol–*n*-butanol–water leads to the conclusion that the tie line for the lowest concentration of ethanol is quite probably in error. On Fig. 2.26, the Bachman coordinates, the data for the dioxane and isopropanol distributions appear very obviously as curves. Figure 2.27 is of the Othmer-

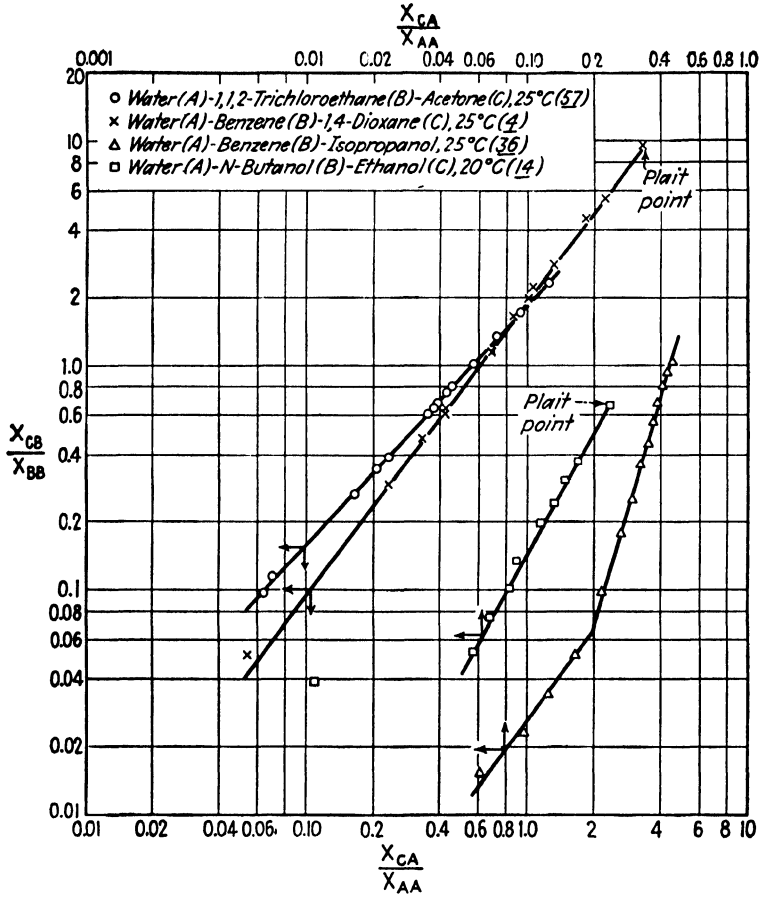



FIG. 2.28. Hand coordinates (22).

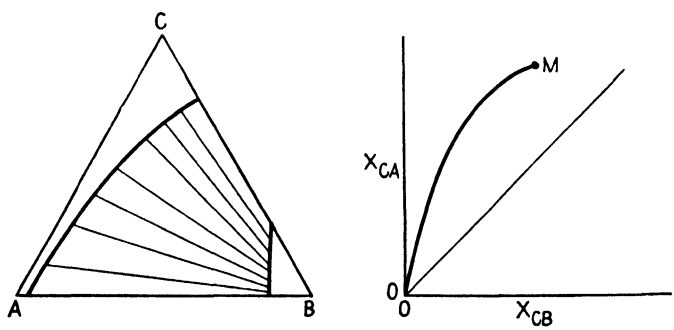



FIG. 2.29. Distribution in a Type 2 system.

Tobias type, and except in the case of isopropanol excellent straight lines are obtained up to plait-point concentrations. These authors have tested this coordinate system with a large number of systems and have shown it to be very useful generally. Figure 2.28, with the Hand type of coordinates, also shows excellent rectilinearity even up to the plait points for all data, with the exception again of the isopropanol distribution. Here the uncertainty of the single point in the ethanol–*n*-butanol–water system is very clear. This plot has been tested with over sixty systems with similar consistently good results (56).

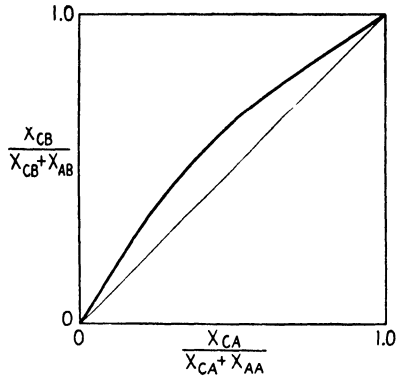



FIG. 2.30. Distribution of *C* between equilibrium layers of a Type 2 system, *B*-free basis.

**Type 2 Systems.** Distribution data for systems of this type will appear in the manner indicated in Fig. 2.29, the point *M* representing the mutual solubility of the *B*–*C* binary. On a *B*-free basis, the distribution of components *A* and *C* give rise to a curve resembling isobaric vapor-liquid equilibria, as in Fig. 2.30. For example, in the case of the system *n*-heptane (*A*)–aniline (*B*)–methylcyclohexane (*C*), Varteressian and Fenske (58) found that at equilibrium

$$\frac{X_{CB}}{X_{AB}} = \beta \frac{X_{CA}}{X_{AA}} \tag{2.14}$$

and

$$\frac{X_{CB}/(X_{CB} + X_{AB})}{1 - X_{CB}/(X_{CB} + X_{AB})} = \beta \frac{X_{CA}/(X_{CA} + X_{AA})}{1 - X_{CA}/(X_{CA} + X_{AA})} \tag{2.15}$$

where $\beta$ in each case equals 1.90, the ratio of osmotic pressures of *A* and *C* when each alone saturates *B*. The similarity of these expressions to that for ideal vapor-liquid equilibria, where $\beta$ is replaced by relative volatility, is striking. There were also several other simple relationships describing distributions of *A* and *C*. Dryden (15) and Darwent and Winkler (13) investigated the forms of these equations further and found several Type 1 systems which could be described in similar fashion, although the relationships are not general for either Type 1 or 2. Brown (10) has studied the application to other Type 2 systems and furthermore pointed out that the plot of Bachman can be made applicable to these systems. There have actually been relatively few Type 2 systems studied, and generalizations are still uncertain.

## FOUR-COMPONENT SYSTEMS

**Representation.** The four components will necessarily require a space model for complete representation of compositions even at constant tem-

perature. One device which has been proposed is the equilateral triangular prism, where the base of the prism is an ordinary triangular representation of one of the ternary systems and the altitude represents the composition with respect to the fourth component. A less confusing representation makes use of a regular tetrahedron (7, 8), with each of the triangular faces representing one ternary combination, as in Fig. 2.31. If necessary, orthogonal projection upon one of the boundary surfaces will permit geometrical construction on ordinary plane triangular coordinates. Thus, if the percentages of $A$, $B$, $C$, and $D$ are, respectively, $X_A$, $X_B$, $X_C$, and $X_D$ at $P$, and if projections are to be made on to the $BCD$ plane, the position of the projected point $P$ on this plane can be defined in terms of percentages of $B, C$, and $D$: $X'_B, X'_C$, and $X'_D$. It is possible to show that

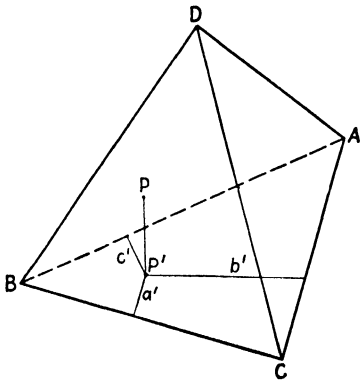



FIG. 2.31. Tetrahedral representation of quaternary systems.

$$X'_B = X_B + \frac{X_A}{3}, \qquad X'_C = X_C + \frac{X_A}{3}, \qquad X'_D = X_D + \frac{X_A}{3} \tag{2.16}$$

There have been very few quaternary systems which have been studied in detail because of the tediousness of the experimental problems. Clearly many combinations of ternary systems are conceivable, resulting in many possibilities for the quaternary equilibria. A system, chloroform–acetone–acetic acid–water at 25°C., which is of considerable interest because it parallels in form many of the petroleum-mixed solvent equilibria, has been determined in some detail by Brancker, Hunter, and Nash (7). This quaternary is made up of the following ternary systems:

1. Chloroform–water–acetic acid (Type 1).
2. Chloroform–water–acetone (Type 1).
3. Chloroform–acetone–acetic acid (completely miscible).
4. Water–acetone–acetic acid (completely miscible).

The system is remarkable in the simplicity of the relationships between the quatenary and various ternary equilibria. Refer to Fig. 2.32. The binodal curve $XGY$ represents the solubility data for chloroform–water–acetic acid, and the line $LK$ is typical of the tie lines in this ternary. Similarly, in the ternary chloroform–water–acetone, the binodal curve is indicated by $XEY$, with tie lines such as $RS$. The three-dimensional surface formed by the two binodal curves and the sloping lines joining them enclose the quaternary heterogeneous region. Any mixture whose composition can be represented by a point underneath this surface exists as two liquid phases, while mix-

tures represented by points outside the surface are homogeneous liquids. Conjugate solutions in the quaternary systems are joined by tie lines, of which the line *QJ* is typical. In this particular system, lines such as *EG*, which outline the profile of the three-dimensional figure, lie in planes perpendicular to the *BCD* plane and are straight. Plane *MNA*, which is formed by the tie line *LK* and the opposite apex *A*, intersects a similar plane *PTD* which includes the tie line *RS*, in a line *VH* which includes the quaternary tie line *QJ*. In this system, therefore, knowledge of the two

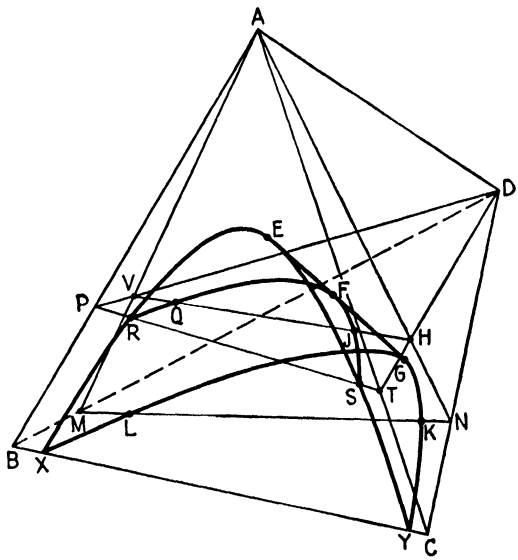



FIG. 2.32. Tie-line relationships in certain quaternary systems.

partially miscible ternary systems alone will serve to establish completely the entire quaternary system. It is not known how general such simplifications are, but it has been shown (8) that certain petroleum-mixed-solvent systems can be represented in a similar manner. Even for such systems, graphical calculations are difficult to make, and, rather than use the orthogonal projections described above, J. C. Smith (49) has suggested that the tie-line data of the two nonconsolute ternaries be plotted on the Hand type of correlation coordinates, giving rise to two straight lines. Quaternary tie lines then appear as points lying between the two binary correlation lines.

Quaternaries made up of two Type 1 and one Type 2 ternary systems are also of interest in liquid extraction. Figure 2.33 is representative of these, and the system naphtha (*A*)–butadiene (*B*)–isobutene (*C*)–furfural (*D*) is typical (48). Only a few quaternary tie lines in this system are known, but it is clear from the ternaries that the simplifications described in the

previous case cannot apply here. Tetrachloroethane ($A$)–acetone ($B$)–isobutanol ($C$)–water ($D$) is another of this type (17) although only the three-dimensional surface in this case has been determined.

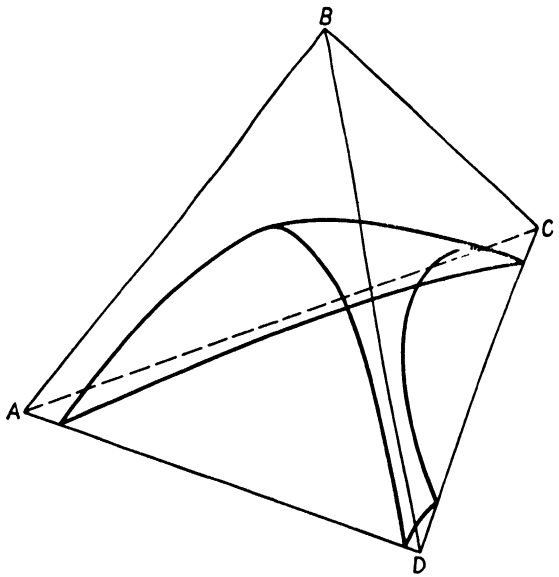



FIG. 2.33. Quaternary system with two immiscible binaries.

## MORE COMPLEX SYSTEMS

Complete graphical representation of the equilibria in systems more complex than the quaternaries is exceedingly difficult. Indeed, in many of the multicomponent systems of industrial importance the number of components is so large that they cannot even be conveniently identified. Fortunately in many of these instances it is possible to group the components according to chemical type and consider the complex mixture as consisting of mixtures of the groups. An example will serve to illustrate the method.

Vegetable oils such as soybean oil consist of a large number of fatty-acid esters of glycerol, some saturated and others unsaturated to various extents. The extent of unsaturation in the mixture which comprises the oil is commonly measured by the "iodine number," the number of centigrams of iodine absorbed by 1 gm. of oil. This is an additive property. In other words, if 100 gm. of an oil of iodine number 50 is mixed with 100 gm. of an oil of iodine number 100, 200 gm. of an oil mixture whose iodine number is 75 would be produced. Iodine numbers for mixtures between 50 and 100 would therefore be a direct indication of the relative amounts of the two original oils present. In separating the high iodine-number fractions from

those of low iodine number, therefore, with furfural as an extracting solvent, iodine number can be substituted for percentage as one of the coordinate scales (40) as in Fig. 2.34. Similarly, viscosity-gravity constant (V.G.C.) can be used for characterizing petroleum oils to their degree of paraffinicity, and this empirical property can be used for simplification of graphical representation. These will be elaborated upon when the corresponding extraction processes are considered.

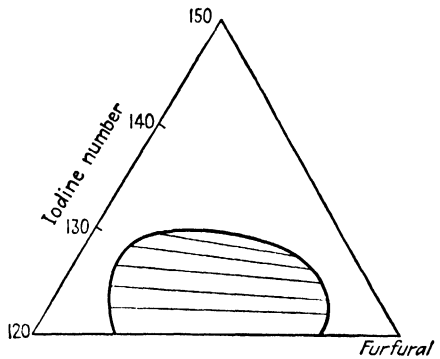



FIG. 2.34. Use of iodine number to characterize vegetable-oil systems.

The possibilities of using similar methods in other situations are numerous. For example, if a mixture of a large number of aldehydes incapable of convenient definition were to be separated by fractional extraction, the percentage of carbonyl oxygen as measured by precipitation with sodium bisulfite might be used as a characterizing property. Simplification of this sort is necessary in any highly complex system.

### Notation for Chapter 2

$A$ = component of a solution.
$a$ = constant.
$B$ = component of a solution.
$b$ = constant.
$C$ = component of a solution.
$D$ = component of a solution.
$F$ = degrees of freedom.
$k$ = constant.
$N$ = number of components.
$m$ = distribution coefficient.
$n$ = constant.
$P$ = number of phases in equilibrium.
$X$ = concentration, weight fraction.
$\alpha$ = degree of dissociation of a simple molecule.
$\alpha'$ = degree of dissociation of a polymolecule.
$\beta$ = constant.

Subscripts:

$A$, $B$, $C$, $D$ refer to components $A$, $B$, $C$, $D$, resp. $X_{AB}$ = weight fraction of $A$ in a $B$-rich solution.
$p$ refers to plait point.

### LITERATURE CITED

1. Bachman, I.: *Ind. Eng. Chem., Anal. Ed.* **12,** 38 (1940).
2. Bancroft, W. D.: *Phys. Rev.* **3,** 120 (1895).

3. Beech, D. G., and S. Glasstone: *J. Chem. Soc.* **1938,** 67.
4. Berndt, R. J., and C. C. Lynch: *J. Am. Chem. Soc.* **66,** 282 (1944).
5. Bogin, C. D.: *Ind. Eng. Chem.* **16,** 380 (1924).
6. Brancker, A. V., T. G. Hunter, and A. W. Nash: *Ind. Eng. Chem., Anal. Ed.* **12,** 35 (1940).
7. ———, ———, and ———: *J. Phys. Chem.* **44,** 683 (1940).
8. ———, ———, and ———: *Ind. Eng. Chem.* **33,** 880 (1941).
9. Briggs, S. W., and E. W. Comings: *Ind. Eng. Chem.* **35,** 411 (1943).
10. Brown, T. F.: *Ind. Eng. Chem.* **40,** 103 (1948).
11. Campbell, J. A.: *Ind. Eng. Chem.* **36,** 1158 (1944).
12. Cox, E. R.: *Ind. Eng. Chem.* **15,** 592 (1923).
13. Darwent, D. DeB., and C. A. Winkler: *J. Phys. Chem.* **47,** 442 (1943).
14. Drouillon, F.: *J. chim. phys.* **22,** 149 (1925).
15. Dryden, C. E.: *Ind. Eng. Chem.* **35,** 492 (1943).
16. Findlay, A., and A. N. Campbell: "The Phase Rule and Its Applications," Longmans, Green & Co., Inc., New York, 1938.
17. Fritzsche, R. H., and D. L. Stockton: *Ind. Eng. Chem.* **38,** 737 (1946).
18. Gibbs, J. Willard: *Trans. Conn. Acad. Arts Sci.* **3,** 152 (1876).
19. *Ibid.*, p. 176.
20. Gibby, C. W.: *J. Chem. Soc.* **1934,** 9.
21. Glasstone, S.: "Textbook of Physical Chemistry," 2d ed., Chap. IX, D. Van Nostrand Company, Inc., New York, 1930.
22. Hand, D. B.: *J. Phys. Chem.* **34,** 1961 (1930).
23. Hendrixson, W. S.: *Z. anorg. Chem.* **13,** 73 (1897).
24. Hill, A. E.: In "A Treatise on Physical Chemistry," H. S. Taylor, Ed., 2d ed., p. 573, D. Van Nostrand Company, Inc., New York, 1930.
25. ———: *J. Am. Chem. Soc.* **44,** 1163 (1922).
26. ——— and F. Miller: *J. Am. Chem. Soc.* **47,** 2702 (1925).
27. Hixson, A. W., and J. B. Bockelman: *Trans. Am. Inst. Chem. Engrs.* **38,** 891 (1942).
28. "International Critical Tables," Vol. III, pp. 393ff., McGraw-Hill Book Company, Inc., New York, 1928.
29. Janecke, E.: *Z. anorg. Chem.* **51,** 132 (1906).
30. Laddha, G. S., and J. M. Smith: *Ind. Eng. Chem.* **40,** 494 (1948).
31. McDonald, H. J.: *J. Am. Chem. Soc.* **62,** 3183 (1940).
32. Meissner, H. P., and C. A. Stokes: *Ind. Eng. Chem.* **36,** 816 (1944).
33. Miller, W. L., and R. H. McPherson: *J. Phys. Chem.* **12,** 706 (1908).
34. Nernst, W.: *Z. physik. Chem.* **8,** 110 (1891).
35. Newman, M., C. B. Hayworth, and R. E. Treybal: *Ind. Eng. Chem.* **41,** 2039 (1949).
36. Olsen, A. L., and E. R. Washburn: *J. Am. Chem. Soc.* **57,** 303 (1935).
37. Othmer, D. F., and P. E. Tobias: *Ind. Eng. Chem.* **34,** 690 (1942).
38. *Ibid.*, p. 693.
39. Palit, S. R., and J. W. McBain: *Ind. Eng. Chem.* **38,** 741 (1946).
40. Ruthruff, R. R., and D. F. Wilcock: *Trans. Am. Inst. Chem. Engrs.* **37,** 649 (1941).
41. Saal, N. J., and W. J. D. Van Dijck: World Petroleum Congress, London, 1933, *Proc.* 2, 352.
42. Schreinemakers, F. A. H.: *Z. physik. Chem.* **25,** 545 (1898).
43. *Ibid.*, **29,** 586 (1899).
44. Sherwood, T. K.: "Absorption and Extraction," p. 242, McGraw-Hill Book Company, Inc., New York, 1937.
45. ——— and C. E. Reed: "Applied Mathematics in Chemical Engineering," pp. 300*ff.*, McGraw-Hill Book Company, Inc., New York, 1939.

46. Smith, A. S.: *Ind. Eng. Chem.* **37,** 185 (1945).
47. ———: *Chem. Eng.* **54,** No. 3, 123 (1947).
48. ——— and T. B. Braun: *Ind. Eng. Chem.* **37,** 1047 (1945).
49. Smith, J. C.: *Ind. Eng. Chem.* **36,** 68 (1944).
50. Tarasenkov, D. N.: *J. Gen. Chem.* (*U.S.S.R.*) **16,** 1583 (1946).
51. ——— and I. A. Paulsen: *J. Gen. Chem.* (*U.S.S.R.*) **8,** 76 (1938).
52. ——— and ———: *Acta Physicochem. U.R.S.S.* **11,** 75 (1939).
53. Taylor, H. S.: "A Treatise on Physical Chemistry," 2d ed., Chap. IX, D. Van Nostrand Company, Inc., New York, 1930.
54. Timmermans, J.: *Z. physik. Chem.* **58,** 159 (1907).
55. Treybal, R. E.: *Ind. Eng. Chem.* **36,** 875 (1944).
56. ———: Unpublished work.
57. ———, L. D. Weber, and J. F. Daley: *Ind. Eng. Chem.* **38,** 817 (1946).
58. Varteressian, K. A., and M. R. Fenske: *Ind. Eng. Chem.* **29,** 270 (1937).

# CHAPTER 3

## PREDICTION OF DISTRIBUTION

In all liquid-extraction process evaluation and equipment design, the importance of having at hand accurate liquid-equilibrium data cannot be overemphasized. As will be shown later, the nature of the flowsheets used in a process, knowledge of the rates at which extraction will occur, decisions as to the amount of separating solvent to employ, and detailed information respecting concentrations of solutions throughout the process — all these depend upon knowledge of the phase diagram in some detail. Since relatively few ternary, and far fewer quaternary, systems have been thoroughly investigated, it will usually be necessary to gather the data experimentally when new processes are considered before complete design details can be established. If the feasibility of making a separation by liquid-extraction methods is being investigated for the first time, it will be desirable to have at hand as many sets of equilibrium data as possible in order that the relative value of various solvents can be compared. However, it is clearly desirable to be able to predict the salient features of the phase diagrams without resort to the laboratory from properties of the substances involved which are readily available in the literature. In this manner a good many solvents which at first might be considered useful can frequently be eliminated and considerable time and money saved by restricting subsequent laboratory work to those systems which appear most promising. None of the methods of prediction is capable of a high order of accuracy, unfortunately, but nevertheless they are most useful. Even a qualitative indication of the direction of distribution of a solute between two solvents is at times of great value.

### IDEAL SOLUTIONS

One of the most useful concepts for present purposes is that of the "ideal solution." There are four important characteristics of such solutions, all interrelated:

1. Mixing of the constituents causes no change in the average intermolecular forces of attraction.
2. The volume of the solution is an additive property of the volume of the constituents over the entire range of composition.
3. Mixing of the constituents in any proportion results in neither absorption nor evolution of heat.

4. The total vapor pressure of the solution is a linear function of the composition, expressed in mole fractions, over the entire range of compositions.

Consideration of these characteristics makes it clear that only very special liquid pairs could conceivably form ideal solutions. It would be necessary that the molecules of the constituents be very similar in every respect, for example in structure, size, and chemical nature. Thus, solutions of optical isomers, adjacent members of an homologous series, and similar mixtures would be expected to be nearly ideal, but actually all solutions can at best only approach ideality as a limit. Solutions which form immiscible liquid phases are of necessity extremely nonideal, and extraction operations depend upon this. The extent to which solutions depart from ideality is manifested by deviations of the properties of the solutions from the characteristics listed above, and a study of these deviations will permit us to some extent to predict their behavior in extraction operations. The most useful characteristics of the ideal solution for these purposes is that of vapor pressure, since considerable information has now been accumulated for many mixtures on this and related properties such as boiling points of solutions, azeotropism, and vapor-liquid equilibria. Classifications of compounds according to the effect of intermolecular forces on properties of mixtures also provide much useful material, but the second and third characteristics in the list above are of limited value owing to lack of experimental data to which we can refer.

**Raoult's Law.** In its simplest form, as originally defined, Raoult's law states that for liquid solutions which are ideal, and under such conditions that the vapor phase follows the ideal gas law, the partial pressure $\bar{p}$ of any constituent of a liquid solution equals the product of its vapor pressure $p$ in the pure state by its mole fraction in the solution $x$. For a binary solution,

$$\bar{p}_A = x_A p_A, \qquad \bar{p}_B = x_B p_B = (1 - x_A) p_B \tag{3.1}$$

Since the total vapor pressure is the sum of the partial pressures of the constituents,

$$p_t = \bar{p}_A + \bar{p}_B = x_A p_A + (1 - x_A) p_B \tag{3.2}$$

and it is seen that the total pressure is a linear function of the liquid composition. The vapor composition will then be

$$y_A = \frac{\bar{p}_A}{p_t} = \frac{x_A p_A}{p_t}, \qquad y_B = 1 - y_A = \frac{(1 - x_A) p_B}{p_t} \tag{3.3}$$

The above relationships can be very satisfactorily shown graphically, as in Fig. 3.1, where the lines drawn are all straight lines. Now the mole fraction of a component in any mixture is directly proportional to the number of molecules of the component present. Any molecules in the vapor above a liquid solution may be conceived as having escaped from

the liquid, and their concentration in the vapor may be looked upon as a measure of their *escaping tendency* (25). Thus, an alternative statement of Raoult's law which is sometimes convenient is: the escaping tendency of the molecules of an ideal solution is directly proportional to their concentration in the liquid.

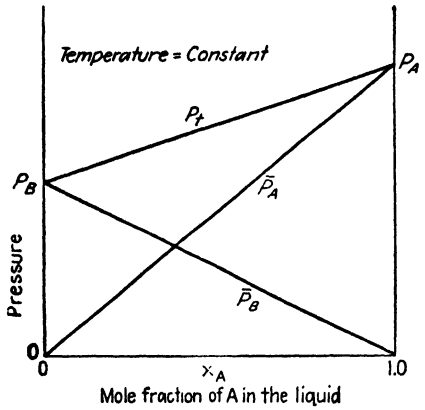



FIG. 3.1. Raoult's law for a binary solution.

**Illustration 1.** Mixtures of *n*-pentane and *n*-hexane may be expected to form nearly ideal solutions. Calculate the composition of the vapor in equilibrium with a liquid containing 0.3 mole fraction pentane at 25°C.

*Solution.* The vapor pressures of pure pentane (*A*) and hexane (*B*) are, resp., $p_A = 508$ mm. Hg and $p_B = 149$ mm. Hg at 25°C. Since $x_A = 0.3$, by Eq. (3.1) the partial pressures of the constituents are

$$\bar{p}_A = 0.3(508) = 152.4 \text{ mm. Hg}$$
$$\bar{p}_B = 0.7(149) = 104.3 \text{ mm. Hg}$$

The total pressure of the vapor, $p_t = 152.4 + 104.3 = 256.7$ mm. Hg. Therefore [Eq. (3.3)], the mole fraction of pentane in the vapor becomes $y_A = 152.4/256.7 = 0.594$, and that of hexane $= y_B = 104.3/256.7 = 0.406$.

**Fugacity.** [*Pure Substances.* Under extreme conditions of temperature and pressure, it is not permissible to assume that the perfect gas law will apply. In order to retain the simple appearance of the equations and functions with which we must deal under such circumstances, Lewis (24) introduced the concept of fugacity, the use of which is very convenient. At constant temperature, for a pure substance (9),

$$dF = v\,dp \tag{3.4}$$

Under circumstances such that the ideal gas law is applicable,

$$v = \frac{RT}{p} \tag{3.5}$$

and therefore

$$dF = \frac{RT\,dp}{p} = RT\,d\ln p \tag{3.6}$$

The fugacity $f$ of the substance is defined in such a manner as to preserve the form of this equation:

$$dF = RT\,d\ln f = v\,dp \tag{3.7}$$

Integration between two conditions of pressure at constant temperature then gives

$$F - F^0 = RT\ln\frac{f}{f^0} = \int_{p^0}^{p} v\,dp \tag{3.8}$$

where the superscript 0 refers to some arbitrarily defined standard state for reference purposes. It is generally convenient to set $f^0 = p^0$ under conditions such that the substance is an ideal gas. Thus, $p^0$ can be some conveniently low pressure, ordinarily 1 atm. The fugacity may be looked upon as a sort of corrected pressure which will describe the behavior of an actual gas in the manner of an ideal gas. It may be satisfactorily calculated for most purposes from generalized plots of the fugacity as a function of reduced temperature and pressure (9, 18). The ratio $f/f^0$ is defined as activity $a$.

**Solutions:** Raoult's law in terms of fugacities is an improvement over the original form, since it does not require the vapor phase to be ideal:

$$\bar{f}_A = x_A f_A \tag{3.9}$$

where $f_A$ = fugacity of pure liquid $A$ at the temperature and pressure of the solution

$\bar{f}_A$ = fugacity of component $A$ in solution, and in the vapor in equilibrium with the solution

At equilibrium, the fugacity of a component is the same in all phases (9). For solutions, activity is defined in the same fashion as for pure substances, *i.e.*,

$$RT \ln a = RT \ln \frac{\bar{f}}{f^0} = \bar{F} - \bar{F}^0 \tag{3.10}$$

$$a = \frac{f}{f^0} \tag{3.11}$$

where $f^0$ is the fugacity at a standard state. Several standard states are in common use, depending upon the nature of the solution:

1. For solutions of nonelectrolytes, the standard state is most conveniently taken as that of the pure substance, at the temperature of the solution, and either at 1.0 atm. pressure, the vapor pressure of the substance at the prevailing temperature, or the pressure of the solution. For most purposes, where conditions are far removed from the critical state and partial molal volumes are low, the effect on activity of choosing either pressure designation is negligible.

2. For solutions of electrolytes, a standard state referred to infinite dilution is sometimes convenient at the pressures indicated above.

If the pure liquid is the standard state, Raoult's law becomes

$$a_A = \frac{\bar{f}_A}{f_A^0} = x_A, \qquad a_B = x_B \tag{3.12}$$

Since at equilibrium in heterogeneous systems the fugacity of a component is the same in all phases, then if the same standard state for a substance is chosen for each phase, the activities of the substance in all phases are equal. The ratio $a/x$ is termed activity coefficient $\gamma$ and for ideal solutions

$$\gamma_A = \gamma_B = 1.0 \tag{3.13}$$

## NONIDEAL BINARY MIXTURES

Deviation from ideality of real liquid solutions manifests itself by departure of the various characteristics such as partial pressure, fugacity, activity, and activity coefficient, from the simple linear relationships previously shown. Of these, perhaps the most convenient to study is the activity coefficient $\gamma$. Thus, for a binary solution of $A$ and $B$,

$$\gamma_A = \frac{a_A}{x_A} = \frac{\bar{f}_A}{x_A f_A^0}, \qquad \gamma_B = \frac{a_B}{x_B} = \frac{\bar{f}_B}{x_B f_B^0} \tag{3.14}$$

where the standard-state fugacities $f_A^0$ and $f_B^0$ are those of the pure components at the temperature and pressure of the solution. Ordinarily it is also satisfactory to use the fugacity of the pure liquids at their own vapor pressure. Under conditions such that the perfect gas laws are adequate to describe the behavior of the gas phase,

$$\gamma_A = \frac{a_A}{x_A} = \frac{\bar{p}_A}{x_A p_A} = \frac{y_A p_t}{x_A p_A}, \qquad \gamma_B = \frac{a_B}{x_B} = \frac{\bar{p}_B}{x_B p_B} = \frac{y_B p_t}{x_B p_B} \tag{3.15}$$

The activity coefficient is consequently the ratio of the actual fugacity, partial pressure, or escaping tendency, to the ideal value of fugacity, partial pressure, or escaping tendency, respectively, at the indicated liquid concentration. If the activity coefficient is greater than 1.0, the escaping tendency is abnormally large, and a positive† deviation from Raoult's law is indicated; if less than 1.0, the escaping tendency is lower than that for an ideal solution, and we have negative† deviations from Raoult's law.

**Illustration 2.** At 760 mm. Hg total pressure, a solution of ethanol and ethyl acetate containing 0.30 mole fraction ethanol boils at 72.2°C., and the equilibrium vapor contains 0.356 mole fraction ethanol. Calculate the activity coefficients and activities of the components, assuming that the perfect gas laws apply.

*Solution.* At 72.2°C., the vapor pressures of the pure components are:

Ethanol: $p_A = 591.6$ mm. Hg

Ethyl acetate: $p_A = 639.7$ mm. Hg

Furthermore,

$$x_A = 0.30, \qquad x_B = 1.0 - 0.30 = 0.70$$
$$y_A = 0.356, \qquad y_B = 1.0 - 0.356 = 0.644$$

Substitution in Eq. (3.15):

Ethanol:
$$\gamma_A = \frac{0.356(760)}{0.30(591.6)} = 1.524$$
$$\therefore a_A = \gamma_A x_A = 1.524(0.30) = 0.657$$

Ethyl acetate:
$$\gamma_B = \frac{0.644(760)}{0.70(639.7)} = 1.093$$
$$\therefore a_B = \gamma_B x_B = 1.093(0.70) = 0.765$$

† The terms "positive" and "negative" refer to the sign of the logarithm of $\gamma$.

Where deviations from the ideal gas law may not be ignored, the method utilized by Benedict, *et al.* (2) and Mertes and Colburn (27) is convenient. They express the activity coefficient as

$$\gamma_A = \frac{y_A p_t}{x_A p_A} e^{\frac{(p_A - p_t)(V_A - B_A)}{RT}} \tag{3.16}$$

where $V_A$ = molal volume of liquid $A$

$B_A$ = second virial coefficient of the equation of state for component $A$, $v_A = RT/p_t + B_A$. It may also be conveniently obtained from compressibility factors, $B_A = RT/p_t(Z_A - 1)$, and, if necessary, generalized plots of compressibility factors (18)

This assumes that there are insignificant volume changes on mixing the liquid components.

**Illustration 3.** Benedict, *et al.* (2) report that at 760.0 mm. Hg, 64.1°C., the liquid and vapor equilibrium compositions for the system methanol ($A$)–toluene ($B$) are, resp., $x_A = 0.692$ and $y_A = 0.829$. Calculate the toluene activity coefficient.

*Solution.*

$p_t$ = total pressure = 760.0 mm. Hg

$T$ = temp. = 64.1 + 273.1 = 337.2°K.

$x_B$ = 1 − 0.692 = 0.308 mole fraction toluene

$y_B$ = 1 − 0.829 = 0.171 mole fraction toluene

$p_B$ = vapor pressure of toluene at 64.1°C. = 163.55 mm. Hg

Critical consts. for toluene = 593.7°K. and 41.6 atm.

Reduced temp. = 337.2/593.7 = 0.568

Reduced pressure = 760.0/41.6(760) = 0.0240

$Z_B$ = compressibility factor = 0.9700, from a generalized chart (18)

$R$ = 62,370 mm. Hg (cu. cm.)/(gm. mole)(°K.)

$$B_B = \frac{RT}{p_t}(Z_B - 1) = \frac{62{,}370(337.2)(0.9700-1)}{760.0}$$

$$= -830 \text{ cu. cm./gm. mole}$$

(Better values are obtainable by use of an equation of state more specific for toluene than the generalized compressibility factors.)

$V_B$ = molar vol. of liquid toluene at 64.1°C. = 111.7 cu. cm./gm. mole

$$e^{\frac{(p_B - p_t)(V_B - B_B)}{RT}} = e^{\frac{(163.55 - 760.0)(111.7 + 830)}{62{,}370(337.2)}} = 0.9735$$

By Eq. (3.16),

$$\gamma_B = \frac{0.171(760.0)}{0.308(163.55)}(0.9735) = 2.511$$

**Typical Systems.** Figures 3.2 through 3.6 have been prepared to illustrate the appearance of typical partial pressure, activity, and activity coefficient curves for various types of systems. Note that a logarithmic scale is used for activity coefficient.

Figure 3.2 is perhaps typical of by far the great majority of cases which are encountered, showing positive Raoult's law deviations. If the positive deviations are sufficiently great in a system where the vapor pressures of the pure components are not far apart, then the total pressure $p_t$ rises

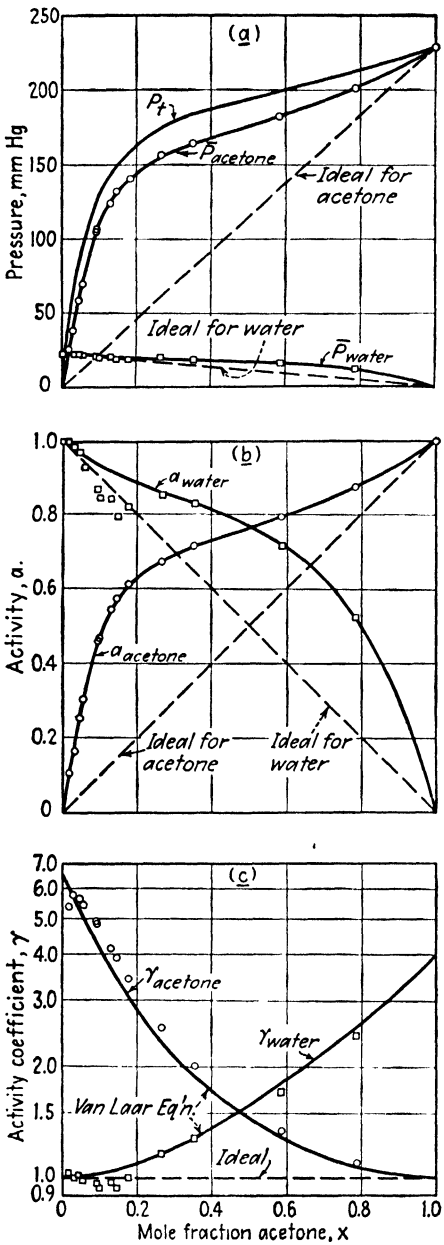



FIG. 3.2. Partial pressures (*a*), activities (*b*), and activity coefficients (c) for the system acetone–water at 25°C. [*Data of Beare, McVicar, and Ferguson, J. Phys. Chem.* **34**, 1310 (1930).] Activity coefficients fitted with two-suffix Van Laar equations: $A_{AB} = \log 6.5$, $A_{BA} = \log 4.0$

through a maximum as in Fig. 3.3, and an azeotrope is formed. Since at the azeotropic composition $x = y$, then

$$\gamma_A = \frac{p_t}{p_A}, \qquad \gamma_B = \frac{p_t}{p_B} \tag{3.17}$$

If the escaping tendencies of the two components are so great that they have difficulty in dissolving in one another, limited miscibility as in Fig. 3.4 results. Here, between the concentrations $x_1$ and $x_2$, two liquid layers are formed whose concentrations are $x_1$ and $x_2$, and since the layers are in equilibrium, the partial pressure and activity of each component is the same in each layer. The total pressure curve contains a flat maximum, a condition which has been termed "heteroazeotropic." Figure 3.5 shows data of a type which is relatively rare, with both negative and positive deviations, while in the case of Fig. 3.6, the negative deviations are sufficiently great that an azeotrope is formed.

In the case of all these systems, it should be noted that as the solution becomes more concentrated in any component, or as $x$ for one component approaches 1.0, the properties of the solution approach ideality. Thus the curves of partial pressure and activity approach the ideal line tangentially near $x = 1.0$, and the activity coefficients approach 1.0 tangentially. This is characteristic and may be used as a test of the soundness of the experimental data. Furthermore, the data for activity coeffi-

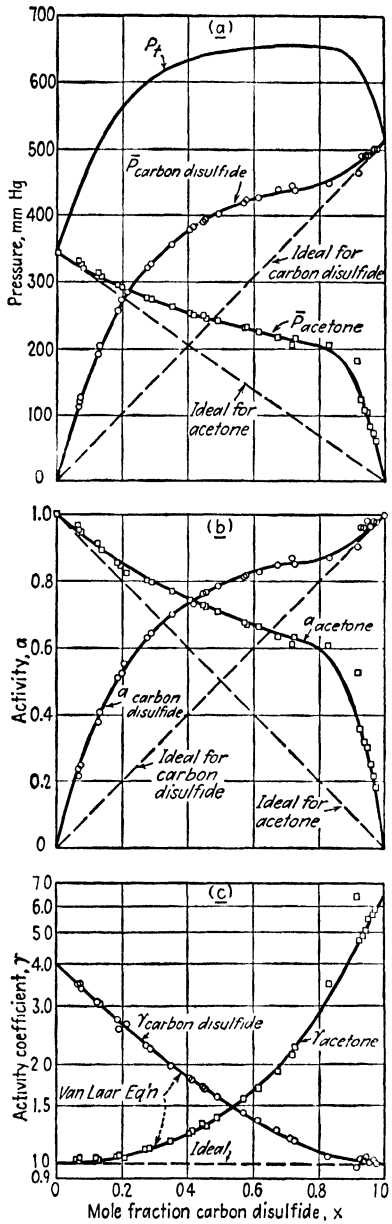



FIG. 3.3. Partial pressures (*a*), activities (*b*), and activity coefficients (*c*) for the system carbon disulfide–acetone at 35.17°C. [*Data of Zawidzki, Z. Physik. Chem.* **35**, 129 (1900).] Activity coefficients fitted by two-suffix Van Laar equations: $A_{AB}$ = log 4.0, $A_{BA}$ = log 6.6

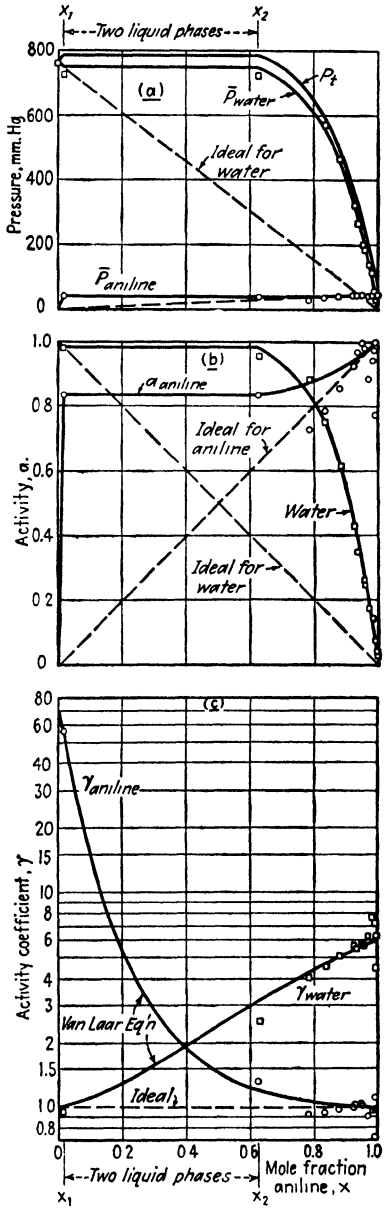



FIG. 3.4. Partial pressures (*a*), activities (*b*), and activity coefficients (*c*), for the system aniline–water, at 100°C. [*Data of Griswold, Andres, Arnett, and Garland, Ind. Eng. Chem.* **32**, 878 (1940).] Activity coefficients fitted by two-suffix Van Laar equations: $A_{AB}$ = log 71.0, $A_{BA}$ = log 6.0

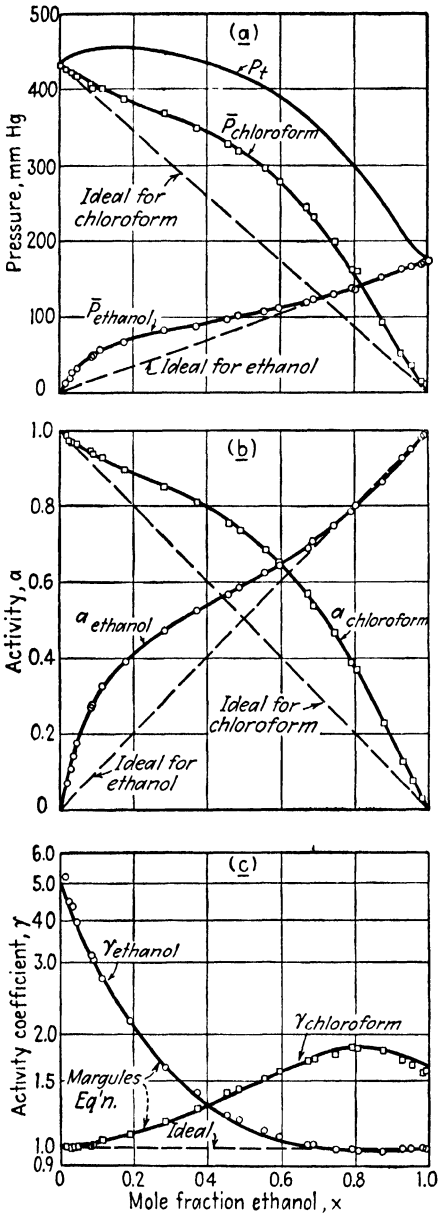



FIG. 3.5. Partial pressures (*a*), activities (*b*), and activity coefficients (*c*) for the system ethanol–chloroform at 45°C. [*Data of Scatchard and Raymond, J. Am. Chem. Soc.* **60,** 1278 (1938).] Activity coefficients fitted by three-suffix Margules equations: $A_{AB}$ = log 5.0, $A_{BA}$ = log 1.65

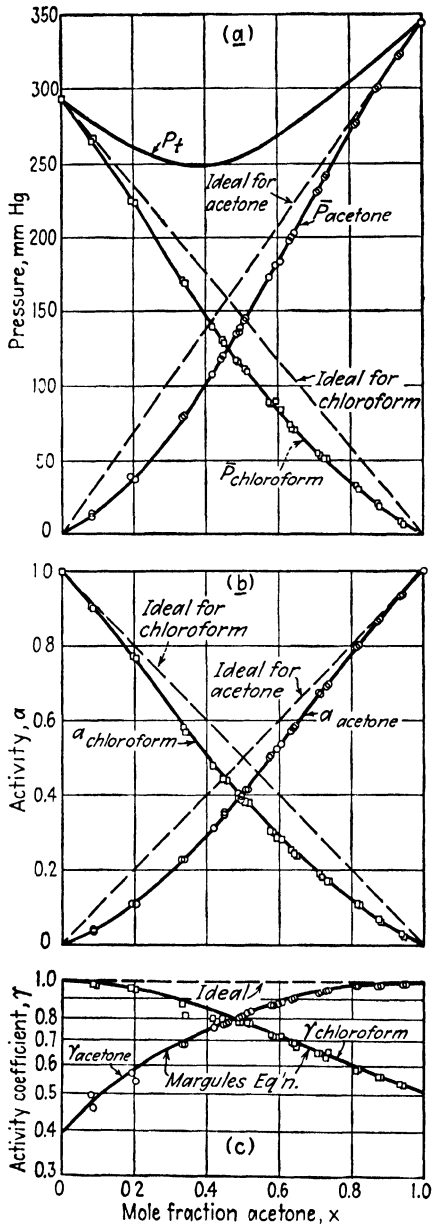



FIG. 3.6. Partial pressures (*a*), activities (*b*), and activity coefficients (*c*) for the system acetone–chloroform at 35.17°C. [*Data of Zawidzki, Z. Physik. Chem.* **35,** 129 (1900).] Activity coefficients fitted by three-suffix Margules equations: $A_{AB}$ = log 0.39, $A_{BA}$ = log 0.51

cient become more erratic and scatter badly as the solution concentration approaches $x = 0$ or 1.0. The activity coefficient is very sensitive to even small errors in measurement, and the experimental difficulties in making measurements on very dilute or highly concentrated solutions are considerable. Therefore it is important that not too much confidence be placed in a single value of activity coefficient for very dilute or very concentrated solutions.

In cases where vapor association, or electrolytic dissociation, occurs, the activity coefficients calculated in the ordinary fashion do not approach Raoult's law as the mole fraction approaches 1.0 and show other unusual behavior. The systems acetic acid–water, sodium chloride–water, and acetaldehyde–water are typical of these.

**The Gibbs-Duhem Equation.** In the manner that is applicable to any extensive property of a solution, we may write (18)

$$x_A\left(\frac{\partial \bar{F}_A}{\partial x_A}\right)_{T,p} + x_B\left(\frac{\partial \bar{F}_B}{\partial x_A}\right)_{T,p} + \cdots = 0 \tag{3.18}$$

Since, from Eq. (3.10), at constant temperature,

$$\partial \bar{F} = RT\partial \ln f, \tag{3.19}$$

Equation (3.18) becomes

$$x_A\left(\frac{\partial \ln \bar{f}_A}{\partial x_A}\right)_{T,p} + x_B\left(\frac{\partial \ln \bar{f}_B}{\partial x_A}\right)_{T,p} + \cdots = 0 \tag{3.20}$$

For binary solutions,

$$x_A + x_B = 1.0 \tag{3.21}$$

and

$$dx_A = -dx_B \tag{3.22}$$

Therefore,

$$x_A\left(\frac{\partial \ln \bar{f}_A}{\partial x_A}\right)_{T,p} = x_B\left(\frac{\partial \ln \bar{f}_B}{\partial x_B}\right)_{T,p} \tag{3.23}$$

which is the Gibbs-Duhem equation. It may also be written in terms of activity coefficients:

$$x_A\left(\frac{\partial \ln \gamma_A}{\partial x_A}\right)_{T,p} = x_B\left(\frac{\partial \ln \gamma_B}{\partial x_B}\right)_{T,p} \tag{3.24}$$

This relationship may be used to test the thermodynamic consistency of activity coefficient data (5, 9, 18), for which purpose we may put it in the form

$$\frac{[(\partial \ln \gamma_A)/\partial x_A]_{T,p}}{(\partial \ln \gamma_B/\partial x_A)_{T,p}} = -\frac{x_B}{x_A} \tag{3.25}$$

Thus, the ratio of slopes of the log $\gamma$ vs. $x_A$ curves should be in the ratio $(-x_B/x_A)$. When the activity coefficients are determined by means of vapor-pressure data, the restrictions of both constant temperature and constant pressure are impossible ones to fulfill. As will be pointed out

however, the effect of temperature and the corresponding pressure on activity coefficients is frequently small, and Eq. (3.25) may be written

$$\frac{(d \log \gamma_A)/dx_A}{(d \log \gamma_B)/dx_A} = -\frac{x_B}{x_A} \tag{3.26}$$

and for most situations used either for constant temperature or constant pressure. Measurements which fail to abide by Eq. (3.26) may be criticized for thermodynamic inconsistency and accepted with corresponding reservations. Furthermore, the integrated forms (9),

$$\log \gamma_A = -\int_{x_A=1}^{x_A=x_A} \frac{x_B}{x_A} d \log \gamma_B \tag{3.27}$$

and

$$\log \gamma_B = -\int_{x_A=0}^{x_A=x_A} \frac{x_A}{x_B} d \log \gamma_A \tag{3.28}$$

are useful in determining values for either activity coefficient curve if the other is known. Thus, by Eq. (3.27), we may plot $x_B/x_A$ as ordinate against log $\gamma_B$ as abscissa, and graphically integrate from $x_A = 1$ (or $x_B/x_A = 0$) to $x_A$, whence the area under the curve equals log $\gamma_A$. Similarly $\gamma_B$ can be established from $\gamma_A$ by Eq. (3.28). Such procedures are also helpful in arriving at self-consistent curves to describe activity coefficient data which scatter badly. Further discussion is to be found in the work of Carlson and Colburn (5).

**Integrations of the Gibbs-Duhem Equation.** For $n_A$ moles of component $A$, the decrease in free energy when transferred from the pure state to solution in $B$ is, according to Eq. (3.10)

$$n_A(\bar{F}_A - F_A^0) = n_A RT \ln \frac{\bar{f}_A}{f_A^0} \tag{3.29}$$

which for an ideal solution, since $f_A/f_A^0 = x_A$, becomes

$$n_A(\bar{F}_A - F_A^0) = n_A RT \ln x_A \tag{3.30}$$

$$\therefore n_A\bar{F}_A = n_A RT \ln x_A + n_A F_A^0 \tag{3.31}$$

Similarly, for $n_B$ moles of component $B$,

$$n_B(\bar{F}_B - F_B^0) = n_B RT \ln x_B \tag{3.32}$$

$$n_B\bar{F}_B = n_B RT \ln x_B + n_B F_B^0 \tag{3.33}$$

and the total free energy of the solution becomes

$$\begin{aligned} \mathbf{F} &= (n_A\bar{F}_A + n_B\bar{F}_B)_{\text{ideal}} \\ &= n_A RT \ln x_A + n_B RT \ln x_B + n_A F_A^0 + n_B F_B^0 \end{aligned} \tag{3.34}$$

For a nonideal solution,

$$\frac{\bar{f}}{f^0} = \gamma x \tag{3.14}$$

and a similar development leads to

$$(n_A\bar{F}_A + n_B\bar{F}_B)_{\text{nonideal}} = n_ART \ln x_A + n_BRT \ln x_B + n_AF_A^0 + n_BF_B^0 + n_ART \ln \gamma_A + n_BRT \ln \gamma_B \quad (3.35)$$

The difference in the total free energies for the ideal and nonideal cases is termed the excess free energy of the nonideal solution $\mathbf{F}_E$ (31). Thus,

$$\mathbf{F}_E = n_ART \ln \gamma_A + n_BRT \ln \gamma_B \quad (3.36)$$

and

$$\mathbf{F} = n_ART \ln x_A + n_BRT \ln x_B + n_AF_A^0 + n_BF_B^0 + \mathbf{F}_E \quad (3.37)$$

Differentiation of Eq. (3.37) with respect to $n_A$:

$$\frac{\partial \mathbf{F}}{\partial n_A} = \bar{F}_A = RT \ln x_A + F_A^0 + \frac{\partial \mathbf{F}_E}{\partial n_A} = RT \ln x_A + F_A^0 + RT \ln \gamma_A \quad (3.38)$$

$$\therefore RT \ln \gamma_A = \frac{\partial \mathbf{F}_E}{\partial n_A} \quad (3.39)$$

or

$$RT \ln \gamma_A = \frac{\partial (n_A + n_B)F_E}{\partial n_A} \quad (3.40)$$

and

$$RT \ln \gamma_B = \frac{\partial (n_A + n_B)F_E}{\partial n_B} \quad (3.41)$$

Wohl (35) has shown that all of the common integrations of the Gibbs-Duhem equations are simplifications of an equation relating the contributions to the excess free energy of interactions of the unlike molecules in groups of two, three, four, etc., the ultimate size of the groups considered characterizing the resulting equation. Thus, if molecular groups of two and three are considered, a "three-suffix" equation results. For a three-suffix equation and a binary mixture of $A$ and $B$,

$$\frac{F_E}{2.3RT} = \text{sum of effects of molecular groups of } A \text{ and } B, \text{ of } A, A, \text{ and } B, \text{ and of } A, B, \text{ and } B \quad (3.42)$$

where empirical terms are used to express the effects of the various molecular groups. Thus,

$$\frac{F_E}{2.3RT} = x_Ax_Bk_{AB} + x_Bx_Ak_{BA} + x_Ax_Ax_Bk_{AAB} + x_Ax_Bx_Ak_{ABA} + x_Bx_Ax_Ak_{BAA} + x_Ax_Bx_Bk_{ABB} + x_Bx_Ax_Bk_{BAB} + x_Bx_Bx_Ak_{BBA} \quad (3.43)$$

where the subscripts of the constants $k$ indicate merely the type of concentration term associated with each. Since order of multiplication is unimportant, $x_Ax_Bk_{AB} = x_Bx_Ak_{BA}$, $x_Ax_Ax_Bk_{AAB} = x_Ax_Bx_Ak_{ABA}$, etc., and therefore

$$\frac{F_E}{2.3RT} = 2k_{AB}x_Ax_B + 3k_{AAB}x_A^2x_B + 3k_{ABB}x_Ax_B^2 \quad (3.44)$$

or since $x_A + x_B = 1.0$,

$$\frac{F_E}{2.3RT} = 2k_{AB}x_Ax_B(x_A + x_B) + 3k_{AAB}x_A^2x_B + 3k_{ABB}x_Ax_B^2 \tag{3.45}$$

Letting

$$A_{AB} = 2k_{AB} + 3k_{ABB} \tag{3.46}$$

and

$$A_{BA} = 2k_{AB} + 3k_{AAB} \tag{3.47}$$

$$\therefore \frac{F_E}{2.3RT} = x_Ax_B(x_AA_{BA} + x_BA_{AB}) \tag{3.48}$$

Since

$$\frac{n_A}{n_A + n_B} = x_A, \quad \text{and} \quad \frac{n_B}{n_A + n_B} = x_B$$

therefore

$$\frac{(n_A + n_B)F_E}{2.3RT} = \frac{n_An_B}{n_A + n_B}\left(\frac{n_AA_{BA}}{n_A + n_B} + \frac{n_BA_{AB}}{n_A + n_B}\right) \tag{3.49}$$

Differentiation in accordance with Eq. (3.40) then leads to

$$\log \gamma_A = x_B^2[A_{AB} + 2(A_{BA} - A_{AB})x_A] \tag{3.50}$$

and

$$\log \gamma_B = x_A^2[A_{BA} + 2(A_{AB} - A_{BA})x_B] \tag{3.51}$$

These are the three-suffix *Margules equations*, which, since $x_A + x_B = 1$, may also be written (5)

$$\begin{cases} \log \gamma_A = (2A_{BA} - A_{AB})x_B^2 + 2(A_{AB} - A_{BA})x_B^3 & (3.52) \\ \log \gamma_B = (2A_{AB} - A_{BA})x_A^2 + 2(A_{BA} - A_{AB})x_A^3 & (3.53) \end{cases}$$

Or they may be solved for the constants

$$\begin{cases} A_{AB} = \dfrac{(x_B - x_A)\log \gamma_A}{x_B^2} + \dfrac{2 \log \gamma_B}{x_A} & (3.54) \\ A_{BA} = \dfrac{(x_A - x_B)\log \gamma_B}{x_A^2} + \dfrac{2 \log \gamma_A}{x_B} & (3.55) \end{cases}$$

If $x_A = 0 (x_B = 1)$, $\log \gamma_A = A_{AB}$, or

$$A_{AB} = \left.\begin{array}{l}\text{limit of } \log \gamma_A \text{ as } x_A \to 0, \text{ or} \\ \text{terminal value of } \log \gamma_A, \text{ or } \log \gamma_A'\end{array}\right\} \tag{3.56}$$

Similarly,

$$A_{BA} = \left.\begin{array}{l}\text{limit of } \log \gamma_B \text{ as } x_B \to 0, \text{ or} \\ \text{terminal value of } \log \gamma_B, \text{ or } \log \gamma_B'\end{array}\right\} \tag{3.57}$$

As examples of the use of these equations to fit activity-coefficient data, refer to Figs. 3.5 and 3.6, where the activity coefficient–mole fraction curves drawn are given by Eqs. (3.52) and (3.53), with the indicated values of the constants $A_{AB}$ and $A_{BA}$.

Other equations may be worked out on the basis of different assumptions respecting the size of the molecular groups which affect the excess free

energy and the relative magnitudes of the molar volumes of the constituents of the solution. The most important of these for present purposes are:

The two-suffix *van Laar equations* (5, 23):

$$\begin{cases} \log \gamma_A = \dfrac{A_{AB}}{[1 + (A_{AB}x_A/A_{BA}x_B)]^2} & (3.58) \\ \log \gamma_B = \dfrac{A_{BA}}{[1 + (A_{BA}x_B/A_{AB}x_A)]^2} & (3.59) \end{cases}$$

or

$$\begin{cases} A_{AB} = \log \gamma_A \left[1 + \left(\dfrac{x_B \log \gamma_B}{x_A \log \gamma_A}\right)\right]^2 & (3.60) \\ A_{BA} = \log \gamma_B \left[1 + \left(\dfrac{x_A \log \gamma_A}{x_B \log \gamma_B}\right)\right]^2 & (3.61) \end{cases}$$

Figures 3.2, 3.3, and 3.4 show examples of the use of these equations to fit activity-coefficient data.

The three-suffix *Scatchard-Hamer* equations (5, 30, 31, 32, 35):

$$\begin{cases} \log \gamma_A = z_B^2 \left[A_{AB} + 2\left(A_{BA}\dfrac{V_A}{V_B} - A_{AB}\right)z_A\right] & (3.62) \\ \log \gamma_B = z_A^2 \left[A_{BA} + 2\left(A_{AB}\dfrac{V_B}{V_A} - A_{BA}\right)z_B\right] & (3.63) \end{cases}$$

or

$$\begin{cases} A_{AB} = \dfrac{2V_A}{z_A V_B} \log \gamma_B - \dfrac{(2z_A - 1) \log \gamma_A}{z_B^2} & (3.64) \\ A_{BA} = \dfrac{2V_B}{z_B V_A} \log \gamma_A - \dfrac{(2z_B - 1) \log \gamma_B}{z_A^2} & (3.65) \end{cases}$$

where $z$ = volume fraction based on the volumes of the pure components
$V$ = molar volume of the pure constituent

$$z_A = \frac{V_A x_A}{V_A x_A + V_B x_B}, \qquad z_B = \frac{V_B x_B}{V_A x_A + V_B x_B} \tag{3.66}$$

In each of these cases, differentiation of the equations shows that they are true integrations of the Gibbs-Duhem equation, and the values of $A_{AB}$ and $A_{BA}$ are the terminal values of $\log \gamma_A$ and $\log \gamma_B$ [Eqs. (3.56) and (3.57)]. More complex equations with constants other than the terminal $\log \gamma$ values are also possible (35).

Redlich and Kister (29) have shown that

$$\int_{x=0}^{x_A=1.0} \log\left(\frac{\gamma_A}{\gamma_B}\right) dx_A = 0 \tag{3.67}$$

and that

$$\log\left(\frac{\gamma_A}{\gamma_B}\right) = M(1 - 2x_A) + N[6x_A(1 - x_A) - 1] + S(1 - 2x_A)[1 - 8x_A(1 - x_A)] \tag{3.68}$$

where $M$, $N$, and $S$ are constants may be used to represent experimental data. A plot of log $(\gamma_A/\gamma_B)$ against $x_A$ is consequently a convenient method of smoothing and correlating vapor-liquid equilibrium data. The constants may be determined from such a plot very readily, and the net area between the curve representing the data and the line log $(\gamma_A/\gamma_B) = 0$ must, by Eq. (3.67), equal zero. If $S = 0$, the equation becomes identical with the Margules equations previously given.

**Limitations.** 1. The *Margules* equations are quantitatively most useful for relatively symmetrical systems, *i.e.*, where $A_{AB}$ nearly equals $A_{BA}$. They are very flexible in that they can show maximum or minimum values of log $\gamma$† with concentration. Differentiation of the equation shows that a maximum (or minimum) can be expected $A_{BA}/A_{AB} > 2.0$. Wohl has shown, however, that for systems of such dissymmetry the Margules equations fail quantitatively to follow the observed data and that a better criterion for the probable appearance of a maximum is when $A_{BA}/A_{AB} > 2 + (2.3A_{BA}/4)$. It is then clear that for systems of considerable dissymmetry without maxima the Margules equations will be inapplicable. If $A_{AB} = A_{BA}$, the equations reduce to the simple forms

$$\log \gamma_A = A_{AB}x_B^2, \qquad \log \gamma_B = A_{BA}x_A^2 \tag{3.69}$$

2. The *van Laar* equations can satisfactorily follow data showing high values of $A_{AB}$ and $A_{BA}$ and greater dissymmetry than the Margules equations, but very large ratios of $A_{BA}$ to $A_{AB}$ cannot be handled. They fit cases where $A_{BA}/A_{AB}$ is in the neighborhood of 2 better than the Margules equations. These equations are more limited in the shapes of curves that can be obtained, however, in that they cannot show maxima or minima or change in sign of log $\gamma$ with changing concentration. If $A_{BA} = A_{AB}$, Eq. (3.69) results, and consequently for nearly symmetrical systems there is little choice to be made between the van Laar or Margules equations.

3. For unsymmetrical systems beyond the capabilities of the van Laar equations, the *Scatchard-Hamer* equations, although less convenient, are better. If $V_A = V_B$, they reduce to the Margules equations, while if $A_{AB}/A_{BA} = V_A/V_B$, they reduce to those of van Laar. Carlson and Colburn (5) consequently suggest that the ratio of $V_A/V_B$ may be taken as a guide as to which of the equations are applicable. For systems that cannot be handled by any of these, the more complex equations suggested by Wohl (35) may be tried.

4. As has been pointed out, the equations are all integrations of the Gibbs-Duhem relationship. They consequently cannot be applied to systems which when treated in the ordinary fashion apparently do not follow this basic relation, as in the case of dissociation of electrolytes in solution.

† If log $\gamma_A$ shows a maximum, then log $\gamma_B$ shows a minimum at the same concentration.

**Effect of Temperature.** The dependency of activity coefficient upon temperature is readily derived from the basic thermodynamic relationships (5, 18, 27):

$$\left(\frac{\partial \ln \gamma_A}{\partial T}\right)_p = -\frac{\bar{H}_A - H_A^0}{RT^2} \tag{3.70}$$

where $\bar{H}_A$ = partial molal enthalpy of component $A$ in soln.
$H_A^0$ = molal enthalpy of pure component $A$ at the same temp.
This may be simplified to

$$\frac{d \log \gamma_A}{d(1/T)} = \frac{\Delta H_S}{2.303R} \tag{3.71}$$

where $\Delta H_S$ = partial molal heat of solution of $A$. A similar equation may be written for component $B$. At infinite dilution, Eq. (3.71) becomes

$$\frac{dA_{AB}}{d(1/T)} = \frac{\Delta H_S'}{2.303R} \tag{3.72}$$

where $\Delta H_S'$ = heat of solution of $A$ at infinite dilution. Plotting $\log \gamma_A$ against $1/T$ at any value of $x_A$ should therefore produce a curve whose slope is related to the differential heat of solution, or, at $x_A = 0$, to the heat of solution at infinite dilution. Conversely, it is possible to estimate the effect of temperature on the activity coefficients, and for this purpose Eq. (3.72) is most useful. Unfortunately, not too many heat-of-solution data are available.

Ordinarily, solutions which exhibit positive deviations from Raoult's law are formed from their constituents with an absorption of heat. $\Delta H_S$ is positive, therefore, and $\gamma_A$ will be smaller at higher temperatures. For mixtures with negative deviations, the $\Delta H_S$ is ordinarily negative. In both cases, therefore, the solutions ordinarily more nearly approach Raoult's law as the temperature is increased. Obvious exceptions to this rule are systems with lower critical solution temperatures, where, at least in the neighborhood of the lower C.S.T., the Raoult's law deviations become greater with increasing temperature.

Benedict, *et al.* (2), and many others have included the effect of temperature as $T \log \gamma$ when expressing $\gamma$ as functions of $x$. At values of $x_A = 0$, this quantity becomes $TA_{AB}$ (27), which leads to the simple approximation

$$\frac{A_{AB_1}}{A_{AB_2}} = \frac{T_2}{T_1} \tag{3.73}$$

This simplification cannot be general but could serve as a useful approximation if more reliable data are lacking. Berg and McKinnis (3) have proposed another empirical method for so-called "regular" solutions.

Data for a typical system are shown in Fig. 3.7, where the activity coefficients for ethanol in aqueous solution at 20, 40, 55, and 75°C. (21),

as well as values calculated from constant-pressure vapor-liquid equilibria at 1 atm. over the temperature range 78.3 to 100°C. (22), are plotted. Clearly in this system the variation of activity coefficient with temperature

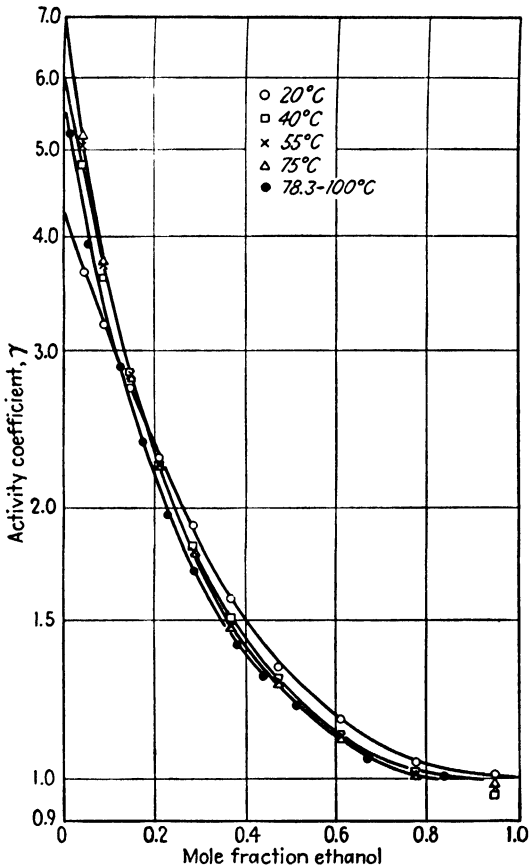



FIG. 3.7. Effect of temperature on activity coefficients of ethanol in aqueous solutions.

is not great. This will be the case for most systems, and for present purposes the temperature dependency can be frequently ignored. Figure 3.8 shows the values of $\log \gamma_A$ at $x_A = 0$, or $A_{AB}$, for this system as a function of temperature in accordance with Eq. (3.72).

**Illustration 4.** From the value of $A_{AB}$ at 40°C. for ethanol ($A$)–water ($B$) and heat-of-solution data, estimate the value of $A_{AB}$ at 55°C., and compare with observed data.

*Solution.* $A_{AB}$ at 40°C. (Fig. 3.7) = log 5.90 = 0.7709. "International Critical Tables" (Vol. V) lists integral heat-of-solution data for ethanol in water for 0, 17.33, and 42.05°C. as a function of ethanol concentration. Extrapolation of these data to zero concentration of ethanol results in the following heats of solution at infinite dilution:

| $t$°C. | 0 | 17.33 | 42.05 |
|---|---|---|---|
| $\Delta H_s$, cal./gm. mole | −3820 | −3010 | −2030 |

From Eq. (3.72),

$$A_{AB_1} = A_{AB_2} + \int_{\frac{1}{T_2}}^{\frac{1}{T_1}} \frac{\Delta H'_S}{2.303R}\, d\left(\frac{1}{T}\right)$$

$$\therefore A_{AB} \text{ at } 55°\text{C.} = 0.7709 + \frac{1}{2.303(1.987)} \int_{0.003195}^{0.00305} \Delta H'_S\, d\left(\frac{1}{T}\right)$$

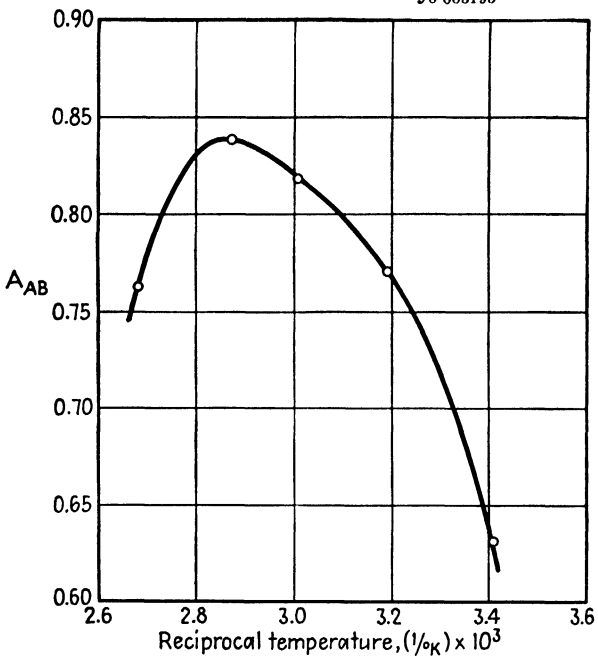



FIG. 3.8. Temperature dependency of $A_{AB}$ for ethanol ($A$)–water ($B$).

The integration is performed graphically by plotting $\Delta H'_S$ against $1/T$, Fig. 3.9, and determining the area under the curve between $1/T = 0.00305$ and $0.003195$. The area is 0.270 cal./(gm. mole)(°K).

$$\therefore A_{AB} \text{ at } 55°\text{C.} = 0.7709 + \frac{0.270}{2.303(1.987)}$$

$= 0.829$, which corresponds to $\gamma_A$ at $(x_A = 0) = 6.75$. These results may be compared with the observed values, 0.8195 and 6.60, resp.

Moderate temperature changes result in such minor changes in activity coefficient that constant-pressure data are ordinarily satisfactory for application of the various integrated forms of the Gibbs-Duhem equation.

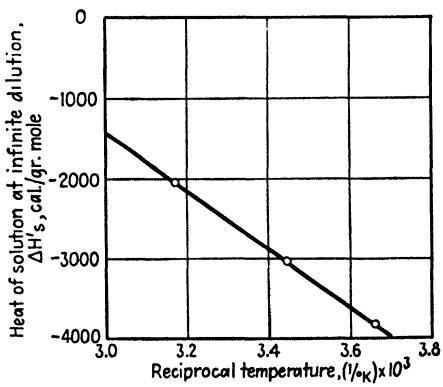



FIG. 3.9. Heat of solution of ethanol in water at infinite dilution.

**Applications of the Integrated Equations.** The usefulness of the Gibbs-Duhem equation for establishing the thermodynamic consistency of, and for smoothing, data has been pointed out. The various integrated forms are probably most useful for extending limited data, sometimes from even single measurements, and it is these applications that are most important for present purposes.

1. *Calculation of Activity-coefficient Curves from a Single Vapor-Liquid Datum.* If a single vapor-liquid equilibrium measurement has been made ($p_t$, $x$, and $y$), the activity coefficients may be readily calculated by Eqs. (3.14) or (3.15), concentrations and activity coefficients may be substituted in the appropriate Gibbs-Duhem equation, and the constants $A_{AB}$ and $A_{BA}$ computed. The integrated equations may then be used to calculate activity coefficients of each component of the solution over the entire concentration range. Greatest precision will result if the single datum is known at a value of $x$ between approximately 0.25 and 0.75. A special case, which frequently arises, is knowledge of the composition, temperature, and pressure of an azeotrope. For an azeotrope, $x = y$, and consequently

$$\gamma_A = \frac{p_t}{p_A}, \qquad \gamma_B = \frac{p_t}{p_B} \tag{3.17}$$

The recent indexed compilation of Horsley (17) is most useful for obtaining data of this sort.

**Illustration 5.** An azeotrope is reported (17) for the system ethyl acetate ($A$)–ethanol ($B$) as follows: 760 mm. Hg, 71.8°C., 30.8 wt. per cent ethanol. From this, calculate the van Laar constants and activity coefficients for the system. Compare these with activity coefficients calculated from complete vapor-liquid equilibria at 1 atm.

*Solution.* 30.8 wt. per cent ethanol = 0.46 mole fraction ethanol.

$$x_B = 0.460$$
$$x_A = 1 - 0.46 = 0.540 \text{ mole fraction ethyl acetate}$$

At 71.8°C., the vapor pressure of ethyl acetate = $p_A$ = 631 mm. Hg, and that of ethanol = $p_B$ = 581 mm. Hg. $p_t$ = 760 mm. Hg. By Eq. (3.17), at the azeotrope

$$\gamma_A = \frac{p_t}{p_A} = \frac{760}{631} = 1.204$$
$$\gamma_B = \frac{p_t}{p_B} = \frac{760}{581} = 1.307$$

By Eqs. (3.60) and (3.61):

$$A_{AB} = \log 1.204 \left[1 + \frac{0.460}{0.540}\left(\frac{\log 1.307}{\log 1.204}\right)\right]^2 = 0.4029$$
$$A_{BA} = \log 1.307 \left[1 + \frac{0.540}{0.460}\left(\frac{\log 1.204}{\log 1.307}\right)\right]^2 = 0.3848$$
$$\frac{A_{AB}}{A_{BA}} = \frac{0.4029}{0.3848} = 1.047$$

The van Laar equations [Eqs. (3.58), (3.59)] are therefore

$$\log \gamma_A = \frac{0.4029}{[1 + (1.047x_A/x_B)]^2}, \qquad \log \gamma_B = \frac{0.3848}{[1 + (x_B/1.047x_A)]^2}$$

Figure 3.10 is a comparison of activity coefficients calculated from these equations with those calculated from the vapor-liquid data of Furnas and Leighton [*Ind. Eng. Chem.* **29**, 709 (1937)] at 760 mm. Hg.

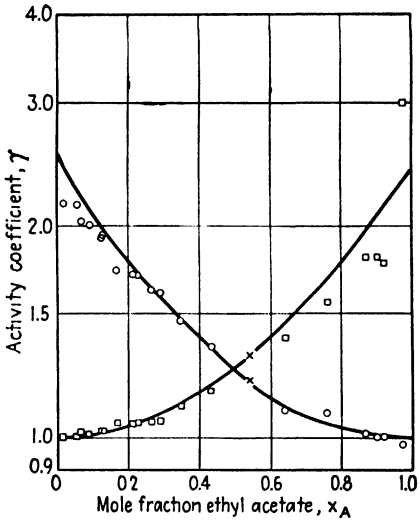



FIG. 3.10. Activity coefficients for ethyl acetate–ethanol. $X$ = azeotrope. ○, □ = data of Furnas and Leighton. [*Ind. Eng. Chem.* **29**, 709 (1937).] Curves calculated from azeotrope.

2. *Calculation of Activity-coefficient Curves from Boiling Points of Solutions or Isothermal Total-pressure Data.* Frequently, boiling points or total pressures of solutions as a function of concentration are known, without information concerning the concentration of the equilibrium vapor. If the appropriate integrated equation can be chosen, it is not difficult to determine the activity coefficients of each component over the entire concentration range by following a procedure suggested by Carlson and Colburn (5). From Eq. (3.15),

$$\gamma_A = \frac{\bar{p}_A}{x_A p_A} = \frac{p_t - \bar{p}_B}{x_A p_A} = \frac{p_t - \gamma_B p_B x_B}{x_A p_A} \tag{3.74}$$

and

$$\gamma_B = \frac{p_t - \gamma_A p_A x_A}{x_B p_B} \tag{3.75}$$

Since, as $x_B$ approaches 1.0, $\gamma_B$ also approaches 1.0, then as a first approximation,

$$\gamma_A(\text{as } x_A \to 0) = \frac{p_t - p_B x_B}{x_A p_A} \tag{3.76}$$

Similarly,

$$\gamma_B(\text{as } x_B \to 0) = \frac{p_t - p_A x_A}{x_B p_B} \tag{3.77}$$

Knowing the boiling points of solutions dilute in component $A$ permits calculation of approximate values of $\gamma_A$. By plotting these on semilogarithmic paper against $x_A$, extrapolation of the curve will give an approximate value of $\gamma_A$ at $x_A = 0$, or $A_{AB}$. Similarly, a value of $A_{BA}$ can be obtained. Substitution in the appropriate integrated Gibbs-Duhem equation permits better estimation of the activity coefficients in the dilute range, and in this way, by successive approximations, reliable values of $A_{AB}$ and $A_{BA}$ are obtained. The activity coefficients over the entire concentration range may then be calculated.

**Illustration 6.** "International Critical Tables" (Vol. III) reports total pressures of solutions of ethanol ($A$)–toluene ($B$) at 32.3°C. as follows:

| $x_A$ | 0 | 0.0420 | 0.1775 | 0.3089 | 0.4613 | 0.5765 |
|---|---|---|---|---|---|---|
| $p_t$, mm. Hg | 93.0 | 141.2 | 214.8 | 233.1 | 242.1 | 244.2 |
| $x_A$ | 0.6680 | 0.7627 | 0.8369 | 0.8802 | 0.9599 | 1.000 |
| $p_t$ | 249.2 | 248.2 | 244.4 | 243.0 | 230.9 | 219.5 |

Calculate the van Laar constants from these data.

*Solution.* At 32.3°C., $p_A = 219.5$ mm. Hg, $p_B = 93.0$ mm. Hg. Eq. (3.76):

$$\gamma_A(\text{at } x_A \to 0) = \frac{p_t - 93.0x_B}{219.5x_A}$$

as a first approximation. Therefore, approximate values of $\gamma_A$ may be computed as follows:

| $x_A$ | $x_B$ | $93.0x_B$ | $219.5x_A$ | $p_t - 93.0x_B$ | Approx. $\gamma_A$ |
|---|---|---|---|---|---|
| 0.0420 | 0.9580 | 89.0 | 9.22 | 52.2 | 5.67 |
| 0.1775 | 0.8225 | 76.5 | 38 98 | 138.3 | 3.55 |
| 0.3089 | 0.6911 | 64.3 | 67.9 | 168.8 | 2.485 |

The approximate values of $\gamma_A$ are plotted on semilogarithmic paper against $x_A$, and by extrapolation, the value of $\gamma_A$ at ($x_A = 0$) is 6.65. A trial value of $A_{AB} = \log 6.65 = 0.8228$. Similarly, approximate values of $\gamma_B$ are computed from Eq. (3.77):

| $x_A$ | $x_B$ | $93.0x_B$ | $219.5x_A$ | $p_t - 219.5x_A$ | Approx. $\gamma_B$ |
|---|---|---|---|---|---|
| 0.9599 | 0.0401 | 3.73 | 211 | 19.9 | 5.35 |
| 0.8802 | 0.1198 | 11.14 | 193.3 | 49.7 | 4.46 |
| 0.8369 | 0.1631 | 15.19 | 183.9 | 60.5 | 3.99 |

In a manner similar to that for $\gamma_A$, a trial value of $A_{BA}$ is found to be $\log 5.88 = 0.7694$. The trial values of $A_{AB}$ and $A_{BA}$ are tested by computing $\gamma$'s, using the van Laar equations, and with these calculating $p_t$ from the relationship

$$p_t = \gamma_A p_A x_A + \gamma_B p_B x_B$$

The results of these calculations are:

| $x_A$ | $\gamma_A$ | $\gamma_B$ | $p_t$ calculated, mm. Hg |
|---|---|---|---|
| 0.0420 | 5.624 | 1.003 | 141.3 |
| 0.3089 | 2.382 | 1.204 | 239.1 |
| 0.5765 | 1.368 | 1.873 | 246.7 |
| 0.7627 | 1.102 | 2.884 | 247.8 |
| 0.8802 | 1.025 | 4.036 | 242.9 |
| 0.9599 | 1.002 | 5.176 | 230.3 |

For most purposes, the computed values of $p_t$ agree satisfactorily with the observed data, and the trial values of $A_{AB}$ and $A_{BA}$ may be considered final. Better values may be obtained by repeating the calculations, using Eqs. (3.76) and (3.77) together with the values of $\gamma_A$ and $\gamma_B$ computed above.

3. *Calculation of Activity Coefficients from Compositions of Liquid and Vapor at Known Pressures, without Knowledge of Temperature.* A method of calculation is suggested by Carlson and Colburn (5). As a first approximation, a temperature is found by assuming that Raoult's law applies to the component present in the larger amount. This temperature permits a first approximation of the activity coefficients of the component present in lesser amount, and plotting these on semilogarithmic coordinates permits a first approximation of $A_{AB}$ and $A_{BA}$. Substitution in the appropriate integrated form of the Gibbs-Duhem equation will give more reliable activity coefficients, and by successive approximations final values of $A_{AB}$ and $A_{BA}$ are obtained.

4. *Calculation of Activity Coefficients from Mutual Solubility Data* (5, 7, 31). As the components of a solution become more and more dissimilar chemically, their solutions show greater and greater deviations from Raoult's law. Large positive deviations ultimately lead to partial immiscibility. Thus, in the systems alcohol–water, we observe that methyl, ethyl, and propyl alcohols are completely miscible but with increasing deviations from Raoult's law. Butyl alcohol, with very large deviations when mixed with water, is only partially soluble. Similar observations can be made in the ketone–water systems, with acetone–water showing moderate deviations and complete miscibility, while methyl ethyl ketone and water show a solubility gap and large positive deviations.

In any two phases at equilibrium, including two liquid phases, the fugacities of each component are the same in the two phases. Provided that the same standard state for a substance is chosen for its condition in each phase, the activities of the substance in each phase are also equal. Thus,

$$a_{AA} = a_{AB}, \qquad a_{BA} = a_{BB} \tag{3.78}$$

Consequently,

$$\frac{x_{AA}}{x_{AB}} = \frac{\gamma_{AB}}{\gamma_{AA}}, \qquad \frac{x_{BA}}{x_{BB}} = \frac{\gamma_{BB}}{\gamma_{BA}} \tag{3.79}$$

Over the range of concentrations between the solubility limits the apparent activity coefficients will vary inversely as the concentrations based on the mixture as a whole. Elimination of $\gamma$'s between Eq. (3.79) and any of the integrated Gibbs-Duhem equations therefore permits the estimation of $A_{AB}$ and $A_{BA}$ from the mutual solubility. Thus, the Margules equations lead to

$$A_{AB} = \frac{\log \dfrac{x_{AB}}{x_{AA}}}{\left(2\dfrac{A_{BA}}{A_{AB}} - 1\right)\left(x_{BA}^2 - x_{BB}^2\right) - 2\left(\dfrac{A_{BA}}{A_{AB}} - 1\right)\left(x_{BA}^3 - x_{BB}^3\right)} \tag{3.80}$$

$$\frac{A_{AB}}{A_{BA}} = \frac{2[(x_{BA}^2 - x_{BB}^2) - (x_{BA}^3 - x_{BB}^3)]\log\dfrac{x_{BB}}{x_{BA}} + [(x_{AA}^2 - x_{AB}^2) - 2(x_{AA}^3 - x_{AB}^3)]\log\dfrac{x_{AB}}{x_{AA}}}{2[(x_{AA}^2 - x_{AB}^2) - (x_{AA}^3 - x_{AB}^3)]\log\dfrac{x_{AB}}{x_{AA}} + [(x_{BA}^2 - x_{BB}^2) - 2(x_{BA}^3 - x_{BB}^3)]\log\dfrac{x_{BB}}{x_{BA}}} \tag{3.81}$$

The van Laar equations give

$$A_{AB} = \frac{\log \frac{x_{AB}}{x_{AA}}}{\frac{1}{\left(1 + \frac{A_{AB}x_{AA}}{A_{BA}x_{BA}}\right)^2} - \frac{1}{\left(1 + \frac{A_{AB}x_{AB}}{A_{BA}x_{BB}}\right)^2}} \tag{3.82}$$

$$\frac{A_{AB}}{A_{BA}} = \frac{\left(\frac{x_{AA}}{x_{BA}} + \frac{x_{AB}}{x_{BB}}\right)\left(\frac{\log \frac{x_{AB}}{x_{AA}}}{\log \frac{x_{BA}}{x_{BB}}}\right) - 2}{\frac{x_{AA}}{x_{BA}} + \frac{x_{AB}}{x_{BB}} - \frac{2x_{AA}x_{AB} \log \frac{x_{AB}}{x_{AA}}}{x_{BA}x_{BB} \log \frac{x_{BA}}{x_{BB}}}} \tag{3.83}$$

The Scatchard-Hamer equations give

$$A_{AB} = \frac{\log \frac{x_{AB}}{x_{AA}}}{\left(\frac{2A_{BA}V_A}{A_{AB}V_B} - 1\right)\left(z_{BA}^2 - z_{BB}^2\right) - 2\left(\frac{A_{BA}V_A}{A_{AB}V_B} - 1\right)\left(z_{BA}^3 - z_{BB}^3\right)} \tag{3.84}$$

$$\frac{A_{AB}}{A_{BA}} = \frac{2\frac{V_A}{V_B}[(z_{BA}^2 - z_{BB}^2) - (z_{BA}^3 - z_{BB}^3)]\log \frac{x_{BB}}{x_{BA}} + [(z_{AA}^2 - z_{AB}^2) - 2(z_{AA}^3 - z_{AB}^3)]\log \frac{x_{AB}}{x_{AA}}}{2\frac{V_B}{V_A}[(z_{AA}^2 - z_{AB}^2) - (z_{AA}^3 - z_{AB}^3)]\log \frac{x_{AB}}{x_{AA}} + [(z_{BA}^2 - z_{BB}^2) - 2(z_{BA}^3 - z_{BB}^3)]\log \frac{x_{BB}}{x_{BA}}} \tag{3.85}$$

In Eqs. (3.80) to (3.85), the concentrations are those of the equilibrium saturated solutions. In each case, the second of the equation pairs permits calculation of $A_{AB}/A_{BA}$ from the data, and the first then gives $A_{AB}$. Colburn and Schoenborn (7) have given a graphical solution of the van Laar set. A similar graphical solution could be worked out for the Margules equations, but the additional parameter of $V_A/V_B$ in the Scatchard-Hamer equations would make such a method awkward.

For systems of moderately symmetrical solubility, *i.e.*, where $x_{AB}$ is nearly equal to $x_{AA}$, $A_{AB}$ will nearly equal $A_{BA}$, and either the Margules or van Laar equations would be expected to be applicable. For moderate dissymmetry, the van Laar equations ought to be better, whereas for strong dissymmetry the Scatchard-Hamer equations should be used. As the mutual solubility decreases, these equations show larger and larger values of $A_{AB}$ and $A_{BA}$ and correspondingly increasing activity coefficients.

At the critical-solution point, since $x_{AA} = x_{AB}$ and $x_{BA} = x_{BB}$, Eqs. (3.80) to (3.85) become indeterminate. Hildebrand (15) has shown, however, that at the critical point $(d \ln a)/dx$ and $(d^2 \ln a)/dx^2$ both equal zero. Applying these criteria to the van Laar equations, as an example, there result

$$\frac{A_{AB}}{A_{BA}} = \frac{1 - x_A^2}{2x_A - x_A^2} \tag{3.86}$$

and

$$A_{AB} = \frac{5.862(1 - x_A)^2}{(2 - x_A)^2(1 - x_A^2)} \tag{3.87}$$

which then may be used with critical-solution data. For example, if the system is symmetrical, so that the critical-solution composition is $x = 0.5$, the $A_{AB} = A_{BA} = 0.868$.

Activity coefficients calculated by these methods agree fairly well for systems where the original equations, *i.e.*, Eqs. (3.50) to (3.66), apply. Carlson and Colburn (5) and Colburn, Schoenborn, and Shilling (8) have shown that the van Laar constants cannot be calculated from solubility data for *n*-butanol–water and isobutanol–water, but the van Laar equations do not satisfactorily describe the activity coefficients obtained from vapor-liquid data in these systems either.

**Illustration 7.** The mutual solubility of methyl ethyl ketone ($A$) and water ($B$) at 40°C. are 18.6 and 90.1 wt. per cent ketone (21). Calculate the constants $A_{AB}$ and $A_{BA}$ for the system, and compare with those calculated from vapor-liquid data.

*Solution. a. Calculation from solubility data.* At 18.6% methyl ethyl ketone and 81.4% water, the mole fractions of ketone and water are 0.054 and 0.946, resp. At 90.1% ketone and 9.9% water, the mole fractions of ketone and water are 0.695 and 0.305, resp. Therefore,

Water layer: $x_{AB} = 0.054, \quad x_{BB} = 0.946$
Ketone layer: $x_{AA} = 0.695, \quad x_{BA} = 0.305$

Since the solubility is moderately unsymmetrical, the van Laar equations will be used. Eq. (3.83):

$$\frac{A_{AB}}{A_{BA}} = \frac{\left(\frac{0.695}{0.305} + \frac{0.054}{0.946}\right)\left(\frac{\log \frac{0.054}{0.695}}{\log \frac{0.305}{0.946}}\right) - 2}{\frac{0.695}{0.305} + \frac{0.054}{0.946} - \frac{2(0.695)(0.054)\log \frac{0.054}{0.695}}{(0.305)(0.946)\log \frac{0.305}{0.946}}} = 1.860$$

Eq. (3.82):

$$A_{AB} = \frac{\log \frac{0.054}{0.695}}{\frac{1}{[1 + 1.86(0.695/0.305)]^2} - \frac{1}{[1 + 1.86(0.054/0.946)]^2}} = 1.455$$

$$\therefore A_{BA} = \frac{1.455}{1.860} = 0.781$$

These correspond to $\gamma_A$ at $(x_A = 0) = 28\ 51$
$\gamma_B$ at $(x_A = 1) = 6.04$

*b. Calculation from vapor-liquid data.* Othmer and Benenati [*Ind. Eng. Chem.* **37**, 299 (1945)] report vapor-liquid data for the system at several total pressures. At 200 mm. Hg, the temperatures most closely approach 40°C., and these will be used. The

table lists the reported temperatures and compositions, and activity coefficients calculated by Eq. (3.15).

| $t$°C. | $x_A$ | $y_A$ | $\gamma_A$ | $\gamma_B$ |
|---|---|---|---|---|
| 41.5 | 1.000 | 1.000 | 1.000 | — |
| 40.6 | 0.903 | 0.825 | 1.009 | 6.31 |
| 40.0 | 0.813 | 0.763 | 1.065 | 4.59 |
| 39.9 | 0.777 | 0.750 | 1.102 | 4.06 |
| 39.8 | 0.674 | 0.726 | 1.237 | 3.07 |
| 41.3 | 0.038 | 0.709 | 20.0 | 1.021 |
| 66.1 | 0 | 0 | — | 1.000 |

A semilogarithmic plot of $\gamma_A$ and $\gamma_B$ against $x_A$ shows that at $x_A = 0$, $\gamma_A = 29$, and $\log \gamma_A = A_{AB} = 1.462$; and at $x_A = 1$, $\gamma_B = 8.2$, and $\log \gamma_B = A_{BA} = 0.914$. These compare very favorably with the results of the solubility calculations.

**Illustration 8.** The critical-solution point for methyl ethyl ketone ($A$) and water ($B$) is 45 wt. per cent ketone, at 150°C. (21). Calculate the van Laar constants at this temperature.

*Solution.* At 45 wt. per cent methyl ethyl ketone, $x_A = 0.1696$ mole fraction ketone. Substitution in Eq. (3.86):

$$\frac{A_{AB}}{A_{BA}} = \frac{(1 - 0.1696)^2}{2(0.1696) - (0.1696)^2} = 3.125$$

Eq. (3.87):
$$A_{AB} = \frac{5.862(1 - 0.1696)^2}{(2 - 0.1696)^2[1 - (0.1696)^2]} = 1.258$$

$$\therefore A_{BA} = \frac{1.258}{3.125} = 0.402$$

Comparison of these constants with those of the previous example will illustrate again the effect of temperature on activity coefficients.

## NONIDEAL TERNARY MIXTURES

The general principles established for ideal solutions, such as Raoult's law in its various forms, are of course applicable to solutions of any number of components. Similarly, the Gibbs-Duhem equation is applicable to nonideal solutions of any number of components, and as in the case of binary mixtures various relationships can be worked out relating the activity coefficients for ternary mixtures. This problem has now been attacked from several points of view, a most excellent summary of which is presented by Wohl (35). His most important results pertinent to the problem at hand are summarized here.

**Two-suffix Ternaries Composed of Three Symmetrical Binaries.** The equations for this case, worked out by Benedict, *et al.* (2) are:

$$\log \gamma_A = A_{AB}x_B^2 + A_{AC}x_C^2 + x_Bx_C(A_{AB} + A_{AC} - A_{BC}) \quad (3.88)$$

$$\log \gamma_B = A_{AB}x_A^2 + A_{BC}x_C^2 + x_Ax_C(A_{AB} + A_{BC} - A_{AC}) \quad (3.89)$$

$$\log \gamma_C = A_{AC}x_A^2 + A_{BC}x_B^2 + x_Ax_B(A_{AC} + A_{BC} - A_{AB}) \quad (3.90)$$

The constants in these equations are those obtained from the end values of the activity coefficients of the three binary systems, each of which is symmetrical:

$$\begin{aligned} A_{AB} &= \text{limit of } \log \gamma_A \text{ as } x_A \to 0 \text{ and } x_B \to 1 \\ &= \text{limit of } \log \gamma_B \text{ as } x_B \to 0 \text{ and } x_A \to 1 \end{aligned} \tag{3.91}$$

$$\begin{aligned} A_{AC} &= \text{limit of } \log \gamma_A \text{ as } x_A \to 0 \text{ and } x_C \to 1 \\ &= \text{limit of } \log \gamma_C \text{ as } x_C \to 0 \text{ and } x_A \to 1 \end{aligned} \tag{3.92}$$

$$\begin{aligned} A_{BC} &= \text{limit of } \log \gamma_B \text{ as } x_B \to 0 \text{ and } x_C \to 1 \\ &= \text{limit of } \log \gamma_C \text{ as } x_C \to 0 \text{ and } x_B \to 1 \end{aligned} \tag{3.93}$$

Since there are no additional constants which are characteristic only of the ternary systems, then knowledge of the three binary systems alone permits calculation of the ternary-mixture activity coefficients. It is most important to note that, for even this most simple of situations, ordinary interpolation of the binary-solution data is not possible. Simple interpolation of the log $\gamma$'s would be valid only if the $-A_{BC}$, $-A_{AC}$, and $-A_{AB}$ terms in the equations were omitted. If, as is ordinarily the case, the constants are positive, values of log $\gamma$ will be lower than the arithmetic average of values from the binaries. Linear interpolation of log $\gamma_A$ will be valid only if the $B$–$C$ mixtures are ideal.

**Two-suffix van Laar Equations.** These are perhaps the next most simple equations:

$$\log \gamma_A = \frac{x_B^2 A_{AB}\left(\frac{A_{BA}}{A_{AB}}\right)^2 + x_C^2 A_{AC}\left(\frac{A_{CA}}{A_{AC}}\right)^2 + x_B x_C \left(\frac{A_{BA}}{A_{AB}}\right)\left(\frac{A_{CA}}{A_{AC}}\right)\left[A_{AB} + A_{AC} - A_{CB}\left(\frac{A_{AC}}{A_{CA}}\right)\right]}{\left[x_A + x_B\left(\frac{A_{BA}}{A_{AB}}\right) + x_C\left(\frac{A_{CA}}{A_{AC}}\right)\right]^2} \tag{3.94}$$

The expressions for log $\gamma_B$ can be obtained by a "rotation" principle, *i.e.*, by substituting subscripts $B$ for $A$, $C$ for $B$, and $A$ for $C$ throughout the equation. Thus in the equation for log $\gamma_B$, $x_B$ in Eq. (3.94) is changed to $x_C$, $A_{AB}$ to $A_{BC}$, $A_{AC}$ to $A_{BA}$, etc. Similarly, in that for $\gamma_C$, $x_C$ in Eq. (3.94) is changed to $x_B$, $A_{BA}$ to $A_{AC}$, etc. The constants are again defined in terms of binary systems only:

$$\left.\begin{aligned} A_{AB} &= \text{limit of } \log \gamma_A \text{ as } x_A \to 0,\ x_B \to 1 \\ A_{BA} &= \text{limit of } \log \gamma_B \text{ as } x_B \to 0,\ x_A \to 1 \end{aligned}\right\} \text{Binary } A\text{–}B$$

$$\left.\begin{aligned} A_{AC} &= \text{limit of } \log \gamma_A \text{ as } x_A \to 0,\ x_C \to 1 \\ A_{CA} &= \text{limit of } \log \gamma_C \text{ as } x_C \to 0,\ x_A \to 1 \end{aligned}\right\} \text{Binary } A\text{–}C \tag{3.95}$$

$$\left.\begin{aligned} A_{BC} &= \text{limit of } \log \gamma_B \text{ as } x_B \to 0,\ x_C \to 1 \\ A_{CB} &= \text{limit of } \log \gamma_C \text{ as } x_C \to 0,\ x_B \to 1 \end{aligned}\right\} \text{Binary } B\text{–}C$$

Wohl has shown that these equations are limited to those cases where

$$\frac{A_{CB}}{A_{BC}} = \left(\frac{A_{CA}}{A_{AC}}\right)\left(\frac{A_{AB}}{A_{BA}}\right) \tag{3.96}$$

a limitation which may not be too serious. As in the previous case, the ternary data can be predicted from information on the binary systems alone.

**Equations Containing Ternary Constants.** In the more complex cases, constants derivable from ternary data are included in the equations, which are in turn more generally useful. Thus,

$$\log \gamma_A = z_B^2[A_{AB} + 2z_A(A_{BA}\frac{q_A}{q_B} - A_{AB})] + z_C^2[A_{AC} + 2z_A(A_{CA}\frac{q_A}{q_C} - A_{AC})] + z_B z_C[A_{BA}\frac{q_A}{q_B} + A_{AC} - A_{CB}\frac{q_A}{q_C} + 2z_A(A_{CA}\frac{q_A}{q_C} - A_{AC}) + 2z_C(A_{CB}\frac{q_A}{q_C} - A_{BC}\frac{q_A}{q_B} - C(1 - 2z_A)] \quad (3.97)$$

If, in this equation, various values are assigned to the "$q$ fractions," the equations resulting are as follows:

$\frac{q_A}{q_B} = \frac{V_A}{V_B}$; $\frac{q_A}{q_C} = \frac{V_A}{V_C}$: three-suffix Scatchard-Hamer equations

$\frac{q_A}{q_B} = \frac{A_{AB}}{A_{BA}}$; $\frac{q_A}{q_C} = \frac{A_{AC}}{A_{CA}}$: three-suffix van Laar equations [use restricted by Eq. (3.96)]

$\frac{q_A}{q_B} = \frac{q_A}{q_C} = 1$; $z$ replaced by $x$: three-suffix Margules equations

In each of these cases, equations for $\log \gamma_B$ and $\log \gamma_C$ can be obtained from Eq. (3.97) by changing subscripts in accordance with the rotation principle previously described. The $A$ constants are defined by Eq. (3.95), and a ternary constant $C$, requiring at least one ternary measurement, is included. In the absence of ternary data, Colburn (6) has suggested as an approximation that $C$ can be estimated in the following manner:

$$C = \tfrac{1}{2}[(A_{BA} - A_{AB}) + (A_{AC} - A_{CA}) + (A_{CB} - A_{BC})] \quad (3.98)$$

The general applicability of these equations may be inferred from the discussion of the corresponding binary equations.

More complex equations containing additional constants are also presented by Wohl. A convenient graphical approximation of the ternary data from binaries is offered by Scheibel and Friedland (33).

## PREDICTION OF DISTRIBUTION

It will be recalled, as pointed out at the beginning of the chapter, that it is desirable to be able to predict the distribution of a solute between partially miscible solvents from a minimum of data. The discussion presented above now offers a means of attacking this problem in fairly systematic fashion. In what follows, $B$ is considered the extracting solvent for removing a distributed substance $C$ from $A$–$C$ solutions.

As previously indicated, provided that the same standard state is chosen for a substance for its condition in each phase, the activities of the substance in each phase at equilibrium are equal:

$$a_{CA} = a_{CB}, \qquad a_{AA} = a_{AB}, \qquad a_{BA} = a_{BB} \tag{3.99}$$

Also,

$$a_{CA} = \gamma_{CA}x_{CA}, \qquad a_{CB} = \gamma_{CB}x_{CB}, \text{ etc.} \tag{3.100}$$

The general procedure which presumably could be followed would be to establish values of activity coefficients in the three binary systems ($A$–$B$, $A$–$C$, and $B$–$C$) from data of the sort previously described, using the binary integrated forms of the Gibbs-Duhem equation to assist in extending meager data as necessary. From these, predictions of activity coefficients and activities in the ternary systems can be made by use of the ternary integrated Gibbs-Duhem equations. Equilibrium ternary liquid layers then exist where activities of all three components are equal. Reference to Fig. 3.11 will make the last step clearer.

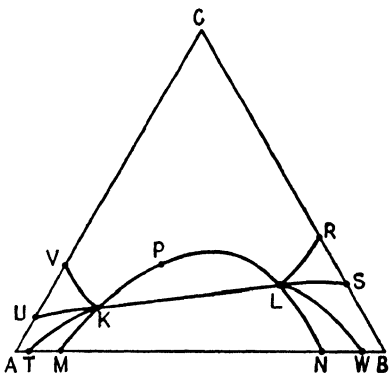


FIG. 3.11. Activities in ternary systems.

Here there is shown a typical ternary liquid-phase diagram for a Type 1 system, with an heterogeneous area $MKPLN$ and a typical tie line $KL$. The activities of $A$, $B$, and $C$ in the solution at $K$ must equal those of $A$, $B$, and $C$, respectively, in the solution at $L$. Lines $VK$ and $LR$ represent solutions of constant activity of $C$. Similarly, $TK$ and $LS$ are solutions of constant activity of $B$, and $UK$ and $LW$ those of constant activity of $A$. By means of the ternary activity-coefficient equations it should be possible to locate points such as $K$ and $L$ where the three constant activity curves intersect. In this fashion it should be possible to locate both the tie lines and the solubility curve.

Unfortunately, the activity-coefficient equations cannot conveniently be made explicit in terms of $x$, and the location of the constant activity curves on the triangular diagram is possible only by a lengthy series of interpolations. Location of the triple intersection points becomes an even more difficult trial-and-error procedure. While this can be done, for practical purposes use of the ternary activity-coefficient equations is ordinarily limited to cases where the solubility curve of the ternary liquid system is known. For such a situation, the calculations become relatively simple, since it is then merely necessary to compute activities of $C$ along the solubility curve and to join equal values on opposite sides of the curve by the tie lines.

**Illustration 9.** Predict the distribution in the Type 1 system water ($A$)–ethyl acetate ($B$)–ethanol ($C$), at 20°C.

*Solution. Ethyl acetate ($B$)–ethanol ($C$).* Refer to Illustration 5 and Fig. 3.10. The vapor-liquid data at 1 atm. of Furnas and Leighton (*loc. cit.*) are plotted as activity coefficients. Smooth curves drawn through the points and extended to the $\gamma$ axes give

$$A_{CB} = \log 2.20 = 0.3424$$
$$A_{BC} = \log 2.30 = 0.3617$$

(NOTE: These are not the constants calculated from azeotropic data.)

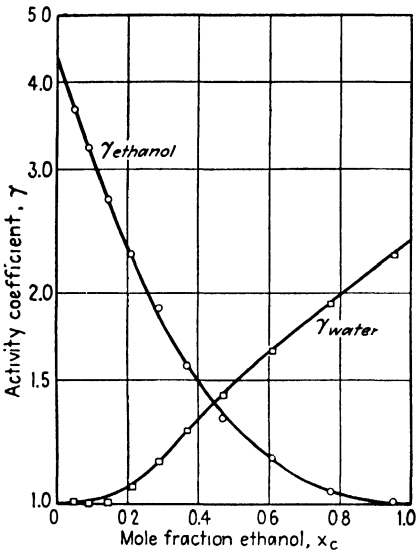



FIG. 3.12. Activity coefficients for ethanol–water, 20°C.

*Water ($A$)–ethanol ($C$).* Vapor-liquid data at 20°C. are available in "International Critical Tables," Vol. III. These have been calculated in the form of activity coefficients and are plotted in Fig. 3.12. Extension of the curves to the $\gamma$ axes gives

$$A_{CA} = \log 4.30 = 0.6334$$
$$A_{AC} = \log 2.40 = 0.3802$$

*Water ($A$)–ethyl acetate ($B$).* Solubility data for this binary are available in "International Critical Tables," Vol. III. At 20°C., the saturated solutions contain 7.94 and 96.99 wt. per cent ethyl acetate. These concentrations correspond to the following mole fractions:

$$x_{BA} = 0.01738, \quad x_{AA} = 0.9826$$
$$x_{BB} = 0.8679, \quad x_{AB} = 0.1321$$

Using the van Laar equations, Eq. (3.83):

$$\frac{A_{AB}}{A_{BA}} = \frac{\left(\frac{0.9826}{0.01738} + \frac{0.1321}{0.8679}\right)\left(\frac{\log \frac{0.1321}{0.9826}}{\log \frac{0.01738}{0.8679}}\right) - 2}{\frac{0.9826}{0.01738} + \frac{0.1321}{0.8679} - \frac{2(0.9826)(0.1321)\log \frac{0.1321}{0.9826}}{(0.01738)(0.8679)\log \frac{0.01738}{0.8679}}} = 0.565$$

Eq. (3.82):

$$A_{AB} = \frac{\log \frac{0.1321}{0.9826}}{\frac{1}{\left[1 + 0.565\left(\frac{0.9826}{0.01738}\right)\right]^2} - \frac{1}{\left[1 + 0.565\left(\frac{0.1321}{0.8679}\right)\right]^2}} = 1.030$$

$$\therefore A_{BA} = \frac{1.030}{0.565} = 1.788$$

Summary:

$$A_{CA} = 0.6334 \quad A_{CB} = 0.3424 \quad A_{AB} = 1.030$$
$$A_{AC} = 0.3802 \quad A_{BC} = 0.3617 \quad A_{BA} = 1.788$$

Eq. (3.96):

$$\frac{A_{CB}}{A_{BC}} = \left(\frac{A_{CA}}{A_{AC}}\right)\left(\frac{A_{AB}}{A_{BA}}\right)$$

$$\frac{0.3424}{0.3617} = \left(\frac{0.6334}{0.3802}\right)\left(\frac{1.030}{1.780}\right)$$

$$0.948 = 0.960$$

This is sufficiently close to an equality that the two-suffix ternary van Laar equations can be used [Eq. (3.94)].

$$\therefore \log \gamma_C = \frac{x_A^2 A_{CA}\left(\frac{A_{AC}}{A_{CA}}\right)^2 + x_B^2 A_{CB}\left(\frac{A_{BC}}{A_{CB}}\right)^2 + x_A x_B\left(\frac{A_{AC}}{A_{CA}}\right)\left(\frac{A_{BC}}{A_{CB}}\right)\left[A_{CA} + A_{CB} - A_{BA}\left(\frac{A_{CB}}{A_{BC}}\right)\right]}{\left[x_C + x_A\left(\frac{A_{AC}}{A_{CA}}\right) + x_B\left(\frac{A_{BC}}{A_{CB}}\right)\right]^2}$$

Substitution of the constants leads to

$$\log \gamma_C = \frac{0.2285x_A^2 + 0.3815x_B^2 - 0.455x_A x_B}{(x_C + 0.601x_A + 1.055x_B)^2}$$

Beech and Glasstone (*J. Chem. Soc.* **1938**, 67) provide ternary-solubility data for this system at 20°C. In the table below, their weight fractions have been converted to mole fractions and $\gamma_C$ calculated from the above equation. Activities $a_C$ are calculated from the relation $a_C = \gamma_C x_C$.

| | $x_A$ | $x_B$ | $x_C$ | $\gamma_C$ | $a_C$ |
|---|---|---|---|---|---|
| | | | $x_{CA}$ | $\gamma_{CA}$ | $a_{CA}$ |
| Water-rich layer | 0.983 | 0.01738 | 0 | 3.767 | 0 |
| | 0.966 | 0.01772 | 0.01718 | 3.468 | 0.0596 |
| | 0.947 | 0.01939 | 0.0335 | 3.225 | 0.1081 |
| | 0.932 | 0.02185 | 0.0473 | 2.992 | 0.1416 |
| | 0.909 | 0.02635 | 0.0645 | 2.742 | 0.1770 |
| | 0.886 | 0.0335 | 0.0812 | 2.477 | 0.2008 |
| | 0.847 | 0.0496 | 0.1034 | 2.136 | 0.2211 |
| | | | $x_{CB}$ | $\gamma_{CB}$ | $a_{CB}$ |
| Ester-rich layer | 0 1321 | 0 8679 | 0 | 1.745 | 0 |
| | 0.1520 | 0.815 | 0.0330 | 1.619 | 0.0534 |
| | 0.2055 | 0.711 | 0.0837 | 1.407 | 0.1179 |
| | 0.2545 | 0.634 | 0.1110 | 1.285 | 0.1427 |
| | 0.294 | 0.569 | 0.1368 | 1.204 | 0.1650 |
| | 0.396 | 0.437 | 0.1678 | 1.097 | 0.1840 |
| | 0.522 | 0.303 | 0.1754 | 1.095 | 0.1925 |

A plot of $a_{CA}$ vs. $x_{CA}$ and of $a_{CB}$ vs. $x_{CB}$ is shown in Fig. 3.13. Equilibrium values of $x_{CA}$ and $x_{CB}$ are read at constant values of activity:

| $x_{CA}$ | 0 | 0.01 | 0.02 | 0.03 | 0.04 | 0.05 | 0.06 | 0.07 | 0.08 |
|---|---|---|---|---|---|---|---|---|---|
| $x_{CB}$ | 0 | 0.0225 | 0.044 | 0.066 | 0.089 | 0.115 | 0.140 | 0.168 | 0.183 |

These are plotted as the curve on Fig. 3.14 and compared with the measured equilibrium data of Beech and Glasstone (*loc. cit.*) plotted as points. The agreement between predicted and observed data is seen to be very satisfactory.

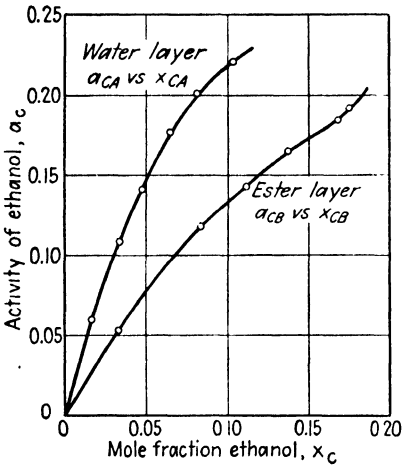



FIG. 3.13. Calculated activities of ethanol in the system water (*A*)–ethyl acetate (*B*)–ethanol (*C*).

**Illustration 10.** Predict the distribution in the Type 2 system *n*-heptane (*A*)–aniline (*B*)–cyclohexane (*C*), at 25°C.

*Solution. n-Heptane (A)–aniline (B).* Mutual-solubility data are available from Hunter and Brown [*Ind. Eng. Chem.* **39**, 1343 (1947)]: at 25°C.

Heptane-rich solution:

93.20 wt. per cent heptane, $x_{AA} = 0.9272$
6.80 wt. per cent aniline, $x_{BA} = 0.0728$

Aniline-rich solution:

6.50 wt. per cent heptane, $x_{AB} = 0.0607$
93.50 wt. per cent aniline, $x_{BB} = 0.9393$

Substitution of these data in the van Laar equations [Eqs. (3.82) to (3.83)] give

$$A_{AB} = 1.359, \qquad A_{BA} = 1.290$$

*Aniline (B)–cyclohexane (C).* Mutual-solubility data of Hunter and Brown (*loc. cit.*) are used: at 25°C.,

Cyclohexane-rich solution:

83.50 wt. per cent cyclohexane, $x_{CC} = 0.8488$
16.50 wt. per cent aniline, $x_{BC} = 0.1512$

Aniline-rich solution:

26.20 wt. per cent cyclohexane, $x_{CB} = 0.2820$
73.80 wt. per cent aniline, $x_{BB} = 0.7180$

The van Laar equations [Eqs. (3.82) to (3.83)] give

$$A_{BC} = 1.120, \qquad A_{CB} = 0.867$$

*n-Heptane (A)–cyclohexane (C).* No data are available, but it is not unreasonable to assume this system nearly ideal.

$$A_{CA} = A_{AC} = 0, \qquad \frac{A_{CA}}{A_{AC}} = 1.0$$

The same ternary van Laar equation is used as in Illustration 9. After substitution and simplification, it becomes

$$\log \gamma_C = \frac{1.447x_B^2 - 0.1691x_Ax_B}{(x_C + x_A + 1.292x_B)^2}$$

Ternary-solubility data at 25°C. of Hunter and Brown (*loc. cit.*) are used in the manner of Illustration 9 to calculate activity coefficients and activities.

| | $x_A$ | $x_B$ | $x_C$ | $\gamma_C$ | $a_C$ |
|---|---|---|---|---|---|
| | | | $x_{CA}$ | $\gamma_{CA}$ | $a_{CA}$ |
| Hydrocarbon-rich layer | 0.9272 | 0.0728 | 0 | 0.9920 | 0 |
| | 0.687 | 0.0850 | 0.227 | 0.9992 | 0.227 |
| | 0.667 | 0.0835 | 0.249 | 1.0015 | 0.250 |
| | 0.426 | 0.1019 | 0.472 | 1.0165 | 0.480 |
| | 0.248 | 0.1210 | 0.630 | 1.0355 | 0.652 |
| | 0.1248 | 0.1428 | 0.731 | 1.058 | 0.774 |
| | 0 | 0.1512 | 0.8488 | 1.0725 | 0.910 |
| | | | $x_{CB}$ | $\gamma_{CB}$ | $a_{CB}$ |
| Aniline-rich layer | 0.0607 | 0.9393 | 0 | 6.046 | 0 |
| | 0.0368 | 0.853 | 0.1098 | 4.721 | 0.518 |
| | 0.0219 | 0.785 | 0.1938 | 3.681 | 0.714 |
| | 0 | 0.718 | 0.282 | 3.251 | 0.916 |

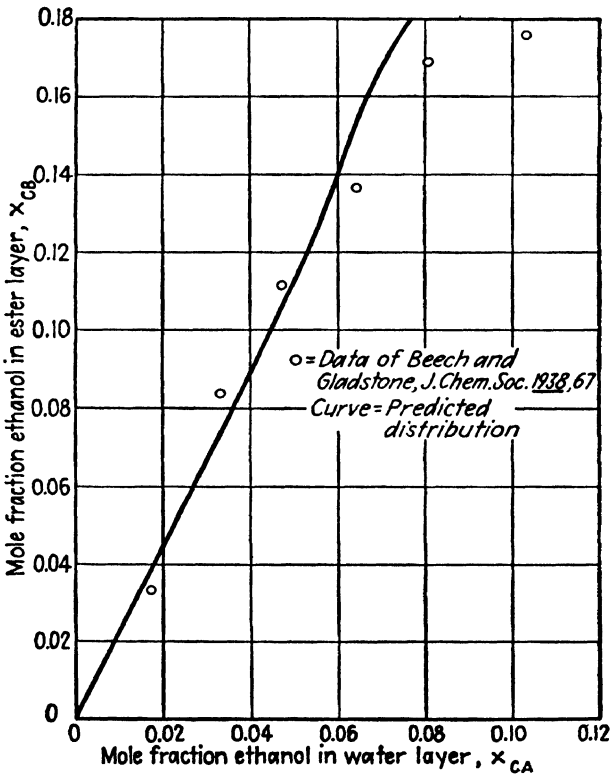



FIG. 3.14. Distribution of ethanol between water and ethyl acetate, 20°C.

Figure 3.15 shows the plot of $a_{CA}$ vs. $x_{CA}$ and $a_{CB}$ vs. $x_{CB}$, from which equilibrium values of $x_{CA}$ and $x_{CB}$ were read at equal values of activity, as follows:

| $x_{CA}$ | 0.280 | 0.480 | 0.600 | 0.705 | 0.795 | 0.849 |
|---|---|---|---|---|---|---|
| $x_{CB}$ | 0.05 | 0.10 | 0.15 | 0.20 | 0.25 | 0.282 |

Figure 3.16 shows these data as a curve, compared with the measured tie-line concentrations of Hunter and Brown. While agreement is not so good as in the previous illustration, it should be noted that the entire prediction was based only on solubilities in two of the three binaries. Furthermore, there is some question concerning the accuracy of the aniline-heptane solubility since it is not in exact agreement with the measurements of Varteressian and Fenske [*Ind. Eng. Chem.* **29**, 270 (1937)]. For use in these types of calculations, very accurate data are desirable.

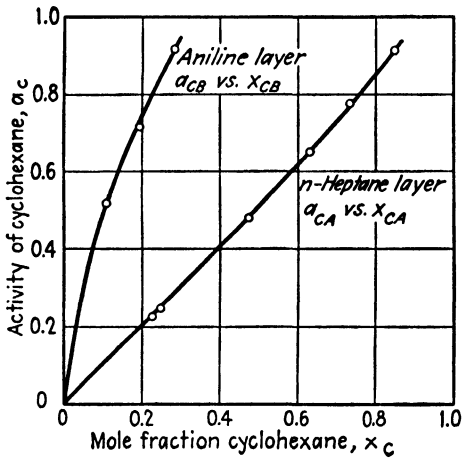



FIG. 3.15. Calculated activities of cyclohexane in the system *n*-heptane (*A*)–aniline (*B*)–cyclohexane (*C*).

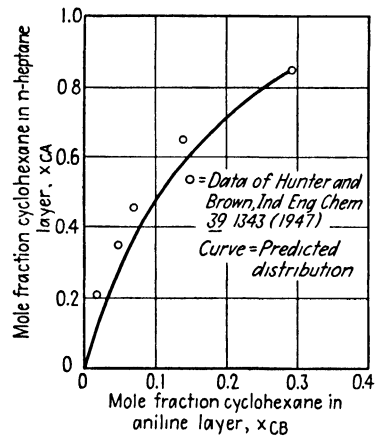



FIG. 3.16. Distribution of cyclohexane between *n*-heptane and aniline, 25°C.

**Selectivity.** It will be shown later (Chap. 4) that for purposes of obtaining a successful extraction process, the "selectivity" of a solvent is a more important index of its usefulness than the simple distribution coefficient of the consolute substance. As will be shown, selectivity of $B$ for $C$ is defined as follows:

$$\beta = \frac{x_{CB}/x_{AB}}{x_{CA}/x_{AA}} \tag{3.101}$$

where the concentrations are those in the equilibrium layers. Since $x = a/\gamma$, and since at equilibrium $a_{CB} = a_{CA}$ and $a_{AB} = a_{AA}$, then

$$\beta = \frac{\gamma_{CA}/\gamma_{AA}}{\gamma_{CB}/\gamma_{AB}} \tag{3.102}$$

Consequently this important quantity can be estimated from the data accumulated in the course of predicting the distribution. For a satisfactory process, $\beta$ must exceed unity.

**Illustration 11.** Predict selectivities in the system water ($A$)–ethyl acetate ($B$)–ethanol ($C$), at 20°C.

*Solution.* Refer to Illustration 9. The various $A$ constants have been calculated, as well as values of $\gamma_C$ in $A$- and $B$-rich solutions. In addition, values of $\gamma_A$ in these solutions are required. For these, use Eq. (3.94) with the data of Illustration 9. After simplification, Eq. (3.94) becomes

$$\log \gamma_A = \frac{3.10x_B^2 + 1.054x_C^2 + 3.48x_Bx_C}{(x_A + 1.735x_B + 1.665x_C)^2}$$

With this equation, values of $\gamma_A$ were calculated for each point on the solubility curve listed in Illustration 9. In order to obtain equilibrium values of $\gamma_A$ and $\gamma_C$ in the $A$- and $B$-rich solutions, plots were made of $\gamma_{CA}$ vs. $x_{CA}$, $\gamma_{CB}$ vs. $x_{CB}$, $\gamma_{AA}$ vs. $x_{CA}$, and $\gamma_{AB}$ vs. $x_{CB}$. From these, values of $\gamma$ were read at concentrations corresponding to the predicted values of $x_{CA}$ and $x_{CB}$ of Illustration 9, as listed below. Values of $\beta$ were calculated from these by Eq. (3.102).

| $x_{CA}$ | $\gamma_{CA}$ | $\gamma_{AA}$ | $x_{CB}$ predicted | $\gamma_{CB}$ | $\gamma_{AB}$ | Predicted $\beta = \frac{\gamma_{CA}\gamma_{AB}}{\gamma_{AA}\gamma_{CB}}$ |
|---|---|---|---|---|---|---|
| 0 | 3.765 | 1.002 | 0 | 1.745 | 7.45 | 16.03 |
| 0.01 | 3.600 | 1.004 | 0.0225 | 1.660 | 6.97 | 15.08 |
| 0.02 | 3.450 | 1.006 | 0.044 | 1.570 | 6.40 | 13.98 |
| 0.03 | 3.280 | 1.009 | 0.066 | 1.480 | 5.77 | 12.67 |
| 0.04 | 3.116 | 1.013 | 0.089 | 1.380 | 5.05 | 11.23 |
| 0.05 | 2.953 | 1.0175 | 0.115 | 1.275 | 4.30 | 9.78 |
| 0.06 | 2.790 | 1.023 | 0.140 | 1.179 | 3.60 | 8.34 |
| 0.07 | 2.630 | 1.030 | 0.168 | 1.100 | 2.60 | 6.03 |
| 0 08 | 2.477 | 1.039 | 0.183 | 1 090 | 1.20 | 2.62 |

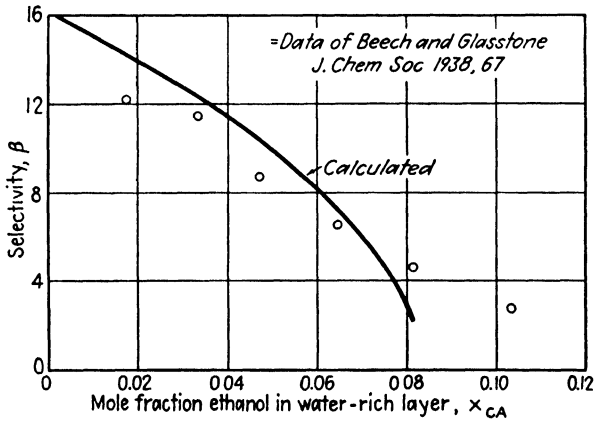



FIG. 3.17. Comparison of predicted and observed selectivities, ethanol–water–ethyl acetate, 20°C.

Values of the predicted $\beta$ are plotted against $x_{CA}$ in Fig. 3.17 as a curve, together with $\beta$ calculated from the tie-line data of Beech and Glasstone (*loc. cit.*) by Eq. (3.101). Agreement is seen to be very satisfactory, and since $\beta$ is greater than unity, ethyl acetate is a selective solvent for extracting ethanol from its water solutions.

**Neglect of Solvent Solubility.** In many instances, because of lack of ternary-solubility data, or merely in order to simplify the computations, the assumption is made that the mutual solubility of the relatively immiscible solvents has no effect on the activity of the distributed substance. Thus, if an estimate of the distribution of ethanol between benzene and water were to be made, one might ignore the mutual solubility of benzene and water and the corresponding effects on the activity of the ethanol. In such cases the activity coefficients of the distributed substance $C$ in the binary solutions $AC$ and $BC$ may be calculated or estimated from limited data by the binary activity-coefficient equations. Activities in the binaries are then calculated and equilibrium values of $x_{CA}$ and $x_{CB}$ determined at equal values of activities of $C$ (15). This method has been investigated fairly thoroughly (34), and it has been shown that in cases where the solvents $A$ and $B$ are very immiscible it can be expected to give moderately good results at low concentrations of the distributed substance $C$. In cases where the solvents show appreciable miscibility, a qualitative indication of the direction of distribution only can be relied upon.

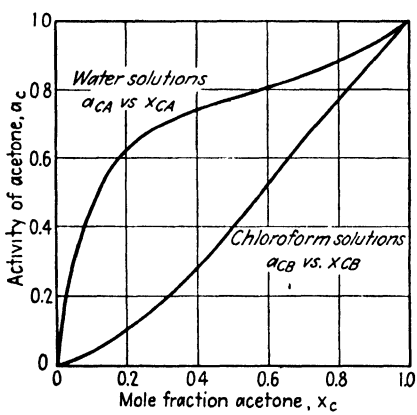



FIG. 3.18. Activities of acetone in the systems acetone ($C$)–water ($A$) and acetone ($C$)–chloroform ($B$).

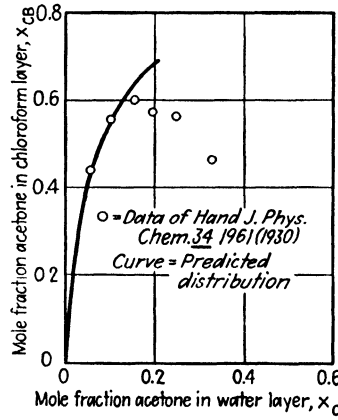



FIG. 3.19. Distribution of acetone between water and chloroform, 25°C.

**Illustration 12.** Predict the distribution of acetone ($C$) between water ($A$) and chloroform ($B$), ignoring the mutual solubility of water and chloroform.

*Solution. Acetone–water.* Activity coefficients and activities for acetone are plotted in Fig. 3.2 at 25°C.

*Acetone–chloroform.* Activity coefficients and activities for acetone are plotted in Fig. 3.6 at 35.17°C.

The activities of acetone in the two binary solutions are plotted, as in Fig. 3.18. Ignoring the mutual solubility of water and chloroform in the ternary mixtures, equilibrium concentrations of acetone in the two layers are estimated by reading concentrations at equal values of acetone activity, as follows:

| $x_{CA}$ | 0 | 0.01 | 0.03 | 0.06 | 0.08 | 0.10 | 0.15 | 0.2 |
|---|---|---|---|---|---|---|---|---|
| $x_{CB}$ | 0 | 0.137 | 0.305 | 0.44 | 0.495 | 0.550 | 0.635 | 0.680 |

The predicted distribution curve and the measured values of Hand (14) for 25°C. are compared in Fig. 3.19. Agreement is seen to be good at low acetone concentrations, but as the mutual solubility of the nonconsolute components is increased by higher acetone concentrations, the method fails to give good results. Nevertheless, the conclusion is reached that the equilibrium distribution strongly favors the chloroform layer, and even this qualitative information can be most useful.

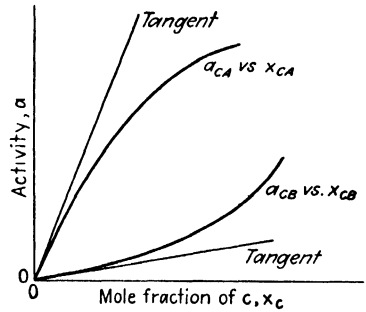



FIG. 3.20. Initial slopes of the activity-concentration curves.

**Distribution Coefficients at Low Concentrations.** If the solvents $A$ and $B$ are substantially insoluble, so that the effect on the distribution of $C$ is small, then the equations of the tangents drawn to the activity curves at the origin of the plot (Fig. 3.20) are

$$a_{CA} = \gamma'_{CA} x_{CA} \tag{3.103}$$

and

$$a_{CB} = \gamma'_{CB} x_{CB} \tag{3.104}$$

where $\gamma'_{CA}$ = activity coefficient of $C$ in the $A$–$C$ binary at $x_{CA} = 0$
$\gamma'_{CB}$ = activity coefficient of $C$ in the $B$–$C$ binary at $x_{CB} = 0$
Therefore, at equal activities for equilibrium solutions, and at zero concentration of $C$,

$$\gamma'_{CA} x'_{CA} = \gamma'_{CB} x'_{CB} \tag{3.105}$$

The initial slope of the distribution curve, or the distribution coefficient at zero concentration of $C$ becomes

$$\frac{x'_{CB}}{x'_{CA}} = \frac{\gamma'_{CA}}{\gamma'_{CB}} = m' \tag{3.106}$$

Since $\log \gamma'_{CA} = A_{CA}$ and $\log \gamma'_{CB} = A_{CB}$, then

$$\frac{x'_{CB}}{x'_{CA}} = m' = 10^{(A_{CA} - A_{CB})} \tag{3.107}$$

or

$$\log \frac{x'_{CB}}{x'_{CA}} = \log m' = A_{CA} - A_{CB} \tag{3.108}$$

Equations (3.106) to (3.108) offer very quick indications of the direction of distribution, which information is often sufficient to eliminate further consideration of a system for liquid-extraction purposes.

The selectivity at low concentrations can also be easily approximated. Combining Eqs. (3.101) and (3.106), we obtain

$$\beta' = m' \frac{x_{AA}}{x_{AB}} \tag{3.109}$$

where $\beta'$ = selectivity of $B$ for $C$ at zero $C$ concentration. It can therefore be estimated from the distribution coefficient at zero $C$ concentration and the mutual solubility of the liquids $A$ and $B$.

**Illustration 13.** Predict the initial distribution coefficient and selectivity for the system water ($A$)–ethyl acetate ($B$)–isopropanol ($C$).

*Solution. Isopropanol (C)–ethyl acetate (B).* An azeotrope for this system is reported ("International Critical Tables") at 74.8°C., 760 mm. Hg, with $x_C = 0.305$.

At 74.8°C., the vapor pressure of isopropanol = $p_C$ = 560.4 mm. Hg, and that of ethyl acetate = $p_B$ = 698.0 mm. Hg.

Eq. (3.17): $$\gamma_C = \frac{760}{560.4} = 1.356, \qquad \gamma_B = \frac{760}{698.0} = 1.089$$

The van Laar constant [Eq. (3.60)] is therefore $A_{CB} = 0.3548$.

$$\therefore \gamma'_{CB} \text{ at } (x_C = 0) = \text{antilog } 0.3548 = 2.26$$

*Isopropanol (C)–water (A).* Vapor-liquid data at 760 mm. Hg are reported by Brunjes and Bogart [*Ind. Eng. Chem.* **35,** 255 (1943)]. Their activity coefficients, when extrapolated to $x_C = 0$, give $\gamma'_{CA} = 11.7$. Therefore, Eq. (3.106):

$$m' = \text{initial distribution coefficient} = \frac{x'_{CB}}{x'_{CA}} = \frac{\gamma'_{CA}}{\gamma'_{CB}} = \frac{11.7}{2.26} = 5.17$$

The mutual solubility of water in ethyl acetate at 20°C. is $x_{AA} = 0.9826$ (water layer), $x_{AB} = 0.1321$ (ester layer) ("International Critical Tables").

Therefore, Eq. (3.109):

$$\beta' = \text{initial selectivity of ethyl acetate for isopropanol}$$
$$= m' \frac{x_{AA}}{x_{AB}} = 5.17 \frac{0.9826}{0.1321} = 38.4$$

These may be compared with observed data of Beech and Glasstone (*J. Chem. Soc.* **1938,** 67), at 20°C. The tangent to their distribution curve in mole fraction units at $x_C = 0$ has a slope $m' = 4.9$. Selectivities calculated from their data, when extrapolated to $x_C = 0$, give $\beta' = 37$.

Equation (3.106) has been shown (34) to be the basis of the tie-line correlation of Hand, Eq. (2.11). Since in the binary $B$–$C$, $x_{CB} = x_{CB}/x_{BB}$ as $x_{CB}$ approaches zero, Eq. (3.106) can be written

$$\frac{x'_{CB}}{x_{BB}} = \frac{\gamma'_{CA}}{\gamma'_{CB}} \frac{x'_{CA}}{x_{AA}} \tag{3.110}$$

An exponent is then introduced to account for mutual solubility of the solvents at concentrations of $C$ other than zero:

$$\frac{x_{CB}}{x_{BB}} = r \left(\frac{x_{CA}}{x_{AA}}\right)^n \tag{3.111}$$

where $r$ and $n$ are constants. This is Eq. (2.11) expressed in terms of mole fractions. The values of $n$ for the two equations are the same, while the coefficients are related in the following manner:

$$k = r \frac{MW_C}{MW_B} \left(\frac{MW_A}{MW_C}\right)^n \tag{3.112}$$

For some systems, $n = 1$, in which case $r = m'$ and can be calculated by Eq. (3.106).

**Concentration Units.** Predictions of distribution thus far described are based on mole fraction concentration units. It should be noted that distribution coefficients in terms of weight fractions are different from those in terms of mole fractions, although ordinarily the direction of distribution is the same for both unit systems. In a few cases, where there is an unusual combination of molecular weights, this will not be the case. For example, in the system ethanol–ethyl acetate–water, higher concentrations of ethanol are in the water-rich layer on a weight basis but in the ester layer on a mole basis. Where the ternary-solubility curve is available, corrections from one system to another can easily be made. If the distribution is estimated from data on the binaries alone, then at zero concentration of $C$,

$$\frac{X'_{CB}}{X'_{CA}} = \frac{x'_{CB}}{x'_{CA}}\left[\frac{(X'_{AB}/MW_A) + (X'_{BB}/MW_B)}{(X'_{AA}/MW_A) + (X'_{BA}/MW_B)}\right] \tag{3.113}$$

where $X'_{AA}$, $X'_{BB}$, $X'_{AB}$, and $X'_{BA}$ are the mutual solubilities of $A$ and $B$. If $A$ and $B$ can be considered practically insoluble, so that $X'_{BB} = X'_{AA} = 1$, and $X'_{AB} = X'_{BA} = 0$, then approximately

$$\frac{X'_{CB}}{X'_{CA}} = \frac{x'_{CB}}{x'_{CA}}\frac{MW_A}{MW_B} \tag{3.114}$$

Selectivity, it should be noted, is independent of whether weight or mole fractions are used in its definition.

**Illustration 14.** Predict the initial distribution coefficient in the water ($A$)–ethyl acetate ($B$)–isopropanol ($C$) system at 20°C. in terms of weight fraction concentration units.

*Solution.* Refer to Illustration 13. $x'_{CB}/x'_{CA}$ was estimated from vapor-liquid data to be 5.17. The mutual solubility of ethyl acetate and water at 20°C. in terms of weight fractions are

$X'_{BA}$ = 0.0794 wt. fraction ester, $X'_{AA}$ = 0.9206 wt. fraction water
$X'_{BB}$ = 0.9699 wt. fraction ester, $X'_{AB}$ = 0.0301 wt. fraction water

$MW_B$ = mol. wt. of ethyl acetate = 88.06
$MW_A$ = mol. wt. of water = 18.02

Therefore, Eq. (3.113):

$$\frac{X'_{CB}}{X'_{CA}} = 5.17\left[\frac{(0.0301/18.02) + (0.9699/88.06)}{(0.9206/18.02) + (0.0794/88.06)}\right] = 1.26$$

The data of Beech and Glasstone (*loc. cit.*) show $X'_{CB}/X'_{CA} = 1.20$.

## QUATERNARY SYSTEMS

In the process known as fractional extraction, two substances are simultaneously distributed between two relatively insoluble solvents, thus forming a quaternary system. In such a situation, let $B$ and $C$ be

the distributed substances, $A$ and $D$ the insoluble solvents. The distribution coefficients are then

$$m_B = \frac{x_{BA}}{x_{BD}}, \qquad m_C = \frac{x_{CA}}{x_{CD}} \tag{3.115}$$

Selectivity in such a system is then defined as

$$\beta = \frac{m_B}{m_C} = \frac{x_{BA}x_{CD}}{x_{CA}x_{BD}} \tag{3.116}$$

and, since at equilibrium the activities of each distributed substance is the same in all phases,

$$\beta = \frac{\gamma_{CA}\gamma_{BD}}{\gamma_{CD}\gamma_{BA}} \tag{3.117}$$

It is not yet possible to calculate quaternary activity coefficients in as reliable a fashion as for binary and ternary systems, and at best $\beta$ may be estimated from ternary or binary data on the assumption that the various distributions which occur will not influence the activity coefficients. Thus $\gamma_{CA}/\gamma_{CD}$ might be calculated from the binary data of the systems $C$–$A$ and $C$–$D$, or the ternary $A$–$C$–$D$. It is best to limit such estimates of $\beta$ to systems where solvent miscibility and concentration of distributed substances are low.

### OTHER AIDS IN PREDICTION OF DISTRIBUTION

In the absence of data with which to calculate activities, the direction of distribution can nevertheless frequently be estimated by other means. These will ordinarily provide only qualitative indication, however, and are in some cases less reliable than the methods previously described.

**Critical Solution Temperature.** Figure 3.21 shows a typical ternary system including the temperature coordinate, with each of the binaries exhibiting an upper C.S.T. Suppose for the moment that each binary-solubility curve is completely symmetrical. We have seen that under these circumstances [Eqs. (3.86) and (3.87)] the $A$ constants of the van Laar equations for each binary will all be equal at the respective C.S.T.'s. Assuming that, as is ordinarily the case, the heat of solution for each binary is less at higher temperatures, each binary will become more ideal as the temperature is increased. It follows that at any temperature, the activity coefficients will be lowest in the $B$–$C$ binary, intermediate in the $C$–$A$ binary, and highest in the $A$–$B$ binary. Consider now the Type 1 system at temperature $t_1$. From our conclusions respecting the activity coefficients, it is apparent that $C$ will favor the $B$-rich phase, and consequently of the two nonconsolute solvents $A$ and $B$, the more selective solvent ($B$) will be that which has the lower C.S.T. with the distributed substance $C$.

In the case of the Type 2 system at temperature $t_2$, where $A$ might be used to separate $B$ and $C$, consideration of the activity coefficients shows that the system $A$–$C$ has lower escaping tendencies than the system $A$–$B$. Consequently $A$ will preferentially extract $C$. The solvent will be more selective toward the substance with which it has the lower C.S.T. Similar reasoning can be applied to systems which have lower C.S.T.'s.

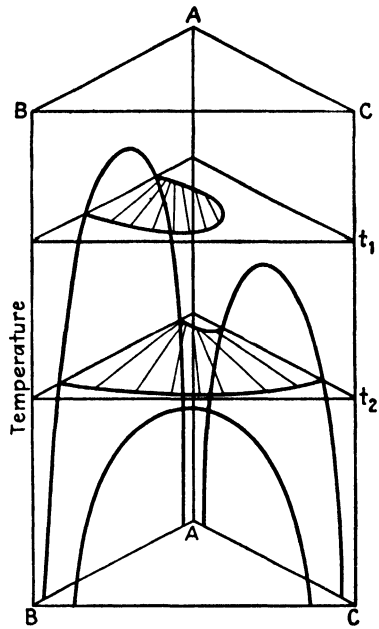



FIG. 3.21. Critical solution temperature and selectivity.

While these principles are generally sound, other factors will influence the distribution in actual situations. For example, the variation of heat of solution with temperature differs with different solutions, and solubility curves are rarely symmetrical. Consequently, critical solution temperatures can give only a rough indication of distribution which cannot always be relied upon. Elgin (11) has stated that it can be used safely only for "regular" solutions, those whose entropy of mixing approximates that for ideal solutions.

In the extraction of undesirable constituents from petroleum fractions, Francis (13) has shown the usefulness of this attack, and has critically reviewed earlier compilations of C.S.T. data. The selective solvent ability of aniline is frequently used as an indication of the effectiveness of such extraction processes, and the so-called "aniline point" is a measure of this. Aniline point is defined as the temperature at which a mixture of equal volumes of aniline and hydrocarbon separates into two saturated liquid layers. While this is not necessarily the C.S.T. since the solubility curves are not exactly symmetrical, Francis has shown that it will approximate it very closely. A large number of aniline points for different hydrocarbons have been recorded, as well as the C.S.T.'s of hydrocarbons with other solvents (13, 36). Francis has used essentially the difference in C.S.T. for a solvent with two types of hydrocarbons as an indication of the selectivity of the solvent in separating the hydrocarbons and has shown the effect on this of chemical structure of the solvent. Similarly, Drew and Hixson (10) and Hixson and Bockelmann (16) have shown the relationship between C.S.T. of propane with various fatty acids and their esters and the selective ability of propane as a solvent in separating them.

TABLE 3.1. RELATIONSHIP BETWEEN SELECTIVITY AND CRITICAL-SOLUTION TEMPERATURE

| | Component | | | C.S.T., °C. | | | Selectivity, $\beta$ | |
|---|---|---|---|---|---|---|---|---|
| | *A* | *B* | *C* | *A*–*B* | *A*–*C* | *B*–*C* | *A* for *C* | *B* for *C* |
| Type 1 | Aniline | *n*-Hexane | Methyl-cyclopentane | 68.8 upper | 34.5 upper | None | 1.37 at 45°C.[1] | 7.54 at 45°C.[1] |
| | Propane | Refined cottonseed oil | Oleic acid* | 66.2 lower | 91.1 lower | None | 2.05 at 85°C.[2] | 23 to 15 at low acid concn. 85°C.[2] |
| | | | | | | | | *A* for *B* |
| Type 2 | Aniline | *n*-Heptane | Methyl-cyclohexane | 70 upper | 41 upper | None | 1.90 at 25°C.[3] | 0.537 at 25°C.[3] |
| | Aniline | *n*-Heptane | Cyclohexane | 70 upper | 31 upper | None | 1.46 at 25°C.[4] | 0.757 at 25°C.[4] |
| | Aniline | *n*-Hexane | Methyl-cyclopentane | 68.8 upper | 34.5 upper | None | 1.20 at 25°C.<br>1.14 at 34.5°C.[1] | 0.849 at 25°C.<br>0.862 at 34.5°C.[1] |
| | Propane | Stearic acid | Palmitic acid | 91.4 lower | 96.9 lower | None | 1.0 at 98°C.[5] | 1.0 at 98°C.[5] |
| | Propane | Refined cottonseed oil | Oleic acid* | 66.2 lower | 91.1 lower | None | 3.08 at 98.5°C.[2] | 0.322 at 98.5°C.[2] |

[1] Darwent and Winkler, *J. Phys. Chem.* **47,** 442 (1943).
[2] Hixson and Bockelman, *Trans. Am. Inst. Chem. Engrs.* **38,** 891 (1942).
[3] Varteressian and Fenske, *Ind. Eng. Chem.* **29,** 270 (1937).
[4] Hunter and Brown, *Ind. Eng. Chem.* **39,** 1343 (1947).
[5] Drew and Hixson, *Trans. Am. Inst. Chem. Engrs.* **40,** 675 (1944).

*See Fig. 2.14.

Table 3.1 lists several examples of the application of these principles. In each case the components are designated in accordance with Fig. 3.21, and, except for one system, the selectivities expected on the basis of critical solution temperatures actually materialize. In the case of propane–stearic acid–palmitic acid, the inability of propane to extract either of the acids selectively is reflected in the very small difference in C.S.T.'s. Note further that, on the basis of the C.S.T.'s alone, it would be expected that the selectivity of aniline for cyclohexane in the presence of heptane would be greater than that for methylcyclohexane, but that the reverse is true.

**Hydrogen Bonding and Internal Pressure.** It is clear from what has been considered that the extent to which mixtures deviate from ideality governs the distribution of a solute between two solvents. It is now possible to predict the nature of the deviation from ideality of mixtures of substances on the basis of their hydrogen-bonding potentialities and internal pressures.

The molecules of many substances are polar, that is, they exhibit a dipole moment caused by unequal sharing of the electrons of the covalent bonds of the atoms. For example, in the case of an alcohol molecule, the electron pair which makes up the bond between oxygen and hydrogen lies closer to the oxygen:

$$R - \bar{O}: \overset{\bullet}{\underset{\bullet}{\overset{+}{H}}}$$

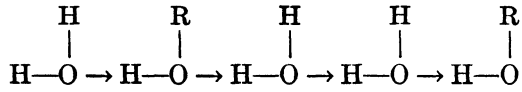
Consequently the hydrogen portion of the molecule is relatively positively charged and the remainder negatively. The dipole moment is a measure of this phenomenon. Occasionally, molecules contain several dipole moment-forming groups which, because of symmetrical arrangement, cancel each other, and a low dipole moment results. Polar molecules tend to associate, with coordination of hydrogen between the negative parts of adjacent molecules:

$$\begin{array}{cccccccc} & R & & R & & R & & R \\ & | & & | & & | & & | \\ H-O & \rightarrow & H-O & \rightarrow & H-O & \rightarrow & H-O & \end{array}$$

Similarly, hydrogen can coordinate between nitrogen or fluorine, as well as oxygen, and these are termed "donor" atoms. Hydrogen can also coordinate between any of the donor atoms and carbon, provided that there is a sufficiently effective negative grouping attached to the carbon. Some of these bondings are strong and others comparatively weak.

Solution of a substance into one which associates through hydrogen bonding may involve either breaking the hydrogen bonds or forming new ones. Thus, if an alcohol dissolves in water, the hydrogen bonds between water molecules and between alcohol molecules may be broken and new

bonds formed between alcohol and water molecules; we may obtain a configuration of the following sort:



If the size of the hydrocarbon chain of the alcohol is great, the water-to-water hydrogen bonding is so strong that the barely negative portion of the alcohol is relatively unimportant. The alcohol then does not dissolve appreciably. An excellent description of the role of the hydrogen bond in such cases is provided by McElvain (26).

Ewell, Harrison, and Berg (12) have classified liquids into five groupings, based on their possibilities of forming hydrogen bonds. Their listing is reproduced in Table 3.2. They have also pointed out that when liquids are mixed, positive deviations from Raoult's law result if hydrogen bonds are broken, negative if they are formed. The extent to which the hydrogen bonds are involved will, in general, indicate the extent of the Raoult's law deviations. Table 3.3 reproduces their summary of these effects.

TABLE 3.2. CLASSIFICATION OF LIQUIDS ACCORDING TO HYDROGEN BONDING*

Class I

Liquids capable of forming three-dimensional networks of strong hydrogen bonds, *e.g.*, water, glycol, glycerol, amino alcohols, hydroxylamine, hydroxy acids, polyphenols, amides, etc. Compounds such as nitromethane and acetonitrile also form three-dimensional networks of hydrogen bonds, but the bonds are much weaker than those involving OH and NH groups. Therefore these types of compounds are placed in Class II.

Class II

Other liquids composed of molecules containing both active hydrogen atoms and donor atoms (oxygen, nitrogen, and fluorine), *e.g.*, alcohols, acids, phenols, primary and secondary amines, oximes, nitro compounds with $\alpha$-hydrogen atoms, nitriles with $\alpha$-hydrogen atoms, ammonia, hydrazine, hydrogen fluoride, hydrogen cyanide, etc.

Class III

Liquids composed of molecules containing donor atoms but no active hydrogen atoms, *e.g.*, ethers, ketones, aldehydes, esters, tertiary amines (including pyridine type), nitro compounds and nitriles without $\alpha$-hydrogen atoms, etc.

Class IV

Liquids composed of molecules containing active hydrogen atoms but no donor atoms. These are molecules having two or three chlorine atoms on the same carbon as a hydrogen atom, or one chlorine on the same carbon atom and one or more chlorine atoms on adjacent carbon atoms, *e.g.*, $CHCl_3$, $CH_2Cl_2$, $CH_3CHCl_2$, $CH_2Cl—CH_2Cl$, $CH_2Cl—CHCl—CH_2Cl$, $CH_2Cl—CHCl_2$, etc.

Class V

All other liquids, *i.e.*, liquids having no hydrogen-bond-forming capabilities, *e.g.*, hydrocarbons, carbon disulfide, sulfides, mercaptans, halohydrocarbons not in Class IV, nonmetallic elements such as iodine, phosphorus, and sulfur.

*Ewell, Harrison, and Berg, *Ind. Eng. Chem.* **36**, 871 (1944). With permission of the American Chemical Society.

TABLE 3.3. DEVIATIONS FROM IDEALITY BASED ON HYDROGEN BONDING*

| Classes | Hydrogen bonding | Deviations |
|---|---|---|
| I + V<br>II + V | Hydrogen bonds broken only | Always + deviations; I + V, frequently limited solubility |
| III + IV | Hydrogen bonds formed only | Always − deviations |
| I + IV<br>II + IV | Hydrogen bonds both broken and formed, but dissociation of Class I or II liquid is the more important effect | Always + deviations; I + IV, frequently limited solubility |
| I + I<br>I + II<br>I + III<br>II + II<br>II + III | Hydrogen bonds both broken and formed | Usually + deviations, very complicated groups, some − deviations give some maximum azeotropes |
| III + III<br>III + V<br>IV + IV<br>IV + V<br>V + V | No hydrogen bonds involved | Quasi-ideal systems, always + deviations or ideal; azeotropes, if any, will be minima |

*Ewell, Harrison, and Berg, *Ind. Eng. Chem.* **36**, 871 (1944). With permission of the American Chemical Society.

It will be noted that for all mixtures of Class III, IV, and V liquids, with the exception of Class III with Class IV, no hydrogen bonds are involved. Hildebrand (15) and Scatchard (30) show that in such cases deviations from Raoult's law are a function of the square of the difference in square roots of the internal pressures of the constituents, the importance of this effect being minimized when hydrogen bonding is extensive. Large deviations for such solutions, in other words, result from large differences in internal pressures. The internal pressure, in turn, can be estimated from the heat of vaporization and molar volumes:

$$p_i = \frac{41.3\,\Delta E_v}{V} = \frac{41.3(\Delta H_v - RT)}{V} \tag{3.118}$$

where $p_i$ = internal pressure, atm.
$\Delta E_v$ = internal energy of vaporization, cal./gm. mole
$\Delta H_v$ = enthalpy of vaporization, cal./gm. mole
$R$ = the gas const., 1.987 cal./(gm. mole)(°K)
$T$ = abs. temp., °K
$V$ = molar vol. of the liquid, cu. cm./gm. mole

Table 3.4 is a short list of internal pressures for substances included in Class III, IV, and V liquids, arranged in order of magnitude of internal pres-

TABLE 3.4. INTERNAL PRESSURES AT 25°C.

| Substance | Class | Internal pressure, atm. |
|---|---|---|
| *n*-Pentane | V | 2,020 |
| *n*-Heptane | V | 2,230 |
| Ethyl ether | III | 2,285 |
| *n*-Octane | V | 2,330 |
| Cyclohexane | V | 2,860 |
| Carbon tetrachloride | V | 3,030 |
| Cyclohexane | V | 3,110 |
| Toluene | V | 3,270 |
| Ethyl acetate | III | 3,370 |
| Benzene | V | 3,440 |
| Chloroform | IV | 3,510 |
| Chlorobenzene | V | 3,840 |
| 1,4-Dioxane | III | 3,860 |
| Acetone | III | 3,920 |
| Tetrachloroethane | V | 3,930 |
| Carbon disulfide | V | 4,120 |

sure. The enthalpy of vaporization used in calculating these were taken from various tabulations (21, 28) or estimated if necessary by usual methods (19). The farther apart two substances are on the list, the greater should be the deviations from ideality of their solutions.

**Illustration 15.** Recommend a solvent potentially useful for extracting acetone from its aqueous solutions.

*Solution.* Acetone is a Class III liquid and water a Class I liquid (Table 3.2). Aqueous acetone solutions can be expected to give positive deviations from Raoult's law (Table 3.3). For a most favorable distribution coefficient, therefore, solutions of acetone in the extracting solvent should show negative deviations. Table 3.3 indicates that liquids of Class IV, such as certain of the chlorinated hydrocarbons, should provide favorable distribution coefficients. Halohydrocarbons of Class V would also be satisfactory, since their acetone solutions would show at most weakly positive deviations. Typical distribution coefficients are indicated in the following tabulation:

| Solvent | Class | Distribution coefficient, $\left(\frac{\text{acetone in solvent layer}}{\text{acetone in water layer}}\right)$ at low concentrations | |
|---|---|---|---|
| | | Weight per cent | Mole per cent |
| Chloroform | IV | 1.83 at 25°C. | 7.85 at 25°C. |
| 1,1,2-Trichloroethane | IV | 1.47 at 25°C. | 14.58 at 25°C. |
| Monochlorobenzene | V | 1.0 at 25–26°C. | 5.91 at 25°C. |
| Tetrachloroethane | V | 2.37 at 25–26°C. | 18.2 at 25°C. |

**Consideration other than distribution coefficient alone must be kept in mind before a solvent is chosen, however, as indicated in Chap. 4.**

**Illustration 16.** Predict the direction of distribution of acetic acid between benzene and water.

*Solution.* Acetic acid (Class II)–benzene (Class V) solutions should show strong positive Raoult's law deviations, or large escaping tendency for the acid. Acetic acid (Class II)–water (Class I) solutions should show less strong positive deviations, or a lesser escaping tendency for the acid. On distribution, the acetic acid should favor the water-rich phase. This is confirmed by the data of Hand (14), at 25°C., which show a distribution coefficient of 30.4 in weight per cent units at low acid concentrations, favoring the water phase.

**Illustration 17.** Predict the direction of the distribution of 1,6-diphenylhexane (Class V) between furfural (Class III) and docosane (Class V), at 45°C.

*Solution.* Since in both furfural–diphenylhexane and docosane–diphenylhexane solutions, hydrogen bonds are not involved, recourse can be had to internal-pressure data to indicate the distribution.

*Furfural:* Mol. wt. = 96.03
Density at 45°C. = 1.133
$\therefore V = \frac{96.03}{1.133} = 84.8$ cu. cm./gm. mole
$\Delta H_v = 12{,}140$ cal./gm. mole at 45°C. (estd.)
$\therefore p_i$ [Eq. (3.118)] $= 41.3\left[\frac{12{,}140 - 1.987(45 + 273)}{84.8}\right]$
$= 1{,}218$ atm.

*Docosane:* Mol. wt. = 310.36
Density at 44°C. = 0.7782
$\therefore V = 391$ cu. cm./gm. mole
$\Delta H_v = 15{,}440$ cal./gm. mole at 45°C. (estd.)
$\therefore p_i$ [Eq. (3.118)] = 1,565 atm.

*1,6-Diphenylhexane:* Mol. wt. = 238
Density at 45°C. = 0.95 (estd.)
$\therefore V = 251$ cu. cm./gm. mole
$\Delta H_v = 16{,}250$ cal./gm. mole at 45°C. (estd.)
$\therefore p_i$ [Eq. (3.118)] = 2,575 atm.

$\Delta p_i$ for diphenylhexane–furfural $= 2{,}575 - 1{,}218 = 1{,}357$ atm.
$\Delta p_i$ for diphenylhexane–docosane $= 2{,}575 - 1{,}565 = 1{,}010$ atm.

$\therefore$ The furfural solutions should show the larger + deviations, and diphenylhexane should favor the docosane-rich phase on distribution.

This is confirmed by Briggs and Comings [*Ind. Eng. Chem.* **35**, 411 (1943)] whose data at 45°C. show distribution coefficients of 1.021 and 2.72 in weight and mole per cents, resp., at low concentrations of diphenylhexane.

### Notation for Chapter 3

$A$ = constant in Margules, van Laar, and Scatchard equations
= limit of $\log \gamma$ as $x \to 0$.
= component of a solution.
$a$ = activity.
$B$ = component of a solution.
= second virial coefficient of the equation of state $v = (RT/p_i) + B$, cu. cm./gm. mole.

$C$ = component of a solution.
= constant [Eq. (3.97)].
$D$ = component of a solution.
$d$ = differential operator.
$\Delta E_v$ = internal energy of vaporization, cal./gm. mole.
$e$ = base of natural logarithms = 2.7183.
$F$ = free energy, cal./gm. mole.
$\bar{F}$ = partial free energy of a substance in solution, cal./gm. mole.
$\mathbf{F}$ = total free energy of a solution, cal.
$F_E$ = excess free energy of a nonideal solution, cal./gm. mole.
$\mathbf{F}_E$ = total excess free energy of a nonideal solution, cal.
$f$ = fugacity of a pure substance, atm.
$\bar{f}$ = partial fugacity of a substance in solution, atm.
$H°$ = enthalpy of a pure substance, cal./gm. mole.
$\bar{H}$ = partial enthalpy of a substance in solution, cal./gm. mole.
$\Delta H_S$ = partial heat of solution, cal./gm. mole.
$\Delta H_v$ = enthalpy of vaporization, cal./gm. mole.
$k$ = constant.
ln = natural logarithm.
log = common logarithm.
$M$ = constant.
$m$ = distribution coefficient = ratio of concentrations of solute in equilibrium liquid phases.
$MW$ = molecular weight.
$N$ = constant.
$n$ = number of moles of a component.
= constant [Eq. (3.111), (3.112)].
$p$ = pressure; vapor pressure of a pure substance, atm.
$\bar{p}$ = partial pressure of a component of a solution, atm.
$p_i$ = internal pressure, atm.
$q$ = arbitrary factor for Eq. (3.97).
$R$ = universal gas constant, cal./gm. mole °K.
$r$ = constant.
$S$ = constant.
$T$ = absolute temperature, °K.
$V$ = specific volume of a liquid, cu. cm./gm. mole.
$v$ = specific volume of a gas, cu. cm./gm. mole.
$x$ = mole fraction in a liquid.
$X$ = weight fraction in a liquid.
$y$ = mole fraction in a gas or vapor.
$Z$ = compressibility factor in the equation of state $pv = ZRT$.
$z$ = volume fraction, based on volumes of pure components.
$\beta$ = selectivity.
$\gamma$ = activity coefficient.
$\partial$ = partial differential operator.

Subscripts:

$A$ = component $A$.
$B$ = component $B$.
$C$ = component $C$.
$D$ = component $D$.
$AB$ = component $A$ in a $B$-rich solution, etc.

Superscripts:

° = standard state.

′ = zero concentration.

## LITERATURE CITED


1. Beech, D. G., and S. Glasstone: *J. Chem. Soc.* **1938,** 67.
2. Benedict, M., C. A. Johnson, E. Solomon, and L. C. Rubin: *Trans. Am. Inst. Chem. Engrs.* **41,** 371 (1945).
3. Berg, C., and A. C. McKinnis: *Ind. Eng. Chem.* **40,** 1309 (1948).
4. Briggs, S. W., and E. W. Comings: *Ind. Eng. Chem.* **35,** 411 (1943).
5. Carlson, H. C., and A. P. Colburn: *Ind. Eng. Chem.* **34,** 581 (1942).
6. Colburn, A. P.: "Azeotropic and Extractive Distillation," paper presented at the Am. Soc. Eng. Educ. Summer School, Madison, Wis., 1948.
7. ——— and E. M. Schoenborn: *Trans. Am. Inst. Chem. Engrs.* **41,** 421 (1945).
8. ———, ———, and D. Shilling: *Ind. Eng. Chem.* **35,** 1250 (1943).
9. Dodge, B. F.: "Chemical Engineering Thermodynamics," McGraw-Hill Book Company, Inc., New York, 1944.
10. Drew, D. A., and A. N. Hixson: *Trans. Am. Inst. Chem. Engrs.* **40,** 675 (1944).
11. Elgin, J. C.: *Ind. Eng. Chem.* **39,** 23 (1947).
12. Ewell, R. H., J. M. Harrison, and L. Berg: *Ind. Eng. Chem.* **36,** 871 (1944).
13. Francis, A. W.: *Ind. Eng. Chem.* **36,** 764, 1096 (1944).
14. Hand, D. B.: *J. Phys. Chem.* **34,** 1961 (1930).
15. Hildebrand, J. H.: "Solubility of Non-electrolytes," 2d ed., Reinhold Publishing Corporation, New York, 1936.
16. Hixson, A. W., and J. B. Bockelmann: *Trans. Am. Inst. Chem. Engrs.* **38,** 891 (1942).
17. Horsley, L. H.: *Ind. Eng. Chem., Anal. Ed.* **19,** 508 (1947); **21,** 831 (1949).
18. Hougen, O. A., and K. M. Watson: "Chemical Process Principles," Part 2, John Wiley & Sons, Inc., New York, 1947.
19. ——— and ———: *Ibid.*, Part 1.
20. Hunter, T. G., and T. Brown: *Ind. Eng. Chem.* **39,** 1343 (1947).
21. "International Critical Tables," McGraw-Hill Book Company, Inc., New York, 1926.
22. Jones, C. A., A. P. Colburn, and E. M. Schoenborn: *Ind. Eng. Chem.* **35,** 666 (1943).
23. Laar, J. J. van: *Z. physik. Chem.* **72,** 723 (1910); **185,** 35 (1929).
24. Lewis, G. N.: *Proc. Am. Acad. Arts Sci.* **37,** 49 (1901).
25. ——— and M. Randall: "Thermodynamics and the Free Energy of Chemical Substances," McGraw-Hill Book Company, Inc., New York, 1923.
26. McElvain, S. M.: "The Characterization of Organic Compounds," Chap. III, The Macmillan Company, New York, 1946.
27. Mertes, T. S., and A. P. Colburn: *Ind. Eng. Chem.* **39,** 787 (1947).
28. Perry, J. H., Ed.: "Chemical Engineers' Handbook," 3d ed. (1950), McGraw-Hill Book Company, Inc., New York, 1941.
29. Redlich, O., and A. T. Kister: *Ind. Eng. Chem.* **40,** 341 (1948).
30. Scatchard, G.: *Chem. Rev.* **8,** 321 (1931).
31. ——— and W. J. Hamer: *J. Am. Chem. Soc.* **57,** 1805 (1935).
32. ——— and S. S. Prentiss: *J. Am. Chem. Soc.* **56,** 1486 (1934).
33. Scheibel, E. G., and D. Friedland: *Ind. Eng. Chem.* **39,** 1329 (1947).
34. Treybal, R. E.: *Ind. Eng. Chem.* **36,** 875 (1944).
35. Wohl, K.: *Trans. Am. Inst. Chem. Engrs.* **42,** 215 (1946).
36. Woodburn, H. M., K. Smith, and H. Tetervsky: *Ind. Eng. Chem.* **36,** 588 (1944).

# CHAPTER 4

## CHOICE OF SOLVENT

In choosing a solvent for a liquid-extraction process, there are several principles which can be used as a guide. These are frequently conflicting, and certainly no single substance would ordinarily possess every desirable characteristic. Compromises must be made, and in what follows an attempt will be made to indicate the relative importance of the various factors to be considered.

**Selectivity.** This is the first property ordinarily studied in deciding the applicability of a solvent, and it refers to the ability of a solvent to extract one component of a solution in preference to another. The most desirable solvent from this point of view would dissolve a maximum of one component and a minimum of the other.

Consider the ternary system of Fig. 4.1, where point $M$ represents a solution of $A$ and $C$ which it is planned to separate by use of solvent $B$. Let us follow the course of a simple extraction process on this diagram. Upon addition of $B$ to the solution $M$, point $S$ would represent the composition of the resulting two-phase mixture as a whole. After vigorous agitation to ensure the attainment of equilibrium and settling of the liquid layers, the two insoluble equilibrium layers at $R$ and $T$ would result. The line $RT$ is, of course, a tie line joining the conjugate concentrations. It is customary in extraction operations to remove the solvent $B$ from the two solutions and recover the extracted substances in solvent-free form. If $B$ is removed completely from $R$, the binary solution at $D$ results, while $E$ represents the solvent-free solution corresponding to $T$. By this procedure, the original solution at $M$ has been separated into two solutions at $D$ and $E$, the first of these richer in $A$ and the second richer in $C$. It is obviously desirable that $E$ and $D$ be a maximum distance apart if the operation is to be most effective.

If, for the same system, $A$ is used as a solvent to separate a solution of $C$ and $B$, as shown in Fig. 4.2, it is clear that while a separation is indeed possible since the ultimate solutions $E$ and $D$ still have different compositions, the separation has not been nearly so effective as that first described. Obviously the direction of tie-line slope has been responsible for the difference. Indeed, it is entirely conceivable that in Fig. 4.2 the tie line utilized by the operation would coincide precisely with the line $AM$ representing the original addition of solvent, in which case the solutions when stripped

of solvent $A$ would both have compositions identical with the original mixture. We may say, in the example shown, that $B$ is more selective in separating solutions of $A$ and $C$ than $A$ for solutions of $B$ and $C$. Similarly, several solvents for separating the same binary pair may be compared. As a rough guide, an extended tie line will intersect that side of the triangle representing binary mixtures of distributed substance and the more selective of the two nonconsolutes.

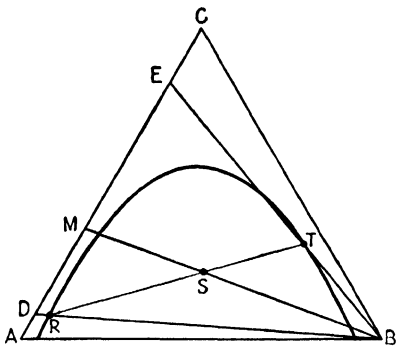



FIG. 4.1. Selective extraction of $C$ from $A$ by means of solvent $B$.

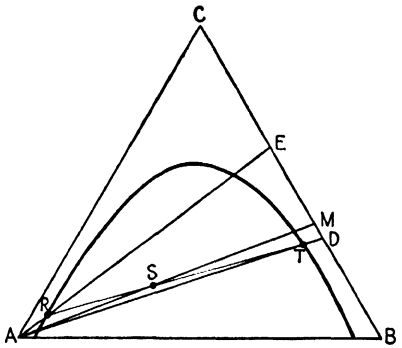



FIG. 4.2. Selective extraction of $C$ from $B$ by means of solvent $A$.

Quantitatively, the property of selectivity may be demonstrated more satisfactorily by plotting the concentrations of the distributed substance $C$ in corresponding solutions at $D$ and $E$ against each other, or, in other words, by plotting a distribution curve for $C$ on a solvent-free basis. Two selectivity diagrams of this sort may be prepared for each ternary, depending upon which nonconsolute is considered the solvent. The curves so obtained are somewhat similar to simple distribution curves in that they start at the origin of the diagram, ordinarily but not necessarily pass through a maximum, and finish on the 45° diagonal at the plait point. The more highly selective the solvent, the greater will be the space between the 45° diagonal and the curve. If the curve coincides with the 45° diagonal, no separation is possible. In many respects, these curves are analogous to the constant-pressure McCabe-Thiele diagrams used for vapor-liquid equilibria in distillation studies (8).

Figure 4.3 shows typical selectivity curves for two systems of the type shown in Fig. 4.1: benzene–water–ethanol at 25°C. (9) and ethyl acetate–water–ethanol at 20°C. (1), ethanol being the distributed substance in each case. In these systems, a simple distribution curve indicates that the distribution of the ethanol favors the water layers in both cases. Figure 4.3 shows that at low concentrations water is much more selective for separating ethanol from benzene than is benzene for separating ethanol and water. Similarly in the ethyl acetate systems, water is the more selective solvent.

However, if a choice were to be made between benzene and ethyl acetate as solvents for separating ethanol and water, clearly benzene is the more selective of the two. Other considerations, however, might show neither to be very desirable.

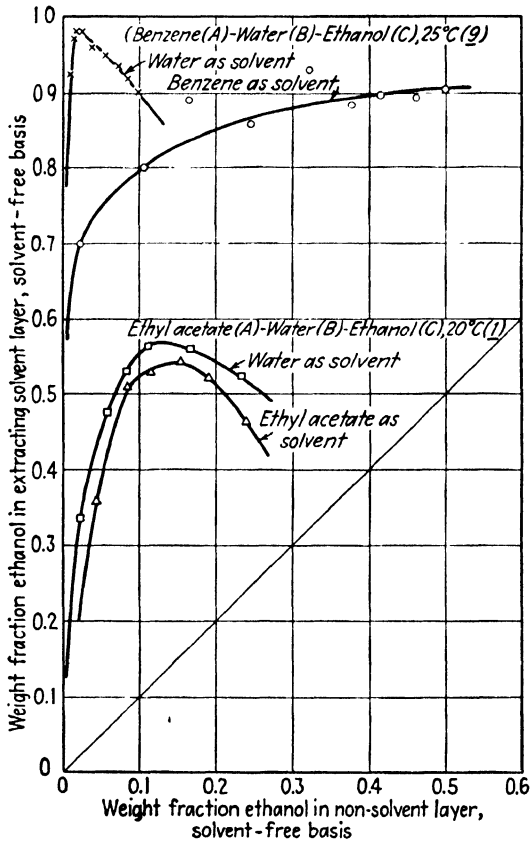



FIG. 4.3. Selectivity diagrams, Type 1 systems.

In Type 2 ternary systems, similar comparisons of the selectivity of solvents are possible. In the case of Fig. 4.4, $B$ is the solvent that is used to separate solutions of $A$ and $C$, and the diagram is lettered in the same manner as Fig. 4.1. Consequently the selectivity diagram is plotted as concentrations of $C$ in the equilibrium phases on a $B$-free basis. Selectivities are ordinarily somewhat lower in this type of system than in those of Type 1, and two examples are shown in Fig. 4.5.

As in the case of vapor-liquid equilibria, numerical values of the selectivity, designated as $\beta$, are desirable, and these may be calculated in the same fashion as the analogous property, relative volatility, for distillation processes (8). Thus, the selectivity $\beta$ of $B$ for $C$ is defined as follows:

$$\frac{\dfrac{X_{CB}}{X_{CB}+X_{AB}}}{1-\dfrac{X_{CB}}{X_{CB}+X_{AB}}}=\beta\frac{\dfrac{X_{CA}}{X_{CA}+X_{AA}}}{1-\dfrac{X_{CA}}{X_{CA}+X_{AA}}} \tag{4.1}$$

or more simply,

$$\beta=\frac{X_{CB}X_{AA}}{X_{CA}X_{AB}} \tag{4.2}$$

Similarly, the selectivity of $A$ for $C$ is

$$\beta=\frac{X_{CA}X_{BB}}{X_{CB}X_{BA}} \tag{4.3}$$

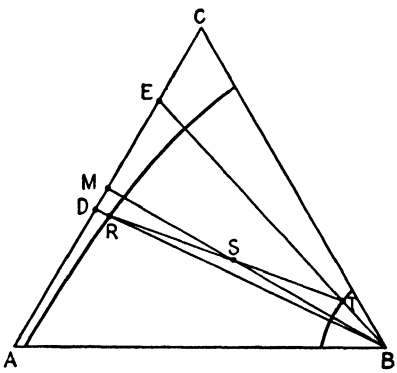



FIG. 4.4. Selective extraction in Type 2 systems.

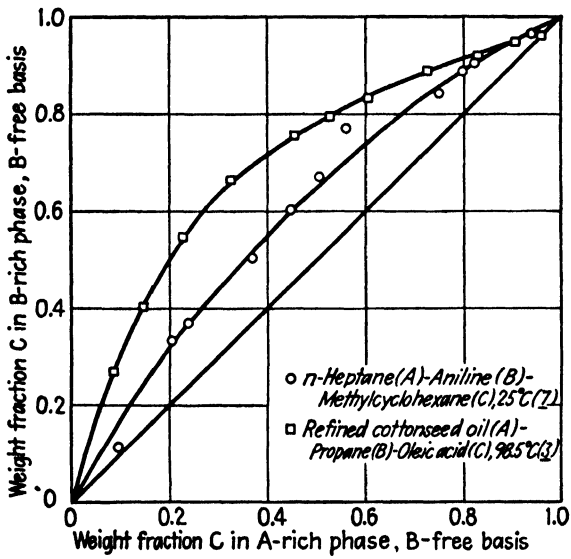



FIG. 4.5. Selectivity diagrams for Type 2 systems.

The concentrations for the $A$- and $B$-rich phases are equilibrium concentrations, and the numerical value for $\beta$ will be the same whether weight or mole fraction units are used for concentration. Like relative volatility, $\beta$ has been shown to be substantially constant for a few systems (2, 7),

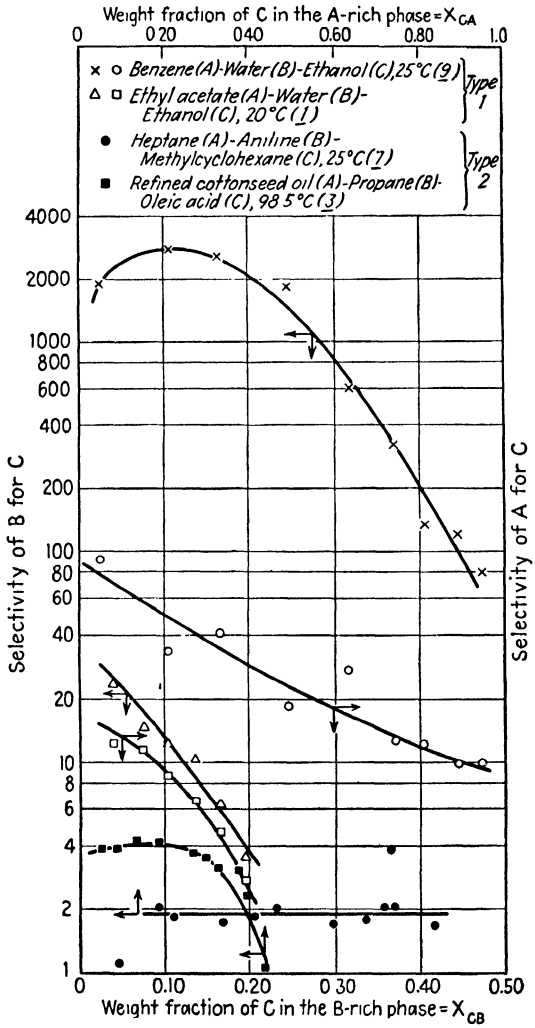



FIG. 4.6. Selectivities in Type 1 and Type 2 systems.

in which case it can be used as a correlating device for tie-line data [Eqs. (2.14), (2.15)]. In most cases, $\beta$ varies widely with concentrations, as shown in Fig. 4.6, where selectivities for the systems of Figs. 4.3 and 4.5 are shown.

The importance of good selectivity for extraction processes parallels that of relative volatility for distillation. Practical processes require that $\beta$ exceed unity, the more so the better. Selectivities close to unity will result in large plant equipment, large numbers of extraction contacts or stages, and in general, costly investment and operation. If $\beta = 1$, separation is impossible.

Combining Eqs. (2.7) and (4.2), we see that selectivity of $B$ for $C$ is related to the distribution coefficient in the following manner:

$$\beta = m\frac{X_{AA}}{X_{AB}} \tag{4.4}$$

Since $X_{AA}/X_{AB}$ is always greater than unity, then for systems with a favorable distribution coefficient ($m > 1$), $\beta$ will always exceed unity. Systems with an unfavorable distribution coefficient ($m < 1$) or systems for which $m$ varies from less than 1 to greater than 1 (characterized by a reversal of tie-line slopes) will not necessarily give values of $\beta$ less than unity except if the mutual solubility of the nonconsolutes $A$ and $B$ is considerable.

In quaternary systems, where $B$ and $C$ are distributed between immiscible solvents $A$ and $D$, the selectivity and distribution coefficients are related in the following manner:

$$m_B = \frac{X_{BA}}{X_{BD}}, \qquad m_C = \frac{X_{CA}}{X_{CD}} \tag{4.5}$$

and

$$\beta = \frac{m_B}{m_C} = \frac{X_{BA}X_{CD}}{X_{CA}X_{BD}} \tag{4.6}$$

where $\beta$ is the selectivity of the solvent pair for $B$. As with ternary systems, $\beta$ must exceed unity for a successful process.

**Recoverability.** In all liquid-extraction processes, it is necessary to remove the extracting solvent from the two products resulting from the separation. This is important not only to avoid contamination of the products with the solvent but also to permit reuse of the solvent in order to reduce the cost of operation. In practically every instance, the recovery process is ultimately one of fractional distillation, and the relative volatility of the solvent and substance to be separated must be high in order that this may be carried out inexpensively. The existence in the system of azeotropes involving the solvent must be checked particularly, since their presence may prevent separation of the solvent by ordinary distillation means. A very complete, indexed list of azeotropes which has recently been compiled is most convenient for at least initial studies of recoverability (4). The question as to whether the solvent or the components which are separated by the extraction process should be the more volatile is an important one. In most extraction processes, the quantity of solvent

used is greater than that of the desired products. If, in the recovery by distillation, the solvent is the more volatile, large quantities will be vaporized and the process will be costly. Therefore in such cases it is preferable that the solvent be the less volatile, and distillation will involve vaporization of the desired products which are present in smaller amounts. If the solvent is very selective, it is possible that very small amounts will be used, in which case it may be advantageous if the solvent is the more volatile. If the solute in the solvent-containing solution is nonvolatile, it may be necessary to recover the solvent by evaporation. In either case, if the solvent must be vaporized, its latent heat of vaporization should be low to reduce the cost of recovery.

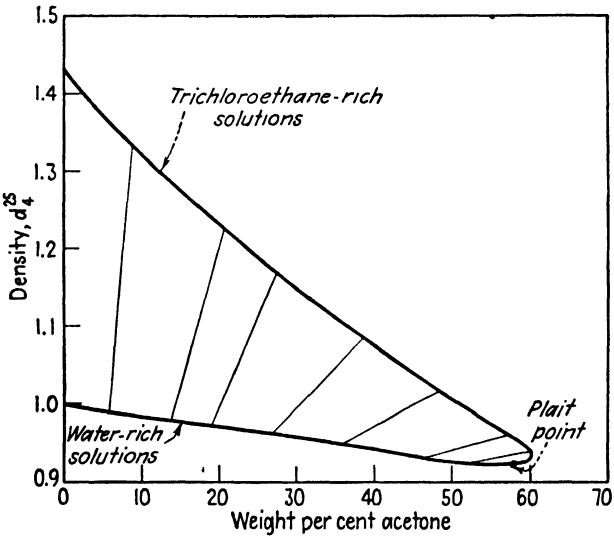



FIG. 4.7. Densities of equilibrium solutions in the system water (*A*)–1,1,2-trichloroethane (*B*)–acetone (*C*), at 25°C. (6).

The possibilities of using methods of solvent-product separation other than vaporization should not be overlooked. Crystallization of the product from the solvent solution and removal of the solute by adsorption are occasionally worth serious investigation.

**Density.** A difference in densities of the contacted phases is essential and should be as great as possible. Not only is the rate of disengaging of the immiscible layers thereby enhanced, but also the capacity of the contacting equipment is increased. It is insufficient to examine merely the relative densities of the solution to be extracted and the pure extracting solvent, since on admixture mutual solubility of the two will alter the densities; for continuous contacting equipment, it is important to be certain that a satisfactory density difference for the contacted phases exists

throughout the entire range of the contemplated process. Figures 4.7 and 4.8 indicate desirable and potentially undesirable situations respectively. In Fig. 4.7, the densities of saturated layers in the Type 1 system acetone–1,1,2-trichloroethane–water (acetone as distributed substance) are plotted, with equilibrium layers joined by tie lines (6). The densities of the water-rich layers are always less than those of trichloroethane-rich layers, but the change in density difference with acetone concentration is necessarily great, since at the plait point the densities of the conjugate solutions are identical. Figure 4.8 is the same sort of plot for the Type 2 system methyl ethyl ketone–water–trichloroethylene (5). Note that here a

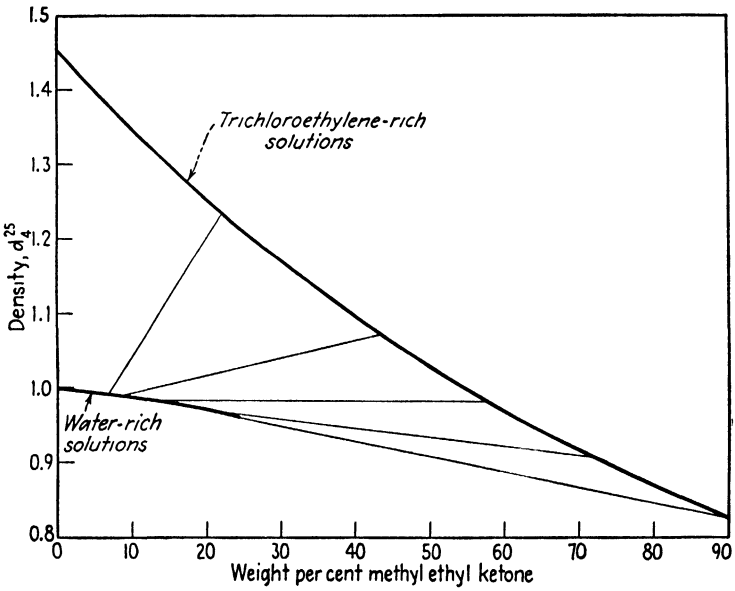



FIG. 4.8. Densities of equilibrium solutions in the system water (*A*)–trichloroethylene (*B*)–methyl ethyl ketone (*C*), at 25°C. (5).

reversal of sign in the density difference between equilibrium layers occurs, and while a stagewise contacting operation could work across the conjugate solutions of equal density, a continuous contacting operation could not.

**Interfacial Tension.** The interfacial tension between immiscible phases which must be settled or disengaged should preferably be high for rapid action. Too high an interfacial tension on the other hand may lead to difficulties in the adequate dispersion of one liquid in the other, while too low a value may lead to the formation of stable emulsions. Unfortunately, relatively few liquid interfacial-tension measurements for complete ternary systems have been made. As an extremely rough guide, the differences in the surface tensions with air of the contacted liquids may be used to estimate the order of magnitude of interfacial tension, but this will be at

best a very crude indication. In Type 1 systems, the interfacial tension between equilibrium layers will fall to zero at the plait point.

**Chemical Reactivity.** Chemical reactions between solvent and components of the solution yielding products extraneous to the process are undesirable, since only in their absence will the yield of products be high and complete solvent recovery be possible. On occasion, the formation of a chemical compound as part of the extraction process may be considered desirable, since then the rate and even the extent of extraction may be enhanced. Ordinarily any such reaction product should be capable of easy decomposition so that solvent recovery is possible, unless the reaction product itself is the desired substance. Polymerization, condensation, or decomposition of the solvent at any temperature attained in the process, including the recovery equipment, is not desirable.

**Mutual Solubility with Solution to Be Extracted.** The extracting solvent and solution to be extracted should be highly immiscible. In a Type 1

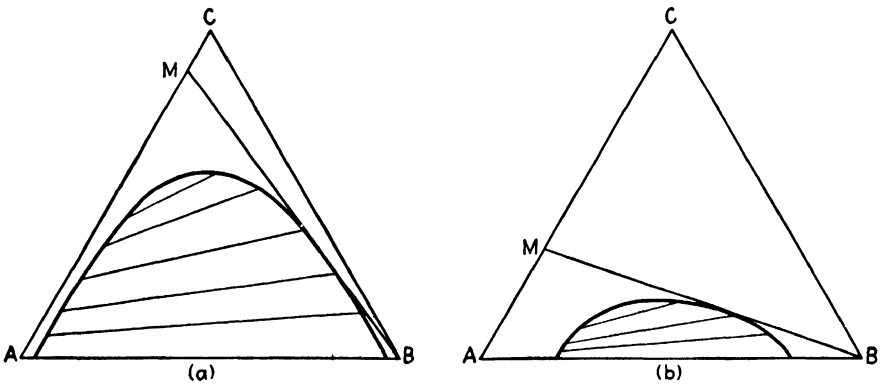



FIG. 4.9. Effect of solvent solubility on extraction.

system, for example, this will ordinarily mean that high concentrations of distributed solute can be attained before complete solution of the immiscible liquid occurs. This in turn increases the ultimate extent of separation possible, as indicated in Fig. 4.9. In both of the systems shown, it is possible to use component $B$ for separating solutions of $A$ and $C$ within the limits of pure $A$ to $M$, since only in this range of concentration will immiscibility occur on addition of $B$. Clearly the possibilities with the system ($a$) are much greater than those with the system ($b$). Furthermore, solvent recovery in highly insoluble systems is simpler, and, for a given distribution coefficient, the selectivity will be better [Eq. (4.4)].

**Corrosiveness.** In order to reduce the cost of equipment, the solvent should cause no severe corrosion difficulties with common materials of construction. Expensive alloys and other unusual materials should not be required.

**Viscosity.** Low power requirements for pumping, high heat-transfer rates, high rates of extraction, and general ease of handling are corollaries of low viscosity, and hence this is a desirable property of solvents in extraction processes.

**Vapor Pressure.** The vapor pressure of a proposed solvent should be sufficiently low so that storage and extraction operations are possible at atmospheric or at most only moderately high pressure. This requirement may of course conflict with the requirement of high relative volatility with the solution being extracted, and a compromise may be necessary.

**Freezing Point.** The solvent should have a sufficiently low freezing point so that it may be conveniently stored and otherwise handled at outdoor temperatures in cold weather.

**Inflammability.** Low inflammability is of course desirable for reasons of safety, and the flash point is frequently used as a numerical indication of the property. If the solvent can be burned, it should have a high flash point and close concentration limits for explosive mixtures with air.

**Toxicity.** Highly poisonous materials are difficult to handle industrially. Unless elaborate plant safety devices are planned, with frequent medical inspection of personnel, the more toxic substances must be avoided.

**Cost.** Low cost and ready availability in adequate quantities usually parallel each other and are of course desirable solvent attributes. While it is true that solvents are recovered from product solutions, nevertheless make-up solvent to replace inevitable process losses must be expected. Furthermore, large quantities of expensive solvent which are retained in the plant represent sizable sums invested. Interest on such money is chargeable directly to the process.

Of all the desirable properties described, favorable selectivity, recoverability, interfacial tension, density, and chemical reactivity are essential for the process even to be carried out. The remaining properties, while not necessary from the technical point of view, must be given consideration in good engineering work and in cost estimation.

### Notation for Chapter 4

$\beta$ = selectivity, defined by Eqs. (4.1) and (4.2).
$m$ = distribution coefficient = ratio of concentration of a solute in equilibrium liquid phases.
$X$ = concentration, weight fraction.

Subscripts:
$A, B, C, D$ = components $A$, $B$, $C$, and $D$, resp.
$AB$ = $A$ in a $B$-rich solution.

### LITERATURE CITED

1. Beech, D. G., and S. Glasstone: *J. Chem. Soc.* **1938,** 67.
2. Brown, T. F.: *Ind. Eng. Chem.* **40,** 103 (1948).

3. Hixson, A. W., and J. B. Bockelman: *Trans. Am. Inst. Chem. Engrs.* **38,** 891 (1942).
4. Horsley, L. H.: *Ind. Eng. Chem., Anal. Ed.* **19,** 508 (1947); **21,** 831 (1949).
5. Newman, M., C. B. Hayworth, and R. E. Treybal: *Ind. Eng. Chem.* **41,** 2039 (1949).
6. Treybal, R. E., L. D. Weber, and J. F. Daley: *Ind. Eng. Chem.* **38,** 817 (1946).
7. Varteressian, K. A., and M. R. Fenske: *Ind. Eng. Chem.* **29,** 270 (1937).
8. Walker, W. H., W. K. Lewis, W. H. McAdams, and E. R. Gilliland: "Principles of Chemical Engineering," 3d ed., Chap. XVI, McGraw-Hill Book Company, Inc., New York, 1937.
9. Washburn, E. R., V. Huizda, and R. Vold: *J. Am. Chem. Soc.* **53,** 3237 (1931).

# CHAPTER 5

## DIFFUSION AND MASS TRANSFER

Consider a liquid flowing through a pipe. Extensive study of the velocity distribution in such a fluid has revealed that at the pipe wall the fluid is motionless and that at increasing distances from the pipe wall the fluid velocity gradually increases, reaching a maximum value at the center. Near the pipe wall the flow is viscous or laminar, characterized by a velocity which is a linear function of the distance from the pipe wall, with no general mixing in the direction of the pipe radius. If the average velocity is sufficiently large, laminar flow is confined to a relatively thin layer adjacent to the pipe wall. In the central core of the fluid, flow is turbulent, characterized by eddy currents with large velocity components perpendicular to the axis of the pipe and considerable mixing of the fluid in the direction of the pipe radius. Similar phenomena are observed whenever fluids move rapidly past solid boundaries of any sort and also when the boundary is an interface between two immiscible fluids, although in the latter case the relative interfacial velocity in the two phases and not the absolute velocity is zero.

In extraction processes, where moving immiscible liquids are brought into contact for the purpose of causing the diffusion of a substance from one liquid to the other across the phase boundary, it is clear that the diffusing substance must pass through various portions of the fluid that are in viscous or turbulent flow. The rates at which the diffusion occurs through these zones are of major importance in determining the size of equipment for carrying out the extraction.

### MOLECULAR DIFFUSION

Molecular diffusion is the mechanism of transfer of a substance either through a fluid which is motionless or, if the fluid is in laminar flow, in a direction perpendicular to the velocity of the fluid. The phenomenon has been studied from many points of view, frequently conflicting, the most important of which are those of Fick and of Maxwell-Stefan. Fick (7) applied the well-known Fourier equation for rate of heat flow to the problem of diffusion. Unfortunately the mechanism of the two processes is not identical, since in the penetration of a liquid by a diffusing solute there will necessarily be displacement of the liquid and consequent volume changes arising for which the Fourier equation does not account. As an approxi-

mation, however, the Fick concept is very useful, particularly since the Fourier equation has been integrated for many situations which parallel problems in diffusion. Maxwell (17) and later Stefan (27) considered the simultaneous movement of both components of the solution through which the solute is diffusing and arrived at equations which are much more general. These have been reviewed and extended by Lewis and Chang (15), Sherwood (24), and Arnold (2).

**Maxwell-Stefan Concept.** In substance, the resistance to diffusion of component $A$ through a solution of $A$ and $B$ is assumed to be proportional to the relative velocity of $A$ with respect to $B$, $u_A - u_B$; to the distance $dl$ through which the diffusion occurs; and to the number of molecules of $A$ and $B$ in the path of the diffusion, in turn proportional to the concentrations $c_A$ and $c_B$. The resistance must be overcome by a concentration gradient in the direction of diffusion $dc_A$. Thus,

$$dc_A = -bc_Ac_B(u_A - u_B)dl \tag{5.1}$$

This basic equation may then be integrated for various situations.

1. *Equimolal Counterdiffusion.* This leads to Fick's law. If $N_A$ and $N_B$ are the number of moles of $A$ and $B$, respectively, diffusing per unit time through a cross section $S$,

$$N_A = c_Au_AS, \qquad N_B = c_Bu_BS \tag{5.2}$$

and

$$N_A = -N_B \tag{5.3}$$

Substitution in Eq. (5.1) then leads to

$$N_A = -\frac{S}{b(c_A + c_B)}\frac{dc_A}{dl} \tag{5.4}$$

The diffusion coefficient, or diffusivity $D$ is defined as

$$D_A = \frac{1}{b(c_A + c_B)}, \tag{5.5}$$

whence

$$N_A = -D_AS\frac{dc_A}{dl} \tag{5.6}$$

which is Fick's law.

2. *Steady-state Conditions* ($N_A$ = *constant*), *One Component Stationary or Not Diffusing* ($u_B = 0$). Equation (5.1) then becomes

$$dc_A = -bc_Ac_Bu_Adl \tag{5.7}$$

$$\therefore dc_A = -\frac{bN_Ac_Bdl}{S} = -\frac{N_Ac_B\,dl}{SD_A(c_A + c_B)} \tag{5.8}$$

Integration of Eq. (5.8) then depends upon the effect of concentration on the volume of the liquid solution and upon $D$.

*a.* Solution very dilute ($c_A << c_B$), $D$ = const. (24).

$$\frac{c_B}{c_A + c_B} = \text{const.} \tag{5.9}$$

and

$$\int_{c_{A_2}}^{c_{A_1}} dc_A = -\frac{N_A c_B}{SD_A(c_A + c_B)} \int_{l_2}^{l_1} dl \tag{5.10}$$

$$c_{A_1} - c_{A_2} = -\frac{N_A c_B (l_1 - l_2)}{SD_A(c_A + c_B)} \tag{5.11}$$

Letting $(l_2 - l_1) = l$, (5.12)

$$N_A = \frac{D_A S}{l}\left(\frac{c_A + c_B}{c_B}\right)(c_{A_1} - c_{A_2}) \tag{5.13}$$

*b.* The volume of the solution is an additive function of the volumes of the constituents, $D$ = const. (15, 24).

$$c_A + c_B = c = \text{const.} \tag{5.14}$$

$$dc_A = -dc_B \tag{5.15}$$

Therefore,

$$dc_A = -dc_B = -\frac{N_A c_B\, dl}{SD_A c} \tag{5.16}$$

$$cD_A \int_{c_{B_2}}^{c_{B_1}} \frac{dc_B}{c_B} = \frac{N_A}{S} \int_{l_2}^{l_1} dl \tag{5.17}$$

$$cD_A \ln \frac{c_{B_1}}{c_{B_2}} = \frac{N_A}{S}(l_1 - l_2) \tag{5.18}$$

Define

$$c_{BM} = \frac{c_{B_1} - c_{B_2}}{\ln \frac{c_{B_1}}{c_{B_2}}} \tag{5.19}$$

$$\therefore \frac{cD_A(c_{B_1} - c_{B_2})}{c_{BM}} = \frac{N_A}{S}(l_1 - l_2) \tag{5.20}$$

Since

$$c_{B_1} + c_{A_1} = c_{B_2} + c_{A_2} \tag{5.14}$$

and

$$(l_2 - l_1) = l \tag{5.12}$$

$$\therefore \frac{cD_A(c_{A_1} - c_{A_2})}{c_{BM}} = \frac{N_A l}{S} \tag{5.21}$$

or

$$N_A = \frac{D_A S c}{c_{BM} l}(c_{A_1} - c_{A_2}) \tag{5.22}$$

Converting to mole fraction units $x$ for concentration,

$$c_A = x_A c, \qquad c_{BM} = x_{BM} c \tag{5.23}$$

$$N_A = \frac{D_A S c}{x_{BM} l}(x_{A_1} - x_{A_2}) \tag{5.24}$$

Since

$$c = \frac{\rho}{MW_M} \tag{5.25}$$

$$\therefore N_A = \frac{D_A S \rho}{x_{BM} MW_M l}(x_{A_1} - x_{A_2}) \tag{5.26}$$

Equations (5.22), (5.24), and (5.26) are most useful for ordinary purposes, and moderate variations in $c$ are usually taken care of by use of an average, $c = (c_1 + c_2)/2$.

**Illustration 1.** Calculate the rate of diffusion of ethanol across a film of water solution 0.2 cm. thick at 20°C., when the concentrations on either side of the film are 14 and 9.6 wt. per cent ethanol. Under these conditions, the diffusivity of the ethanol may be taken as $0.74 \times 10^{-5}$ sq. cm./sec.

*Solution.* Use Eq. (5.22). Mol. wt. ethanol = 46.05, mol. wt. water = 18.02. At 20°C., the density of the 14% solution = 0.9764 gm./cu. cm.

Consequently,

$$c_{A_1} = \frac{0.9764(0.14)}{46.05} = 0.00297 \frac{\text{gm. mole ethanol}}{\text{cu. cm. soln.}}$$

$$c_{B_1} = \frac{0.9764(0.86)}{18.02} = 0.0466 \frac{\text{gm. mole water}}{\text{cu. cm. soln.}}$$

$$c_1 = 0.00297 + 0.0466 = 0.0496 \frac{\text{gm. mole}}{\text{cu. cm. soln.}}$$

The density of the 9.6% solution = 0.9824 gm./cu. cm.

$$c_{A_2} = \frac{0.9824(0.096)}{46.05} = 0.00205 \frac{\text{gm. mole ethanol}}{\text{cu. cm. soln.}}$$

$$c_{B_2} = \frac{0.9824(0.904)}{18.02} = 0.0492 \frac{\text{gm. mole water}}{\text{cu. cm. soln.}}$$

$$c_2 = 0.00205 + 0.0492 = 0.0513 \frac{\text{gm. mole}}{\text{cu. cm. soln.}}$$

$$c_{BM} = \frac{c_{B_1} - c_{B_2}}{\ln (c_{B_1}/c_{B_2})} = \frac{0.0466 - 0.0492}{\ln (0.0466/0.0492)} = 0.0485 \frac{\text{gm. mole}}{\text{cu. cm.}}$$

$$c = \frac{c_1 + c_2}{2} = \frac{0.0496 + 0.0513}{2} = 0.0505 \frac{\text{gm mole}}{\text{cu. cm.}}$$

$$l = 0.2 \text{ cm.}$$

$$\therefore \frac{N_A}{S} = \frac{D_A c (c_{A_1} - c_{A_2})}{c_{BM} l} = \frac{0.74(10^{-5})(0.0505)(0.00297 - 0.00205)}{0.0485(0.2)}$$

$$= 3.54 \times 10^{-8} \text{ gm. mole ethanol/sq. cm. cross section}$$

3. *Unsteady-state Conditions.* Arnold (2) has integrated the Maxwell-Stefan equation for gaseous diffusion in the case of the "semi-infinite column," or diffusion from a plane at which the concentrations are kept constant into a space filled with gas extending to infinity, both for vaporization of a liquid into a gas and absorption of a gas by a liquid. It is possible that the resulting equations could be applied successfully to liquid diffusion for similar circumstances, provided that an assumption analogous to Dalton's law for gases can be made and that $D$ is assumed to remain constant. The direct application to extraction operations of such equa-

tions is unlikely, but it could be useful in the experimental determination of the diffusivity.

There is perhaps more direct application for an integration of the diffusion equation for unsteady-state diffusion from spheres, since frequently extraction operations involve the dispersion of one liquid in the form of more or less spherical drops into another immiscible liquid. Isolated drops rising or falling through the continuous liquid will undergo unsteady-state extraction of their solute. Newman (21) presents the integration of the Fick equation for this case, for a sphere with an initial uniform concentration of solute $c_A^0$, a constant surface concentration $c_{A_1}$, and a radius $r$. The fraction unextracted at any time $\theta$, when the final average concentration is $w_A$, is given by

$$\frac{w_A - c_{A_1}}{c_A^0 - c_{A_1}} = \frac{6}{\pi^2}\left(e^{\frac{-D_A\theta\pi^2}{r^2}} + \tfrac{1}{4}e^{\frac{-4D_A\theta\pi^2}{r^2}} + \tfrac{1}{9}e^{\frac{-9D_A\theta\pi^2}{r^2}} + \cdots\right) \quad (5.27)$$

Numerical solutions of the equation are given by Newman.

**Experimental Determination of Diffusivity.** Reviews of the various methods of determining $D$ are given by Williams and Cady (33) and Cohen and Bruins (3). Two general techniques are used: (*a*) those in which average concentrations are determined in different zones of a liquid by sampling and analysis after diffusion of a solute into the various zones has occurred, and (*b*) those in which the course of the diffusion is followed without disturbing the liquid, using optical or similar means of analysis. Aside from the obvious requirements of constant temperature and absence of vibration and eddy currents, the various experimental techniques require means of obtaining a sharp demarcation between the dilute and concentrated solutions at the beginning of the experiment. Cohen and Bruins (3) and others accomplished this by placing several plates in contact with each other, each with a hole bored through it. These were so arranged that by rotating the plates the holes would line up to form a diffusion column. A concentrated solution in the hole of one plate could then be rotated into contact with solvent in the other holes with a minimum of disturbance. At the end of the experiment, rotating the plates would effectively slice samples from the diffusion column without disturbance of the liquid. McBain and Liu (18) and others have used a porous, sintered, glass membrane to separate the concentrated and dilute solutions, with the concentration gradient and diffusion confined to the pores of the membrane. Gels have frequently been used to keep the solutions free of eddy currents and to facilitate the clean slicing of samples, but it is doubtful whether the rate of diffusion through a gel is the same as through a solution. The data resulting from these experiments have almost invariably been converted to diffusivities by application of several integrated forms of Fick's law. Since the diffusivities in liquid solutions are functions

of concentration, unless the concentration gradient has been kept small the resulting diffusivities are average values over the range of concentration encountered, rather than "instantaneous" values. Many data are tabulated in the "International Critical Tables" (Vol. V, pp. 63–75).

**Empirical Estimation of Diffusivities for Nonelectrolytes.** *Dilute Solutions.* Two reasonably successful approaches have been made to the problem of estimation of diffusivities in the absence of measured data, based on an extension of the kinetic theory to liquids and on the theory of absolute reaction rates.

1. *Kinetic theory approach.* By application of the kinetic theory of gases to the liquid phase, Arnold (1) obtained an expression of $D$ paralleling in form that obtained previously for gases:

$$D_A = \frac{0.0100\sqrt{\frac{1}{MW_A} + \frac{1}{MW_B}}}{A_A A_B \mu_B^{1/2}(V_A^{1/3} + V_B^{1/3})^2} \text{ at } 20°\text{C.}\dagger \qquad (5.28)$$

where $MW$ = mol. wt.
$\mu$ = viscosity at 20°C., centipoises
$V$ = molar vol. at the boiling point, cu. cm./gm. mole
$A$ = abnormality factor
$D$ = diffusivity at 20°C., sq. cm./sec.
Subscripts $A$ and $B$ refer to the diffusing solute and the solvent, resp.

The equation is limited to very dilute solutions, to a temperature of 20°C., and to diffusion through relatively low-boiling solvents.

TABLE 5.1. ATOMIC AND MOLECULAR VOLUMES

| Atomic vol. | | Mol. vol. | |
|---|---|---|---|
| Carbon | 14.8 | $H_2$ | 14.3 |
| Hydrogen | 3.7 | $O_2$ | 25.6 |
| Chlorine | 24.6 | $N_2$ | 31.2 |
| Bromine | 27.0 | Air | 29.9 |
| Iodine | 37.0 | CO | 30.7 |
| Sulfur | 25.6 | $CO_2$ | 34.0 |
| Nitrogen | 15.6 | $SO_2$ | 44.8 |
| Nitrogen in primary amines | 10.5 | NO | 23.6 |
| Nitrogen in secondary amines | 12.0 | $N_2O$ | 36.4 |
| Oxygen | 7.4 | $NH_3$ | 25.8 |
| Oxygen in methyl esters | 9.1 | $H_2O$ | 18.9 |
| Oxygen in higher esters | 11.0 | $H_2S$ | 32.9 |
| Oxygen in acids | 12.0 | COS | 51.5 |
| Oxygen in methyl ethers | 9.9 | $Cl_2$ | 48.4 |
| Oxygen in higher ethers | 11.0 | $Br_2$ | 53.2 |
| Benzene ring: subtract | 15 | $I_2$ | 71.5 |
| Naphthalene ring: subtract | 30 | | |

† The listed units must be used in Eq. (5.28).

Values of $V$ can be obtained conveniently from Kopp's law, which states that $V$ is an additive function of the atomic volumes of the constituents of a molecule. The contributions of each atom given by Le Bas are used by Arnold, and these are listed in Table 5.1. For complex molecules, these are then added together. Thus, for toluene $C_7H_8$, $V = 7(14.8) + 8(3.7) - 15 = 118.2$. For the smaller molecules such as those of the gases, the table lists directly the values to be used. The abnormality factors $A_A$ and $A_B$ are corrections included in the equation to account for "association," or unduly large intermolecular attraction. Values of $A_B$ are strictly functions of the solvent, paralleling in numerical magnitude the association factors obtained from other anomalous properties of liquids, and are listed

TABLE 5.2. $A_B$, ABNORMALITY FACTORS FOR SOLVENT*

| Solvent | $A_B$ |
|---|---|
| Ethyl ether | 0.90 |
| Benzene | 1.0 |
| Toluene | 1.0 |
| Acetone | 1.15 |
| Water | 4.70 |
| Methanol | 2.0 |
| Ethanol | 2.0 |
| Propanol | 1.36 |
| Amyl alcohol | 1.36 |
| *m*-Xylene | 0.97 |
| Chloroform | 1.0 |
| Carbon tetrachloride | 0.94 |
| Carbon disulfide | 1.0 |
| Ethyl acetate | 1.06 |
| Heptane | 0.66 |
| Acetic acid | 1.86 |
| Ethyl benzoate | 1.0 |
| Nitrobenzene | 1.35 |

* J. H. Arnold, *J. Am. Chem. Soc.* **52**, 3937 (1930). With permission of the American Chemical Society.

in Table 5.2. Values of $A_A$ represent abnormality of the solute and are somewhat dependent upon the value of $A_B$ for the solvent, as indicated in Table 5.3. Additional substances are given by Arnold.

For short ranges in temperature, Arnold recommends that the temperature effect on $D$ be estimated by the expression

$$D = D_{0°C.}(1 + bt)\dagger \tag{5.29}$$

and

$$b = 0.020\left(\frac{\mu_B}{\rho_B^{2/3}}\right)^{1/2}\dagger \tag{5.30}$$

† The listed units must be used in Eqs. (5.29) and (5.30).

TABLE 5.3. $A_A$, ABNORMALITY FACTORS FOR SOLUTES*

| Solute | Solvent | | | |
|---|---|---|---|---|
| | Benzene $A_B = 1$ | Methanol $A_B = 2$ | Ethanol $A_B = 2$ | Water $A_B = 4.7$ |
| Formic acid | 1.29 | 1.53 | | 1.32 |
| Acetic acid | 1.38 | 1.53 | | 1.27 |
| Chloracetic acid | 1.42 | 1.28 | | |
| Benzoic acid | 1.32 | 1.26 | | |
| Propanol | 1.42 | | | 1.16 |
| Amyl alcohol | 1.29 | 1.29 | 1.31 | 1.16 |
| Phenol | 1.32 | 1.35 | | 1.21 |
| Chlorophenol | 1.26 | 1.26 | | |
| Chloroform | | | 0.89 | |
| Stearic acid | | | 0.96 | |
| Pyridine | | 1.26 | 1.07 | 1.60 |
| Allyl alcohol | | 1.27 | 1.42 | 1.17 |
| Acetamide | | 1.54 | 2.08 | 1.15 |
| Glycerol | | 1.65 | 2.15 | 1.25 |
| Methanol | | | | 1.19 |
| Ethanol | | | | 1.24 |
| Glucose | | | | 1.27 |
| Aniline | | | | 1.23 |

* J. H. Arnold, *J. Am. Chem. Soc.* **52**, 3937 (1930). With permission of the American Chemical Society.

where $D$ = diffusivity at temp. $t$
$D_{0°C.}$ = diffusivity at 0°C.
$t$ = temp., °C.
$\mu_B$ = solvent viscosity at 20°C., centipoises
$\rho_B$ = solvent density at 20°C., gm./cu. cm.

It is an observed fact that the larger the value of $D$, the less is its temperature dependence, although Eqs. (5.29) and (5.30) do not include this effect.

Figure 5.1 compares some observed values of $D$ with those calculated by the Arnold correlation.

2. *Absolute-rate-theory Approach.* Eyring and others (6, 8, 14, 23, 29) have extended the theory of absolute rates to the problem of liquid diffusion and viscosity with considerable success. Viscosity is a measure of the force per unit area required to overcome the frictional resistance between two layers of molecules of a liquid in maintaining unit relative velocity of the two layers. In diffusion, molecules of the diffusing solute move past those

of the solvent, and a force must be applied to maintain their velocity. The phenomena are thus closely related.

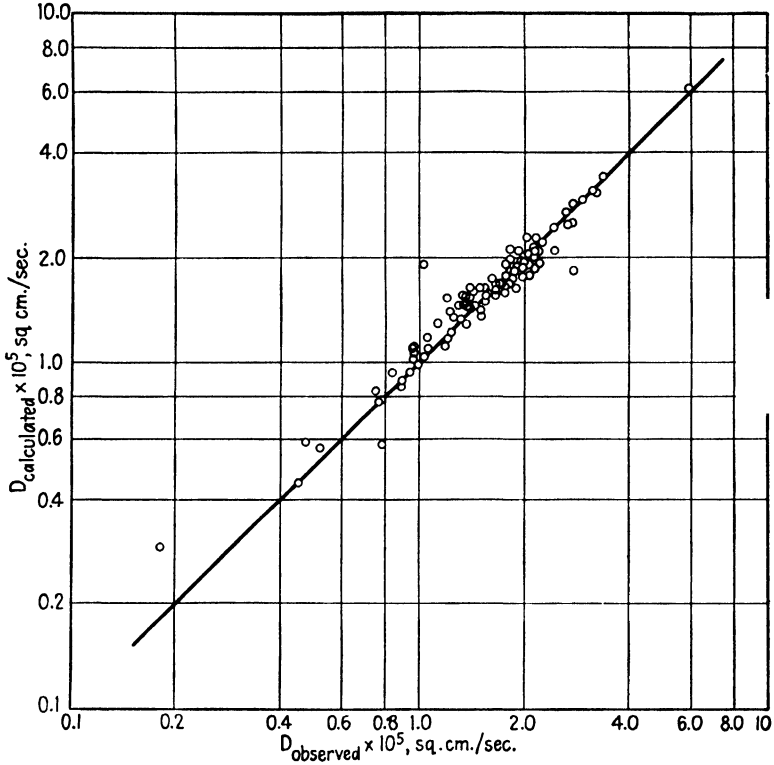



FIG. 5.1. Comparison of observed diffusivities with those calculated by the method of Arnold (1).

In the Eyring concept, a liquid is regarded as being made up of a continuum of matter interspersed with holes. The same energy is required to make a hole in the liquid the size of a molecule as the energy of vaporization per molecule. Thus, per mole,

$$\Delta E_V = \Delta H_V - RT \tag{5.31}$$

where $\Delta E_V$ = energy to make a hole
$\Delta H_V$ = enthalpy of vaporization
$RT$ = external work of vaporization for an ideal gas

Movement of one layer of a liquid relative to another requires the movement of molecules from one equilibrium position to another, for which it is necessary that a hole be available. This in turn requires expenditure of energy to make the hole. This concept leads to the relationship

$$\mu = \frac{\lambda_1 \mathbf{k} T}{\lambda_2 \lambda_3 \lambda^2 k'} \tag{5.32}$$

where $\lambda_1$ = distance between two layers of molecules
$\lambda_2$ = distance between adjacent molecules in the direction of movement
$\lambda_3$ = average distance between adjacent molecules in a direction perpendicular to the movement
$\lambda$ = distance between equilibrium positions in the direction of movement
$\mathbf{k}$ = Boltzmann const.
$k'$ = specific rate const.

Application of the theory of absolute rates then leads to

$$\mu = k'' c^{E_{vis}/RT} \tag{5.33}$$

where $k''$ = a constant including the molar volume, energy of vaporization, and temperature
$E_{vis}$ = energy of activation for viscous flow

$k''$ is fairly independent of temperature, and hence a plot of log $\mu$ vs. $1/T$ will result in a reasonably good straight line for most liquids, the slope of which will permit determination of $E_{vis}$. It has been found that

$$E_{vis} = \frac{\Delta E_V}{n} \tag{5.34}$$

where $n$ = a number, between 3 and 4 for most unassociated liquids, but for highly associated liquids such as water it is somewhat lower and varies with temperature. This indicates that the hole-size required for the movement of a molecule is only $\frac{1}{3}$ to $\frac{1}{4}$ that of the molecule itself.

Diffusion, as indicated above, is a related problem, differing however in the fact that molecules of different sizes are involved. Many years ago, Einstein (5), in considering the Brownian movement of colloids where the particles are very large in comparison to the molecules of the solvent and assuming that Stokes' law described the motion of the particles, arrived at what is known as the Stokes-Einstein equation:

$$D_A = \frac{\mathbf{k}T}{6\pi r_A \mu_B} \tag{5.35}$$

This relation has been found inadequate to describe ordinary diffusion data perfectly, since the Stokes' law assumption that the liquid through which the diffusing molecules move is continuous is inapplicable when the molecules of the diffusing solute actually approach those of the solvent in size.

Application of the Eyring "hole" theory for ideal liquids leads to

$$D_A = \lambda^2 k' \tag{5.36}$$

and on the assumption that $\lambda$ and $k'$ for diffusion and viscosity are the same,

$$D_A = \frac{\lambda_1 \mathbf{k}T}{\lambda_2 \lambda_3 \mu_B} \tag{5.37}$$

which parallels in form the Stokes-Einstein equation. Clearly the quantity $\lambda_1/\lambda_2\lambda_3$ is related to the molar volume, and hence the product $D\mu$ should be a function of the molar volume of the system. Furthermore, it is known that the temperature coefficient for the diffusion of large molecules is the same as the temperature coefficient of viscosity of the solvent, indicating that the Stokes-Einstein equation is a limiting case of Eq. (5.37). This is interpreted as meaning that in the case of large diffusing molecules the rate is determined by a jump of the solvent molecule from one equilibrium position to another, followed by movement of the diffusing molecule into the space thus made available.

The theory of absolute rates, when applied to the rate constant $k'$, then leads to

$$D_A = k'''e^{-E_{\text{diff}}/RT} \tag{5.38}$$

where $k'''$ = a constant including $\lambda$, $\mathbf{k}$, temp., and the free vol. of the liquid
$E_{\text{diff}}$ = energy of activation for diffusion

Since $k'''$ is substantially independent of temperature, a plot of $\log D$ vs. $1/T$ results in reasonably good straight lines.

Because of the similarity of the diffusion and viscosity phenomena, the energies of activation of the two processes are apparently the same, so that

$$E_{\text{diff}} = E_{\text{vis}} = \frac{\Delta E_V}{n} \tag{5.39}$$

and $E_{\text{diff}}$ can thus be calculated either from latent heats of vaporization or from the temperature dependency of viscosity. Since two unlike molecules are involved, it has been found that $\Delta E_V$ should be calculated from the values for the pure constituents by the relationship

$$\Delta E_V = (x_A \Delta E_{V_A}^{1/2} + x_B \Delta E_{V_B}^{1/2})^2 \tag{5.40}$$

Thus, by a combination of Eqs. (5.38), (5.39), and (5.40), a single determination of $D$ permits estimates of the constant $k'''$ and hence the temperature dependency of $D$.

Direct application of Eq. (5.38) by determination of $k'''$ from its constituent constants leads to values of $D$ which are too large, differing from the observed values by a factor frequently larger than 2. Wilke (32) has employed an empirical modification, however, which permits much closer estimates of $D$. Rearranging Eq. (5.37) to read

$$\frac{T}{D_A\mu_B} = \frac{\lambda_2\lambda_3}{\lambda_1\mathbf{k}} = F_A\dagger \tag{5.41}$$

where $T$ = temp., °K
$D_A$ = diffusivity of $A$, sq. cm./sec.,
$\mu_B$ = viscosity of solvent, centipoises

† The listed units must be used in Eq. (5.41).

Wilke found that $F$ for a given solvent correlated well as a function of the molal volume of the solute. The effect of different solvents is expressed through a parameter $\phi$ which at values of solute molal volumes less than 150 cu. cm./gm. mole equals the ratio of $F$ for the solvent to $F$ for water at constant molal volume of solute. Furthermore, $F$ for a given solution is

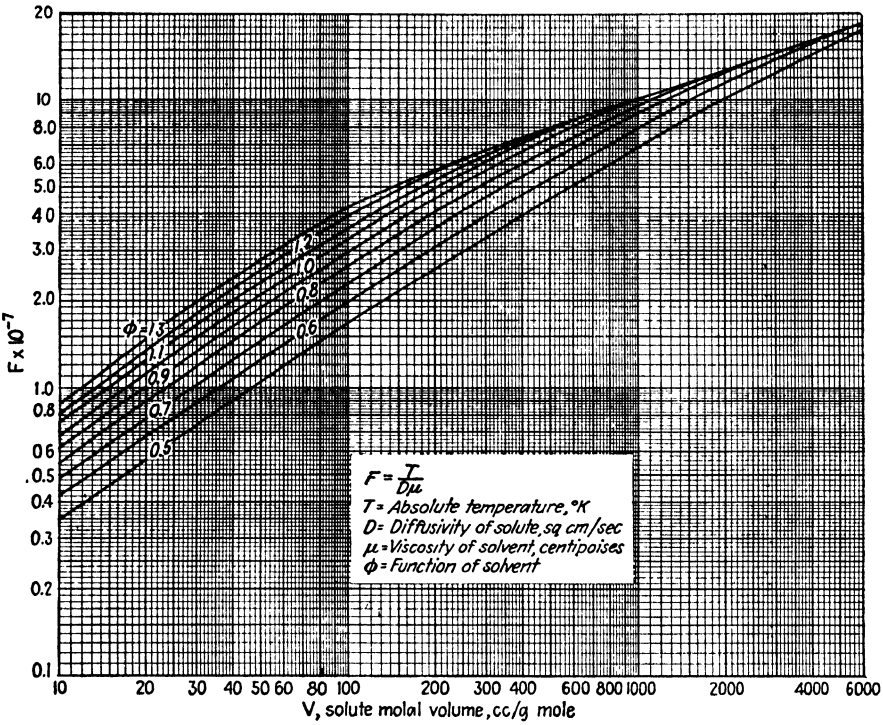



FIG. 5.2. Diffusivity correlation for dilute solutions of nonelectrolytes. C. R. Wilke [*Chem. Eng. Progress* **45**, 218 (1949). *Reproduced with the permission of the American Institute of Chemical Engineers.*]

relatively independent of temperature. Figure 5.2 summarizes the Wilke correlation. The solute molal volume $V_A$ should be calculated from the data of Table 5.1, in the manner described for the Arnold correlation. Values of $\phi$ for water, methanol, and benzene are 1.0, 0.82, and 0.70, respectively. Values of $\phi$ for other solvents may be obtained by plotting all available data for diffusion in the solvent on the figure and drawing the best line through the plotted points. In the absence of such data, it is recommended that $\phi$ be taken as 0.9. Figure 5.3 compares observed data with those calculated by the Wilke method.

*Concentrated Solutions.* Powell, Roseveare, and Eyring (23) have shown that in concentrated, nonideal solutions, the diffusivity will be a function of the activity of the solute in the solution:

$$D_{A\text{conced}} = D_{A\text{dil}}\left(\frac{d \ln a_A}{d \ln x_A}\right) = D_{A\text{dil}}\left(1 + \frac{d \ln \gamma_A}{d \ln x_A}\right) \tag{5.42}$$

where $\gamma_A$ = the activity coefficient of $A$
$a_A$ = the activity of $A = x_A\gamma_A$

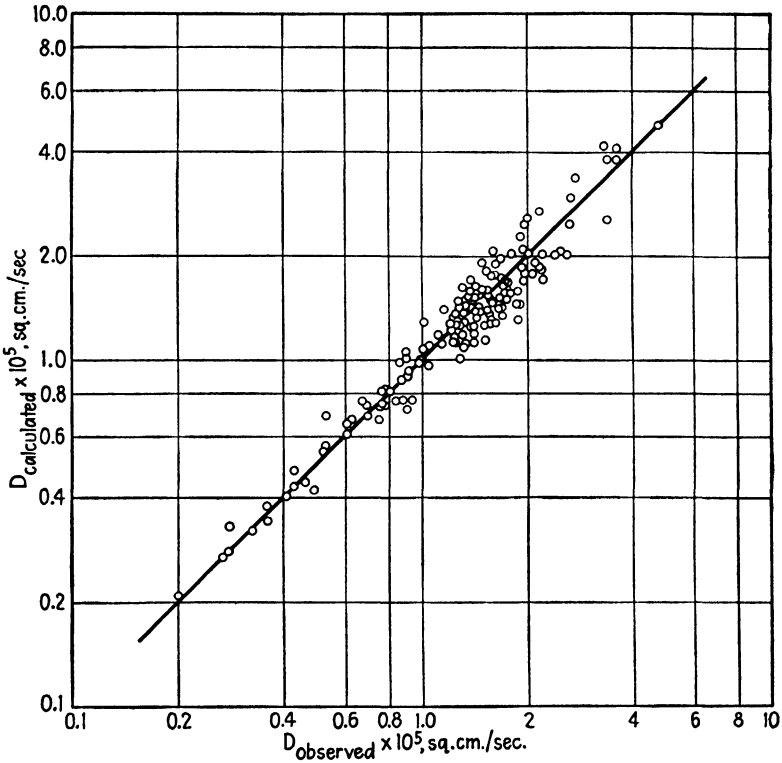



FIG. 5.3. Comparison of observed diffusivities with those calculated by the method of Wilke (32). (*With permission of the American Institute of Chemical Engineers.*)

Substituting from Eq. (5.37),

$$(D_A\mu)_{\text{conced}} = \frac{\lambda_1 \mathbf{k} T}{\lambda_2\lambda_3} \frac{d \ln a_A}{d \ln x_A} \tag{5.43}$$

If mean values of $\lambda_1$ and $\lambda_2\lambda_3$ are used, and if these vary linearly with mole fraction concentration, it follows that the quantity

$$\frac{(D_A\mu)_{\text{conced}}}{d \ln a_A / d \ln x_A}$$

should be a linear function of mole fraction concentration at constant temperature, which has been shown to be the case for several systems.

This relationship may be expressed in the following convenient manner (32):

$$\left(\frac{D_A\mu}{T}\right)_{\text{concd}} = \left[\left(\frac{1}{F_A} - \frac{1}{F_B}\right)x_A + \frac{1}{F_A}\right]\frac{d \ln a_A}{d \ln x_A}\dagger \tag{5.44}$$

where $(D_A\mu/T)_{\text{concd}}$ = the value of this group in a solution of mole fraction $x_A$. $\mu$ refers to the solution

$F_A = T/D_A\mu_B$ of $A$ in a dilute solution of $A$ in $B$

$F_B = T/D_B\mu_A$ of $B$ in a dilute solution of $B$ in $A$

Values of $F_A$ and $F_B$ may be estimated from Fig. 5.2. The quantity $d \ln a_A/d \ln x_A$ is easily obtained as the slope of a log-log plot of activity of $A$ against mole fraction of $A$, which in turn may be obtained from vapor pressure or other data as indicated in Chap. 3. $[1 + (d \log \gamma_A/d \log x_A)]$ may be substituted for $d \ln a_A/d \ln x_A$.

**Illustration 2.** Estimate the diffusivity of ethanol in dilute aqueous solution at 15°C., and compare with the observed value.

*Solution. Arnold's method:*

At 20°C.,
$$D_A = \frac{0.0100\sqrt{\frac{1}{MW_A} + \frac{1}{MW_B}}}{A_A A_B \mu_B^{1/2}(V_A^{1/3} + V_B^{1/3})^2} \tag{5.28}$$

$MW_A$ = mol. wt. ethanol = 46.05

$MW_B$ = mol. wt. water = 18.02

$A_B$ = 4.70 (Table 5.2)

$A_A$ = 1.24 (Table 5.3)

$\mu_B$ = viscosity of water = 1.005 centipoises at 20°C.

$V_A$ = 2(14.8) + 6(3.7) + 7.4 = 59.2 (Table 5.1)

$V_B$ = 18.9 (Table 5.1)

$\therefore D_{\text{ethanol}}$ at 20°C., dilute solution

$$= \frac{0.0100\sqrt{\frac{1}{46.05} + \frac{1}{18.02}}}{1.24(4.70)(1.005)^{1/2}(59.2^{1/3} + 18.9^{1/3})^2}$$

$$= 1.165 \times 10^{-5} \text{ sq. cm./sec.}$$

$$b = 0.020\left(\frac{\mu_B}{\rho_B^{2/3}}\right)^{1/2} \tag{5.30}$$

$\rho_B$ = density of water = 0.9982 gm./cu. cm. at 20°C.

$$b = 0.020\left[\frac{1.005}{(0.9982)^{2/3}}\right]^{1/2} = 0.020$$

From Eq. (5.29):

$$D \text{ at } t_1 = D \text{ at } t_2\left(\frac{1 + bt_1}{1 + bt_2}\right)$$

$$D_{\text{ethanol}} \text{ at } 15°\text{C.} = (1.165 \times 10^{-5})\left[\frac{1 + 0.02(15)}{1 + 0.02(20)}\right]$$

$$= 1.08 \times 10^{-5} \text{ sq. cm./sec.}$$

*Wilke method:* $V_A = 59.2$

From Fig. 5.2, at $\phi = 1.0$ for water, $F_A = 2.35 \times 10^7 = T/D_A\mu_B$. At 15°C., $\mu_B$ = 1.1404 centipoises, $T$ = 288°K.

† The units used in Eq. (5.41) are required for Eq. (5.44).

$$\therefore D_{\text{ethanol}} = \frac{T}{2.35(10^7)\mu_B} = \frac{288}{2.35(10^7)(1.1404)}$$
$$= 1.07 \times 10^{-5} \text{ sq. cm./sec.}$$

"International Critical Tables" (Vol. V, p. 70) lists $D$ at 15°C. for ethanol in water at zero concentration as $1.00 \times 10^{-5}$ sq. cm./sec.

**Illustration 3.** Estimate the diffusivity of ethanol in water as a function of concentration, at 10°C., and compare with the observed data.

*Solution.*

$$\left(\frac{D_A\mu}{T}\right)_{\text{concd}} = \left[\left(\frac{1}{F_A} - \frac{1}{F_B}\right)x_A + \frac{1}{F_A}\right]\left(1 + \frac{d \log \gamma_A}{d \log x_A}\right) \qquad (5.44)$$

From Fig. 5.2, with $V_A = 59.2$, $\phi = 1.0$ for water, $F_A = 2.35 \times 10^7$. With $V_B = 18.9$, $\phi = 0.9$ (estimated for ethanol), $F_B = 0.95 \times 10^7$. At 10°C., $T = 283$°K.

Activity coefficients for ethanol-in-water solution were taken from the data of Chap. 3, Fig. 3.7. These were plotted as $\log \gamma_A$ vs. $\log x_A$ and the slopes of the resulting curve measured at various values of $x_A$. The viscosity of ethanol-water solutions at 10°C. were taken from the "International Critical Tables" (Vol. V, p. 22). The tabulated data and calculations are listed below.

| $x_A$ | $\frac{d \log \gamma_A}{d \log x_A}$ | $\left(\frac{1}{F_A} - \frac{1}{F_B}\right)x_A + \frac{1}{F_A}$ | $\left(\frac{D_A\mu}{T}\right)_{\text{concd}}$ by Eq. (5.44) | $\mu$, viscosity of soln., 10°C., centipoises | Calculated $D_{\text{ethanol}}$, sq. cm./sec. |
|---|---|---|---|---|---|
| 0.0 | —— | —— | —— | 1.308 | $0.921 \times 10^{-5}$ |
| 0.02 | −0.0875 | $0.4124 \times 10^{-7}$ | $0.376 \times 10^{-7}$ | 1.60 | $0.665 \times 10^{-5}$ |
| 0.0416 | −0.123 | $0.3989 \times 10^{-7}$ | $0.350 \times 10^{-7}$ | 2.16 | $0.458 \times 10^{-5}$ |
| 0.0899 | −0.270 | $0.3686 \times 10^{-7}$ | $0.2965 \times 10^{-7}$ | 3.24 | $0.235 \times 10^{-5}$ |
| 0.1439 | −0.442 | $0.3347 \times 10^{-7}$ | $0.1863 \times 10^{-7}$ | 4.10 | $0.1287 \times 10^{-5}$ |

The "International Critical Tables" (Vol. V, p. 70) lists diffusivities for ethanol in water solution at 10°C., up to a concentration of 3.75 gm. mole ethanol/liter. The concentrations were converted to mole fractions using density data from "Chemical Engineers' Handbook" (McGraw-Hill Book Company, Inc., New York, 2d edition, page 439). Calculated and observed data are compared in Fig. 5.4.

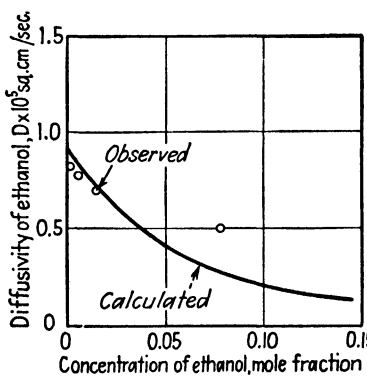



FIG. 5.4. Diffusivity of ethanol in water solutions, 10°C.

**Illustration 4.** The diffusivity of mannitol in water at 20°C. (in dilute solution) is listed in the "International Critical Tables," Vol. V, p. 71, as $0.56 \times 10^{-5}$ sq. cm./sec. Estimate the diffusivity of mannitol at various temperatures up to 70°C., and compare with the observed data.

*Solution.* By Eq. (5.39), $E_{\text{diff}} = E_{\text{vis}}$. Since the solution is dilute, the temperature variation of the viscosity of water can be used to predict the temperature dependency of $D$. According to Eqs. (5.33) and (5.38), semilogarithmic plots of $\mu$ and $D$ against $1/T$ should have slopes which are equal but opposite in sign. Accordingly, in Fig. 5.5, the viscosity

of water was plotted against $1/T$ from the data of "Chemical Engineers' Handbook." The $D$ for mannitol at 20°C. was plotted (the cross symbol in the figure), and a curve whose slope is equal to that of the viscosity curve but opposite in sign was drawn through this point. This curve gives predicted values of $D$ at any temperature and may be compared with the observed data included in the figure. Thus, at 70°C., the predicted $D$ is $1.47 \times 10^{-5}$ sq. cm./sec., and the observed value is $1.56 \times 10^{-5}$ ("International Critical Tables," Vol. V, p. 71).

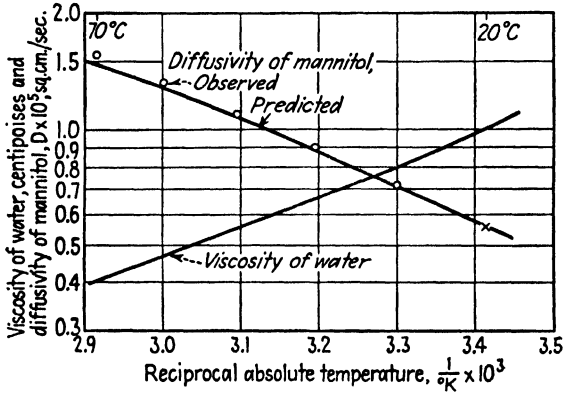



FIG. 5.5. Effect of temperature on the diffusivity of mannitol in water solution.

Alternatively, the Wilke observation that $F_A = T/D_{A\mu B}$ is relatively independent of temperature can be utilized. Since the solution is very dilute, $\mu_B$ is the viscosity of water. At 20°C.,

$$F_A = \frac{273 + 20}{(0.56 \times 10^{-5})(1.005)} = 520 \times 10^5$$

At 70°C.,

$$\mu \text{ for water} = 0.4061 \text{ centipoise}$$

$$\therefore D \text{ at } 70°\text{C.} = \frac{T}{F_{A\mu B'}} = \frac{273 + 70}{(520 \times 10^5)(0.4061)} = 1.62 \times 10^{-5} \frac{\text{sq. cm.}}{\text{sec.}}$$

**Diffusivities of Electrolytes.** *Dilute Solutions.* The diffusion of an electrolyte is complicated by the dissociation of the molecule into ions. Conductivity measurements indicate that the various ions have different mobilities, and consequently it might be assumed that the various ions might diffuse at different rates. This would lead, however, to high local concentrations of positively and negatively charged ions, and the electrostatic forces resulting would slow down the fast ions and speed up the slow. As a result, the ions actually diffuse at equal speeds, and the solution remains electrically neutral. Since the ions are smaller than the undissociated molecules, they diffuse at greater rates.

For complete dissociation, Nernst (20) showed that at infinite dilution the diffusivity of an electrolyte is related to the ionic mobilities in the following manner:

$$D_{\text{dil}} = \frac{R'T\text{U}^+\text{U}^-}{\text{U}^+ + \text{U}^-}\left(\frac{1}{Z^+} + \frac{1}{Z^-}\right)^\dagger \tag{5.45}$$

† The listed units should be used in Eq. (5.45).

where $U^+$ and $U^-$ = absolute velocities of the cation and anion, resp., cm./sec., under a force of 1 dyne at infinite dilution
$Z^+$ and $Z^-$ = valences of the cation and anion, resp.
$R'$ = the gas const., $8.314 \times 10^7$ ergs/(gm. mole) (°K)
$D_{dil}$ = diffusivity at infinite dilution, sq. cm./sec.
$T$ = temp., °K

The ionic velocities, in turn, may be obtained from conductance measurements. Table 5.4 lists values from such sources, recalculated from the tabulation of Partington (22).

TABLE 5.4. IONIC VELOCITIES U AT INFINITE DILUTION, 18°C. CM./SEC. DYNE

| Cation | $U^+ \times 10^{17}$ | $\alpha \times 10^4$ | Anion | $U^- \times 10^{17}$ | $\alpha \times 10^4$ |
|---|---|---|---|---|---|
| $Li^+$ | 35.8 | 265 | $F^-$ | 50.1 | 238 |
| $Na^+$ | 46.6 | 244 | $Cl^-$ | 70.4 | 216 |
| $Ag^+$ | 58.0 | 229 | $I^-$ | 71.6 | 213 |
| $K^+$ | 69.4 | 217 | $Br^-$ | 72.7 | 215 |
| $Tl^+$ | 70.8 | 215 | $SCN^-$ | 60.9 | 221 |
| $Rb^+$ | 72.5 | 214 | $IO_3^-$ | 36.5 | 234 |
| $Cs^+$ | 73.0 | 212 | $C_2H_3O_2^-$ | 37.6* | 238 |
| $H^+$ | 337. | 154 | $ClO_3^-$ | 59.2 | 215 |
| $NH_4^+$ | 69.5 | 222 | $BrO_3^-$ | 51.1 | |
| $\frac{1}{2}Be^{++}$ | 30.1 | | $IO_4^-$ | 51.6 | |
| $\frac{1}{2}Mn^{++}$ | 47.2 | | $ClO_4^-$ | 68.8 | |
| $\frac{1}{2}Co^{++}$ | 46.2 | | $NO_3^-$ | 66.4 | |
| $\frac{1}{2}Ni^{++}$ | 47.2 | | $OH^-$ | 187. | 180 |
| $\frac{1}{2}Fe^{++}$ | 48.3 | | $\frac{1}{2}C_2O_4^{--}$ | 67.6 | 231 |
| $\frac{1}{3}Fe^{+++}$ | 65.5 | | $\frac{1}{2}SO_4^{--}$ | 73.5 | 227 |
| $\frac{1}{3}Cr^{+++}$ | 48.4 | | $\frac{1}{2}CrO_4^{--}$ | 77.4* | |
| $\frac{1}{2}Mg^{++}$ | 49.3 | 256 | $\frac{1}{2}CO_3^{--}$ | 64.5* | 270 |
| $\frac{1}{2}Zn^{++}$ | 50.5 | 254 | $\frac{1}{4}Fe(CN)_6^{----}$ | 102. | |
| $\frac{1}{2}Cu^{++}$ | 49.3 | | | | |
| $\frac{1}{2}Cd^{++}$ | 49.9 | 245 | | | |
| $\frac{1}{2}Sr^{++}$ | 55.7 | 247 | | | |
| $\frac{1}{2}Ca^{++}$ | 55.7 | 247 | | | |
| $\frac{1}{2}Ba^{++}$ | 59.5 | 239 | | | |
| $\frac{1}{2}Pb^{++}$ | 65.3 | 240 | | | |
| $\frac{1}{2}Ra^{++}$ | 62.4 | 239 | | | |
| $\frac{1}{3}Al^{+++}$ | 43.0 | | | | |
| $\frac{1}{3}La^{+++}$ | 65.5 | | | | |
| $\frac{1}{3}Sm^{+++}$ | 57.5 | | | | |
| $\frac{1}{4}Th^{++++}$ | 25.3 | | | | |

Thus, $U_{Li^+} = 35.8 \times 10^{-17}$, $\alpha = 0.0265$.

$\alpha$ = temperature coefficient: $U_{t_2} = U_{t_1}\left[\frac{2 + \alpha(t_2 - t_1)}{2 - \alpha(t_2 - t_1)}\right]$, $t$ in °C.

* Uncertain.

*Concentrated Solutions.* For concentrated solutions, corrections involving activity coefficients and the effect of concentration on the ion mobilities must be included:

$$D_{\text{concd}} = D_{\text{dil}}\left(1 + \frac{\mathbf{m}\partial \ln \gamma_{\pm}}{\partial \mathbf{m}}\right) f(\mathbf{m}) \tag{5.46}$$

where $\mathbf{m}$ = molality of the solution
$\gamma_{\pm}$ = mean ionic activity coefficients referred to molality
$f(\mathbf{m})$ = a correction for effect of concentration on ionic mobilities

At low concentrations, the activity-coefficient term is by far the more important of the corrections. Attempts to evaluate $f(\mathbf{m})$ from theoretical principles are reviewed in detail by Harned (10) and Harned and Owen (11), who show that they have not been particularly useful at high concentrations. Gordon (9) has had considerable success using an empirical evaluation, however:

$$f(\mathbf{m}) = \frac{1}{c_B \overline{V}_B} \frac{\mu_B}{\mu}\dagger \tag{5.47}$$

where $\overline{V}_B$ = the partial molal vol. of the water in solution, cubic centimeters per gram mole
$c_B$ = the number of gram moles of water per cu. cm. of solution
$\mu_B$ = viscosity of water
$\mu$ = viscosity of the solution

This approximation is particularly good in the case of electrolytes dissociating into two univalent ions but less successful for those of higher valences.

**Illustration 5.** Estimate the diffusivity of sodium chloride in water as a function of concentration at 18°C., and compare with observed data.

*Solution.* $D$ at infinite dilution is calculated from ionic mobilities using Eq. (5.45). At 18°C., $U^+$ for $Na^+ = 46.6 \times 10^{-17}$ cm./sec. dyne, $U^-$ for $Cl^- = 70.4 \times 10^{-17}$ cm./sec. dyne } Table 5.4.

$$T = 273 + 18 = 291°\text{K}$$
$$Z^+ = Z^- = 1$$
$$\therefore D_{\text{dil}} = \frac{8.314(10^7)(291)(46.6)(70.4)(10^{-17})^2}{(46.6 + 70.4)10^{-17}}\left(\frac{1}{1} + \frac{1}{1}\right)$$
$$= 1.356 \times 10^{-5} \text{ sq. cm./sec.}$$

Correction for concentration is made by combining Eqs. (5.46) and (5.47).

$$D = D_{\text{dil}}\left(1 + \frac{\mathbf{m}\partial \ln \gamma_{\pm}}{\partial \mathbf{m}}\right) \frac{1}{c_B \overline{V}_B} \frac{\mu_B}{\mu}$$

Mean ionic activity coefficients $\gamma_{\pm}$ at various molalities $\mathbf{m}$ are given at 25°C. by Glasstone ("Thermodynamics for Chemists," p. 402, D. Van Nostrand Company, Inc., N.Y., 1947). These are corrected to 18°C. as follows:

$$\log \frac{\gamma_{18°\text{C}}}{\gamma_{25°\text{C}}} = \frac{\bar{L}_A}{4.576\,\nu}\left(\frac{1}{273 + 18} - \frac{1}{273 + 25}\right)$$

† The listed units should be used in Eq. (5.47).

where $\nu$ number of ions = 2 for NaCl, and $\bar{L}_A$ the relative partial molal enthalpy of NaCl in solution, calories/gm. mole. Values of $\bar{L}_A$ are listed by Lewis and Randall ("Thermodynamics and the Free Energy of Chemical Substances," p. 92, McGraw-Hill Book Company, Inc., New York, 1923). The term $[1 + (\mathbf{m}\partial \ln \gamma_\pm/\partial \mathbf{m})]$ is evaluated as $[1 + (d \log \gamma_\pm/d \log \mathbf{m})]$ by plotting $\log \gamma_\pm$ against $\log \mathbf{m}$ and determining the slopes of the resulting curve at various values of $\mathbf{m}$. Differentiation of empirical expressions for $\gamma_\pm$ as a function of $\mathbf{m}$ is another method of obtaining this quantity.

Values of $c_B$ for various molalities were calculated from density data of "Chemical Engineers' Handbook" (McGraw-Hill Book Company, Inc., New York, 1950). Partial molal volumes $\bar{V}_B$ were calculated from these density data by the method of tangent intercepts described by Lewis and Randall (*loc. cit.*, p. 39). Relative viscosities $\mu/\mu_B$ are available for NaCl solutions at 18°C. in "International Critical Tables" (Vol. V, p. 15). The accompanying tabulation summarizes the results of the various calculations, and Fig. 5.6 compares the calculated results with the experimental data as reported in "International Critical Tables" (Vol. V, p. 67).

| m, molality NaCl | $\gamma_\pm$, 25°C. | $\bar{L}_A$, 18°C. cal./gm. mole | $\gamma_\pm$, 18°C. | $1 + \frac{d \log \gamma_\pm}{d \log m}$ | $c_B$, gm. moles $H_2O$/cu. cm. | $\bar{V}_B$, cu. cm./gm. mole | $\frac{\mu_B}{\mu}$ | $D \times 10^5$ sq. cm./sec. (calculated) |
|---|---|---|---|---|---|---|---|---|
| 0.001 | 0.966 | | 0.966 | 0.979 | 0.0555 | 18.05 | 1.00 | 1.327 |
| 0.005 | 0.929 | | 0.929 | 0.968 | 0.0555 | 18.05 | 1.00 | 1.313 |
| 0.01 | 0.904 | | 0.904 | 0.958 | 0.0555 | 18.05 | 1.00 | 1.300 |
| 0.02 | 0.875 | | 0.875 | 0.943 | 0.0555 | 18.05 | 0.998 | 1.278 |
| 0.05 | 0.823 | −5 | 0.823 | 0.922 | 0.0554 | 18.05 | 0.995 | 1.244 |
| 0.1 | 0.778 | −12 | 0.778 | 0.915 | 0.0553 | 18.05 | 0.992 | 1.230 |
| 0.2 | 0.732 | −30 | 0.732 | 0.915 | 0.0552 | 18.05 | 0.983 | 1.222 |
| 0.5 | 0.679 | −122 | 0.676 | 0.915 | 0.0549 | 18.03 | 0.962 | 1.205 |
| 1.0 | 0.656 | −332 | 0.651 | 0.995 | 0.0544 | 18.00 | 0.922 | 1.265 |
| 2.0 | 0.670 | −561 | 0.662 | 1.080 | 0.0533 | 17.95 | 0.838 | 1.280 |
| 3.0 | 0.719 | −738 | 0.708 | 1.174 | 0.0524 | 17.91 | 0.753 | 1.278 |

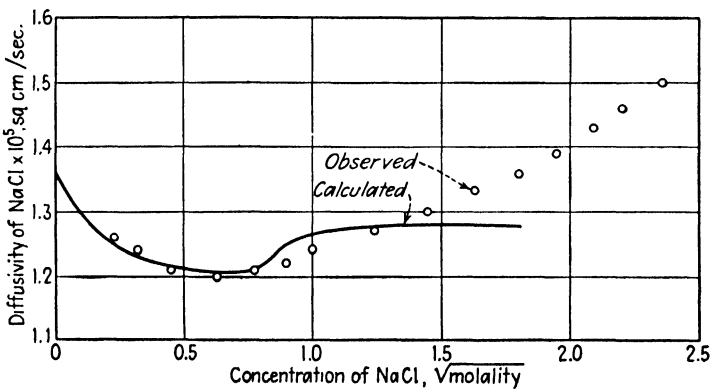



FIG. 5.6. Diffusivity of NaCl in water solution, 18° C.

Figure 5.7 shows the results of other calculations of the same type, compared with reported data for concentrations ranging from 0.01 to 0.2 normal, where the correction $f(\mathbf{m})$ is practically equal to unity, and temperatures ranging from 10 to 18°C. Each plotted point represents a different electrolyte. At these concentrations agreement between observed and calculated results are obviously excellent.

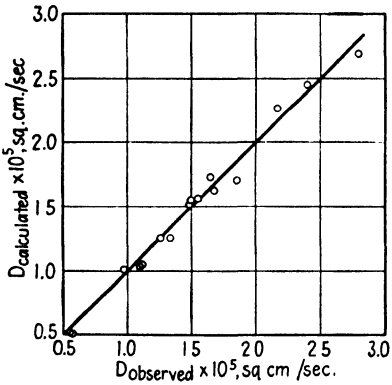



FIG. 5.7. Comparison of observed and predicted diffusivities of strong electrolytes in water solution.

These methods cannot be employed for weak electrolytes, where the properties of the solution cannot be approximated from the properties of the individual ions. The presence of large concentrations of undissociated molecules which diffuse at a slower rate than the ions prevents direct application of the methods described, and no satisfactory substitute is as yet available.

## EDDY DIFFUSION

The transfer of matter through a fluid flowing in turbulent flow is a much more complicated process than molecular diffusion, and its analysis depends primarily upon our understanding of the flow phenomenon. In turbulent flow, eddies exist within the body of the fluid which carry with them any dissolved solute in bulk. Since the velocities of the eddies are great in comparison to the velocities of molecular diffusion, it is to be expected that eddy diffusion, or the transfer of the solute under such conditions, is much the more rapid process.

As Dryden (4) emphasizes, turbulence is a lack of uniformity in the flow conditions, characterized by an irregular fluctuation of the fluid velocity at any point from instant to instant. Two factors are ordinarily required to express the degree of turbulence in quantitative fashion, the *intensity* and the *scale*. Intensity is defined as the root-mean-square fluctuation of velocity at any point. The scale relates the fluctuations at different points within the fluid at the same instant and has been quantitatively defined by Taylor (28) as the area under a curve of the correlation between the velocity fluctuation at two points taken perpendicular to the line joining the points plotted against the distance between the points. The scale may be taken as the size of an eddy.

Provided that the distances considered are large in comparison to the scale, or eddy size, the rate of eddy diffusion should be proportional to the concentration gradient. On this basis, Sherwood and others (13, 25, 26)

have been successful in treating eddy diffusion in terms of an eddy diffusivity $E$ defined in a manner analogous to Fick's law for molecular diffusion:

$$N_A = -E_A S \frac{dc_A}{dl} \tag{5.48}$$

Sherwood's work with eddy diffusion in gases (26, 30) has shown that the eddy diffusivity is constant over the central core of a gas stream in turbulent flow and, as was to be expected, is not only much larger numerically than the molecular diffusivity (of the order of 100 times as great as the gaseous $D$) but also independent of the molecular weight of the diffusing substance except in so far as the turbulence of the stream is thereby affected. Kalinske and Pien (13), working with the eddy diffusion of HCl in liquid water, obtained values of $E$ of the order of $10^{12}$ times as great as the molecular diffusivity in liquid water.

Since the transfer of the diffusing solute is a bulk transfer rather than the slow, molecular diffusion, the nature of the eddying and the velocity gradient in the fluid should provide a means of estimating the eddy diffusivity Thus, if viscosity is defined by the following equation for laminar flow:

$$\tau = \mu \frac{dv}{dl} \tag{5.49}$$

where $\tau$ = the shearing stress

$dv/dl$ = the velocity gradient in the fluid

then by analogy an eddy viscosity $\epsilon$ for turbulent flow can be defined (19) as

$$\tau = (\mu + \epsilon) \frac{dv}{dl} \tag{5.50}$$

and $\epsilon$ should be obtainable from measurements of velocity gradients. By analogy to a similar treatment for heat transfer (4, 19, 26) it can further be shown that $E$ should equal $\epsilon/\rho$. In the case of certain gaseous diffusion experiments (26), $E = 1.6\ (\epsilon/\rho)$, while in the eddy diffusion of HCl in liquid water (13) where the velocity gradient could not be measured accurately, it is reported that values of $E$ compared well with those of $\epsilon/\rho$. Much work remains to be done before eddy diffusivities can be calculated with confidence.

## MASS-TRANSFER COEFFICIENTS

The complete diffusion process ordinarily occurs through successive regions of a fluid in laminar and turbulent flow. It is to be expected that in the laminar-flow region the rate of diffusion would be proportional to $D$, while in the turbulent region proportional to $E$. In the region between those strictly in laminar and turbulent flow, the nature of the change from laminar flow to turbulence is obviously of importance. The Prandtl-Taylor concept of a strictly laminar film with a well-defined boundary

separating it from the turbulent region has been shown to be incorrect, and there exists instead a gradual change from one condition to the other. Many attempts to account for this change have been made, and an excellent review of the developments as they apply to diffusion problems is provided by Sherwood (25). In view of our relative lack of knowledge concerning the eddy-diffusion process, it seems best at present to describe the rate of diffusion by expressions paralleling those for molecular diffusion, and attempt to include the effects of both phenomena by use of a fictitious laminar film whose thickness, the "effective" film thickness, is sufficient to account for the total resistance to mass transfer. Thus, Eqs. (5.22) and (5.24) become

$$N_A = \frac{D_A Sc(c_{A_1} - c_{A_2})}{c_{BM}l} = \frac{D_A Sc(x_{A_1} - x_{A_2})}{x_{BM}l} \tag{5.51}$$

where l is the effective film thickness for combined molecular and eddy diffusion. Equation (5.51) may be simplified by introducing a mass-transfer film coefficient $k$ as follows:

$$k = \frac{D_A}{x_{BM}l} \tag{5.52a}$$

and

$$N_A = kS(c_{A_1} - c_{A_2}) = kSc(x_{A_1} - x_{A_2}) \tag{5.52b}$$

**Two-film Concept.** Let us now apply this concept to a typical transfer of a solute from one liquid to another nonconsolute liquid in contact with it, under steady-state conditions. Assuming both liquids to be in motion in a general direction parallel to the interface between them, there will exist concentration gradients in both phases which act as driving forces for the transfer, and the resistance to diffusion can be represented by an effective film thickness for each phase. This picture of the complete mass-transfer process was first introduced by Whitman (16, 31), who also postulated that at the interface itself equilibrium would be established. The concentrations in each phase on either side of the interface and immediately in contact with it would be such that they correspond to an indefinitely long time of contact. There is no direct evidence to prove the latter concept; indeed there have been a few experiments reported indicating the contrary (12). Nevertheless the general conclusions based on the assumption appear to be valid.

Figure 5.8 indicates graphically the situation just described. Here concentration of the diffusing substance is plotted as a function of the distance through the two-phase system. The interfacial surface between the liquids is imagined to be in a plane perpendicular to that of the paper and is thus seen only as a line. The two liquid phases are designated as $E$ and $R$, and the subscripts on the concentration terms $c$ refer to the various positions in the system, $i$ for interface, $E$ and $R$ for the main portion

of the corresponding phases. It is understood that only concentrations of the distributed, diffusing substance are being considered. In the $R$ phase, $c_R$ is the average, main-body concentration of diffusing substance such as would be obtained by analyzing a sample of the mixed liquid. By virtue of the concentration gradient $c_R - c_{Ri}$, the diffusing substance is transferred through the eddy- and laminar-flow portions of the $R$ phase to the interface, the equivalent molecular diffusional resistance for which is represented by the effective film thickness $l_R$. Equilibrium concentrations pertain at the interface, so that $c_{Ei}$ is in equilibrium with $c_{Ri}$, the relationship between them given by the equilibrium-distribution curve for the system. There is consequently no diffusional resistance at the interface, and the diffusing substance passes into the $E$ phase. The concentration gradient $c_{Ei} - c_E$ then provides the driving force for diffusion into the main body of the $E$ phase, where the average concentration is $c_E$. The equivalent molecular diffusional resistance is represented by the effective film thickness $l_E$.

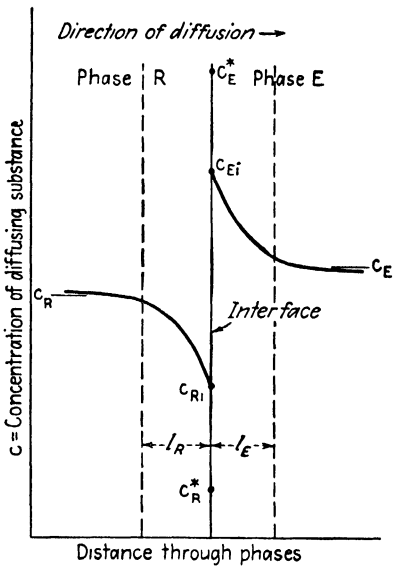



FIG. 5.8. Concentration gradients.

It might at first be thought that the concentration difference $c_{Ei} - c_R$ would represent a barrier or a concentration gradient operating in a direction such as to oppose the forward movement of the diffusing substance. It should be recalled, however, that if all portions of the two phases were in equilibrium, so that the concentrations of the distributed substance were represented by horizontal lines at $c_{Ri}$ in the $R$ phase and $c_{Ei}$ in the $E$ phase, the concentration difference $c_{Ei} - c_{Ri}$ would still exist, and yet there would be no net diffusion from $E$ to $R$. The apparent concentration barrier would disappear if activities were used rather than concentrations, and the driving forces of Fig. 5.8 would be represented by a continuous drop as we moved from $R$ to $E$.

It is instructive to plot the concentrations on a distribution diagram, as in Fig. 5.9. The equilibrium-distribution curve will contain the point $(c_{Ei},c_{Ri})$, and the point represented by main-body concentrations $(c_E,c_R)$ will be below the equilibrium curve. The driving-force concentration gradients for each phase are indicated as $\Delta c_E$ and $\Delta c_R$, respectively. In applying Eq. (5.52*b*), let us consider the differential rate of transfer $dN$ which will occur through differential interfacial surface $dS$. Further,

since the thickness of the fictitious film through which most of the concentration gradient occurs is very small, so that the solute content of the films is negligible with respect to the total solute present, under steady-state conditions the rate of transfer of solute through the $E$ phase equals that through the $R$ phase. Consequently,

$$\left.\begin{aligned} dN &= k_R\,dS(c_R - c_{Ri}) = k_E\,dS(c_{Ei} - c_E) \\ &= k_R\,dS\,\Delta c_R = k_E\,dS\,\Delta c_E \\ &= k_R\,dSc(x_R - x_{Ri}) = k_E\,dSc(x_{Ei} - x_E) \end{aligned}\right\} \tag{5.53}$$

$$\frac{k_R}{k_E} = \frac{c_{Ei} - c_E}{c_R - c_{Ri}} = \frac{\Delta c_E}{\Delta c_R} \tag{5.54}$$

**Over-all Coefficients.** In most practical situations, the ratio $k_R/k_E$ is not known. Ordinary sampling of the liquids and analysis will give the coordinates $c_E$ and $c_R$ on Fig. 5.9, but it is ordinarily impossible to approach the

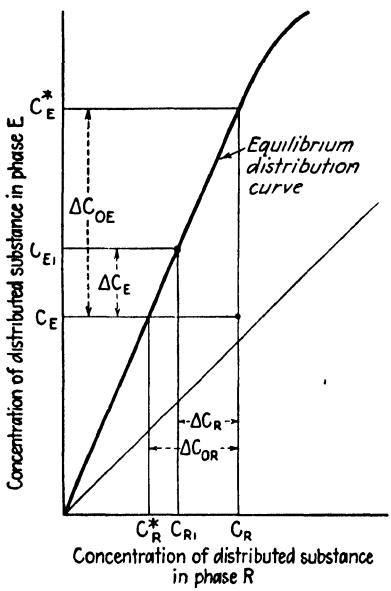



FIG. 5.9. Over-all and individual film driving forces.

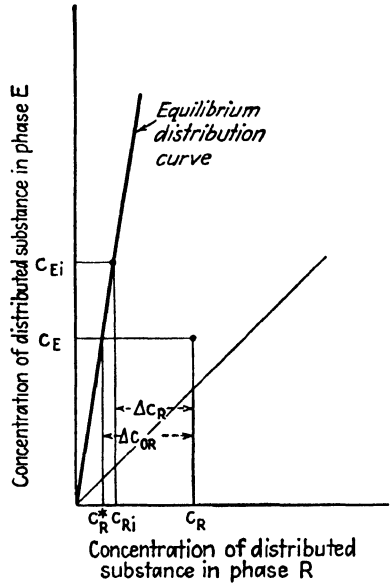



FIG. 5.10. Principal diffusional resistance in phase $R$.

interface sufficiently closely and to sample the liquids accurately enough so that $c_{Ei}$ and $c_{Ri}$ can be determined. The true film driving forces $\Delta c_E$ and $\Delta c_R$ cannot then be obtained. If the equilibrium-distribution curve is a straight line, so that at all concentrations encountered $c_{Ei}$ is proportional to $c_{Ri}$,

$$c_{Ei} = mc_{Ri} \tag{5.55}$$

we may define a concentration $c_E^*$ which would be in equilibrium with $c_R$:

$$c_E^* = mc_R \tag{5.56}$$

We may then represent the complete transfer process in both phases in the following manner:

$$dN = K_E\, dS(c_E^* - c_E) = K_E\, dS\, \Delta c_{OE} \tag{5.57}$$

where $K_E$ is an over-all mass-transfer coefficient based on an over-all concentration gradient $\Delta c_{OE}$ in the $E$ phase. Similarly $c_R^*$ is defined as a concentration in equilibrium with $c_E$,

$$c_E = mc_R^* \tag{5.58}$$

and

$$dN = K_R\, dS(c_R - c_R^*) = K_R\, dS\, \Delta c_{OR} \tag{5.59}$$

where $K_R$ is an over-all mass-transfer coefficient based on an over-all concentration gradient in the $R$ phase.

Elimination of $c_{Ei}$, $c_{Ri}$, and $c_R$ from Eqs. (5.53), (5.55), and (5.56) (16) results in

$$dN = \frac{1}{(1/k_E) + (m/k_R)}\, dS(c_E^* - c_E) \tag{5.60}$$

Comparison with Eq. (5.57) shows therefore that

$$\frac{1}{K_E} = \frac{1}{k_E} + \frac{m}{k_R} \tag{5.61}$$

Similarly,

$$\frac{1}{K_R} = \frac{1}{k_R} + \frac{1}{mk_E} \tag{5.62}$$

and the terms $1/k_E$, $m/k_R$, $1/k_R$, and $1/mk_E$ may be considered the resistances of the individual films. If the equilibrium distribution of the diffusing substance strongly favors the $E$ phase, $m$ will be very large; provided $k_E$ and $k_R$ are of comparable order of magnitude, $K_R$ will nearly equal $k_R$, and we may conclude that the principal resistance to diffusion lies in the $R$ phase. Graphical interpretation of such a situation is shown in Fig. 5.10,

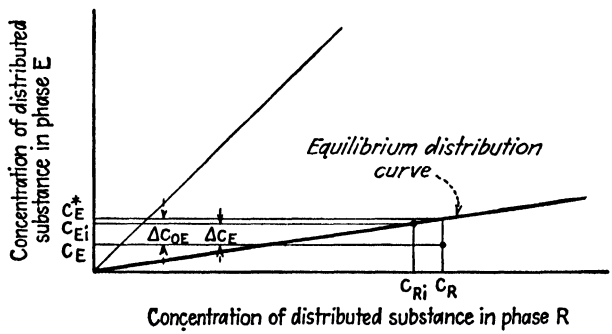



FIG. 5.11. Principal diffusional resistance in phase $E$.

where $\Delta c_{OR}$ is very nearly equal to $\Delta c_R$. In such instances Eq. (5.59) is ordinarily used to describe the operations. Similarly if $m$ is very small and the distributed substance favors the $R$ phase, $K_E$ will nearly equal $k_E$, the resistance in the $E$-phase controls, and Eq. (5.57) is used. Figure 5.11 represents this situation.

In continuously operating extraction processes, each phase undergoes wide concentration changes as it flows through the equipment. The point on the concentration diagrams whose coordinates are $(c_R,c_E)$ therefore represents only one position in such equipment, and the rate equations (Eqs. (5.53), (5.57), and (5.59)) are "instantaneous," or point conditions. In applying them to actual operations, therefore, they will have to be integrated over the concentration range which the liquids experience. Clearly if the simple distribution law, Eq. (5.55), is not applicable, wide variation with concentration of the over-all coefficients $K_E$ and $K_R$ can be expected even if $k_E$ and $k_R$ remain constant. Since the factors upon which $k_E$ and $k_R$ depend are also likely to vary, the use of the over-all coefficients is definitely limited.

### Notation for Chapter 5

Since this chapter deals largely with diffusivities and in most cases these are reported and used in C.G.S. units, the following table lists only C.G.S. units for the various quantities. Most of the equations of the chapter can be used with consistent English units as well, except where there have been included certain dimensional constants. These are all marked.

$A$ = abnormality factor, Eq. (5.28).
$a$ = activity.
$b$ = temperature coefficient of diffusivity, Eqs. (5.29), (5.30).
$c$ = concentration, gm. moles/cu. cm.
$D$ = molecular diffusivity, or diffusion coefficient, sq. cm./sec.
$d$ = differential operator.
$E$ = eddy diffusivity, sq. cm./sec.
$E_{\text{diff}}$ = energy of activation for diffusion, cal./gm. mole.
$E_{\text{vis}}$ = energy of activation for viscous flow, cal./gm. mole.
$\Delta E_V$ = internal energy of vaporization, cal./gm. mole.
$e$ = base of natural logarithms, 2.7183.
$F$ = defined by Eq. (5.41), °K sec./sq. cm. centipoises.
$f$ = function.
$\Delta H_V$ = enthalpy of vaporization, cal./gm. mole.
$K$ = over-all mass transfer coefficient, $\frac{\text{gm. moles}}{\text{sec. sq. cm. (gm. moles/cu. cm.)}}$.
$k$ = mass transfer film coefficient, $\frac{\text{gm. moles}}{\text{sec. sq. cm. (gm. moles/cu. cm.)}}$.
$\mathbf{k}$ = Boltzmann constant, $1.38 \times 10^{-16}$ ergs/°K.
$k'$ = specific rate constant for viscous flow and diffusion.
$k''$ = constant.
$k'''$ = constant.
$\bar{L}$ = relative partial molal enthalpy, cal./gm. mole.
$l$ = distance in direction of diffusion, cm.
$\mathbf{l}$ = effective or fictitious film thickness, cm.
ln = natural logarithm.
log = common logarithm.
$MW$ = molecular weight.
$m$ = distribution coefficient, for concentrations expressed as gm. moles/cu. cm.

$\mathbf{m}$ = concentration, molality.
$N$ = rate of diffusion or mass transfer, gm. moles/sec.
$n$ = constant.
$R$ = the gas constant, 1.987 cal./(gm. mole)(°K).
$R'$ = the gas constant, $8.314 \times 10^7$ ergs/(gm. mole)(°K).
$r$ = radius of a sphere, cm.
$S$ = cross-sectional area perpendicular to the direction of diffusion, sq. cm.
$T$ = absolute temperature, °K.
$t$ = temperature, °C.
U = absolute velocity of an ion at infinite dilution, cm./sec. dyne.
$u$ = velocity of diffusion, cm./sec.
$V$ = molal volume, cu. cm./gm. mole.
$\overline{V}$ = partial molal volume, cu. cm./gm. mole.
$v$ = average velocity in a fluid in the general direction of flow, cm./sec.
$w$ = final average liquid concentration, gm. moles/cu. cm.
$x$ = concentration, mole fraction.
$Z$ = valence of an ion.
$\alpha$ = temperature coefficient of ionic velocity (Table 5.4).
$\gamma$ = activity coefficient.
$\gamma\pm$ = mean ionic activity coefficient for an electrolyte, referred to molality.
$\epsilon$ = eddy viscosity, gm/cm. sec.
$\theta$ = time, sec.
$\lambda, \lambda_1, \lambda_2, \lambda_3$ = intermolecular distances, Eq. (5.32), cm.
$\mu$ = viscosity, gm./cm. sec. In Eqs. (5.28), (5.30), (5.41), and (5.44), and in Fig. 5.2, the unit must be centipoises.
$\nu$ = number of ions per molecule.
$\pi$ = 3.14159.
$\rho$ = density, gm./cu. cm.
$\tau$ = shearing stress parallel to direction of flow, gm./cm. sec.
$\phi$ = $F$ for a solvent/$F$ for water (Fig. 5.2).
$\partial$ = partial differential operator.

Subscripts:

$A$ = component $A$, the diffusing substance.
$B$ = component $B$, the solvent.
$E$ = phase $E$.
$i$ = interface.
$M$ = mean.
$O$ = over-all.
$R$ = phase $R$.
dil = dilute, infinite dilution
concd = concentrated.
1, 2 = positions 1 and 2, resp.

Superscripts:

0 = initial.
+ = cation.
− = anion.

## LITERATURE CITED


1. Arnold, J. H.: *J. Am. Chem. Soc.* **52,** 3937 (1930).
2. ———: *Trans. Am. Inst. Chem. Engrs.* **40,** 361 (1944).
3. Cohen, E., and H. R. Bruins: *Z. physik. Chem.* **103,** 337 (1923).
4. Dryden, H. L.: *Ind. Eng. Chem.* **31,** 416 (1939).
5. Einstein, A.: *Ann. Physik.* **17,** 549 (1905); **19,** 371 (1906).
6. Eyring, H.: *J. Chem. Phys.* **4,** 283 (1936).
7. Fick, A.: *Ann. Physik.* **94,** 59 (1855).
8. Glasstone, S., K. J. Laidler, and H. Eyring: "The Theory of Rate Processes," McGraw-Hill Book Company, Inc., New York, 1941.
9. Gordon, A. R.: *J. Chem. Phys.* **5,** 522 (1937).
10. Harned, H. S.: *Chem. Rev.* **40,** 461 (1947).
11. ——— and B. O. Owen: "The Physical Chemistry of Electrolytic Solutions," Reinhold Publishing Corporation, New York, 1943.
12. Higbie, L.: *Trans. Am. Inst. Chem. Engrs.* **31,** 365 (1935).
13. Kalinske, A. A., and C. L. Pien: *Ind. Eng. Chem.* **36,** 220 (1944).
14. Kincaid, J. F., H. Eyring, and A. E. Stearn: *Chem. Rev.* **28,** 301 (1941).
15. Lewis, W. K., and K. C. Chang: *Trans. Am. Inst. Chem. Engrs.* **21,** 135 (1928).
16. Lewis, W. K., and W. G. Whitman: *Ind. Eng. Chem.* **16,** 1215 (1924).
17. Maxwell, J. C.: *Phil. Trans. Royal Soc.* **157,** 49 (1866).
18. McBain, J. W., and T. H. Liu: *J. Am. Chem. Soc.* **53,** 59 (1931).
19. Murphree, E. V.: *Ind. Eng. Chem.* **24,** 727 (1932).
20. Nernst, W.: *Z. physik. Chem.* **2,** 613 (1888).
21. Newman, A. B.: *Trans. Am. Inst. Chem. Engrs.* **27,** 310 (1931).
22. Partington, J. R.: In "Treatise on Physical Chemistry," H. S. Taylor, Ed., 2d ed., p. 673, D. Van Nostrand Company, Inc., New York, 1930.
23. Powell, R. E., W. E. Roseveare, and H. Eyring: *Ind. Eng. Chem.* **33,** 430 (1941).
24. Sherwood, T. K.: "Absorption and Extraction," McGraw-Hill Book Company, Inc., New York, 1937.
25. ———: *Trans. Am. Inst. Chem. Engrs.* **36,** 817 (1940).
26. ——— and B. B. Woertz: *Trans. Am. Inst. Chem. Engrs.* **35,** 517 (1939).
27. Stefan, J.: *Wien. Sitzungsber.* **63,** 63 (1871).
28. Taylor, G. I.: *Proc. Roy. Soc.* (*London*) **A 151** (873), 421 (1935); **A 156** (888), 307 (1936).
29. Taylor, H. S.: *J. Chem. Phys.* **6,** 331 (1938).
30. Towle, W. L., and T. K. Sherwood: *Ind. Eng. Chem.* **31,** 457 (1939).
31. Whitman, W. G.: *Chem. Met. Eng.* **29,** 147 (1923).
32. Wilke, C. R.: *Chem. Eng. Progress* **45,** 218 (1949).
33. Williams, J. W., and L. C. Cady: *Chem. Rev.* **14,** 171 (1934).

# CHAPTER 6

## METHODS OF CALCULATION I. STAGEWISE CONTACT WITH A SINGLE SOLVENT

The separation of the components of a solution by extraction may be brought about in a number of ways, depending upon the nature of the solvent system and the physical arrangement of the apparatus employed. A convenient classification is the following:

1. Single solvent systems, including all those which consist of, or which may be reduced to the equivalent of, three components: the two to be separated, and the solvent.
   *a*. Stagewise contact. In this category are included those arrangements of equipment where solvent and mixture to be separated are intimately contacted, allowed to approach equilibrium, and separated. The operation may then be repeated and with a variety of flowsheets.
   *b*. Continuous contact. This includes arrangements where solvent and mixture to be separated are continuously in contact within the equipment for the entire operation. Equilibrium is not ordinarily approached.
2. Mixed solvents. This includes those arrangements employing a solvent solution consisting of at least two components, where the solubility relationships are such that simplification to the equivalent of a ternary system is not feasible.
   *a*. Stagewise contact.
   *b*. Continuous contact.
3. Double solvents (fractional extraction). This category includes those arrangements where the mixture to be separated is distributed between two immiscible solvents. The systems contain at least four components.
   *a*. Stagewise contact.
   *b*. Continuous contact.

In this chapter only stagewise contact with single solvents is considered.

**Distillation Analogy.** In studying the various processes of extraction, it is frequently helpful to keep in mind the parallel processes of distillation, which are generally more familiar. The analogy between the two methods of separation has been pointed out by several writers (13, 14). In distillation processes, a mixture of two substances is separated by creation of two

phases, one liquid and one vapor, by the addition of heat, and the separation is brought about by virtue of the fact that the relative concentration of the substances is different in the two phases. Subsequent condensation of the vapor phase is brought about by removal of heat. In extraction, two liquid phases are formed by the addition of an immiscible solvent, which then becomes the analog of heat. Since the relative concentration of the substances to be separated is different in the two phases, physical settling of the liquid layers produces the desired degree of separation. Removal of solvent from the solvent-rich phase is then analogous to condensation of the vapor in the case of distillation. Table 6.1 indicates the analogous situations.

TABLE 6.1. EXTRACTION-DISTILLATION ANALOGY

| Operation or Condition in Extraction | Distillation Analogy |
|---|---|
| Addition of solvent | Addition of heat |
| Solvent mixer | Reboiler |
| Removal of solvent | Removal of heat |
| Solvent separator | Condenser |
| Solvent-rich solution saturated with solvent | Vapor at the boiling point |
| Solvent-rich solution containing more solvent than that required to saturate it | Superheated vapor |
| Solvent-lean solution, containing less solvent than that required to saturate it | Liquid below the boiling point |
| Solvent-lean solution saturated with solvent | Liquid at the boiling point |
| Two-phase liquid mixture | Mixture of liquid and vapor |
| Selectivity | Relative volatility |
| Change of temperature | Change of pressure |

**Definitions.** A *stage* is a mechanical device or series of devices wherein the solution to be separated and an immiscible solvent are intimately mixed, allowed to approach equilibrium, and then settled or separated into two immiscible liquid phases which are then withdrawn. The solvent-rich phase leaving the stage is termed the *extract*, the solvent-lean phase the

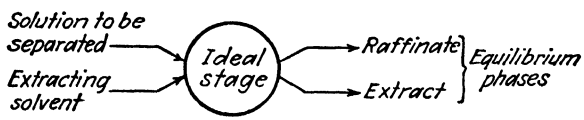



FIG. 6.1. The ideal stage.

*raffinate*. A *theoretical* or *ideal* stage is one where contact between phases is sufficiently intimate and maintained for a sufficient period of time that distribution equilibrium is established, so that raffinate and extract are equilibrium solutions. Although there are many varieties and combinations of mixers and settlers used for this purpose, in this chapter the ideal stage will be designated diagrammatically by a circular figure, as in Fig. 6.1.

**Design Diagrams.** The interrelationship among the phase equilibria, number of stages, and concentrations and weights of various streams in an extraction process can best be worked out graphically on a diagram showing the phase equilibria. Many types of diagrams can be used, and certain coordinate systems are more convenient than others, depending upon the nature of the phase equilibria and the process. Three types will be considered here:

1. *Triangular Coordinates.* Customarily, ternary-phase-equilibrium data are described in the literature on triangular diagrams, and since they are capable of depicting all concentration characteristics of such systems, they are most useful. The general properties of these coordinates are described in Chap. 2, to which reference should now be made. In connection with the use of such diagrams in this chapter, the following scheme of notation will be applied:

$A$, $B$, and $C$ will represent the three pure components of the ternary system. $A$ and $C$ are the principal components of the solution to be separated, $B$ the pure extracting solvent. In Type 1 ternary systems, $A$ and $B$ are partially miscible; in Type 2 systems, the pairs $A$–$B$ and $B$–$C$ are partially miscible. The symbols will also represent the weight of these components. Thus, $A$ will mean $A$ pounds of component $A$, $B$ will mean $B$ pounds of component $B$, etc. $F$, $E$, and $R$ will designate feed, extract, and raffinate solutions, respectively, both with respect to weight and composition. Thus, the symbol $F$ will represent $F$ pounds of a feed solution of composition indicated by point $F$ on the triangular diagram. Other solutions and mixtures will be designated by appropriate symbols, in each case the symbol representing not only the weight but also the composition as indicated on the phase diagram. Weight fraction compositions will be designated by $X$ with appropriate subscripts as described in Chap. 2. Thus, $X_{AB}$ = weight fraction of $A$ in a $B$-rich solution, $X_{CE}$ = weight fraction of $C$ in the extract, $X_{BF}$ = weight fraction of $B$ in the feed, etc. It should be noted that moles and mole fractions may be substituted throughout for weights and weight fractions, if desired.

Stages are numbered, and when these numbers are used as subscripts they ordinarily indicate streams issuing from the indicated stage. Thus, $X_{CR_2}$ = weight fraction of $C$ in the raffinate from stage 2. $R_n$ = weight of raffinate from the $n$th stage, etc.

The length of a line on a phase diagram between two points $O$ and $P$ will be represented by $\overline{OP}$, as in Fig. 6.2*a*. A mixture at $O$, when added to one at $P$, results in a new mixture at $K$ on the straight line $OP$, such that

$$\frac{O}{P} = \frac{\overline{KP}}{\overline{OK}} \tag{6.1}$$

Similarly, removing $P$ from $K$ yields $O$ on the line $PK$ extended. Tie lines will be shown lighter in weight than other construction lines.

2. *Janecke Diagram.* This system of coordinates, described in Chap. 2, involves plotting **X**, the weight fraction of $C$ on a $B$-free basis as abscissa against $N$, the weight of $B$ per unit weight of $B$-free solution as ordinate, as in Fig. 6.2*b*. Thus,

$$\mathbf{X} = \frac{X_C}{X_A + X_C}, \qquad N = \frac{X_B}{X_A + X_C} \tag{6.2}$$

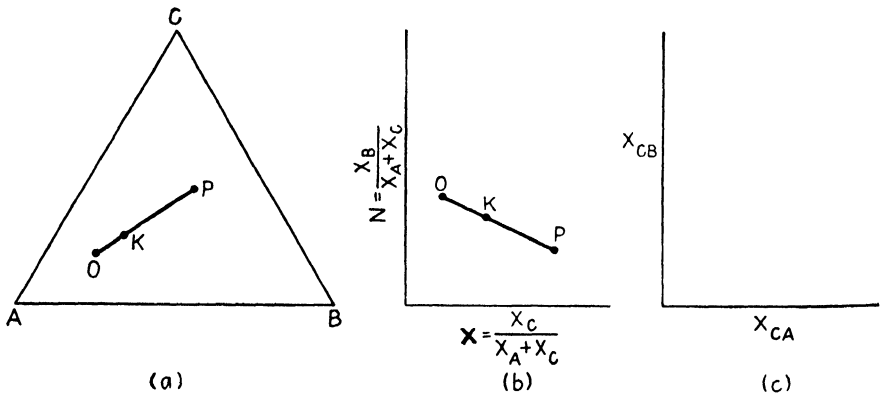



FIG. 6.2. Coordinate systems for extraction calculations. (*a*) triangular, (*b*) Janecke, (*c*) distribution.

As in the case of triangular diagrams, the symbols $E$, $A$, $R$, etc. will represent both weight and composition as indicated on the diagram of liquids $E$, $A$, and $R$. Boldface symbols will represent the $B$-free weights of the designated streams. Thus, $\mathbf{R}_2$ represents the combined weight of $A$ and $C$ in the raffinate from stage 2. The total and $B$-free weights of a stream $P$ are related in the following manner:

$$P = \mathbf{P}(1 + N_P) \tag{6.3}$$

The weight of $B$ in the solution $P$ will be

$$B_P = \mathbf{P}N_P \tag{6.4}$$

The length of the line between points $O$ and $P$ will be indicated by $\overline{OP}$ and, as in the case of triangular coordinates, moles and mole fractions may be used in place of weights and weight fractions.

On the Janecke diagram, as on triangular coordinates, if a mixture at $O$ is added to one at $P$, the resulting mixture $K$ will be on the straight line $OP$, and the weights are in the following relationship:

$$\frac{\mathbf{O}}{\mathbf{P}} = \frac{\overline{KP}}{\overline{OK}} \tag{6.5}$$

Likewise, removing $P$ from $K$ results in $O$ on the line $PK$ extended. Tie lines and construction lines will be shown light and heavy, respectively.

3. *Simple Distribution Diagram.* On these coordinates $X_{CA}$ is plotted as abscissa against $X_{CB}$ as ordinate, as in Fig. 6.2*c*. Modification of these coordinates, in cases where the liquids $A$ and $B$ may be considered substantially insoluble, will be described as they are needed.

Calculations may ordinarily be worked out on any of these diagrams, but for certain systems, because of overcrowding of the phase relationships in a given region of the plot, one or the other of the diagrams may not be convenient for graphical computation. It is therefore desirable to be familiar with the use of all. Properties of the diagrams other than those used here, the complete interrelationship between them, and other useful coordinate systems are described at length in a series of articles by Randall and Longtin (13).

**Flowsheet Arrangements.** Stagewise single-solvent extraction can be brought about in several fashions, depending upon the arrangement of the stages, each yielding different results. Thus, we have

1. Single contact. This involves the use of a single stage, where solution to be separated and extracting solvent are contacted once and extract and raffinate phases separated. Operation may be batchwise or continuous. The distillation analog is flash vaporization or equilibrium distillation.

2. Differential extraction. This is a batch operation wherein a definite amount of solution to be extracted is contacted with differential portions of extracting solvent, the differential portions of extract being removed as fast as formed. The operation is exactly analogous to differential distillation and has been termed "cocurrent infinite stage" by Varteressian and Fenske (22).

3. Cocurrent multiple contact. This may be batch or continuous and is an extension of the single contact wherein the raffinate is contacted repeatedly with fresh extracting solvent. In the limit represented by an infinite number of stages, this becomes the same as differential extraction.

4. Countercurrent multiple contact. This method involves the use of a cascade of stages, extracting solvent and solution to be extracted entering at opposite ends of the cascade. Extracts and raffinates flow countercurrently. The operation is more analogous to gas absorption than to any distillation practice. It is necessarily continuous but may be simulated in batch fashion, in the laboratory for example, as "pseudo countercurrent multiple contact."

5. Countercurrent multiple contact with reflux. This is a continuous operation analogous to fractional distillation. A cascade of stages is employed, with feed solution to be separated customarily entering somewhere in the middle of the cascade and extracting solvent at one end. Extract and raffinate phases flow countercurrently, with reflux provided at both ends of the cascade. Alternatively, reflux may be used only at one end of the cascade, corresponding to the enriching or stripping practices of distillation.

## SINGLE CONTACT

**Triangular Coordinates.** The flowsheet, with indicated weights of the various streams, is shown in Fig. 6.3*a* (22). While ordinarily the solution to be extracted consists solely of a mixture of $A$ and $C$, and the extracting solvent is pure $B$, in the general case all three components will be present in

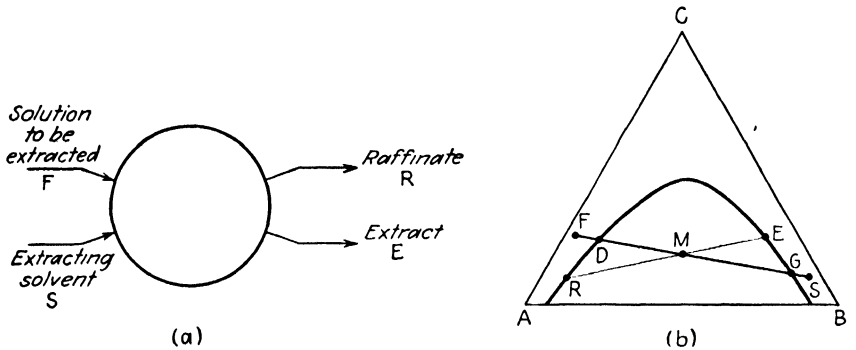



FIG. 6.3. Single-contact extraction.

these streams, as indicated by the positions of the points $F$ and $S$ on Fig. 6.3*b*. Here the curve $RDEG$ is a typical binodal-solubility curve of a Type 1 system, enclosing an area of two liquid phases. A material balance for the operation is

$$F + S = R + E = M \tag{6.6}$$

$M$, representing the mixture of feed and solvent, is in the two-liquid-phase region, as indicated on the diagram. Its location can be determined graphically on the line $FS$ through the relationship

$$\frac{F}{S} = \frac{\overline{MS}}{\overline{FM}} \tag{6.7}$$

or analytically by calculating its composition by material balances. Thus, a $C$ balance is

$$FX_{CF} + SX_{CS} = MX_{CM} \tag{6.8}$$

from which

$$X_{CM} = \frac{FX_{CF} + SX_{CS}}{M} = \frac{FX_{CF} + SX_{CS}}{F + S} \tag{6.9}$$

Similarly, by a $B$ balance,

$$X_{BM} = \frac{FX_{BF} + SX_{BS}}{M} = \frac{FX_{BF} + SX_{BS}}{F + S} \tag{6.10}$$

Equations (6.9) and (6.10) will locate point $M$. Alternatively, to determine the quantity of solvent needed for a given feed in order to produce a predetermined $M$, Eq. (6.10) may be solved for $S$:

$$S = \frac{F(X_{BM} - X_{BF})}{X_{BS} - X_{BM}} \tag{6.11}$$

In the mixer of the ideal stage, equilibrium is established, so that the two-phase mixture $M$ produces extract and raffinate solutions $E$ and $R$, the products of the operation, located on opposite ends of the tie line through $M$. The compositions of the streams $E$ and $R$ must be determined graphically on the diagram (which may involve trial-and-error tie-line interpolation). Their weights may be computed either graphically,

$$\frac{R}{E} = \frac{\overline{EM}}{\overline{RM}} \tag{6.12}$$

or by material balance. Thus, a $C$ balance:

$$EX_{CE} + RX_{CR} = MX_{CM} \tag{6.13}$$

Solving simultaneously with Eq. (6.6) gives

$$E = \frac{M(X_{CM} - X_{CR})}{X_{CE} - X_{CR}} \tag{6.14}$$

Equation (6.6) then permits calculation of $R$.

In the operation of such a plant, it is clear that if the mixture $M$ is not within the two-liquid-phase area, no separation by extraction will occur. Consequently there is a minimum amount of solvent which will locate $M$ at point $D$, given by

$$S_{\min} = F\left(\frac{\overline{FD}}{\overline{DS}}\right) = \frac{F(X_{BD} - X_{BF})}{X_{BS} - X_{BD}} \tag{6.15}$$

which results in a maximum of raffinate of composition $D$ and no extract. There is also a maximum amount which will locate $M$ at $G$,

$$S_{\max} = F\left(\frac{\overline{GF}}{\overline{GS}}\right) = \frac{F(X_{BG} - X_{BF})}{X_{BS} - X_{BG}} \tag{6.16}$$

resulting in a maximum of extract of composition $G$ and no raffinate. A real plant must use an amount of solvent between these limits.

**Stage Efficiency.** The theoretical stage produces as effluent two streams, extract and raffinate, which are in equilibrium. However, if agitation is inadequate or if insufficient time of contact is maintained between solvent and solution to be extracted, the streams issuing from the stage will not be in equilibrium, or, as it is expressed, the stage efficiency is less than 100 per cent. Refer to Fig. 6.4. When solvent $S$ is added to feed $F$, at first two saturated phases at $D$ and $G$ are very

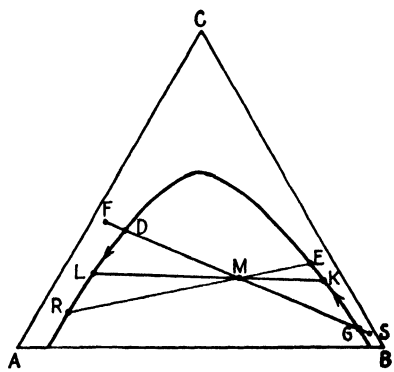



FIG. 6.4. Diffusion in a theoretical stage.

quickly produced (6), which will be dispersed one within the other if agitation is sufficiently vigorous. Diffusion of the various components of the mixture, a relatively slow process, then gradually changes the compositions of the phases along the solubility curve through $L$ and $K$, eventually to $R$ and $E$ at opposite ends of the tie line through $M$, representing the mixture as a whole. Only if the compositions $R$ and $E$ are realized is the stage considered a theoretical stage.

**Solvent Recovery.** Although not strictly part of the extraction operation, all such separations are ordinarily followed by removal of solvent from the extract and raffinate solutions to give the finished products. Figure 6.5 shows a typical extraction solvent recovery scheme. Distillation is

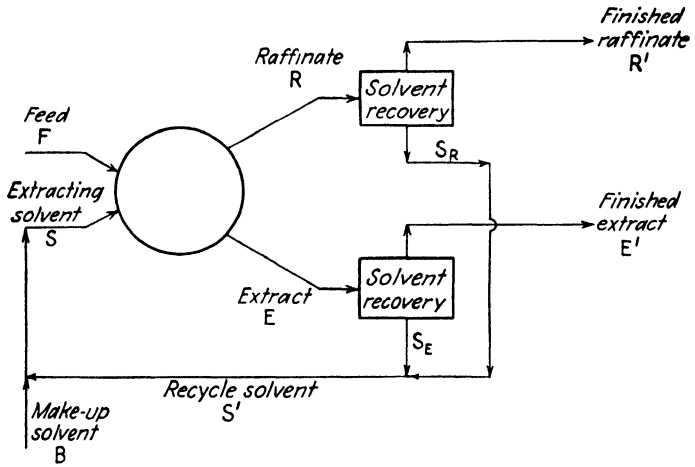



FIG. 6.5. Single-contact extraction with solvent recovery.

ordinarily used to remove the solvent from the solutions, and if it is assumed that relative volatilities are comparatively low so that incomplete solvent separation results, two recovered solvents, $S_E$ from the extract and $S_R$ from the raffinate, are produced. The finished products $E'$ and $R'$ also carry some of the unremoved solvent. The recovered solvents are mixed to give the recycle solvent $S'$, make-up solvent (usually pure $B$) is added to balance the loss of solvent in the finished streams $E'$ and $R'$, and the resulting mixture $S$ used again in extraction.

The entire series of operations can be followed conveniently on the triangular diagram, as in Fig. 6.6. When solvent $S_R$ is removed from raffinate $R$, finished raffinate $R'$ results. Material balances on the raffinate solvent recovery:

Over-all: $$R' + S_R = R \tag{6.17}$$

Component $B$: $$R'X_{BR'} + S_RX_{BS_R} = RX_{BR} \tag{6.18}$$

Solving simultaneously,

$$R' = \frac{R(X_{BS_R} - X_{BR})}{X_{BS_R} - X_{BR'}} \tag{6.19}$$

Similarly, removal of solvent $S_E$ from extract $E$ results in finished extract $E'$, the quantity of which may be calculated in a similar manner:

$$E' = \frac{E(X_{BS_E} - X_{BE})}{X_{BS_E} - X_{BE'}} \tag{6.20}$$

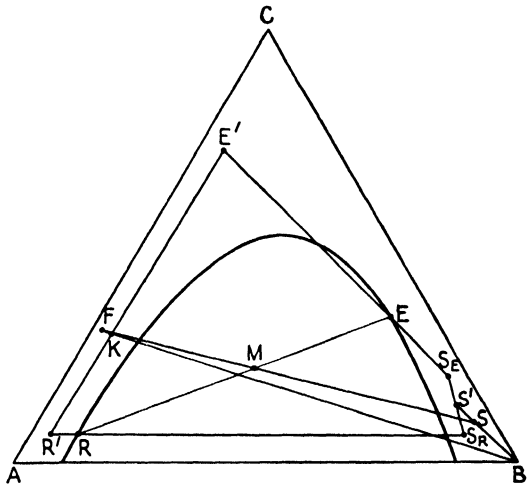



FIG. 6.6. Single-contact extraction with solvent recovery.

If desired, the products $R'$and $E'$ may be computed graphically:

$$R' = R\left(\frac{\overline{RS}_R}{\overline{R'S}_R}\right), \qquad E' = E\left(\frac{\overline{ES}_E}{\overline{E'S}_E}\right) \tag{6.21}$$

Further,

$$S_R = R - R' \tag{6.22}$$

and

$$S_E = E - E' \tag{6.23}$$

Recycle solvent:

$$S' = S_R + S_E \tag{6.24}$$

Extraction solvent:

$$S = S' + B \tag{6.25}$$

For the plant as a whole, including extraction and solvent recovery,

$$F + B = E' + R' = K \tag{6.26}$$

$B$ balance:

$$FX_{BF} + B = E'X_{BE'} + R'X_{BR'} \tag{6.27}$$

Consequently the make-up solvent is

$$B = E'X_{BE'} + R'X_{BR'} - FX_{BF} \tag{6.28}$$

As a result of the complete operation, therefore, the feed $F$ has been separated into two solutions, one at $E'$ rich in $C$, the other at $R'$, rich in $A$.

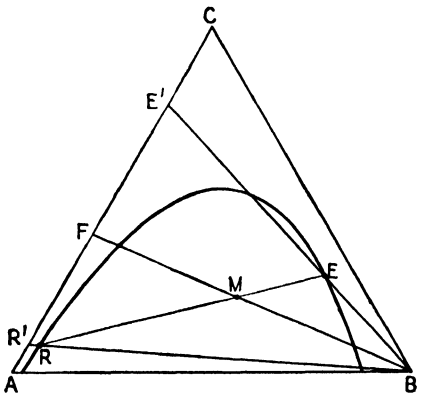



FIG. 6.7. Simplified diagram for single-contact extraction with solvent recovery.

In the frequently arising situation where the feed consists solely of $A$ and $C$, where pure $B$ is the solvent and solvent recovery is substantially complete so that

$$S = S_E + S_R = B \quad (6.29)$$

the diagram is much simplified, as in Fig. 6.7. For such a situation, $E'$ and $R'$ are on the $A$–$C$ axis of the diagram, and all of the equations developed above apply with the additional simplifications that $X_{BS} = X_{BB} = 1$, and $X_{CS} = X_{BF} = X_{BE'} = X_{BR'} = 0$.

Consider the situation described in the diagram of Fig. 6.8*a*. The point $E'$, where $E'B$ is tangent to the binodal curve, is clearly the maximum possible concentration of $C$ in a finished extract, and can be realized for all feeds with $C$ concentrations between $X_{CF'}$ and $X_{CE'}$. It is also clear that $X_{CE'}$ in this diagram represents the maximum concentration of $C$ in any feed that can be processed. Similarly, referring to Fig. 6.8*b*, the maximum

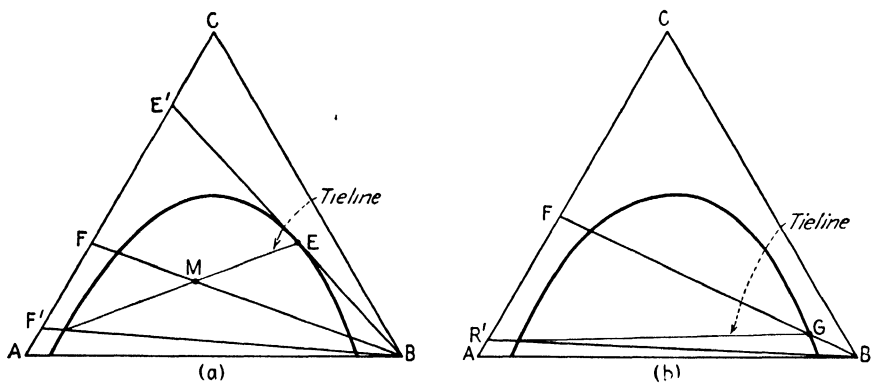



FIG. 6.8. Maximum concentrations: (*a*) extract, (*b*) raffinate.

possible concentration of $A$ in the finished raffinate $R'$ is obtained by using the maximum amount of solvent with zero yield of raffinate. There is no absolute upper limit to the $A$ concentration in the raffinate, but the actual maximum depends on the feed composition.

Type 2 ternary systems are handled in the same fashion as those of Type 1, and the construction diagrams for the general and simplified cases are

shown in Fig. 6.9. All the equations previously developed apply. For such systems there is no absolute upper limit to the purity of $C$ in the finished extract or of $A$ in the finished raffinate, with the actual maxima for a given feed depending upon the tie lines through points G and D.

**Janecke Diagram.** Calculations for the flowsheet of Fig. 6.4 can be followed on the Janecke diagram if it is recalled that the $B$-free weights of the various streams are **F, S, E, E′, R, R′,** $\mathbf{S}_E$, $\mathbf{S}_R$, and **S′**. For the feed stream, the coordinates are $N_F$(lb. $B$)/(lb. $A$ + lb. $C$), $\mathbf{X}_F$(lb. $C$)/(lb. $A$ + lb. $C$), etc. Figure 6.10 shows the construction for a Type 1 system (the construction is identical for Type 2 systems, but the solubility curve has the appearance shown in Fig. 2.20*b*. Points $F$ and $S$ corresponding to feed and extracting solvent are first located, and the point $M$ located on the line $FS$ either graphically,

$$\frac{\mathbf{F}}{\mathbf{S}} = \frac{\overline{MS}}{\overline{FM}} \tag{6.30}$$

or analytically by a series of material balances. Thus,

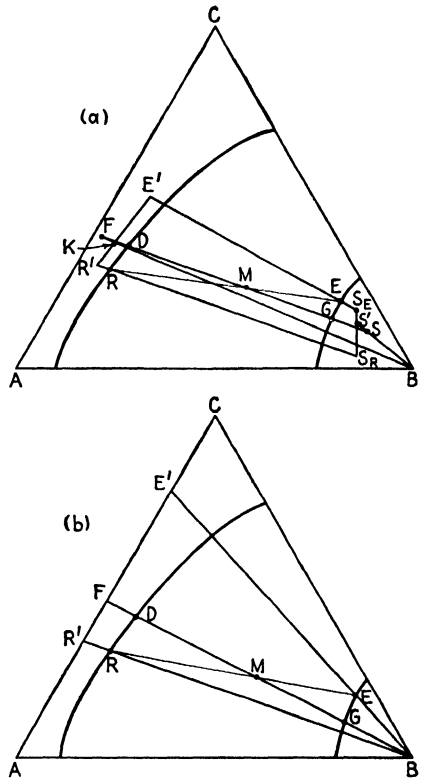



FIG. 6.9. Single-contact extraction with solvent recovery, Type 2 systems: (*a*) general case, (*b*) simplified case.

$(A + C)$ balance: $$\mathbf{F} + \mathbf{S} = \mathbf{E} + \mathbf{R} = \mathbf{M} \tag{6.31}$$

$B$ balance: $$\mathbf{F}N_F + \mathbf{S}N_S = \mathbf{M}N_M \tag{6.32}$$

$$\therefore N_M = \frac{\mathbf{F}N_F + \mathbf{S}N_S}{\mathbf{M}} = \frac{\mathbf{F}N_F + \mathbf{S}N_S}{\mathbf{F} + \mathbf{S}} \tag{6.33}$$

$C$ balance: $$\mathbf{F}\mathbf{X}_F + \mathbf{S}\mathbf{X}_S = \mathbf{M}\mathbf{X}_M \tag{6.34}$$

$$\mathbf{X}_M = \frac{\mathbf{F}\mathbf{X}_F + \mathbf{S}\mathbf{X}_S}{\mathbf{M}} = \frac{\mathbf{F}\mathbf{X}_F + \mathbf{S}\mathbf{X}_S}{\mathbf{F} + \mathbf{S}} \tag{6.35}$$

Equations (6.33) and (6.35) give the coordinates of $M$, with which the point may be located. In case the amount of solvent must be determined in

order to provide a predetermined location for $M$, Eq. (6.33) may be solved for **S**:

$$\mathbf{S} = \frac{\mathbf{F}(N_M - N_F)}{N_S - N_M} \tag{6.36}$$

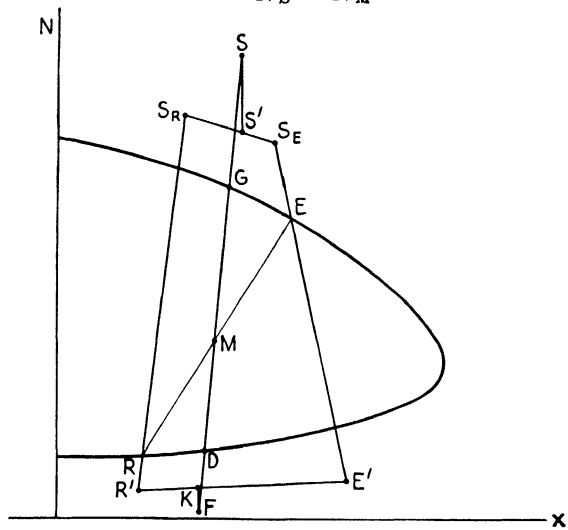



FIG. 6.10. Single-contact extraction and solvent recovery on Janecke coordinates.

Extract and raffinate concentrations are found graphically by locating the tie line through $M$, as shown in the figure. The weights of these streams may be calculated graphically:

$$\frac{\mathbf{R}}{\mathbf{E}} = \frac{\overline{EM}}{\overline{MR}} \tag{6.37}$$

or by material balances:

$B$ balance: $$\mathbf{E}N_E + \mathbf{R}N_R = \mathbf{M}N_M \tag{6.38}$$

Solving simultaneously with Eq. (6.31),

$$\mathbf{E} = \mathbf{M}\left(\frac{N_M - N_R}{N_E - N_R}\right) \tag{6.39}$$

Equation (6.31) then permits calculation of **R**.

The minimum amount of solvent that can be used will place $M$ at point $D$ (Fig. 6.9):

$$\mathbf{S}_{\min} = \frac{\mathbf{F}(N_D - N_F)}{N_S - N_D} \tag{6.40}$$

The maximum amount of solvent places $M$ at $G$:

$$\mathbf{S}_{\max} = \frac{\mathbf{F}(N_G - N_F)}{N_S - N_G} \tag{6.41}$$

As before, real plants must use solvent quantities between these limits.

**Solvent Recovery.** As in the case of the triangular coordinates, the finished raffinate $R'$ results from removal of solvent $S_R$ from raffinate $R$.

$(A + C)$ balance: $$\mathbf{S}_R + \mathbf{R}' = \mathbf{R} \tag{6.42}$$

$B$ balance: $$\mathbf{S}_R N_{S_R} + \mathbf{R}' N_{R'} = \mathbf{R} N_R \tag{6.43}$$

$$\therefore \mathbf{R}' = \frac{\mathbf{R}(N_R - N_{S_R})}{N_{R'} - N_{S_R}} \tag{6.44}$$

Similarly,

$$\mathbf{E}' = \frac{\mathbf{E}(N_E - N_{S_E})}{N_{E'} - N_{S_E}} \tag{6.45}$$

and

$$\mathbf{S}_E + \mathbf{E}' = \mathbf{E} \tag{6.46}$$

The recycle solvent: $$\mathbf{S}' = \mathbf{S}_E + \mathbf{S}_R \tag{6.47}$$

$$\mathbf{S}' N_{S'} = \mathbf{S}_E N_{S_E} + \mathbf{S}_R N_{S_R} \tag{6.48}$$

$$\mathbf{S}' \mathbf{X}_{S'} = \mathbf{S}_E \mathbf{X}_{S_E} + \mathbf{S}_R \mathbf{X}_{S_R} \tag{6.49}$$

$S'$ is fortified by addition of pure $B$, to give the extraction solvent $S$. On Fig. 6.10, the addition of pure $B$, for which $N_B = \infty$, is shown by the vertical line $S'S$. Consequently $\mathbf{X}_{S'} = \mathbf{X}_S$, $\mathbf{S} = \mathbf{S}'$, and make-up solvent $B$:

$$B = \mathbf{S}(N_S - N_{S'}) \tag{6.50}$$

For the plant as a whole,

$$F + B = R' + E' = K \tag{6.51}$$

Consequently point $K$ is on the line $R'E'$, vertically above (or below) $F$, so that $\mathbf{X}_K = \mathbf{X}_F$. Further, the make-up solvent $B$ can be calculated by a plant $B$ balance:

$$B = \mathbf{E}' N_{E'} + \mathbf{R}' N_{R'} - \mathbf{F} N_F \tag{6.52}$$

Having calculated the $B$-free weights of all streams, the total weights and $B$ content may be determined by Eqs. (6.3) and (6.4).

In the simplified case, feed and finished extract and raffinate solutions are $B$-free, and pure $B$ is the extracting solvent. Refer to Fig. 6.11. Addition of solvent to the feed is shown by the vertical line $FM$ and removal of solvent from raffinate and extract streams by vertical lines $RR'$ and $EE'$. Equations (6.31) to (6.35), (6.37) to (6.39) all apply, with the simplification that

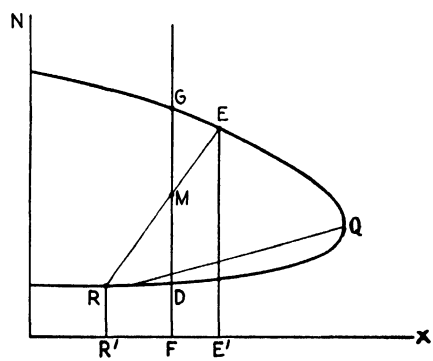



FIG. 6.11. Single-contact extraction, simplified case.

$\mathbf{S} = 0$, $N_S = \infty$, $\mathbf{S}N_S = B$, $\mathbf{X}_S = 0$, $\mathbf{F} = \mathbf{M}$, $\mathbf{E}' = \mathbf{E}$, $\mathbf{R}' = \mathbf{R}$. In place of Eqs. (6.36), (6.40), and (6.41), $B$ may be calculated by

$$B = \mathbf{F}(N_M - N_F) \tag{6.53}$$

$$B_{\min} = \mathbf{F}(N_D - N_F) \tag{6.54}$$

$$B_{\max} = \mathbf{F}(N_G - N_F) \tag{6.55}$$

Figure 6.11 also shows that the maximum possible concentration of $C$ in a finished extract will result when sufficient solvent is used to give an extract at $Q$, the point of maximum abscissa on the solubility curve.

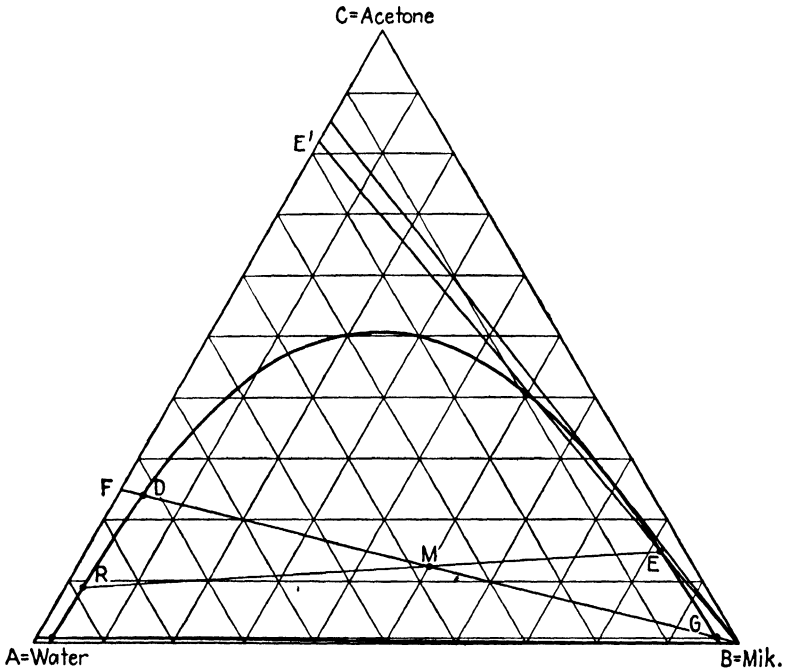



FIG. 6.12. Solution of Illustration 1. Acetone–water–methyl isobutyl ketone at 25° C. [*Ind. Eng. Chem.* **33**, 1240 (1941)].

**Types of Problems.** The principal quantities in the extraction process are $F$, $X_F$, $E$, $X_E$, $R$, $X_R$, $S$, and $X_S$. Of these, $F$, $X_F$, and $X_S$ are ordinarily fixed by the process. Only one of the remaining quantities can be arbitrarily fixed, whereupon the remainder are no longer under control but are determined by the characteristics of the equilibrium diagram.

**Distribution Diagram.** Although computations for single-contact extraction can be carried out on distribution-diagram coordinates, it is inconvenient because a trial-and-error solution is required; hence description of this method is omitted.

**Illustration 1.** One hundred pounds of a solution containing 25% acetone ($C$), 75% water ($A$) by weight are to be extracted with methyl isobutyl ketone (MIK) ($B$) at

25°C. Calculate (*a*) minimum quantity of solvent, (*b*) maximum quantity of solvent, (*c*) the weights of solvent-free extract and raffinate for 100 lb. of solvent and the per cent acetone extracted, (*d*) the maximum possible purity of *C* in the finished extract, and (*e*) the maximum possible purity of *A* in the raffinate.

*Solution.* Equilibrium data of Othmer, White, and Treuger will be used [*Ind. Eng. Chem.* **33**, 1240 (1941)]. Calculations will be made on triangular and Janecke coordinates.

*a.* Triangular coordinates (Fig. 6.12). Point *F* corresponding to the feed solution is located. Pure *B* is the solvent. The minimum quantity of solvent will give a mixture with the feed at *D*. $F = 100$; $X_{BD} = 0.036$.

Eq. (6.15):

$$S_{\min} = B_{\min} = \frac{F(X_{BD} - X_{BF})}{X_{BS} - X_{BD}} = \frac{100(0.036 - 0)}{1 - 0.036} = 3.74 \text{ lb.} \quad \textit{Ans.}$$

Janecke diagram (Fig. 6.13):

$$\mathbf{X}_F = \frac{25}{100} = 0.25,$$
$$N_F = 0,$$
$$\mathbf{F} = 100 \text{ lb.},$$
$$N_D = 0.04$$

Eq. (6.54):

$$B_{\min} = \mathbf{F}(N_D - N_F) = 100(0.04 - 0) = 4 \text{ lb.} \quad \textit{Ans.}$$

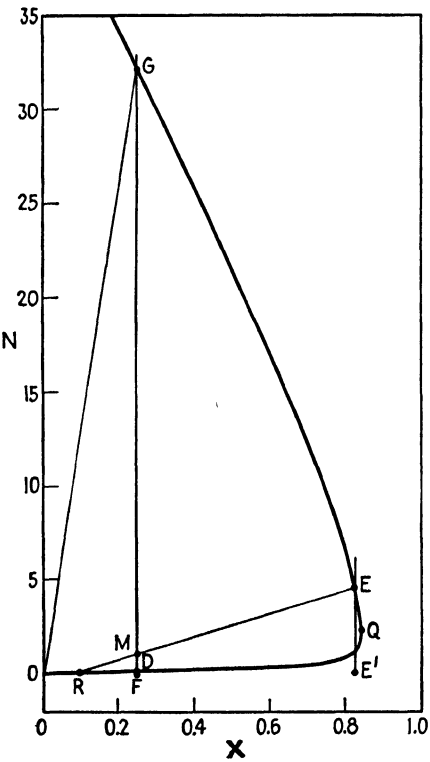



FIG. 6.13. Solution of Illustration 1 on Janecke coordinates.

(NOTE: Discrepancies by the two methods are due entirely to errors incurred in graphical construction.)

*b.* Triangular coordinates. Maximum solvent will give a mixture with the feed at *G*. $X_{BG} = 0.97$.

Eq. (6.16): $$B_{\max} = \frac{F(X_{BG} - X_{BF})}{X_{BS} - X_{BG}} = \frac{100(0.97 - 0)}{1 - 0.97} = 3{,}210 \text{ lb.} \quad \textit{Ans.}$$

Janecke diagram: $N_G = 32$.

Eq. (6.55): $$B_{\max} = \mathbf{F}(N_G - N_F) = 100(32 - 0) = 3{,}200 \text{ lb.} \quad \textit{Ans.}$$

*c.* Triangular coordinates. $S = B = 100$ lb.

Eq. (6.6): $$F + S = M = E + R$$
$$100 + 100 = M = 200 \text{ lb.}$$

Eq. (6.10): $$X_{BM} = \frac{FX_{BF} + SX_{BS}}{M} = \frac{100(0) + 100(1)}{200} = 0.50$$

Locate point $M$. $X_{CM} = 0.125$. Locate the tie line through $M$ with the help of a tie-line correlation curve and the available data, to give points $E$ and $R$. From the graph, $X_{CE} = 0.15$, $X_{BE} = 0.818$; $X_{CR} = 0.09$, $X_{BR} = 0.023$.

Eq. (6.14): $$E = \frac{M(X_{CM} - X_{CR})}{X_{CE} - X_{CR}} = \frac{200(0.125 - 0.09)}{0.15 - 0.09} = 116.8 \text{ lb.}$$

Eq. (6.6): $$R = M - E = 200 - 116.8 = 83.2 \text{ lb.}$$

Lines $BE$ and $BR$ are extended to $E'$ and $R'$. From the graph, $X_{CR'} = 0.093$, $X_{BR'} = 0$; $X_{CE'} = 0.829$, $E_{BE'} = 0$.

Eq. (6.20): $$E' = \frac{E(X_{BS_E} - X_{BE})}{X_{BS_E} - X_{BE'}} = \frac{116.8(1 - 0.818)}{1.0 - 0} = 21.3 \text{ lb.} \quad Ans.$$

$$R' = F - E' = 100 - 21.3 = 78.7 \text{ lb.} \quad Ans.$$

Per cent of the acetone of the feed which was extracted $= \frac{E'X_{CE'}}{FX_{CF}}(100)$

$$= \frac{21.3(0.829)(100)}{100(0.25)}$$

$$= 70.5\%. \quad Ans.$$

Janecke diagram:

$B = 100$ lb., $\mathbf{S} = 0$, $SN_S = B$, $\mathbf{X}_S = 0$, $\mathbf{M} = \mathbf{F} = 100$ lb.

Eq. (6.33): $$N_M = \frac{\mathbf{F}N_F + \mathbf{S}N_S}{\mathbf{M}} = \frac{100(0) + 100}{100} = 1.0$$

Eq. (6.35): $$\mathbf{X}_M = \frac{\mathbf{F}\mathbf{X}_F + \mathbf{S}\mathbf{X}_S}{\mathbf{M}} = \mathbf{X}_F = 0.25$$

After locating the point $M$ and the tie line, the coordinates of $E$ and $R$ are obtained: $N_E = 4.55$, $N_R = 0.0235$.

Eq. (6.39): $$\mathbf{E} = \frac{\mathbf{M}(N_M - N_R)}{N_E - N_R} = \frac{100(1 - 0.0235)}{4.55 - 0.0235} = 21.5 \text{ lb.} = E' \quad Ans.$$

Eq. (6.31): $\mathbf{R} = \mathbf{M} - \mathbf{E} = 100 - 21.5 = 78.5$ lb. $= R'$ *Ans.*

Eq. (6.3): $E = \mathbf{E}(1 + N_E) = 21.5(1 + 4.55) = 119.3$ lb.
$R = \mathbf{R}(1 + N_R) = 78.5(1 + 0.0235) = 80.3$ lb.

*d.* Triangular coordinates. Draw the tangent from $B$ to the binodal curve. The corresponding $X_{CE'} = 0.852$, or 85.2% acetone. *Ans.*

Janecke diagram. The greatest value of $\mathbf{X}_C$ on the binodal curve at $Q$ is 0.840. This corresponds to 84.0% acetone. *Ans.*

*e.* Triangular coordinates. Draw the tie line through $G$, locating the corresponding $R$ and $R'$. $X_{AR'}$ for this point $= 0.995$, or 99.5% water. *Ans.*

Janecke diagram. The tie line through $G$ gives $\mathbf{X}_{CR} = \mathbf{X}_{CR'} = 0.005$, corresponding to 0.5% acetone or 99.5% water. *Ans.*

Part (*c*) of Illustration 1 was recalculated for quantities of solvent other than the 100 lb. used in the illustration, with the interesting results shown in Fig. 6.14. The percentage of acetone extracted from the feed rises rapidly with increasing solvent up to roughly 90 per cent with 300 lb. solvent/100 lb. feed Additional solvent results in little additional extraction and correspondingly greater dilutions of the extract. The maximum

concentration of acetone in the solvent-free extract occurs at point P. These curves are fairly typical of calculations with this type of system, although it must be kept in mind that with other systems different equilibria may have great influence.

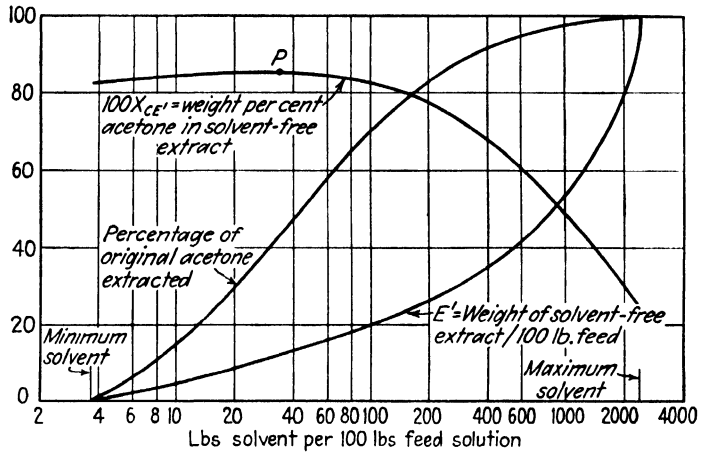



FIG. 6.14 Extraction of a 25 per cent acetone–water solution with methyl isobutyl ketone at 25°C.

## DIFFERENTIAL EXTRACTION

Differential extraction, as previously pointed out, is analogous in many respects to differential distillation. It is not used industrially and is of interest principally as a laboratory procedure and because it represents the limiting result of increasing the number of stages of a cocurrent extraction. Like its distillation counterpart, actual operations can probably only approach the more or less ideal situation described below.

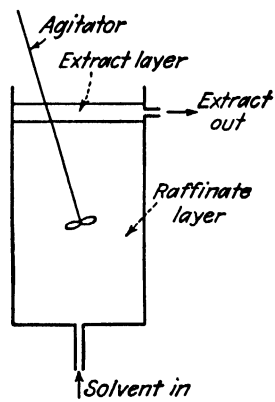



FIG. 6.15. Differential extraction.

Imagine the container of Fig. 6.15 filled initially with a solution $F$ to be extracted. Solvent $S$ is admitted slowly to the bottom of the container (if the solvent has a lower specific gravity than the solution). If the initial solution is not saturated, *i.e.*, not located on the binodal curve of a phase diagram, the first portions of solvent added will dissolve until the solution is saturated. Further addition of solvent results in the formation of an extract layer which collects at the top where it is immediately withdrawn. Thorough agitation should be maintained within the vessel so that the extract leaving is at all times in equilibrium with the raffinate solution remaining behind.

Calculations will be described in connection with the triangular coordinates of Fig. 6.16. The solvent required to saturate the feed $F$, bringing it to the condition of $R_0$, will be by a $B$ balance,

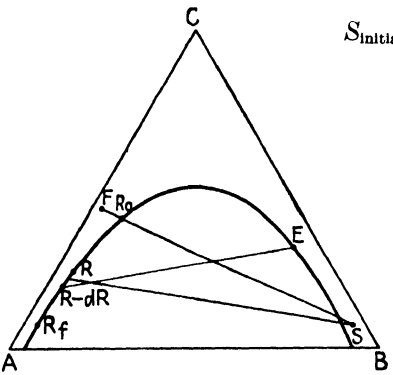



FIG. 6.16. Differential extraction on triangular coordinates.

$$S_{\text{initial}} = F\left(\frac{\overline{FR_0}}{\overline{R_0S}}\right) = \frac{F(X_{BR_0} - X_{BF})}{X_{BS} - X_{BR_0}} \tag{6.56}$$

At a later stage in the process, after extract has begun to form, let the raffinate in the container be $R$. By addition of a differential amount of solvent $dS$ the raffinate layer is reduced by an amount $dR$, producing an extract layer at $E$ of an amount $dE$, at the opposite end of a tie line. The new raffinate, $R-dR$, has a composition $X_{AR}-dX_{AR}$, $X_{BR}-dX_{BR}$, $X_{CR}-dX_{CR}$. A total material balance for the process:

$$R + dS = (R - dR) + dE \tag{6.57}$$

$$dS = dE - dR \tag{6.58}$$

$C$ balance:

$$RX_{CR} + X_{CS}\,dS = (R - dR)(X_{CR} - dX_{CR}) + X_{CE}\,dE \tag{6.59}$$

$$X_{CS}\,dS = X_{CE}\,dE - R\,dX_{CR} - X_{CR}\,dR \tag{6.60}$$

$A$ balance:

$$RX_{AR} + X_{AS}\,dS = (R - dR)(X_{AR} - dX_{AR}) + X_{AE}\,dE \tag{6.61}$$

$$X_{AS}\,dS = X_{AE}\,dE - R\,dX_{AR} - X_{AR}\,dR \tag{6.62}$$

Eliminating $dS$ and $dE$ from Eqs. (6.58), (6.60), and (6.62),

$$\frac{dR}{R} = \frac{dX_{CR}/(X_{CS} - X_{CE}) - dX_{AR}/(X_{AS} - X_{AE})}{(X_{CS} - X_{CR})/(X_{CS} - X_{CE}) - (X_{AS} - X_{AR})/(X_{AS} - X_{AE})} \tag{6.63}$$

Integrating between appropriate limits,

$$\ln\frac{R_0}{R_f} = \int_{R_f}^{R_0}\frac{dR}{R} = \int_{X_{CR_f}}^{X_{CR_0}} \frac{dX_{CR}}{(X_{CS} - X_{CE})\left[\dfrac{(X_{CS} - X_{CR})}{(X_{CS} - X_{CE})} - \dfrac{(X_{AS} - X_{AR})}{(X_{AS} - X_{AE})}\right]}$$

$$- \int_{X_{AR_f}}^{X_{AR_0}} \frac{dX_{AR}}{(X_{AS} - X_{AE})[(X_{CS} - X_{CR})/(X_{CS} - X_{CE}) - (X_{AS} - X_{AR})/(X_{AS} - X_{AE})]} \tag{6.64}$$

This is analogous to Rayleigh's law for distillation and may be evaluated graphically. The first integral is the area under a curve of $X_{CR}$ as abscissa,

$$\frac{1}{(X_{CS} - X_{CE})[(X_{CS} - X_{CR})/(X_{CS} - X_{CE}) - (X_{AS} - X_{AR})/(X_{AS} - X_{AE})]}$$

as ordinate, the concentrations ($X_{CE}$,$X_{AE}$) and ($X_{CR}$,$X_{AR}$) being taken on opposite ends of tie lines. The second integral can be evaluated graphically in similar fashion.

$E_f$, the final extract which is a composite of all the extracts withdrawn (not in equilibrium with $R_f$), can be obtained by eliminating $dS$ from Eqs. (6.58) and (6.60):

$$dE = \frac{dR(X_{CS} - X_{CR}) - R\,dX_{CR}}{X_{CS} - X_{CE}} \tag{6.65}$$

Since $X_{CS}$ is a constant,

$$E_f = \int_0^{E_f} dE = \int_{(X_{CS} - X_{CR_f})R_f}^{(X_{CS} - X_{CR_0})R_0} \frac{d[(X_{CS} - X_{CR})R]}{X_{CS} - X_{CE}} \tag{6.66}$$

This can be evaluated by determining the area under a curve of $1/(X_{CS} - X_{CE})$ as ordinate, $(X_{CS} - X_{CR})R$ as abscissa, obtaining the data during the evaluation of Eq. (6.64). To obtain the solvent used,

$$S_f = E_f + R_f - R_0 \tag{6.67}$$

To this should be added the initial solvent required to saturate feed, Eq. (6.56). The final composite extract composition can be obtained by a series of material balances:

$$X_{CE_f} = \frac{S_f X_{CS} + R_0 X_{CR_0} - R_f X_{CR_f}}{E_f} \tag{6.68}$$

$$X_{AE_f} = \frac{S_f X_{AS} + R_0 X_{AR_0} - R_f X_{AR_f}}{E_f} \tag{6.69}$$

$$X_{BE_f} = 1 - X_{CE_f} - X_{AE_f} \tag{6.70}$$

For the special case where the solvent is pure $B$ (3, 22), $X_{CS} = X_{AS} = 0$, Eq. (6.64) reduces to

$$\ln \frac{R_0}{R_f} = \int_{X_{CR_f}}^{X_{CR_0}} \frac{dX_{CR}}{X_{CE}\left(\dfrac{X_{AR}}{X_{AE}} - \dfrac{X_{CR}}{X_{CE}}\right)} - \int_{X_{AR_f}}^{X_{AR_0}} \frac{dX_{AR}}{X_{AE}\left(\dfrac{X_{AR}}{X_{AE}} - \dfrac{X_{CR}}{X_{CE}}\right)} \tag{6.71}$$

and Eq. (6.66) becomes

$$E_f = \int_{R_f X_{CR_f}}^{R_0 X_{CR_0}} \frac{d(X_{CR}R)}{X_{CE}} \tag{6.72}$$

For certain Type 2 systems,

$$\beta = \frac{X_{CE}}{X_{AE}} \cdot \frac{X_{AR}}{X_{CR}} = \text{const.} \tag{6.73}$$

where $\beta$ = selectivity, as described in Chaps. 2 and 4. For this special case and for pure $B$ as solvent (23), substitution in Eq. (6.71) leads to

$$\ln \frac{R_0}{R_f} = \frac{1}{\beta - 1}\left(\ln \frac{X_{CR_0}}{X_{CR_f}} - \beta \ln \frac{X_{AR_0}}{X_{AR_f}}\right) \tag{6.74}$$

which is analogous to the integration of Rayleigh's law for distillation at constant relative volatility.

**Illustration 2.** One hundred pounds of a 50% acetone ($C$)–50% water ($A$) solution is to be reduced to 10% acetone by differential extraction with 1,1,2-trichloroethane at 25°C. Calculate the quantity of solvent required and the concentrations and weights of extract and raffinate.

*Solution.* Equilibrium data are available [Treybal, Weber, and Daley, *Ind. Eng. Chem.* **38,** 817 (1946)]. See Fig. 6.17. Point $F$ corresponding to the initial solution is

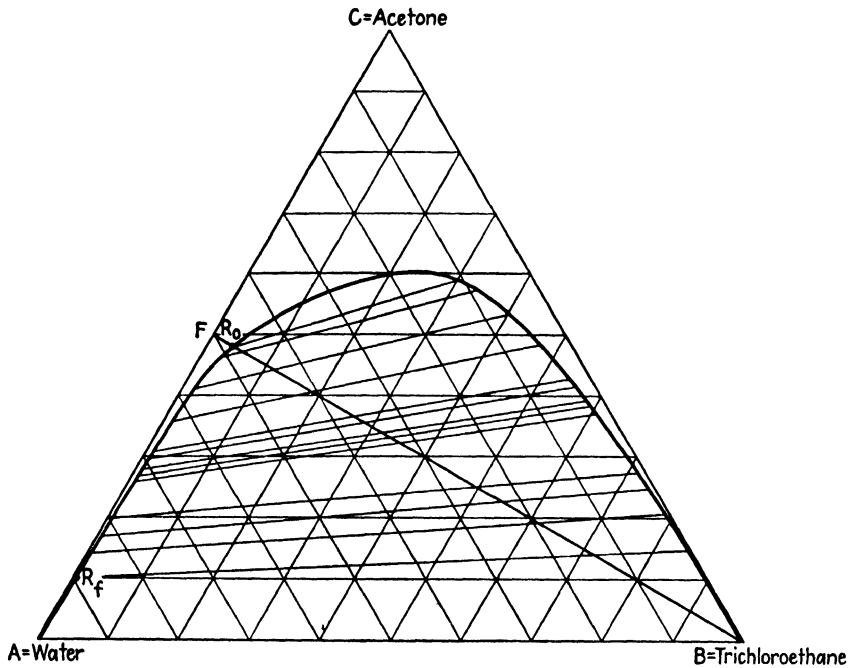



FIG. 6.17. Differential extraction in the system acetone–water–trichloroethane. [*Equilibria from Ind. Eng. Chem.* **38,** 817 (1946).]

located and line $FB$ drawn, thus locating $R_0$. $F = 100$ lb.; $S = B$; $X_{BF} = 0$; $X_{BS} = X_{BB} = 1.0$; $X_{BR_0} = 0.045$, $X_{CR_0} = 0.478$, $X_{AR_0} = 0.477$. $R_f$ is located on the solubility curve at 10% acetone. $X_{CR_f} = 0.100$, $X_{AR_f} = 0.895$.

(Eq. 6.56): $$B_{\text{initial}} = \frac{F(X_{BR_0} - X_{BF})}{(X_{BS} - X_{BR_0})} = \frac{100(0.045 - 0)}{(1.0 - 0.045)} = 4.71 \text{ lb.}$$

$$\therefore R_0 = 100 + 4.71 = 104.7 \text{ lb.}$$

Eq. (6.71): $$\ln \frac{R_0}{R} = \ln \frac{104.7}{R} = \int_{X_{CR}}^{X_{CR_0}=0.478} \frac{dX_{CR}}{X_{CE}[(X_{AR}/X_{AE}) - (X_{CR}/X_{CE})]} - \int_{X_{AR}}^{X_{AR_0}=0.477} \frac{dX_{AR}}{X_{AE}[(X_{AR}/X_{AE}) - (X_{CR}/X_{CE})]}$$

Tie lines are drawn on the figure corresponding to the computations to be made, a portion of which are tabulated on page 145. Data of columns 1 to 4 are taken from the ends of the

| (1) | (2) | (3) | (4) | (5) | (6) | (7) | (8) | (9) | (10) |
|---|---|---|---|---|---|---|---|---|---|
| $X_{CR}$ | $X_{AR}$ | $X_{CE}$ | $X_{AE}$ | $\frac{1}{X_{CE}\left(\frac{X_{AR}}{X_{AE}}-\frac{X_{CR}}{X_{CE}}\right)}$ | $\frac{1}{X_{AE}\left(\frac{X_{AR}}{X_{AE}}-\frac{X_{CR}}{X_{CE}}\right)}$ | $\ln\frac{104.7}{R}$ | $R$ | $X_{CR}R$ | $\frac{1}{X_{CR}}$ |
| 0.478 | 0.477 | 0.592 | 0.107 | 0.463 | 3.44 | 0 | 104.7 | 50.0 | 1.690 |
| 0.409 | 0.5700 | 0.5395 | 0.0605 | 0.2135 | 1.905 | 0.2379 | 82.6 | 33.8 | 1.853 |
| 0.3088 | 0.6795 | 0.4297 | 0.0311 | 0.1100 | 1.52 | 0.4274 | 68.3 | 21.1 | 2.325 |
| 0.2763 | 0.7133 | 0.3939 | 0.0240 | 0.0878 | 1.437 | 0.4807 | 64.8 | 17.91 | 2.54 |
| 0.2600 | 0.7300 | 0.3706 | 0.0209 | 0.0788 | 1.395 | 0.5057 | 63.2 | 16.43 | 2.795 |
| 0.1704 | 0.8223 | 0.2514 | 0.0110 | 0.0536 | 1.227 | 0.6328 | 55.5 | 9.46 | 3.98 |
| 0.1000 | 0.895 | 0.150 | 0.0060 | 0.0470 | 1.123 | 0.7217 | 51.0 | 5.10 | 6.67 |

tie lines. Graphical integration of a plot of column 1 vs. column 5 gives the value of the first integral of the equation, and integration of a plot of column 2 vs. column 6 gives the second. Combining these according to the equation gives column 7. Column 8 then lists the value of $R$ corresponding to each value of $X_{CR}$. The value of $R_f$, where $X_{CR} = X_{CR_f} = 0.100$, is then 51.0 lb. *Ans.*

Eq. (6.72): $$E_f = \int_{R_f X_{CR_f}}^{R_0 X_{CR_0}} \frac{d(X_{CR}R)}{X_{CE}} = \int_{51\ 0(0\ 100)}^{104\ 7(0\ 478)} \frac{d(X_{CR}R)}{X_{CE}}$$

The integral is evaluated graphically by plotting column 9 vs. column 10. The area under the curve $= E_f = 112.2$ lb. *Ans.*

Eq. (6.67): $S_f = B_f = E_f + R_f - R_0 = 112.2 + 51.0 - 104.7 = 58.5$ lb. *Ans.*

Total solvent $= B_f + B_{\text{initial}} = 58.5 + 4.71$

$= 63.2$ lb. *Ans.*

By Eqs. (6.68) to (6.70), the concentrations for $E_f$ are then calculated to be $X_{CE_f} = 0.400$, $X_{AE_f} = 0.0383$, $X_{BE_f} = 0.562$, which falls in the two-phase region. The composite extract will form two liquid layers.

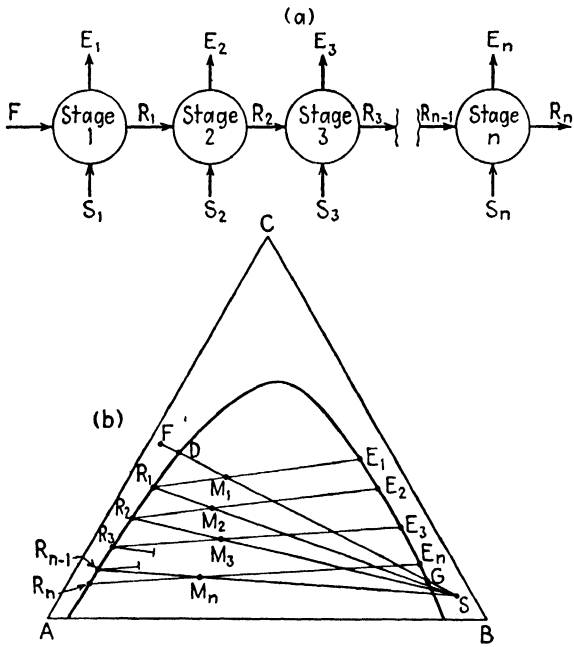



FIG. 6.18. Cocurrent multiple contact.

## COCURRENT MULTIPLE CONTACT

This process is an extension of single-contact extraction, wherein the raffinate from the first stage is extracted with fresh solvent of the same composition in successive stages, as the flowsheet of Fig. 6.18*a* indicates, the concentration of $C$ in the raffinate thus being further reduced. Different quantities of solvent may be used in the various stages.

The methods of calculation are more or less obvious from the construction

on the triangular coordinates of Fig. 6.18*b*. Each raffinate becomes the feed to the succeeding stage. Accordingly, Eqs. (6.6) to (6.16) for single-stage contact all apply exactly for the first stage of cocurrent multiple contact, with the substitution of $S_1$, $E_1$, $R_1$, and $M_1$ for $S$, $E$, $R$, and $M$, respectively. Similarly, for any other stage, the $m$th for example, Eqs. (6.6) to (6.14) apply with the substitution of $R_{m-1}$ for $F$, and $R_m$, $E_m$, $M_m$, and $S_m$ for $R$, $E$, $M$, and $S$, respectively. For all but the first stage, since

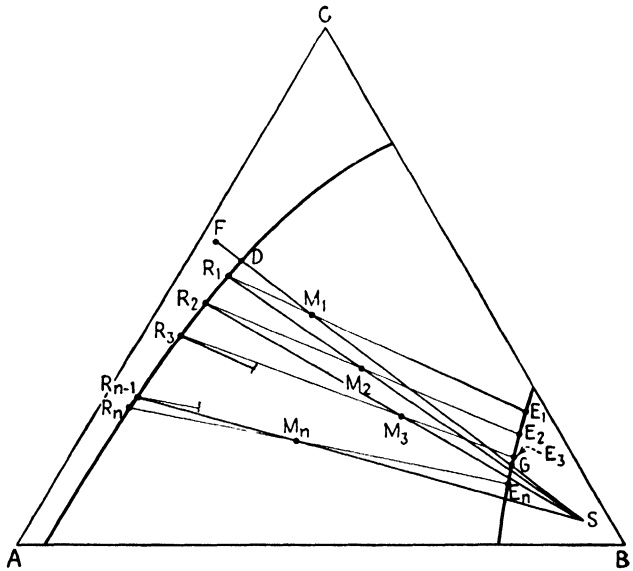



FIG. 6.19. Cocurrent multiple contact in a Type 2 system.

the feeds to each are necessarily saturated solutions, there is no minimum amount of solvent. The maximum solvent for any stage, as for single contact, must be such that the combined feed-solvent mixture forms two liquid phases. Construction for a Type 2 system is shown in Fig. 6.19.

**Solvent Recovery.** Only a single raffinate, that from the last stage $n$, is treated for solvent recovery. The extracts from all stages are ordinarily combined and the mixture then treated for solvent recovery, although individual extracts may be treated separately if so desired. Refer to Fig. 6.20. The flowsheet and construction are the same for single contact except that a combined extract $E$ is prepared:

$$E = E_1 + E_2 + E_3 + \cdots + E_n \tag{6.75}$$

$$X_{CE} = \frac{E_1X_{CE_1} + E_2X_{CE_2} + E_3X_{CE_3} + \cdots + E_nX_{CE_n}}{E} \tag{6.76}$$

$$X_{BE} = \frac{E_1X_{BE_1} + E_2X_{BE_2} + E_3X_{BE_3} + \cdots + E_nX_{BE_n}}{E} \tag{6.77}$$

Since the solubility curve is ordinarily concave downward, as shown, $E$ will be in the two-liquid-phase region. All equations previously derived, Eqs. (6.17) to (6.28), apply. Extension to cases where pure solvent $B$ is used and completely recovered is obvious and need not be described.

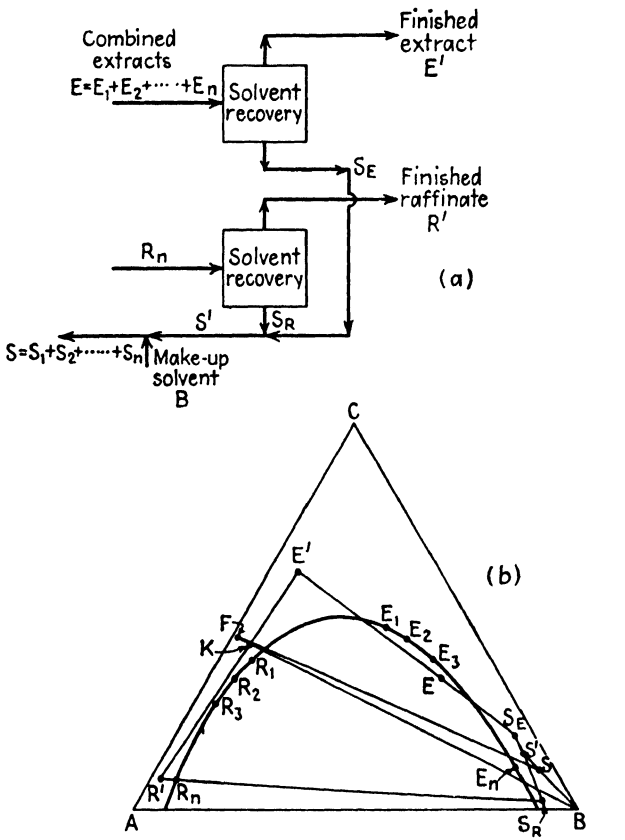



FIG. 6.20. Solvent recovery for cocurrent multiple contact.

**Purity of Products.** The maximum purity of $A$ in the raffinate will be given by an operation in which the $n$th tie line, corresponding to the last stage, passes through $S$ when extended. This necessarily requires $n$ to be infinity. The absolute maximum purity of $C$ in the solvent-stripped extract will correspond to the case for single contact (tangency of solvent-removal line to the solubility curve for the combined extracts). Since $E$ ordinarily falls within the two-liquid-phase area, this cannot usually be realized, however.

**Janecke Diagram.** Construction on these coordinates is indicated in Fig. 6.21, which also includes the solvent-recovery lines. Calculations again are simply an extension of the case for single contact, Eqs. (6.30) to

(6.39) applying with the substitution of $\mathbf{S}_m$, $\mathbf{E}_m$, $\mathbf{R}_m$, $\mathbf{M}_m$, and $\mathbf{R}_{m-1}$ for **S**, **E**, **R**, **M**, and **F** for any stage $m$. Similarly, Eqs. (6.42) to (6.52) apply directly, with

$$\mathbf{E} = \mathbf{E}_1 + \mathbf{E}_2 + \mathbf{E}_3 + \cdots + \mathbf{E}_n \tag{6.78}$$

$$\mathbf{E}N_E = \mathbf{E}_1 N_{E_1} + \mathbf{E}_2 N_{E_2} + \mathbf{E}_3 N_{E_3} + \cdots + \mathbf{E}_n N_{E_n} \tag{6.79}$$

and

$$\mathbf{X}_E = \frac{\mathbf{E}_1\mathbf{X}_{E_1} + \mathbf{E}_2\mathbf{X}_{E_2} + \mathbf{E}_3\mathbf{X}_{E_3} + \cdots + \mathbf{E}_n\mathbf{X}_{E_n}}{\mathbf{E}} \tag{6.80}$$

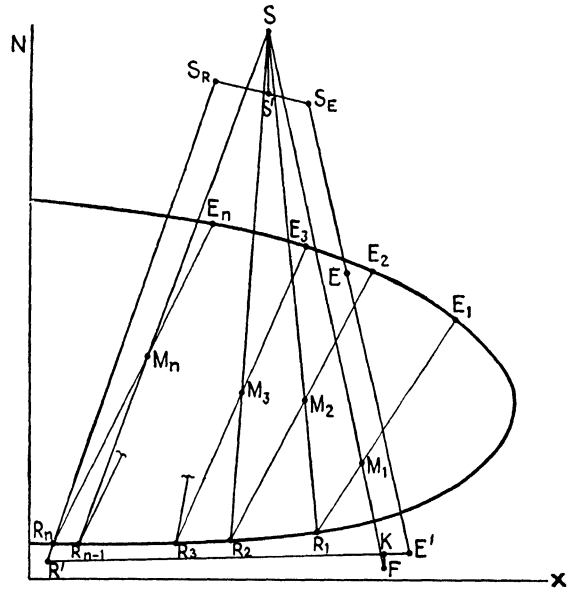


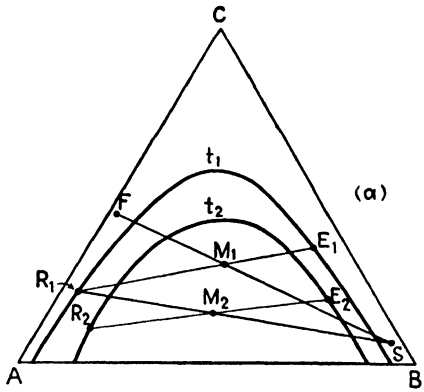

FIG. 6.21. Cocurrent multiple contact with solvent recovery, Janecke coordinates.

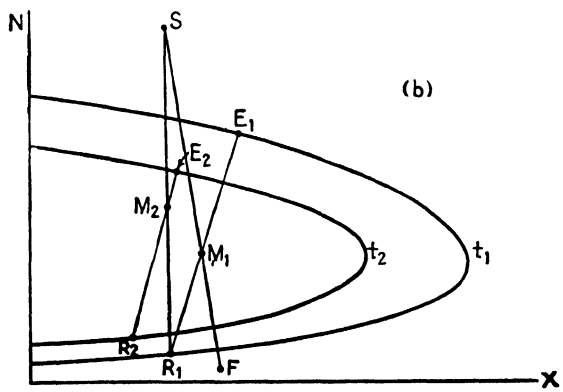
Extension to cases where pure $B$ is the solvent means that construction lines for the stages radiating from $S$ and the solvent-recovery lines all become vertical.

**Varying Temperature.** If equilibrium and other considerations make it desirable to use different temperatures in each stage, the construction is modified in either coordinate system to include appropriate solubility curves and tie lines for each stage, as shown in Fig. 6.22. Here a two-stage plant uses temperatures $t_1$ and $t_2$ for the separate stages. The equations indicated above all apply as before.

**Types of Problems.** Concentrations of solvent and feed and amount of feed are ordinarily fixed by the process. The principal additional variables are then the total amount of solvent, the proportioning of solvent among the stages, the number of stages, and extract and raffinate compositions. One may in addition to the fixed items mentioned above specify

ı) the number of stages and the quantity of solvent for each stage, (*b*) ex-act or raffinate compositions for each stage together with the number of ages, (*c*) final raffinate composition and total solvent with the proportion ) be used for each stage, (*d*) final raffinate composition, number of stages,




IG. 6.22. Two-stage contact, each stage at a separate temperature: (*a*) triangular, b) Janecke coordinates.

nd the proportioning of the total solvent among the stages. The last two equire trial-and-error solutions to the problems. For a fixed amount of olvent and infinite stages, the net result will be the same as for differential xtraction.

**Stage Efficiency.** Each stage of the plant will behave in the manner lescribed previously for single-stage contact, producing equilibrium extracts nd raffinates only if agitation is thorough and time of contact adequate. For a real plant, it may be found that $m$ real stages are required to produce ı final raffinate composition for which only $n$ theoretical stages are com-puted. Then,

$$\text{Per cent over-all stage efficiency} = \frac{n \text{ theoretical stages}}{m \text{ real stages}} (100) \quad (6.81)$$

**Immiscible Solvents.** If the liquids $A$ and $B$ may be considered completely immiscible, or at least if their solubility does not change over the range of concentration of distributed substance $C$ under the process conditions, calculations may be conveniently simplified (2). Assume that $A$ lb. of component $A$ is contained in the feed and all the raffinates and that

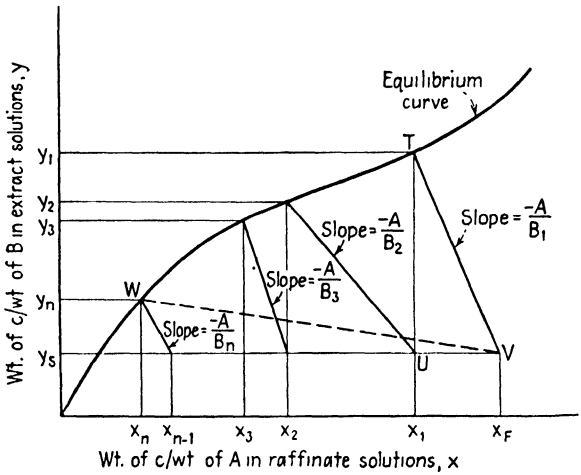



FIG. 6.23. Cocurrent multiple contact with immiscible solvents.

the $B$ content of the extract from any stage equals that in the extracting solvent to the stage. We may then define a coordinate system $y = X_{CB}/X_{BB}$ for extract solutions, $x = X_{CA}/X_{AA}$ for raffinate solutions, and plot an equilibrium-distribution curve at the temperature of the extraction operation, as in Fig. 6.23. The extract from the $m$th stage will then have the concentration $y_m$, and the raffinate $x_m$. The $C$ concentration of the solvent and feed will be $y_s$ and $x_F$. The total weights of the various streams then become

$$F = A(1 + x_F) \tag{6.82}$$

$$S_m = B_m(1 + y_S) \tag{6.83}$$

$$R_m = A(1 + x_m) \tag{6.84}$$

$$E_m = B_m(1 + y_m) \tag{6.85}$$

For any stage $m$, we may make the following $C$ balance:

$$Ax_{m-1} + B_m y_S = B_m y_m + Ax_m \tag{6.86}$$

or

$$\frac{y_m - y_S}{x_m - x_{m-1}} = -\frac{A}{B_m} \tag{6.87}$$

Equation (6.87) is the equation of a straight line on the coordinates of Fig. 6.23 of slope $-(A/B_m)$, passing through the two points whose coordi-

nates are $(x_m,y_m)$ and $(x_{m-1},y_S)$. Since the effluent streams from a theoretical stage are at equilibrium, the point $(x_m,y_m)$ is on the equilibrium-distribution curve. For the first stage, therefore, a line of slope $-(A/B_1)$ is erected from point $V(x_F,y_S)$ which will intersect the equilibrium curve at $T(x_1,y_1)$. The second stage is constructed from point $U$, etc., until the final extract and raffinate concentrations are reached at $W$. The same reduction in raffinate concentration could be obtained in a single stage represented by the line $WV$ at a corresponding increase in solvent consumption.

The same diagram and method of construction can be frequently used with other concentration units. Thus, if the solutions are dilute in $C$, without appreciable change in density throughout the operation, $x$ and $y$ may be expressed as weight of $C$/unit volume of solution, in which case $F, S, E$, and $R$ are measured in volumes; or as $x$ = weight of $C$/volume of $A$, $y$ = weight of $C$/volume of $B$, in which case $A$ and $B$ are measured in volumes.

**Distribution Law.** In the special case where solvents are immiscible and the distribution law holds,

$$y_m = \mathbf{m}x_m \tag{6.88}$$

where $\mathbf{m}$ is the constant distribution coefficient, and if further $y_S = 0$ and equal quantities of solvent $B$ are used in each stage, then the first contact is represented by

$$-\frac{A}{B} = \frac{y_1}{x_1 - x_F} = \frac{\mathbf{m}x_1}{x_1 - x_F} \tag{6.89}$$

or

$$x_1 = \frac{x_F}{(\mathbf{m}B/A) + 1} \tag{6.90}$$

Similarly, the second contact becomes

$$-\frac{A}{B} = \frac{y_2}{x_2 - x_1} = \frac{\mathbf{m}x_2}{x_2 - \left[\dfrac{x_F}{(\mathbf{m}B/A) + 1}\right]} \tag{6.91}$$

or

$$x_2 = \frac{x_F}{[(\mathbf{m}B/A) + 1]^2} \tag{6.92}$$

Similarly for $n$ stages,

$$x_n = \frac{x_F}{[(\mathbf{m}B/A) + 1]^n} \tag{6.93}$$

It may be concluded from Eq. (6.93) that for a given total amount of solvent $B_t$, the larger the value of $n$ the greater will be the amount of extraction or the smaller the value of $x_n$. Further, equal subdivision of the solvent among the stages results in more effective extraction than unequal (20). If the total available solvent $B_t$ is divided into $n$ equal portions for $n$ stages, $x_n$

will not approach zero as $n$ is increased to infinity as a limit (1, 4), but instead

$$\lim_{n\to\infty} \frac{x_n}{x_F} = e^{-\frac{mB_t}{A}} \tag{6.94}$$

Use of an extremely large number of stages is rarely warranted, since it has been shown (1, 15) that if $B_t$ is fixed, at least 94 per cent of the maximum removal possible will be attained with five stages. Equation (6.93) may be solved for $n$ for convenience in solving certain problems:

$$n = \frac{\log (x_n/x_F)}{\log [A/(mB + A)]} \tag{6.95}$$

and it has been put in convenient chart and nomograph form (11, 12, 21).

**Illustration 3.** One hundred pounds of a 50% acetone ($C$)–50% water ($A$) solution is to be reduced to a 10% solution of acetone by extraction with 1,1,2-trichloroethane ($B$) in a cocurrent multiple-contact extraction system. Twenty-five pounds of solvent is to be used in each stage. Calculate the number of stages and concentration of extracts. The temperature is to be 25°C.

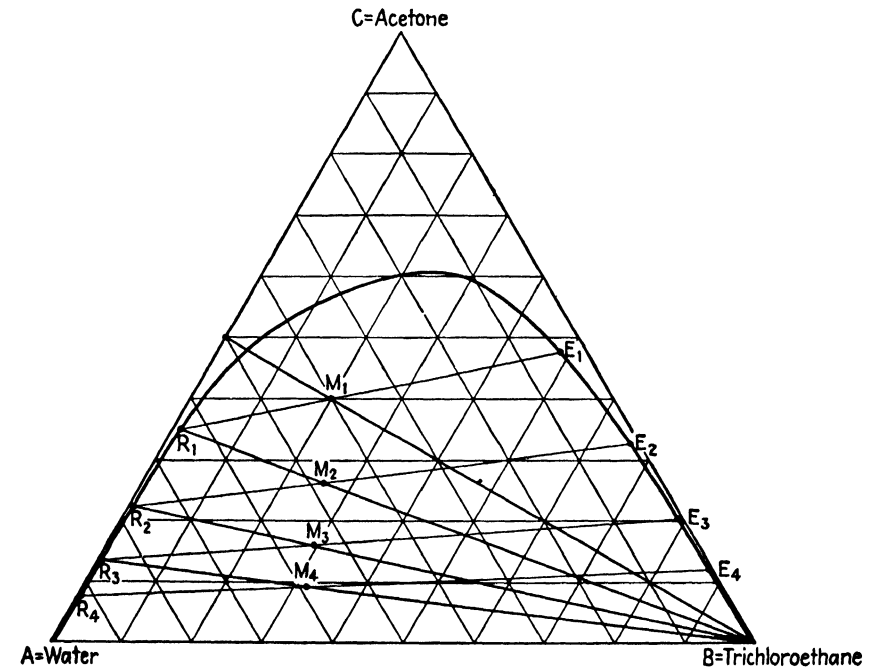



FIG. 6.24. Extraction of acetone from water with trichloroethane using cocurrent multiple contact.

*Solution.* Equilibrium data are available [*Ind. Eng. Chem.* **38**, 817 (1946)]. Refer to Fig. 6.24. $F$ = 100 lb., $X_{CF}$ = 0.50, $X_{BF}$ = 0, $S$ = 25 lb. (for each stage), $X_{CS}$ = 0, $X_{BS}$ = 1.0.

For stage 1, Eq. (6.9):

$$X_{CM_1} = \frac{FX_{CF} + S_1X_{CS}}{F + S_1} = \frac{100(0.50) + 0}{100 + 125} = 0.40$$

Eq. (6.10):

$$X_{BM_1} = \frac{FX_{BF} + S_1X_{BS}}{F + S_1} = \frac{0 + 25(1.0)}{100 + 25} = 0.20$$

$M_1$ can therefore be located. $M_1 = F + S_1 = 100 + 25 = 125$ lb. The tie line through $M_1$ is located by trial, with the help of a tie-line correlation. From the figure, the coordinates of $R_1$ are $X_{CR_1} = 0.35$, $X_{AR_1} = 0.64$, $X_{BR_1} = 0.02$. Those for $E_1$ are $X_{CE_1} = 0.475$, $X_{AE_1} = 0.04$, $X_{BE_1} = 0.485$.

Eq. (6.14): $$E_1 = \frac{M_1(X_{CM_1} - X_{CR_1})}{(X_{CE_1} - X_{CR_1})} = \frac{125(0.40 - 0.35)}{(0.475 - 0.35)} = 50 \text{ lb.}$$

Eq. (6.6): $$R_1 = M_1 - E_1 = 125 - 50 = 75 \text{ lb.}$$

Similarly for the additional stages, resulting in the following data:

| | $X_C$ | $X_A$ | $X_B$ | Lb. |
|---|---|---|---|---|
| $M_2$ | 0.262 | 0.480 | 0.258 | 100. |
| $R_2$ | 0.223 | 0.769 | 0.008 | 61.8 |
| $E_2$ | 0.325 | 0.013 | 0.662 | 38.2 |
| $M_3$ | 0.159 | 0.547 | 0.294 | 86.8 |
| $R_3$ | 0.134 | 0.860 | 0.006 | 55.8 |
| $E_3$ | 0.204 | 0.007 | 0.789 | 31.0 |
| $M_4$ | 0.0925 | 0.5945 | 0.313 | 80.8 |
| $R_4$ | 0.075 | 0.920 | 0.005 | 50.3 |
| $E_4$ | 0.120 | 0.005 | 0.875 | 30.5 |

Since $X_{CR_3} = 0.134$ and $X_{CR_4} = 0.075$, whereas the desired raffinate from the last stage is $X_{CR} = 0.10$, then three stages are too few, four too many. About 3.5 stages are required. There are three alternatives: (*a*) use three stages and slightly more solvent per stage, determining the quantity to be used by trial until $X_{CR_3} = 0.10$, (*b*) use four stages and slightly less solvent, again with a trial-and-error procedure, or (*c*) accept the 7.5% acetone in the final raffinate. Note that if the over-all stage efficiency were (3.5/4)100 = 87.5%, four real stages would be satisfactory.

Accepting alternative (*c*), the final raffinate = 50.3 lb., containing 0.075(50.3) = 3.77 lb. acetone, 50.3(0.005) = 0.25 lb. solvent, and 50.3(0.92) = 46.3 lb. water. The final extract $E$ = the combined extracts = 50 + 38.2 + 31.0 + 30.5 = 149.7 lb., containing the extracted acetone, 50 − 3.77 = 46.2 lb. acetone.

$$X_{CE} = \frac{46.2}{149.7} = 0.309$$

$$X_{BE} = \frac{100 \text{ lb. total solvent} - 0.25 \text{ lb. in raffinate}}{149.7} = 0.666$$

and the point $E$ can be located on the diagram as shown.

**Illustration 4.** The acetaldehyde ($C$) in 100 lb/hr. of a 4.5% solution in toluene ($A$) is to be extracted in a five-stage cocurrent plant with 25 lb. water ($B$)/hr. as solvent in each stage. Calculate the extent of extraction.

*Solution.* Equilibrium data of Othmer and Tobias [*Ind. Eng. Chem.* **34**, 690 (1942)], at 17°C. will be used. Up to 15% acetaldehyde, toluene-water mixtures may be considered practically insoluble. The equilibrium data are plotted in Fig. 6.25 on $x$-$y$ coordinates, where $x$ = lb. acetaldehyde/lb. toluene, $y$ = lb. acetaldehyde/lb. water. Basis: 1 hr.

Acetaldehyde in feed = 100(0.045) = 4.5 lb.
Toluene in feed = 100 − 4.5 = 95.5 lb. = $A$
Water per stage = $B$ = 25 lb.

$y_S = 0$, $x_F = 4.5/95.5 = 0.0471$ lb. acetaldehyde/lb. toluene

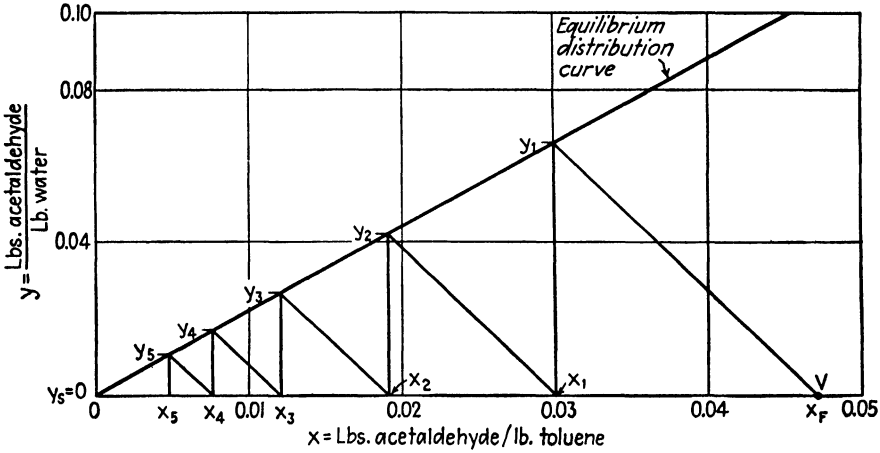



FIG. 6.25. Extraction of acetaldehyde from toluene with water.

Slope of stage lines for all stages $= -(A/B) = -95.5/25 = -3.82$. From point $V$ on the figure, representing solvent and feed, a line of slope −3.82 is drawn representing the first stage. Other stage lines, totaling 5, are drawn as indicated. From the figure, $x_5 = 0.0048$ lb. acetaldehyde/lb. toluene in the final raffinate, corresponding to (0.0048/1.0048)(100) = 0.477% acetaldehyde. Acetaldehyde extracted

$$A(x_F - x_5) = 95.5(0.0471 - 0.0048) = 4.04 \text{ lb.}$$

or 89.8% of that in the feed. The total solvent = 5(25) = 125 lb. water. The concentration of acetaldehyde in a composite extract = [4.04/(125 + 4.04)](100) = 3.13%.

Alternatively, for this case the distribution law holds, and $\mathbf{m} = y_m/x_m = 2.20$.

Eq. (6.93): $$x_5 = \frac{x_F}{(\mathbf{m}B/A + 1)^n} = \frac{0.0471}{\left[\dfrac{2.20(25)}{95.5} + 1\right]^5} = 0.00486$$

For the same extraction in a single stage,

Eq. (6.89): $$-\frac{A}{B} = \frac{\mathbf{m}x_1}{x_1 - x_F}$$

$$-\frac{95.5}{B} = \frac{2.20(0.00486)}{0.00486 - 0.0471}$$

$$B = 368 \text{ lb. water}$$

The resulting extract would have an acetaldehyde concentration $= y_1 = \mathbf{m}x_1 =$ 2.20(0.00486) = 0.0107, or 1.06% acetaldehyde.

## COUNTERCURRENT MULTIPLE CONTACT

In this type of extraction, a cascade of stages is employed, with feed and solvent entering at opposite ends of the cascade, raffinate and extract solutions flowing countercurrently, as in Fig. 6.26.

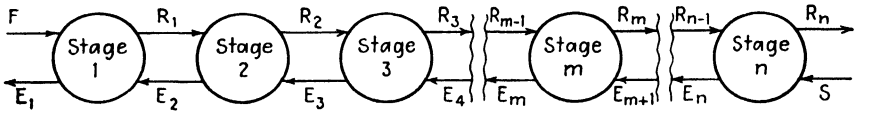



FIG. 6.26. Flowsheet for countercurrent multiple-contact extraction.

**Triangular Coordinates.** Refer to Fig. 6.27 (2, 6). Assume that the location of $F$, $E_1$, $R_n$, and $S$ are known. A material balance for the entire plant is

$$F + S = E_1 + R_n = M \tag{6.96}$$

or

$$F - E_1 = R_n - S = O \tag{6.97}$$

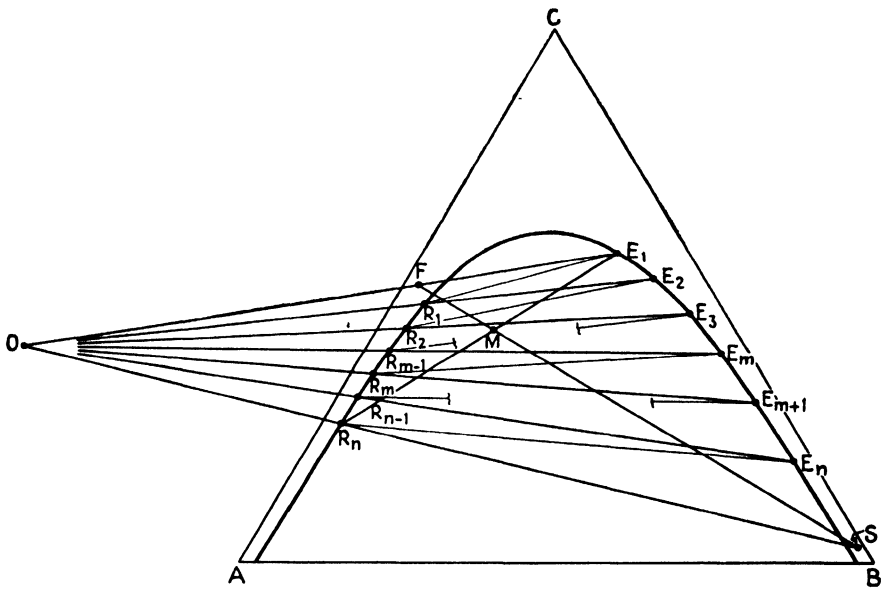



FIG. 6.27. Countercurrent multiple contact.

Point $O$, the operating point, may then be located by extending the lines $E_1F$ and $SR_n$ to intersection. A material balance for stages 1 through $m$:

$$F + E_{m+1} = E_1 + R_m \tag{6.98}$$

or

$$F - E_1 = R_m - E_{m+1} = O \tag{6.99}$$

For the $m$th stage,

$$R_{m-1} + E_{m+1} = R_m + E_m \tag{6.100}$$

$$R_{m-1} - E_m = R_m - E_{m+1} = O \tag{6.101}$$

Consideration of Eqs. (6.99) and (6.101) shows that any extract $E_{m+1}$ can be located from any raffinate $R_m$ by extending the line $OR_m$ to the $B$-rich solubility curve. As with all ideal stages, extract $E_m$ and raffinate $R_m$ will be in equilibrium and on opposite ends of a tie line. Consequently $R_1$ may be located at the opposite end of a tie line through $E_1$, $E_2$ by line $OR_1$ extended, $R_2$ by a tie line through $E_2$, etc. The operating point $O$ may be located either on the feed or solvent side of the triangle, depending upon the relative amounts of feed and solvent and the slope of the tie lines.

$M$ may be calculated and its coordinates determined by Eqs. (6.7), (6.9), and (6.10). $E_1$ and $R_n$ may be determined by combining Eq. (6.96) with a $C$ balance:

$$E_1 = \frac{M(X_{CM} - X_{CR_n})}{X_{CE_1} - X_{CR_n}} \tag{6.102}$$

For any stage $m$, the total material balance of Eq. (6.100) may be rearranged to give

$$E_{m+1} = R_m + E_m - R_{m-1} \tag{6.103}$$

An $A$ balance for stage $m$:

$$R_{m-1}X_{AR_{m-1}} + E_{m+1}X_{AE_{m+1}} = R_mX_{AR_m} + E_mX_{AE_m} \tag{6.104}$$

Combining the last two equations:

$$R_m = \frac{R_{m-1}(X_{AR_{m-1}} - X_{AE_{m+1}}) + E_m(X_{AE_{m+1}} - X_{AE_m})}{X_{AR_m} - X_{AE_{m+1}}} \tag{6.105}$$

Thus we may calculate $R_1$ by Eq. (6.105) by letting $m - 1 = F$ and $m = 1$; $E_2$ by Eq. (6.99) with $m = 1$; $R_2$ by Eq. (6.105) with $m = 2$; $E_3$ by Eq. (6.99) with $m = 2$, etc. In this fashion all extracts and raffinates may be determined after the necessary concentrations are read from the triangular diagram.

**Limitations on Amount of Solvent.** It is clear from the construction of Fig. 6.27 that if an extended tie line passed through the operating point $O$, the stepwise determination of stages could necessarily not pass beyond this tie line, and an infinite number of stages would be required even to reach it, a condition known in distillation as a "pinch." For a real plant, the line $R_nS$ may not, therefore, coincide with a tie line, else a pinch will occur at the solvent end of the plant. The farther point $O$ is from $R_n$, the greater the amount of solvent indicated. The procedure for determining the minimum solvent can therefore be outlined (refer to Fig. 6.28). Draw line $R_nS$ extended, and extend all tie lines to intersection with the line $R_nS$. The intersection farthest from $R_n$ (tie line $HJ$ in the figure, with intersection at $O'$) corresponds to the minimum solvent. A real operating point $O$, with a correspondingly greater amount of solvent, must be chosen. In most cases, a tie line $DG$ which passes through $F$ will locate the minimum-solvent operating point but not in the example shown. If the tie lines

slope downward toward the $B$ apex, their intersections with $R_nS$ will be on the solvent side of the triangle, in which case the nearer the intersection to point $S$ the greater the indicated amount of solvent.

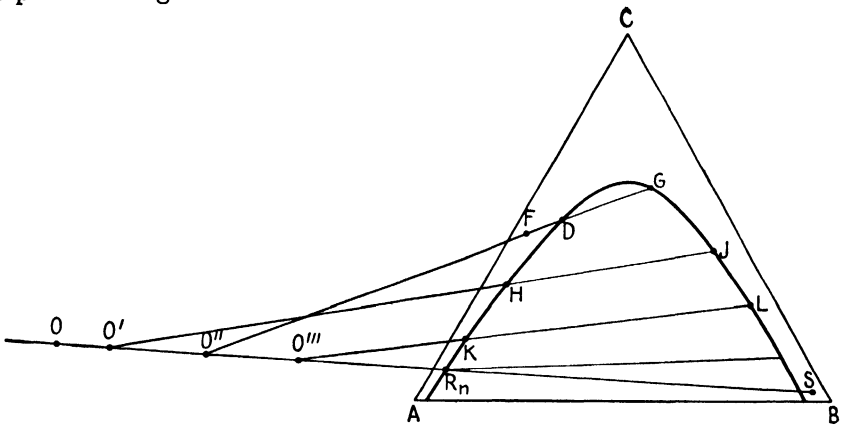



FIG. 6.28. Minimum solvent in countercurrent multiple contact.

The maximum amount of solvent will be such that the feed solution is entirely dissolved, as in the case for a single-contact operation.

**Solvent Recovery.** Since but a single raffinate and a single extract are the products of this type of operation, solvent-recovery calculations are identical with those of the single-contact operation described previously. The maximum purity of $C$ in the finished extract will accordingly result if the solvent-removal line $E_1S_E$ is tangent to the binodal curve.

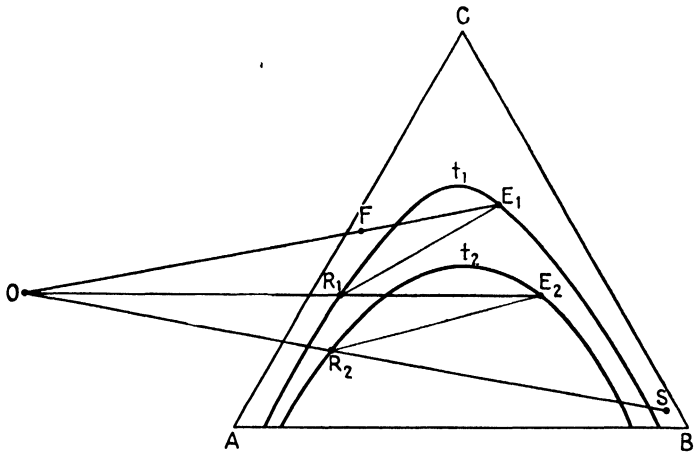



FIG. 6.29. Two-stage countercurrent contact at different temperatures.

**Varying Temperature.** Operations with the various stages at different temperatures are easily followed on triangular coordinates (6), using tie lines and solubility curves for each stage corresponding to the temperature

of the stage. The equations presented earlier all apply, and Fig. 6.29 shows a typical construction for a two-stage plant with temperatures $t_1$ and $t_2$ for the stages.

**Distribution Diagram.** If the number of stages is large, calculations are frequently more conveniently made on a simple distribution diagram ($X_{CA}$ vs. $X_{CB}$) in conjunction with triangular coordinates (22). A $C$ balance for stages 1 through $m$:

$$FX_{CF} + E_{m+1}X_{CE_{m+1}} = E_1X_{CE_1} + R_mX_{CR_m} \tag{6.106}$$

Rearranging,

$$X_{CE_{m+1}} = \frac{E_1X_{CE_1}}{E_{m+1}} - \frac{FX_{CF}}{E_{m+1}} + \frac{R_mX_{CR_m}}{E_{m+1}} \tag{6.107}$$

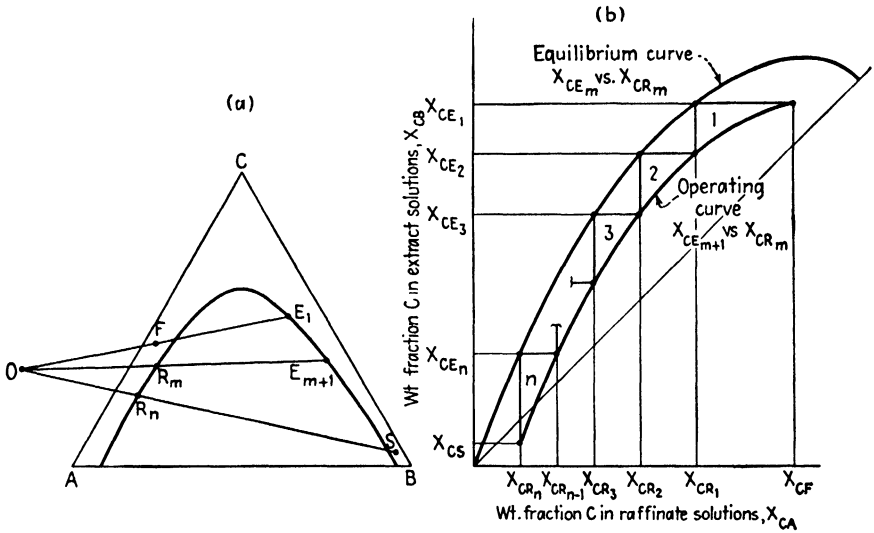



FIG. 6.30. Countercurrent multiple contact on rectangular coordinates.

Equation (6.107) is that of a curve, the operating curve, on $X_{CA}$ vs. $X_{CB}$ coordinates relating $X_{CE_{m+1}}$ with $X_{CR_m}$, since $E_1$, $X_{CE_1}$, $F$, and $X_{CF}$ are constants for any plant. Refer to Fig. 6.30*b*, on which is plotted an equilibrium distribution curve $X_{CE_m}$ vs. $X_{CR_m}$, corresponding to the equilibrium data of Fig. 6.30*a*. From the operating point $O$, lines such as $OE_{m+1}$ are drawn at random, giving corresponding coordinates of $R_m$ and $E_{m+1}$. These need not coincide with the stage lines used previously. The coordinates are transferred to the distribution diagram to form the operating curve. Stepwise construction between operating and equilibrium curves then show the stages and the corresponding raffinate and extract concentrations. Minimum solvent conditions (infinite stages) are indicated on the diagram of Fig. 6.30*b* by the operating curve touching the equilibrium curve, which then "pinches" the steps representing the stages. It should be noted,

however, that if the $C$ concentration at the plait point is less than $X_{CF}$, the operating and equilibrium curves will cross, as shown in the two-stage construction of Fig. 6.31. A similar configuration was pointed out to occur in an analogous gas-absorption operation by Randall and Longtin (13).

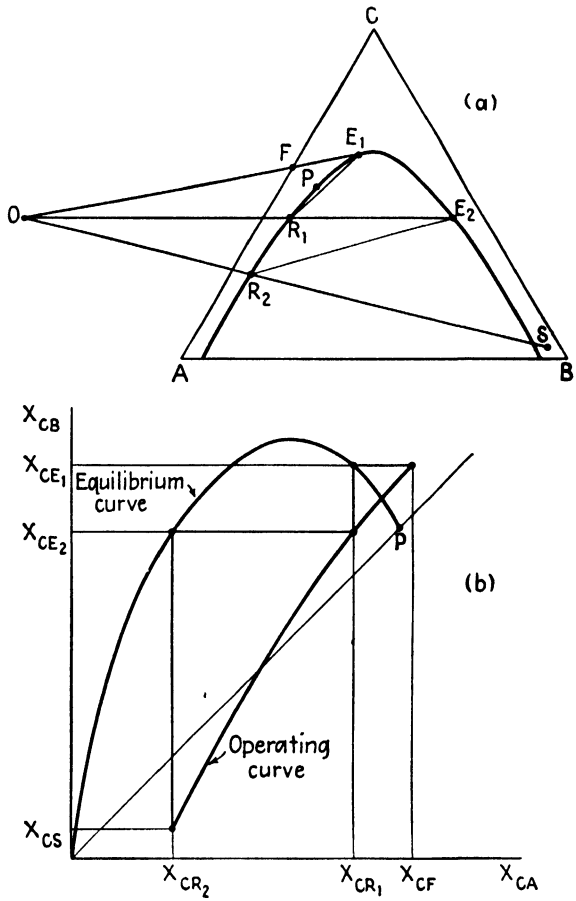



FIG. 6.31. Crossing of operating and equilibrium curves.

**Janecke Coordinates.** Construction for a typical Type 2 system is shown in Fig. 6.32. Having located points $F$, $S$, $E_1$, and $R_n$, point $M$ may be located graphically and by Eqs. (6.30) to (6.35). For the entire plant,

$$\mathbf{F} + \mathbf{S} = \mathbf{E}_1 + \mathbf{R}_n = \mathbf{M} \tag{6.108}$$

$$\mathbf{F} - \mathbf{E}_1 = \mathbf{R}_n - \mathbf{S} \tag{6.109}$$

For stage 1 through $m$:

$$\mathbf{F} + \mathbf{E}_{m+1} = \mathbf{E}_1 + \mathbf{R}_m \tag{6.110}$$

$$\mathbf{F} - \mathbf{E}_1 = \mathbf{R}_m - \mathbf{E}_{m+1} \tag{6.111}$$

$$\therefore \mathbf{F} - \mathbf{E}_1 = \mathbf{R}_m - \mathbf{E}_{m+1} = \mathbf{R}_n - \mathbf{S} = \mathbf{O} \tag{6.112}$$

and the operating point $O$ is common for all stages. It is located graphically by intersection of lines $E_1F$ and $SR_n$ extended or by its coordinates. A solvent balance

$$\mathbf{F}N_F - \mathbf{E}_1 N_{E_1} = \mathbf{O}N_O = \mathbf{R}_n N_{R_n} - \mathbf{S}N_S \tag{6.113}$$

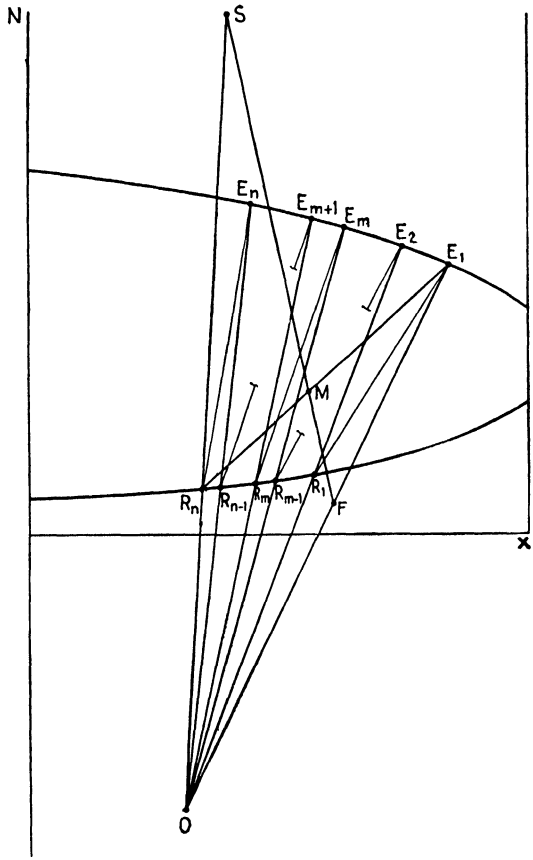



FIG. 6.32. Countercurrent multiple contact on Janecke coordinates.

from which

$$N_O = \frac{\mathbf{F}N_F - \mathbf{E}_1 N_{E_1}}{\mathbf{F} - \mathbf{E}_1} = \frac{\mathbf{R}_n N_{R_n} - \mathbf{S}N_S}{\mathbf{R}_n - \mathbf{S}} \tag{6.114}$$

A $C$ balance:

$$\mathbf{F}X_F - \mathbf{E}_1 X_{E_1} = \mathbf{O}X_O = \mathbf{R}_n X_{R_n} - \mathbf{S}X_S \tag{6.115}$$

whence

$$X_O = \frac{\mathbf{F}X_F - \mathbf{E}_1 X_{E_1}}{\mathbf{F} - \mathbf{E}_1} = \frac{\mathbf{R}_n X_{R_n} - \mathbf{S}X_S}{{}_n - \mathbf{S}} \tag{6.116}$$

Stages are determined by lines radiating from $O$ and tie lines used alternatively, in the manner of the construction on triangular coordinates. $\mathbf{M}$ can be calculated from Eq. (6.108). Then

$$\mathbf{E}_1 = \mathbf{M}\left(\frac{N_M - N_{R_n}}{N_{E_1} - N_{R_n}}\right) \tag{6.117}$$

and

$$\mathbf{R}_n = \mathbf{M} - \mathbf{E}_1 \tag{6.118}$$

For any stage,

$$\mathbf{R}_{m+1} + \mathbf{E}_{m+1} = \mathbf{R}_m + \mathbf{E}_m \tag{6.119}$$

$$\mathbf{R}_{m-1}N_{R_{m-1}} + \mathbf{E}_{m+1}N_{E_{m+1}} = \mathbf{R}_m N_{R_m} + \mathbf{E}_m N_{E_m} \tag{6.120}$$

from which

$$\mathbf{R}_m = \frac{\mathbf{R}_{m-1}(N_{R_{m-1}} - N_{E_{m+1}}) + \mathbf{E}_m(N_{E_{m+1}} - N_{E_m})}{N_{R_m} - N_{E_{m+1}}} \tag{6.121}$$

Equations (6.121) and (6.111) used alternately will permit calculation of the weights of the various extracts and raffinates. Solvent recovery is identical with that for single contact, and if pure $B$ is the solvent, $\mathbf{X}_O = \mathbf{X}_{R_n}$, and lines $SF$ and $SR_n$ are vertical since $S$ is at infinity.

**Types of Problems.** Ordinarily $F$, $X_F$, and $X_S$ are fixed by the process. The major remaining variables, amount of solvent $S$, number of stages $n$, and extract and raffinate compositions $X_{E_1}$ and $X_{R_n}$, may be additionally specified in pairs as follows: ($a$) $S$ and $n$: locate $E_1$ graphically by trial and error, $R_n$ by $E_1M$ extended, and fit the requisite number of stages on the diagram so that $R_n$ and $E_n$ fall on the ends of a tie line; ($b$) $n$ and either $X_{E_1}$ or $X_{R_n}$: determine $S$ by trial and error until the number of stages exactly fits as before; ($c$) $S$ and either $X_{E_1}$ or $X_{R_n}$: locate $M$, and either $X_{R_n}$ or $X_{E_1}$, $O$, and determine $n$ by direct calculation; ($d$) $X_{R_n}$ and $X_{E_1}$: locate $R_n$, $E_1$, $M$, $O$, and calculate $S$ and $n$ directly.

**Illustration 5.** One hundred pounds per hour of a 50% acetone ($C$)-50% water ($A$) solution is to be reduced to 10% acetone with 30 lb./hr. of 1,1,2-trichloroethane as solvent in a countercurrent multiple contact operation at 25°C. Determine the number of stages and concentrations and weights of the various streams.

*Solution.* Equilibrium data are available in *Ind. Eng. Chem.* **38,** 817 (1946). Refer to Fig. 6.33. Points $F$, $S$ (pure $B$), and $R_n$ are located. Basis: 1 hr.

$$F = 100 \text{ lb.}, \quad B = S = 30 \text{ lb.}, \quad X_{BF} = 0, \quad X_{BS} = X_{BB} = 1.0$$

Eq. (6.10): $$X_{BM} = \frac{FX_{BF} + SX_{BS}}{F + S} = \frac{100(0) + 30(1.0)}{100 + 30} = 0.231$$

$$M = F + S = 100 + 30 = 130 \text{ lb.}$$

Point $M$ is located on line $FB$, and line $R_nM$ is extended to locate $E_1$. Lines $E_1F$ and $BR_n$ are extended to intersection to locate point $O$. $R_1$ is located by the tie line through

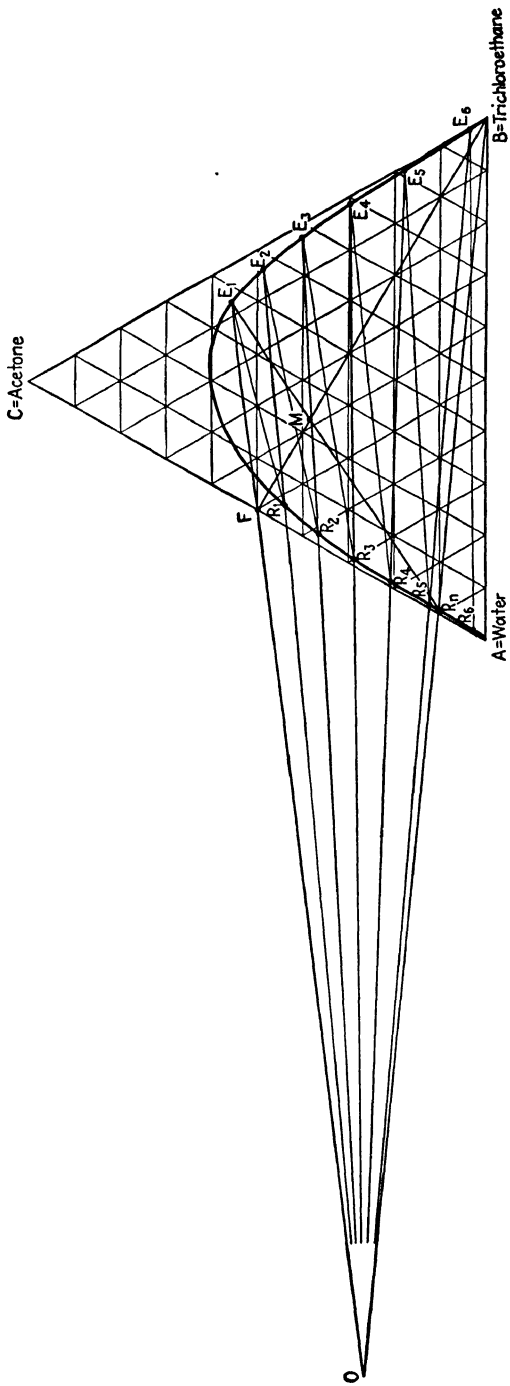



FIG. 6.33. Extraction of acetone from water with trichloroethane by countercurrent multiple contact.

$E_1$, $E_2$ by line $OR_1$ extended, $R_2$ by the tie line through $E_2$, etc. The following concentrations are obtained from the figure:

| Stage no. | 1 | 2 | 3 | 4 | 5 | 6 |
|---|---|---|---|---|---|---|
| Extract, $X_{CE}$ | 0.557 | 0.489 | 0.403 | 0.300 | 0.180 | 0.038 |
| Raffinate, $X_{CR}$ | 0.438 | 0.363 | 0.287 | 0.206 | 0.120 | 0.025 |

Since the desired $X_{CR_n} = 0.10$, approximately 5.2 theoretical stages are required. Adjustment of the quantity of solvent by trial to give exactly five or six stages can be made. The 5.2 will be accepted here.

Eq. (6.102): $$E_1 = \frac{M(X_{CM} - X_{CR_n})}{(X_{CE_1} - X_{CR_n})} = \frac{130(0.384 - 0.10)}{(0.557 - 0.10)} = 80.8 \text{ lb.}$$

Eq. (6.96): $R_n = M - E_1 = 130 - 80.8 = 49.2$ lb. (10% acetone)

Acetone unextracted = 49.2(0.10) = 4.92 lb.

Acetone extracted = 50 − 4.92 = 45.1 lb., or 90.2% of that in the feed.

For stage 1, Eq. (6.105):

$$R_1 = \frac{F(X_{AF} - X_{AE_2}) + E_1(X_{AE_2} - X_{AE_1})}{X_{AR_1} - X_{AE_2}}$$

$$= \frac{100(0.50 - 0.044) + 80.8(0.044 - 0.073)}{0.531 - 0.044} = 89.0 \text{ lb.}$$

Eq. (6.99): $$E_2 = R_1 - F + E_1 = 89.0 - 100 + 80.8 = 69.8 \text{ lb.}$$

For stage 2, Eq. (6.105):

$$R_2 = \frac{R_1(X_{AR_1} - X_{AE_3}) + E_2(X_{AE_3} - X_{AE_2})}{X_{AR_2} - X_{AE_3}}$$

$$= \frac{89.0(0.531 - 0.027) + 69.8(0.027 - 0.044)}{0.622 - 0.027} = 73.5 \text{ lb.}$$

Eq. (6.99): $$E_3 = R_2 - F + E_1 = 73.5 - 100 + 80.8 = 54.3 \text{ lb.}$$

In similar fashion the remaining extract and raffinate weights may be calculated.

It is now possible to set up a comparison of a typical extraction by the three processes of differential, cocurrent, and countercurrent contact. The calculations described in Illustrations 3 and 5 were supplemented by determining the number of stages and extract compositions for amounts of solvent other than those considered previously. In each case, the same feed, final raffinate, and solvent compositions were used. The results are summarized in Fig. 6.34. It is seen that for a given number of stages less solvent is required in countercurrent operation, with less extract solution resulting and consequent higher solute concentration in the extract, except for a single stage where both operations are identical. Increasing the number of stages beyond 5 results in relatively small changes. The limiting condition ($\infty$ stages) for the countercurrent case was determined by the methods described for minimum solvent, for the cocurrent case by the re-

sults of Illustration 2 for differential extraction. Curves of this sort may differ considerably from those shown, depending upon the equilibrium data and feed and solvent compositions. See for example those of Varteressian and Fenske (22).

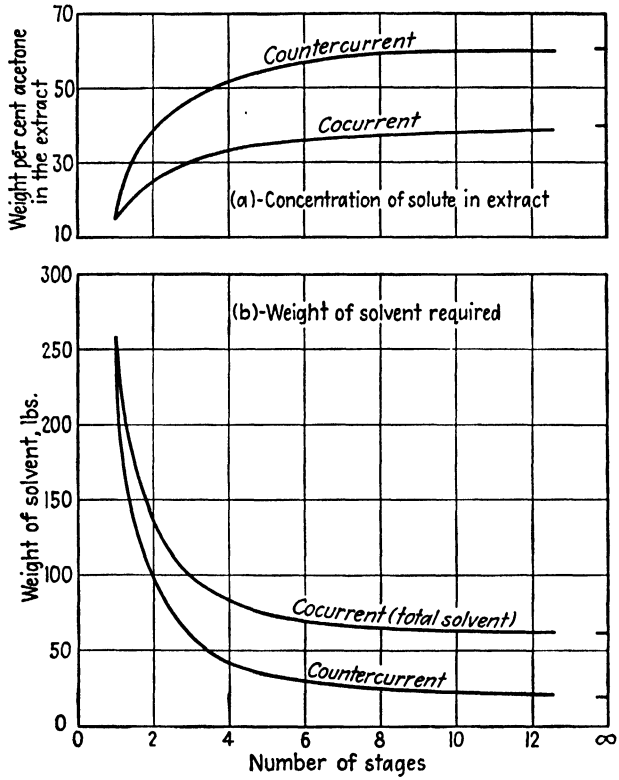



FIG. 6.34. Extraction of acetone from water by trichloroethane.

**Illustration 6.** One hundred pounds per hour of a feed solution containing 30% isopropanol ($C$), 70% water ($A$) are to be extracted by countercurrent multiple contact with pure benzene ($B$) as solvent at 25°C. The saturated final raffinate is to contain 2% isopropanol. Determine the minimum quantity of solvent that may be used.

*Solution.* Equilibrium data of Olsen and Washburn [*J. Am. Chem. Soc.* **57**, 303 (1935)] are used. See Fig. 6.35, where several of the tie lines are indicated. Basis: 1 hr.

$$F = 100 \text{ lb.}, \quad X_{CF} = 0.30, \quad X_{AF} = 0.70$$
$$X_{BS} = X_{BB} = 1.0, \quad S = B, \quad X_{CR_n} = 0.02$$

$F$ and $R_n$ are located on the diagram and the line $BR_n$ extended is drawn. The tie lines in this system slope downward toward the $A$ apex above about 24% isopropanol, downward toward the $B$ apex below. Tie line $HJ$ is parallel to line $BR_n$.

Extension of tie line $DG$, which passes through $F$, intersects the line $BR_n$ at $O'$. The operating point may therefore not lie between $O'$ and $R_n$. Any operating point to the left of $O'$ will be unsatisfactory, since it will represent an intersection of line $BR_n$ with

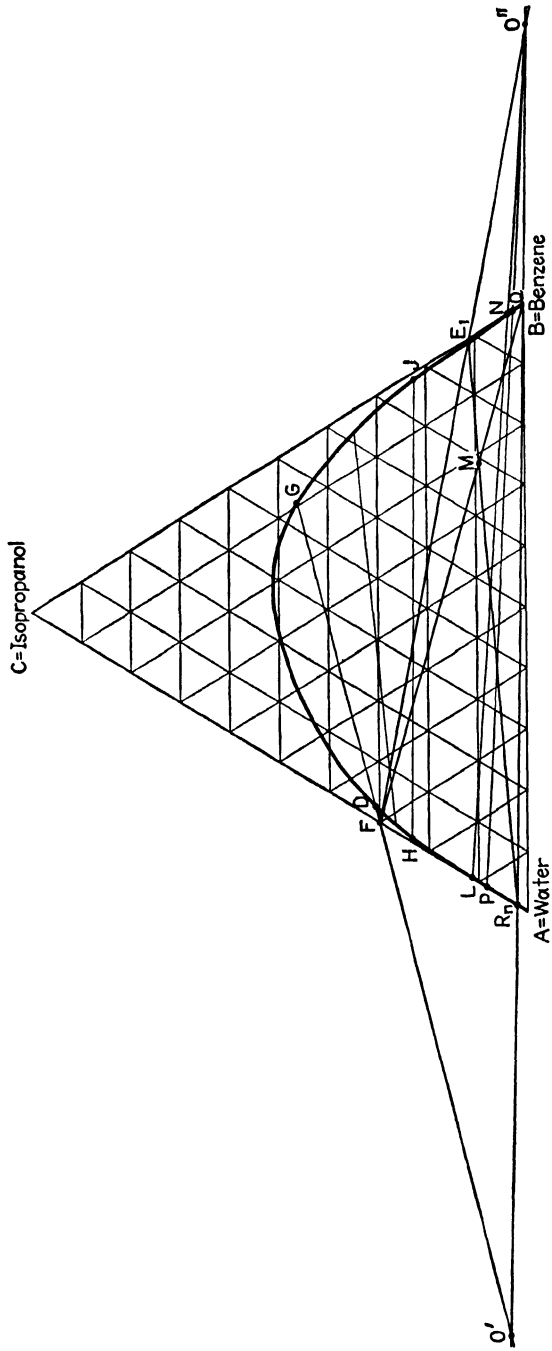



FIG. 6.35. Minimum solvent in the system water–isopropanol–benzene.

some tie line between $DG$ and $HJ$. Tie lines below $HJ$ intersect line $R_nB$ to the right of $B$, and the nearer the operating point to $B$ on this extension, the greater the amount of solvent indicated. Tie lines $LN$ and $PQ$, when extended, both intersect $R_nB$ at $O''$, the nearest to $B$. Tie lines below $PQ$ and between $LN$ and $HJ$ all intersect $R_nB$ farther to the right. The point $O''$ therefore represents the operating point for minimum solvent.

Draw $O''F$, intersecting the solubility curve at $E_1$. Draw $BF$ and $R_nE_1$, to intersect at $M$. $X_{BM} = 0.69$.

$$\therefore \text{ Eq. (6.11)}: \quad S = B = \frac{F(X_{BM} - X_{BF})}{(X_{BS} - X_{BM})} = \frac{100(0.69 - 0)}{(1.0 - 0.69)} = 222 \text{ lb.}$$

This is the minimum solvent rate per hour. A real operating point between $O''$ and $B$ must be chosen.

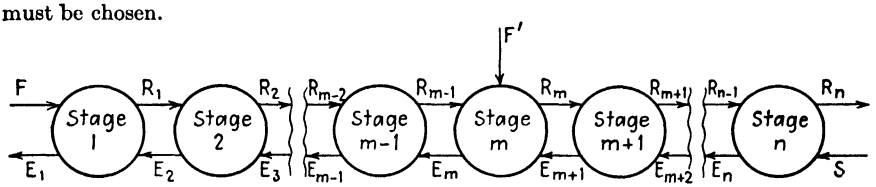



FIG. 6.36. Multiple feed in a countercurrent extraction.

**Multiple Feed.** The problem of two or more feed solutions of different compositions, both of which are to be extracted in the same cascade of stages to give a single raffinate and extract occasionally arises. Consider, for example, the flowsheet of Fig. 6.36, with two feed solutions, $F$ and $F'$. Feed $F'$ has a $C$ concentration between that of $F$ and $R_n$ and so can be introduced into the cascade conveniently at the point where the raffinate concentration corresponds most closely to that of $F'$.

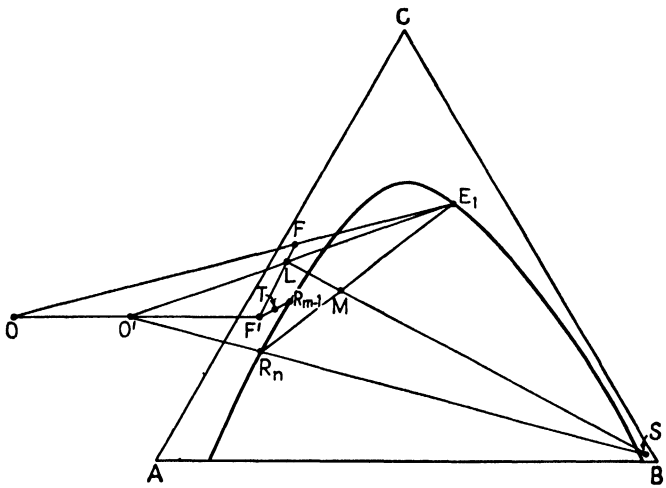



FIG. 6.37. Multiple feed in a countercurrent extraction.

Refer to Fig. 6.37, where the principal relationships are shown on triangular coordinates. A material balance for the entire plant is

$$F + F' + S = E_1 + R_n = M \tag{6.122}$$

or, letting $F + F' = L$, and rearranging,

$$F + F' - E_1 = L - E_1 = R_n - S = O' \tag{6.123}$$

Therefore, an operating point $O'$ is established, much as with a single feed, using the combined feeds $L$ together with $E_1$, $R_n$, and $S$. A material balance for stages $m$ through $n$ is

$$F' + R_{m-1} + S = R_n + E_m \tag{6.124}$$

or

$$F' + R_{m-1} - E_m = R_n - S = O' \tag{6.125}$$

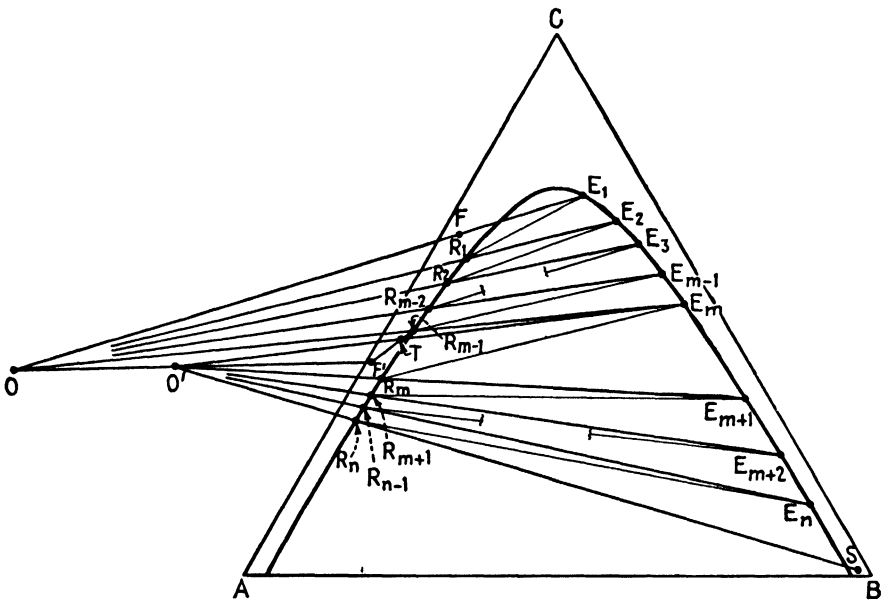



FIG. 6.38. Stage relationships with multiple feed.

Consequently the operating point $O'$ is used for all stages between $m$ and $n$ in the manner as for a single feed. For convenience, we may consider the feed to stage $m$ as a combination of $R_{m-1}$ and $F'$, $R_{m-1} + F' = T$, and calculations can be made for this end of the cascade exactly as before. For stages 1 through $m - 1$, the material balance is

$$F + E_m = R_{m-1} + E_1 \tag{6.126}$$

or

$$F - E_1 = R_{n-1} - E_m = O \tag{6.127}$$

Consequently an operating point $O$ is used for stages 1 through $m - 1$. Combining Eqs. (6.123) and (6.127),

$$O + F' = R_n - S = O' \tag{6.128}$$

from which we see that $O'$ is on the line $F'O$. The complete construction, including that for the stages, is shown in Fig. 6.38. Operating point $O$

is used for stages 1 through $m - 1$. The next stage $m$ has a $C$ concentration for the raffinate such that $X_{CF'}$ is between $X_{CR_m}$ and $X_{CR_{m-1}}$. Operating point $O'$ is therefore used for stages $m$ through $n$.

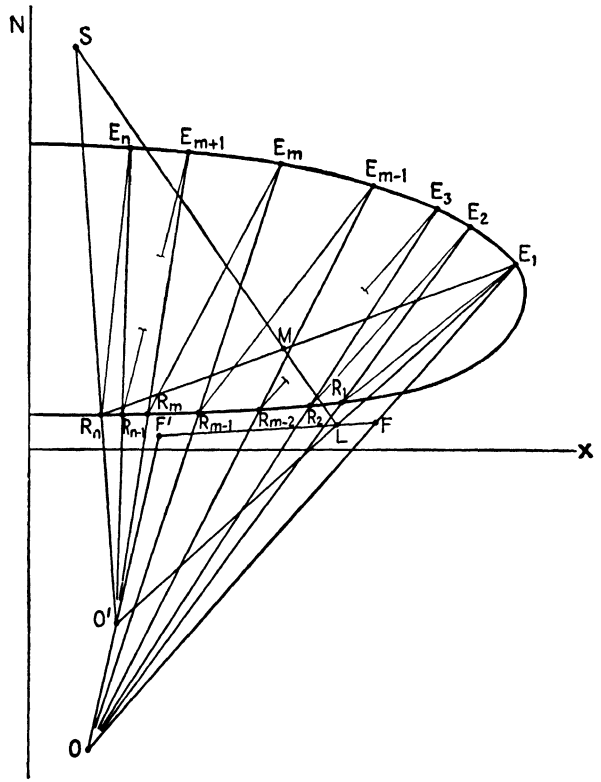



FIG. 6.39. Multiple feed, countercurrent extraction, Janecke coordinates.

The construction on Janecke coordinates is shown on Fig. 6.39, and on distribution coordinates on Fig. 6.40. The operating curve on the latter will show a discontinuity at $X_{CF'}$, the upper part having been obtained by drawing random lines from $O$ (Fig. 6.38), the lower part by drawing them from $O'$.

**Illustration 7.** Two solutions, feed $F$ at the rate of 100 lb./hr. containing 50% acetone, 50% water, and feed $F'$ at the rate of 100 lb./hr. containing 25% acetone, 75% water, are to be extracted in a countercurrent system with 50 lb./hr. of 1,1,2-trichloroethane at 25°C. to give a raffinate containing 10% acetone. Calculate the number of stages and the stage into which the feed $F'$ should be introduced.

*Solution.* The equilibrium data used previously [*Ind. Eng. Chem.* **38**, 817 (1946)] is again applicable. See Fig. 6.41. Basis: 1 hr.

$$F = 100 \text{ lb.}, \quad X_{CF} = 0.50, \quad X_{AF} = 0.50. \quad F' = 100 \text{ lb.},$$
$$X_{CF'} = 0.25, \quad X_{AF'} = 0.75, \quad L = F + F' = 200 \text{ lb.}$$

$$X_{CL} = \frac{FX_{CF} + F'X_{CF'}}{F + F'} = \frac{100(0.50) + 100(0.25)}{100 + 100} = 0.375$$

$S = B = 50$ lb., $X_{BS} = X_{BB} = 1.00$. $R_n$ is saturated, $X_{CR_n} = 0.10$. Locate $B$, $F$, $F'$, $L$, and $R_n$, and draw line $LB$. To locate $M$,

$$X_{BM} = \frac{LX_{BL} + BX_{BS}}{L + S} = \frac{200(0) + 50(1)}{200 + 50} = 0.200$$
$$M = L + S = 250 \text{ lb.}$$

Locate $M$ on line $LB$. Locate $E_1$ by extending $R_nM$ to the saturation curve. Locate operating point $O'$ at the intersection of $E_1L$ and $BR_n$ extended. Extend $O'F'$ and $FE_1$ to intersect with $O$.

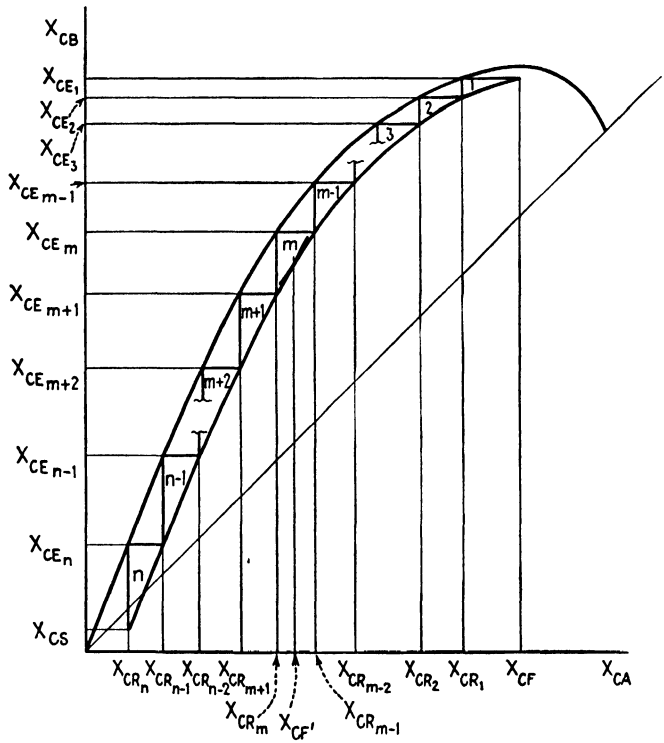



FIG. 6.40. Multiple feed, countercurrent extraction, rectangular coordinates.

The stages are determined on the distribution coordinates of Fig. 6.42. The upper operating curve is established by drawing random lines from $O$, and plotting $X_{CE}$ vs. $X_{CR}$ at the intersection of these with the saturation curve. The lower operating curve is similarly established using point $O'$. The stepwise construction indicates the stages. Total theoretical stages = 8.7, with feed $F'$ introduced between the fourth and fifth from the feed-$F$ end of the cascade.

Eq. (6.102): $$E_1 = \frac{M(X_{CM} - X_{CR_n})}{X_{CE_1} - X_{CR_n}} = \frac{250(0.30 - 0.10)}{0.523 - 0.10} = 118.1 \text{ lb.}$$

Eq. (6.123): $$R_n = L - E_1 + S = 200 - 118.1 + 50 = 131.9 \text{ lb.}$$

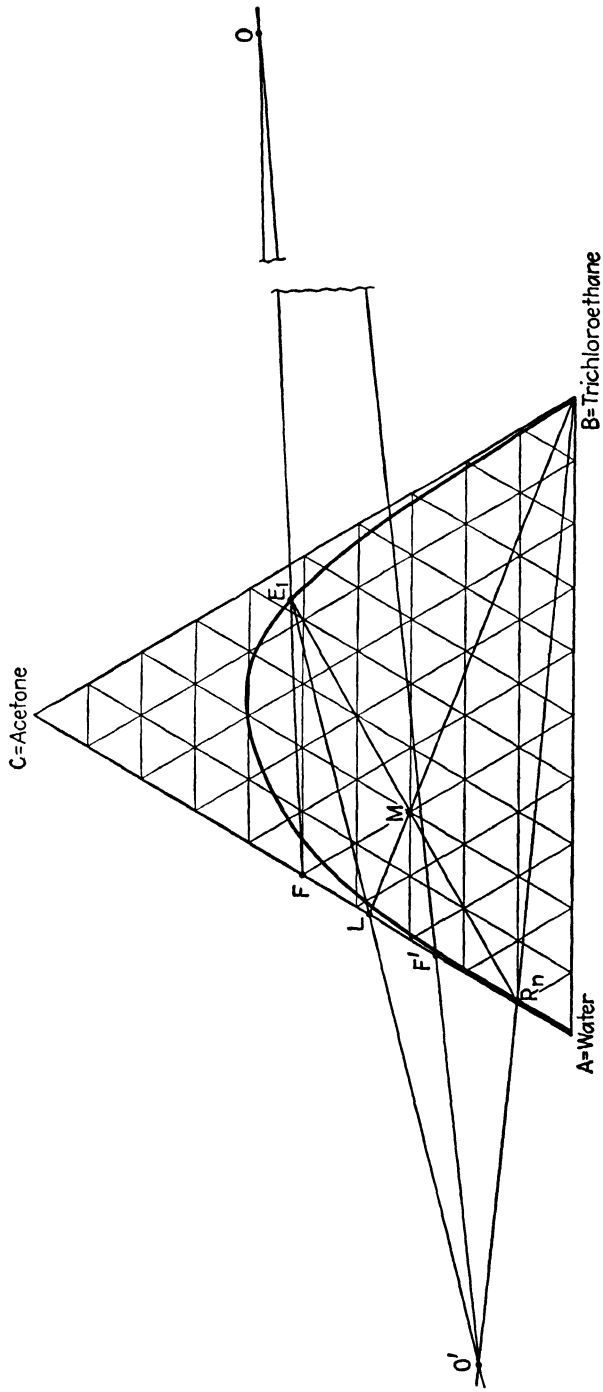



FIG. 6.41. Principal relationships for Illustration 7.

**Immiscible Solvents.** As in the case of cocurrent extraction, considerable simplification results if we may consider the liquids $A$ and $B$ substantially insoluble over the range of $C$ concentrations experienced in the extraction (2, 5). The same notation will be used as in the previous case,

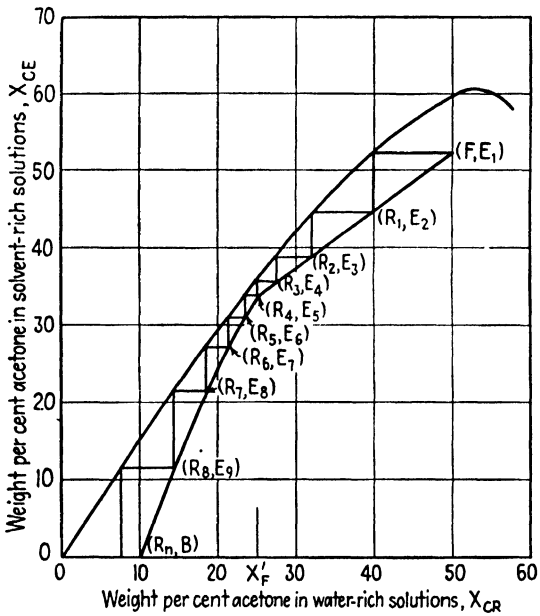



FIG. 6.42. Stage construction for Illustration 7.

$y = X_{CB}/X_{BB}$, $x = X_{CA}/X_{AA}$, etc., with the $A$ content of the feed and all raffinates remaining constant and the $B$ content of solvent and all extracts constant. A $C$ balance for stages 1 through $m$ is

$$Ax_F + By_{m+1} = Ax_m + By_1 \tag{6.129}$$

which may be rearranged to

$$y_{m+1} = \frac{A}{B}x_m + y_1 - \frac{A}{B}x_F \tag{6.130}$$

The latter is an equation of a straight line, $y_{m+1}$ vs. $x_m$, of slope $A/B$, since $y_1$ and $x_F$ are constants for a given plant. Since $m$ represents any stage, the line (an "operating line") is applicable to the entire plant and may be drawn between the two points whose coordinates are $(x_F,y_1)$ and $(x_n,y_S)$, as on Fig. 6.43. Since the equilibrium curve represents the relationship between $x_m$ and $y_m$, the stages can be represented by steps drawn between the equilibrium curve and the operating line, as shown.

A common problem is one where $A$, $x_F$, $x_n$, and $y_S$ are fixed. The operating line must then start at point $G$ (Fig. 6.43) and end on the line whose

abscissa is $x_F$, at an ordinate depending upon the solvent rate. At high solvent rates the operating line will be relatively flat, and few stages will be required. At low solvent rates, the reverse is true. Decreasing the solvent rate will ultimately bring the operating line to point $D$ on the figure, for which the number of stages is infinite, corresponding to the minimum solvent rate. It should be noted that, prior to this, should the operating line become tangent to the equilibrium curve at any point between $x_n$ and $x_F$, its slope will then indicate the minimum solvent rate.

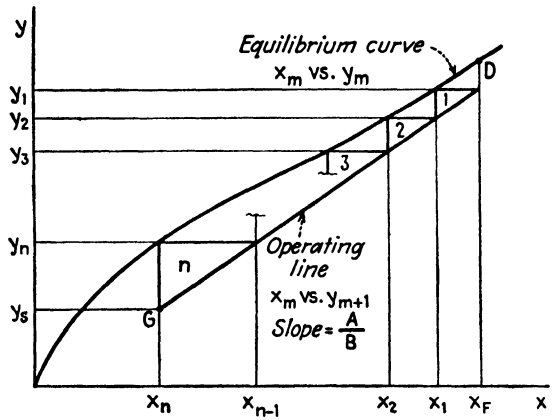



FIG. 6.43. Countercurrent multiple contact with immiscible solvents.

**Distribution Law.** If in addition to solvent immiscibility the distribution law [Eq. (6.88)] also applies, further simplification is possible. A material balance around stages $m + 1$ through $n$ is

$$Ax_m + By_S = Ax_n + By_{m+1} \tag{6.131}$$

Substituting Eq. (6.88) in the form $y_{m+1} = \mathbf{m}x_{m+1}$, and rearranging:

$$x_{m+1} - x_m\left(\frac{A}{\mathbf{m}B}\right) = \left(\frac{A}{\mathbf{m}B}\right)\left(y_S\frac{B}{A} - x_n\right) \tag{6.132}$$

The last equation may be so solved as to eliminate the concentrations of the raffinates of adjacent stages by the calculus of finite differences (19). If $\mathbf{m}B/A \neq 1$,

$$x_m = \frac{(B/A)(\mathbf{m}x_F - y_1)}{(\mathbf{m}B/A) - 1}\left(\frac{1}{\mathbf{m}B/A}\right)^m + \frac{(B/A)y_S - x_n}{(\mathbf{m}B/A) - 1} \tag{6.133}$$

which may be used to calculate intermediate raffinate concentrations without the necessity for graphical work.

Refer to Fig. 6.44. For a fixed value of $x_F$, $y_S$, and $y_1$, the operating line must start on a line of $y_S$ ordinate and terminate at point $K$. If the ratio of the slope of the equilibrium curve to that of the operating line $\mathbf{m}B/A$

is greater than unity, the final raffinate concentration will be the least for $\infty$ stages, and the operating line $GK$ results. For such a situation, the extent of extraction $x_F - (y_S/\mathrm{m})$ is the greatest. If in a real plant of $n$ stages, the extent of extraction is $x_F - x_n$, then

$$\frac{x_F - x_n}{x_F - y_S/\mathrm{m}} = \frac{(\mathrm{m}B/A)^{n+1} - (\mathrm{m}B/A)}{(\mathrm{m}B/A)^{n+1} - 1} \tag{6.134}$$

which is defined by Tiller (19) as the "relative extraction efficiency" of the plant. This relationship exactly parallels another derived for gas-absorption operations by Kremser (9) and modified by Souders and Brown (17). It is most effective in the graphical form prepared by Sherwood (16), Fig. 6.45, where solution of the equation for $n$ is readily made. The figure also permits ready determination of the minimum solvent ratio by use of the line $n = \infty$. The quantity $\mathrm{m}B/A$, which appears so frequently in developments of this sort, is termed the "extraction factor."

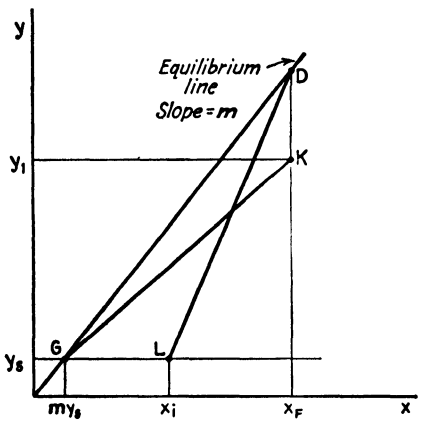



FIG. 6.44. Limiting extraction for distribution law cases.

If, on the other hand, $\mathrm{m}B/A$ is fixed at a value less than unity, the extent of extraction is definitely limited, giving rise to an operating line $LD$ (Fig. 6.44) with the "pinch" at the feed end of the cascade. A real plant must have a value of $x_n$ greater than $x_i$. Tiller (19) redefines relative extraction efficiency for this case as

$$\frac{x_F - x_n}{x_F - x_i} = \frac{1 - (\mathrm{m}B/A)^n}{1 - (\mathrm{m}B/A)^{n+1}} \tag{6.135}$$

For $\mathrm{m}B/A = 1$, by differentiation of numerator and denominator to resolve the indeterminate, the relative efficiency becomes $n/(n + 1)$.

**Illustration 8.** One hundred pounds per hour of a 4.5% solution of acetaldehyde ($C$) in toluene ($A$) is to be extracted with water ($B$) in a five-stage countercurrent plant to give the same raffinate concentration as in Illustration 4, 0.0048 lb. acetaldehyde/lb. toluene. Calculate the water rate required.

*Solution.* Basis: 1 hr. The equilibrium data of Illustration 4 will serve. See Fig. 6.46.

$$x_F = \frac{4.5}{100 - 4.5} = 0.0471 \text{ lb. acetaldehyde/lb. toluene}$$
$$A = 100 - 4.5 = 95.5 \text{ lb. toluene}$$
$$y_S = 0 \text{ lb. acetaldehyde/lb. water}$$
$$x_6 = 0.0048$$

The operating line is located by trial and error until five stages just fit between operating line and equilibrium curve. From the figure, $y_1 = 0.079$ lb. acetaldehyde/lb. water (corresponding to 7.33% acetaldehyde by weight). The slope of the operating line =

$$\frac{A}{B} = \frac{95.5}{B} = \frac{y_1 - y_S}{x_F - x_5} = \frac{0.079 - 0}{0.0471 - 0.0048}$$

$B = 51.1$ lb. water *Ans.*

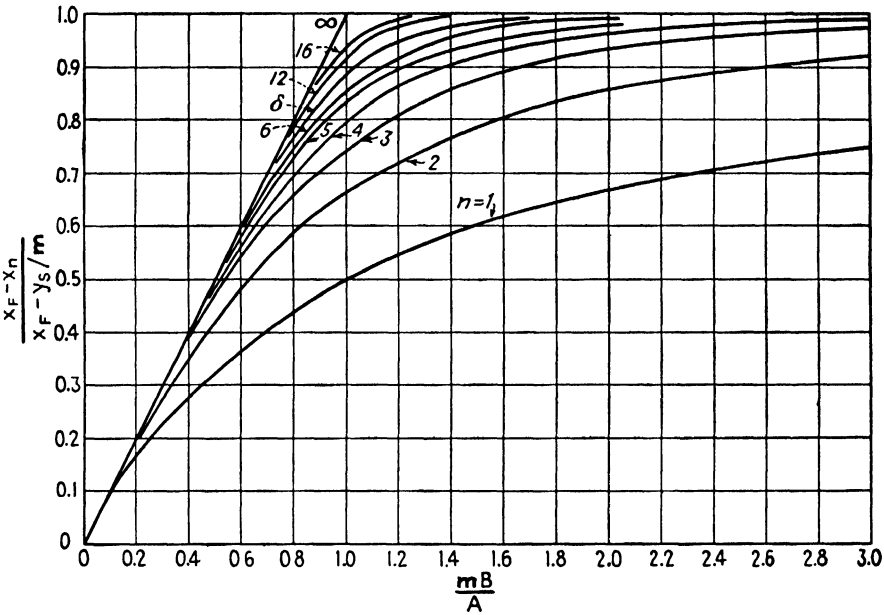



FIG. 6.45. Plot of Eq. (6.134). (*After Sherwood.*)

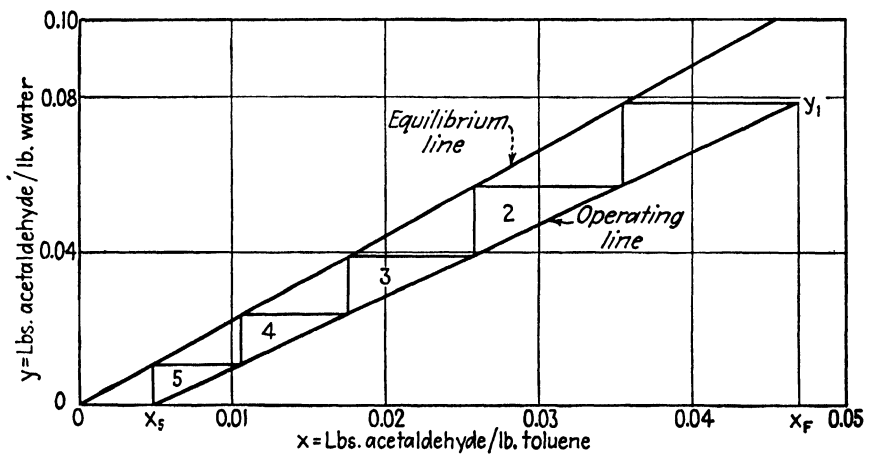



FIG. 6.46. Countercurrent extraction of acetaldehyde from toluene with water.

Alternatively, since the slope of the equilibrium curve is constant, $\mathbf{m} = 2.2$,

$$\frac{x_F - x_5}{x_F - y_S/\mathbf{m}} = \frac{0.0471 - 0.0048}{0.0471 - 0} = 0.896$$

From Fig. 6.45, at $n = 5$, $\frac{\mathbf{m}B}{A} = 1.18$.

$$\therefore B = \frac{A}{\mathbf{m}}(1.18) = \frac{95.5(1.18)}{2.2} = 51.1 \text{ lb. water} \quad Ans.$$

**Batchwise Operation.** The operation as described is necessarily continuous. Its effects can be approached batchwise in the laboratory by a complicated manipulation of stages, described by Jantzen (8) and Hunter and Nash (7) who evaluate the percentage approach to the true countercurrent effect in terms of the number of stages used and their arrangement.

## COUNTERCURRENT MULTIPLE CONTACT WITH REFLUX

Extension of a simple countercurrent operation to one involving the use of reflux provides a process which is analogous in its essentials to the rectification type of distillation. Whereas in the extraction operations described previously the richest extract leaving the plant was nearly in equilibrium with the feed solution, by proper use of reflux it is possible not only to separate systems showing unfavorable distribution coefficients but also to enrich the extract beyond that which is merely in equilibrium with the feed (7, 14, 18).

Consider the flowsheet of Fig. 6.47. The feed solution $F$ is separated into an extract product $P_E$ and a raffinate product $P_R$, both relatively far removed in composition from the feed. Stages 1 through $(f - 1)$ serve to increase the $C$ content of the extract, providing a primary product $E_1$. After removal of either all or most of the solvent to give a solution $E'$, the final extract product $P_E$ is withdrawn, allowing a portion of the stream $R_0$ to return to the plant as extract reflux flowing countercurrently to the enriching extract. The solvent separator (analogous to the condenser in rectification) is customarily a distillation device, and it removes sufficient solvent so that $E_1$ and $E'$ are at least on opposite sides of the solubility curve describing the ternary equilibria. $E'$, $R_0$, and $P_E$ are all of the same composition and may or may not be saturated (located on the solubility curve).

Stages $f + 1$ through $n$ constitute the raffinate stripping section of the cascade, where the raffinate solution is exhausted of its $C$ content. The primary raffinate product $R_n$ is divided into two streams: $P_R$, the saturated raffinate product, may be further treated to remove solvent and to provide the finished raffinate $P_R'$, and operation not concerned with the extraction operation; and $R_n'$, which when mixed with the extracting solvent $S$, provides the raffinate reflux $E_{n+1}$. $R_n$, $R_n'$, and $P_R$ are of the same composi-

tion, and sufficient solvent $S$ must be added at least to bring the composition of $E_{n+1}$ to the opposite side of the solubility curve but not so much that complete miscibility results in stage $n$. The entire operation is necessarily continuous; a batchwise series of operations can at best only approach it in net effect.

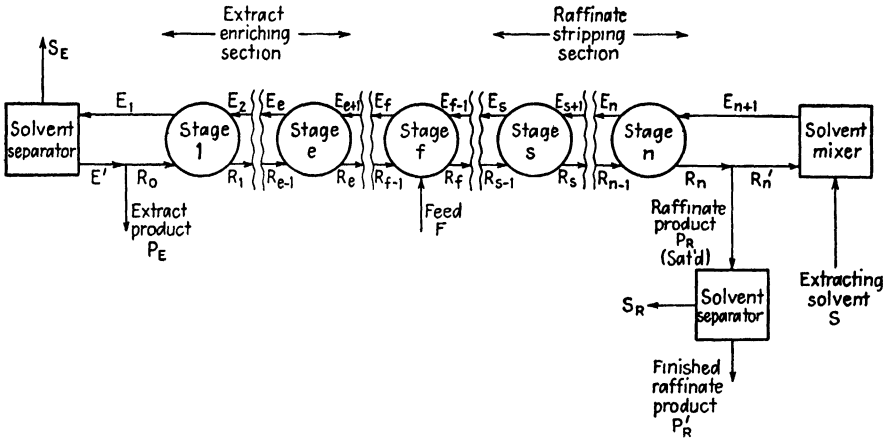



FIG. 6.47. Flowsheet for countercurrent multiple contact with extract and raffinate reflux.

**Extract End.** The computations will first be described in connection with triangular coordinates (23), Fig. 6.48. A material balance around the solvent separator shows

$$E_1 = S_E + E' \tag{6.136}$$

while a similar balance including the reflux stream is

$$E_1 = S_E + P_E + R_0 \tag{6.137}$$

Let

$$S_E + P_E = Q \tag{6.138}$$

$$\therefore E_1 = Q + R_0 \tag{6.139}$$

$Q$ is therefore on the line $S_E E'$, between $E_1$ and $S_E$. A material balance about the entire extract end of the plant including any stage $e$ in the extract-enriching section is

$$E_{e+1} = S_E + P_E + R_e \tag{6.140}$$

$$\therefore S_E + P_E = Q = E_{e+1} - R_e \tag{6.141}$$

and consequently $Q$ represents the net flow in the direction of the extract end of the plant, for all stages from 1 through $(f - 1)$. A line on the triangular coordinates radiating from $Q$ into the body of the triangle will cut the $B$-rich solubility curve at a concentration corresponding to the extract entering a given stage, while it cuts the $A$-rich solubility curve at a concentration corresponding to the raffinate from the same stage. Since for

any stage extract $E_e$ and raffinate $R_e$ are in equilibrium and are located on opposite ends of a tie line, the stepwise construction of alternate tie lines and lines from $Q$ as on Fig. 6.48 will establish all concentrations and the number of stages from 1 through $(f-1)$. From a consideration of Eq. (6.141),

$$\frac{R_e}{Q} = \frac{\overline{E_{e+1}Q}}{\overline{R_eE_{e+1}}} \tag{6.142}$$

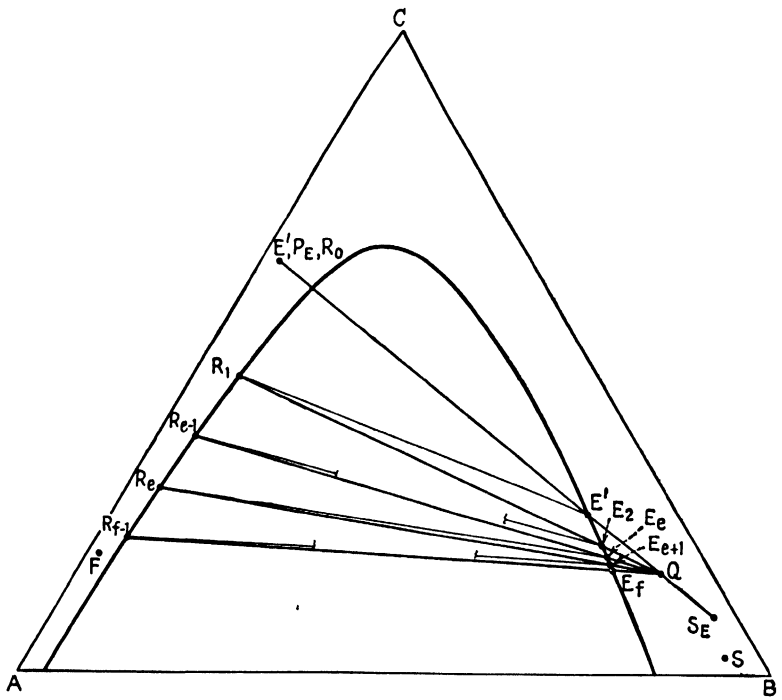



FIG. 6.48. Extract end of the countercurrent extraction with reflux.

Since

$$\overline{R_eE_{e+1}} + \overline{E_{e+1}Q} = \overline{R_eQ} \tag{6.143}$$

by combining Eqs. (6.142) and (6.143), we have

$$\frac{R_e}{E_{e+1}} = \frac{\overline{E_{e+1}Q}}{\overline{R_eQ}} = \frac{X_{AE_{e+1}} - X_{AQ}}{X_{AR_e} - X_{AQ}} \tag{6.144}$$

for any enriching stage. Analogous to rectification practice, this may be termed the internal reflux ratio, which will vary from stage to stage. At the end of the section,

$$\frac{R_0}{E_1} = \frac{\overline{E_1Q}}{\overline{R_0Q}} \tag{6.145}$$

$$\frac{S_E}{P_E} = \frac{\overline{P_EQ}}{\overline{QS_E}} \tag{6.146}$$

and

$$\overline{P_E Q} + \overline{Q S_E} = \overline{P_E S_E} \tag{6.147}$$

Combining Eqs. (6.145) to (6.147), and noting that $R_0$ and $P_E$ have the same location on the diagram,

$$\frac{R_0}{P_E} = \left(\frac{\overline{E_1 Q}}{\overline{P_E E_1}}\right)\left(\frac{\overline{P_E S_E}}{\overline{Q S_E}}\right) \tag{6.148}$$

which is the external reflux ratio at the extract end. Alternatively

$$\frac{R_0}{P_E} = \frac{(X_{AE_1} - X_{AQ})(X_{AP_E} - X_{AS_E})}{(X_{AP_E} - X_{AE_1})(X_{AQ} - X_{AS_E})} \tag{6.149}$$

The point $Q$ is therefore so located on line $S_E P_E$ as to give the desired reflux ratio.

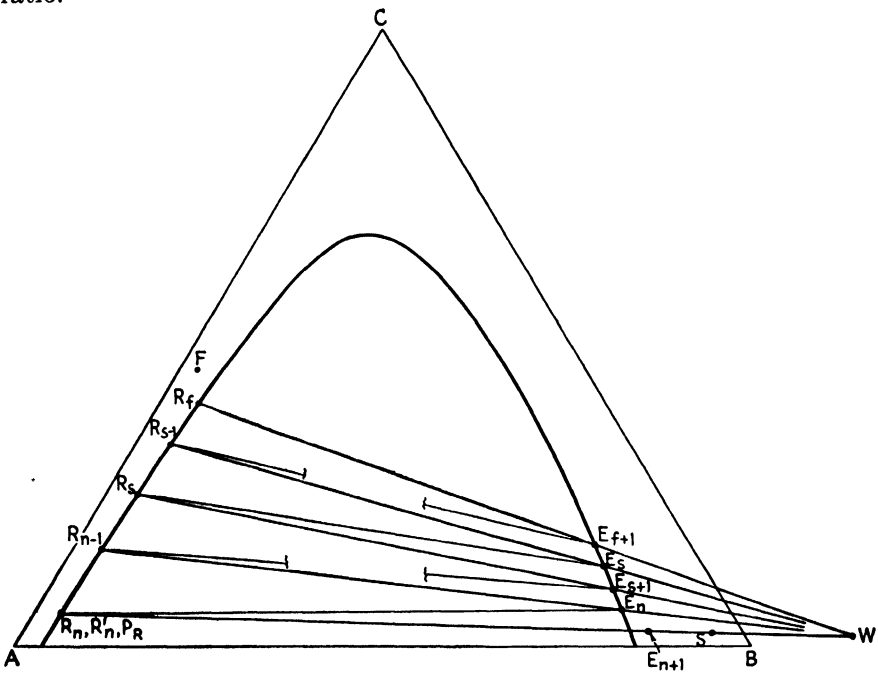



FIG. 6.49. Raffinate end of the countercurrent extraction with reflux.

**Raffinate End.** Refer to Fig. 6.49(23). A material balance around the solvent mixer

$$R'_n + S = E_{n+1} \tag{6.150}$$

Similarly, including $R_n$,

$$R_n + S = E_{n+1} + P_R \tag{6.151}$$

Let

$$S - P_R = W \tag{6.152}$$

$$\therefore E_{n+1} = R_n + W \tag{6.153}$$

A material balance around the entire raffinate end of the plant and including stage $(s + 1)$:

$$R_s + S = E_{s+1} + P_R \tag{6.154}$$

or

$$S - P_R = W = E_{s+1} - R_s \tag{6.155}$$

Since $s$ is any stage in the stripping section, a line radiating from $W$ will cut the $A$-rich side of the solubility curve at a concentration corresponding to the raffinate, leaving a given stage and the $B$-rich side at a concentration corresponding to the extract entering that stage. Since, as before, extract and raffinate from the same stage are located on opposite ends of a tie line, the stepwise construction shown permits determination of the number of stages from $(f + 1)$ through $n$, and all pertinent concentrations. For any stage $s$, Eq. (6.155) indicates that

$$\frac{R_s}{W} = \frac{\overline{E_{s+1}W}}{\overline{R_sE_{s+1}}} \tag{6.156}$$

Combining Eqs. (6.155) and (6.156):

$$\frac{R_s}{E_{s+1}} = \frac{\overline{E_{s+1}W}}{\overline{R_sW}} = \frac{X_{AE_{s+1}} - X_{AW}}{X_{AR_s} - X_{AW}} \tag{6.157}$$

the internal reflux ratio for the stripping section, varying from stage to stage. The fictitious $X_{AW}$ may be calculated from Eq. (6.152), using an $A$ balance. Specifically, at the end of the cascade

$$\frac{R_n}{E_{n+1}} = \frac{\overline{E_{n+1}W}}{\overline{R_nW}} \tag{6.158}$$

$$\frac{W}{P_R} = \frac{\overline{SP_R}}{\overline{SW}} \tag{6.159}$$

and

$$\overline{SP_R} + \overline{SW} = \overline{P_RW} \tag{6.160}$$

Combining Eqs. (6.150), (6.159), and (6.160), and noting that $R'_n$ and $P_R$ have the same location on the triangular diagram:

$$\frac{R'_n}{P_R} = \left(\frac{\overline{E_{n+1}S}}{\overline{P_RE_{n+1}}}\right)\left(\frac{\overline{P_RW}}{\overline{SW}}\right) \tag{6.161}$$

the external raffinate reflux ratio. Alternatively,

$$\frac{R'_n}{P_R} = \frac{(X_{AE_{n+1}} - X_{AS})(X_{AP_R} - X_{AW})}{(X_{AP_R} - X_{AE_{n+1}})(X_{AS} - X_{AW})} \tag{6.162}$$

The point $W$ is therefore located on the line $P_RS$ to satisfy a predetermined reflux ratio.

As in a distillation column, reflux ratios at both ends of the cascade may not both be set arbitrarily. Refer to Fig. 6.50. A material balance about the feed stage $f$:

$$E_{f+1} + R_{f-1} + F = E_f + R_f \tag{6.163}$$

or

$$E_{f+1} - R_f + F = E_f - R_{f-1} \tag{6.164}$$

For the entire raffinate-stripping section:

$$R_f + S = E_{f+1} + P_R \tag{6.165}$$

or

$$S - P_R = W = E_{f+1} - R_f \tag{6.166}$$

For the entire extract-enriching section:

$$E_f = S_E + P_E + R_{f-1} \tag{6.167}$$

or

$$S_E + P_E = Q = E_f - R_{f-1} \tag{6.168}$$

Combining Eqs. (6.164), (6.166), and (6.168),

$$W + F = Q \tag{6.169}$$

and point $Q$ must be on the line $FW$. Letting $E_f + R_f = K$, and $R_{f-1} + F = J$, we have from Eq. (6.163):

$$J + E_{f+1} = K \tag{6.170}$$

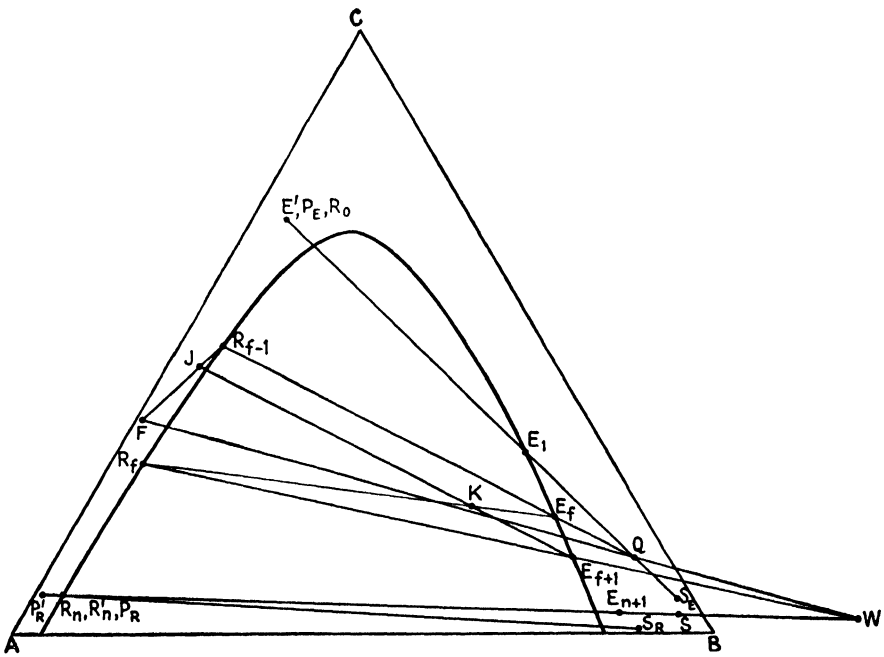



FIG. 6.50. Feed-stage construction.

These relationships are shown on Fig. 6.50. The entire stage construction for the plant is now clear. Starting with stage 1, $Q$ is used as an operating point until a tie line (from $E_f$) crosses the line $FQ$. From stage $f$ through $n$, $W$ is the operating point. The diagram also shows the removal of solvent from $P_R$, although this is not part of the extraction operation.

**Minimum Reflux Ratio.** From a consideration of the stepwise construction of alternating tie lines and radiating lines from $Q$ and $W$, it is clear that should the extension of any tie line in the extract-enriching section pass through $Q$, or in the raffinate-stripping section through $W$, it would require an infinite number of stages merely to reach this tie line by the stepwise procedure. Equation (6.148) indicates that the nearer $Q$ lies to $S_E$, the larger the reflux ratio. For the extract-enriching section, therefore, the

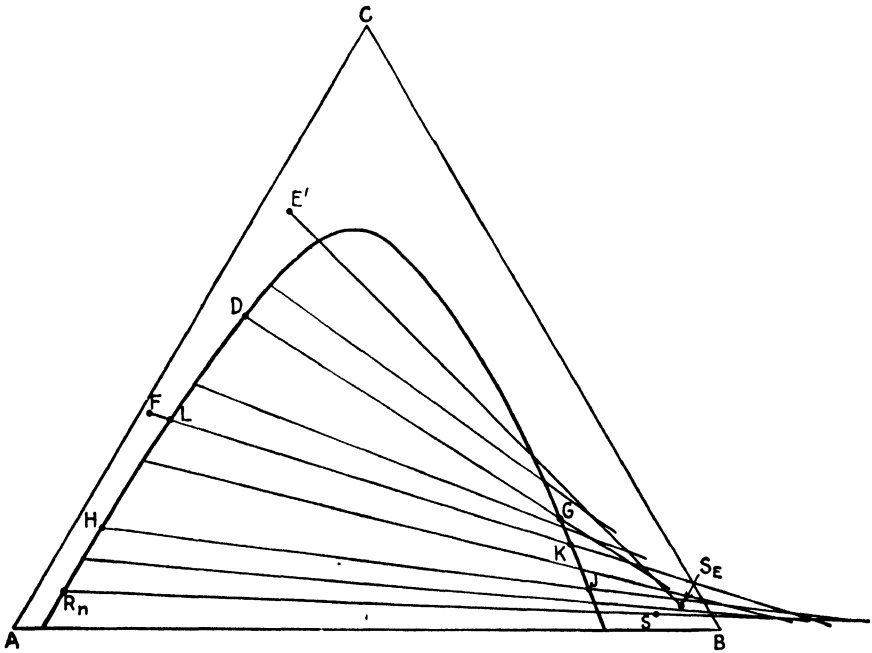



FIG. 6.51. Determination of the minimum reflux ratio.

minimum possible reflux ratio still requiring infinite stages would place $Q$ at the intersection which is nearest $S_E$ of an extended tie line in this section and line $E'S_E$, such as tie line $DG$, Fig. 6.51. Similarly in the raffinate-stripping section, Eq. (6.161) indicates that the nearer $W$ is located to $S$, the larger the reflux ratio. Consequently the minimum possible reflux ratio will be such that $W$ is at the intersection which is nearest to $S$ of an extended tie line and line $R_nS$, such as tie line $HJ$, Fig. 6.51. Since Eq. (6.169) must likewise be satisfied, either $Q$ or $W$ must be placed at one of these intersections and the other adjusted so that $F$, $Q$, and $W$ are on the same straight line. Equations (6.144), (6.148), (6.157), and (6.161) then give the minimum reflux ratios for the case at hand. In many instances, the minimum reflux ratio will be established simultaneously for both sections of the cascade by the tie line $LK$ which when extended passes through $F$

(23), but not in the case illustrated in Fig. 6.51. In an actual plant, $W$ must be nearer $S$, and $Q$ nearer $S_E$, than the positions thus chosen.

**Total Reflux.** For the least number of stages, corresponding to total reflux or infinite reflux ratio, no raffinate product or extract product is withdrawn from the plant. To maintain the material balance, $F$ and consequently the capacity of the plant must be zero. $R_n = R'_n$, $R_0 = E'$, $S = S_E$, and points $Q$ and $W$ both coincide with $S$ on the triangular diagram. The construction is shown on Fig. 6.52.

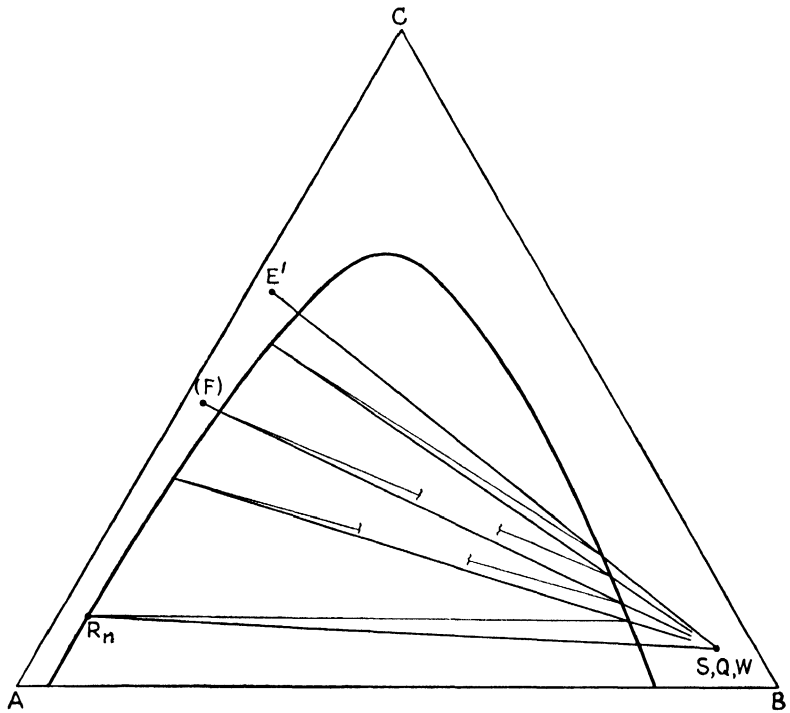



FIG. 6.52. Infinite reflux ratio and minimum stages

**Optimum Reflux Ratio.** For any plant, the number of stages will vary regularly in a manner dependent upon the ternary equilibria and feed, solvent, and product compositions, from the minimum number at total reflux to infinity at minimum reflux ratio. The cost of the stages thus at first decreases rapidly as reflux ratio increases, but since their capacity must increase at high reflux ratios, their cost passes through a minimum. Simultaneously the quantity of liquids to be handled, solvent inventory, and the cost of solvent recovery per unit of feed handled increases continually with reflux ratio, with consequent increasing operating cost. The total cost per unit of feed, which is the sum of investment and operating cost, will therefore show a minimum at what is termed the optimum reflux ratio.

**Pure $B$ as Solvent.** A simple case frequently arising is one where the solvent is pure $B$, $F$ contains no $B$, and the solvent removed at the extract end of the plant is pure $B$. The equations previously presented all apply, and the construction diagram is altered so that $F$ is on the $A$–$C$ axis, and $S$ on the $B$ apex. The change requires no further explanation. Other modifications, such as the use of different temperatures in the various stages, are obvious from what has been described in connection with the other methods of extraction.

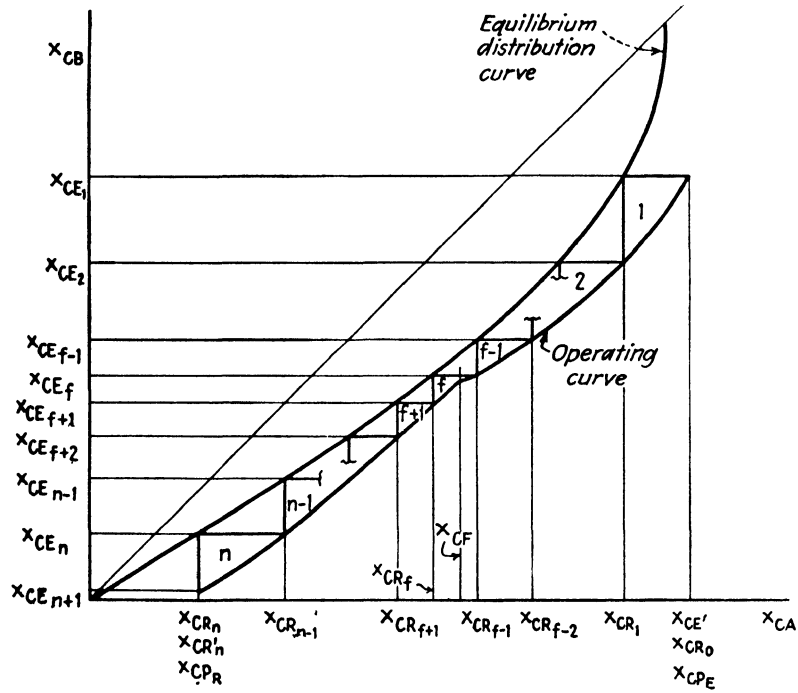



FIG. 6.53. Countercurrent extraction with reflux on distribution coordinates.

**Distribution Coordinates.** Where the number of stages is very large, transfer of the stage calculations to $X_{CA}$ vs. $X_{CB}$ coordinates is useful. The general principles are the same as for countercurrent extraction without reflux. Random lines are drawn on [illegible] coordinates from the operating points $Q$ and $W$, and the concentrations at the intersections of these lines with the solubility curve plotted as an operating curve, as in Fig. 6.53. The discontinuity in this curve occurs as the transition is made from $Q$ to $W$ as operating points. The stages are then stepped off. Minimum reflux conditions will appear as in Fig. 6.54, where the pinch is shown in the extract-enriching section. The pinch may, of course, occur at the feed or in the raffinate-stripping section. The condition of total reflux, with minimum stages, is indicated in Fig. 6.55.

**Janecke Coordinates** (10). Because of crowding on the triangular coordinates, the rectangular plot of Janecke is particularly useful for this case since the calculator is not limited to the single size of graph paper

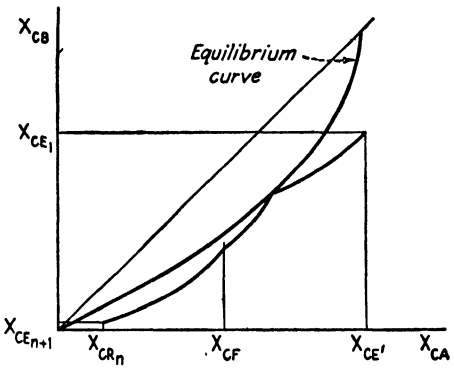



FIG. 6.54. Minimum reflux for countercurrent multiple contact.

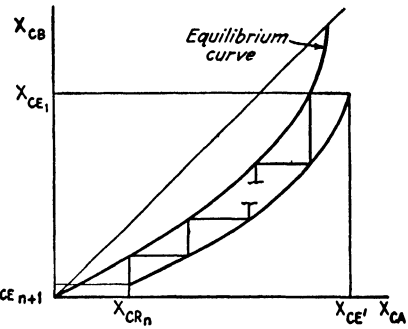



FIG. 6.55. Total reflux, minimum stages.

ordinarily available for the former. Refer to Figs. 6.47 and 6.56. At the extract end of the plant, an $(A + C)$ balance about the solvent separator is

$$\mathbf{E}_1 = \mathbf{S}_E + \mathbf{E}' \tag{6.171}$$

and for $B$:

$$\mathbf{E}_1 N_{E_1} = \mathbf{S}_E N_{S_E} + \mathbf{E}' N_{E'} \tag{6.172}$$

Similarly, including the raffinate reflux,

$$\mathbf{E}_1 = \mathbf{S}_E + \mathbf{P}_E + \mathbf{R}_0 \tag{6.173}$$

$$\mathbf{E}_1 N_{E_1} = \mathbf{S}_E N_{S_E} + \mathbf{P}_E N_{P_E} + \mathbf{R}_0 N_{R_0} \tag{6.174}$$

Allowing

$$\mathbf{Q} = \mathbf{S}_E + \mathbf{P}_E \tag{6.175}$$

then

$$\mathbf{E}_1 = \mathbf{Q} + \mathbf{R}_0 \tag{6.176}$$

which places point $Q$ on lines $S_E P_E$ between $S_E$ and $E_1$. For the entire extract end of the plant including stage $e$:

$$\mathbf{E}_{e+1} = \mathbf{S}_E + \mathbf{P}_E + \mathbf{R}_e \tag{6.177}$$

or

$$\mathbf{S}_E + \mathbf{P}_E = \mathbf{Q} = \mathbf{E}_{e+1} - \mathbf{R}_e \tag{6.178}$$

Consequently point $Q$ is the operating point for stage construction in the extract-enriching section. Tie lines, as usual, connect raffinate and extract from the same stage. As in the case of triangular coordinates, the internal reflux ratio is

$$\frac{\mathbf{R}_e}{\mathbf{E}_{e+1}} = \frac{\overline{E_{e+1}Q}}{\overline{R_e Q}} = \frac{N_Q - N_{E_{e+1}}}{N_Q - N_{R_e}} \tag{6.179}$$

The external extract reflux becomes

$$\frac{\mathbf{R}_0}{\mathbf{P}_E} = \left(\frac{\overline{E_1Q}}{\overline{P_EE_1}}\right)\left(\frac{\overline{P_ES_E}}{\overline{QS_E}}\right) = \frac{(N_Q - N_{E_1})(N_{S_E} - N_{P_E})}{(N_{E_1} - N_{P_E})(N_{S_E} - N_Q)} \tag{6.180}$$

In the special case that the solvent removed at the extract end is pure $B$, $S_E = B$, line $E_1Q$ is vertical, and

$$\frac{\mathbf{R}_0}{\mathbf{P}_E} = \frac{\overline{E_1Q}}{\overline{P_EE_1}} = \frac{N_Q - N_{E_1}}{N_{E_1} - N_{P_E}} \tag{6.181}$$

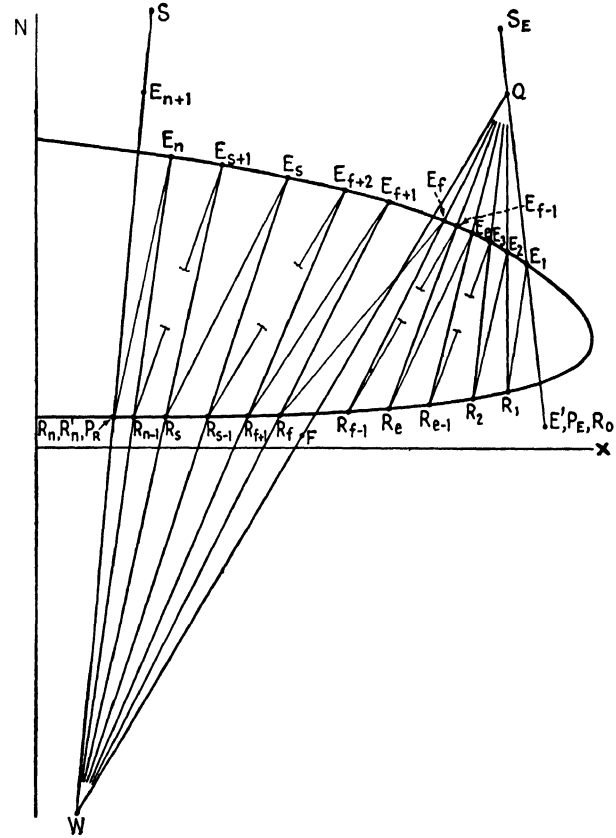



FIG. 6.56. Countercurrent multiple contact with extract and raffinate reflux, Janecke coordinates.

The coordinates of $Q$ may be established from its defining equation. A $B$ balance:

$$\mathbf{Q}N_Q = \mathbf{S}_EN_{S_E} + \mathbf{P}_EN_{P_E} \tag{6.182}$$

whence

$$N_Q = \frac{\mathbf{S}_EN_{S_E} + \mathbf{P}_EN_{P_E}}{\mathbf{S}_E + \mathbf{P}_E} \tag{6.183}$$

A $C$ balance leads to

$$\mathbf{X}_Q = \frac{\mathbf{S}_E\mathbf{X}_{S_E} + \mathbf{P}_E\mathbf{X}_{P_E}}{\mathbf{S}_E + \mathbf{P}_E} \tag{6.184}$$

For pure $B$ removed at the extract separator, $\mathbf{S}_E = 0$, $N_{S_E} = \infty$, $\mathbf{S}_E N_{S_E} = B_E$, and

$$N_Q = \frac{B_E}{\mathbf{P}_E} + N_{P_E}, \qquad \mathbf{X}_Q = \mathbf{X}_{P_E} \tag{6.185}$$

At the raffinate end of the plant, a material balance for $(A + C)$ around the solvent mixer is

$$\mathbf{R}'_n + \mathbf{S} = \mathbf{E}_{n+1} \tag{6.186}$$

and for $B$:

$$\mathbf{R}'_n N_{R'_n} + \mathbf{S}N_S = \mathbf{E}_{n+1}N_{E_{n+1}} \tag{6.187}$$

Including the raffinate product, the balances become

$$\mathbf{R}_n + \mathbf{S} = \mathbf{E}_{n+1} + \mathbf{P}_R \tag{6.188}$$

and

$$\mathbf{R}_n N_{R_n} + \mathbf{S}N_S = \mathbf{E}_{n+1}N_{E_{n+1}} + \mathbf{P}_R N_{P_R} \tag{6.189}$$

Letting

$$\mathbf{W} = \mathbf{S} - \mathbf{P}_R \tag{6.190}$$

then

$$\mathbf{E}_{n+1} = \mathbf{R}_n + \mathbf{W} \tag{6.191}$$

For the entire raffinate-stripping section through stage $s + 1$:

$$\mathbf{R}_s + \mathbf{S} = \mathbf{E}_{s+1} + \mathbf{P}_R \tag{6.192}$$

or

$$\mathbf{S} - \mathbf{P}_R = \mathbf{W} = \mathbf{E}_{s+1} - \mathbf{R}_s \tag{6.193}$$

Point $W$ is then the operating point for stage construction lines in the raffinate-stripping section, with tie lines joining extract and raffinate from the same stage, as in Fig. 6.56. The internal reflux ratio becomes

$$\frac{\mathbf{R}_s}{\mathbf{E}_{s+1}} = \frac{\overline{E_{s+1}W}}{\overline{R_sW}} = \frac{N_{E_{s+1}} - N_W}{N_{R_s} - N_W} \tag{6.194}$$

and the external reflux ratio

$$\frac{\mathbf{R}'_n}{\mathbf{P}_R} = \left(\frac{\overline{E_{n+1}S}}{\overline{P_RE_{n+1}}}\right)\left(\frac{\overline{P_RW}}{\overline{SW}}\right) = \frac{(N_S - N_{E_{n+1}})(N_{P_R} - N_W)}{(N_{E_{n+1}} - N_{P_R})(N_S - N_W)} \tag{6.195}$$

In the special case that the extraction solvent is pure $B$, line $E_{n+1}W$ is vertical, and

$$\frac{\mathbf{R}'_n}{\mathbf{P}_R} = \frac{\overline{P_RW}}{\overline{P_RE_{n+1}}} = \frac{N_{P_R} - N_W}{N_{E_{n+1}} - N_{P_R}} \tag{6.196}$$

The coordinates of $W$, as for $Q$, are found by material balances. For component $B$:

$$\mathbf{W}N_W = \mathbf{S}N_S - \mathbf{P}_R N_{P_R} \tag{6.197}$$

$$\therefore N_W = \frac{\mathbf{S}N_S - \mathbf{P}_R N_{P_R}}{\mathbf{S} - \mathbf{P}_R} \tag{6.198}$$

Similarly,

$$\mathbf{X}_W = \frac{\mathbf{S}\mathbf{X}_S - \mathbf{P}_R\mathbf{X}_{P_R}}{\mathbf{S} - \mathbf{P}_R} \tag{6.199}$$

If the solvent added to the mixer is pure $B$, $\mathbf{S} = 0$, $N_S = \infty$, $\mathbf{S}N_S = B_R$, whence

$$N_W = N_{P_R} - \frac{B_R}{\mathbf{P}_R}, \qquad \mathbf{X}_W = \mathbf{X}_{P_R} \tag{6.200}$$

For the entire plant, a non-$B$ balance becomes

$$\mathbf{F} + \mathbf{S} = \mathbf{P}_R + \mathbf{P}_E + \mathbf{S}_E \tag{6.201}$$

or, rearranging and substituting Eqs. (6.175) and (6.190):

$$\mathbf{F} + \mathbf{W} = \mathbf{Q} \tag{6.202}$$

The reflux ratios at the opposite ends of the plant are therefore not independent; only one may be arbitrarily fixed. For component $B$:

$$\mathbf{F}N_F + \mathbf{W}N_W = \mathbf{Q}N_Q \tag{6.203}$$

For component $C$:

$$\mathbf{F}\mathbf{X}_F + \mathbf{W}\mathbf{X}_W = \mathbf{Q}\mathbf{X}_Q \tag{6.204}$$

Solving Eqs. (6.202) to (6.204) simultaneously:

$$\frac{N_Q - N_F}{N_F - N_W} = \frac{\mathbf{X}_Q - \mathbf{X}_F}{\mathbf{X}_F - \mathbf{X}_W} \tag{6.205}$$

which is convenient for the analytical determination of the coordinates of $Q$ or $W$.

**Minimum Reflux Ratio.** The general principles are the same as for triangular coordinates. If any tie line in the extract-enriching section passes through point $Q$ when extended, an infinite number of stages are required to reach this tie line. Similarly, an extended tie line in the raffinate-stripping section passing through point $W$ leads to infinite stages. The nearer $Q$ lies to $S_E$, the greater the extract reflux [Eq. (6.180)]; the farther $W$ from $P_R$, the greater the raffinate reflux [Eq. (6.195)]. The procedure for minimum reflux ratio may then be briefly outlined (refer to Fig. 6.57). Extend all tie lines in the extract-enriching section to intersection with line $E'S_E$ and note the intersection nearest $S_E$, point $D$ on the figure. Extend all tie lines in the raffinate-stripping section to intersection with line $SP_R$ and note the one farthest from $S$, point $G$ on the figure. Choose one of these, $G$ for $W$ or $D$ for $Q$, consistent with the facts that $F$, $W$, and $Q$ must be on the same straight line and that $Q$ may not be lower than $D$ nor $W$ higher than $G$. Equations (6.180) and (6.195) then give the minimum reflux ratio. In most instances, the tie line $HJ$, which when extended passes through $F$, will locate simultaneously $W$ and $Q$ for minimum reflux but not in the case illustrated.

**Total Reflux.** For the least number of stages, the capacity of the plant for feed solution is zero, and no products are withdrawn. $S$, $S_E$, $Q$, and $W$ coincide as on Fig. 6.58. For pure solvent $B$ into the solvent mixer, $S$ will be at infinity and the radiating stage construction lines become vertical.

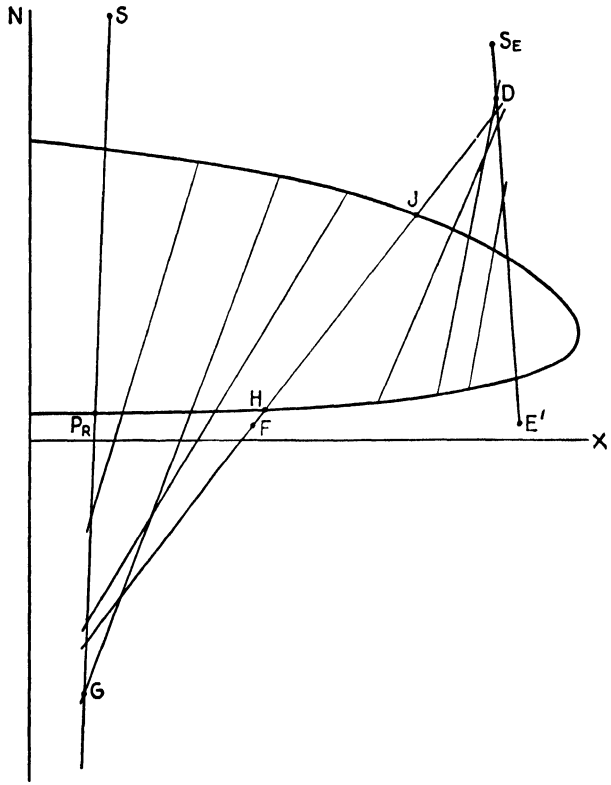



FIG. 6.57. Determination of minimum reflux ratio.

**Type 2 Systems.** Computations thus far described include diagrams for Type 1 systems only. The arrangement of the graphical work and the equations all apply exactly for Type 2 systems. However, whereas in the case of Type 2 systems use of reflux and pure $B$ as extracting solvent will make possible the production of raffinate and extract products containing as nearly pure $A$ and $C$, respectively, as desired, for Type 1 systems only the raffinate may be enriched to such an extent. The maximum purity of $C$ in the extract will be limited to a solvent-separation line $S_E E'$ which is tangent to the binodal curve.

**Illustration 9.** One hundred moles per hour of a solution containing 47.5 mole per cent *n*-hexane ($A$), 47.5 mole per cent methylcyclopentane ($C$), 5 mole per cent aniline ($B$) are to be separated into a solution containing 95 mole per cent hexane, and one containing 5 mole per cent hexane, both on an aniline-free basis. Pure aniline is to be the solvent

and the temperature is to be 25°C. Pure aniline will be removed in the solvent separators, leaving aniline-free products. Raffinate reflux $E_{n+1}$ is to be saturated. Determine (*a*) the minimum number of stages, (*b*) the minimum reflux ratios, and (*c*) the number of stages and important flow quantities for an extract reflux ratio of 2.2 times the minimum.

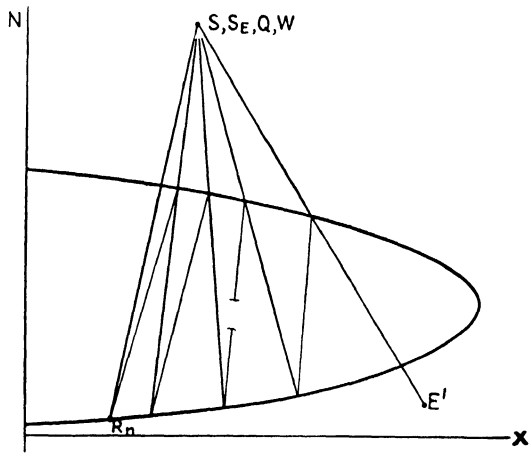



FIG. 6.58. Total reflux, minimum stages.

*Solution.* The system is one of Type 2, for which equilibrium data are given by Darwent and Winkler [*J. Phys. Chem.* **47**, 442 (1943)]. The calculations will be made on Janecke coordinates using mole rather than weight values, Figs. 6.59 and 6.60. Thus, $N$ = moles $B$/moles $(A + C)$, $\mathbf{X}$ = moles $C$/moles $(A + C)$, etc. Basis: 1 hr.

$$a.\ \mathbf{X}_F = \frac{47.5}{(47.5 + 47.5)} = 0.500, \qquad N_F = \frac{5}{95} = 0.0527$$

$$F = 100 \text{ moles}, \qquad \mathbf{F} = \frac{F}{(1 + N_F)} = \frac{100}{(1 + 0.0527)} = 95 \text{ moles}$$

$$S = B, \qquad S_E = B_E, \qquad S_R = B_R \cdot \mathbf{X}_{P'_R} = 0.05, \qquad N_{P'_R} = 0$$

Locate $P_R$ on the saturation curve by a vertical line from $P'_R$, Fig. 6.59. $\mathbf{X}_{P_R} = 0.05$, $N_{P_R} = 0.0753$, with the same coordinates for $R_n$ and $R'_n$. $\mathbf{X}_{P_E} = 0.95$, $N_{P_E} = 0$, with the same coordinates for $E'$ and $R_0$. Since pure aniline ($B$) is the solvent, the minimum number of stages is determined by using vertical stage construction lines together with the tie lines, as in Fig. 6.59. The minimum number of stages is 14.5.

*b.* $\mathbf{X}_Q = \mathbf{X}_{P_E}$ since pure $B$ is removed at the extract end of the plant. $\mathbf{X}_W = \mathbf{X}_{P_R}$ since pure $B$ is added to the solvent mixer. For this system, the tie line which when extended passes through $F$ provides the position of $Q$ and $W$ for minimum reflux. From Fig. 6.59, $N_Q = 40.0$, $N_W = -39.7$, $N_{E_1} = 6.34$, $N_{E_{n+1}} = 13.50$. An $A + C$ balance, entire extraction plant:

$$\mathbf{F} = \mathbf{P}_E + \mathbf{P}_R$$
$$95 = \mathbf{P}_E + \mathbf{P}_R$$

A $C$ balance:

$$\mathbf{F}\mathbf{X}_F = \mathbf{P}_E\mathbf{X}_{P_E} + \mathbf{P}_R\mathbf{X}_{P_R}$$
$$95(0.500) = \mathbf{P}_E(0.95) + \mathbf{P}_R(0.05)$$

Solving simultaneously,

$$\mathbf{P}_E = \mathbf{P}_R = 47.5 \text{ moles}$$

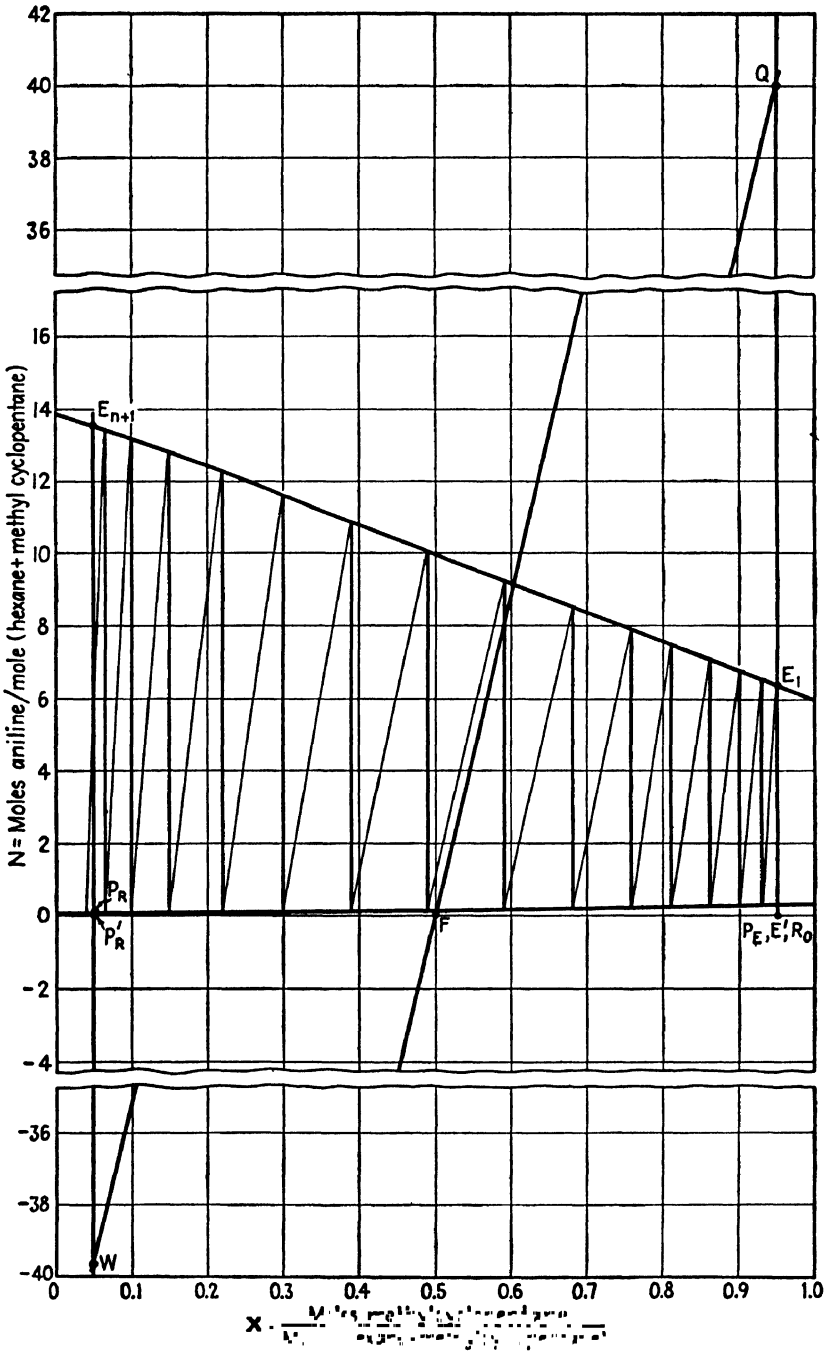



FIG. 6.59. Minimum reflux ratio and minimum stages, Illustration 9.

Eq. (6.181):
$$\frac{\mathbf{R}_0}{\mathbf{P}_E} = \frac{N_Q - N_{E_1}}{N_{E_1} - N_{P_E}} = \frac{40.0 - 6.34}{6.34 - 0}$$
$$= 5.32 \frac{\text{moles extract reflux}}{\text{mole extract product}}$$
$$= \text{minimum reflux ratio}$$

Eq. (6.196):
$$\frac{\mathbf{R}_n'}{\mathbf{P}_R} = \frac{N_{P_R} - N_W}{N_{E_{n+1}} - N_{P_R}} = \frac{0.0753 + 39.7}{13.50 - 0.0753}$$
$$= 2.96 \frac{\text{moles raffinate reflux}}{\text{mole raffinate product}}$$
$$= \text{minimum reflux ratio}$$

*c.* For 2.2 times the minimum extract ratio, $\mathbf{R}_0/\mathbf{P}_E = 2.2(5.32) = 11.70$ (moles extract reflux/mole extract product).

Eq. (6.181):
$$11.70 = \frac{N_Q - N_{E_1}}{N_{E_1} - N_{P_E}} = \frac{N_Q - 6.34}{6.34 - 0}$$
$$N_Q = 80.0$$

Relocate $Q$, Fig. 6.60. Draw line $QF$ to locate $W$, or calculate $N_W$ by Eq. (6.205).

$$\frac{N_Q - N_F}{N_F - N_W} = \frac{\mathbf{X}_Q - \mathbf{X}_F}{\mathbf{X}_F - \mathbf{X}_W}$$
$$\frac{80.0 - 0.0527}{0.0527 - N_W} = \frac{0.95 - 0.50}{0.50 - 0.05}$$
$$N_W = -79.90$$

With $W$ and $Q$ as operating points, the stages are constructed. Twenty theoretical stages are required, with the feed entering the tenth from the extract end.

Eq. (6.185): $B_E = \mathbf{P}_E(N_Q - N_{P_E}) = 47.5(80 - 0) = 3{,}800$ moles of solvent from the extract-solvent separator

Eq. (6.200): $B_R = \mathbf{P}_R(N_{P_R} - N_W) = 47.5(0.0753 + 79.90) = 3{,}798$ moles of solvent into the solvent mixer

Solvent balance:
$$\mathbf{F}N_F + B_R = \mathbf{P}_E N_{P_E} + \mathbf{P}_R N_{P_R} + B_E$$
$$95(0.0527) + 3{,}798 = 47.5(0) + 47.5(0.0753) + 3{,}800$$
$$3{,}803 \equiv 3{,}803.$$

$\mathbf{R}_0 = 11.70\ \mathbf{P}_E = 11.70(47.5) = 555$ moles
$R_0 = \mathbf{R}_0(1 + N_{R_0}) = 555(1 + 0) = 555$ moles
$\mathbf{E}' = \mathbf{P}_E + \mathbf{R}_0 = 47.5 + 555 = 602.5$ moles
$E' = \mathbf{E}'(1 + N_{E'}) = 602.5(1 + 0) = 602.5$ moles
$\mathbf{E}_1 = \mathbf{E}' = 602.5$ moles
$E_1 = \mathbf{E}_1(1 + N_{E_1}) = 602.5(1 + 6.34) = 4{,}420$ moles

Eq. (6.179):
$$\frac{\mathbf{R}_1}{\mathbf{E}_2} = \frac{(N_Q - N_{E_2})}{(N_Q - N_{R_1})} = \frac{(80.0 - 6.50)}{(80.0 - 0.27)} = 0.923$$

Eq. (6.177):
$$\mathbf{E}_2 = \mathbf{S}_E + \mathbf{P}_E + \mathbf{R}_1 = 0 + 47.5 + \mathbf{R}_1$$

Solving simultaneously,

$\mathbf{E}_2 = 617$ moles, $\mathbf{R}_1 = 569.5$ moles
$E_2 = \mathbf{E}_2(1 + N_{E_2}) = 617(1 + 6.50) = 4{,}620$ moles
$R_1 = \mathbf{R}_1(1 + N_{R_1}) = 569.5(1 + 0.27) = 761$ moles

Extract and raffinate quantities for the remaining stages in the extract-enriching section may be similarly computed.

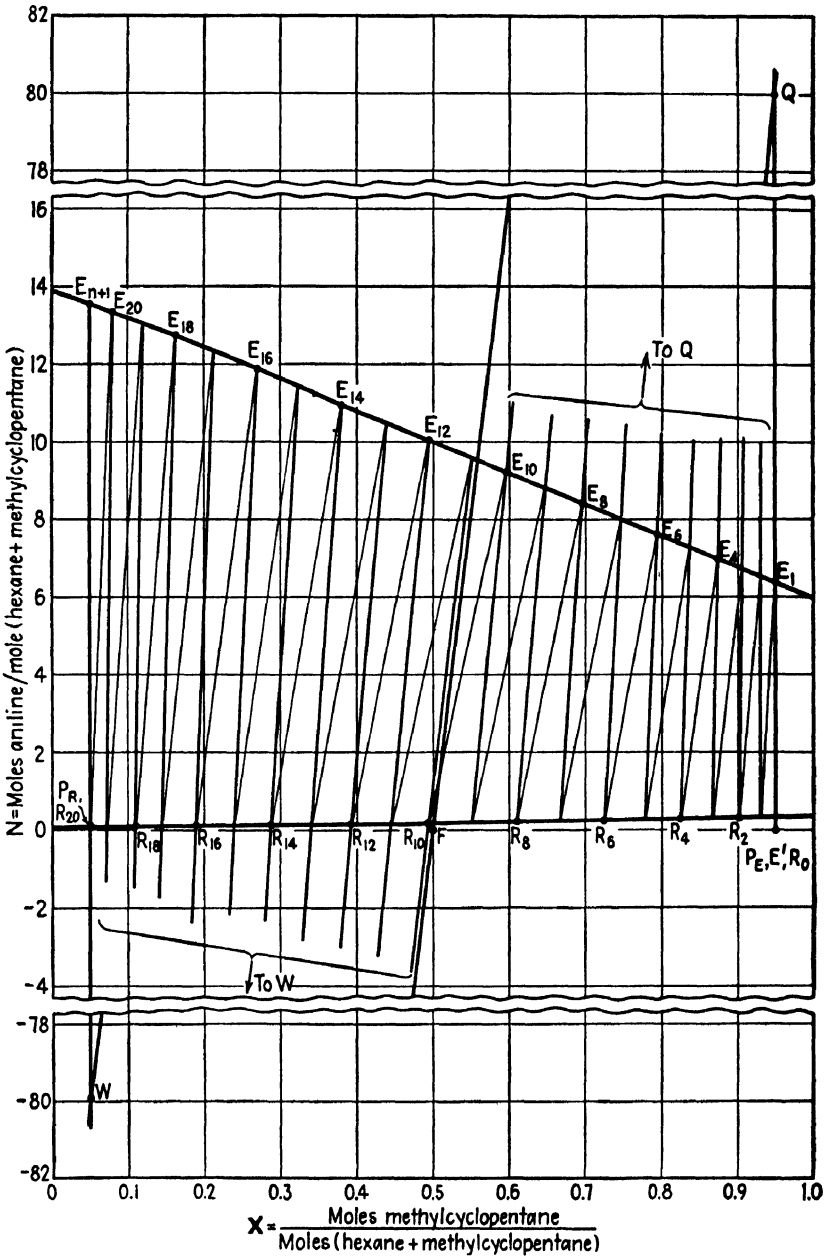



FIG. 6.60. Illustration 9. Stages for 2.2 times the minimum extract reflux ratio.

Eq. (6.196): $$\frac{\mathbf{R}'_n}{\mathbf{P}_R} = \frac{(N_{P_R} - N_W)}{(N_{E_{n+1}} - N_{P_R})} = \frac{(0.0753 + 79.90)}{(13.50 - 0.0753)} = 5.95$$

$$\mathbf{R}'_n = 5.95(\mathbf{P}_R) = 5.95(47.5) = 283 \text{ moles}$$

$$R'_n = \mathbf{R}'_n(1 + N_{R'_n}) = 283(1 + 0.0753) = 304 \text{ moles}$$

$$\mathbf{R}_{20} = \mathbf{R}'_n + \mathbf{P}_R = 304 + 47.5 = 351.5 \text{ moles}$$

$$R_{20} = \mathbf{R}_{20}(1 + N_{R_{20}}) = 351.5(1 + 0.0753) = 378 \text{ moles}$$

Eq. (6.186): $$\mathbf{E}_{n+1} = \mathbf{R}'_n + \mathbf{S} = 283 + 0 = 283 \text{ moles}$$

$$E_{n+1} = \mathbf{E}_{n+1}(1 + N_{E_{n+1}}) = 283(1 + 13.50) = 4{,}100 \text{ moles}$$

Eq. (6.194): $$\frac{\mathbf{R}_{19}}{\mathbf{E}_{20}} = \frac{(N_{E_{20}} - N_W)}{(N_{R_{19}} - N_W)} = \frac{(13.40 + 79.90)}{(0.075 + 79.90)} = 1.170$$

Eq. (6.192): $$\mathbf{R}_{19} = \mathbf{E}_{20} + \mathbf{P}_R - \mathbf{S} = \mathbf{E}_{20} + 47.5 - 0$$

Solving simultaneously,

$$\mathbf{R}_{19} = 327 \text{ moles}, \qquad \mathbf{E}_{20} = 279.5 \text{ moles}$$

$$R_{19} = \mathbf{R}_{19}(1 + N_{R_{19}}) = 327(1 + 0.075) = 352 \text{ moles}$$

$$E_{20} = \mathbf{E}_{20}(1 + N_{E_{20}}) = 279.5(1 + 13.40) = 4{,}020 \text{ moles}$$

In similar fashion, extract and raffinate quantities for stages in the raffinate-stripping section may be determined.

$$\mathbf{P}'_R = \mathbf{P}_R = 47.5 \text{ moles}, \qquad P'_R = \mathbf{P}'_R = 47.5 \text{ moles}$$

The solvent removed in the raffinate-solvent separator is then

$$\mathbf{P}_R(N_{P_R} - N_{P'_R}) = 47.5(0.0753 - 0) = 3.58 \text{ moles}.$$

**Extract Reflux Only.** Should the feed be extremely weak in component $C$, or if the distribution coefficient for $C$ is very unfavorable for the solvent chosen at $C$ concentrations above that in the feed, it is possible to operate with extract reflux only (7, 14, 18), as with the flowsheet of Fig. 6.61. At

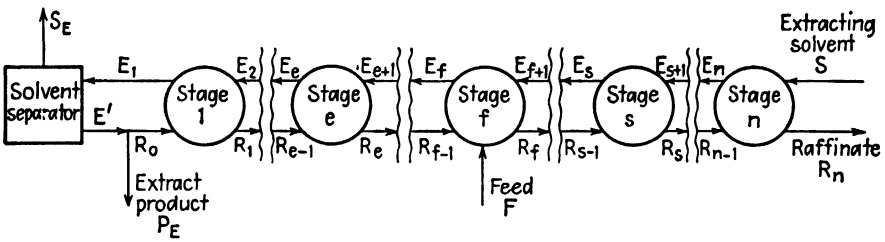



FIG. 6.61. Countercurrent extraction with extract reflux.

the raffinate end of the cascade, solvent $S$ and what was extract reflux $E_{n+1}$ now coincide. Raffinate $R_n$ and what was $P_R$ are the same not only in composition but also in amount. Except for the interrelation between the extracts $E_1$ and $E'$, the product $P_E$, and reflux $R_0$, the entire arrangement is the same as for countercurrent contact with two feeds ($F$ and $R_0$). Omitting stages $(f + 1)$ through $n$ would provide an operation analogous to the use of a rectification section only in a distillation column.

A material balance about the raffinate end of the plant, including stages $f + 1$ through $n$ is

$$S + R_f = E_{f+1} + R_n \tag{6.206}$$

$$S - R_n = E_{f+1} - R_f = W \tag{6.207}$$

For stages $(s + 1)$ through $n$:

$$S + R_s = E_{s+1} + R_n \tag{6.208}$$

$$S - R_n = E_{s+1} - R_s = W \tag{6.209}$$

About the feed stage $f$:

$$E_{f+1} + R_{f-1} + F = E_f + R_f \tag{6.210}$$

$$E_{f+1} - R_f = E_f - R_{f-1} - F \tag{6.211}$$

$$W = Q - F \tag{6.212}$$

Consequently the raffinate operating point $W$, Fig. 6.62, lies at the intersections of $E_{f+1} - R_f$, $E_{s+1} - R_s$, and $Q - F$. The extract enriching section is the same as in the previous case. The entire construction diagram

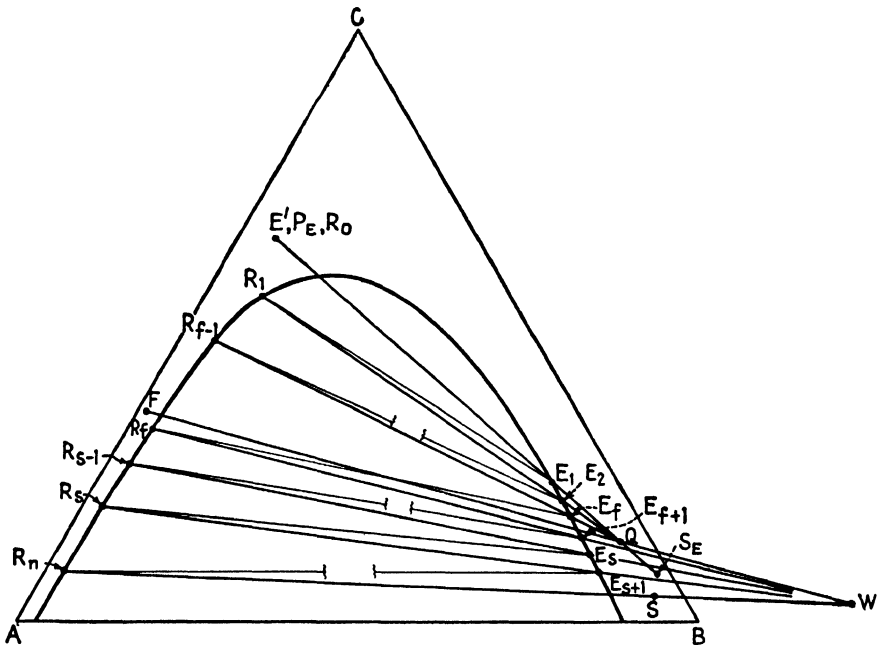



FIG. 6.62. Countercurrent extraction with extract reflux.

is essentially the same as before, with the exception that points $S$ and $E_{n+1}$ coincide at $S$.

Especially with feeds rich in $C$ and with Type 1 systems, the use of extract reflux does not always give improvement over the results expected for ordinary countercurrent contact, since frequently it happens that a higher finished extract $C$ concentration can be obtained without it.

**Raffinate Reflux Only.** Operation with raffinate reflux only is analogous to the use of a stripping section in a distillation column (7, 14, 18), Fig. 6.63. Since solvent removal from the final extract produces the richest

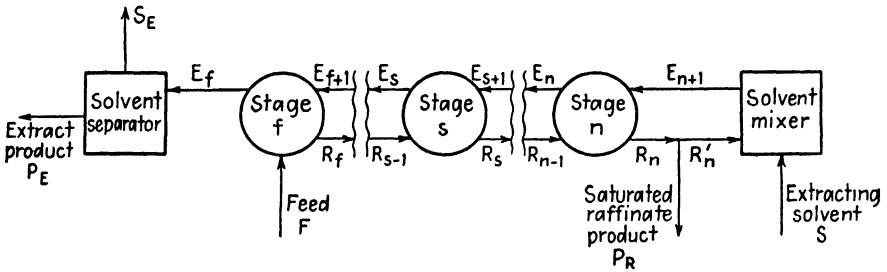



FIG. 6.63. Countercurrent extraction with raffinate reflux.

finished extract when the solvent-removal line $S_E P_E$ is tangent to the binodal curve (Fig. 6.64), it happens frequently that extract reflux is unnecessary, while raffinate reflux is useful for cases of poor distribution coefficient of the distributed substance at $C$ concentrations below that in the feed.

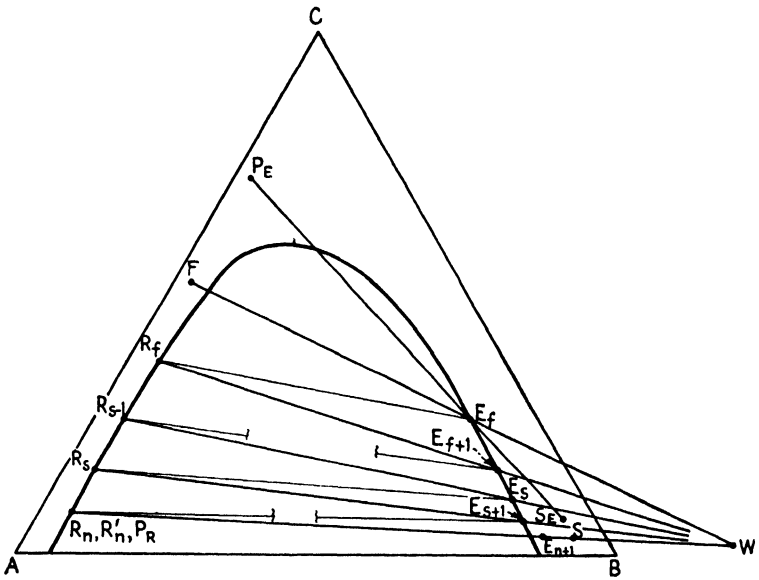



FIG. 6.64. Countercurrent extraction with raffinate reflux.

A material balance for the entire extraction plant, not including the solvent separator:

$$S + F = E_f + P_R \tag{6.213}$$

$$S - P_R = E_f - F = W \tag{6.214}$$

For the raffinate-stripping section, including stage $(s + 1)$:

$$S + R_s = E_{s+1} + P_R \tag{6.215}$$

$$E_{s+1} - R_s = S - P_R = W \tag{6.216}$$

For the extract solvent removal:

$$E_f = S_E + P_E = Q \tag{6.217}$$

The construction is shown in Fig. 6.64. $Q$ and $E_f$ coincide at $E_f$ [Eq. (6.217)], and the raffinate-stripping section is identical with the arrangement involving both reflux streams.

The Janecke diagrams for both of the cases just described are obvious from the description of the triangular coordinate construction and need no additional explanation. See also the following illustration.

**Illustration 10.** One hundred pounds per hour of a feed solution containing 25% ethanol ($C$), 75% water ($A$), is to be reduced to 2% ethanol (saturated) with ethyl ether ($B$) as solvent. Twice the minimum raffinate reflux ratio is to be used, and the reflux $E_{n+1}$ is to be saturated. The temperature is to be 25°C. Calculate the number of stages and amount of solvent required.

*Solution.* The equilibrium data are available in "International Critical Tables" (Vol. III, p. 405). Because of crowding on triangular coordinates, the Janecke diagram will be used, Fig. 6.65. Basis: 1 hr. $\mathbf{F} = 100$ lb., $\mathbf{X}_F = 25/100 = 0.25$, $N_F = 0$. For a saturated raffinate product, $X_{CP_R} = 0.02$, $X_{AP_R} = 0.92$, $X_{BP_R} = 0.06$. $\mathbf{X}_{P_R} = \mathbf{X}_{R_n} = \mathbf{X}_{R'_n} = 0.02/0.94 = 0.0213$, $N_{P_R} = N_{R_n} = N_{R'_n} = 0.06/0.94 = 0.0639$. Since pure ether is the solvent, $\mathbf{X}_{E_{n+1}} = \mathbf{X}_{P_R} = 0.0213$, $N_{E_{n+1}} = 73.9$. The plait point and tie lines to the right of $F$, Fig. 6.65, are so located that extract reflux would not appreciably increase the value of $\mathbf{X}$ for the final extract. Therefore only raffinate reflux will be used (Fig. 6.63).

For minimum raffinate reflux, tie lines to the left of $F$ are extended. Tie line $DG$ intersects line $E_{n+1}P_R$ at the lowest value, $N_W = -1.8$.

Eq. (6.196):
$$\frac{\mathbf{R}'_n}{\mathbf{P}_R} = \frac{(N_{P_R} - N_W)}{(N_{E_{n+1}} - N_{P_R})} = \frac{(0.0639 + 1.8)}{(73.9 - 0.0639)} = 0.0253$$

For twice the minimum raffinate reflux ratio,

$$\frac{\mathbf{R}'_n}{\mathbf{P}_R} = 2(0.0253) = 0.0506 = \frac{(0.0639 - N_W)}{(73.9 - 0.0639)}$$

$$N_W = -3.67$$

Extension of line $WF$ gives $E_f$, and $N_{E_f} = 7.1$, $\mathbf{X}_{E_f} = 0.673$. With $W$ as operating point, five theoretical stages are required. For the entire plant,

$$\mathbf{F} = \mathbf{P}_R + \mathbf{E}_f$$

A $C$ balance:

$$25 = 0.02\mathbf{P}_R + \mathbf{E}_f$$

Solving simultaneously,

$$\mathbf{P}_R = 64.75 \text{ lb.}, \quad \mathbf{E}_f = 35.25.$$

$$P_R = \mathbf{P}_R(1 + N_{P_R}) = 64.75(1 + 0.0639) = 69.5 \text{ lb.}$$

$$E_f = \mathbf{E}_f(1 + N_{E_f}) = 35.25(1 + 7.1) = 286 \text{ lb.}$$

$$\mathbf{R}'_n = 0.0506P_R = 0.0506(64.75) = 3.28 \text{ lb.}$$

$$R'_n = \mathbf{R}'_n(1 + N_{R'_n}) = 3.28(1 + 0.0639) = 3.52 \text{ lb.}$$

Solvent to the mixer $= B_R = \mathbf{P}_R(N_{P_R} - N_W) = 64.75(0.0639 + 3.67) = 242$ lb.

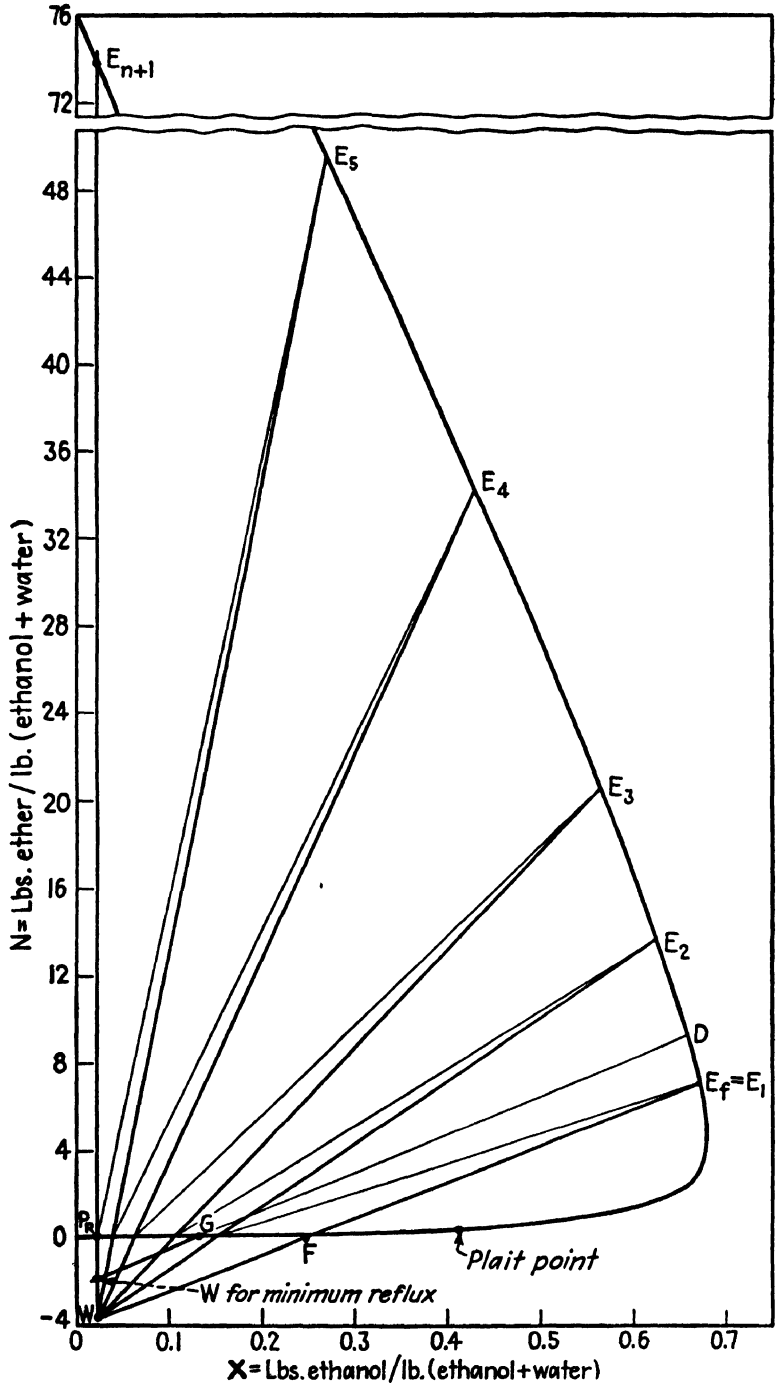



FIG. 6.65. Solution to Illustration 10.

**Constant Selectivity** (22, 23). For some Type 2 systems, the selectivity $\beta$ as defined by Eq. (4.2) is constant. Recalling that $A$-rich solutions are raffinates, $B$-rich solutions extracts, and that the selectivity is determined by equilibrium concentrations, we may write Eq. (4.2) for any stage $m$ as

$$\frac{X_{CE_m}}{X_{AE_m}} = \beta \frac{X_{CR_m}}{X_{AR_m}} \tag{6.218}$$

which leads to simplification of the calculations for total and minimum reflux.

Confining the discussion to cases where pure $B$ is the solvent, and where feed and products are saturated with solvent on the $A$-rich solubility curve, material balances for total reflux around the solvent mixer and stage $n$ are (Fig. 6.47):

$$R_{n-1} = E_n + B \tag{6.219}$$

$$R_{n-1}X_{CR_{n-1}} = E_nX_{CE_n} \tag{6.220}$$

$$R_{n-1}X_{AR_{n-1}} = E_nX_{AE_n} \tag{6.221}$$

Combining Eqs. (6.218), (6.220), and (6.221),

$$\frac{X_{CR_{n-1}}}{X_{AR_{n-1}}} = \frac{X_{CE_n}}{X_{AE_n}} = \beta \frac{X_{CR_n}}{X_{AR_n}} \tag{6.222}$$

Similarly, for stage $(n - 1)$,

$$\frac{X_{CR_{n-2}}}{X_{AR_{n-2}}} = \beta \frac{X_{CR_{n-1}}}{X_{AR_{n-1}}} = \beta^2 \left(\frac{X_{CR_n}}{X_{AR_n}}\right) \tag{6.223}$$

and for the entire raffinate-stripping section,

$$\frac{X_{CF}}{X_{AF}} = \beta^{s_{\min}} \left(\frac{X_{CP_R}}{X_{AP_R}}\right) \tag{6.224}$$

where $s_{\min}$ is the number of stripping stages at total reflux. In the same fashion, consideration of the enriching section leads to

$$\frac{X_{CP_E}}{X_{AP_E}} = \beta^{e_{\min}} \left(\frac{X_{CF}}{X_{AF}}\right) \tag{6.225}$$

where $e_{\min}$ is the number of enriching stages at total reflux. Since

$$s_{\min} + e_{\min} = n_{\min} \tag{6.226}$$

then

$$\frac{X_{CP_E}}{X_{AP_E}} = \beta^{n_{\min}} \left(\frac{X_{CP_R}}{X_{AP_R}}\right) \tag{6.227}$$

or

$$n_{\min} = \frac{\log \left[(X_{CP_E}/X_{AP_E})(X_{AP_R}/X_{CP_R})\right]}{\log \beta} \tag{6.228}$$

At minimum reflux ratio for such systems, the pinch occurs at the feed stage. A total material balance of the extract end of the plant through stage $f-1$, with pure $B$ as the solvent removed, is

$$E_f = B_E + P_E - R_{f-1} \tag{6.229}$$

For component $C$:

$$E_f X_{CE_f} = P_E X_{CP_E} + R_{f-1} X_{CR_{f-1}} \tag{6.230}$$

and for component $A$:

$$E_f X_{AE_f} = P_E X_{AP_E} + R_{f-1} X_{AR_{f-1}} \tag{6.231}$$

Eliminating $E_f$ from Eqs. (6.230) and (6.231), and rearranging,

$$\frac{R_{f-1}}{P_E} = \frac{X_{AP_E} X_{CE_f} - X_{CP_E} X_{AE_f}}{X_{CR_{f-1}} X_{AE_f} - X_{AR_{f-1}} X_{CE_f}} \tag{6.232}$$

But $X_{AE_f} = X_{CE_f} X_{AR_f}/\beta X_{CR_f}$, with the pinch at the feed stage, $X_{CR_f} = X_{CR_{f-1}}$, $X_{AR_f} = X_{AR_{f-1}}$; and if the feed is saturated, $X_{CR_f} = X_{CF}$, $X_{AR_f} = X_{AF}$. Substitution in Eq. (6.232) then leads to

$$\left(\frac{R_{f-1}}{P_E}\right)_{\min} = \frac{1}{\beta - 1}\left(\frac{X_{CP_E}}{X_{C_F}} - \beta \frac{X_{AP_E}}{X_{AF}}\right) \tag{6.233}$$

**Illustration 11.** A solution containing 50% *n*-heptane ($A$), 50% cyclohexane ($C$) (on a solvent-free basis) is to be separated into a raffinate containing 95% heptane and an extract containing 95% cyclohexane (both percentages on a solvent-free basis), with aniline ($B$) as the extracting solvent at 25°C., in a countercurrent multiple contact system with reflux. Feed, reflux, and product streams are to be saturated with solvent, and pure solvent will be added at the mixer and removed from the extract solvent separator. Determine the minimum number of stages and the minimum reflux ratio.

*Solution.* The equilibrium data for this Type 2 system [Hunter and Brown, *Ind. Eng. Chem.* **39**, 1343 (1947)] show $\beta$ to be nearly constant with an average value of 1.4. The saturated compositions, taken from the phase diagram, are as follows: $X_{CF} = 0.447$, $X_{AF} = 0.447$; $X_{CP_E} = 0.80$, $X_{AP_E} = 0.042$; $X_{CP_R} = 0.046$, $X_{AP_R} = 0.871$.

*a.* Minimum stages: Eq. (6.228):

$$n_{\min} = \frac{\log\left[\left(\frac{X_{CP_E}}{X_{AP_E}}\right)\left(\frac{X_{AP_R}}{X_{CP_R}}\right)\right]}{\log \beta} = \frac{\log\left[\left(\frac{0.80}{0.042}\right)\left(\frac{0.871}{0.046}\right)\right]}{\log 1.4} = 17.5$$

*b.* Minimum reflux ratio: Eq. (6.233):

$$\left(\frac{R_{f-1}}{P_E}\right)_{\min} = \frac{1}{\beta - 1}\left(\frac{X_{CP_E}}{X_{CF}} - \beta \frac{X_{AP_E}}{X_{AF}}\right)$$

$$= \frac{1}{1.4 - 1}\left[\frac{0.80}{0.447} - 1.4\left(\frac{0.042}{0.447}\right)\right] = 4.15 \text{ lb. raffinate into the feed stage per lb. extract product}$$

Since the internal reflux ratio is not constant from stage to stage, the ratio $R_0/P_E$ can be calculated by a series of material balances together with a consideration of the phase equilibria. Basis: 100 lb. saturated feed. A complete plant material balance:

$$F + B_R = P_E + P_R + B_E$$

Component $C$:

$$100(0.447) = P_E(0.80) + P_R(0.046)$$

Component $A$:

$$100(0.447) = P_E(0.042) + P_R(0.871)$$

Solving simultaneously,

$$P_R = 48.6 \text{ lb.}, \qquad P_E = 53.0 \text{ lb.}$$
$$R_{f-1} = 4.15P_E = 4.15(53.0) = 220 \text{ lb.}$$

At minimum reflux ratio, $R_f$, $R_{f-1}$, and $F$ have the same compositions. Therefore $E_f$ is in equilibrium with $F$.

Eq. (6.218):
$$\frac{X_{CE_f}}{X_{AE_f}} = \beta \frac{X_{CF}}{X_{AF}} = 1.4 \left(\frac{0.447}{0.447}\right) = 1.4$$

Reference to the phase diagram shows $X_{CE_f} = 0.068$.

Eq. (6.168):
$$B_E + P_E = E_f - R_{f-1}$$
$$B_E + 53.0 = E_f - 220$$

$C$ balance:

$$53.0(0.80) = E_f(0.068) - 220(0.447)$$

Solving simultaneously,

$$E_f = 2{,}070 \text{ lb.}, \qquad B_E = 1{,}797 \text{ lb.}$$

$E_1$ is found on a phase diagram as a saturated solution on line $BP_E$, so that $X_{CE_1} = 0.215$. Further, $X_{CR_0} = X_{CP_E}$.

Eq. (6.137):
$$E_1 = B_E + P_E + R_0$$
$$E_1 = 1797 + 53.0 + R_0$$

$C$ balance:

$$E_1(0.215) = 53.0(0.80) + R_0(0.80)$$

Solving simultaneously,

$$E_1 = 2{,}457 \text{ lb.}, \qquad R_0 = 607 \text{ lb.}$$

$$\therefore \left(\frac{R_0}{P_E}\right)_{\min} = \frac{607}{53.0} = 11.45$$

### Notation for Chapter 6

A symbol representing a solution denotes not only the composition but also the weight of the solution. Throughout, moles and mole fraction may be substituted for weights and weight fraction.

$A$ = component $A$.
$B$ = component $B$, the principal component of the extracting solvent.
$C$ = component $C$.
$d$ = differential operator.
$E$ = extract solution.
$\mathbf{E}$ = extract solution, $B$-free basis.
$e$ = a stage in the extract-enriching section of a cascade.
$F$ = feed solution.
$\mathbf{F}$ = feed solution, $B$-free basis.
ln = natural logarithm.
log = common logarithm.
$m$ = any stage of a cascade.
$\mathbf{m}$ = distribution coefficient, $y/x$ at equilibrium.
$N$ = weight fraction of $B$ in a solution, $B$-free basis $X_B/(X_A + X_C)$.

$n$ = total number of stages in a cascade; the last stage.
$P_E$ = extract product.
$\mathbf{P}_E$ = extract product, $B$-free basis.
$P_R$ = raffinate product.
$\mathbf{P}_R$ = raffinate product, $B$-free basis.
$R$ = raffinate solution.
$\mathbf{R}$ = raffinate solution, $B$-free basis.
$S$ = extracting solvent.
$\mathbf{S}$ = extracting solvent, $B$-free basis.
$S_E$ = solvent removed from the extract.
$\mathbf{S}_E$ = solvent removed from the extract, $B$-free basis.
$S_R$ = solvent removed from the raffinate.
$\mathbf{S}_R$ = solvent removed from the raffinate, $B$-free basis.
$s$ = a stage in the raffinate-stripping section of a cascade.
$X$ = weight fraction.
$\mathbf{X}$ = weight fraction of $C$, $B$-free basis $X_C/(X_A + X_C)$.
$x = X_{CA}/X_{AA}$.
$y = X_{CB}/X_{BB}$.
$\beta$ = selectivity of $B$ for $C$.

Subscripts:

$A, B, C$ = components $A$, $B$, $C$.
$E$ = extract.
$e$ = stage $e$.
$F$ = feed.
$f$ = feed stage.
max = maximum.
min = minimum.
$R$ = raffinate.
$S$ = solvent.
$s$ = stage $s$.
$t$ = total
1, 2, etc. = stage 1, 2, etc.

## LITERATURE CITED


1. Evans, T. W.: *Ind. Eng. Chem.* **26,** 439 (1934).
2. _____: *Ind. Eng. Chem.* **26,** 860 (1934).
3. _____: *J. Chem. Education* **14,** 408 (1937).
4. Griffin, C. W.: *Ind. Eng. Chem., Anal. Ed.* **6,** 40 (1934).
5. Hunter, T. G., and A. W. Nash: *J. Soc. Chem. Ind.* **51,** 285T (1932).
6. _____ and _____: *J. Soc. Chem. Ind.* **53,** 95T (1934).
7. _____ and _____: *Ind. Eng. Chem.* **27,** 836 (1935).
8. Jantzen, E.: "Das fraktionierte Destillieren und das fraktionierte Verteilen," Dechema Monograph Vol. 5, No. 48, Berlin, Verlag Chemie, 1932.
9. Kremser, A.: *Nat. Petroleum News* **22,** No. 21, 42 (May 21, 1930).
10. Maloney, J. O., and A. E. Schubert: *Trans. Am. Inst. Chem. Engrs.* **36,** 741 (1940).
11. Nord, M.: *Ind. Eng. Chem.* **38,** 560 (1946).
12. Perry, J. H.: Ed., "Chemical Engineers' Handbook," 3d ed., McGraw-Hill Book Company, Inc., New York, 1950.
13. Randall, M., and B. Longtin: *Ind. Eng. Chem.* **30,** 1063, 1188, 1311 (1938); **31,** 908, 1295 (1939); **32,** 125 (1940).

14. Saal, R. N. J., and W. J. D. Van Dijck: *World Petroleum Congr.*, London, 1933, Proc. 2, 352.
15. Sharefkin, J. G., and J. M. Wolfe: *J. Chem. Education* **21**, 449 (1944).
16. Sherwood, T. K.: "Absorption and Extraction," McGraw-Hill Book Company, Inc., New York, 1937.
17. Souders, M., and G. G. Brown: *Ind. Eng. Chem.* **24**, 519 (1932).
18. Thiele, E. W.: *Ind. Eng. Chem.* **27**, 392 (1935).
19. Tiller, F. M.: *Chem. Eng. Progress* **45**, 391 (1949).
20. Underwood, A. J. V.: *J. Soc. Chem. Ind.* **47**, 805T (1928).
21. ———: *Ind. Chemist* **10**, 128 (1934).
22. Varteressian K. A., and M. R. Fenske: *Ind. Eng. Chem.* **28**, 1353 (1936).
23. ——— and ———: *Ind. Eng. Chem.* **29**, 270 (1937).

# CHAPTER 7

## METHODS OF CALCULATION II. STAGEWISE CONTACT WITH MIXED AND DOUBLE SOLVENTS

In the case of four or more components, difficulties in the calculations for the number of stages arise from the necessarily complicated diagrams required for the representation of the equilibria and, even more restricting, almost complete lack of the equilibrium data themselves. In consequence, designs are frequently made on the basis of laboratory experiments rather than by direct computation from the phase relationships. The simple flowsheets applied to the simpler systems can be handled, however.

### MIXED SOLVENTS

Mixed-solvent liquid extraction includes those operations where the extracting solvent is itself a homogeneous solution, so that there are a minimum of four components comprising the entire system: two components to be separated and two forming the extracting solvent. Solvent solutions are used in order to bring about a modification of the effects produced by a single solvent, such as improvement of the selectivity, lowering of the freezing point of the solvent, etc. The simplest of these systems, to which the following description is limited, involves only one partially miscible pair of components and certain unusual relationships among the ternary and quaternary equilibria. These are described in detail in Chap. 2 and Fig. 2.32, to which reference should now be made. While it has not yet been demonstrated that all systems of this general type can be similarly described, it is known that certain mixed-solvent-petroleum combinations do conform, and consequently this case is of industrial importance.

**Single-contact Extraction.** These calculations were first described by Hunter (10). Refer to Fig. 7.1. On tetrahedral diagrams of this sort, the geometrical rules applicable to mixtures on ternary triangular diagrams apply. Consequently, if feed solution $F$, a solution of components $A$ and $B$, is extracted with solvent $S$, a solution of $C$ and $D$, the point $M$ representing the mixture as a whole is on the straight line $FS$, such that

$$\frac{F}{S} = \frac{\overline{MS}}{\overline{FM}} \tag{7.1}$$

$$F + S = M \tag{7.2}$$

Since $M$ is within the two-liquid-phase portion of the diagram, two equilibrium solutions, raffinate $R$ and extract $E$, located on opposite ends of the quaternary tie line result:

$$R + E = M \tag{7.3}$$

$$\frac{R}{E} = \frac{\overline{EM}}{\overline{MR}} \tag{7.4}$$

The problem is then one of locating the points $R$ and $E$. As previously pointed out (Chap. 2) the quaternary tie lines can be located at the intersection of two planes, one passing through apex $D$ and a tie line $R'E'$ in the

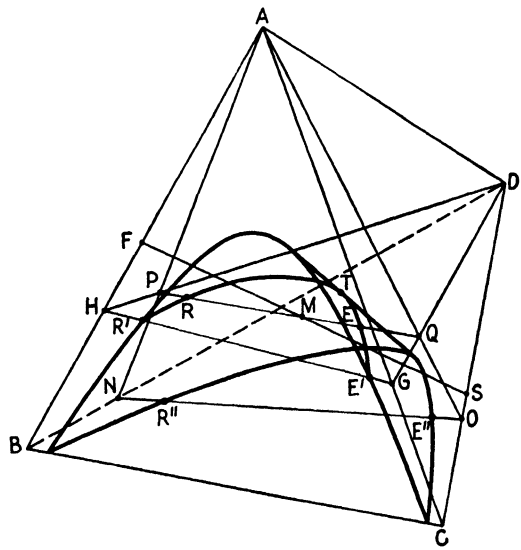



FIG. 7.1. Single-contact extraction with a mixed solvent.

ternary $ABC$, the other through apex $A$ and tie line $R''E''$ in the ternary $BCD$. We may therefore consider the mixing of feed and solvent as having occurred in two separate steps (Fig. 7.2): (*a*) addition of $C$ to $F$ to give $M'$,

$$\frac{F}{C} = \frac{\overline{M'C}}{\overline{FM'}} \tag{7.5}$$

$$F + C = M' \tag{7.6}$$

and (*b*) addition of $D$ to $M'$ to give $M$,

$$\frac{D}{M'} = \frac{\overline{MM'}}{\overline{DM}} \tag{7.7}$$

$$D + M' = M \tag{7.8}$$

In each case, the amounts of $C$ and $D$ used are the same as that originally in $S$,

$$C + D = S \tag{7.9}$$

$$\frac{C}{D} = \frac{\overline{SD}}{\overline{CS}} \tag{7.10}$$

It is then necessary to locate the quaternary tie line $RE$ passing through point $M$, which involves first locating ternary tie line $R''E''$. The inter-

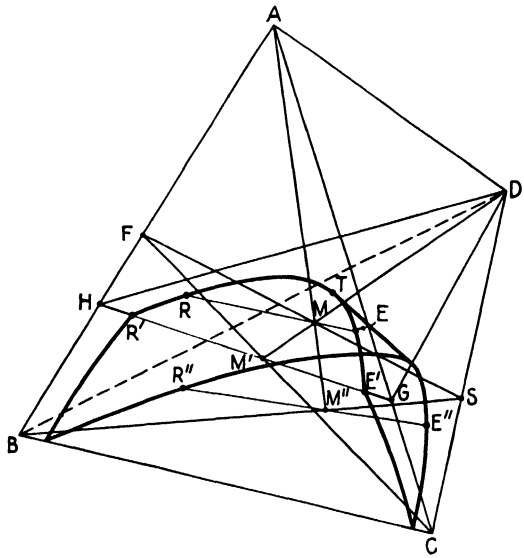



FIG. 7.2. Stepwise addition of solvents.

section of the planes $R''E''A$ and $R'E'D$ will then give $RE$. Were all the $A$ to be removed from $M$, the result would be $M''$, which is necessarily in the plane $R''E''A$ and on the tie line $R''E''$. In turn, point $M''$ may be established by mixing $S$ with the proper amount of $B$,

$$B = FX_{BF} = MX_{BM} \tag{7.11}$$

Then

$$S + B = M'' \tag{7.12}$$

$$\frac{S}{B} = \frac{\overline{BM''}}{\overline{M''S}} \tag{7.13}$$

In the ternary $BDS$, tie line $R''E''$ is then determined, permitting the location of quaternary tie line $RE$.

The solvent-free finished raffinate and extract, $R'''$ and $E'''$, can be determined (Fig. 7.3) by considering the removal of $S$ from $R$ and $E$ in two separate steps: ($a$) removal of $D$ from $R$ and $E$ to produce ternary mixtures $K$ and $L$, and ($b$) removal of $C$ from $K$ and $L$ to leave $R'''$ and $E'''$, thus completing the entire extraction operation.

Actual computations cannot of course be made on the tetrahedral space diagram. Instead it is necessary to work with orthogonal projections of the various points and curves, most conveniently projections on the base *BCD*. Throughout these calculations, the same letter in the various figures consistently designates a given point, and points projected on the *BCD* plane are indicated by the lower-case counterparts of the letters designating the original point. Thus $m$ is the projection of $M$, etc. If the

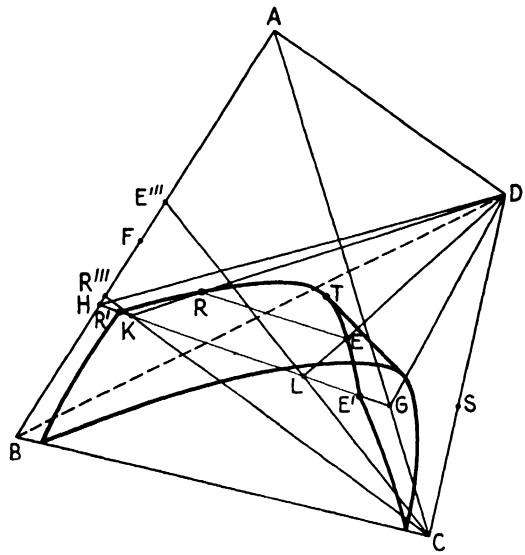



FIG. 7 3. Removal of solvents from raffinate and extract.

quaternary coordinates of a point $P$ are $X_{AP}$, $X_{BP}$, $X_{CP}$, and $X_{DP}$, where $X$ represents weight fraction, then the coordinates of $p$, the orthogonal projection of $P$ on plane $BCD$, will be $X_{Bp}$, $X_{Cp}$, and $X_{Dp}$, which may be evaluated from the relationship (Chap. 2):

$$X_{Bp} = X_{BP} + \frac{X_{AP}}{3}, \quad X_{Cp} = X_{CP} + \frac{X_{AP}}{3}, \quad X_{Dp} = X_{DP} + \frac{X_{AP}}{3} \tag{7.14}$$

In this way, projected coordinates may be computed and points plotted on the *BCD* plane. The various steps are numbered for convenient reference and are given in the order in which the calculations should be made (10).

1. Refer to Fig. 7.4. Point $f$, the projection of $F$, is located on line $Ba$ by calculation of its coordinates through Eq. (7.14). The coordinates of $M$ are calculated from the material balances:

$$M = F + S \tag{7.2}$$

$$X_{CM} = \frac{FX_{CF} + SX_{CS}}{M}, \text{ etc.} \tag{7.15}$$

and hence point $m$ may be located (on line $fS$). Similarly the coordinates of $M'$ are computed by Eq. (7.6) and

$$X_{CM'} = \frac{FX_{CF} + CX_{CC}}{M'}, \text{ etc.} \tag{7.16}$$

Point $m'$ is then plotted on line $fC$. Point $m$ is at the intersection of lines $m'D$ and $fS$.

2. From the ternary equilibria for the system $ABC$, $R'$ and $E'$ are computed by the methods of Chap. 6, and $r'$ and $e'$ located on Fig. 7.4.

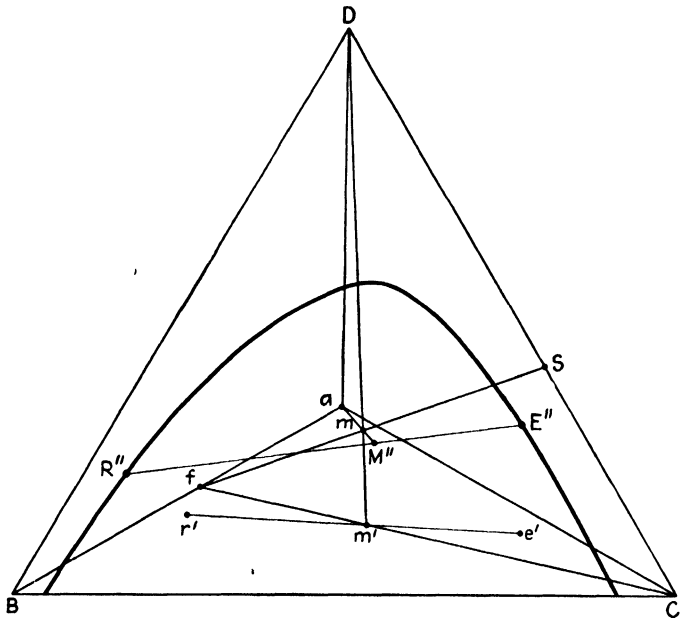



FIG. 7.4. Single contact with a mixed solvent, in projection.

3. $M''$ is located at the intersection of lines $BS$ and $aM$, Fig. 7.4. Tie line $R''E''$ in the ternary system $BCD$ is then located through $M''$ by the methods of Chap. 6.

4. The intersection $PQ$ of the planes $R'E'D$ and $R''E''A$ (Fig. 7.5) is located by

*a*. Extending $r'e'$ to $g$ and $h$, and drawing $Dh$ and $Dg$.

*b*. Extending $R''E''$ to $N$ and $O$ and drawing $aN$ and $aO$.

*c*. Locating $p$ at the intersection of $Dh$ and $aN$, and $q$ at the intersection of $Dg$ and $aO$. Draw line $pq$, the projection of $PQ$.

Tie-line projection $re$ then lies on $pq$ and to locate it requires a projection of the quaternary solubility curve $R'RTEE'$.

5. Refer to Fig. 7.6, where the device for locating point $Z$ on the quaternary solubility curve is indicated. Plane $YJW$, containing point $Z$, is

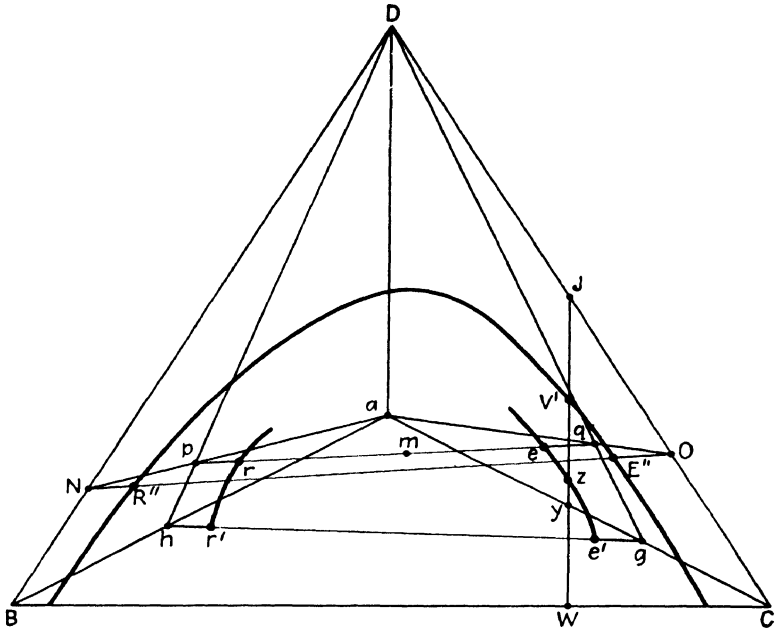



FIG. 7 5. Location of raffinate and extract, in projection.

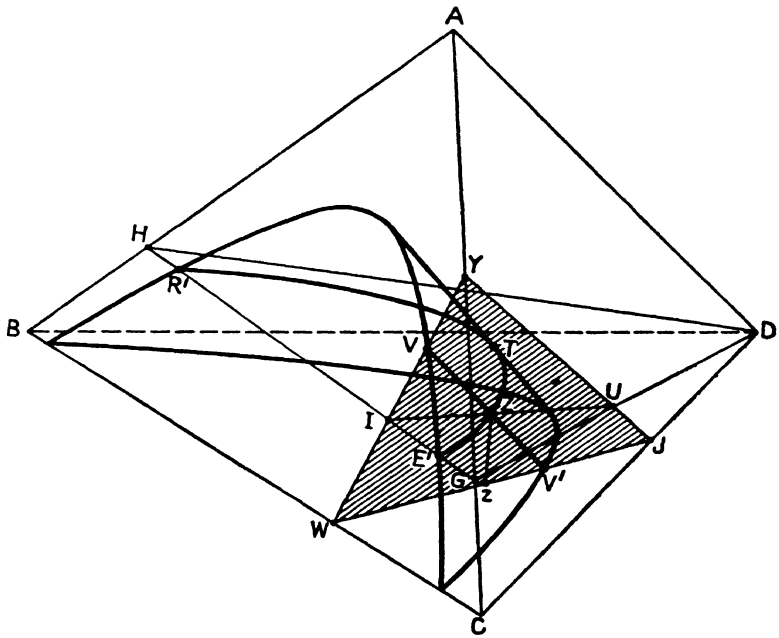



FIG. 7.6. Projection of quaternary equilibria.

perpendicular to plane $BCD$ and to line $BC$. Lines $WJ$ and $YW$ are therefore perpendicular to line $BC$, and $z$, the projection of $Z$, is on line $WJ$. The detailed construction to locate $z$ is outlined as follows:

*a*. On Fig. 7.5, any line $WJ$ is drawn, perpendicular to $BC$, intersecting the ternary solubility curve at $V'$. Lengths $WJ$ and $WV'$ are measured.

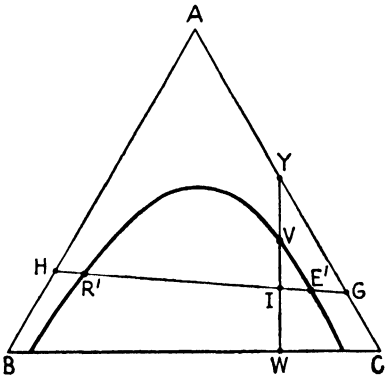



FIG. 7.7. Intersection of plane $YJW$ with the base $ABC$.

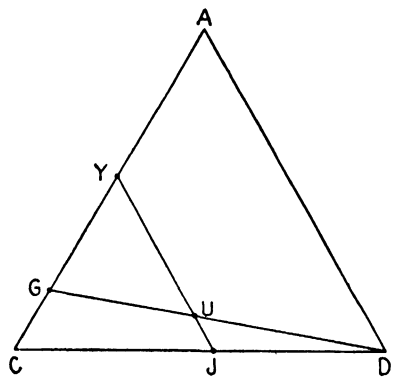



FIG. 7.8. Intersection of plane $YJW$ with the base $ACD$.

*b*. On a separate sheet, the base $ABC$ with its ternary solubility curve is drawn (Fig. 7.7). $W$ is located on line $BC$, and the perpendicular line $YW$ is erected. The intersection of $YW$ with the solubility curve is at $V$, and the lengths $VW$ and $YW$ are measured. The tie line $R'E'$ is drawn, which intersects line $YW$ at $I$. The length $IW$ is measured. $R'E'$ is extended to $H$ and $G$.

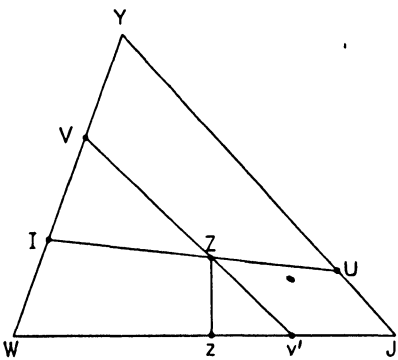



FIG. 7.9. Location of the intersection of plane $YJW$ with the quaternary solubility curve.

*c*. On a separate sheet, base $ACD$ is drawn (Fig. 7.8). Points $Y$, $G$, and $J$ are marked. The lines $YJ$ and $GD$ are drawn to intersect at $U$. The lengths $YU$ and $YJ$ are measured.

*d*. On a separate sheet (Fig. 7.9), a line of length $WJ$ is drawn and the position of $V'$ marked (see *a* above). Since the lengths $YW$ and $YJ$ are known (see *b* and *c*), triangle $YJW$ is constructed. Points $V$ and $I$ are located on line $YW$ (see *b*), as well as points $U$ and $V'$ (see *a* and *c*). Lines $VV'$ and $IU$ are drawn to locate the intersection $Z$. A perpendicular is dropped from $Z$ to line $WJ$ to locate $z$. The length $Wz$ is measured and transferred to Fig. 7.5.

The entire procedure is repeated sufficiently often to permit drawing the

projected quaternary-solubility curve on Fig. 7.5, which intersects line $pq$ at $r$ and $e$, as shown.

6. The coordinates of $r$ and $e$ are then read. To determine the coordinates of $R$, draw line $Dr$ on Fig. 7.5 (not shown), which intersects line $hg$ at $k$. Line $Ck$ is drawn and extended to intersect line $aB$ at $r'''$. The lengths $Br'''$ and $r'''a$ are measured. Since $r'''$ is the projection of the solvent-free raffinate,

$$\frac{\overline{Br'''}}{\overline{r'''a}} = \frac{X_{AR}'''}{X_{BR}'''} = \frac{X_{AR}}{X_{BR}} \tag{7.17}$$

Solving Eqs. (7.14) and (7.15) simultaneously then gives the coordinates of $R$. Those of $E$ are determined in a similar manner.

The calculations are necessarily tedious, and if a great number are to be made, the analytical methods of Wiegand (19) or the suggestions of Smith (16) are helpful.

It must be emphasized again that the methods described are applicable only when the simple relationships between the various ternary and quaternary equilibria pertain and would have to be modified considerably for more complicated situations as knowledge of the equilibria in these systems is acquired. Similarly extraction calculations involving the more complex flowsheets must still be developed, although the case of cocurrent multiple contact can be handled as a simple extension of single contact where the raffinates are progressively put through the same procedure. Further developments, for example, operations wherein one of the solvents is progressively removed as the extraction proceeds from stage to stage (17), cannot at this time be conveniently evaluated.

**Illustration 1.** One hundred pounds of a 20% acetone ($A$), 80% chloroform ($B$), solution are to be extracted in a single-contact process with 100 lb. of a mixed solvent consisting of 65% water ($C$), 35% acetic acid ($D$), at 25°C. Calculate the weights and compositions of extract and raffinate.

*Solution.* Equilibria for the ternary and quaternary systems are reported by Brancker, Hunter, and Nash [*J. Phys. Chem.* **44**, 683 (1940)]. The system is one of the type described above, and consequently only the ternary data are actually necessary. The computations are made in the order described above and are numbered accordingly. Standard triangular coordinates measuring 9.1 in. on a side were used, and distances were measured with a strip of 20-to-the-inch graph paper. Diagrams are not reproduced since they appear almost exactly as Figs. 7.4, 7.5, 7.7, 7.8, and 7.9. Figs. 7.4 and 7.5 are made on one diagram and will be referred to as Fig. 7.4.

1. $X_{AF} = 0.20$, $X_{BF} = 0.80$, $X_{CF} = X_{DF} = 0$.

Eq. (7.14): $$X_{Bf} = X_{BF} + \frac{X_{AF}}{3} = 0.80 + \frac{0.20}{3} = 0.867$$

Similarly,

$$X_{Cf} = 0.067, \qquad X_{Df} = 0.067$$

Point $f$ is plotted on plane $BCD$ (Fig. 7.4). It falls on line $Ba$.

$$X_{AS} = X_{BS} = 0, \qquad X_{CS} = 0.65, \qquad X_{DS} = 0.35$$

Point $S$ is plotted on plane $BCD$ (Fig. 7.4), and line $fS$ is drawn.

$$F = 100 \text{ lb.}, \qquad S = 100 \text{ lb.}$$

Eq. (7.2): $$M = F + S = 100 + 100 = 200 \text{ lb.}$$

Eq. (7.15): $$X_{CM} = \frac{FX_{CF} + SX_{CS}}{M} = \frac{100(0) + 100(0.65)}{200} = 0.325$$

$$X_{AM} = \frac{FX_{AF} + SX_{AS}}{M} = \frac{100(0.20) + 100(0)}{200} = 0.100$$

Eq. (7.14): $$X_{Cm} = X_{CM} + \frac{X_{AM}}{3} = 0.325 + \frac{0.100}{3} = 0.358$$

Point $m$ is plotted on line $fS$ (Fig. 7.4).

Weight of $C$ in solvent $S = SX_{CS} = 100(0.65) = 65$ lb.

Eq. (7.6): $$M' = F + C = 100 + 65 = 165 \text{ lb.}$$

Eq. (7.16): $$X_{CM'} = \frac{FX_{CF} + CX_{CC}}{M'} = \frac{100(0) + 65(1.0)}{165} = 0.394$$

$$X_{AM'} = \frac{FX_{AF} + CX_{AC}}{M'} = \frac{100(0.20) + 65(0)}{165} = 0.1212$$

Eq. (7.14): $$X_{Cm'} = X_{CM'} + \frac{X_{AM'}}{3} = 0.394 + \frac{0.1212}{3} = 0.4344$$

Line $fC$ is drawn, and point $m'$ plotted on $fC$ (Fig. 7.4). (As a check, $m$ should fall on line $Dm'$.)

2. On plane $ABC$ (Fig. 7.7), point $M'$ is plotted. Tie line $R'E'$ is drawn through $M'$, located by trial and error with the help of a distribution curve. From the plot, $X_{AR'} = 0.166$, $X_{CR'} = 0.010$, $X_{BR'} = 0.824$, $X_{DR'} = 0$; $X_{AE'} = 0.060$, $X_{BE'} = 0.010$, $X_{CE'} = 0.930$, $X_{DE'} = 0$.

Eq. (7.14): $$X_{Cr'} = X_{CR'} + \frac{X_{AR'}}{3} = 0.010 + \frac{0.166}{3} = 0.0653$$

Similarly,

$$X_{Br'} = 0.879, \qquad X_{Dr'} = 0.0553$$

Point $r'$ is plotted on plane $BCD$ (Fig. 7.4). In like fashion, $X_{Ce'} = 0.950$, $X_{Be'} = 0.030$, $X_{De'} = 0.020$. Point $e'$ is plotted on plane $BCD$ (Fig. 7.4). As a check, line $r'e'$ must pass through point $m'$.

3. On plane $BCD$ (Fig. 7.4), lines $BS$ and $am$ are drawn. The latter is extended to intersect line $BS$ at $M''$. Tie line $R''E''$ is located through $M''$ by trial and error, with the aid of a distribution curve. $X_{BR''} = 0.902$, $X_{CR''} = 0.012$, $X_{DR''} = 0.086$; $X_{BE''} = 0.020$, $X_{CE''} = 0.689$, $X_{DE''} = 0.291$.

4. *a.* On Fig. 7.4, line $r'e'$ is extended to $g$ and $h$ and lines $gD$ and $hD$ drawn.
   *b.* Line $R''E''$ is extended to $N$ and $O$ and lines $aN$ and $aO$ drawn.
   *c.* Point $p$ is located at the intersection of $aN$ and $hD$, point $q$ at the intersection of $gD$ and $aO$. Line $pq$ is drawn. As a check, line $pq$ must pass through point $m$.

5. *a.* On Fig. 7.4, $W$ is chosen at $X_{DW} = 0$, $X_{CW} = 0.75$, $X_{BW} = 0.25$, and line $WJ$ is drawn perpendicular to line $BC$. $X_{CJ} = 0.500$, $X_{DJ} = 0.500$. The intersection of line $WJ$ with $BCD$ ternary-solubility curve is marked $V'$. $X_{DV'} = 0.407$, $X_{CV'} = 0.547$. $\overline{WJ} = 3.95$ in., $\overline{WV'} = 3.22$ in.
   *b.* On Fig. 7.7, $W$ is located, and line $YW$ drawn perpendicular to line $BC$. $X_{AY} = 0.50$, $X_{BY} = 0$, $X_{CY} = 0.50$. Points $V$ and $I$ are located. $X_{AV} = 0.420$, $X_{CV} = 0.540$; $X_{AI} = 0.085$, $X_{CI} = 0.708$. $\overline{VW} = 3.31$ in., $\overline{YW} = 3.95$ in., $\overline{IW} = 0.67$ in. Tie line $R'E'$ is extended to $H$ and $G$. $X_{AG} = 0.058$, $X_{CG} = 0.942$; $X_{AH} = 0.168$, $X_{BG} = 0.832$.
   *c.* Base $ACD$ is drawn (Fig. 7.8). Points $Y$, $G$, and $J$ are marked, and lines $YJ$ and $GD$ are drawn to intersect at $U$. $\overline{YU} = 4.30$ in., $\overline{YJ} = 4.57$ in.

*d.* With the lengths of the lines $WJ$, $WY$, and $YJ$ known, triangle $WJY$ is constructed (Fig. 7.9). Points $V'$, $V$, $I$, and $U$ are located. Lines $VV'$ and $JU$ are drawn to intersect at $Z$. Point $z$ is located by dropping a perpendicular from $Z$ to line $WJ$. $\overline{Wz} = 3.00$ in. Point $z$ is marked on Fig. 7.4. $X_{Dz} = 0.381$, $X_{Cz} = 0.560$. Step 5 is repeated with the following results:

| $X_{CW}$ | $X_{BW}$ | $X_{Cz}$ | $X_{Dz}$ |
|---|---|---|---|
| 0.875 | 0.125 | 0.790 | 0.170 |
| 0 820 | 0.180 | 0.679 | 0.285 |

The quaternary-solubility curve is located in projection by drawing a curve through the points $z$; it intersects line $pq$ at $e$: $X_{Be} = 0.038$, $X_{Ce} = 0.667$, $X_{De} = 0.295$.

6. Line $D$ is extended to intersect line $hg$ at point $l$. Line $Cl$ is extended to intersect line $Ba$ at $e'''$. $\overline{Be'''} = 3.27$ in., $\overline{ae'''} = 1.95$ in.

Eq. (7.17):
$$\frac{\overline{Be'''}}{\overline{ae'''}} = \frac{X_{AE}}{X_{BE}} = \frac{3.27}{1.95} = 1.678$$

Eq. (7.14):
$$X_{BE} = X_{Be} - \frac{X_{AE}}{3} = 0.038 - \frac{X_{AE}}{3}$$

Solving simultaneously,
$$X_{AE} = 0.0409, \qquad X_{BE} = 0.0244$$

Eq. (7.14):
$$X_{CE} = X_{Ce} - \frac{X_{AE}}{3} = 0.667 - \frac{0.0409}{3} = 0.6534$$

Similarly,
$$X_{DE} = 0.2814$$

To obtain the coordinates of $R$, step 5 is repeated. Figure 7.8 is changed to become base $ABD$, and point $H$ is used instead of point $G$.

| $X_{CW}$ | $X_{BW}$ | $X_{Cz}$ | $X_{Dz}$ |
|---|---|---|---|
| 0.125 | 0.875 | 0.067 | 0.118 |
| 0.175 | 0.825 | 0.071 | 0.206 |

The projection of the quaternary curve is drawn through the two points $z$ and point $r'$. It intersects line $pq$ at $r$: $X_{Br} = 0.807$, $X_{Cr} = 0.067$, $X_{Dr} = 0.126$. Line $Dr$ is drawn to intersect line $hg$ at $k$; line $Ck$ is drawn to intersect line $Ba$ at $r'''$. $\overline{Br'''} = 0.87$ in., $\overline{ar'''} = 0.435$ in. By a procedure similar to that for the extract, $X_{AR} = 0.1514$, $X_{BR} = 0.757$, $X_{CR} = 0.0165$, $X_{DR} = 0.0751$.

Eq. (7.3):
$$R + E = M = 200 \text{ lb.}$$

$C$ balance:
$$RX_{CR} + EX_{CE} = MX_{CM}$$
$$R(0.0165) + E(0.6534) = 200(0.325)$$

Solving simultaneously,
$$R = 103.1 \text{ lb.}, \qquad E = 96.9 \text{ lb.}$$

The solvent-free products in this case have the compositions $X_{AR'''} = 0.1668$ and $X_{AE'''} = 0.626$. It is interesting to note that if this extraction were carried out with 100 lb. of water only as the solvent, the solvent-free products would analyze $X_{AR'''} = 0.1507$, $X_{AE'''} = 0.835$. The single solvent is more effective than the mixed solvent in this case, even though the distribution coefficient is unfavorable.

## DOUBLE SOLVENTS (FRACTIONAL EXTRACTION)

Double-solvent operations involve the distribution of a mixture, components $B$ and $C$, between the immiscible solvents $A$ and $D$, where $B$ and $C$ are both soluble in both $A$ and $D$. One of the solvents, for example solvent $A$, is usually chosen so as preferentially to extract component $B$, while solvent $D$ preferentially extracts component $C$. In this manner the separa-

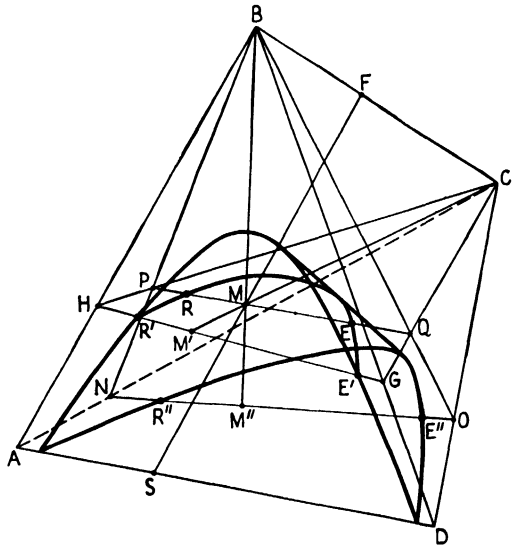



FIG. 7.10. Single-contact extraction with a double solvent.

tion is enhanced, and consequently double-solvent systems are usually employed where $B$ and $C$ are ordinarily separated with difficulty. Our knowledge of the equilibria in such systems is extremely sketchy, and in most cases resort must be had to actual laboratory extraction data.

**Single-stage Contact, Batchwise or Continuous.** Should the entire quaternary equilibria for the system be of the type described for mixed solvents, Fig. 7.1, the calculations for single-stage contact can be made entirely rigorously. Refer to Fig. 7.10, which represents equilibria of the type previously described, relettered to conform to the present process. Feed $F$, a mixture of $B$ and $C$, is extracted with incompletely soluble solvents $A$ and $D$, used in such proportions that together they are represented by $S$.

$$A + D = S \tag{7.18}$$

$$X_{AS} = \frac{A}{S}, \qquad X_{DS} = \frac{D}{S} \tag{7.19}$$

On mixture of the feed with the double solvent, $M$ results, in the two-liquid-phase region. The two equilibrium solutions then formed are $R$ and $E$, at

the ends of the quaternary tie line through $M$. As in the case of mixed solvents, tie line $RE$ can be located by determining the tie line $R'E'$ which passes through $M'$ in the base $ABD$, where $M'$ is the $C$-free composition corresponding to $M$, and tie line $R''E''$ through $M''$ in the base $ACD$, where $M''$ is the $B$-free composition corresponding to $M$. Tie line $R'E'$ and apex $C$ form plane $HGC$ which intersects plane $NOB$, formed from tie line $R''E''$ and apex $B$, in line $PQ$ which contains the quaternary tie line.

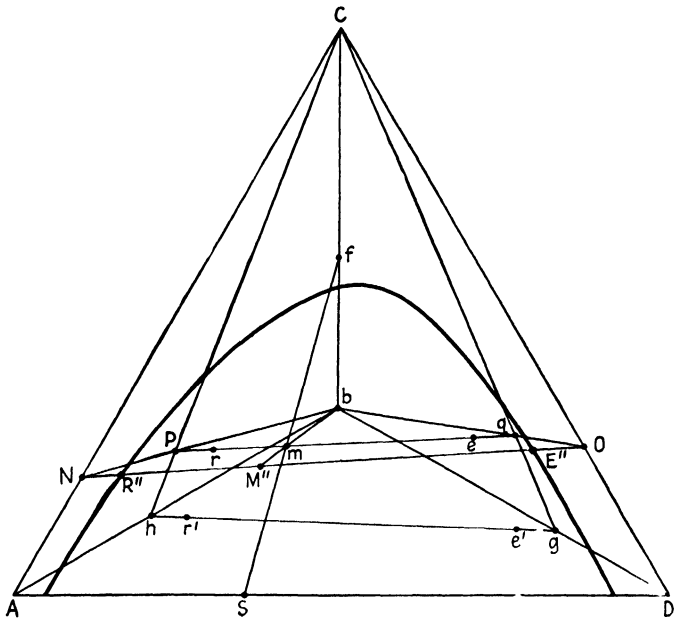



FIG. 7.11. Single-contact extraction with a double solvent, in projection.

As before, the calculations are made largely in projection, as in Fig. 7.11, on base $ACD$ where projected points are indicated by the lower-case letters corresponding to the points in the three-dimensional figure. Addition of double solvent to feed permits calculation of the coordinates of $M$, and hence of $m$. Point $m$ is thus located on line $fS$. The coordinates of $M''$ are determined and plotted (on line $bm$ extended). Ternary tie line $R''E''$ is then located through $m''$. The coordinates of $M'$ are calculated, plotted on base $ABD$ (not shown), tie line $R'E'$ located through $M'$, and points $r'$ and $e'$ plotted on Fig. 7.11. Line $r'e'$ is extended to $h$ and $g$, and lines $Ch$ and $Cg$ drawn. $R''E''$ is extended to $N$ and $O$, and lines $bN$ and $bO$ drawn. Point $p$ is located at the intersection of $bN$ and $Ch$, $q$ at the intersection of $bO$ and $Cg$. Line $pq$ then contains the tie-line projection $re$, which is located in the manner previously described for mixed solvents.

Solvent removal from the product solutions $E$ and $R$ can be followed in a

stepwise manner on Fig. 7.12. Removal of $A$ from $R$ leaves $K$ on the base $BDC$, from which $D$ is removed to produce the finished product $R''$ on line $BC$. In similar fashion, $E'''$ is the finished product corresponding to $E$. It is probably easier to calculate the coordinates of $E'''$ and $R'''$ than to locate these points geometrically.

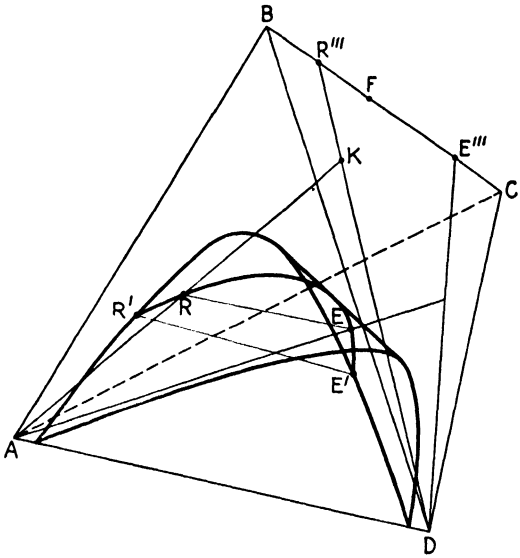



FIG. 7.12. Removal of double solvent from products.

**Illustration 2.** One hundred pounds of a solution containing 36% acetone ($B$), 64% acetic acid ($C$), are extracted in a single contact with a double solvent consisting of 60 lb. of chloroform ($A$) and 40 lb. of water ($D$), at 25°C. Calculate the weights and compositions of the solvent-free products.

*Solution.* The equilibrium data of Illustration 1 are used. Basis: 100 lb. of feed. $F = 100$ lb., $X_{BF} = 0.36$, $X_{CF} = 0.64$.

Eq. (7.14): $$X_{Cf} = X_{CF} + \frac{X_{BF}}{3} = 0.64 + \frac{0.36}{3} = 0.76$$

Point $f$ is plotted on plane $ACD$ (Fig. 7.11), on line $bC$. $S = 100$ lb., $X_{AS} = 0.60$, $X_{DS} = 0.40$. Point $S$ is plotted on line $AD$ (Fig. 7.11).

$$M = S + F = 100 + 100 = 200 \text{ lb.}$$

$$X_{AM} = \frac{FX_{AF} + SX_{AS}}{M} = \frac{100(0) + 100(0.60)}{200} = 0.30$$

Similarly,

$$X_{BM} = 0.18, \qquad X_{CM} = 0.32, \qquad X_{DM} = 0.20$$

Eq. (7.14): $$X_{Am} = X_{AM} + \frac{X_{BM}}{3} = 0.30 + \frac{0.18}{3} = 0.36$$

Similarly,

$$X_{Cm} = 0.38, \qquad X_{Dm} = 0.26$$

and point $m$ is plotted on Fig. 7.11. As a check, it must fall on line $fS$.

$$C \text{ in the feed} = FX_{CF} = 100(0.64) = 64 \text{ lb.}$$

$$\therefore M' = M - C = 200 - 64 = 136 \text{ lb.}$$

$$X_{AM'} = X_{AM}\frac{M}{M'} = 0.30\frac{200}{136} = 0.441$$

Similarly,

$$X_{BM'} = 0.265, \qquad X_{DM'} = 0.294$$

Point $M'$ is plotted on base $ABD$ (not shown). Tie line $R'E'$ is located through $M'$ by trial with the help of a distribution curve.

$R'$: $X_{AR'} = 0.658, \quad X_{BR'} = 0.327, \quad X_{DR'} = 0.015$

$$X_{Ar'} = X_{AR'} + \frac{X_{BR'}}{3} = 0.658 + \frac{0.327}{3} = 0.767$$

Similarly,

$$X_{Cr'} = 0.109, \qquad X_{Dr'} = 0.124$$

$E'$: $X_{AE'} = 0.013, \quad X_{BE'} = 0.147, \quad X_{DE'} = 0.840$

$$X_{Ae'} = X_{AE'} + \frac{X_{BE'}}{3} = 0.013 + \frac{0.147}{3} = 0.062$$

Similarly,

$$X_{Ce'} = 0.049, \qquad X_{De'} = 0.889$$

Points $e'$ and $r'$ are plotted on Fig. 7.11, line $e'r'$ extended to $h$ and $g$, and lines $Ch$ and $Cg$ drawn.

$$B \text{ in the feed} = FX_{BF} = 100(0.36) = 36 \text{ lb.}$$

$$M'' = M - B = 200 - 36 = 164 \text{ lb.}$$

$$X_{AM''} = X_{AM}\frac{M}{M''} = 0.30\frac{200}{164} = 0.366$$

Similarly,

$$X_{CM''} = 0.390, \qquad X_{DM''} = 0.244$$

Point $M''$ is plotted on base $ACD$ (Fig. 7.11), and tie line $R''E''$ located.

$R''$: $X_{AR''} = 0.744, \quad X_{CR''} = 0.226, \quad X_{DR''} = 0.030$

$E''$: $X_{AE''} = 0.164, \quad X_{CE''} = 0.455, \quad X_{DE''} = 0.381$

Line $R''E''$ is extended to $N$ and $O$, and lines $bN$ and $bO$ drawn. Points $p$ and $q$ are located, and line $pq$ drawn. The intersections of the quaternary-solubility curve with $pq$, which determine the coordinates of points $E$ and $R$, are located in exactly the same fashion as steps 5 and 6 of Illustration 1, with the following results:

$R$: $X_{AR} = 0.425, \quad X_{BR} = 0.228, \quad X_{CR} = 0.241, \quad X_{DR} = 0.106$

$E$: $X_{AE} = 0.191, \quad X_{BE} = 0.136, \quad X_{CE} = 0.390, \quad X_{DE} = 0.283$

The coordinates of $R'''$ must then be

$$X_{BR'''} = \frac{X_{BR}}{X_{BR} + X_{CR}} = \frac{0.228}{0.228 + 0.241} = 0.486$$

$$X_{CR'''} = 1 - X_{BR'''} = 1 - 0.486 = 0.514$$

Similarly,

$$X_{BE'''} = \frac{X_{BE}}{X_{BE} + X_{CE}} = \frac{0.136}{0.136 + 0.390} = 0.258$$

$$X_{CE'''} = 1 - X_{BE'''} = 1 - 0.258 = 0.742$$

Lack of the complete equilibrium data usually requires the assumption that the substances to be separated ($B$ and $C$) distribute themselves individually and independently according to their respective distribution coefficients $\mathbf{m}_B$ and $\mathbf{m}_C$ which remain constant. This in turn necessarily requires that (*a*) the solvents $A$ and $D$ are either substantially immiscible

or are saturated with each other prior to use, (*b*) that addition of $B$ and $C$ does not alter their insolubility, and (*c*) that the concentrations of $B$ and $C$ are always low.

Thus, on mixing feed $F$ with solvents $A$ and $D$ and upon reaching equilibrium, the weight of $B$ in the resulting $A$-rich phase will be $(A/X_{AA})(X_{BA})$, and in the $D$-rich phase $(D/X_{DD})(X_{BD})$. A $B$ balance is therefore

$$FX_{BF} = \frac{A}{X_{AA}}(X_{BA}) + \frac{D}{X_{DD}}(X_{BD}) \tag{7.20}$$

In similar fashion, a $C$ balance is

$$FX_{CF} = \frac{A}{X_{AA}}(X_{CA}) + \frac{D}{X_{DD}}(X_{CD}) \tag{7.21}$$

Furthermore, for insoluble solvents,

$$X_{AA} + X_{BA} + X_{CA} = 1 \tag{7.22}$$

$$X_{BD} + X_{CD} + X_{DD} = 1 \tag{7.23}$$

$$\mathbf{m}_B = \frac{X_{BA}}{X_{BD}} \tag{7.24}$$

and

$$\mathbf{m}_C = \frac{X_{CA}}{X_{CD}} \tag{7.25}$$

Solving Eqs. (7.20) to (7.25) simultaneously permits calculation of the concentrations at equilibrium. If, as will frequently happen, the solutions are so dilute that $X_{AA}$ and $X_{DD}$ are for all practical purposes equal to unity, Eqs. (7.20) and (7.21) reduce to

$$FX_{BF} = AX_{BA} + DX_{BD} \tag{7.26}$$

and

$$FX_{CF} = AX_{CA} + DX_{CD} \tag{7.27}$$

which may be used with Eqs. (7.24) and (7.25) to give the equilibrium concentrations. Should $\mathbf{m}_B$ and $\mathbf{m}_C$ vary with concentration, a trial-and-error calculation is necessary. For dilute solutions, the equations may also be used with $X$ defined as weight of solution per unit volume, with $F$, $A$, and $D$ defined as volumes.

For a successful separation, the selectivity $\beta$, as previously defined,

$$\beta = \frac{\mathbf{m}_B}{\mathbf{m}_C} = \frac{X_{BA}X_{CD}}{X_{CA}X_{BD}} \tag{3.116}$$

must exceed unity, the more so the better. Ordinarily, $\beta$ will be greater the more dilute the solutions. At the same time the product $\mathbf{m}_B\mathbf{m}_C$ should not be far removed from unity else the low concentration in one of the solvents will require excessive amounts of that solvent, thus aggravating the

solvent-recovery problem. Solvent pairs should be chosen with these considerations in mind. $A$ and $D$ may themselves be solutions, if thereby the distribution coefficients are improved. Van Dijck and Schaafsma (18) offer a convenient illustration: if equal parts of *o*- and *p*-oxybenzaldehyde are to be separated into two products, one rich in the ortho, the other rich in the para compound, each product at the same purity, 85 per cent aqueous ethanol and an aromatic-free gasoline may be used as a solvent pair. However, approximately 16 times as much gasoline as ethanol will be required, which produces an exceedingly low concentration in the gasoline phase. Replacing the gasoline with a mixture of 40 per cent benzene, 60 per cent gasoline would increase the equilibrium concentrations of both solutes in the hydrocarbon phase considerably but will also cause too great a mutual solubility with the ethanol. If in addition, however, the ethanol is diluted to a 50 per cent concentration with water, the insolubility of the solvents is preserved, the equilibrium concentration of both solutes in the ethanol phase is reduced, and the selectivity is still favorable. As a consequence, a solvent ratio of 1.6 rather than 16 may be employed. Similarly, in separating mixtures of organic acids or bases, aqueous solutions may be buffered to alter the ionization constants of the solute, thus altering the distribution coefficients (7). See also the work of Garwin and Hixson (9), and McKee (14).

Let $p_B$ represent the fraction of the $B$ in the feed entering the $A$-rich phase, $q_B$ that entering the $D$-rich phase (3). Thus, for dilute solution,

$$\frac{p_B}{q_B} = \frac{p_B}{1 - p_B} = \frac{AX_{BA}}{DX_{BD}} = \frac{A\mathbf{m}_B}{D} \tag{7.28}$$

$$p_B = \frac{A\mathbf{m}_B/D}{1 + (A\mathbf{m}_B/D)} = 1 - q_B \tag{7.29}$$

Similarly, $p_C$ and $q_C$ are the fractions of the $C$ in the feed entering the $A$- and $D$-rich phases, respectively, so that

$$p_C = \frac{A\mathbf{m}_C/D}{1 + (A\mathbf{m}_C/D)} = 1 - q_C \tag{7.30}$$

Combining Eqs. (7.29) and (7.30),

$$\frac{p_B}{p_C} = \frac{1 + (D/A\mathbf{m}_C)}{1 + (D/A\mathbf{m}_B)} \tag{7.31}$$

The quantity $A\mathbf{m}/D$ is the familiar "extraction factor." Consideration of Eq. (7.31) shows that for $\mathbf{m}_B > \mathbf{m}_C$, large values of $D/A$ increase $p_B/p_C$, ultimately to $\mathbf{m}_B/\mathbf{m}_C$. Rearrangement of Eq. (7.31),

$$\frac{A}{D} = \frac{(1/\mathbf{m}_C) - (p_B/p_C\mathbf{m}_B)}{(p_B/p_C) - 1} \tag{7.32}$$

permits calculation of the solvent ratio for any desired value of $p_B/p_C$. For a symmetrical separation, *i.e.*, where the fraction of $B$ entering phase $A$ equals that of $C$ entering $D$,

$$p_B = q_C = 1 - p_C \tag{7.33}$$

whence

$$\frac{Am_B/D}{1 + (Am_B/D)} = 1 - \frac{(Am_C/D)}{1 + (Am_C/D)} \tag{7.34}$$

from which

$$\frac{A}{D} = \sqrt{\frac{1}{m_B m_C}} \tag{7.35}$$

or

$$\frac{Am_B}{D} = \sqrt{\beta}, \qquad \frac{Am_C}{D} = \sqrt{\frac{1}{\beta}} \tag{7.36}$$

If we define the degree of separation between components $B$ and $C$ as $(p_B - p_C)$ (2), then

$$p_B - p_C = \frac{Am_B/D}{1 + (Am_B/D)} - \frac{Am_C/D}{1 + (Am_C/D)} \tag{7.37}$$

The differential, $d(p_B - p_C)/d\left(\frac{A}{D}\right)$, of Eq. (7.37) when set equal to zero results in Eq. (7.35). In other words, the degree of separation as so defined is a maximum when the solvent ratio is given by Eq. (7.35).

**Illustration 3.** Scheibel (15) reports the simultaneous distribution of para ($B$)- and ortho ($C$)-chloronitrobenzene between the double-solvent pair Skellysolve (a mixture of heptanes) ($A$) and methanol (containing 15% water by volume) ($D$). When 50 gm. of solute was distributed between 250 cu. cm. of each of the solvents, $m_B = 1.33$ and $m_C = 0.82$, values which are substantially constant with varying ratios of the distributed substances. The solvents are substantially immiscible. What will be the solvent-free product compositions when 100 lb. of a mixture containing 33.5% para-, 66.5% ortho-chloronitrobenzene are distributed in a single-stage extraction with these solvents to give (*a*) a symmetrical separation and (*b*) products of equal purity? What quantities of the solvents should be used?

*Solution.* *a.* For symmetrical separation,

Eq. (7.35) $$\frac{A}{D} = \sqrt{\frac{1}{m_B m_C}} = \sqrt{\frac{1}{(1.33)(0.82)}} = 0.959 \frac{\text{cu. ft. heptane}}{\text{cu. ft. methanol}}$$

$$\frac{Am_B}{D} = 0.959(1.33) = 1.276$$

$$\frac{Am_C}{D} = 0.959(0.82) = 0.786$$

Eq. (7.29): $$p_B = \frac{Am_B/D}{1 + (Am_B/D)} = \frac{1.276}{1 + 1.276} = 0.560$$

$$p_C = \frac{Am_C/D}{1 + (Am_C/D)} = \frac{0.786}{1 + 0.786} = 0.440 (= 1 - 0.560)$$

Basis: 100 lb. feed, containing 33.5 lb. para-, 66.5 lb. ortho-chloronitrobenzene. The $A$-rich layer will contain

0.560(33.5) = 18.78 lb. para; 39.1%, solvent-free.
0.440(66.5) = 29.3 lb. ortho; 60.9%, solvent-free.

The *B*-rich layer will contain

$$33.5 - 18.78 = 14.76 \text{ lb. para; } 28.4\%, \text{ solvent-free.}$$
$$66.5 - 29.3 = 37.2 \text{ lb. ortho; } 71.6\%, \text{ solvent-free.}$$

To be reasonably certain that the distribution data will apply, the solute concentrations should approximate those of the experiments, 500 cu. cm. total solvent/50 gm. solute.

$\therefore$ (500/50)(100)(454)(1/28,320) = 16 cu. ft. total solvent should be used, of which (0.959/1.959)(16) = 7.84 cu. ft. should be heptane.

*b*. Let $X_{BA}$, $X_{BD}$, $X_{CA}$, $X_{CD}$ be expressed in pounds solute per cubic foot solvent, $A$ and $D$ in cu. ft.

$$\therefore 33.5 = AX_{BA} + DX_{BD}$$
$$66.5 = AX_{CA} + DX_{CD}$$
$$m_B = 1.33 = \frac{X_{BA}}{X_{BD}}$$
$$m_C = 0.82 = \frac{X_{CA}}{X_{CD}}$$

For the same total solute concentration as in *a*,

$$A + D = 16$$

For equal purities,

$$\frac{X_{BA}}{X_{BA} + X_{CA}} = \frac{X_{CD}}{X_{BD} + X_{CD}}$$

The six equations set the conditions for the problem. Simultaneous solution reveals $A$ to be negative, and further study of the equations shows that no real solution is possible with any quantity of total solvent. Hence with this feed composition, equal purities of products cannot be obtained.

**Batchwise Extraction, Multiple Stage.** This operation, usually a laboratory procedure, can be carried out in two ways. The immiscible solvents may be continuously pumped through the various stages in countercurrent flow, and the batch of mixture to be separated may be suddenly introduced near the center of the cascade. The result is an unsteady-state operation, the solutes leaving the opposite ends of the cascade in ratios different from that in the feed and in amounts varying with time. Such an operation has been considered in some detail by Martin and Synge (13) and Cornish *et al.* (4).

On the other hand, the discontinuous batch operation of the type described in Fig. 7.13 is more readily carried out. Here the mixture $(B + C)$ to be separated is introduced into stage $g$ at the top of the figure, together with the immiscible solvents $A$ and $D$. The $A$-rich layer resulting then passes to stage $h$ to be extracted with additional $D$, the $D$-rich layer to stage $j$ for contacting with additional $A$, etc. The operation may be stopped at any point or may be carried through the diamond-shaped arrangement shown. Additional stages may of course be used. The use of $n$ portions of each solvent in such an operation can be handled in the laboratory with $n$ separating funnels as stages. If $n$ is large, the operations are cumbersome at best, and recourse may be had to the ingenious laboratory device fashioned by Craig (5, 8) which permits large numbers of ex-

tractions to be made rapidly with small amounts of solvent, according to various arrangements of the stages. The device operates on a principle similar to that used in the Cohen-Bruins apparatus for measuring diffusivities described in Chap. 5: two metal plates containing matching holes for

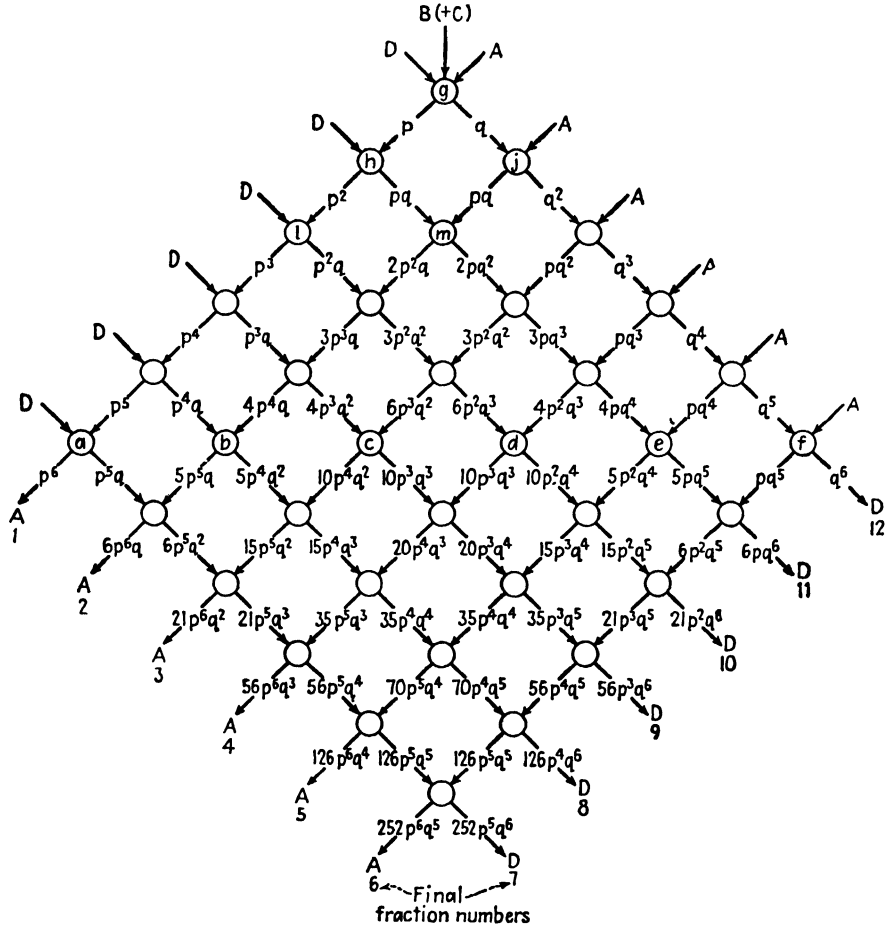



FIG. 7.13. Discontinuous batchwise multistage extraction with a double solvent. (*Bush and Densen.*)

the upper and lower solvent layers, respectively, are placed in contact; shaking the apparatus brings about equilibrium, and after the solvent layers are settled, rotation of one plate with respect to the other separates the layers and brings each into contact with another hole containing solvent.

Several thorough studies have been made of the discontinuous batch extraction (3, 5, 6, 7, 11, 12, 20). The Bush and Densen (3) treatment is described here. Refer to Fig. 7.13, and let the simplifying assumptions re-

specting solvent immiscibility and constancy of distribution coefficients apply. Further, let the solvents $A$ and $D$ each be divided into $n$ equal portions (in the figure, $n = 6$). If $B$ alone were distributed between the solvents, the products from stage $g$ would contain the fraction $p_B$ of the original $B$ in the $A$ layer, the fraction $q_B$ in the $D$ layer, the previous definitions of $p$ and $q$ still applying. If the same distribution occurs in all stages, *i.e.*, if $\mathbf{m}_B$ is constant, then the fraction of $B$ in the $A$ layer from stage $h$ will be $p_B p_B$ or $p_B^2$, that from stage $j$ will be $p_B q_B$, and that from stage $m$ will be $p_B(p_B q_B + p_B q_B) = 2p_B^2 q_B$. Similarly the fraction of the original $B$ leaving other stages may be calculated. If in addition solute $C$ is simultaneously distributed the same fractions (with $C$ as subscripts) apply to solute $C$.

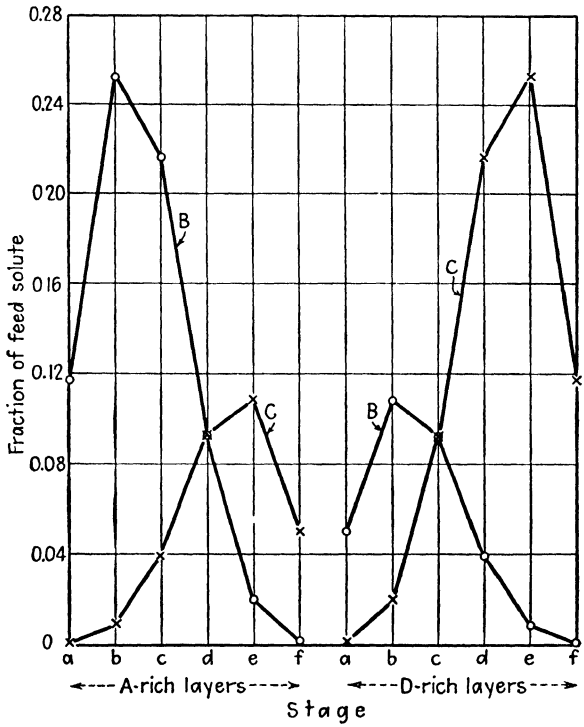



FIG. 7.14. Distribution of solute in discontinuous multistage extraction after 21 stages. $n = 6$, $p_B = q_C = 0.7$.

If the extractions are stopped at a horizontal series of stages in the diagram, such as at stages $a$, $b$, $c$, etc., the fractions of each solute in the various layers may be calculated from the binomial expansion of $(p + q)^n$. The distribution of each solute in the various product layers may then be compared. For example, suppose we have the symmetrical distribution $p_B = 0.7$, $q_B = 1 - 0.7 = 0.3$, $p_C = 0.3$, $q_C = 1 - 0.3 = 0.7$, and $n = 6$ as in Fig. 7.13. Figure 7.14 then shows the fractions of the original solutes

in each of the layers from stages $a$ through $f$. It is seen that component $B$ tends to concentrate in the $A$-rich layers, particularly in that from stage $b$, while component $C$ tends to concentrate in the $D$ layers, especially that from stage $e$. If we define $\mathbf{p}$ and $\mathbf{q}$ as the fractions of original solute in the $A$- and $D$-rich layers, respectively, after several extractions, then $\mathbf{p}_B - \mathbf{p}_C = 0.2436$ for stage $b$, and $\mathbf{q}_C - \mathbf{q}_B = 0.2436$ for stage $e$, the greatest values obtained for any single final stage. If the $A$-rich layers of stages $a$ through $d$ are composited, $\mathbf{p}_B - \mathbf{p}_C = 0.6785 - 0.1415 = 0.5370$, while for stages $a$ through $e$, $\mathbf{p}_B - \mathbf{p}_C = 0.7000 - 0.3000 = 0.4000$. Similar figures result for quantities $\mathbf{q}_C - \mathbf{q}_B$ for composited $D$ layers, and these may be used as an indication of the degree of separation.

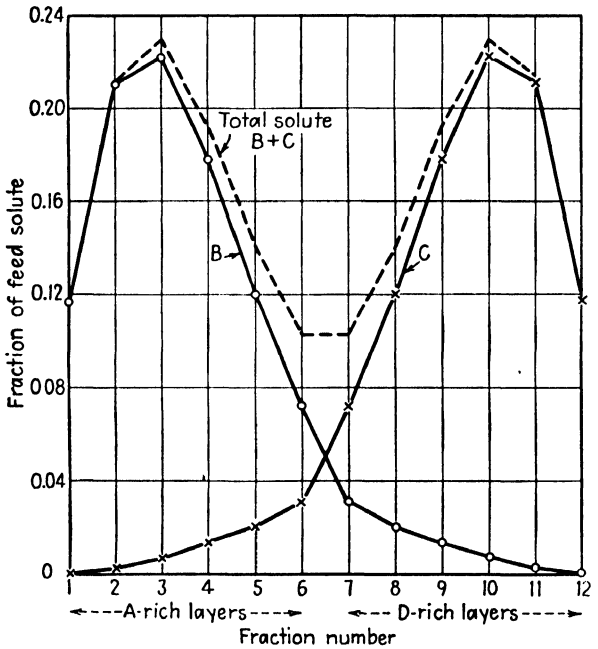



FIG. 7.15. Distribution of solute in discontinuous multistage extraction after 36 stages. $n = 6$, $p_B = q_C = 0.7$.

On the other hand, if the extractions are continued through the diagonal stages to yield fractions 1 through 12 (a total of $n^2$ extractions, 36 in the case of Fig. 7.13), the fractions of each of the original solutes in each of the product layers are given by the series

$$p^n + \frac{n!}{(n-1)!}p^n q + \frac{(n+1)!}{2!(n-1)!}p^n q^2 + \frac{(n+2)!}{3!(n-1)!}p^n q^3 + \cdots + \frac{(2n-2)!}{(n-1)!(n-1)!}p^n q^{n-1}$$

for the $A$-rich solutions, and

$$\frac{(2n-2)!}{(n-1)!(n-1)!}q^n p^{n-1} + \cdots + \frac{(n+2)!}{3!(n-1)!}q^n p^3 + \frac{(n+1)!}{2!(n-1)!}q^n p^2 + \frac{n!}{(n-1)!}q^n p + q^n$$

for the $D$-rich solutions. With these we can calculate distributions of the solutes in the products for this arrangement. As before, if $p_B = p_C = 0.7$, $p_C = q_B = 0.3$, and $n = 6$, the final fractions contain the amounts shown in Fig. 7.15. Fractions 3 and 10 show the highest degree of separation for any single fractions, $\mathbf{p}_B - \mathbf{p}_C = 0.2147$ for fraction 3, $\mathbf{q}_C - \mathbf{q}_B = 0.2147$ for fraction 10. A composite of all $A$-rich solutions, fractions 1 through 6, shows $\mathbf{p}_B - \mathbf{p}_C$ to be $0.9217 - 0.0783 = 0.8434$, the same value for $\mathbf{q}_C - \mathbf{q}_B$ for a composite of all the $D$-layers of fractions 7 through 12. These show not only higher total recoveries of the individual solutes in a single solvent but also greater degrees of separation than for the operation which stops at the horizontal stages $a$ through $f$. The sum of the ordinates on either curve will equal unity, and if the dividing line for compositing be taken at the intersection of the two curves, an over-all measure of the degree of separation can be taken as

$$\text{Degree of separation} = 2 - \frac{\left\{\begin{array}{l}\text{sum of fractions of } B \text{ to the right}\\ \text{of the intersection of the curves}\\ + \text{ sum of fractions of } C \text{ to the left}\\ \text{of the intersection}\end{array}\right.}{2} \qquad (7.38)$$

In the example discussed, this value is 0.9217.

It should be recalled that the symmetrical separations ($p_B = q_C$) just described require the ratios of the solvents to be fixed in accordance with Eqs. (7.35) or (7.36), and in such cases curves of the type of Fig. 7.15 are always mirror images of each other. In other cases, they are lopsided or distorted. For example, for $\mathbf{m}_B = 4.0$ and $\mathbf{m}_C = 0.735$, $A/D$ for a symmetrical separation will be 0.583 [Eq. (7.35)], $p_B = 0.7$ [Eq. (7.29)], and the curves of Fig. 7.15 result if $n = 6$. If instead a solvent ratio $A/D = 1.0$ is used, $p_B = 0.8$ [Eq. (7.29)], $p_C = 0.424$ [Eq. (7.30)], and for $n = 6$ with the arrangement of Fig. 7.13, we get the distributions shown in Fig. 7.16. If after removal of solvent composites of fractions on either side of the point of intersection (*i.e.*, 1 to 4 inclusive, and 5 to 12 inclusive) are made, the degree of separation as defined in Eq. (7.38) becomes 0.8919. The symmetrical separation will always result in higher values of the degree of separation than any other, although advantages are sometimes to be found in the nonsymmetrical. For example, in the case of Fig. 7.16, compositing all $D$-rich fractions will give $C$ in purer form than for the symmetrical

separation although at a sacrifice of yield. Similarly, using unequal numbers of portions of the two solvents ($n_A \neq n_D$) can be advantageous.

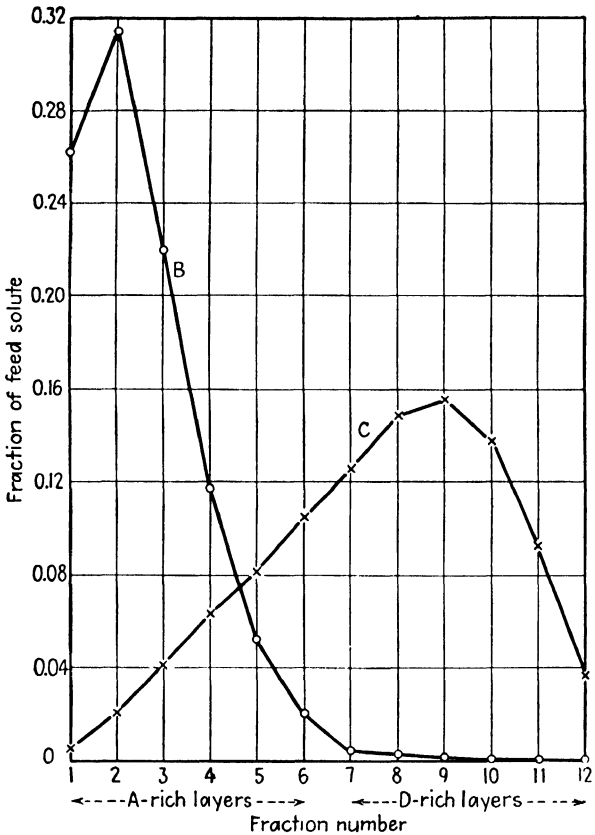



FIG. 7.16. Distribution of solute in discontinuous multistage extraction after 36 stages, $n = 6$, $p_B = 0.8$, $p_C = 0.424$.

Estimates of extractions can be made quickly with the assistance of Fig. 7.17, which relates the fraction of either solute which has accumulated in the composited $A$-rich layers with the number of stages in a diamond-shaped plan. For symmetrical separations, the abscissa for $p_B$ is the degree of separation as defined by Eq. (7.38).

**Illustration 4.** $p$-Nitrobenzoic acid ($B$) and $o$-nitrobenzoic acid ($C$) distribute between chloroform ($A$) and water ($D$) (mutually saturated solvents) with distribution coefficients $\mathbf{m}_B = 1.71$ and $\mathbf{m}_C = 0.27$ at concentrations of 0.0015 gm. mole/liter in the $A$-rich layer, at 25°C. ("International Critical Tables," Vol. III, p. 429). On the assumption that the distributions are independent of each other, calculate the separation obtainable for various numbers of stages and for a symmetrical separation, starting with a 50–50 mixture of $B$ and $C$.

*Solution.* For a symmetrical separation,

Eq. (7.35):
$$\frac{A}{D} = \sqrt{\frac{1}{m_B m_C}} = \sqrt{\frac{1}{(1.71)(0.27)}}$$
$$= 1.47 \frac{\text{liters } CHCl_3\text{-rich solvent}}{\text{liters } H_2O\text{-rich solvent}}$$

Eq. (7.29):
$$p_B = \frac{Am_B/D}{1 + (Am_B/D)} = \frac{1.47(1.71)}{1 + 1.47(1.71)} = 0.715$$

Eq. (7.30):
$$p_C = \frac{Am_C/D}{1 + (Am_C/D)} = \frac{1.47(0.27)}{1 + 1.47(0.27)} = 0.2845$$

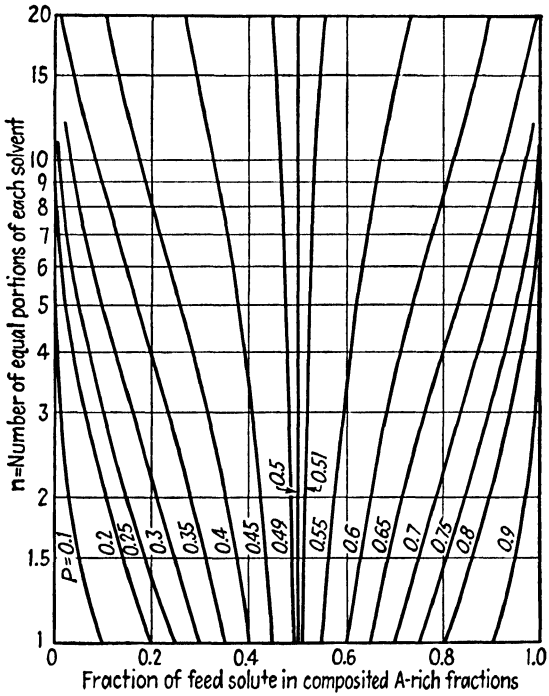



FIG. 7.17. Distribution of solute in discontinuous multistage extraction for $n^2$ stages. (*Bush and Densen.*)

Refer to Fig. 7.17. At $n = 5$ (25 stages, arranged as in Fig. 7.13, each solvent divided into five equal portions), and at $p_B = 0.715$, the fraction of $B$ in the composited $A$-rich phase is 0.91, and for $p_C = 0.2845$, the fraction of $C$ in the $A$-rich phase is 0.09.
Basis: 1 gm. feed mixture = 0.5 gm. $B$, 0.5 gm. $C$.
$B$ in composited $A$-rich phase = 0.91(0.5) = 0.455 gm. (91%)
$C$ in composited $A$-rich phase = 0.09(0.05) = 0.045 gm. (9%)
The degree of separation is 0.91. Similarly for other values of $n$, the following results are obtained:

| $n$ | 1 | 2 | 4 | 5 | 8 | 10 |
|---|---|---|---|---|---|---|
| Degree of separation | 0.715 | 0.80 | 0.89 | 0.91 | 0.96 | 0.995 |

**Illustration 5.** From a mixture containing 40% of $p(B)$- and 60% of $o(C)$-nitrobenzoic acids, it is desired to obtain a mixture analyzing 95% $B$, 5% $C$, with 80% recovery of $B$, in a 25-stage extraction arranged as in Fig. 7.13, using chloroform ($A$) and water ($D$). What solvent ratio should be used?

*Solution.* Distribution coefficients are given in Illustration 4.

Basis: 1 gm. mixture, containing 0.4000 gm. $B$, 0.6000 gm. $C$.

The composited $A$-rich solutions must contain $0.8(0.4000) = 0.3200$ gm. $B$, and $0.3200(5/95) = 0.01685$ gm. $C$.

$$\therefore \text{Fraction of } B \text{ in composited } A\text{-rich solution} = \frac{0.3200}{0.4000} = 0.80$$

$$\text{Fraction of } C \text{ in composited } A\text{-rich solution} = \frac{0.01685}{0.6000} = 0.0281$$

From Fig. 7.17, at $n = 5$, $p_B = 0.635$, $p_C = 0.22$.

$$\text{Eq. (7.32):} \quad \frac{A}{D} = \frac{[(1/\mathbf{m}_C) - (p_B/p_C\mathbf{m}_B)]}{(p_B/p_C) - 1} = \frac{[1/0.27 - 0.635/0.22(1.71)]}{[(0.635/0.22) - 1]}$$

$$= 1.068 \frac{\text{liters } CHCl_3}{\text{liter } H_2O}$$

This extraction procedure is useful in the laboratory not only for making actual separations of mixtures but for analytical purposes as well. For example, an unknown mixture can be subjected to a fractionation of the arrangement shown in Fig. 7.13 and the total solute content of the final fractions determined by weighing the residues after solvent evaporation. If a curve plotted from the resulting data, such as the broken curve of Fig. 7.15, shows two or more peaks, it is first-hand evidence that the original solute is a mixture and not pure. Such a curve can provide preliminary information for subsequent separation procedures.

**Illustration 6.** One gram of a mixture, when fractionated according to the scheme of Fig. 7.13 with a solvent ratio $A/D = 0.583$, gave the broken curve of Fig. 7.15. The total solute content of fractions 2 and 3 were 0.2148 gm. and 0.2297 gm., resp. Make a first estimate of the distribution coefficient of one of the components of the mixture.

*Solution.* Assume the $C$ content of the fractions are negligible, in view of the nature of the peaks of the curve.

$$\therefore \frac{\text{Weight of fraction 3}}{\text{Weight of fraction 2}} = \frac{21 p_B^5 q_B^2}{6 p_B^5 q_B} = \frac{21}{6} q_B = \frac{0.2297}{0.2148}$$

$$\therefore q_B = 0.3055, \qquad p_B = 1 - q_B = 0.6945 \text{ (first estimate)}$$

$$\text{Eq. (7.28):} \quad \mathbf{m}_B = \frac{D}{A}\frac{p_B}{q_B} = \frac{1}{0.583}\frac{0.6945}{0.3055} = 3.90 \text{ (first estimate)}$$

The curves were originally drawn for $\mathbf{m}_B = 4.0$ with this solvent ratio. Similarly $\mathbf{m}_C$ could be estimated, and with the help of Fig. 7.17, an extraction procedure to separate the mixture more or less completely could be planned.

**Continuous Countercurrent Multistage Fractional Extraction.** The industrial process utilizing the double-solvent principles is continuous and is carried out according to the flowsheet of Fig. 7.18 (2, 15). The feed, consisting principally of a mixture of $B$ and $C$ to be separated, is introduced into the central portion of a cascade of stages, $1'$ to 1. To facilitate

handling of the feed, it may be mixed with or dissolved in relatively small portions of solvents $A_F$ and $D_F$. The principal portions of the solvents, which may contain dissolved solute remaining from a solvent-recovery operation or solute returned as reflux, are introduced into the extremities of the cascade as shown and are either substantially immiscible or mutually saturated with each other before use.

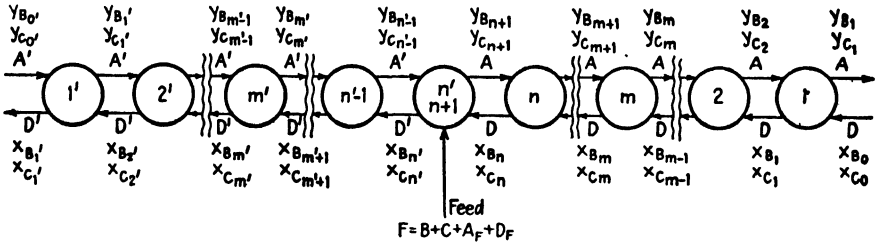



FIG. 7.18. Countercurrent multiple contact with a double-solvent-fractional extraction.

$$A = A' + A_F, \qquad D' = D + D_F \tag{7.39}$$

and $A$, $A'$, $D$, $D'$ are constant from stage to stage. Concentrations of the solutes in the $A$ phase ($y$) and the $D$ phase ($x$) are expressed according to the following scheme:

$$x_B = \frac{X_{BD}}{X_{DD}}, \qquad x_C = \frac{X_{CD}}{X_{DD}}, \qquad y_B = \frac{X_{BA}}{X_{AA}}, \qquad y_C = \frac{X_{CA}}{X_{AA}} \tag{7.40}$$

where $X$ is weight fraction, in which case $A$ and $D$ are expressed as weights per unit time. Alternatively, $x$ and $y$ may be made mole ratios or weights per unit volume, for which $A$ and $D$ should be expressed as moles or volumes per unit time, respectively. The equilibrium-distribution coefficients are described as

$$\mathbf{m}_B = \frac{y_B}{x_B}, \qquad \mathbf{m}_C = \frac{y_C}{x_C} \tag{7.41}$$

and are assumed independent of each other.

A material balance for component $B$, stages $1'$ through $m'$, inclusive:

$$A'y_{B_0'} + D'x_{B_{m'+1}} = A'y_{B_{m'}} + D'x_{B_1'} \tag{7.42}$$

$$\frac{D'}{A'} = \frac{y_{B_{m'}} - y_{B_0'}}{x_{B_{m'+1}} - x_{B_1'}} \tag{7.43}$$

This is the equation of a straight line of slope $D'/A'$ on $x_B - y_B$ coordinates, the operating line, passing through the points $(x_{B_1'}, y_{B_0'})$ representing the end of the cascade, and $(x_{B_{m'+1}}, y_{B_{m'}})$ representing any stage to the left of the feed. It is shown as line $MN$ on Fig. 7.19, along with the equilibrium-distribution curve $y_B = \mathbf{m}_B x_B$, where $\mathbf{m}_B$ is not necessarily constant. The operating line represents the relationship between concentrations in the $A$-rich phase

leaving any stage and that in the $D$-rich phase entering that stage. The equilibrium curve, on the other hand, represents the relationship between the concentrations in the two solutions leaving the same stage. Between

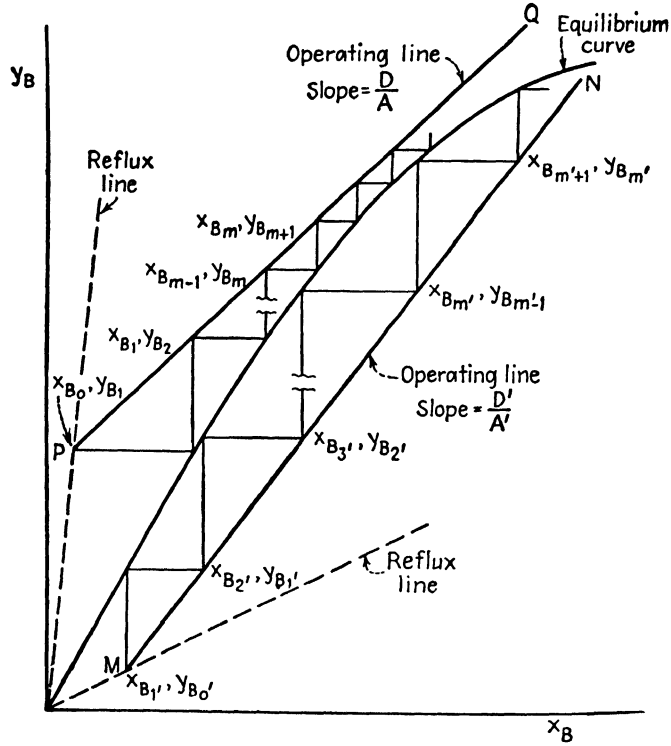



FIG. 7.19. Stage construction, component $B$.

them they provide the stepwise construction shown in the figure for the stages to the left of the feed, each step representing one theoretical stage. Similarly, a $B$ balance for stages $m$ through 1, inclusive:

$$Ay_{B_{m+1}} + Dx_{B_0} = Ay_{B_1} + Dx_{B_m} \tag{7.44}$$

$$\frac{D}{A} = \frac{y_{B_{m+1}} - y_{B_1}}{x_{B_m} - x_{B_0}} \tag{7.45}$$

a straight line of slope $D/A$, through $(x_{B_0},y_{B_1})$ and $(x_{B_m},y_{B_{m+1}})$, shown as line $PQ$, Fig. 7.19. This figure then permits the determination of the stagewise change in concentrations of component $B$, below the equilibrium curve for the stages to the left of the feed, above for the stages to the right.

For component $C$, stages $1'$ through $m'$:

$$A'y_{C_{0'}} + D'x_{C_{m'+1}} = A'y_{C_{m'}} + D'x_{C_{1'}} \tag{7.46}$$

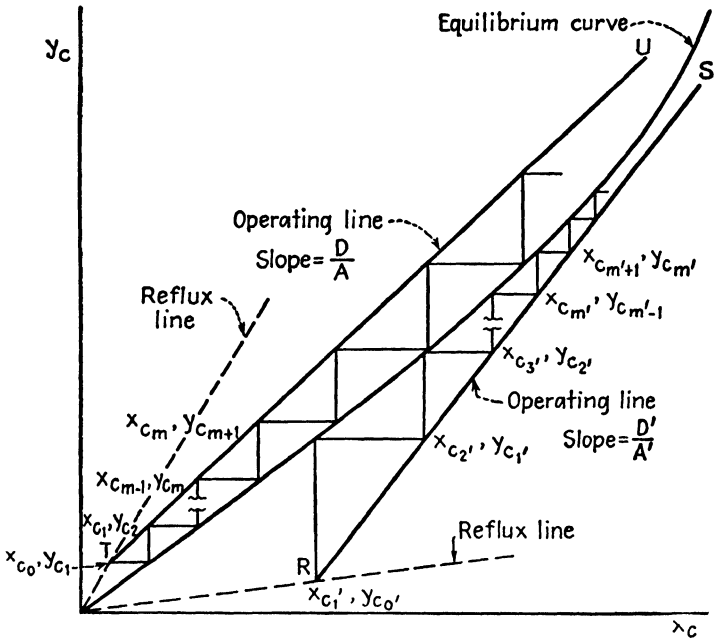
$$\frac{D'}{A'} = \frac{y_{C_{m'}} - y_{C_{0'}}}{y_{C_{m'+1}} - x_{C_{1'}}} \tag{7.47}$$

a line of slope $D'/A'$ through points $(x_{C_1'}, y_{C_0'})$ and $(x_{C_{m'+1}}, y_{C_{m'}})$, shown as line $RS$ on Fig. 7.20. For stages $m$ through 1:

$$Ay_{C_{m+1}} + Dx_{C_0} = Ay_{C_1} + Dx_{C_m} \tag{7.48}$$

$$\frac{D}{A} = \frac{y_{C_{m+1}} - y_{C_1}}{x_{C_m} - x_{C_0}} \tag{7.49}$$

a line of slope $D/A$ through $(x_{C_0}, y_{C_1})$ and $(x_{C_m}, y_{C_{m+1}})$, line $TU$ on Fig. 7.20. This figure then permits the determination of the stagewise concentration changes for $C$, as shown.


Equilibrium curve
U
S
Operating line
Slope= D/A
Reflux line
Operating line
Slope= D'/A'
Reflux line
R
T
T
T

cients. If $\mathbf{m}_B$ and $\mathbf{m}_C$ are constant, the equilibrium curves are straight lines. If no solvent is introduced with the feed, the four operating lines are all parallel. On the other hand, if the number of stages is fixed and final concentrations in the product solutions are to be determined, the operating lines must be located by trial to permit fitting the required number of stages on the plots. In this latter case, matching of component concentrations is carried out directly on Figs. 7.19 and 7.20. It is important that computed concentrations at the feed stage do not exceed the solubility limits.

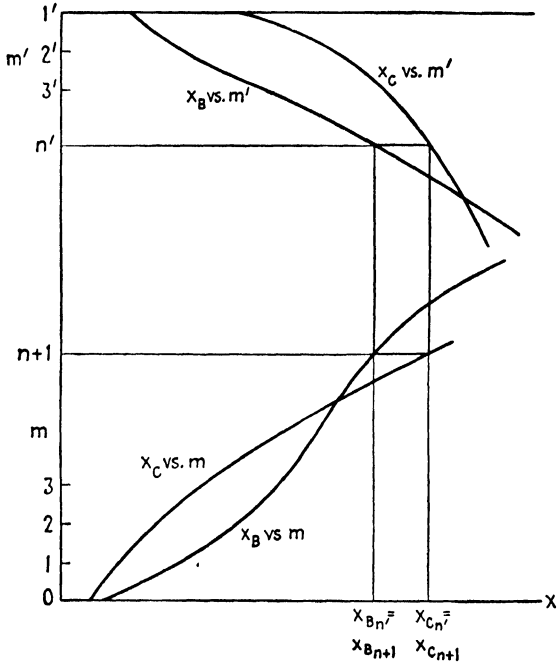



FIG. 7.21. Matching of components at the feed stage.

For a given total amount of the solvents, the number of stages will be fewer if all solvent is introduced at the ends of the cascade rather than partly with the feed, since then the slope of the operating lines $MN$ and $RS$ will be smaller, and that of the lines $PQ$ and $TU$ greater (Figs. 7.19 and 7.20).

**Illustration 7.** Scheibel (15) reports the separation of *p*(*B*)- and *o*(*C*)-chloronitrobenzene with the double-solvent system heptane (*A*), 86.7% aqueous methanol (*D*) in a countercurrent plant as follows (Run 5): Feed = 5.35 lb./hr. of a mixture of 37.5% para isomer, 62.5% ortho isomer, diluted with 0.08 cu. ft./hr. of heptane. Fresh heptane = 3.04 cu. ft./hr., fresh methanol = 2.83 cu. ft./hr., fed to the extremities of the cascade. The heptane-rich product contained 1.96 lb./hr. of solute analyzing 81.7% para, 18.3% ortho; the methanol-rich product 3.39 lb./hr. of solute analyzing 12.0%

para, 88.0% ortho isomer. The distribution coefficients are $m_B = 1.10$ and $m_C = 0.679$, in lb./cu. ft. concentration units. Mutual solubility of the solvents is negligible. Calculate the number of theoretical stages to which the extraction plant is equivalent.

*Solution.* Define $x$ and $y$ in terms of lb. solute/cu. ft. solvent, $A$ and $D$ in cu. ft./hr.

$$A' = 3.04, \quad A_F = 0.08, \quad A = 3.12 \text{ cu. ft./hr. heptane}$$
$$D_F = 0, \quad D' = D = 2.83 \text{ cu. ft./hr. methanol}$$
$$\frac{D'}{A'} = \frac{2.83}{3.04} = 0.930, \quad \frac{D}{A} = \frac{2.83}{3.12} = 0.907$$

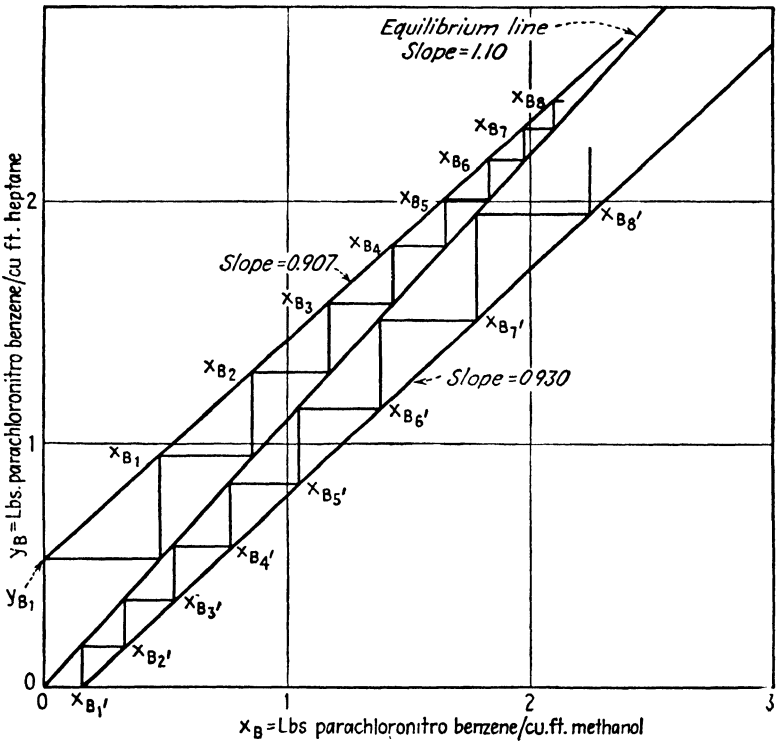



FIG. 7.22. Illustration 7. Stage construction for component $B$.

Since the solvents introduced into the ends of the cascade contain no solute, $x_{B_0} = x_{C_0} = y_{B_0'} = y_{C_0'} = 0$.

Heptane-rich product:

$$y_{B_1} = \frac{1.96(0.817)}{3.12} = 0.512 \text{ lb. } B/\text{cu. ft. } A$$

$$y_{C_1} = \frac{1.96(0.183)}{3.12} = 0.1153 \text{ lb. } C/\text{cu. ft. } A$$

Methanol-rich product:

$$x_{B_1'} = \frac{3.39(0.120)}{2.83} = 0.1441 \text{ lb. } B/\text{cu. ft. } D$$

$$x_{C_1'} = \frac{3.39(0.880)}{2.83} = 1.052 \text{ lb. } B/\text{cu. ft. } D$$

Operating lines and equilibrium curves are plotted on Figs. 7.22 and 7.23, stages are stepped off, and the concentration $x$ plotted against stage number on Fig. 7.24. Match-

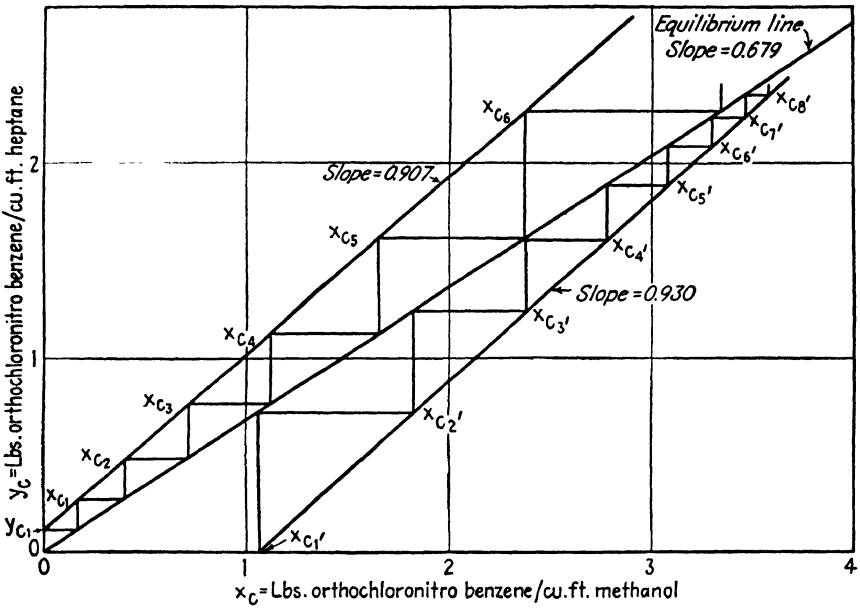



FIG. 7.23. Illustration 7. Stage construction for component $C$.

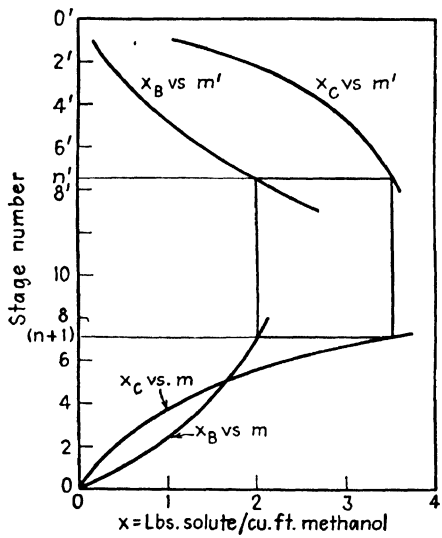



FIG. 7.24. Illustration 7. Matching of stages and concentrations.

ing stage numbers and concentrations show $n' = 7.5$, $n + 1 = 7.1$. The total number of theoretical stages is therefore $n' + n = 7.5 + 6.1 = 13.6$. *Ans.*

The simplifying conditions that (*a*) $A_F = D_F = 0$, (*b*) $\mathbf{m}_B$ and $\mathbf{m}_C$ are constants, and (*c*) solvents $A$ and $D$ initially contain no solute frequently pertain. For such a situation, stages 1′ through $(n' - 1)$ may be considered separately from the remainder of the plant as simply a countercurrent extraction of the type considered in Chap. 6, with $A$ as the extracting solvent and $D$ the solution being extracted. Applying Eq. (6.134), therefore, we obtain for either component

$$\frac{x_{n'} - x_{1'}}{x_{n'} - y_{0'}/\mathbf{m}} = \frac{x_{n'} - x_{1'}}{x_{n'}} = \frac{\left(\frac{\mathbf{m}A}{D}\right)^{n'} - \left(\frac{\mathbf{m}A}{D}\right)}{\left(\frac{\mathbf{m}A}{D}\right)^{n'} - 1} \tag{7.50}$$

$$x_{n'} = x_{1'}\left[\frac{\left(\frac{\mathbf{m}A}{D}\right)^{n'} - 1}{\left(\frac{\mathbf{m}A}{D}\right) - 1}\right] \tag{7.51}$$

Similarly, for stages 1 through $n$, where the extraction is in the opposite direction, Eq. (6.135) may be applied:

$$\frac{y_{n+1} - y_1}{y_{n+1} - \mathbf{m}x_0} = \frac{y_{n+1} - y_1}{y_{n+1}} = \frac{1 - \left(\frac{\mathbf{m}A}{D}\right)^{n}}{1 - \left(\frac{\mathbf{m}A}{D}\right)^{n+1}} \tag{7.52}$$

$$y_{n+1} = y_1\left[\frac{1 - \left(\frac{\mathbf{m}A}{D}\right)^{n+1}}{\left(\frac{\mathbf{m}A}{D}\right)^{n}\left(1 - \frac{\mathbf{m}A}{D}\right)}\right] \tag{7.53}$$

Equations (7.51) and (7.53) are particularly useful in determining the number of stages where $n'$ and $n$ are very large, since they permit calculation of the concentrations near the feed stage without the necessity of obtaining those at intermediate stages. At stage $n'$,

$$y_{n+1} = \mathbf{m}x_{n'} \tag{7.54}$$

and we may substitute Eqs. (7.51) and (7.53):

$$y_1\left[\frac{1 - \left(\frac{\mathbf{m}A}{D}\right)^{n+1}}{\left(\frac{\mathbf{m}A}{D}\right)^{n}\left(1 - \frac{\mathbf{m}A}{D}\right)}\right] = \mathbf{m}x_{1'}\left[\frac{\left(\frac{\mathbf{m}A}{D}\right)^{n'} - 1}{\left(\frac{\mathbf{m}A}{D}\right) - 1}\right] \tag{7.55}$$

Rearranging and multiplying through by $A/D$,

$$\frac{Ay_1}{Dx_{1'}} = \frac{\left[\left(\frac{mA}{D}\right)^{n'} - 1\right]\left(\frac{mA}{D}\right)^{n+1}}{\left(\frac{mA}{D}\right)^{n+1} - 1} = \frac{\mathbf{p}}{1-\mathbf{p}} = \frac{\mathbf{p}}{\mathbf{q}} \tag{7.56}$$

where $\mathbf{p}$ is the fraction of the solute in the feed which passes into the final $A$-rich product, and $\mathbf{q}$ is that which passes into the $D$-rich product. Solving for $\mathbf{p}$,

$$\mathbf{p} = \frac{\left(\frac{mA}{D}\right)^{n'+n+1} - \left(\frac{mA}{D}\right)^{n+1}}{\left(\frac{mA}{D}\right)^{n'+n+1} - 1} \tag{7.57}$$

Bartels and Kleiman (2) present several graphical solutions of Eq. (7.57) for certain values of $n' + n$ and $n'/n$. Unfortunately it cannot be solved directly for $n'$ and $n$; it is most useful when $n'$ and $n$ are known.

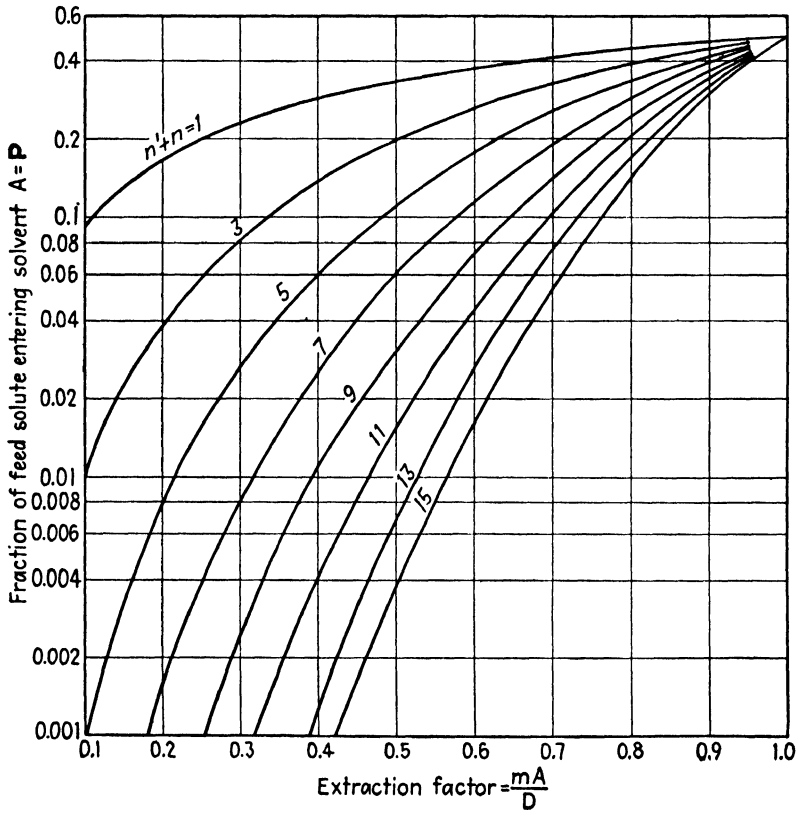



FIG. 7.25. Fractional extraction with central feed ($n' = n + 1$); solvents enter solute-free.

For a symmetrical separation, $\mathbf{p}_B = \mathbf{q}_C$, and it can be shown that, at least for cases where $n' = n + 1$ (central feed), that this will occur if Eqs. (7.35) and (7.36) define the ratio $A/D$. For $n' = n + 1$,

$$\mathbf{p} = \frac{(\mathbf{m}A/D)^{2n'} - (\mathbf{m}A/D)^{n'}}{(\mathbf{m}A/D)^{2n'} - 1} \tag{7.58}$$

a convenient graphical solution for which is shown in Figs. 7.25 and 7.26.

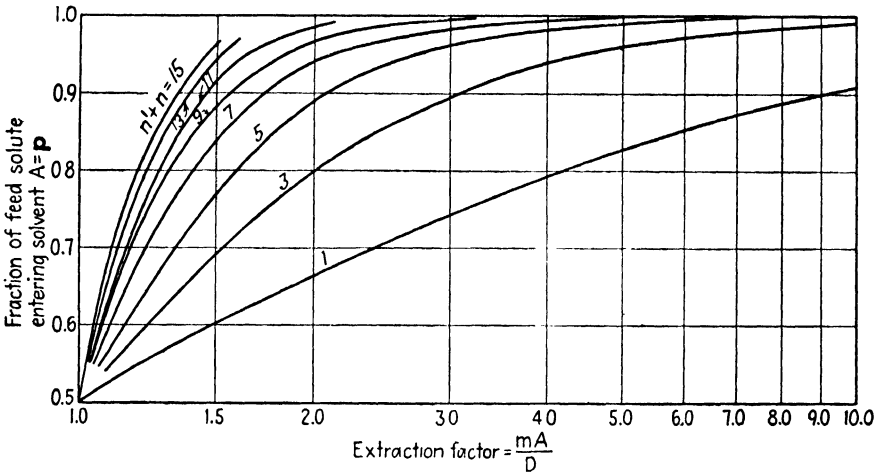



FIG. 7.26. Fractional extraction with central feed ($n' = n + 1$); solvents enter solute-free.

**Illustration 8.** Van Dijck and Schaafsma (18) report on the simultaneous distribution of para ($B$)- and ortho ($C$)-ethoxy aniline between the double solvent 50% aqueous ethanol ($A$), hydrocarbon (50% gasoline, 50% benzene) ($D$). When 20 gm. of mixture is distributed between 100 cu. cm. each of the solvents, $\mathbf{m}_B = 4.85$, $\mathbf{m}_C = 0.74$. Assuming that the distribution coefficients are constant and independent, (*a*) what purity of products will be obtained for a solvent ratio of 1 : 1 by volume for a feed consisting of a 50–50 mixture of the solutes introduced centrally into a five-stage cascade? (*b*) What purity will result for a five-stage cascade where $n' = 2$, $n = 3$? (*c*) What solvent ratio is required for a symmetrical separation?

*Solution.*

*a.* $$\frac{D}{A} = \frac{D'}{A'} = 1, \qquad n' + n = 5$$

Component $B$: $\dfrac{\mathbf{m}_B A}{D} = 4.85$. From Fig. 7.26, $\mathbf{p}_B = 0.99$

Component $C$: $\dfrac{\mathbf{m}_C A}{D} = 0.74$. From Fig. 7.25, $\mathbf{p}_C = 0.103$

Basis: 1 lb. feed = 0.50 lb. $B$, 0.50 lb. $C$.

$A$-rich product: $B = 0.50(0.99) = 0.495$ lb. (90.6%)
$C = 0.50(0.103) = 0.0515$ lb. (9.4%)

$D$-rich product: $B = 0.5 - 0.495 = 0.005$ lb. (1.1%)
$C = 0.5 - 0.0515 = 0.4485$ lb. (98.9%)

*b.* Use Eq. (7.57):

Component $B$:
$$\mathfrak{p}_B = \frac{[(4.85)^6 - (4.85)^4]}{[(4.85)^6 - 1]} = 0.957$$
$$\mathfrak{p}_C = \frac{[(0.74)^6 - (0.74)^4]}{[(0.74)^6 - 1]} = 0.1623$$

In the manner of (*a*), the $A$-rich product contains 0.4785 lb. $B$ (85.5%), 0.0812 lb. $C$ (14.5%); the $D$-rich product 0.0215 lb. $B$ (4.9%), 0.4188 lb. $C$ (95.1%).

*c.* Eq. (7.35):
$$\frac{A}{D} = \sqrt{\frac{1}{\mathfrak{m}_B \mathfrak{m}_C}} = \sqrt{\frac{1}{4.85(0.74)}} = 0.527$$

The number of stages depends upon the per cent recovery and the ratio $n'/(n+1)$. For example, for $n'/(n+1) = 1$, and 97% recovery of $B$, $\mathfrak{m}_B A/D = 4.85(0.527) = 2.56$, and from Fig. 7.26 at $\mathfrak{p}_B = 0.97$, $n' + n = 7$.

**Fractional Extraction with Reflux.** Asselin and Comings (1) describe a process where the $A$-rich solution removed from stage 1 (Fig. 7.18) is split into two streams, one of which is withdrawn as product, while the other is freed of solvent $A$ by evaporation and the solute taken up by solvent $D$ before it enters stage 1 to provide reflux. Similarly, the $D$-rich phase leaving stage 1′ is split into two streams, one of which is the product while the other is freed of solvent by evaporation and the solute taken up by solvent $A$ as it enters stage 1′. At stage 1, let $r$ be the fraction of the $A$-rich phase whose solute is to be returned as reflux. The reflux ratio is then $r/(1-r)$ lb. solute returned per pound solute product. Further,

$$x_{B_0} D = rAy_{B_1}, \qquad x_{C_0} D = rAy_{C_1} \tag{7.59}$$
$$\therefore y_{B_1} = x_{B_0}\left(\frac{D}{rA}\right) \tag{7.60}$$
$$y_{C_1} = x_{C_0}\left(\frac{D}{rA}\right) \tag{7.61}$$

Equation (7.60) is plotted as a broken straight line on Fig. 7.19, the "reflux" line, which passes through the origin and point $(x_{B_0}, y_{B_1})$ and has a slope $D/rA$. Similarly, Eq. (7.61) is a straight line on Fig. 7.20, through the origin and point $(x_{C_0}, y_{C_1})$, of slope $D/rA$.

At stage 1′, if $r'$ is the fraction of the $D$-rich phase which is to provide reflux solute, with a reflux ratio $r'/(1-r')$ lb. solute returned per pound withdrawn, then

$$y_{B_{0'}} A' = r' x_{B_{1'}} D', \qquad y_{C_{0'}} A' = r' x_{C_{1'}} D' \tag{7.62}$$
$$\therefore y_{B_{0'}} = x_{B_{1'}}\left(\frac{r'D'}{A'}\right) \tag{7.63}$$
$$y_{C_{0'}} = x_{C_{1'}}\left(\frac{r'D'}{A'}\right) \tag{7.64}$$

which are reflux lines on Figs. 7.19 and 7.20, through the origins and points $(x_{B_{1'}}, y_{B_{0'}})$ and $(x_{C_{1'}}, y_{C_{0'}})$, respectively, of slope $r'D'/A'$.

The slopes of the reflux lines may be either greater or less than those of the equilibrium curves, and by adjusting the reflux ratios at either end of the cascade it is possible to make stripping or enriching sections of either half of the cascade for either component, $B$ and $C$. Only a detailed study of the equilibria for each system separately can establish the most desirable reflux ratios to be used, or indeed whether reflux is at all desirable.

### Notation for Chapter 7

A symbol representing a solution or mixture denotes not only the composition but also the weight of the solution. Throughout, moles and mole fraction may be substituted for weights and weight fraction.

$A, B, C, D$ = components of a system. In mixed-solvent extraction, $A$ and $B$ are components to be separated, $C$ and $D$ the solvents. In double-solvent extraction, $A$ and $D$ are the solvents, $B$ and $C$ the components to be separated.

$a, b, e, f$, etc. = orthogonal projections of $A$, $B$, $E$, $F$, etc.

$d$ = differential operator.

$E$ = extract.

$F$ = feed mixture.

$M$ = mixture of feed and solvent.

$m$ = A stage in a cascade. Orthogonal projection of $M$.

$m'$ = A stage in a cascade.

$\mathbf{m}$ = distribution coefficient, concentration in $A$-rich soln./concentration in $D$-rich soln. at equilibrium.

$n$ = number of portions into which solvent is divided, in batchwise double-solvent extraction.

= number of stages in part of a cascade for continuous double-solvent extraction.

$n'$ = number of stages in part of a cascade for continuous double-solvent extraction.

$p$ = fraction of the feed solute passing to the $A$-rich solution in a single contact.

$\mathbf{p}$ = same as $p$, but after several extractions.

$q$ = fraction of the feed solute passing to the $D$-rich solution in a single contact.

$\mathbf{q}$ = same as $q$, but after several extractions.

$R$ = raffinate.

$r, r'$ = fraction of solute returned as reflux, in fractional extraction.

$S$ = solvent.

$X$ = concentration, weight fraction.

$x$ = concentration, lb. solute/lb. solvent $D$.

$y$ = concentration, lb. solute/lb. solvent $A$.

$\beta$ = selectivity = $\mathbf{m}_B/\mathbf{m}_C$.

Subscripts:

$A, B, C, D$ = components $A$, $B$, $C$, $D$.

$BM$ = component $B$ in solution $M$.

$CA$ = component $C$ in an $A$-rich solution.

$E$ = extract.

$F$ = feed.

$R$ = raffinate.

$S$ = solvent.

1, 2, 2′, etc. = stages 1, 2, 2′, etc.

## LITERATURE CITED


1. Asselin, G. F., and E. W. Comings: *Ind. Eng. Chem.* **42,** 1198 (1950).
2. Bartels, C. R., and G. Kleiman: *Chem. Eng. Progress* **45,** 589 (1949).
3. Bush, M. T., and P. M. Densen: *Anal. Chem.* **20,** 121 (1948).
4. Cornish, R. E., R. C. Archibald, E. A. Murphy, and H. M. Evans: *Ind. Eng. Chem.* **26,** 397 (1934).
5. Craig, L. C.: *J. Biol. Chem.* **155,** 519 (1944).
6. ———: *Anal. Chem.* **21,** 85 (1949).
7. ———, C. Golumbic, H. Mighton, and E. Titus: *J. Biol. Chem.* **161,** 321 (1945).
8. ——— and O. Post: *Anal. Chem.* **21,** 500 (1949).
9. Garwin, L., and A. N. Hixson: *Ind. Eng. Chem.* **41,** 2303 (1949).
10. Hunter, T. G.: *Ind. Eng. Chem.* **34,** 963 (1942).
11. ——— and A. W. Nash: *Ind. Eng. Chem.* **27,** 836 (1935).
12. Jantzen, E.: "Das fraktionierte Destillieren und das fraktionierte Verteilen," Dechema Monograph Vol. 5, No. 48, Berlin, Verlag Chemie, 1932.
13. Martin, A. J. P., and R. L. M. Synge: *Biochem. J.* **35,** 91 (1941).
14. McKee, R. H.: *Ind. Eng. Chem.* **38,** 382 (1946).
15. Scheibel, E. G.: *Chem. Eng. Progress* **44,** 681, 771 (1948).
16. Smith, J. C.: *Ind. Eng. Chem.* **36,** 68 (1944).
17. Van Dijck, W. J. D.: U.S. Pat. 2, 107, 681 (2/8/38).
18. ——— and A. Schaafsma: U.S. Pat. 2, 245, 945 (6/17/41).
19. Wiegand, J. H.: *Ind. Eng. Chem., Anal. Ed.* **15,** 380 (1943).
20. Williamson, B., and L. C. Craig: *J. Biol. Chem.* **168,** 687 (1947).

# CHAPTER 8

## METHODS OF CALCULATION III. CONTINUOUS COUNTERCURRENT CONTACT

Instead of bringing the solution to be extracted and the extracting solvent into contact in separate stages with intermediate settling, as considered in the two preceding chapters, it is also possible to cause them to flow countercurrently through a vessel, usually a vertical tower, by virtue of their difference in specific gravities. Thus, the solution to be extracted may flow downward, if it is the more dense of the two phases, through an empty tower, filling it completely, while the lighter solvent may be dispersed in the form of a spray at the bottom, the drops rising through the downward flowing raffinate, to be withdrawn at the top. Either phase may be made the dispersed phase. Alternatively, various filling materials, such as packing similar to that used in gas absorption and distillation processes, baffles, and perforated trays, may be installed in the tower to increase the turbulence and otherwise affect the flow characteristics. Operation is necessarily continuous, and at the same time the two immiscible phases are in continuous contact throughout the length of the apparatus. The cross-sectional area of devices of this sort depends upon the quantities of the phases flowing through it. Their height, on the other hand, directly influences the extent of extraction occurring, and it is with this that we are presently concerned.

**Height Equivalent to a Theoretical Stage.** The most obvious method for designing continuous contactors of the type described parallels a simple procedure introduced many years ago for absorption and distillation processes. This involves calculation of the number of ideal or theoretical stages $n$ required to bring about a given extraction by the methods of the previous chapters, and multiplication of $n$ by a factor, the height equivalent to a theoretical stage, H.E.T.S., determined from previous experiment with the system. Thus,

$$H = n(\text{H.E.T.S.}) \tag{8.1}$$

where $H$ is the height of the tower. Previous experience in the case of gas absorption and distillation has proven that fundamentally this method is unsound, since it applies a procedure involving stepwise changes in concentration to an operation where the concentration actually changes differentially with height. As a result, H.E.T.S. is found to vary widely

with such important operating conditions as type of system, rates of flow, and concentration, as well as type of tower used, thus making it necessary to have at hand very specific H.E.T.S. data for the contemplated design. Theoretically, at least, the methods to be described below alleviate this situation considerably, at the expense of a slightly more complex design procedure. Practically, until more experimental information is made available for the application of the preferred methods, the design procedure indicated by Eq. (8.1) is as good as any and is used extensively in practice.

## THE TRANSFER UNIT

**Individual-film Transfer Units.** Consider the extraction tower of Fig. 8.1, where raffinate and extract phases are flowing countercurrently. The raffinate phase, or solution to be extracted, enters at a rate $R_1$ moles/hr. with a concentration of distributed solute $x_{R_1}$ mole fraction, and leaves at a rate $R_2$ with a concentration $x_{R_2}$. $R_2$ is less than $R_1$ by the extent of extraction. Similarly, the extracting solvent forming the extract phase enters at a rate $E_2$ moles/hr., undergoes a concentration change $x_{E_2}$ to $x_{E_1}$, and leaves at a rate $E_1$. Alternatively, concentrations in either phase may be expressed as weight fractions $X$, or pound moles per cubic foot of solution $c$. The cross-sectional area of the tower is $S$ sq. ft., and the total interfacial surface between the phases $A$ sq. ft. Per unit volume of tower, the exposed interfacial surface is $a$ sq. ft./cu. ft. At some position in the tower where raffinate and extract rates are $R$ and $E$, a differential change in concentration of these streams occurs over a differential height $dH$. This change in concentration results from the diffusion of distributed solute from phase $R$ to phase $E$ because of the concentration gradients discussed in detail in Chap. 5. If $N$ is the total transfer of solute, moles per hour, then the rate of transfer for the differential section can be described by application of Eq. (5.53) to the situation at hand (1, 3).

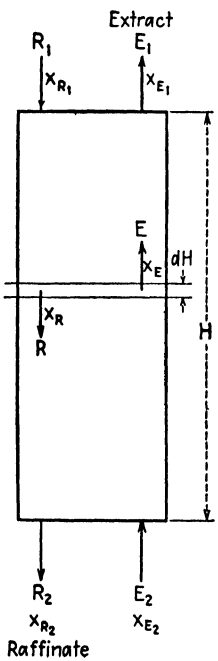



FIG. 8.1. Extraction with continuous countercurrent contact.

$$dN = d(Rx_R) = k_R\, dA c_{RM}(x_R - x_{Ri}) \qquad (8.2)$$

where $c_{RM}$ is the average of the values $c_R$ and $c_{Ri}$. Use of this equation limits the resulting relationships to cases where solvents are completely immiscible or to relatively dilute solutions, since the diffusion upon which Eq. (5.53) is based includes only that of the dissolved solute and not those of the solvents. For lack of anything better, the equations are nevertheless applied to all situations.

The total raffinate rate $R$ varies from one end of the tower to the other, but the solute-free raffinate, $R(1 - x_R)$, remains constant. Consequently,

$$d(Rx_R) = R(1 - x_R)d\left(\frac{x_R}{1 - x_R}\right) = \frac{Rdx_R}{1 - x_R} \tag{8.3}$$

The mass transfer coefficient $k_R$ includes a term $(1 - x_R)_{iM}$ which varies throughout the tower [Eq. (5.52*a*)]. The quantity $k_R(1 - x_R)_{iM}$ is more likely to be constant. In addition, $dA = aSdH$. Eq. (8.2) may thus be modified,

$$\frac{(1 - x_R)_{iM}Rdx_R}{(1 - x_R)} = k_Ra(1 - x_R)_{iM}Sc_{RM}(x_R - x_{Ri})dH \tag{8.4}$$

$$\frac{(1 - x_R)_{iM}dx_R}{(1 - x_R)(x_R - x_{Ri})} = \frac{k_Ra(1 - x_R)_{iM}Sc_{RM}dH}{R} \tag{8.5}$$

Since the terms $(1 - x_R)_{iM}$ and $(1 - x_R)$ are usually nearly unity, the left-hand portion of Eq. (8.5) is essentially the concentration change $dx_R$ experienced per unit of concentration difference $(x_R - x_{Ri})$ causing the change, and represents a measure of the difficulty of the extraction. This in turn is designated as $N_t$, the number of transfer units, which when multiplied by the experimentally determined factor $HTU$, the height per transfer unit, gives the height of the tower. Thus,

$$N_{t_R} = \int_{x_{R_2}}^{x_{R_1}} \frac{(1 - x_R)_{iM}dx_R}{(1 - x_R)(x_R - x_{Ri})} = \int_0^H \frac{dH}{HTU_R} = \frac{H}{HTU_R} \tag{8.6}$$

Consideration of Eqs. (8.5) and (8.6) shows that $HTU_R$ and the mass-transfer coefficient are related:

$$HTU_R = \frac{R}{k_Ra(1 - x_R)_{iM}c_{R_{av}}S} \tag{8.7}$$

In similar fashion, the concentration differences in terms of the extract phase might have been used [Eq. (5.53)], which would have resulted in

$$N_{t_E} = \int_{x_{E_2}}^{x_{E_1}} \frac{(1 - x_E)_{iM}dx_E}{(1 - x_E)(x_{Ei} - x_E)} = \int_0^H \frac{dH}{HTU_E} = \frac{H}{HTU_E} \tag{8.8}$$

$$HTU_E = \frac{E}{k_Ea(1 - x_E)_{iM}c_{E_{av}}S} \tag{8.9}$$

**Over-all Transfer Units.** As explained in Chap. 5, the practical difficulties entering into the use of true equilibrium interfacial concentrations $x_{Ei}$ and $x_{Ri}$ have led to the introduction of over-all mass-transfer coefficients $K_E$ and $K_R$, which express the rate of diffusion in terms of over-all concentration gradients $(x_R - x_R^*)$ and $(x_E^* - x_E)$ [Eqs. (5.57) and (5.59)]. Their use requires that the distribution coefficient,

$$m = \frac{x_{Ei}}{x_{Ri}} = \frac{x_E^*}{x_R} = \frac{x_E}{x_R^*} \tag{8.10}$$

be truly constant over the range of concentrations encountered in the design. This is a serious restriction, and in practice the equations based on the over-all concentration gradients are usually used regardless of the constancy of $m$. Applying Eqs. (5.57) and (5.59) to the present situation, we obtain

$$N_{t_{OR}} = \int_{x_{R_2}}^{x_{R_1}} \frac{(1 - x_R)_{OM}\, dx_R}{(1 - x_R)(x_R - x_R^*)} = \int_{x_{R_2}}^{x_{R_1}} \frac{dx_R}{(1 - x_R) \ln \dfrac{(1 - x_R^*)}{(1 - x_R)}} = \frac{H}{HTU_{OR}} \tag{8.11}$$

$$HTU_{OR} = \frac{R}{K_R a (1 - x_R)_{OM} c_{R_{av}} S} \tag{8.12}$$

and

$$N_{t_{OE}} = \int_{x_{E_2}}^{x_{E_1}} \frac{(1 - x_E)_{OM}\, dx_E}{(1 - x_E)(x_E^* - x_E)} = \int_{x_{E_2}}^{x_{E_1}} \frac{dx_E}{(1 - x_E) \ln \dfrac{(1 - x_E)}{(1 - x_E^*)}} = \frac{H}{HTU_{OE}} \tag{8.13}$$

$$HTU_{OE} = \frac{E}{K_E a (1 - x_E)_{OM} c_{E_{av}} S} \tag{8.14}$$

These equations are then used for design, Eq. (8.11) in cases where the principal diffusional resistance lies in the $R$ phase ($m$ large), Eq. (8.12) in cases where the principal diffusional resistance lies in the $E$ phase ($m$ small).

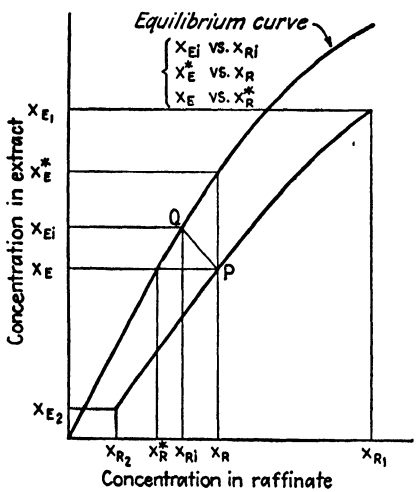



FIG. 8.2. Operating diagram for continuous countercurrent extraction.

To determine the value of $N_{t_{OR}}$ or $N_{t_{OE}}$, graphical integration of the respective expressions is ordinarily required, for which in turn operating diagrams of the sort described in Chap. 6 are prerequisite. Refer to Fig. 8.2 where there is shown an operating diagram, including an equilibrium curve and operating line, directions for obtaining which have previously been described. For any point $P$ on the operating line, the vertical distance to the equilibrium curve gives the over-all concentration difference $(x_E^* - x_E)$, while the horizontal distance gives $(x_R - x_R^*)$. To evaluate $N_{t_{OR}}$, either the quantity $\dfrac{(1 - x_R)_{OM}}{(1 - x_R)(x_R - x_R^*)}$ or the quantity $\dfrac{1}{(1 - x_R) \ln \dfrac{(1 - x_R^*)}{(1 - x_R)}}$

is calculated for as many points on the operating line as required to give a smooth curve when plotted against $x_R$. The area under the resulting curve between the limits $x_{R_1}$ and $x_{R_2}$ is the required value. $N_{t_{OE}}$ may be obtained in a similar manner. Equations (8.6) and (8.8) could be evaluated in the same fashion also, if the position of points corresponding to $Q$ could be located.

**Simplified Graphical Integration.** Considerable effort has been put into the problems of reducing the tedium of the graphical integration for $N_{t_{OR}}$ and $N_{t_{OE}}$. Thus, if $(1 - x_R^*)$ and $(1 - x_R)$ differ by no more than a factor of 2, an arithmetic average rather than a logarithmic average for $(1 - x_R)_{OM}$ incurs an error of 1.5 per cent at the most (8). Thus,

$$(1 - x_R)_{OM} = \frac{(1 - x_R^*) + (1 - x_R)}{2} \tag{8.15}$$

and substitution in Eq. (8.11) leads to

$$N_{t_{OR}} = \int_{x_{R_2}}^{x_{R_1}} \frac{dx_R}{x_R - x_R^*} + \tfrac{1}{2} \ln \frac{1 - x_{R_2}}{1 - x_{R_1}} \tag{8.16}$$

Similarly,

$$N_{t_{OE}} = \int_{x_{E_2}}^{x_{E_1}} \frac{dx_E}{x_E^* - x_E} + \tfrac{1}{2} \ln \frac{1 - x_{E_2}}{1 - x_{E_1}} \tag{8.17}$$

and graphical integration is made of a curve of $1/(x_R - x_R^*)$ vs. $x_R$ for $N_{t_{OR}}$. Weight fractions are usually more convenient than mole fractions, since the triangular equilibrium diagrams from which the operating diagrams are plotted use this unit most frequently. Thus,

$$x = \frac{rX}{rX + 1 - X} \tag{8.18}$$

where $r$ is the ratio of molecular weights of nonsolute to solute. Substitution in Eqs. (8.11) and (8.13) leads to results which are too awkward to use directly, but if the arithmetic rather than logarithmic average is used for $(1 - X)_{OM}$, there is obtained (2)

$$N_{t_{OR}} = \int_{X_{R_2}}^{X_{R_1}} \frac{dX_R}{X - X_R^*} + \frac{1}{2} \ln \frac{1 - X_{R_2}}{1 - X_{R_1}} + \frac{1}{2} \ln \frac{X_{R_2}(r-1) + 1}{X_{R_1}(r-1) + 1} \tag{8.19}$$

and

$$N_{t_{OE}} = \int_{X_{E_2}}^{X_{E_1}} \frac{dX_E}{X_E^* - X_E} + \frac{1}{2} \ln \frac{1 - X_{E_2}}{1 - X_{E_1}} + \frac{1}{2} \ln \frac{X_{E_2}(r-1) + 1}{X_{E_1}(r-1) + 1} \tag{8.20}$$

Weight ratios, $w = X/(1 - X)$, are sometimes convenient since the operating line on the operating diagram is then frequently a straight line. Substitution in Eqs. (8.11) and (8.13) leads to (2)

$$N_{t_{OR}} = \int_{W_{R_2}}^{W_{R_1}} \frac{(1 + rw_R)_{OM}\, dw_R}{(1 + rw_R)(w_R - w_R^*)} = \int_{W_{R_2}}^{W_{R_1}} \frac{dw_R}{w_R - w_R^*} + \tfrac{1}{2} \ln \frac{1 + rw_{R_2}}{1 + rw_{R_1}} \tag{8.21}$$

and

$$N_{t_{OE}} = \int_{W_{E_2}}^{W_{E_1}} \frac{(1 + rw_E)_{OM}\, dw_E}{(1 + rw_E)(w_E^* - w_E)} = \int_{W_{E_2}}^{W_{E_1}} \frac{dw_E}{w_E^* - w_E} + \tfrac{1}{2} \ln \frac{1 + rw_{E_2}}{1 + rw_{E_1}} \quad (8.22)$$

where the right-hand parts of the preceding equations include an approximation equivalent to that of Eq. (8.15). Mole-ratio-concentration units lead to equations identical with Eqs. (8.21) and (8.22) with the exception that $r$ is omitted.

Further simplification can be introduced by evaluation of the integrals of Eqs. (8.16) to (8.22) formally rather than graphically. This can be accomplished with more or less precision depending on the validity of the assumptions necessary to permit formal integration. The various conditions and the results may be outlined as follows:

**1. Dilute Solutions, $m$ Constant** (1, 2, 3). For dilute solutions, $(1 - x_R)$ and $(1 - x_E)$ are nearly unity, and $R$ and $E$ are substantially constant. A material balance over the lower portion of the tower of Fig. 8.1 then becomes approximately

$$R(x_R - x_{R_2}) = E(x_E - x_{E_2}) \quad (8.23)$$

Substitution of $mx_R^*$ for $x_E$ and rearrangement leads to

$$x_R^* = \frac{R}{mE}(x_R - x_{R_2}) + \frac{x_{E_2}}{m} \quad (8.24)$$

This may be substituted in the integral of Eq. (8.16), and the integral evaluated:

$$\int_{x_{R_2}}^{x_{R_1}} \frac{dx_R}{x_R - x_R^*} = \frac{1}{1 - \dfrac{R}{mE}} \ln \left[ \left(1 - \frac{R}{mE}\right) \left( \frac{x_{R_1} - \dfrac{x_{E_2}}{m}}{x_{R_2} - \dfrac{x_{E_2}}{m}} \right) + \frac{R}{mE} \right] \quad (8.25)$$

In a similar manner,

$$\int_{x_{E_2}}^{x_{E_1}} \frac{dx_E}{x_E^* - x_E} = \frac{1}{1 - \dfrac{mE}{R}} \ln \left[ \left(1 - \frac{mE}{R}\right) \left( \frac{x_{E_1} - mx_{R_2}}{x_{E_2} - mx_{R_2}} \right) + \frac{mE}{R} \right] \quad (8.26)$$

Since in practice there are always slight variations in $m$, $E$, and $R$, somewhat more precise results are obtained by using values of these quantities at the dilute end of the system ($m_2$, $E_2$, and $R_2$), since the transfer units are ordinarily concentrated at this end. Equations (8.25) and (8.26) may also be used for the integrals of Eqs. (8.19) and (8.20) provided that $X$ is substituted for $x$, $m$ is defined in terms of $X$, and $E$ and $R$ are expressed in weights per unit time; they may be used for the integrals of Eqs. (8.21) and (8.22) if $w$ is substituted for $x$, $m$ is defined in terms of $w$, and $E$ and $R$ are the weights of the solute-free streams per unit time. A convenient graphical solution is provided in Fig. 8.3.

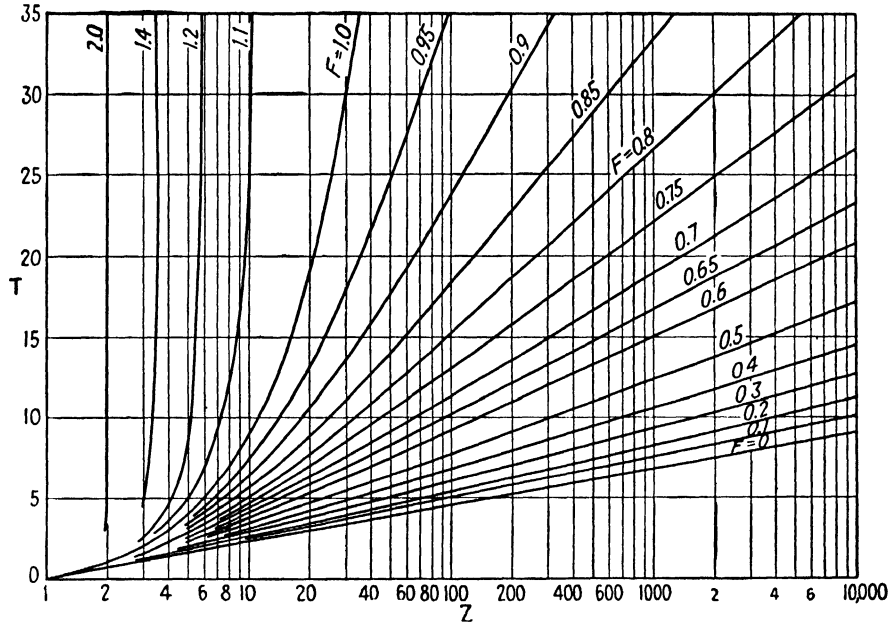



FIG. 8.3. Integration of transfer unit equations. (*With Permission of American Institute of Chemical Engineers*)

| $Z$ | $F$ | $T$ |
|---|---|---|
| $\dfrac{x_{R_1} - (x_{E_2}/m)}{x_{R_2} - (x_{E_2}/m)}$ | $\dfrac{R}{mE}$ | $\displaystyle\int_{x_{R_2}}^{x_{R_1}} \frac{dx_R}{x_R - x_R^*}$ |
| $\left(\dfrac{x_{R_1} - \dfrac{x_{E_2}}{m}}{x_{R_2} - \dfrac{x_{E_2}}{m}}\right)\left(\dfrac{1 - \dfrac{R_2}{m_2E_2}}{1 - \dfrac{x_{R_1}^*}{x_{R_1}}}\right)$ | $\dfrac{R_2}{m_2E_2}$ | |
| $\dfrac{x_{E_1} - mx_{R_2}}{x_{E_2} - mx_{R_2}}$ | $\dfrac{mE}{R}$ | $\displaystyle\int_{x_{E_2}}^{x_{E_1}} \frac{dx_E}{x_E^* - x_E}$ |
| $\left(\dfrac{x_{E_1} - m_2x_{R_2}}{x_{E_2} - m_2x_{R_2}}\right)\left(\dfrac{1 - \dfrac{m_2E_2}{R_2}}{1 - \dfrac{x_{E_1}^*}{x_{E_1}}}\right)$ | $\dfrac{m_2E_2}{R_2}$ | |

**2. More Concentrated Solutions, $m$ = Constant for Dilute Solutions.** Colburn (2) has assumed (*a*) that $m$ may be constant for dilute solutions, whereupon $(x_E^* - x_E)$, for example, is a linear function of $(mx_R - x_E)$, and (*b*) that for more concentrated solutions $(x_E^* - x_E)$ is a function of $(mx_R - x_E)$.[2] By dividing the total extraction into two parts, when each assumption is likely to apply separately, and combining the results, he was able to obtain the following approximations:

$$\int_{x_{R_2}}^{x_{R_1}} \frac{dx_R}{x_R - x_R^*}$$

$$= \frac{1}{1 - \dfrac{R_2}{m_2E_2}} \ln\left[\left(1 - \frac{R_2}{m_2E_2}\right)\left(\frac{x_{R_1} - \dfrac{x_{E_2}}{m_2}}{x_{R_2} - \dfrac{x_{E_2}}{m_2}}\right)\left(\frac{1 - \dfrac{R_2}{m_2E_2}}{1 - \dfrac{x_{R_1}^*}{x_{R_1}}}\right) + \frac{R_2}{m_2E_2}\right] \tag{8.27}$$

$$\int_{x_{E_2}}^{x_{E_1}} \frac{dx_E}{x_E^* - x_E}$$

$$= \frac{1}{1 - \dfrac{m_2E_2}{R_2}} \ln\left[\left(1 - \frac{m_2E_2}{R_2}\right)\left(\frac{x_{E_1} - m_2x_{R_2}}{x_{E_2} - m_2x_{R_2}}\right)\left(\frac{1 - \dfrac{m_2E_2}{R_2}}{1 - \dfrac{x_{E_1}^*}{x_{E_1}}}\right) + \frac{m_2E_2}{R_2}\right] \tag{8.28}$$

Equations (8.27) and (8.28) may be used as well for the integrals of Eqs. (8.19) to (8.22) by substitution of the proper units, as explained in (1) above. The graphical solution of Fig. 8.3 is also applicable. The equations are satisfactory only for cases where the number of transfer units is large (where the value of the abscissa of Fig. 8.3 exceeds approximately 120) and where $R_2/m_2E_2$ [in the case of Eq. (8.27)] or $m_2E_2/R_2$ [in the case of Eq. (8.28)] do not exceed approximately 0.75.

**3. More Concentrated Solutions, $m$ Varies Linearly with $x_R$.** Scheibel and Othmer (5) have evaluated the integrals for this case, and show the results to be applicable to a wide variety of siutations. Their results may be expressed as follows:

$$\int_{x_{R_2}}^{x_{R_1}} \frac{dx_R}{x_R - x_R^*} = \frac{x_{R_1} - x_{R_2}}{s} \ln \frac{u + s}{u - s} \quad \text{if } s^2 \text{ is positive} \tag{8.29a}$$

$$= \frac{x_{R_1} - x_{R_2}}{s} \ln \frac{x_{R_1} - m_2'x_{E_1} + v}{x_{R_2} - m_1'x_{E_2} - v} \quad \text{if } u \text{ nearly equals } s,\ s^2 \text{ positive} \tag{8.29b}$$

$$= \frac{2(x_{R_1} - x_{R_2})}{s'} \tan^{-1} \frac{s'}{u} \quad \text{if } s^2 \text{ is negative} \tag{8.29c}$$

$$\int_{x_{E_2}}^{x_{E_1}} \frac{dx_E}{x_E^* - x_E} = \frac{x_{E_1} - x_{E_2}}{s''} \ln \frac{u' + s''}{u' - s''} \quad \text{if } s''^2 \text{ is positive} \tag{8.30a}$$

$$= \frac{x_{E_1} - x_{E_2}}{s'''} \ln \frac{m_2x_{R_1} - x_{E_1} + v'}{m_1x_{R_2} - x_{E_2} - v'} \quad \text{if } u' \text{ nearly equals } s'',\ s''^2 \text{ positive} \tag{8.30b}$$

$$= \frac{2(x_{E_1} - x_{E_2})}{s'''} \tan^{-1} \frac{s'''}{u'} \quad \text{if } s''^2 \text{ is negative} \tag{8.30c}$$

where $s = \sqrt{(x_{R_1} - x_{R_2} + m_1'x_{E_2} - m_2'x_{E_1})^2 + 4(x_{E_1}x_{R_2} - x_{E_2}x_{R_1})(m_1' - m_2')}$

$s' = \sqrt{4(x_{E_2}x_{R_1} - x_{E_1}x_{R_2})(m_1' - m_2') - (x_{R_1} - x_{R_2} + m_1'x_{E_2} - m_2'x_{E_1})^2}$

$s'' = \sqrt{(x_{E_1} - x_{E_2} + m_1x_{R_2} - m_2x_{R_1})^2 + 4(x_{R_1}x_{E_2} - x_{R_2}x_{E_1})(m_1 - m_2)}$

$s''' = \sqrt{4(x_{R_2}x_{E_1} - x_{R_1}x_{E_2})(m_1 - m_2) - (x_{E_1} - x_{E_2} + m_1x_{R_2} - m_2x_{R_1})^2}$

$$u = x_{R_1} + x_{R_2} - m_2'x_{E_1} - m_1'x_{E_2}$$
$$u' = m_1x_{R_2} + m_2x_{R_1} - x_{E_1} - x_{E_2}$$
$$v = \frac{(x_{E_1}x_{R_2} - x_{E_2}x_{R_1})(m_1' - m_2')}{x_{R_1} - x_{R_2} - m_2'x_{E_1} + m_1'x_{E_2}}$$
$$v' = \frac{(x_{R_1}x_{E_2} - x_{E_2}x_{R_1})(m_1 - m_2)}{m_2x_{R_1} - m_1x_{R_2} - x_{E_1} + x_{E_2}}$$

and for the purposes of these equations,

$$m_1 = \frac{x_{E_1}^*}{x_{R_1}}, \qquad m_2 = \frac{x_{E_2}^*}{x_{R_2}}, \qquad m_1' = \frac{x_{R_1}^*}{x_{E_1}}, \qquad m_2' = \frac{x_{R_2}^*}{x_{E_2}}$$

For cases where equilibrium curve and operating line are very close at the dilute end of the column, with a concentration of transfer units at the end, $m_2$ should be the true slope of the equilibrium curve at $x_{R_2}$, and $m_2'$ that of the reciprocal of the slope at $x_{E_2}$. Other corrections for handling cases of more complicated curvature of equilibrium and operating lines are discussed in detail by Scheibel and Othmer (5). Graphical solutions of Eqs. (8.29) and (8.30) are available (5, 6), and the equations may be applied to the integrals of Eqs. (8.19) to (8.22) by the substitution of the proper units, as outlined in (1) above.

The formal integrations just discussed will be more successful if that for $N_{t_{OR}}$ is used in the case of countercurrent extraction without reflux. If reflux is used, $N_{t_{OR}}$ should be calculated for the stripping section, $N_{t_{OE}}$ for the enriching section.

## MASS-TRANSFER COEFFICIENTS

The mass-transfer coefficients can be used directly for design, without resort to the $HTU$, if desired, by integration of their defining equations. Thus, adapting Eq. (5.59) to the present situation, we have

$$dN = K_RaS(c_R - c_R^*)dH = K_RaSc_{RM}(x_R - x_R^*) \tag{8.31}$$

where the over-all coefficient is defined as $K_Ra$, the $a$-term being ordinarily incapable of separate evaluation.

$$dH = \frac{dN}{K_RaS(c_R - c_R^*)} = \frac{dN}{K_RaSc_{RM}(x_R - x_R^*)} \tag{8.32}$$

But

$$dN = d(Rx_R) = \frac{Rdx_R}{1 - x_R} \tag{8.3}$$

and

$$dN = d\left(\frac{RM_Rc_R}{\rho_R}\right) \tag{8.33}$$

Therefore

$$H = \int_0^H dH = \int_{c_{R_2}}^{c_{R_1}} \frac{d\left(\frac{RM_R c_R}{\rho_R}\right)}{K_R a S(c_R - c_R^*)} \tag{8.34}$$

$$= \int_{x_{R_2}}^{x_{R_1}} \frac{R dx_R}{K_R a S c_{RM}(1 - x_R)(x_R - x_R^*)} \tag{8.35}$$

Thus, the height $H$ may be evaluated by graphical integration either of a plot of $1/[K_R a S(c_R - c_R^*)]$ against $RM_R c_R/\rho_R$, or one of

$$\frac{R}{K_R a S c_{RM}(1 - x_R)(x_R - x_R^*)}$$

against $x_R$, in both cases obtaining the necessary data from operating diagrams in the appropriate concentration units. If the solutions are moderately dilute, the integrals may be conveniently simplified to

$$H = \frac{RM_R}{\rho_R S} \int_{c_{R_2}}^{c_{R_1}} \frac{dc_R}{K_R a(c_R - c_R^*)} = \frac{R}{S c_{R_{av}}} \int_{x_{R_2}}^{x_{R_1}} \frac{dx_R}{K_R a(x - x_R^*)} \tag{8.36}$$

to be used with average values of $R$, $M_R$, and $\rho_R$. Similarly, in terms of $K_E a$,

$$H = \int_{c_{E_2}}^{c_{E_1}} \frac{d(EM_E c_E/\rho_E)}{K_E a S(c_E^* - c_E)} = \frac{EM_E}{\rho_E S} \int_{c_{E_2}}^{c_{E_1}} \frac{dc_E}{K_E a(c_E^* - c_E)} \tag{8.37}$$

and

$$H = \int_{x_{E_2}}^{x_{E_1}} \frac{E dx_E}{K_E a S c_{EM}(1 - x_E)(x_E^* - x_E)} = \frac{E}{S c_{E_{av}}} \int_{x_{E_2}}^{x_{E_1}} \frac{dx_E}{K_E a(x_E^* - x_E)} \tag{8.38}$$

The equations may be written also for the individual-film mass-transfer coefficients $k_R a$ and $k_E a$, using individual-film concentration gradients.

If the solutions are very dilute and the distribution coefficient and mass-transfer coefficients may be considered constant, formal integration of the equations may be carried out as in the case of transfer units. For such a situation,

$$H = \frac{R}{S c_{R_{av}} K_R a} \int_{x_{R_2}}^{x_{R_1}} \frac{dx_R}{x - x_R^*} \tag{8.39}$$

Combining with Eq. (8.24), integrating, and combining the result with a total material balance, there is obtained

$$N = K_R a S H c_{R_{av}}(x_R - x_R^*)_{av} \tag{8.40}$$

where

$$(x_R - x_R^*)_{av} = \frac{(x_{R_1} - x_{R_1}^*) - (x_{R_2} - x_{R_2}^*)}{\ln[(x_{R_1} - x_{R_1}^*)/(x_{R_2} - x_{R_2}^*)]} \tag{8.41}$$

The detailed derivation has been presented many times previously (4, 7). Similarly,

$$\begin{aligned} N &= K_E a S H c_{E_{av}}(x_E^* - x_E)_{av} = K_E a S H(c_E^* - c_E)_{av} \\ &= K_R a S H(c_R - c_R^*)_{av} \end{aligned} \tag{8.42}$$

### OVER-ALL AND INDIVIDUAL-FILM DIFFUSIONAL RESISTANCES

It is useful to establish the relationship between the over-all diffusional resistances generally used in design and those of the individual films. We have already seen the relationship in terms of mass-transfer coefficients in Chap. 5, and Eq. (5.62), adapted to the use of mole-fraction units for $m$, becomes

$$\frac{1}{K_R a} = \frac{1}{k_R a} + \frac{c_{R_{av}}}{m k_E a c_{E_{av}}} \tag{8.43}$$

Multiplying through by $R/[S(1 - x_R)_{OM} c_{R_{av}}]$, each term contains the essentials of the definitions of the various $HTU$'s, and we obtain (3)

$$HTU_{OR} = HTU_R \frac{(1 - x_R)_{iM}}{(1 - x_R)_{OM}} + \left(\frac{R}{mE}\right) HTU_E \frac{(1 - x_E)_{iM}}{(1 - x_R)_{OM}} \tag{8.44}$$

In the special case that the principal diffusional resistance lies in the $R$ phase, $(1 - x_R)_{iM} = (1 - x_R)_{OM}$, and $(1 - x_E)_{iM} = (1 - x_E)$. Equation (8.44) becomes

$$HTU_{OR} = HTU_R + \left(\frac{R}{mE}\right) HTU_E \frac{(1 - x_E)}{(1 - x_R)_{OM}} \tag{8.45}$$

If in addition the solutions are dilute,

$$HTU_{OR} = HTU_R + \left(\frac{R}{mE}\right) HTU_E \tag{8.46}$$

By a similar process, we can arrive at

$$HTU_{OE} = HTU_E + \left(\frac{mE}{R}\right) HTU_R \tag{8.47}$$

for dilute solutions, and the principal resistance in the $E$ phase. These equations are useful, particularly in experimental work, in indicating the controlling importance the group $mE/R$, the extraction factor, has in establishing the location of the principal resistance. Although $HTU_E$ and $HTU_R$ are not constant with varying rates of flow, if we assume that they are of the same order of magnitude, increasing the size of the extraction factor places the principal diffusional resistance in the $R$ phase, while decreasing its size places the principal resistance in the $E$ phase.

The extraction factor, which is essentially the ratio of the slope of the equilibrium curve to that of the operating line, has additional economic significance in establishing the conditions of design. We have seen (Chap. 6) that for a countercurrent extraction, a value of $mE/R$ less than unity definitely limits the extent of extraction even with an infinite number of stages or transfer units. For reduction of the concentration of the solute in the final raffinate to a low value, $mE/R$ must exceed unity. From Fig. 8.3, it is clear that the greater the value of $mE/R$, the fewer will be the number of transfer units required for a given degree of extraction, with con-

sequently lesser costs for the extraction equipment. On the other hand, most extraction operations must be followed by solvent-recovery processes, and with large values of $mE/R$ the extract solution becomes very dilute and solvent recovery is costly. It follows that there will be an optimum value of $mE/R$ for any process, dependent upon the value of the solute being extracted and a variety of other costs, but very likely in the neighborhood of 1.5 to 2.0 (1). Unfortunately for the designer, this is in the range of extraction factors where both film resistances are of importance and the use of over-all $HTU$'s or mass-transfer coefficients under these conditions, without true constancy of $m$ or the individual film resistances, becomes the more risky.

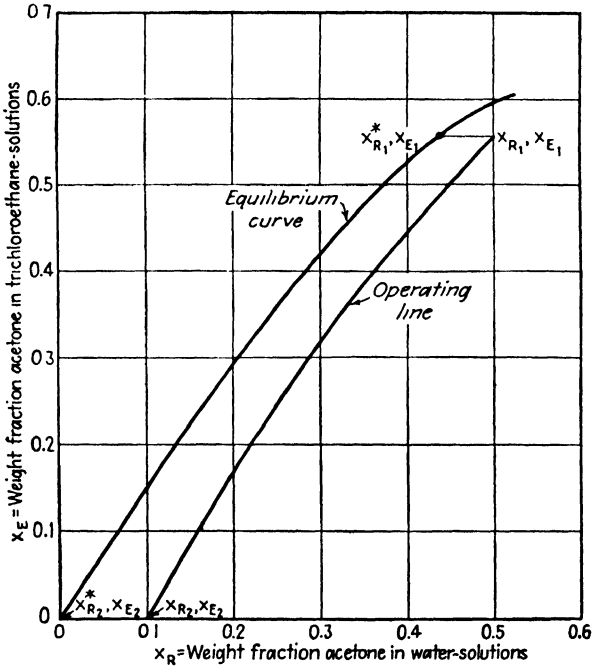



FIG. 8.4. Operating diagram, Illustration 1.

**Illustration 1.** Calculate the number of transfer units $N_{t_{OR}}$ for the extraction of Illustration 5, Chap. 6.

*Solution.* The preliminary computations are completed in the previous illustration. In terms of the notation used here, $R_1 = 100$ lb./hr., $E_2 = 30$ lb./hr. $X_{R_1} = 0.50$, $X_{R_2} = 0.10$, $X_{E_2} = 0$, $X_{E_1} = 0.557$ wt. fraction acetone. On the triangular diagram, Fig. 6.33, the operating point $O$ is located as before. Random lines from $O$ cut the equilibrium solubility curve at concentrations $X_R$ on the water-rich side, $X_E$ on the solvent-rich side, to provide data for the operating line. Equilibrium tie lines provide data for the equilibrium curve. The operating diagram prepared from these data is shown in Fig. 8.4. From this figure,

$$X^*_{R_2} = 0, \qquad 1 - X^*_{R_2} = 1.0, \qquad 1 - X_{R_2} = 0.9$$
$$X^*_{R_1} = 0.435, \qquad 1 - X^*_{R_1} = 0.565, \qquad 1 - X_{R_1} = 0.5$$

Since $(1 - X_R^*)$ and $(1 - X_R)$ at either end of the extraction differ by less than a factor of 2, and since weight fractions have been used, Eq. (8.19) will be used to determine $N_{t_{OR}}$.

$$r = \frac{\text{mol. wt. water}}{\text{mol. wt. acetone}} = \frac{18.02}{58.05} = 0.310$$

Since, from the triangular coordinates of Fig. 6.33, it is obvious that the mutual solubilities of the water and solvent are appreciable at the final extract concentration, the formal integrations should not be used. A curve of $1/(X - X_R^*)$ vs. $X_R$, Fig. 8.5, is prepared from the data of Fig. 8.4. The area under the curve between $X_{R_1} = 0.50$ and $X_{R_2} = 0.10$ is 4.98.

Eq. (8.19):

$$N_{t_{OR}} = \int_{x_{R_2}}^{x_{R_1}} \frac{dX_R}{X_R - X_R^*} + \frac{1}{2}\ln\frac{1 - X_{R_2}}{1 - X_{R_1}} + \frac{1}{2}\ln\frac{X_{R_2}(r-1)+1}{X_{R_1}(r-1)+1}$$

$$= 4.98 + \frac{1}{2}\ln\frac{(1 - 0.10)}{(1 - 0.50)} + \frac{1}{2}\ln\frac{0.10(0.310 - 1) + 1}{0.50(0.310 - 1) + 1}$$

$$= 5.45$$

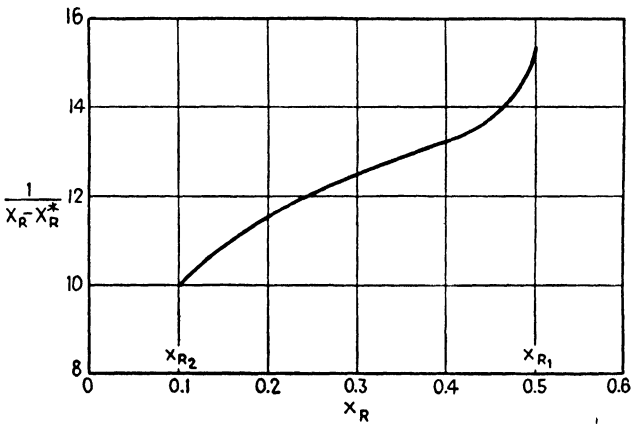



FIG. 8.5. Graphical integration, Illustration 1.

**Illustration 2.** A solution of acetic acid in water containing 10% acid is to be extracted with methyl isobutyl ketone to reduce the concentration to 0.1%. A tower packed with ½-in. carbon Raschig rings is to be used, with the solvent dispersed. The extract is to contain 6.5% acetic acid, and the rate of flow of aqueous solution is to be 30 cu. ft./hr. sq. ft. tower cross section. Mass-transfer rates and equilibrium data are provided by Sherwood, Evans, and Longcor [*Ind. Eng. Chem.* **31**, 1144 (1939)]. Calculate the height of tower required.

*Solution.* At the concentrations used, the solvent and water are substantially immiscible. The operating diagram will be prepared in terms of weight-ratio concentrations, and the number of transfer units determined by Eq. (8.21). $R$ and $E$ will be defined in terms of lb. water and solvent/hr., respectively.

$$r = \frac{\text{mol. wt. ketone}}{\text{mol. wt. acid}} = \frac{100.2}{60.1} = 1.669$$

Basis: 1 hr., 1 sq. ft. tower cross section. Initial acid solution density = 63 lb./cu. ft. Solution to be extracted = 30(63) = 1,890 lb., containing 189 lb. acid, 1,701 lb. water.

$R = 1701$, $w_{R_1} = 0.10/(1 - 0.10) = 0.111$, $w_{R_2} = 0.001/(1 - 0.001) = 0.001$ lb. acid/lb. water.

$$w_{E_1} = \frac{0.065}{(1 - 0.065)} = 0.0695, \qquad w_{E_2} = 0 \text{ lb. acid/lb. solvent}$$

Acetic acid balance:

$$E = \frac{[1701(0.111 - 0.001)]}{0.0695 - 0} = 2{,}690 \text{ lb. solvent (53.8 cu. ft.)}$$

An operating diagram, with equilibrium data of Sherwood, Evans, and Longcor (*loc. cit.*) is plotted in Fig. 8.6. Since the solutions are fairly dilute and the operating line not greatly curved, graphical integration is not necessary. If Eq. (8.27) in conjunction with

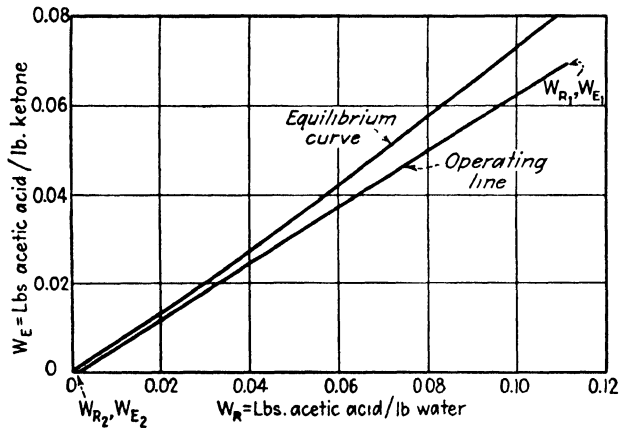



FIG. 8.6. Operating diagram, Illustration 2.

Fig. 8.3 is tried, the abscissa of the figure is found to be 18.65, too low for the method to be used. Therefore use Eq. (8.29), with the substitution of $w$ for $x$ and with $m$ defined in terms of $w$.

$$m_1' = w_{R_1}^*/w_{E_1} = 0.0959/0.0695 = 1.380$$
$$m_2' = \text{reciprocal slope of equilibrium curve (at } w_R = 0) = 1.543$$

$s^2$ is negative. Therefore,

$$s' = \sqrt{4(w_{E_2}w_{R_1} - w_{E_1}w_{R_2})(m_1' - m_2') - (w_{R_1} - w_{R_2} + m_1'w_{E_2} - m_2'w_{E_1})^2}$$
$$= \sqrt{4[0 - 0.0695(0.001)](1.380 - 1.543) - [0.111 - 0.001 + 0 - 1.543(0.0695)]^2}$$
$$= 0.00615$$
$$u = w_{R_1} + w_{R_2} - m_2'w_{E_1} - m_1'w_{E_2} = 0.111 + 0.001 - 1.543(0.0695) - 0$$
$$= 0.0047$$

Eq. (8.29c):

$$\int_{w_{R_2}}^{w_{R_1}} \frac{dw_R}{w_R - w_R^*} = \frac{2(w_{R_1} - w_{R_2})}{s'} \tan^{-1}\frac{s'}{u} = \frac{2(0.111 - 0.001)}{0.00615} \tan^{-1}\left(\frac{0.00615}{0.0047}\right)$$
$$= 35.5$$

(NOTE: Graphical integration, as a check, gave 37.0.)

Eq. (8.21):
$$N_{t_{OR}} = 35.5 + \frac{1}{2}\ln\frac{1 + 1.669(0.001)}{1 + 1.669(0.111)} = 35.2$$

Sherwood, Evans, and Longcor (*loc. cit.*) show $K_Ea$ to be 48 moles/hr. cu. ft. ($\Delta c$) at flow rates of 30 and 53.8 cu. ft./hr. sq. ft. acid and solvent rate, resp. This must be converted to $HTU_{OR}$.

Eq. (5.61): $$\frac{1}{K_E a} = \frac{1}{k_E a} + \frac{m c_{E_{av}}}{k_R a c_{R_{av}}}$$

for $m$ in mole fraction units. Solving simultaneously with Eq. (8.43),

$$K_R a c_{R_{av}} = m K_E a c_{E_{av}}$$

Substitution in Eq. (8.12):

$$HTU_{OR} = \frac{R}{m K_E a c_{E_{av}} (1 - x_R)_{OM} S}$$

where $R$ is in moles/hr.

$R_1 = (189/60) + (1{,}701/18) = 97.7$ moles/hr.

$R_2 = (1.7/60) + (1{,}701/18) = 94.5$ moles/hr.

Average $R = 96.1$ moles/hr.

At $w_{R_1} = 0.111$, $x_{R_1} = 0.0322$, $x^*_{R_1} = 0.0280$ mole fraction.

$(1 - x_{R_1})_{OM}$ = logarithmic average of $(1 - 0.0280)$ and $(1 - 0.0322) = 0.970$.

At $w_{R_2} = 0.001$, $(1 - x_{R_2})_{OM} = 1.00$; Average $(1 - x_R)_{OM} = 0.985$.

The operating line and equilibrium curve are so close that $c_E$ and $c^*_E$ are almost identical.

$$c_{EM_2} = (50 \text{ lb./cu. ft.})/100.2 = 0.499 \text{ lb. moles/cu. ft.}$$

Estimated density of extract = 51 lb./cu. ft.

$$c_{EM_1} = \frac{51(0.065)}{60} + \frac{51(0.935)}{100.2} = 0.530 \text{ lb. moles/cu. ft.}$$

$$c_{E_{av}} = \frac{(c_{EM_1} + c_{EM_2})}{2} = 0.515 \text{ lb. moles/cu. ft.}$$

The average slope of the equilibrium curve over the concentration range involved = $m$ = 3.0.

$$HTU_{OR} = \frac{96.1}{[3.0(48)(0.515)(0.985)1]} = 1.32 \text{ ft.}$$

Eq. (8.11): $H = N_{t_{OR}} HTU_{OR} = 35.2(1.32) = 46.5$ ft., height of tower

### Notation for Chapter 8

$A$ = total interfacial surface between phases, sq. ft.

$a$ = interfacial surface between phases, sq. ft./cu. ft. of tower.

$c$ = concentration, lb. moles/cu. ft.

$c_{av} = (c_{M_1} + c_{M_2})/2$, where $c$ refers to total concentration of all substances present.

$c_M = (c + c_i)/2$ or $(c + c^*)/2$, where $c$ refers to total concentration of all substances present.

$$(c^*_E - c_E)_{av} = \frac{[(c^*_{E_1} - c_{E_1}) - (c^*_{E_2} - c_{E_2})]}{\ln \frac{(c^*_{E_1} - c_{E_1})}{(c^*_{E_2} - c_{E_2})}}, \text{ where } c \text{ refers to solute only}$$

$$(c_R - c^*_R)_{av} = \frac{[(c_{R_1} - c^*_{R_1}) - (c_{R_2} - c^*_{R_2})]}{\ln \frac{(c_{R_1} - c^*_{R_1})}{(c_{R_2} - c^*_{R_2})}}$$

$d$ = differential operator.

$E$ = rate of flow of extract phase, lb. moles/hr.

$H$ = height of tower, ft.

H.E.T.S. = height equivalent to a theoretical stage, ft.

$HTU$ = height of a transfer unit, ft.

$K$ = over-all mass-transfer coefficient, lb. moles/(hr.)(sq. ft.)($\Delta c$).

$Ka$ = over-all mass-transfer coefficient, lb. moles/(hr.)(cu. ft.)($\Delta c$).

$k$ = individual-film mass-transfer coefficient, lb. moles/(hr.)(sq. ft.)($\Delta c$).
$ka$ = individual-film mass-transfer coefficient, lb. moles/(hr.)(cu. ft.)($\Delta c$).
ln = natural logarithm.
$M$ = molecular weight.
$m$ = slope of the equilibrium curve, $x_{E_i}/x_{R_i}$, except in Eqs. (8.29) and (8.30).
$N$ = rate of extraction, lb. moles/hr.
$N_t$ = number of transfer units.
$n$ = number of theoretical stages.
$R$ = rate of flow of raffinate phase, lb. moles/hr.
$r$ = molecular weight of nonsolute/molecular weight of solute.
$S$ = cross-sectional area of tower, sq. ft.
$w$ = concentration, lb. solute/lb. nonsolute = $X/(1 - X)$.
$X$ = concentration of solute, weight fraction.
$x$ = concentration of solute, mole fraction.
$x_R^*$, $x_E^*$ = defined by Eq. (8.10).

$$(x_E^* - x_E)_{av} = \frac{[(x_{E_1}^* - x_{E_1}) - (x_{E_2}^* - x_{E_2})]}{\ln [(x_{E_1}^* - x_{E_1})/(x_{E_2}^* - x_{E_2})]}$$

$$(x_R - x_R^*)_{av} = \frac{[(x_{R_1} - x_{R_1}^*) - (x_{R_2} - x_{R_2}^*)]}{\ln [(x_{R_1} - x_{R_1}^*)/(x_{R_2} - x_R^*)]}$$

$$(1 - x_E)_{iM} = \frac{[(1 - x_E) - (1 - x_{E_i})]}{\ln [(1 - x_E)/(1 - x_{E_i})]}$$

$$(1 - x_R)_{iM} = \frac{[(1 - x_{R_i}) - (1 - x_R)]}{\ln [(1 - x_{R_i})/(1 - x_R)]}$$

$$(1 - x_E)_{OM} = \frac{[(1 - x_E) - (1 - x_E^*)]}{\ln [(1 - x_E)/(1 - x_E^*)]}$$

$$(1 - x_R)_{OM} = \frac{[(1 - x_R^*) - (1 - x_R)]}{\ln [(1 - x_R^*)/(1 - x_R)]}$$

$\rho$ = density, lb./cu. ft.

Subscripts:

1 = that end of a tower where solutions are concentrated.
2 = that end of a tower where solutions are dilute.
av = average.
$E$ = extract.
$i$ = interface.
$M$ = mean.
$O$ = over-all.
$R$ = raffinate.

## LITERATURE CITED

1. Colburn, A. P.: *Trans. Am. Inst. Chem. Engrs.* **35**, 211 (1939).
2. ———: *Ind. Eng. Chem.* **33**, 459 (1941).
3. Elgin, J. C.: In "Chemical Engineers' Handbook," J. H. Perry, Ed., 3d ed., McGraw-Hill Book Company, Inc., New York, 1950.
4. Hunter, T. G., and A. W. Nash: *J. Soc. Chem. Ind.* **51**, 285T (1932).
5. Scheibel, E. G., and D. F. Othmer: *Trans. Am. Inst. Chem. Engrs.* **38**, 339 (1942).
6. ——— and ———: *Ind. Eng. Chem.* **34**, 1200 (1942).
7. Sherwood, T. K.: "Absorption and Extraction," p. 79, McGraw-Hill Book Company, Inc., New York, 1937.
8. Wiegand, J. H.: *Trans. Am. Inst. Chem. Engrs.* **36**, 679 (1940).

# CHAPTER 9

## EQUIPMENT FOR STAGEWISE CONTACT

The various types of equipment for liquid extraction may be classified into two main categories:

1. Those which provide discrete stages, where the liquids are mixed, extraction is allowed to occur, and the insoluble phases are settled and separately removed. At best, the insoluble phases are in equilibrium, and the performance represents that of one ideal or theoretical stage. For results corresponding to the multistage flowsheets of Chaps. 6 and 7, multiple units each providing mixing, settling, and separation must be joined.
2. Those which provide continuous countercurrent contact between the insoluble phases. The equivalent of as many theoretical stages may be built into a single piece of equipment as is desired or is practical, without intermediate removal of the phases. Design calculations are described in Chap. 8.

A few of the latter types combine features of both categories. Only the first will be considered in this chapter.

The discrete stage must provide each of the functions listed in 1 above. It is convenient to classify the equipment according to method of operation as follows:

1. Batch operation
   - *a*. The mixer provides a substantially uniform dispersion of the two liquid phases throughout the mixing vessel, if well designed
   - *b*. Settling of the phases and their separation may occur in the mixing vessel after agitation is stopped or in a separate vessel
2. Continuous operation. Mixing and phase separation must be carried out in separate vessels
   - *a*. The mixer provides mixing in the direction of forward flow, with substantially uniform dispersion
   - *b*. The mixer does not provide mixing in the direction of forward flow ("in-line" mixing). The composition of the phases varies with position in the mixer in the direction of flow

The design of such equipment then requires study of the two major types of mixers and separators. These are considered separately.

### AGITATED VESSELS

Mixers which provide substantially uniform dispersion throughout are represented by the many types of agitated vessels. Agitation might be

provided by rocking or shaking the entire vessel, by bubbling of a gas through the vessel contents, or by circulating the contents from the bottom of the vessel to the top externally by means of a pump. None of these methods is satisfactory industrially, and invariably some form of mechanical internal agitation is necessary. The design of agitators involves consideration of the power requirements and the adequacy of mixing. It is only in the last few years that systematic study has been given the former, and very little has been done with the latter. It seems well established that high power absorption by an agitator is not necessarily accompanied by adequate mixing.

If the mixing vessel is inadequately agitated, the two insoluble liquids will settle out vertically owing to their difference in density. On the other hand, strong circular motion about the axis of the vessel may cause stratification by centrifugal force, with the heavy liquid collecting in a layer around the tank wall. It is clear, therefore, that for adequate mixing the agitator must produce both vertical motion of the liquids to offset the first tendency and radial motion to prevent the second. While adequacy of mixing and dispersion is obviously essential to provide rapid extraction, it is most important that difficultly settleable emulsions do not result. The nature of the circulation produced in an agitated vessel is influenced by tank shape, the presence of stationary objects immersed in the liquid such as baffles, and impeller design, location, and speed (9). The degree of dispersion which results from a given mechanical arrangement depends upon the properties of the tank contents, including density and viscosity of each phase, interfacial tension, and the relative amounts of the two phases.

**Mixing Tanks.** The tank used for the mixer is ordinarily a vertical cylinder with a smooth internal surface, except for baffles, preferably fitted with a dished bottom. Flat-bottomed, square, or rectangular tanks are much less effective (3, 9). The minimum limits for the ratio of liquid depth to tank diameter for adequate circulation has been considered in some detail (8), but for best results the liquid depth should be at least equal to or somewhat greater than the tank diameter.

*Baffles.* For the most effective circulation within the tank, swirl and vortices must be avoided, since the circular flow associated with swirl is not accompanied by the necessary vertical motion. Except in the case of extremely viscous liquids (viscosity $>$ 60,000 centipoises), or where marine propellers are used in an off-center arrangement, vortices will invariably develop with any impeller, and properly arranged baffles are thoroughly effective in eliminating them.

Vertical baffles are narrow, flat strips placed vertically along the walls of the mixer tank, most commonly [illegible] radially, less frequently at an angle to the tank radius. They may be welded or otherwise fastened

directly to the tank wall, or set out from the wall 0.5 to 1.5 in., and should preferably extend for the full liquid depth as in Fig. 9.1*a*. In the case of turbine impellers, it is particularly important that baffles be available in the zone directly opposite the turbine (9). The work of Mack and Kroll (39) has established minimum baffle conditions which produce a "fully baffled state," where swirl is negligible and beyond which additional baffling produces no very great advantage. Four equally spaced vertical baffles, arranged radially, of length equal to the liquid depth and width equal to $\frac{1}{10}$ or $\frac{1}{12}$ of the tank diameter provide this condition.

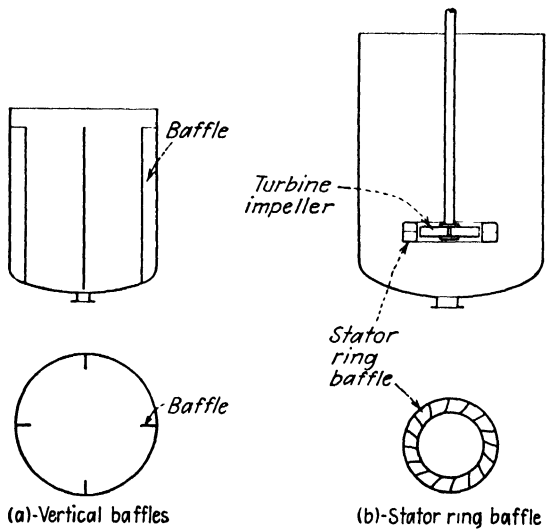



FIG. 9.1. Mixing tank baffles.

Stator ring baffles, used in conjunction with turbine-type impellers, consist of a series of blades arranged on a circular ring mounted in the plane of the turbine, as in Fig. 9.1*b*. The inner diameter is slightly larger than that of the turbine, the outer diameter usually in the neighborhood of one-half that of the tank. The results produced by these are basically different from those produced by vertical baffles, and they serve to develop substantially complete radial flow of the liquid (38). Much higher local turbulence and shear result than with vertical baffles, and care must be exercised in their use with liquids having a tendency to form emulsions.

Draft tubes are cylindrical sleeves placed axially either at the level of a marine propeller or above a turbine impeller. For most mixing operations of the type considered here, they provide nothing that cannot be made available through baffling (38).

*Impellers.* With the exception of a few special designs, impellers may be classified according to the type of flow they induce: tangential (paddle

type), axial (propellers), and radial (turbines). The paddle type produces poor circulation and is not recommended for the purposes at hand.

*Propellers.* These are the most economical impellers for mixing low-viscosity liquids in small tanks (38). Marine types, with two, three, or four blades are usually used, three blades most commonly (Fig. 9.2*a*).

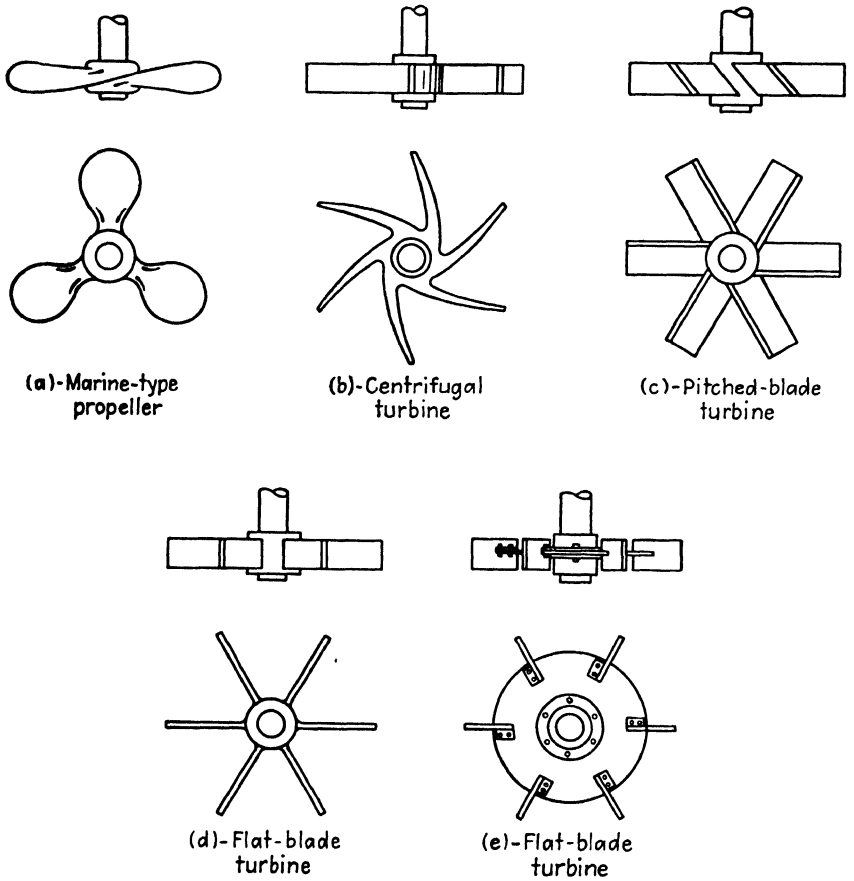



FIG. 9.2. Mixing impellers.

They are rotated in such a manner as to cause downward flow against the bottom of the tank, at speeds usually in the range 100 to 1,000 r.p.m., depending upon the diameter and pitch of the propeller and the nature of the liquids being mixed. The shaft is ordinarily mounted along the axis of the tank, entering from the top, although off-centered entrance at an angle is sometimes used to avoid vortexing without baffles. Bottom steady bearings and auxiliary bearings for eliminating shaft vibration are undesirable and can usually be avoided (9).

*Turbines.* For the most difficult mixing operations, particularly for large quantities of liquids, the "back-sloped" or centrifugal turbine, Fig. 9.2*b*, is most efficient. The blades may or may not be confined between flat peripheral plates. Simpler radial-type blades are also used, with blades attached either directly to the hub or to a horizontal disk as in Fig. 9.2*d,e*. The pitched-blade turbine, Fig. 9.2*c*, is popular, since it combines the action of both propeller and radial-bladed turbines, although neither action is as well developed as with these devices separately. For continuous operation, compartmented vessels such as that shown in Fig. 9.3 may be used conveniently with turbine impellers, to reduce the short-circuiting that may result with a single vessel. Here the holes in the plates which separate the compartments are sufficiently large to permit removal of the impellers for maintenance, and rotating plates attached to the shaft reduce the flow area between compartments to prevent excessive short-circuiting (9). Each compartment may be baffled with vertical or stator ring baffles.

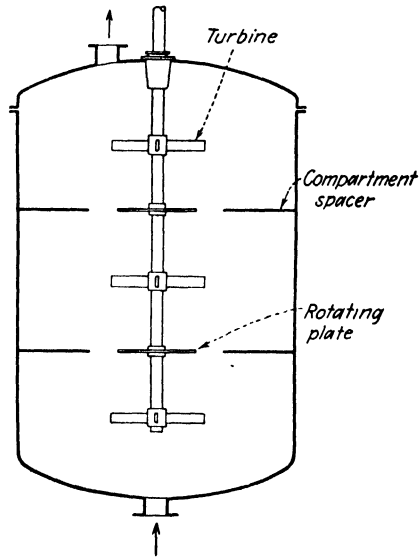



FIG. 9.3. Compartmented agitator for continuous operation.

The diameters of impellers of either the propeller or turbine type are ordinarily one-third the diameter of the mixing tank. They are usually placed between one impeller diameter above the bottom and a similar distance below the liquid surface, the lower position preferred.

**Power for Agitation.** In recent years, considerable study has been given the power requirements for agitation, particularly of single-phase liquids. It has been well established that the power varies as the cube of the speed for fully developed turbulence, so that one measurement of power for a given mixer and liquid will permit prediction of the power at any speed. Reasonably successful correlation of power for agitation under geometrically similar conditions has been made by relating the dimensionless group $\phi = Pg/l^5S^2\mu$ to a modified Reynolds number, $Re = l^2S\rho/\mu$,

where $P$ = power
$l$ = impeller diam.
$S$ = impeller speed
$\mu$ = liquid viscosity
$\rho$ = liquid density
$g$ = gravitational conversion factor

all in consistent units. Alternatively, a power coefficient, $Pg/l^3S^3\rho = \phi/Re$, has been used for correlating purposes and for characterizing impellers. The work of Miller and Mann (46) and Olney and Carlson (52) has established that power data for two-liquid-phase mixtures can be correlated with those of single liquids provided that an average density and viscosity for the mixture are used, as follows:

$$\rho = z_E\rho_E + z_R\rho_R \tag{9.1}$$

$$\mu = \mu_E^{z_E}\mu_R^{z_R} \tag{9.2}$$

where $z$ = the volume fraction of the appropriate phase, although as Miller and Mann point out, an increased viscosity due to emulsion formation may be developed at high agitation intensities which cannot be estimated by Eq. (9.2). Olney and Carlson (52) and Hooker (29) have made beginnings in establishing generalized power correlations for many types of unbaffled agitators, using both single- and two-liquid-phase data, although their correlations must be considered tentative.

Power measurements on several two-liquid-phase systems have been made by Olney and Carlson (52) using an arrowhead turbine agitator with vertical baffles and a centrifugal turbine with a stator ring baffle. The effectiveness of mixing was not considered. The arrowhead-type turbine is not now recommended for such service (41).

**Mixing Effectiveness.** Miller and Mann (46) studied power requirements of seven types of impellers in unbaffled vessels and mixing effectiveness for several systems using a special sampling technique. The effectiveness of mixing was expressed as a mixing index, defined as the average ratio of the volume fraction of the phase in which the sample is poor to the volume fraction of that phase in the vessel as a whole. The index then provides some measure of the uniformity of dispersion throughout the vessel, although it does not measure the fineness of subdivision. Their results for kerosene-water in an unbaffled tank may be summarized as follows: (*a*) mixing index increased with power input per unit volume generally to a maximum at 200 ft. lb./min. (cu. ft.), whereupon it either dropped or leveled off with further increase of power; (*b*) a four-bladed radial turbine and a four-bladed pitched turbine deflecting downward performed best, while a two-bladed propeller was poorest; the performance of all seven types of agitators was surprisingly similar, with mixing indexes ranging up to 0.8 and 0.9 for most; (*c*) impellers operate best if the interface between the phases when at rest is above the impeller; (*d*) measurements on the effect of liquid depth were not conclusive; (*e*) performance depends upon the tendency to form oil-in-water or water-in-oil dispersions. Measurements with other oils and water indicated that power input varies almost directly with density at the same mixing index, but the effect of viscosity was not clearly established. This study of the relation between power and mixing

effectiveness is the most complete available but should be projected to other systems with considerable caution because of the lack of baffling and the lack of information concerning the effect of interfacial tension.

Some indication of the effect of interfacial tension on mixing effectiveness is provided by the data of Hunter (30), who contacted lubricating oil with nitrobenzene in laboratory separatory funnels which were air-agitated. The effectiveness of extraction appears to be best at oil:solvent ratios which tend to give complete miscibility, conditions which correspond to low values of interfacial tension.

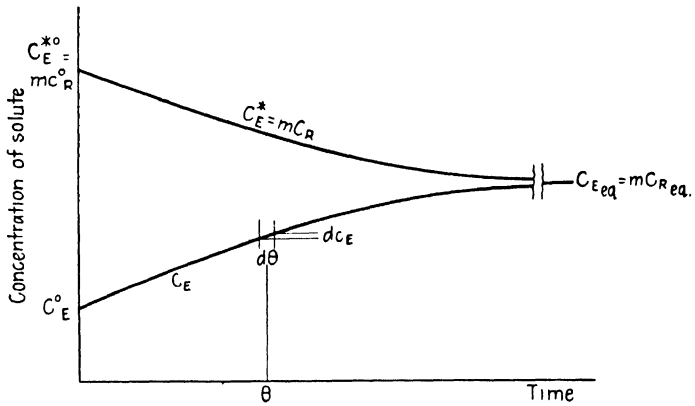



FIG. 9.4. Batch extraction.

**Rate of Extraction.** *Batch Agitators.* Consider the batch extraction of a solute from a raffinate phase by an extract phase in an agitated vessel. At zero time, the concentration of solute in the raffinate phase is $c_R^0$, in the extract phase $c_E^0$. As time passes and extraction proceeds, the concentration in the extract phase will increase, that in the raffinate will decrease, until eventually equilibrium values in each phase, $c_{E\,eq}$ and $c_{R\,eq}$, are reached. We may express the concentration of solute in the raffinate at any time as

$$c_E^* = mc_R \tag{9.3}$$

where $m$ is the distribution coefficient, in the manner of Chap. 5 [Eq. (5.56)], and indicate the variation of concentration with time graphically as in Fig. 9.4. Letting $N$ = the number of moles of solute extracted and $A$ the interfacial area available in the agitator, Eq. (5.57) can be adapted to the situation at any time $\theta$:

$$\frac{dN}{d\theta} = \frac{E\,dc_E}{d\theta} = K_E A(c_E^* - c_E) \tag{9.4}$$

A material balance from zero time to time $\theta$, assuming the amounts of the phases $E$ and $R$ remain constant, is

$$R(c_R^0 - c_R) = E(c_E - c_E^0) \tag{9.5}$$

or

$$c_E^* = mc_R^0 - \frac{mE}{R}(c_E - c_E^0) \tag{9.6}$$

Substituting Eq. (9.6) in Eq. (9.4),

$$\int_{c_E^0}^{c_E} \frac{dc_E}{mc_R^0 + \frac{mE}{R}c_E^0 - c_E\left(1 + \frac{mE}{R}\right)} = \frac{K_E A}{E}\int_0^\theta d\theta \tag{9.7}$$

whence

$$-\frac{1}{1 + (mE/R)} \ln \frac{mc_R - c_E}{mc_R^0 - c_E^0} = \frac{K_E A\theta}{E} \tag{9.8}$$

At equilibrium,

$$c_{E\,\text{eq}} = mc_{R\,\text{eq}} \tag{9.9}$$

and

$$E(c_{E\,\text{eq}} - c_E^0) = R(c_R^0 - c_{R\,\text{eq}}) = R\left(c_R^0 - \frac{c_{E\,\text{eq}}}{m}\right) \tag{9.10}$$

$$\therefore mc_R^0 - c_E^0 = \left(1 + \frac{mE}{R}\right)(c_{E\,\text{eq}} - c_E^0) \tag{9.11}$$

Further,

$$R(c_R - c_{R\,\text{eq}}) = E(c_{E\,\text{eq}} - c_E) \tag{9.12}$$

from which

$$mc_R - c_E = \left(1 + \frac{mE}{R}\right)(c_{E\,\text{eq}} - c_E) \tag{9.13}$$

Combining Eqs. (9.11) and (9.13),

$$\frac{mc_R - c_E}{mc_R^0 - c_E^0} = \frac{c_{E\,\text{eq}} - c_E}{c_{E\,\text{eq}} - c_E^0} = 1 - \frac{E(c_E - c_E^0)}{E(c_{E\,\text{eq}} - c_E^0)} = 1 - \frac{N}{N_{\text{eq}}} = 1 - \mathbf{E} \tag{9.14}$$

where $N_{\text{eq}}$ is the solute transferred after equilibrium is established and $\mathbf{E}$ is the stage efficiency or approach to equilibrium at time $\theta$. Substituting in Eq. (9.8),

$$-\frac{1}{1 + (mE/R)} \ln (1 - \mathbf{E}) = \frac{K_E A\theta}{E} \tag{9.15}$$

Letting $1/(1 + mE/R) = b$ and $K_E A/E = K'$, then

$$\theta = -\frac{b}{K'} \ln (1 - \mathbf{E}) = -K'' \ln (1 - \mathbf{E}) \tag{9.16}$$

where

$$K'' = \frac{E}{[1 + (mE/R)]K_E A} \tag{9.17}$$

Equation (9.16) can also be obtained in terms of a raffinate rate coefficient, in which case $K''$ is defined as

$$K'' = \frac{[1 + (R/mE)]R}{K_R A} \tag{9.18}$$

Equation (9.16) was obtained by Hixson and Smith (27) by a slightly different procedure and tested by extraction of iodine from water with carbon tetrachloride in a series of unbaffled geometrically similar vessels using marine propellers as agitators. Plotting $(1 - N/N_{eq})$ against time on semilogarithmic graph paper yielded straight lines from which the constant $K'$ could be determined. $K'$ was found to vary with speed to a power ranging from 3.8 to 5 depending upon propeller height and with diameter of the mixing vessel. Failure to obtain a correlation between $K'$, vessel diameter, and propeller position is explained by Rushton (53) as being caused by the lack of kinematic and dynamic similarity in the unbaffled vessel. Interfacial tension probably enters as an important variable where vortex and swirl are produced, and dynamic similarity would require the use of different liquids in unbaffled vessels of different sizes.

The general applicability of an equation of the form of Eq. (9.8) was also confirmed for two-liquid-phase systems on a very small scale by Yates and Watson (61), who extracted acetic acid from a very dilute water solution by kerosene in agitated laboratory beakers.

**Rate of Extraction.** *Continuous Extraction.* Extraction by mixing liquids in an agitated vessel with continuous flow will generally be less effective than by a batch process, since it can be shown from Eq. (9.8) that in the batch process the average concentration-difference driving force is the logarithmic mean between that at the beginning and that at the end of the process. In the uniformly mixed continuous agitator, on the other hand, the driving force is that corresponding to the withdrawn products (17). Assuming flow through a continuous mixer in a direction parallel to the axis of the mixer, and assuming thorough mixing in a direction perpendicular to the axis of the tank but none in the direction of flow (an "in-line" mixer with perfect displacement), the continuous process should behave in the manner of a batch process. This situation can be approached as nearly as desired by using several agitated vessels in series for the continuous process, as exemplified by the compartmented vessel of Fig. 9.3.

Macmullin and Weber (40) have investigated this situation mathematically and found that for agitated vessels with uniform dispersion of the liquids throughout,

$$y = e^{-\frac{\theta}{\theta_H}}\left[1 + \frac{\theta}{\theta_H} + \frac{1}{2!}\left(\frac{\theta}{\theta_H}\right)^2 + \cdots + \frac{1}{(n-1)!}\left(\frac{\theta}{\theta_H}\right)^{n-1}\right] \qquad (9.19)$$

where $y$ = the fraction of the stream remaining in the tank for time $\theta$ or longer

$\theta_H$ = the nominal holding time of the tank, vol. of tank/volumetric rate of flow

$n$ = the number of tanks in series

A graphical solution to Eq. (9.19) is provided by Fig. 9.5. The stage efficiency $\mathbf{E}_{av}$ for a series of identical vessels operated continuously is then related to the stage efficiency $\mathbf{E}$ for one of them operated batchwise by

$$\mathbf{E}_{av} = \int_{y=0}^{y=1} \mathbf{E}\, dy \tag{9.20}$$

For $n = 1$, Eqs. (9.16) and (9.19) can be substituted in Eq. (9.20) to yield

$$\mathbf{E}_{av} = 1 - \frac{K''}{K'' + \theta_H} \tag{9.21}$$

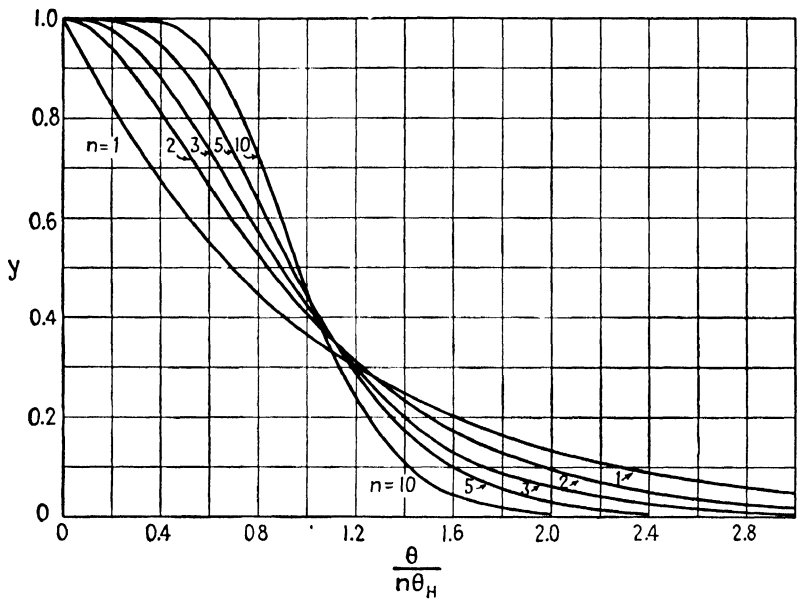



FIG. 9.5. Holding time, continuous-flow tanks in series. (*Macmullin and Weber; with permission of American Institute of Chemical Engineers.*)

where $K''$ is obtained from a batch experiment. For other situations, where for example the form of Eq. (9.16) might not be followed, graphical solution of Eq. (9.20) may be used. Such predictions of efficiency should of course be used with considerable caution because of the assumptions of uniform dispersion and of the absence of an effect on the flow regime in the vessel when changing from batch to continuous operation.

**Illustration 1.** Hixson and Smith (27) report the following data for the batchwise extraction of iodine from water with carbon tetrachloride (diameter of vessel = 21.5 cm.; depth of liquid = 21.5 cm.; volume of liquids: 7,090 cu. cm. water, 709 cu. cm. carbon tetrachloride; propeller speed = 200 r.p.m.):

| $\theta$, min. | 0 | 8 | 13 | 16 | 24 | 30 | 38 | 45 | 52 | $\infty$ |
|---|---|---|---|---|---|---|---|---|---|---|
| $N$, gm. $I_2$ ext'd | 0 | 0.529 | 0.712 | 0.861 | 1.038 | 1.125 | 1.175 | 1.205 | 1.276 | 1.330 |
| $\frac{N}{N_{eq}} = E$ | 0 | 0.397 | 0.535 | 0.647 | 0.780 | 0.845 | 0.883 | 0.906 | 0.958 | 1.000 |

Assuming that dispersion of the two phases was uniform throughout the vessel, estimate the stage efficiency to be expected for a continuous process with the rate of flow of liquids = 8,000 cu. cm./20 min., in the same proportions and the same initial concentration for (*a*) one vessel and (*b*) for two vessels in series.

*Solution.*

*a.* $N$ may be expressed as gm. iodine extracted, in which case $N_{eq} = 1.330$. $N/N_{eq} = E$ is then listed above for each value of $\theta$. $(1 - E)$ is plotted against $\theta$ on semilogarithmic paper, Fig. 9.6, and the best straight line is drawn through the data points. When $(1 - E) = 0.1$, $\theta = 38.6$ min., and substitution in Eq. (9.16) gives $K'' = 16.80$.

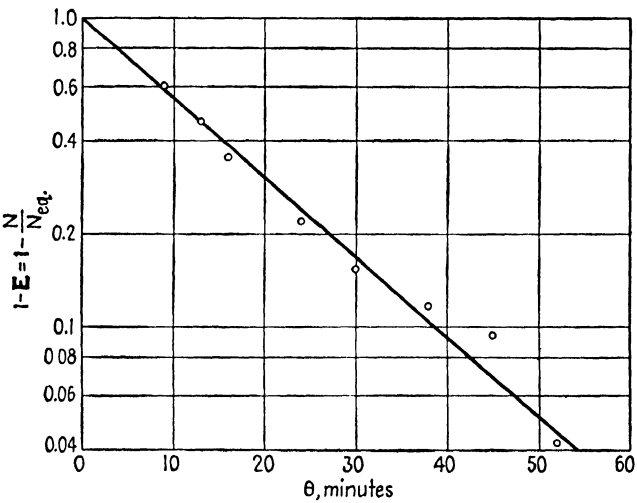



FIG. 9.6. Batch extraction efficiency, Illustration 1.

$$\theta_H = \frac{\text{vol. of vessel}}{\text{rate of flow}} = \frac{(\pi/4)(21.5)^2(21.5)}{\left(\frac{8{,}000}{20}\right)} = 19.50 \text{ min.}$$

Eq. (9.21): $$E_{av} = 1 - \frac{K''}{(K'' + \theta_H)} = 1 - \frac{16.80}{(16.80 + 19.50)} = 0.538$$

*b.* Solution is by graphical integration of Eq. (9.20). Values of $y$ from 0 to 1.0 are chosen, and corresponding values of $\theta/n\theta_H$ are read for $n = 2$ from Fig. 9.5. $\theta$ is calculated for each value of $y$ by letting $n = 2$, $\theta_H = 19.50$ min. For each value of $\theta$, a value

of E is obtained from the curve of Fig. 9.6. The computations are summarized as follows:

| $y$ | $\frac{\theta}{n\theta_H}$ | $\theta$ min. | E |
|---|---|---|---|
| 0 | $\infty$ | $\infty$ | 1 |
| 0.10 | 1.95 | 76.0 | 0.990 |
| 0.20 | 1.50 | 58.5 | 0.969 |
| 0.40 | 1.01 | 39.4 | 0.904 |
| 0.60 | 0.70 | 27.3 | 0.779 |
| 0.80 | 0.41 | 16.0 | 0.615 |
| 0.90 | 0.26 | 10.2 | 0.455 |
| 0.95 | 0.17 | 6.6 | 0.320 |
| 1.00 | 0 | 0 | 0 |

E is plotted against $y$ in Fig. 9.7, and the area under the curve, in accordance with Eq. (9.20), is $E_{av} = 0.787$.

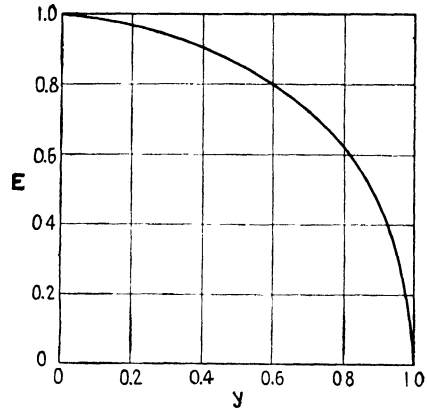



FIG. 9.7. Graphical integration, Illustration 1.

## FLOW MIXERS

Flow mixers, or "in-line" mixers, are devices for bringing about continuous dispersion of one liquid in another while the previously proportioned phases are flowing through the apparatus. They differ from continuously operated agitated vessels in that they have small volumes and consequently provide very little holding time for diffusion to occur. Their use is ordinarily limited to cases where dispersion is not difficult and where equilibrium is rapidly obtained, such as in the case of liquids of low viscosity (less than 100 centipoises). They have been widely used in the refining of light petroleum distillates, where the ratio of quantity of solvent or treating liquid to that of liquid to be treated is small. There are four basic types:

1. Jets, or devices depending upon impingement of one liquid upon the other for intimacy of mixing.
2. Injectors, where the flow of one of the liquids is induced by the flow of the other, at the same time resulting in mixing.
3. Orifices and nozzles, which bring about mixing and dispersion by causing a high degree of turbulence in the stream of the flowing liquids.
4. Devices depending upon mechanical agitation.

These devices are all relatively inexpensive in first cost and will bring about a fairly coarse dispersion economically. Intimate mixing requires fairly great expenditure of pressure drop, however, and consequently they may be expensive to operate.

**Jets.** These are ordinarily the least satisfactory of the flow mixers for bringing about intimate mixing of two immiscible liquids, although they are successful in mixing gases. Their use in extraction is limited to liquids

of low density difference and interfacial tension, where more efficient mixers might cause emulsification. In its simplest form, the jet mixer consists merely of pipes connected in the form of a $Y$, where the two liquids are pumped separately into the branches to flow out together through the stem. More positive breakup of one of the liquids seems almost essential, however.

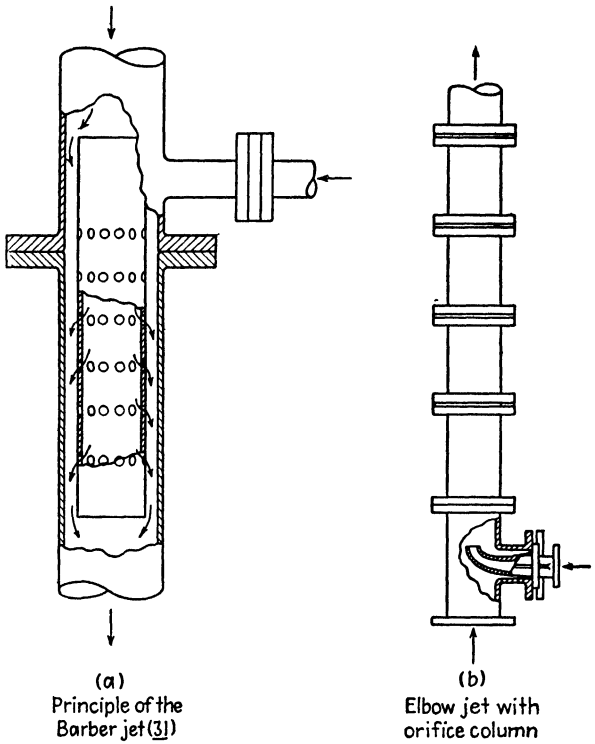



FIG. 9.8. Jet mixers. (*a*) Principle of the Barber jet (31); (*b*) Elbow jet with orifice column. (*Courtesy, The Duriron Co., Inc.*)

The Barber jet described by Hunter and Nash (31), the essentials of which are indicated in Fig. 9.8*a*, disperses one liquid into the other by pumping it through a number of tangentially arranged orifices in the inner concentric tube. The action of a simple jet is further improved by supplementing it with mixing nozzles or orifices of the type described below (13, 30), for example as in Fig. 9.8*b*. There are substantially no data available on the performance of such jets, with the exception of an indication by Hunter (30) that in the removal of phenol from an oil with aqueous alkali, a particular jet brought about between 90 and 100 per cent removal of phenol over a range of flow rates of approximately 200 to 1,000 gal./hr.

One variety of mixer, Fig. 9.9, which can be considered to fall in this category has been eminently successful in providing the initial mixing of oil and solvents in the Duo-Sol process for refining lubricating oils (45).

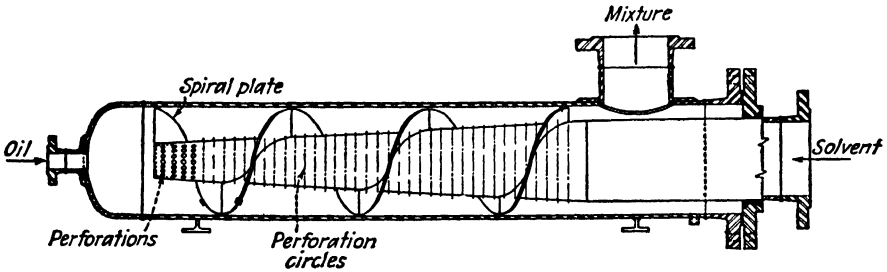



FIG. 9.9. Duo-Sol crude mixer. (*Courtesy, Max B. Miller and Co., Inc.*)

Solvent-rich solution enters the larger nozzle and flows through the perforations at velocities of 16 to 20 ft./sec. The oil enters the smaller nozzle and, as it spirals around the perforated cone, is thoroughly mixed with solvent. The mixture leaves at the top, as shown.

**Injectors.** These devices operate in principle in the manner of the familiar steam injector, the flow of one liquid which is pumped through the device inducing the flow of, and admixture with, the other liquid. The

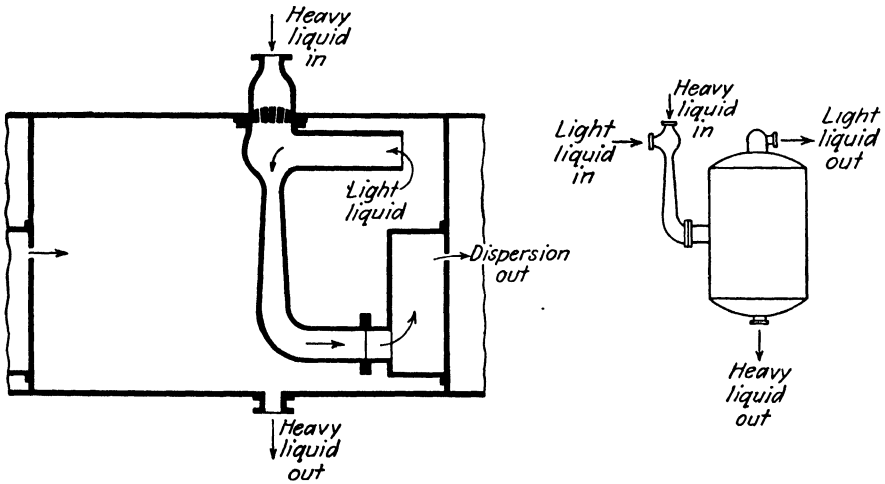



FIG. 9.10. Injector mixer. (*Hampton, U.S. Pat.* 2,091,709.)

mass velocity of the added liquid must be several times that of the main liquid if adequate mixing is to occur (60). One type (24) which has been used is shown in Fig. 9.10*a*, where the injector is incorporated into the settling chamber of the stage. The chamber is filled with a settled mixture of the two insoluble liquids, with the interface roughly at the center.

Heavy liquid from a previous stage is pumped into the injector as shown, thus inducing the flow of light liquid from the settled mixture in the chamber. Mixing occurs in the tapered tube leading from the throat of the injector, and the dispersion is discharged through a slit in the wall of the chamber into the adjoining chamber for settling. Figure 9.10*b* shows a similar arrangement but with the injector mounted externally, and others of the same principle are also possible (44, 56). Such devices thus require only one pump per stage. The basic principles have been recently reviewed by Folsom (20), but no data are available on their effectiveness in mixing immiscible liquids. Morrell and Bergman (50) indicate that they operate well provided that approximately equal quantities of the two liquids are being handled.

In the early installations of the Duo-Sol process for lubricating oil refining, injector mixers similar to those described above were used for mixing the insoluble liquid phases between adjacent stages, but it was found that the mixing which resulted was too thorough to permit settling in a reasonable time for the low interfacial tension encountered. In more recent plants for this process, the liquids are merely pumped through 10 or 15 ft. of piping between stages at velocities in the range from 10 to 16 ft./sec., which results in sufficient turbulence to provide adequate mixing (45).

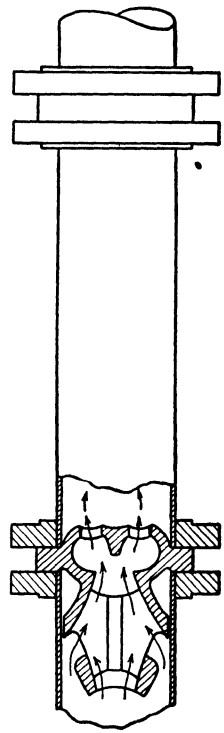


FIG. 9.11. Mixing nozzles. (*Courtesy, The Duriron Co., Inc.*)

**Nozzles and Orifices.** *Nozzle mixers* are relatively simple devices which can be installed in pipe lines, as shown in Fig. 9.11. The two liquids are pumped simultaneously through the nozzle, or through several in series, the mixing depending upon the development of a high degree of turbulence at the expense of the pressure of the liquids entering the nozzle. *Orifice mixers*, Fig. 9.12, operate on the same principle and have been very widely used in the refining of light petroleum distillates. The typical orifice column as used in the petroleum refinery consists of 20 to 30 orifice plates in a pipe line, usually set 12 in. apart (14, 50). The orifice plates contain a number of circular holes, 1.5 to 2.0 in. in diameter, sufficient to produce a pressure drop in the neighborhood of 2 lb./sq. in. for each plate as estimated by ordinary standard orifice equations (50). The velocity of the liquids through the pipe cross section should be fairly low, less than 1 ft./sec., in order to provide some holding time for diffusion to occur. A "knothole" mixer, containing orifices in the shape of a 12-pointed star (62), has been

used, but this seems an unnecessary complication. The orifice plates may be bolted between flanges, welded on a rod which is then introduced into the pipe, or welded into slots cut in the pipe. Construction is simple and inexpensive. A modification, shown in Fig. 9.13, has been used successfully

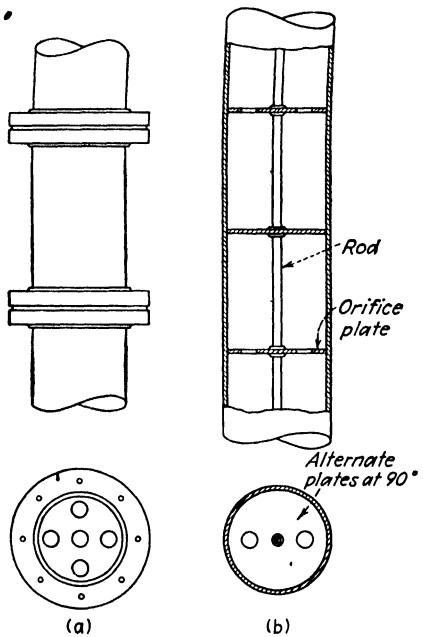



FIG. 9.12. Orifice mixers.

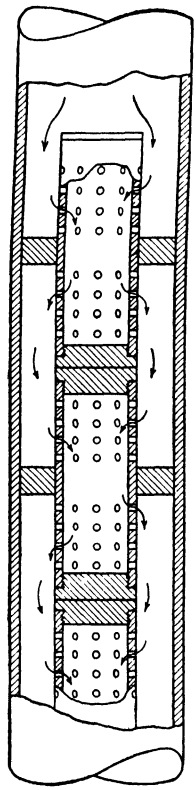


FIG. 9.13. Leaver's mixer (36).

in petroleum work. If interfacial tension is low, as in the presence of surface active agents, even simpler devices will serve. For example, pumping petroleum–salt-water mixtures through a standard globe valve was sufficient in one case to produce such intimate mixing that difficultly separable emulsions resulted (25).

**Centrifugal Pumps.** These have been used as mixers in extraction work, although their field of applicability is small. In the ordinary arrangement, the two liquids to be mixed are fed to the suction side of the pump, and the action of the impeller provides the dispersion; at the same time the liquids are pumped to the settler which follows. If the interfacial tension and density difference are low, the violence of the impeller action is quite likely to produce an emulsion, while if the density difference is large, stratification

with little mixing may result from the strong centrifugal action. Morrell and Bergman (50) suggest pumping the liquids backwards through a centrifugal pump which has had its impeller reduced in diameter. No systematic data are available on performance; Gollmar (22, 23) indicates that they are successful in contacting a mixture of light oil and aqueous gas-works ammonia liquor for removal of phenols.

Figure 9.14 shows a device (16) which uses turbulence developed both by orifices and agitators to bring about mixing. It has been used successfully in the treatment of gasoline with caustic soda solutions. The Stratford mixer (58), which incorporates similar principles, has been successfully used in acid treatment of light petroleum distillates and lubricating oils and subsequent neutralization with caustic solutions.

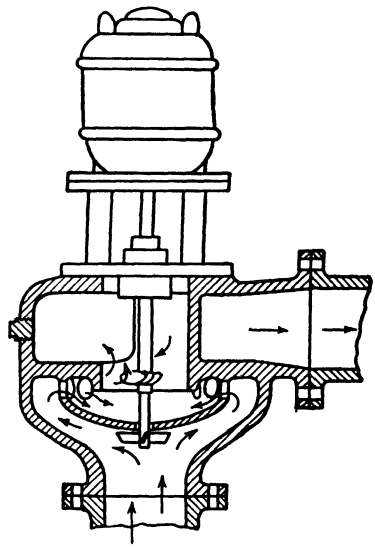


FIG. 9.14. Agitated mixer (16). *(Courtesy, New England Tank and Tower Co.)*

**Baffles.** Baffle mixers have frequently been used in conjunction with each of the flow-mixer types described above to provide longer contact time in the dispersed condition with relatively little expenditure of power. They are essentially orifice mixers with the orifices replaced by segmental baffles, the opening representing ½ to ⅓ of the cross-sectional area of the pipe in which they are installed, and they are placed downstream from the mixer. The more moderate turbulence they create will frequently maintain a dispersion sufficiently well to permit rapid extraction. Alternatively, the downstream pipe may be filled with tower packing such as Raschig rings to accomplish the same purpose (10, 30, 50).

## EMULSIONS

The mixture of immiscible liquids resulting from agitation or mixing are dispersions of one liquid in a continuum of another. It is customary to speak of these as "water-in-oil" or "oil-in-water" emulsions, referring to whether water or oil, respectively, forms the dispersed phase. Even though there may be no aqueous phase present in an extraction process, it is convenient to use this designation to describe the liquids in what follows. The conditions controlling the formation of one type or the other have been the object of considerable study. Since closely packed spheres of uniform size occupy approximately 74 per cent of the total space, it was long considered that emulsions cannot exist which contain more than 74 per cent

by volume of the dispersed phase. Thus, 0 to 26 volume per cent water would produce water-in-oil emulsions, 74 to 100 per cent oil-in-water, with both possible in the range from 26 to 74 per cent. Other factors of great importance influence these proportions, however. The dispersed droplets are ordinarily not uniform in size, nor need they necessarily be perfect spheres. High viscosity of one of the liquids favors its forming the continuous phase. The presence of an emulsifying substance, or surface active agent, is of great influence, and it is generally recognized that the liquid in which the emulsifying agent is soluble has the greater tendency to form the continuous phase. In the absence of emulsifiers, however, it is known that oil-in-water emulsions form more readily with low volumetric ratios of oil to water, and vice versa, and that inversion or change from one phase dispersed to the other will frequently occur on dilution of an emulsion with the continuous phase. Occasionally dual emulsions, where the continuous phase is also present as very small droplets dispersed in the drops of the other, result from partial or arrested inversion. Dilution of a sample of an emulsion will usually indicate to which type it belongs: an emulsion will mix readily with more of continuous phase, with difficulty with additional dispersed phase.

**Stability of Emulsions.** From the point of view of liquid-extraction operations, the stability or permanence of a dispersion is its most important property since it is necessary to separate the phases at each extraction stage. In order for an emulsion to "break," or separate into its phases in bulk, *both* sedimentation *and* coalescence of the droplets of the dispersed phase must occur.

The velocity of rise or fall of isolated liquid drops immersed in another liquid was studied by Bond and Newton (11), who showed that

$$U_\infty = \left(\frac{2\,\Delta\rho g r}{9\mu_C}\right) f\left(\frac{\mu_D}{\mu_C}, \frac{r\sigma}{W}\right) \tag{9.22}$$

where $U_\infty$ = terminal settling velocity of drop in viscous flow
$\mu_C$ = viscosity of the continuous phase
$\mu_D$ = viscosity of the dispersed phase
$r$ = radius of the drops
$\Delta\rho$ = difference in density of the two liquids
$g$ = acceleration due to gravity
$W$ = apparent weight of the drop allowing for buoyancy
$\sigma$ = interfacial tension

all in consistent units. The quantity in the first set of brackets is the familiar Stokes' law for rigid spheres. It was shown that for large drops, $r\sigma/W$ is small and the Stokes' law correction becomes

$$f\left(\frac{\mu_D}{\mu_C}, \frac{r\sigma}{W}\right) = \frac{1 + (\mu_D/\mu_C)}{\frac{2}{3} + (\mu_D/\mu_C)} \tag{9.23}$$

which in turn reaches a maximum value of $\frac{3}{2}$ when $\mu_D/\mu_C$ is small. For small drops, $r\sigma/W$ is large, the correction factor approaches unity, and Stokes' law becomes directly applicable. The interfacial tension becomes of importance when $r\sigma/W$ is approximately unity, although the precise nature of the interfacial tension function was not determined. Equation (9.22) cannot be applied directly to settling of emulsions since coalescence may vary the value of $r$ and because of the close crowding of the drops. It does indicate, however, that settling will be slower the greater the viscosity of the continuous phase, the smaller the density difference, and the smaller the drop size. Most stable emulsions are characterized by maximum particle diameters of the order of 1 to 1.5 microns (6), while diameters of the order of 1 mm. produce relatively coarse dispersions which settle fairly readily (30). The method of agitation may have an influence on the particle size. For example, Herschel (26) and Hunter and Nash (32) found, in agitating certain oils and aniline with water, that with increasing speed of agitation the rate of settling of the resulting dispersions at first decreased, passed through a minimum, and then increased. Similarly, Moore (47) noted that the size of the dispersed drops of a kerosene-aqueous ammonium chloride emulsion stabilized with lampblack passed through a minimum as the time of stirring was increased, and Rushton (54) has observed a critical speed of mixing above which emulsions of water–benzene, water–toluene, water–xylene, and water–methyl isopropyl ketone settled more rapidly.

The only factor causing coalescence is interfacial tension, whereas several oppose it (6, 7). Ordinarily, the greater the interfacial tension, the greater the tendency to coalesce. Interfacial tension will be low for liquids of high mutual solubility and will be lowered by the presence of emulsifying agents. High viscosity of the continuous phase hinders coalescence by decreasing the rate at which the thin film between drops is removed. The formation of tough interfacial films by substances such as certain proteins and other emulsifying agents may prevent coalescence. The presence of minute dust particles, which generally accumulate at the interface when dispersed in two-liquid-phase systems, can prevent coalescence. Certain dispersions are characterized by an electric charge on the droplets, which are then mutually repelled and cannot coalesce. The emulsion will be stable should the combined effects of all of these be stronger than the coalescent tendency of interfacial tension; practically, the presence of an emulsifying agent is almost always necessary for stability.

Stable emulsions must be avoided in liquid extraction, since their destruction requires removal or counteraction of the emulsifying agent responsible for their stability.

**Unstable Emulsions.** Meissner and Chertow (43) have given an excellent description of the appearance of an unstable emulsion during the time immediately following cessation of agitation, which is applicable to the great

majority of cases. As soon as agitation is stopped, the mixture separates by sedimentation and coalescence into two liquid layers (primary break), fairly rapidly unless the viscosity of the continuous phase is large. During this period, three distinct zones are discernible: a layer of light liquid at the top of the container, a layer of heavy liquid at the bottom, and a central portion containing the remaining unsettled emulsion. This period is considered complete when the upper and lower liquid layers have grown to meet at a sharply defined interface, at the expense of the central portion. Both liquid layers may then be clear, but ordinarily one of them, and sometimes both, are cloudy owing to a foglike dispersion of a relatively small quantity of the other phase. The cloud eventually settles out, leaving both layers clear (secondary break), although this process is ordinarily very slow. The phase which is present in the largest volume after primary break is usually clouded and the other clear, both conditions accentuated by increased volume ratio of the two phases. When the volume ratio exceeds approximately 3, corresponding to the 74 per cent packing density of spheres as discussed above, the layer in the minority is ordinarily entirely clear.

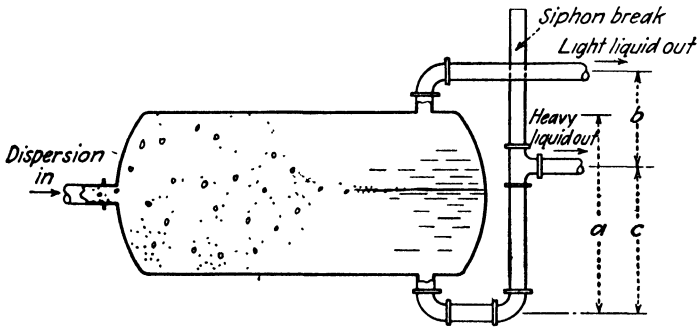



FIG. 9.15. Simple gravity settler.

**Settlers.** Primary break of the emulsion is ordinarily so rapid that merely providing a short period without agitation is usually sufficient to permit phase separation. In batch processes the mixture may be settled in the agitation vessel or in any other convenient tank. In continuous processes the mixture is usually allowed to flow through a vessel of large cross section where turbulence is at a minimum and holding time for settling is provided. The simple gravity settler, as it is called, is an empty tank such as that in Fig. 9.15. The level of the interface within the settler and the level of the heavy liquid in the siphon break adjust themselves so that

$$\bar{a}\rho_h + \Delta p_h = \bar{b}\rho_l + \bar{c}\rho_h + \Delta p_l \tag{9.24}$$

where $\bar{a}$, $\bar{b}$, and $\bar{c}$ = distances as indicated in the figure
$\rho_l$ and $\rho_h$ = density of light and heavy phases, resp.

$\Delta p_h$ = pressure drop in the heavy-liquid exit pipe
$\Delta p_l$ = pressure drop in the light-liquid exit pipe

For satisfactory operation without liquid-level control, the $\Delta p$ terms must be kept either very small or substantially equal, whence the relative height $\bar{c}$ for any desired interface position can be computed by

$$\bar{a}\rho_h = \bar{b}\rho_l + \bar{c}\rho_h \tag{9.25}$$

More positive control over the position of the interface to ensure satisfactory phase separations requires that a control valve operated by a liquid-level controller, in turn actuated by the position of the interface, be installed on the heavy-liquid exit pipe, with elimination of the siphon break. Devices of the sort described have been the subject of many patents [see, for example (19)].

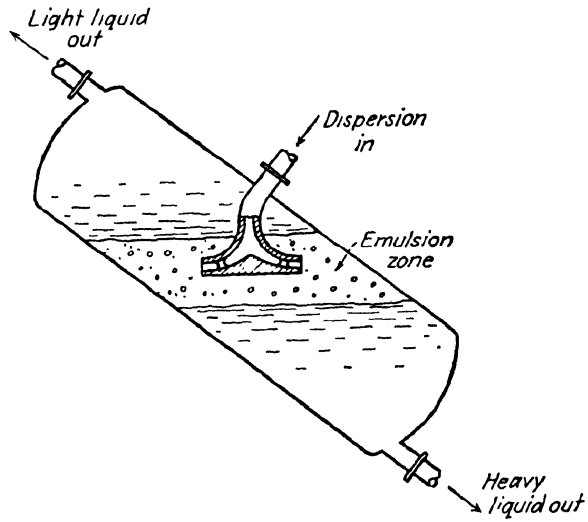



FIG. 9.16. Settler of Edeleanu, *et al.* (18).

Many variations of the simple gravity settler are in use. For example, vertical rather than horizontal settling seems to be more satisfactory in some cases (14), although the horizontal arrangement is usually preferred and would seem more logical. Advantages have been claimed for placing them at an angle, as in Fig. 9.16 (18, 57). Admission of the mixture to be settled at the level of the interface is favored; tangential entrance into a vertical tank, deliberately to produce a gentle swirl which presumably assists the settling has been suggested (37, 50). The device of Edeleanu, *et al.*, Fig. 9.16, reduces the velocity of the dispersion, and hence the turbulence, as it enters the settler. Baffles of various descriptions are frequently introduced to influence the direction of flow so as to cause impingement of the dispersion on the baffles. Baffles are also profitably used to

ensure laminar flow and to reduce the distance through which the dispersed phase must settle, thus reducing the settling time, as in the case of the settler of Burtis and Kirkbride (15), Fig. 9.17. The number of patents concerned with devices of this sort is very large.

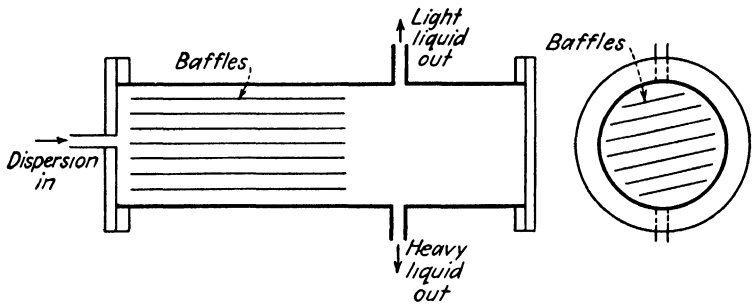



FIG. 9.17. Baffled settler (15).

A settler of unusual design, used in the modern Duo-Sol lubricating-oil refinery plants, is shown in Fig. 9.18. The liquid mixture enters as shown and flows through the narrow tray running down the center of the settler, after having passed through the bank of short pipes which serve to distribute the mixture. Since the height of the tray is only a few inches, settling is

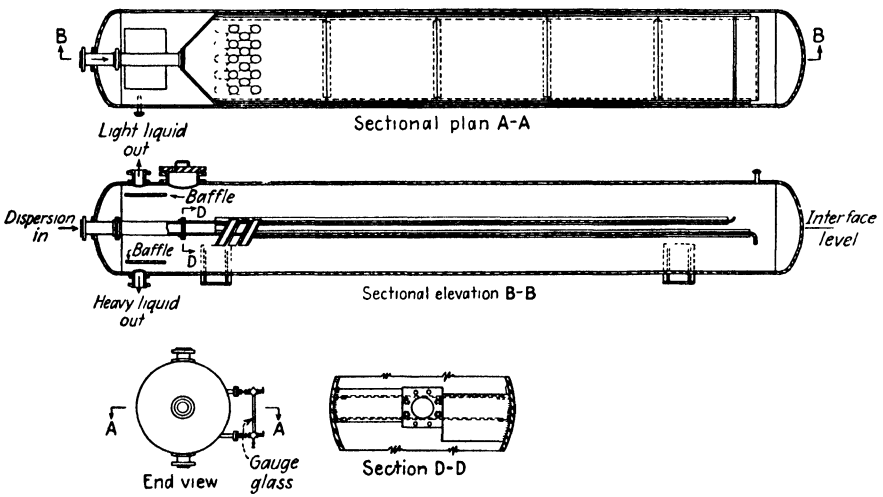



FIG. 9.18. Settler for Duo-Sol process. (*Courtesy, Max B. Miller and Co., Inc.*)

practically entirely complete by the time the mixture reaches the end of the tray. The settled layers either pass through the openings in the tray or around the end. The heavy layer then flows back through the space underneath the tray, the light layer through the space above. Any additional liquid which settles can pass through the short oblique pipes or around the

feed pipe. The liquids are then removed through the baffled openings, as shown.

The Stratford Engineering Corporation's "Decelerating Settler," successfully used in handling two-phase mixtures resulting from acid treatment of petroleum products and for caustic neutralization of acid oils, is shown in Fig. 9.19. This settler is unique in that the flow of emulsion is gradually decelerated by flow through a constantly expanding cross section, ultimately reaching a value of a fraction of an inch per second. Incoming mixture,

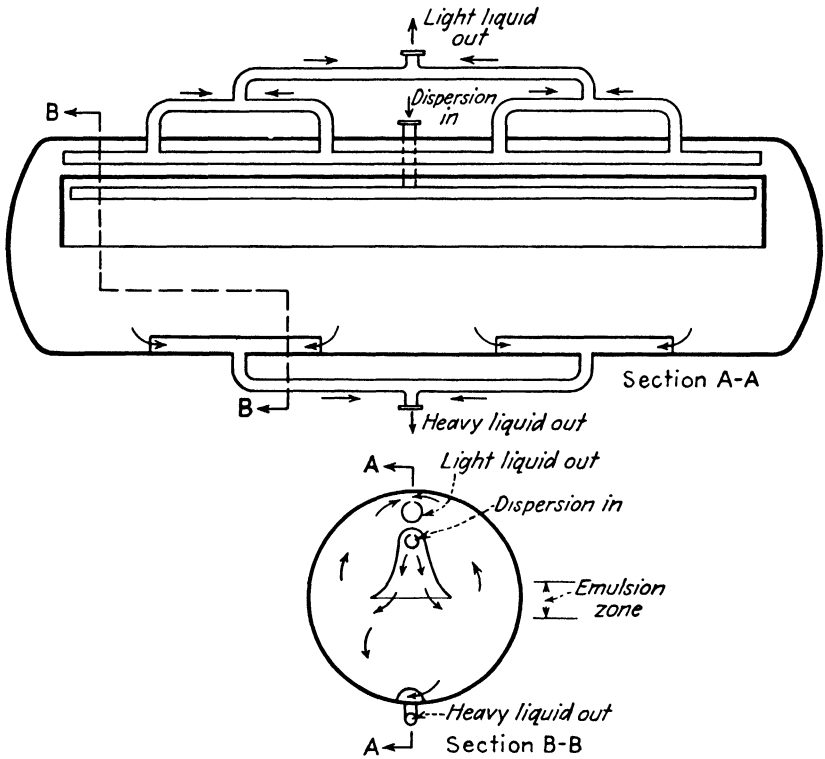



FIG. 9.19. Stratford settler. (*Courtesy, Stratford Engineering Corp.*)

distributed throughout the length of the vessel, enters through a slot in the inlet pipe under the hood, thus eliminating disturbances which would unduly agitate the settling emulsion.

The holding time to be used in the design of such settlers cannot be generally specified, since the time for primary break is so dependent upon the properties of the mixture to be settled, size of drops, and the nature of the previous agitation, as discussed above. Most settlers in the petroleum industry are designed for holding times of 30 min. to 1 hr., although with baffling to ensure laminar flow and small settling distances for the dis-

persed drops these times could frequently be shortened. Since the time of settling of a fog remaining after the primary break is usually considerable, it will rarely be practical to attempt the secondary break in such a settler without previous treatment of the emulsion, especially if additional extraction stages follow. Carry-over of a fog to a subsequent stage ordinarily results in only a small reduction in stage efficiency.

Where settling is slow due to small density difference, high viscosity of the continuous phase, or small particle size, centrifuges can be used to increase the rate. They are expensive machines, however, and can rarely be justified except in cases where the value of the product is high and low hold-up in settling devices is required, as in the case of penicillin extraction. Complete separation still requires coalescence, which is not affected by centrifugal force, and a stable emulsion will be merely concentrated and not broken by centrifuging (5).

**Inducing Coalescence.** Addition of excess of the phase which is dispersed will often bring about rapid coalescence, frequently if dilution is carried out at least to the extent of the 3:1 ratio mentioned previously. Bikerman (7) explains that in the case of water-in-oil petroleum emulsions the frequent success of such procedures is due to the presence of oil-soluble emulsifiers which normally tend to keep the oil as the continuous phase. Dilution beyond the 3:1 ratio, on the other hand, tends to bring about inversion to oil-in-water emulsions, so that as a net result no emulsion is stable.

The observations of Meissner and Chertow (43) with this technique are most informative. They showed that the secondary fog which may be present in the majority phase after primary break may frequently be coalesced and settled by addition of roughly four times its volume of the dispersed phase (the majority phase after the second settling is then likely to be clouded). After studying a large number of two- and three-component systems, it was shown that, with the exception of glycerol-nitrobenzene mixtures, coalescence of the secondary fog resulted when the dispersed phase was polar and did not occur if it was nonpolar. Thus, benzene clouded with a secondary fog of water droplets could be successfully treated by agitation with excess water, whereas water clouded by a benzene fog could not be clarified by addition of benzene. Distribution of hydrochloric acid between the phases, thus introducing a polar substance into both, made both fogs recoverable. Similarly, secondary fogs in either phase of nitrobenzene-water mixtures responded. For systems containing a polar dispersed phase, they suggest operation according to the flowsheet of Fig. 9.20: the dispersion of $A$ and $B$ is settled in settler no. 1, where primary break occurs; the clear $B$ layer is withdrawn, the clouded $A$ layer is agitated with excess $B$ layer; final settling in settler no. 2 then provides clear $A$ and clouded $B$ which is recycled. Other variations of this technique can be devised, but they all require extensive recycling.

Causing the emulsion to flow through a porous substance which has a large ratio of surface to volume but contains relatively large capillary openings, which is preferentially wetted by the dispersed phase, will frequently induce coalescence, possibly owing to mechanical destruction of the surface film surrounding the dispersed phase droplets. Thus, allowing water-in-petroleum emulsions to flow through a bed of excelsior is used extensively as a coalescing process. Beds of steel wool are successful in causing coalescence of the fog of aqueous alkaline solutions dispersed in gasoline (12).

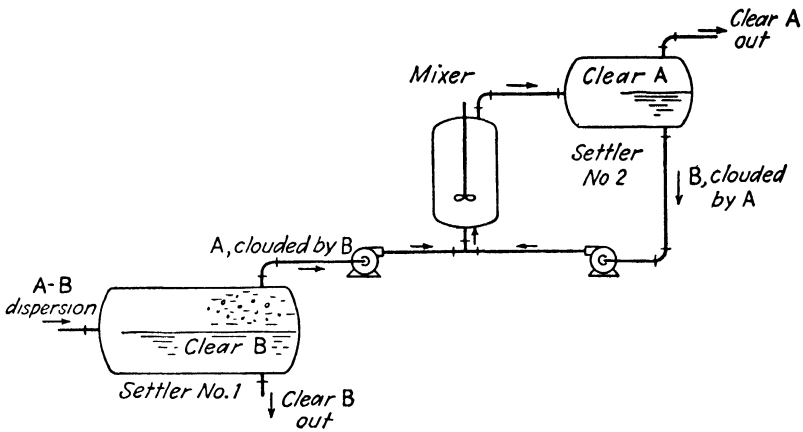



FIG. 9.20. Settling primary and secondary dispersions (43).

Beds of glass fibers (34) or layers of pumice stone (21) are useful. The most complete data on a coalescent device of this sort is provided by Burtis and Kirkbride (15) who report on tests of a Fiberglas bed for coalescing dispersions of salt water in crude petroleum. Their pertinent results can be briefly summarized, to indicate at least the nature of some of the variables which govern such processes: (*a*) efficiency of coalescence decreased with increasing velocity of flow; 0.25 to 1.0 ft./min. superficial velocity is effective, depending upon the properties of the emulsion, particularly water-oil ratio and temperature; (*b*) coalescence improved at elevated temperatures, probably because of reduced viscosity of the oil phase; (*c*) desalting of the oil improved as water-oil ratio increased, but it is not clear that this effect is entirely due to coalescence; (*d*) certain secondary emulsions failed to coalesce; (*e*) a depth of 3 to 4 in. of Fiberglas at a packing density of 13 lb./cu. ft. is ordinarily sufficient. These results were confirmed with a large-scale installation of the same process (25). Beds of coarse wire mesh, and even tower packings such as Raschig rings, have been successfully used as coalescers. These devices may be used immediately following the mixer or agitator, thus decreasing the holding time necessary in the settler which follows.

If the capillary size of a porous substance is very small, then although the liquid which preferentially wets the solid may flow through the capillaries readily, the strong interfacial films which separate the wetting from the nonwetting liquid may block the capillaries for flow of the nonwetting liquid. Sufficient pressure will cause the disruption of the film, permitting the nonwetting liquid to pass through the porous solid, but regulation of the pressure commensurate with the pore size and interfacial tension can permit separation of the phases. For example, the force resisting the distention of the interfacial film at the entrance to a circular capillary of diameter $d_0$ is the product of the circumference of the capillary by the interfacial tension $\sigma$. The force tending to cause disruption is the product of the cross-sectional area of the capillary by the pressure $p$. At equilibrium,

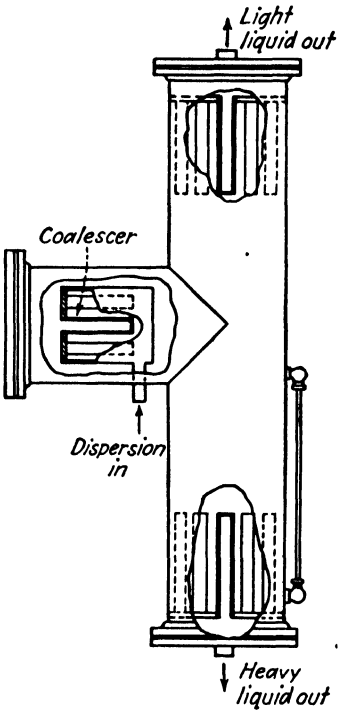



FIG. 9.21. Porous-membrane separator. (*Courtesy, Selas Corp.*)

$$\pi d_0 \sigma = \frac{\pi d_0^2 p}{4} \tag{9.26}$$

Thus, if a benzene-water dispersion, $\sigma = 35$ dynes/cm., is brought into contact with a porous porcelain which is preferentially wetted by water (hydrophilic) and which has been previously wetted, of maximum pore diameter of 2.0 microns (0.0002 cm.), Eq. (9.26) indicates an equilibrium pressure of 700,000 dynes/sq. cm., or 10.2 lb./sq. in. Thus, if the pressure is kept at a value less than 10.2 lb./sq. in., water will flow through the capillaries but the benzene will not, thus effecting the separation. Similarly a hydrophobic porous substance could be operated to permit the flow of benzene but not that of water. Figure 9.21 is a representation of a device which is successful in separating unstable emulsions by use of these principles. The emulsion is first passed through a porous solid for coalescing the dispersed phase, whereupon considerable settling occurs. The heavy liquid then passes through a porous solid of small pore diameter, treated in such a fashion as to be preferentially wetted by the continuous phase. Droplets of dispersed light phase do not pass through but collect and coalesce until large enough to rise to the upper part of the apparatus. The light liquid is handled in similar fashion. The theoretical principles upon which such a device operates have been outlined in some detail (55).

**Stable Emulsions.** The presence of some emulsifying agent is usually

responsible for stability of emulsions, and with a few exceptions this must be destroyed, counteracted, or removed for successful breaking. Berkman and Egloff (6) review in detail the general methods of dealing with stable emulsions, but they present such problems that liquid-extraction operations involving them cannot ordinarily be considered in industrial work.

## MULTIPLE-STAGE PLANTS

A multiple-stage plant will consist of several stages arranged for cocurrent or countercurrent operation, each stage consisting of a combination of at least a mixer and a settler of the types described above. Additional equipment, such as coalescers or centrifuges, may or may not be included, depending upon the difficulty of phase separation. Figure 9.22 shows a typical

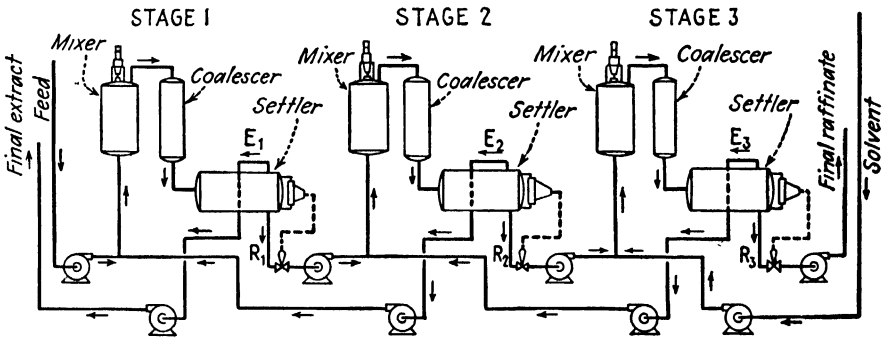



FIG. 9.22. Three-stage countercurrent extraction plant.

arrangement, and it can be appreciated that other types of mixers and settlers could be substituted and that different arrangements are possible. For example, if floor space is at a premium, the settlers can be built one over the other in the form of a tower, with the mixers and pumps on the ground level (22). In others, provided that density differences are sufficiently great, mixers and settlers can be arranged for gravity flow, thus eliminating transfer pumps between stages. The latter method is used in the Holley-Mott plant (2, 28), shown in Fig. 9.23, a design which has been very successful in the treatment of naphthas (1, 59) and in dephenolization of gas-works ammoniacal liquor (51). The interconnections between mixers and settlers for each stage provide for recirculation within the stage, so that relative proportions of the two phases in the mixer are independent of the relative net flows. Flow between stages is entirely due to difference in density of the liquids. The agitators of the mixers are simple, but for the liquids which have been contacted in such plants they are apparently entirely adequate. Morello and Poffenberger (48) described a plant of somewhat similar design. There has recently been made available a centrifugal extractor which is said to accomplish a single-stage extraction

TABLE 9.1. STAGE EFFICIENCIES OF DISCRETE-STAGE PLANTS

| Nature of service | Nature of plant | Nature of liquids | | | | Stage efficiency | Ref. |
|---|---|---|---|---|---|---|---|
| Extraction of phenols from gas ammonia liquor by light creosote oil | 5-stage countercurrent Holley-Mott system. Mixers: 4′3″ diam. by 8′ high, agitators 9″ off-center. Settlers: 9′ diam. by 18′ long, horizontal | Temp. 66–77°F. Sp. gr. gas liquor 1.02, Wash oil 0.94 | | | | | |
| | | Rates, g.p.h. | | Phenols in gas liquor lb./1,000 gal. | | | |
| | | liquor | oil | in | out | | |
| | | 8,000 | 4,000 | 26.6 | 2.3 | 79% | |
| | | 10,000 | 5,000 | 25.8 | 2.0 | 77% | (51) |
| | | 12,000 | 4,500 | 27.3 | 2.7 | 77% | |
| Extraction of phenols from gas ammonia liquor by crude light oil from coke plant | 3-stage countercurrent plant. Mixers: centrifugal pumps | Total phenols in gas liquor In 1.28, out 0.031 gm./liter | | | | ≐ 95% | (23) |
| Extraction of butadiene from $C_4$-hydrocarbons by ammoniacal cuprous acetate solution | Pilot plant. Mixers of the turbine type | ..... ..... | | | | 75–100% | (49) |

| | | | | |
|---|---|---|---|---|
| Extraction of butadiene from $C_4$-hydrocarbons by ammoniacal cuprous acetate solution | 7–8 stage countercurrent plant. Settlers: 6′6″ diam., 30′ long, with 3 horizontal baffles | Sp. gr. aqueous soln. 1.1–1.2. Sp. gr. hydrocarbons 0.61 Temp. 25°F. | 71–100% | (48) |
| Extraction of phenol from water by chlorobenzene | 8-stage plant. Mixer: 2′ by 2′ Settler: 2′ by 10′ | Temp. 110°F. | 75% | (48) |
| Extraction of phenol from water by chlorobenzene | 8-stage plant. Mixer: 8″ by 8″. Settler: 6′ by 1′ | Temp. 110°F. | 75% | (48) |
| Solvent refining of lubricating oils, Duo-Sol process (fractional extraction) | 7–9 stage countercurrent plants. Mixers: Between stages: 10–15′ pipe, with liquid velocities 10–16 ft./sec. Introduction of oil, Fig. 9.9. Settlers: Fig. 9.18. | Naphthenic solvent: cresylic acid (60%) + phenol (40%). Paraffinic solvent: propane | $\doteq$ 100% | (45) |

and separation (33), operating on the principle of the multistage continuous contactor described later.

**Stage Efficiencies.** No extensive studies of the stage efficiencies, or ratio of ideal to real stages, have been made available. Table 9.1 lists typical data on commercial-sized plants, and it appears that stage efficiencies of 75 to 100 per cent are readily obtained. It seems quite probable that to a large extent efficiencies below 100 per cent are due to incomplete

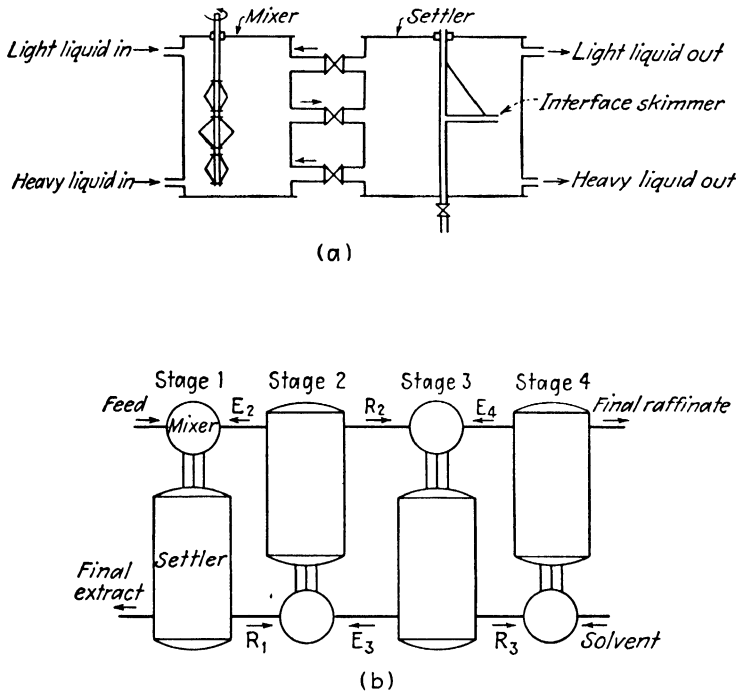



FIG. 9.23. Holley-Mott extraction plant (28). (*a*) Single stage; (*b*) four-stage-countercurrent plant.

settling rather than inadequate mixing in most industrial plants. Despite the more clumsy appearance, the discrete-stage type of plant is frequently favored over the continuous contact devices to be described in the next chapter, since with our present knowledge there is less uncertainty in obtaining the required number of stages.

**Laboratory Equipment.** Useful laboratory equipment for stagewise extraction is described by Knox *et al.* (35), which utilizes packed mixing columns or agitators with settlers much in the manner of large-scale equipment, and whose stage efficiency is apparently 100 per cent (4). For cases where large numbers of stages are required, the device of Martin and Synge (42) is convenient.

## Notation for Chapter 9

Units of the pound-foot-hour system are listed, but consistent units of any system may be used.

$A$ = interfacial area, sq. ft.
$b$ = constant, Eq. (9.16).
$c$ = concentration, lb. moles/cu. ft.
$d$ = differential operator.
$d_0$ = diameter of orifice or capillary, ft.
$E$ = quantity of extract, cu. ft.
$\mathbf{E}$ = fractional stage efficiency.
$e$ = base of natural logarithms, 2.7183.
$f$ = function.
$g$ = gravitational constant = $4.17 \times 10^8$ ft./hr.$^2$.
$K$ = over-all mass-transfer coefficient, lb. moles/hr. (cu. ft.)($\Delta c$)
$K'$ = constant, Eq. (9.16).
$K''$ = constant, Eqs. (9.16), (9.18).
$l$ = impeller diameter, ft.
ln = natural logarithm.
$m$ = distribution coefficient = $c_E/c_R$ at equilibrium.
$N$ = number of lb. moles solute transferred.
$n$ = number of vessels in a series.
$P$ = power, ft. lb./hr.
$p$ = pressure, lb./sq. ft.
$\Delta p$ = difference in pressure, lb./sq. ft.
$R$ = quantity of raffinate, cu. ft.
$r$ = radius of a drop, ft.
$Re$ = modified Reynolds number.
$S$ = impeller speed, revolutions/hr.
$U_\infty$ = terminal settling velocity of a drop, ft./hr.
$W$ = apparent weight of a drop, allowing for buoyancy, lb.
$y$ = fraction of a stream remaining in a vessel for a specified time.
$z$ = concentration, volume fraction.
$\theta$ = time, hr.
$\mu$ = viscosity, lb./ft. hr. = 2.42 (centipoises).
$\pi$ = 3.1416.
$\rho$ = density, lb./cu. ft.
$\Delta\rho$ = difference in density between phases, lb./cu. ft.
$\sigma$ = interfacial tension, lb./ft. = $6.89 \times 10^{-5}$ (dynes/cm.).
$\phi$ = $Pg/l^3S^2\mu$.

Subscripts:

av = average.
$C$ = continuous phase.
$D$ = dispersed phase.
$E$ = extract.
eq = final equilibrium.
$H$ = hold-up.
$h$ = heavy liquid.
$l$ = light liquid.
$R$ = raffinate.

Superscripts:

$^0$ = initial.
$^*$ = at equilibrium.

## LITERATURE CITED


1. Anglo-Persian Oil Co.: *Oil and Gas J.* **29,** No. 42, 96 (1931).
2. Anglo-Persian Oil Co., Ltd., A. E. Holley, and O. E. Mott: Brit. Pat. 321,200 (11/4/29).
3. Asquith, J. P.: *Trans. Inst. Chem. Engrs.* (London) **23,** 10 (1945).
4. Asselin, G. F., and E. W. Comings: *Ind. Eng. Chem.* **42,** 1198 (1950).
5. Ayres, E. E.: *Ind. Eng. Chem.* **13,** 1011 (1921).
6. Berkman, S., and G. Egloff: "Emulsions and Foams," Reinhold Publishing Corporation, New York, 1941.
7. Bikerman, J. J.: "Surface Chemistry," Academic Press, Inc., New York, 1948.
8. Bissell, E. S., H. J. Everett, and J. H. Rushton: *Chem. Met. Eng.* **53,** 118 (January, 1946).
9. ———, H. C. Hesse, H. J. Everett, and J. H. Rushton: *Chem. Eng. Progress* **43,** 649 (1947).
10. Bohm, E.: Brit. Pat. 550,331 (1/4/43).
11. Bond, W. N., and D. A. Newton: *Phil. Mag.* **5,** series 7, 794 (1928).
12. Border, L. E.: *Chem. Met. Eng.* **47,** 776 (1940).
13. Broderson, H. J., and W. E. Bartels: U.S. Pat. 1,594,041 (7/27/26).
14. Burkhard, M. J.: *Chem. Met. Eng.* **32,** 860 (1925).
15. Burtis, T. A., and C. G. Kirkbride: *Trans. Am. Inst. Chem. Engrs.* **42,** 413 (1946).
16. Chase, W. O.: U.S. Pat. 2,183,859 (12/19/39).
17. Colburn, A. P.: *Trans. Am. Inst. Chem. Engrs.* **31,** 457 (1935).
18. Edeleanu, L., K. Pfeiffer, K. Gress, and P. Jodek: U.S. Pat. 1,660,560 (1/17/28).
19. Edwards, W. K.: U.S. Pat. 1,968,131 (7/31/34).
20. Folsom, R. G.: *Chem. Eng. Progress* **44,** 765 (1948).
21. Gard, S. W., B. B. Aldridge, and H. J. Multer: U.S. Pat. 1,665,164 (4/3/28).
22. Gollmar, H. A.: *Ind. Eng. Chem.* **39,** 596 (1947).
23. ———, Koppers Co., Inc.: Personal communication (1950).
24. Hampton, A. C.: U.S. Pat. 2,091,709 (8/31/37).
25. Hayes, J. G., L. A. Hays, and H. S. Wood: *Chem. Eng. Progress* **45,** 235 (1949).
26. Herschel, W. A.: *U.S. Bur. Stds. Tech. Paper* No. 86, February, 1917.
27. Hixson, A. W., and M. I. Smith: *Ind. Eng. Chem.* **41,** 973 (1949).
28. Holley, A. E., and O. E. Mott: U.S. Pat. 1,953,651 (4/3/34).
29. Hooker, T.: *Chem. Eng. Progress,* **44,** 833 (1948).
30. Hunter, T. G.: "Science of Petroleum," A. E. Dunstan, Ed., Vol. 3, p. 1779, Oxford University Press, 1938.
31. ——— and A. W. Nash: *Ind. Chemist* **9,** 245, 263, 313 (1933).
32. ——— and ———: *Trans. Chem. Eng. Congr. of World Power Conf.* (London) **2,** 400 (1937).
33. Kaiser, H. R., Podbielniak, Inc.: Personal communication (1949).
34. Kleinschmidt, R. V.: U.S. Pat. 2,143,015–6 (1/10/39).
35. Knox, W. T., R. L. Weeks, H. J. Hibshman, and J. H. McAteer: *Ind. Eng. Chem.* **39,** 1573 (1947).
36. Leaver, C.: U.S. Pat. 1,733,545 (10/29/29).
37. Linnman, W.: U.S. Pat. 1,958,054 (5/8/34).
38. Lyons, E. J.: *Chem. Eng. Progress* **44,** 341 (1948).
39. Mack, D. E., and A. E. Kroll: *Chem. Eng. Progress* **44,** 189 (1948).
40. Macmullin, R. B., and M. Weber: *Trans. Am. Inst. Chem. Engrs.* **31,** 409 (1935).
41. Mahoney, L. H., Mixing Equipment Co., Inc.: Personal communication (1950).
42. Martin, A. J. P., and R. L. M. Synge: *Biochem. J.* **35,** 91 (1941).
43. Meissner, H. P., and B. Chertow: *Ind. Eng. Chem.* **38,** 856 (1946).

44. Mensing, C. E.: U.S. Pat. 2,405,158 (8/6/46).
45. Miller, Max B., Jr., Max B. Miller and Co., Inc.: Personal communication (1950).
46. Miller, S. A., and C. A. Mann: *Trans. Am. Inst. Chem. Engrs.* **40,** 709 (1944).
47. Moore, W. C.: *J. Am. Chem. Soc.* **41,** 940 (1919).
48. Morello, V. S., and N. Poffenberger: *Ind. Eng. Chem.* **42,** 1021 (1950).
49. Morrell, C. E., W. J. Paltz, W. J. Packie, W. C. Asbury, and C. L. Brown: *Trans. Am. Inst. Chem. Engrs.* **42,** 473 (1946).
50. Morrell, J. C., and D. J. Bergman: *Chem. Met. Eng.* **35,** 211, 291, 350 (1928).
51. Murdoch, D. G., and M. Cuckney: *Trans. Inst. Chem. Engrs.* (London) **24,** 90 (1946).
52. Olney, R. B., and G. J. Carlson: *Chem. Eng. Progress* **43,** 473 (1947).
53. Rushton, J. H.: *Ind. Eng. Chem.* **42,** 74 (1950).
54. ———: Illinois Institute of Technology: Personal communication (1950).
55. Selas Corporation of America: "Physical Separations of Immiscible Fluids," Philadelphia, 1943.
56. Sheldon, H. W.: U.S. Pat. 2,009,347 (7/23/35).
57. Soule, R. P.: U.S. Pat. 1,594,024 (7/27/26).
58. Stratford, C. W.: U.S. Pat. 1,736,018 (11/19/29); 1,815,366 (6/21/31).
59. Thornton, E.: *J. Inst. Pet. Technol.* **19,** 957 (1933).
60. Valentine, K. S., and G. MacLean: In "Chemical Engineers' Handbook," J. H. Perry, Ed., 3d. ed., McGraw-Hill Book Company, Inc., New York, 1950.
61. Yates, P. B., and H. E. Watson: *J. Soc. Chem. Ind.* **59,** 63T (1940).
62. Young, H. W., and A. W. Peake: *Chem. Met. Eng.* **27,** 972 (1922).

CHAPTER 10

# EQUIPMENT FOR CONTINUOUS COUNTERCURRENT CONTACT

Equipment wherein the insoluble liquids flow countercurrently in continuous contact can be built to contain the equivalent of as many stages as desired. In every case, the countercurrent flow is brought about by the difference in densities of the two liquids, and the equipment usually takes the appearance of a vertical tower with or without internal devices to influence the flow pattern. The length of path of travel for the liquids is dependent upon the number of stages required, while the cross-sectional area for flow depends upon the quantities of the liquids to be handled. The number of designs which have been proposed is very large, as evidenced by the considerable patent literature. Only a relatively few major types have had successful industrial application, however. These may to a certain extent be classified according to the method of contacting the liquids, as follows:

1. Film contact, neither liquid dispersed. One liquid is spread over a surface in the form of a film while in contact with the other liquid.

2. Dispersed contact, where one or both liquids are mechanically dispersed to provide increased area for extraction. Dispersion may be brought about by causing one of the liquids to flow through nozzles, orifices, screens, packing, etc., or by agitation. The liquids may be dispersed once or many times after intermediate coalescence.

Such a classification is far from perfect, since in many of the second type film-flow occurs at least in part of the equipment. On the other hand, the second type includes practically all the commercially important equipment and will be considered first.

## EQUIPMENT TYPES

**Spray Towers.** Spray towers are the simplest of the equipment involving dispersion of one of the liquids, and as shown diagrammatically in Fig. 10.1, they are merely empty shells with provisions for introducing and removing the liquids. Consider operation according to Fig. 10.1*a*, where the light liquid is dispersed. Heavy liquid entering at the top through the distributor fills the tower almost completely, flows downward as a continuous phase, and leaves at the bottom. As shown in the figure, it leaves through a loop *b* so as to ensure the tower being filled with liquid. Light liquid enters at the bottom through a distributor which disperses it

into small drops. These rise through the continuous heavy liquid by virtue of their smaller density and collect in a layer $d$ at the top, which then flows out of the tower. The head of heavy liquid at the bottom of the loop $b$ (static pressure + pressure drop due to friction) must balance the head of combined light and heavy liquids in the tower, and the position of the interface $e$ will adjust itself accordingly.

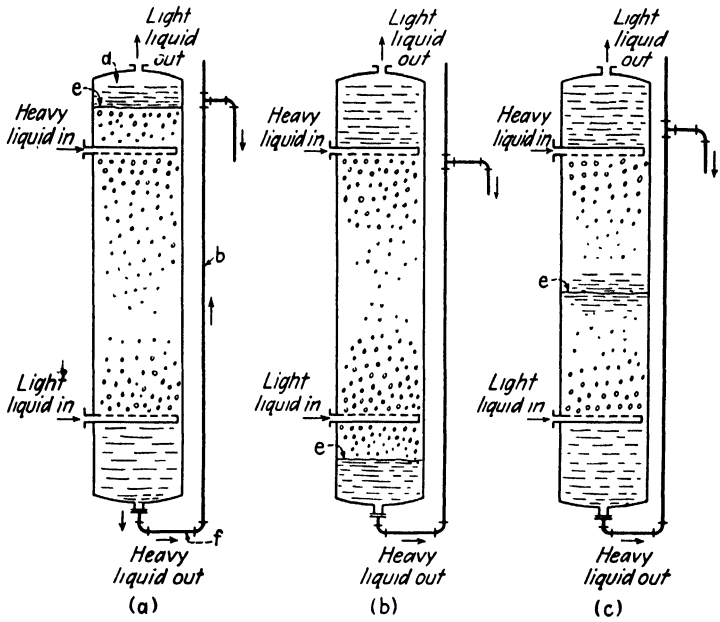



FIG. 10.1. Spray tower.

It is clear that if the loop carrying the heavy liquid out of the tower is lowered, as in Fig. 10.1*b*, the interface $e$ must move downward, and by adjustment of the loop height it can be made to locate itself at the bottom of the tower as shown. The tower then operates with the heavy liquid dispersed into drops. Alternatively, the interface can be regulated so as to remain near the center of the tower, as in Fig. 10.1*c*. The loop arrangement for regulating the position of the interface is used frequently in laboratory and pilot-plant towers, but in industrial practice it is much more satisfactory to regulate the pressure drop through the heavy liquid exit pipe by a valve at $f$, preferably automatically operated by a liquid-level controller actuated by movement of the interface, thus dispensing with the necessity of the loop. The figures show the arrangement for operating with stripping or enriching sections only; if central feed is used, a distributor much like those at the top and bottom of the tower is used to introduce the feed liquid at the desired position in the tower.

Consider again the operation shown in Fig. 10.1*a*, with the rate of flow of heavy liquid fixed while that of light liquid is slowly increased. At low rates for the light liquid, the drops of dispersed phase form regularly at the distributor and rise without interference to collect in the layer at the top. As the rate is increased, drops are formed more frequently and they tend to crowd each other as they rise; the hold-up of dispersed phase increases. Since the pressure drop through the light-liquid exit pipe at the top of the tower increases with increased flow, there will be a tendency for the interface *e* to lower, which can be overcome by raising the loop *b* or by closing down slightly on a valve at *f*. The increased hold-up of dispersed phase reduces the available area for flow of the continuous phase, which must then flow at higher local velocities. As the rate of flow of light liquid is further increased, the hold-up of dispersed phase increases, and the increased velocity of the continuous phase usually causes very erratic movement of the drops. Large eddy currents develop, considerable swirl may occur, and with a glass tower it can be observed that there is considerable recirculation (rise and fall) of the drops. The distributor causes a restriction in the free area for flow of dispersed phase and will ordinarily be the cause of difficulty. Crowding of the drops at this point may result in coalescence into large globules of light liquid which may be carried down into the lower part of the tower. Hold-up of light liquid is thus increased greatly, and large quantities are carried out the exit pipe for the heavy liquid. The tower seems to fill with light liquid, which frequently becomes the continuous phase. The tower is then *flooded*, and satisfactory operation is no longer possible. The same situation will ordinarily arise if the light liquid rate is kept constant and heavy liquid rate is increased, although at very low rates for the light liquid, it may be observed that before flooding occurs appreciable numbers of drops of dispersed phase are carried out with the heavy liquid owing to its high velocity. For each rate of flow of light liquid there is a rate for the heavy liquid beyond which satisfactory operation cannot be maintained.

A great many of the difficulties described above can be avoided if care is taken not to restrict the flow area in the tower and to introduce the continuous phase with a minimum of disturbance to the flow pattern. The column described by Elgin and Blanding (9, 24) is exceptionally satisfactory in this respect and is shown diagrammatically in Fig. 10.2 for operation with light liquid dispersed. At the top, the heavy liquid is introduced in such a manner as not to result in high local velocities. At the bottom, the flared end is constructed preferably with an angle from the vertical not greater than 16°, which results in a gradually decreasing downward velocity of the continuous phase. The annular space between the walls of the expanded bottom section and the distributor should be sufficiently large to reduce the velocity of the continuous phase to from 0.2 to 0.9 its value in

the column proper. In this way formation of the drops at the distributor is not disturbed. With such arrangements, the flow regime for flooding is characterized by high hold-up of dispersed phase in the column, with the mass of drops extending down into the funnel-shaped lower end. Excessive coalescence does not occur nor is the dispersed phase carried out with the heavy liquid, and operation in the flooded state is perfectly feasible. Much higher flow rates are possible than with straight-sided towers. For operation with the heavy phase dispersed, the tower is constructed in upside-down fashion as compared with the arrangement of Fig. 10.2. Other designs embodying these principles have been suggested (15), but none have been so well worked out.

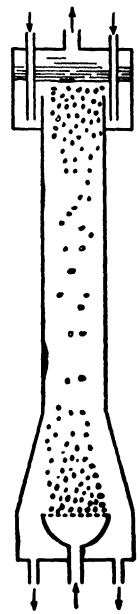


FIG. 10.2. Spray tower of Elgin (24).

The freedom with which the continuous phase can recirculate in the spray tower may lead to a lowering of extraction efficiency because of the lack of true countercurrent flow. This would presumably be aggravated with large tower diameters, and at least in one case (59) several small-diameter towers in parallel were used in preference to one with a large diameter in an attempt to overcome this tendency. Presumably vertical baffling in a single tower would also be helpful.

The simplicity of construction, low cost, ease of cleaning, trouble-free operation, and high flow capacities make the spray tower very attractive, although the height required for a given number of stages will ordinarily be greater than for other types.

**Packed Towers.** In order to increase the turbulence of the flow regime so as to improve extraction rates, the towers are frequently filled with packings of the type commonly used in gas absorption work. Raschig rings, which were early applied to these problems (67), and Berl saddles are most frequently used, and descriptions of these are given in the standard reference works (63). Other packings such as wooden grids (35), lumps of coke (38, 47), and spiral wire work (11) have also been successful. Packing of the type that is dumped at random may be supported on an open screen work, woven of sufficiently heavy wire to support the necessary weight, with openings just small enough to retain the packing pieces. Perforated plates have been used, but they usually offer such restriction to flow that flooding is very likely to occur at the packing support. If the continuous liquid rather than the dispersed preferentially wets the packing support, it is important that the dispersed-phase distributor be embedded in the packing (24), else crowding of the drops of dispersed phase at the support, with coalescence and flooding, is likely to occur. If the continuous phase wets the packing preferentially, the dispersed phase passes through the

tower in droplets. If the dispersed phase wets the packing preferentially, it flows along the packing in rivulets or continuous films. As with spray towers, the interface between phases may be held at any desired level.

Although no systematic study has been made respecting the relative size of the packing particles to be used as compared to the diameter of the tower, it seems reasonable to follow the principles established for gas-absorption work, that the ratio of tower diameter to particle size should not be less than 8:1. This should reduce the tendency toward channeling and would seem particularly important when attempting to obtain design data from experiments with small towers, where the packing density in the pilot plant ought to be the same as that expected in the large tower. It is common practice to arrange the packing in the tower in a series of beds separated by unpacked spaces, as in Fig. 10.3, to provide for redistribution of the liquids should channeling occur. In cases where the dispersed liquid flows in a film over the packing, this practice also provides for redispersion of the liquid and exposure of new surface to contact with the other phase. Cooling or heating coils can conveniently be installed in these open spaces should they be required. For cases where the dispersed phase does not wet the packing support, however, this may lead to flooding difficulties as described above. Baffles at intervals can also be used to circumvent channeling tendencies (10), or one of the liquids may be withdrawn entirely by a collecting device and be redistributed (22).

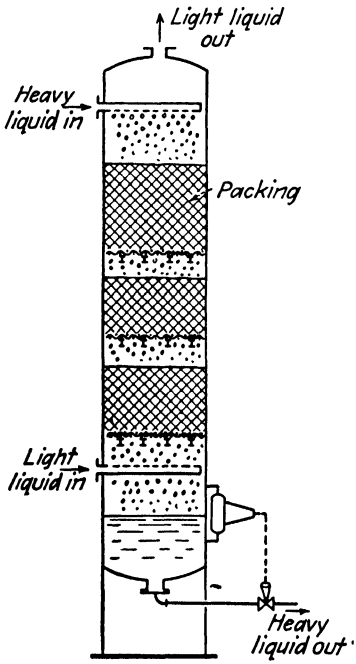



FIG. 10.3. Packed tower.

The approach to flooding in packed towers is usually characterized by increased hold-up of dispersed phase within the packing, with increased coalescence giving the dispersed phase a tendency to become continuous. At flooding, a layer of dispersed phase appears at the inlet to the packing, and further increase in the flow rate causes dispersed phase to flow out the exit pipe for the continuous liquid. Should the packing support offer excessive restriction to flow, however, flooding may occur owing to disturbances at this point at rates of flow considerably below the maximum that can be put through the packing alone. As might be expected, the maximum flow rates for packed towers are considerably less than for spray towers because of the decreased area for flow and the increased tendency

toward coalescence. Higher rates than otherwise can be obtained with the end designs of Elgin (24).

After the spray towers, packed towers are undoubtedly the simplest to construct and are probably the least costly for handling highly corrosive liquids. Where the liquids contain suspended solids, or where solids may be precipitated during the course of extraction, however, the tendency of the packing to clog and the difficulty of cleaning make them less desirable. Packed towers have had extensive application in the solvent refining of lubricating oils, removal of hydrogen sulfide from petroleum fractions, sweetening of naphthas, removal of phenols from gasworks ammoniacal liquors, solvent refining of vegetable oils, and in general chemical recovery in the synthetic organic chemicals industries.

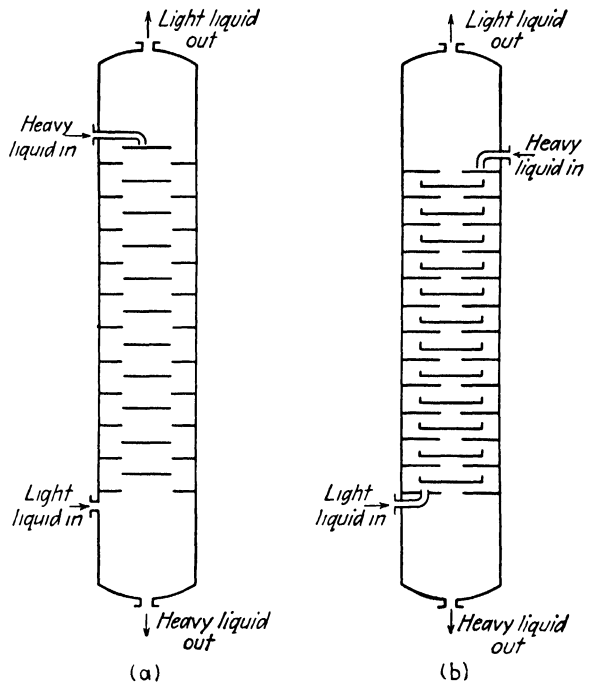



FIG. 10.4. Disk-and-doughnut baffle towers. (*a*) *after Thompson* (80); (*b*) *after Ittner* (44).

**Baffle Towers.** These extractors consist of vertical towers containing horizontal baffles to direct the flow of the liquids. There are three principal types: disk-and-doughnut, side-to-side, and center-to-side.

Disk-and-doughnut baffles consist of alternate annular rings (doughnuts) attached to the shell of the tower and centrally located circular disks supported by spacer rods or by arms extending to the shell (23). In some designs, Fig. 10.4*a*, the disks have the same diameter as that of the opening in the doughnut, as suggested by Thompson (80). In Ittner's arrange-

ment (44), Fig. 10.4*b*, the central opening of the doughnut is relatively small and the disks are provided with lips to form a pool of heavy liquid on the disk. These devices have been in use for years despite the relatively recent dates of the patents. In this type of column, the dispersed liquid flows along the baffle in a thin film and then falls over the edge of the baffle in a broken sheet through the continuous liquid. If interfacial tension and

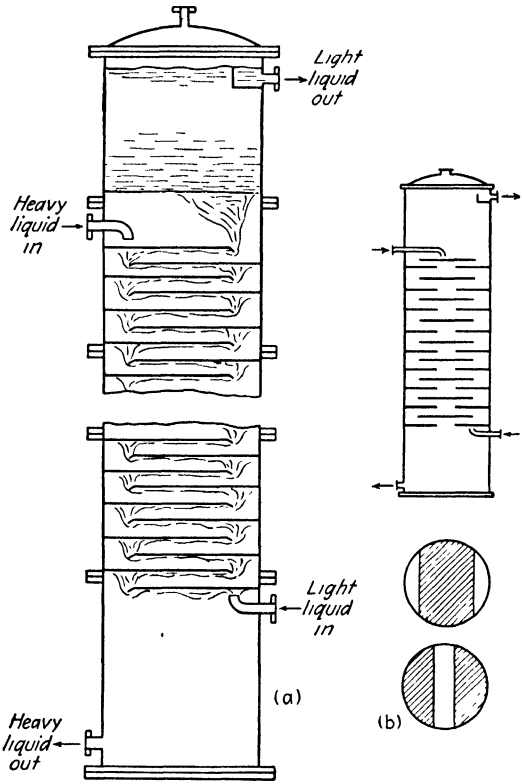



FIG. 10.5. Baffle towers. (*a*) side-to-side; (*b*) center-to-side. (*Courtesy, Vulcan Copper and Supply Co.*)

density difference are low, the tendency for the dispersed liquid to remain in film and sheet form will be considerably lessened, and instead the behavior is more like that of a spray tower with the baffles providing additional turbulence. Coahran's tower (17) provides for radial veins on the upper and lower surface of both disks and doughnuts and slow rotation of the disks which are supported on a central shaft. The agitation thus provided adds to the effectiveness of contact. Still another type, in use for some time for extraction of acetic acid from pyroligneous liquor (59), provides rotating arms attached to the central rotating shaft which scrape accumu-

lated solids from the doughnut baffles and stationary arms attached to the shell which scrape the rotating disks.

Side-to-side flow is provided by the segmental baffle arrangement of Fig. 10.5*a*. In the design shown, the baffles are made with a collar to provide a friction fit in the shell, are kept in place by spacer posts, and are fitted with an edge lip which not only stiffens the baffle but also provides a means of collecting a pool of dispersed liquid on the baffle (33). The center-to-center type, Fig. 10.5*b*, is the same in principle but is used in the larger diameter towers to reduce the length of travel of the liquid film on the baffle. Baffle spacing in these towers is ordinarily 4 to 6 in. The towers are versatile, capable of handling a wide variety of liquids and flow rates, and have had application in the extraction of acetic acid from pyroligneous liquors and from solutions used in cellulose acetate rayon manufacture, in the extraction of caffeine in the food industries, and for general chemical recovery in the synthetic organic chemicals industries.

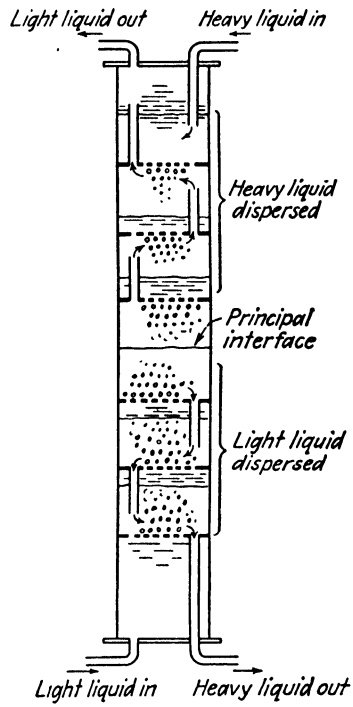



FIG. 10.6. Perforated-plate tower (34).

**Perforated-plate Towers.** In the perforated-plate, or sieve-plate, column, the dispersed phase is repeatedly coalesced and redispersed by causing it to flow through a series of trays in which a large number of small holes have been punched or drilled. In the simplest type, the plates are similar to the side-to-side baffles described above, except that they are perforate. Hunter and Nash (42) describe a successful installation of this type for dephenolating gas liquor consisting of a 46-ft.-high shell, 5 ft. in diameter, in which the baffles each contain two hundred $\frac{1}{16}$-in. holes.

Usually some more positive means of conducting the continuous liquid from tray to tray is provided. In Fig. 10.6, a tower of the type described by Harrington (34), for example, the continuous phase flows across the plates and from plate to plate by means of the pipes provided for that purpose. These pipes extend sufficiently far to be sealed in the layer of continuous liquid on the plate. The dispersed phase collects on the trays in a coalesced layer and bubbles through the perforations of the plate. As shown, the light liquid is dispersed in the lower part of the tower and the heavy in the upper part, although only one of the liquids, preferably that which does not wet the plate, needs be dispersed. When the flow of con-

tinuous liquid is large, in order to reduce the pressure drop through the downcomers or risers, larger cross section for flow can be provided by segmental flow areas (79) as in Fig. 10.7; for still larger diameters, alternate center and side downcomers can be provided. While it is customary to install the pipes or ducts for the continuous phase with a short lip extending beyond the tray from which it leads the liquid, higher flow capacities can be obtained if the pipes are kept flush with the plates (66). These ducts have on occasion been filled with tower packing such as Raschig rings for coalescing any dispersed phase which may be entrained by the continuous phase.

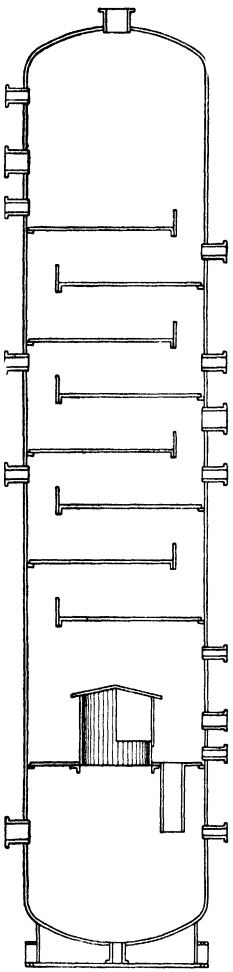


FIG. 10.7. Perforated-plate tower. (*Courtesy, Standard Oil Development Co.*)

Perforation sizes vary from $\frac{1}{16}$ to $\frac{3}{8}$ in. in diameter in practice, and tray spacings from 6 in. to 2 ft. or more. It is observed that at certain flow rates the dispersed phase issues from the perforations in jets, which may reach considerable length before dispersing into droplets. For efficient extraction, the plate spacing should be sufficiently great that these jets are dispersed before they reach the coalesced layer on the next plate. Flooding in the equipment can occur either due to inability to maintain the position of the principal interface between the light and heavy liquids at the end of the tower (or at the center if so operated), or else due to thickening of the coalesced layer on a plate until it reaches the adjacent plate.

Towers of the type described have been extensively used, particularly in petroleum refining where they have been built to diameters of 12 ft. Modifications have been suggested, such as that of Laird (52) which provides for tilting the perforated trays and of van Dijck (83) which involves rapid vibration of the plates. A design which substitutes a fine, wire-mesh screen for the perforated tray (54) has been used in the refining of wood rosin, with a 3-ft.-diameter tower and an 8-in. tray spacing (41).

Designs which utilize a vertically arranged perforated plate have been particularly popular in petroleum-refining work. An early device (56) caused light liquid to collect underneath the plates in a tower and bubble through perforations in a downcomer which led the heavy liquid from plate to plate. A more modern design, Fig. 10.8, is an arrangement successfully used for large-diameter towers. The heavy phase

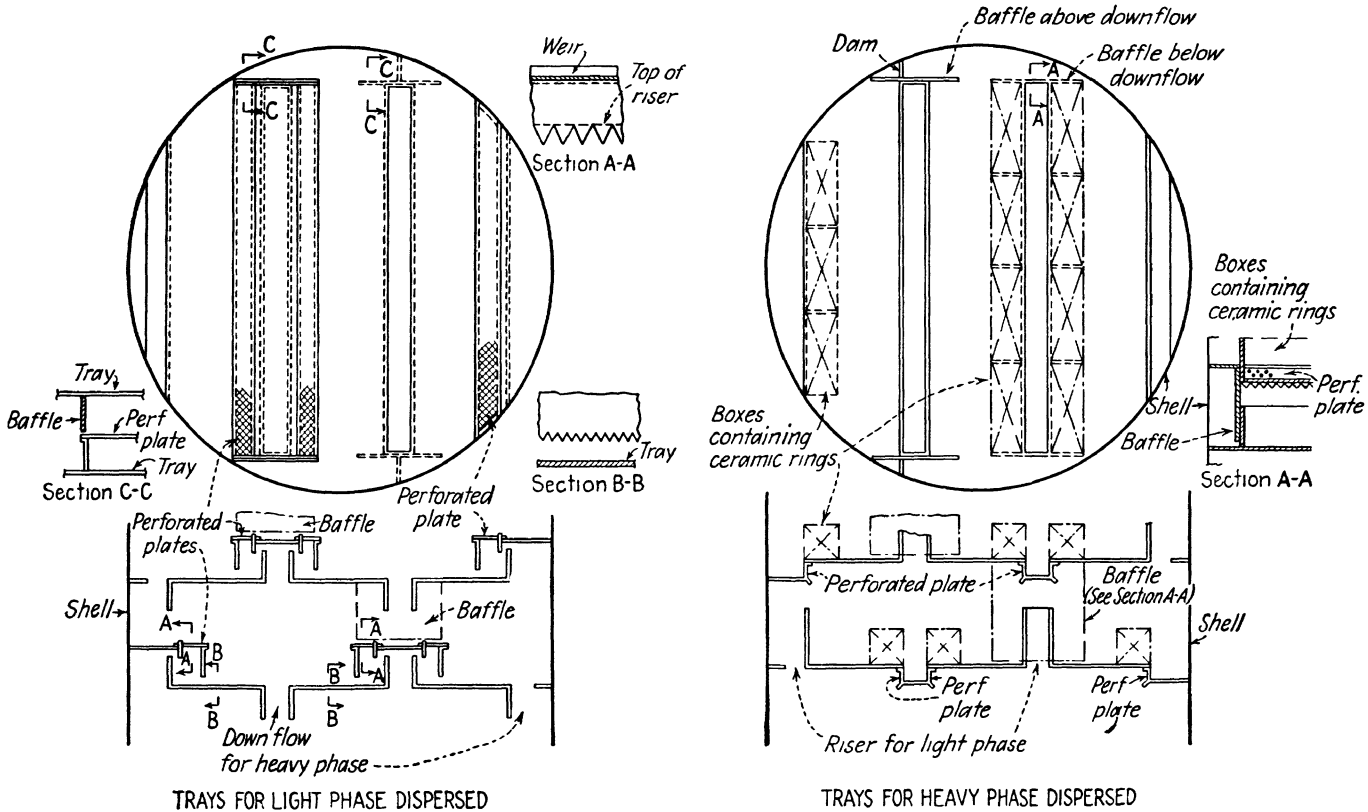



FIG. 10.8. Perforated plates for large-diameter towers. (*Courtesy, M. W. Kellogg Co.*)

is dispersed in the upper section of the tower by trays constructed with vertical perforated plates flanked by boxes containing Raschig rings to coalesce entrained light liquid (4). The light liquid is dispersed by trays with horizontal perforated plates in the lower section of the tower.

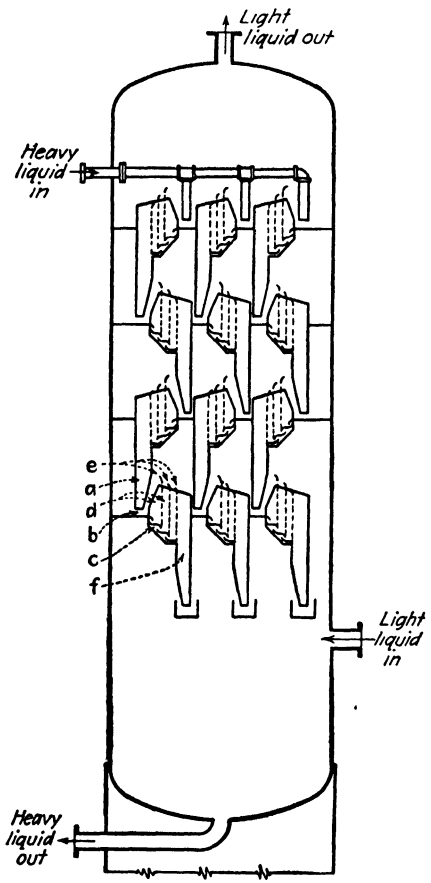



FIG. 10.9. Koch tower. (*Courtesy, Koch Engineering Co., Inc.*)

The Koch tower (50), Fig. 10.9, is an unusual arrangement involving perforations in a vertical plate. This device was originally used for vapor-liquid contact, but several installations for contacting gasoline with caustic sweetening solutions have been made. In a typical tray, heavy liquid flows down the downcomer at *a* and through the opening at *b*. Light liquid flowing upward enters the openings *c*, and through the spaces at *d*, thus sweeping the heavy liquid upward along the vertical perforated plates *e*. The heavy liquid flows through the perforations, falls, and is swept upward again through the next perforated plate, thus experiencing several dispersions. Final disengagement and coalescence take place in the downcomer at *f*.

**Other Dispersion Contactors.** The success of the bubble-cap column in liquid-vapor contacting naturally led to attempts at application in liquid-liquid contacting, and its use for this purpose has been patented (14). No record of commercial installations is recorded. Some early experiments in contacting lubricating oil with dichloroethyl ether by Rogers and Thiele (68) with bubble caps of more or less conventional design showed such low capacity and tray efficiency ($< 33$ per cent), and similarly in contacting water–benzoic acid solutions with benzene by Sherwood (75) (efficiency $< 5$ per cent) that extensive work with these devices has been to some extent discouraged. It is quite possible that if designs were modified to take into consideration the lower density differences and interfacial tensions, and higher viscosities encountered in liquid-liquid contact a successful arrangement could be devised.

A simple but apparently very effective design is described by Allen, *et al.*

(1), used in an experimental tower for contacting high-molecular-weight fatty acids with water, Fig. 10.10. The streams of insoluble liquids must cross at right angles on each tray. In the 5-in.-diameter tower, the trays were spaced at 1 in. A somewhat similar design, but without the risers and downcomers, was suggested by Ittner (44).

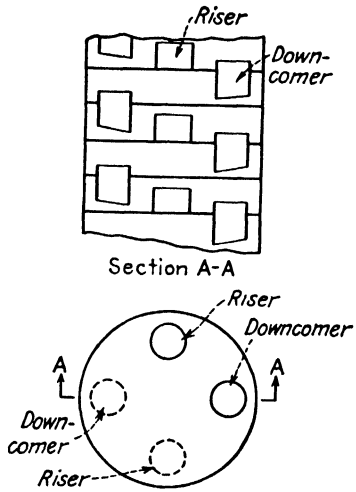



FIG. 10.10. Tray contactor (1). (*Permission, American Institute of Chemical Engineers.*)

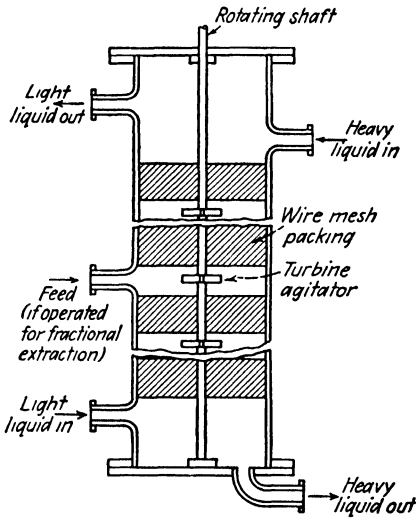



FIG. 10.11. Scheibel column. (*Courtesy, Otto H. York Co., Inc.*)

Although Jantzen (45) early described some highly successful extractions in small-scale equipment fitted with internal agitation for redispersion of the liquids, it is only recently that a successful device in commercial sizes has been produced by Scheibel (72, 73), Fig. 10.11. The agitators are simple four-bladed flat turbines, which operate at speeds up to 600 r.p.m. depending on the materials being extracted. The emulsions produced in the agitator zones are coalesced by the fine wire mesh. Successful operation is apparently sensitive to the design of the mesh, and a specially prepared mesh is used containing 97 to 98 per cent voids. The packed sections may be varied in thickness from 1 in. in laboratory-sized columns to 1 ft. or more in commercial-sized columns. Successful pilot-plant towers of 12 and 14 in. in diameter have been operated.

A laboratory column utilizing alternate agitated sections and settling zones is described by Cornish *et al.* (21). Simpler laboratory devices which also give high extraction efficiencies consist merely of a vertical tube containing a rotating axial rod (62, 74).

**Wetted-wall Equipment.** Wetted-wall equipment resembling that used in gas-absorption studies has been used for laboratory investigations only

in studies where an attempt has been made to control and measure the interfacial area between the immiscible liquids. These devices provide for the heavy liquid to flow down the inside wall of a circular pipe an inch or two in diameter, while the light liquid flows upward as a central core. It is unlikely that devices of this sort will find commercial application, since stable operation is difficult to maintain. Difficulty is encountered with preferential wetting of the wall by the core liquid, tendency of the core liquid to sweep the wall fluid away from the wall, and of the wall fluid to break away and shower down through the core fluid in droplets. Only a limited range of flow rates for either phase is possible.

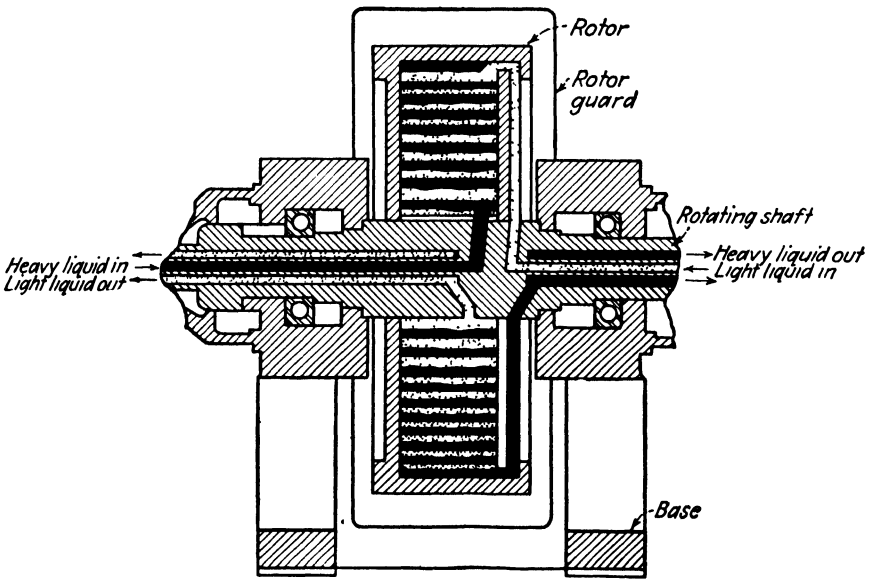



FIG. 10.12. Schematic diagram of liquid flow through Podbielniak extractor. (*Courtesy, Podbielniak, Inc.*)

A variant of the wetted-wall column was designed by Gordon and Zeigler (32) where the heavy liquid flows down an inclined flat plate while the light liquid flows upward in countercurrent. The passages for liquid flow are rectangular in cross section, ½ in. wide, and arranged in parallel. At least one successful installation has been recorded (59).

The Podbielniak centrifugal contactor (64), Fig. 10.12, is a modification which has been singularly successful, however. This device consists principally of a passage, rectangular in cross section and wound in a spiral of 33 turns, through which the liquid flows. The spiral rotor is revolved at speeds between 2,000 and 5,000 r.p.m., depending upon the service conditions. Light liquid is pumped into the machine through the shaft on which the rotor revolves and is led to the periphery of the spiral; heavy liquid

is similarly pumped to the center of the spiral. Owing to the considerable centrifugal force developed by the rotation, the heavy liquid flows countercurrently to the light liquid to the periphery of the spiral from where it is led back to the shaft and out of the machine. In the same fashion the light liquid flows to the center and is likewise removed from the shaft. The machines are made in various sizes capable of handling 500 cu. cm./min. in the laboratory size up to 2,400 gal./hr. of combined liquids for industrial work. At least in some designs, the spiral has been perforate. They are expensive in first cost and to operate but offer the following advantages: a wide range of feed-to-solvent ratios are feasible; low floor-space and headroom requirements; extremely low hold-up (9 gal. in a 2,400-gal./hr. machine); they are almost portable and can be connected in series and in parallel in a variety of ways; they can handle mixtures which tend to emulsify readily. For these reasons they have been widely used for the extraction steps in the manufacture of antibiotic substances such as penicillin, streptomycin, chloromycetin, and bacitracin. Pharmaceutical products such as these can absorb the relatively high costs, and the ease with which the extraction plants can be dismantled and reassembled when process flowsheets are changed make these devices useful in this field.

## FLOW CAPACITIES

**Spray Towers.** Blanding and Elgin (9) have demonstrated conclusively that consistent flooding data can very likely only be obtained with end designs of the type shown in Fig. 10.2. Typical of the data obtained with such towers are those shown in Fig. 10.13, plotted on coordinates suggested by Colburn (18). Study of curves 1, 2, 3, and 4 of this figure, which deal with two systems of similar physical properties, indicates the importance of the diameters of the nozzles used to distribute the dispersed phase, which regulate the drop size. The considerable effect of changing the dispersed phase in the xylene–water system is shown by curves 4 and 5, but in the ketone–water system there is substantially no effect (curve 6). Additional data for the xylene and ketone systems are given by Blanding and Elgin.

The curves for any one system can almost be brought together by dividing the ordinate of Fig. 10.13 by the square root of the prevailing drop diameters, but the correlation is by no means good. The most promising general approach is that of Elgin and Foust (26), who found that flooding in spray towers when finely divided solid particles represented the dispersed phase paralleled the phenomena observed by Blanding and Elgin. Flooding in both cases occurs when the velocity of the individual particles relative to that of the continuous fluid ($U_P + U_C$) is 75 per cent of the free-fall velocity of the particles in the stationary continuous liquid, assuming the particles

to be spherical. The velocity of the particles is related to the superficial velocity of the dispersed phase through the dispersed phase hold-up:

$$H = \frac{U_D}{U_P} \tag{10.1}$$

where $H$ is the fractional volumetric hold-up of dispersed phase and $U_D$ and $U_C$ the superficial velocities of dispersed and continuous phases. In the absence of specific data, Elgin and Foust recommend the correlation of Wilhelm and Kwauk (85) for fluidized beds of solids for estimation of the

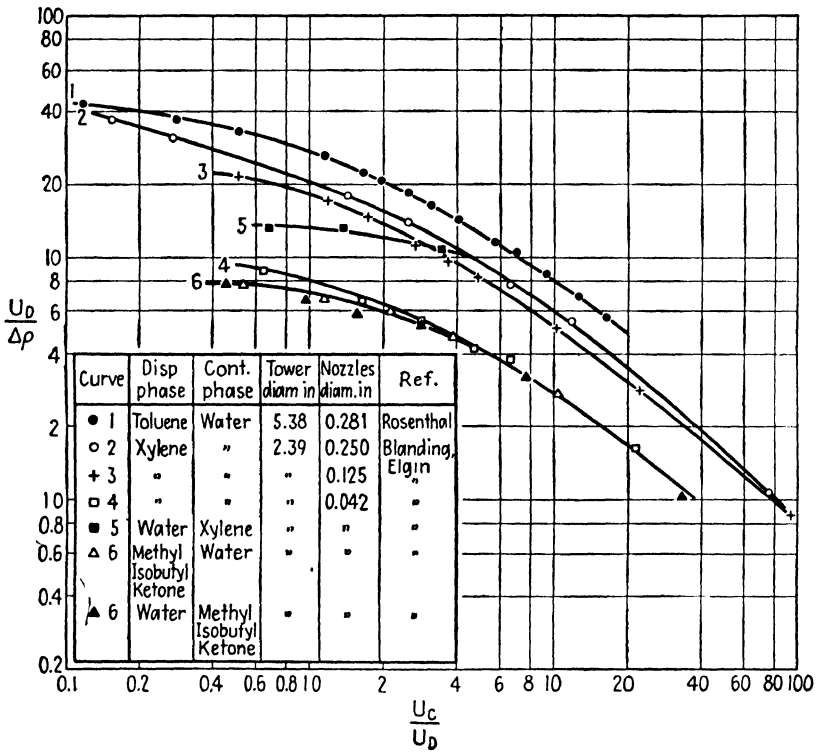



FIG. 10.13. Flooding in spray towers.

hold-up at flooding. This leads to hold-ups in the neighborhood of 0.05, while the few data available (9, 69) indicate values in the range 0.10 to 0.35. Drop sizes for liquids issuing from sharp-edged nozzles into another immiscible liquid can be estimated from the empirical equation of Hayworth and Treybal (36)

$$v + \frac{0.01258v^{0.667}\rho_D u^2}{\Delta\rho} = \frac{1.41(10^{-4})\sigma' d_0}{\Delta\rho} + 0.0553\left(\frac{d_0^{0.747}u^{0.365}\mu'_C{}^{0.186}}{\Delta\rho}\right)^{0.667} \tag{10.2}$$

for velocities through the nozzle not greater than 1 ft./sec.

**Packed Towers.** There are available the results of only three investigations exclusively devoted to the study of the flow phenomena in packed towers. In each case, small towers fitted with the special end designs of Elgin (Fig. 10.2) were used, with packings of ¼-in. and ½-in. size. Unfortunately, no studies are reported for the larger packing sizes which are usually used in industrial towers, and in the case of the ½-in. packings, the packing density is probably somewhat smaller than would be found in large-diameter towers. With minor exceptions the descriptions of the flooding phenomena observed in two of the investigations agree, and the data of these studies can be reconciled.

The studies of Blanding and Elgin (9) were made with ½-in. ceramic saddles, carbon Raschig rings, and clay spheres in a 2.39-in.-diameter tower, using the systems xylene– and methyl isobutyl ketone–water. Flooding velocities were independent of the hole size for the dispersed-phase distributor; the drop size seemed to be regulated by the packing, with a tendency toward coalescence as flooding conditions were approached. It was observed that a plot of the square roots of the linear superficial liquid velocities (based on the empty tower cross section) at flooding against each other gave a straight line for each system. It was later shown (12) that at flooding the simple relationship

$$U_C^{1/2} + U_D^{1/2} = \text{const.} \tag{10.3}$$

holds remarkably well, with a different constant for each system. Thus, with one accurately determined set of flooding velocities, the entire flooding regime for a given system can be approximated.

Breckenfeld and Wilke (12) used a 2.6-in.-diameter tower packed with ¼-in. carbon Raschig rings and ½-in. saddles, and a wide variety of liquids. They established that higher rates of flow at flooding resulted from greater density difference, lower interfacial tension, and lower continuous-phase viscosity. Absolute values of the densities and of the viscosity of the dispersed phase seemed to have no effect over the range of these properties considered. The data were correlated empirically with those of Blanding and Elgin by a modification of a method suggested by Colburn (18), with the introduction of the packing characteristics of surface area ($a$) and fractional void volume ($F$) to permit inclusion of the several shapes and sizes of packing.

All the data of the above studies and a few from that of Ballard and Piret (5) are presented in Fig. 10.14 plotted according to the method of Breckenfeld and Wilke, with the exception that the dispersed-phase velocity is used in the ordinate rather than that of the continuous phase, as originally suggested by Colburn (18). It is believed that this represents an improvement in that not only are all the Blanding and Elgin data brought to a narrower band, but also the range of the ordinate is larger, thus leading to

a curve which is less flat. This correlation must be regarded as tentative and should be used with caution, especially if it is attempted to apply it to larger packing sizes, since the term $a^{0.8}/F^2$ was established on the basis of ¼-in. and ½-in. packings only. Further, liquids of high viscosity and very low interfacial tension have not been studied. It should also be kept

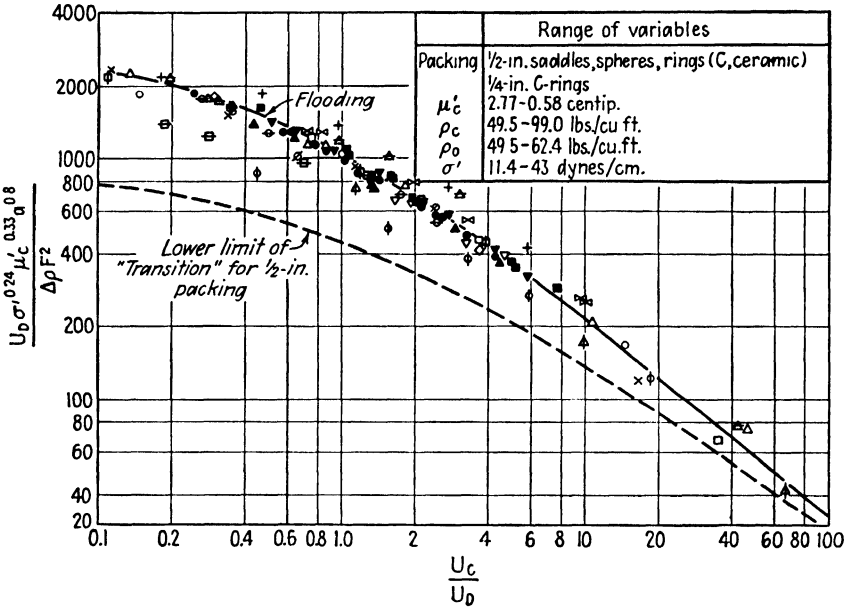



FIG. 10.14. Flooding in packed towers.

in mind that flooding may occur at lower velocities in towers not fitted with the end designs described earlier, or with distributors and packing supports which occupy large portions of the tower cross section.

Ballard and Piret (5), using columns of 2.03 and 3.75 in. in diameter packed with ¼-in. and ½-in. porcelain rings, observed that the ½-in. rings were preferentially wet by the water. If the water was the dispersed phase, the flooding characteristics were similar to those described by the previous investigators. These data are included in Fig. 10.14. On the other hand, if the water was the continuous phase, important changes in the flow regime were noticed at flow rates less than those at flooding, and major attention was given to these. For this case, as the flow rate of dispersed phase was increased, dispersed phase hold-up and the pressure drop for flow increased regularly. At a particular flow rate, a sudden increase in pressure drop was noticed which was followed by considerable coalescence and increased drop size of dispersed liquid. Three separate behaviors were then noticed at higher flow rates, depending upon the interfacial tension, which were not always reproducible. The rate of flow at which the initial

marked enlargement of drop size occurred was defined as a "transition" condition, and the transition data are plotted in Fig. 10.15 according to the coordinates of Fig. 10.14 together with the flooding curve for comparison. Ballard and Piret present a more satisfactory correlation which can be related to gas-liquid flooding but which cannot be conveniently compared

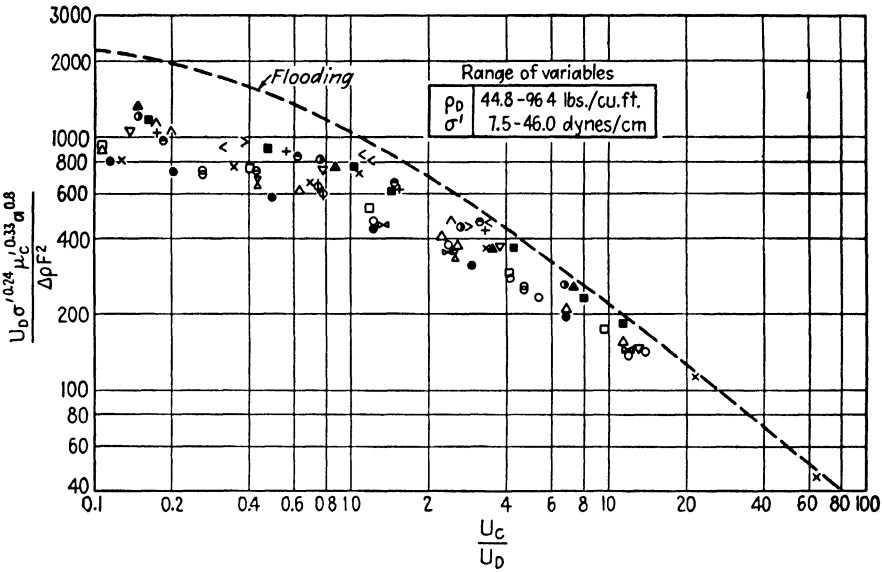



FIG. 10.15. Transition flow, ½-in. rings, water continuous.

with the other liquid-liquid data. With ¼-in. rings, sharply defined flooding was observed, but the data do not correlate with the others for reasons which are not now clear. They are shown separately on simplified coordinates in Fig. 10.16.

The lower limits of excessive coalescence, or transition, for the ½-in. packing have been indicated on Fig. 10.14 as a broken curve. It would appear that design conditions should be chosen below this curve at least, so as to avoid the coalescence which not only reduces interfacial area between the phases but may lead to incipient flooding conditions.

Miscellaneous capacity data for saddle and ring packings, taken largely in small towers during the course of other work, are shown in Fig. 10.17 on simplified coordinates. Lack of complete data on liquid properties precludes attempts to include these on the more general correlation. Since in most instances designers do not have such data as interfacial tension at hand, this plot may be useful in estimating flow capacities for similar liquids. Hold-up data for the dispersed phase in packed columns have been reported for a few cases (2, 3, 70). In general, hold-up increases with increased flow of both phases and is dependent upon whether the dispersed

or continuous phase preferentially wets the packing. The data are too few to permit generalizations.

**Illustration 1.** Acetic acid is to be extracted from water by isopropyl ether in a tower packed with ½-in. carbon Raschig rings, ether dispersed. Flow rates are to be 30 cu. ft./hr. ether, 45 cu. ft./hr. water. Average physical properties are: aqueous phase density $\rho_C = 63.0$ lb./cu. ft., viscosity $\mu'_C = 3.1$ centipoises; ether phase density $\rho_D = 45.6$ lb./cu. ft.; interfacial tension $\sigma' = 13$ dynes/cm. (25). Calculate the diameter of tower to be used.

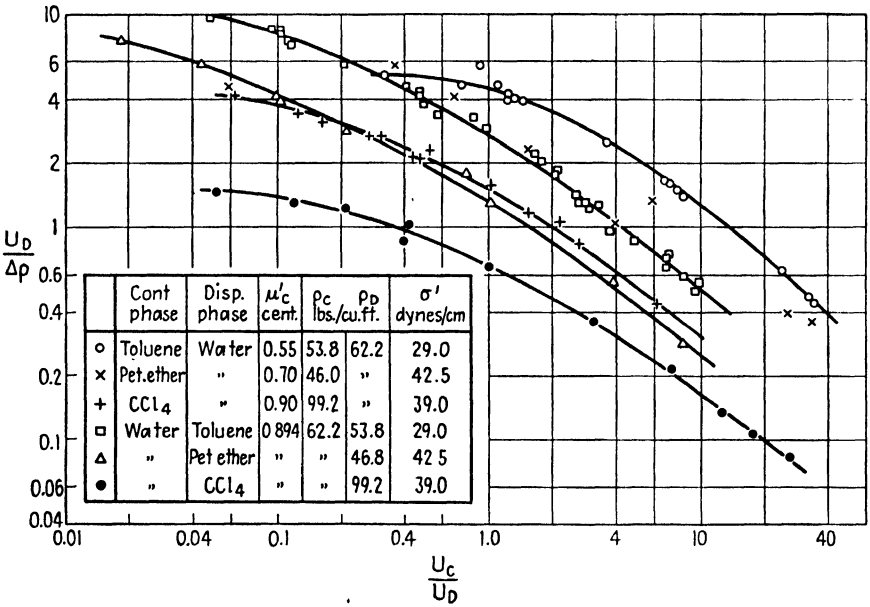



FIG. 10.16. Flooding with ¼-in. rings. (*Data of Ballard and Piret.*)

*Solution.* For ½-in. carbon rings, $a = 114$ sq. ft./cu. ft., $F = 0.74$ fractional void volume. $\Delta\rho = 63.0 - 45.6 = 17.4$ lb./cu. ft. $U_C/U_D$ = ratio of volumetric flow rates = 45/30 = 1.5. From Fig. 10.14, values of the ordinate are 800 at flooding, 380 at transition. An ordinate of 300 will be used to ensure operation below transition.

$$U_D = 300\left(\frac{\Delta\rho F^2}{\sigma'^{0.21}\mu'_C{}^{0.33}a^{0.8}}\right) = 300\left[\frac{17.4(0.74)^2}{(13)^{0.21}(3.1)^{0.33}(114)^{0.8}}\right] = 24.1 \text{ ft./hr.}$$

$$\text{The cross-sectional area for the tower} = \frac{30 \text{ cu. ft./hr. ether}}{(24.1 \text{ ft./hr.})}$$

$$= 1.242 \text{ sq. ft.}$$

This corresponds to a diameter of 1 ft. 3 in.

**Baffle Towers.** Although no systematic study has been made for these extractors, it can be surmised that the important variables would be densities, viscosities, and interfacial tension of the liquids, and baffle shape, relative size, and spacing. A few data for capacities of towers of the type of Fig. 10.5 are indicated in Table 10.1 (33).

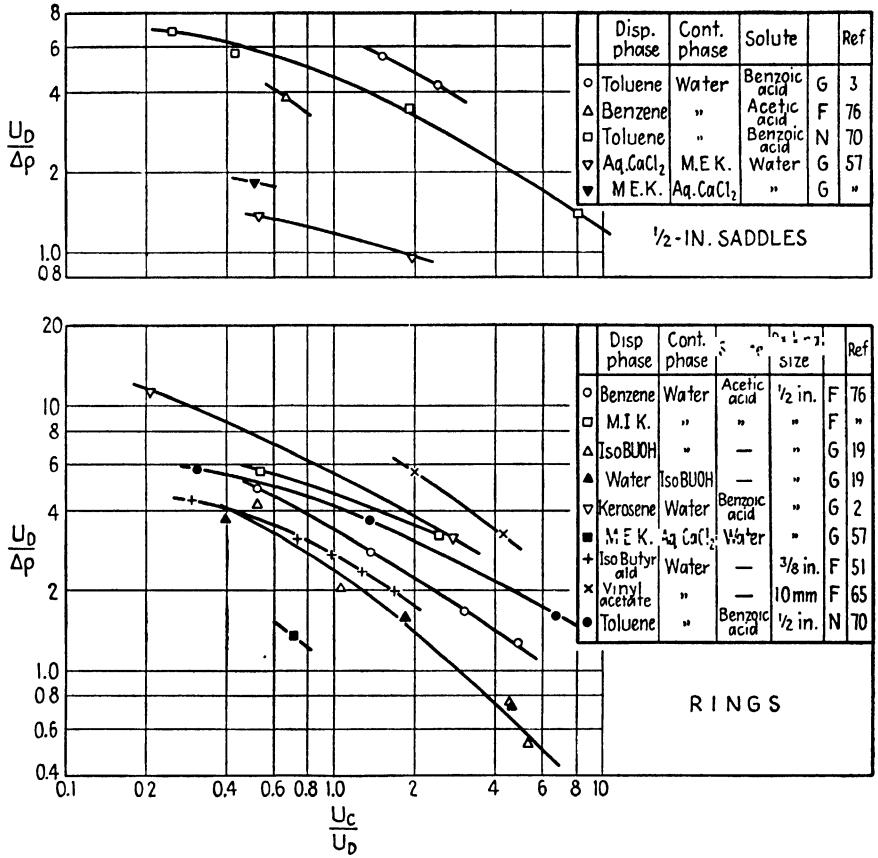



FIG. 10.17. Capacities of packed towers. $G$ = greatest reported, $N$ = on verge of flooding, $F$ = flooded.

TABLE 10.1. CAPACITIES OF BAFFLE TOWERS (33)

| Tower diam., in. | No. of baffles | Baffle spacing, in. | Type of flow | $\Delta\rho$, lb./cu. ft. | Total flow (both liquids) | |
|---|---|---|---|---|---|---|
| | | | | | G.p.h. | Ft./hr. |
| 78 | 103 | 5 | Center-to-side | 12.72 | 16150 | 65 |
| 42 | 104 | 5 | Center-to-side | 13.10 | 5850 | 81.1 |
| 24 | 7 | 1.75 | Center-to-side | 14.35 | 2845 | 121 |
| 26 | 96 | 4 | Side-to-side | 5.99 | 2550 | 92.5 |

**Perforated-plate Towers.** Flooding of these towers may occur either because of inability to maintain an interface at the end of the tower or because of thickening of the layers of dispersed phase on the plates. Tend-

ency toward the former can be controlled by elimination of restrictions to flow. For control of the latter, the plates must be properly designed. Since the flow of the liquids through the tower is entirely due to their difference in densities, the driving force required to overcome the various resistances is developed by displacement of the continuous phase by the dispersed phase, resulting in a layer of dispersed phase on each plate. The displacement required for flow of dispersed phase through the perforations can be estimated from the ordinary equation for flow through an orifice (55, 66):

$$h_0 = \frac{\rho_D[1 - (S_0/S_t)^2]U_0^2}{2g\,\Delta\rho\,C_0^2} \tag{10.4}$$

where $h_0$ = continuous phase displacement
$\rho_D$ = density of dispersed phase
$\Delta\rho$ = difference in density of the phases
$S_0$ = cross-sectional area of the perforations
$S_t$ = cross-sectional area of the tower
$U_0$ = velocity of dispersed phase through the perforations
$C_0$ = orifice const.

all in consistent units. The displacement required to overcome resistance to flow of the continuous phase through the downspouts (or risers) can be estimated from the contraction and expansion losses on entering and leaving the downspouts together with the friction loss for flow through the pipe (55). The contraction and expansion losses, for downspout cross sections of 5 per cent or less of the column cross section, will equal approximately 1.5 velocity heads (66):

$$h_{ce} = \frac{\rho_C}{\Delta\rho}\left(\frac{1.5U_d^2}{2g}\right) \tag{10.5}$$

where $h_{ce}$ = continuous phase displacement
$\rho_C$ = continuous phase density
$U_d$ = velocity through the downspout

The displacement due to friction in the downspout $h_f$ can be computed by standard methods (63). For a case where the dispersed phase preferentially wets the perforated plate, the total displacement is the sum, $h_0 + h_{ce} + h_f$. On the other hand, if the continuous phase preferentially wets the plate, a pressure must be developed merely to start the dispersed phase through the perforations against interfacial tension, which can be calculated from Eq. (9.26). Expressing the pressure in terms of continuous-phase displacement, this becomes

$$h_\sigma = \frac{4\sigma}{\Delta\rho d_0} \tag{10.6}$$

For this case the thickness of dispersed phase will be either $h_\sigma$ or the sum $h_0 + h_{ce} + h_f$, whichever is greater. Additional resistance to flow can pre-

sumably be expected if the thickness of the dispersed layer becomes so great that it leaves little room for continuous phase flow across the plate or if the clearance between the bottom of the downspout and the plate it feeds is too small. These cannot be conveniently estimated.

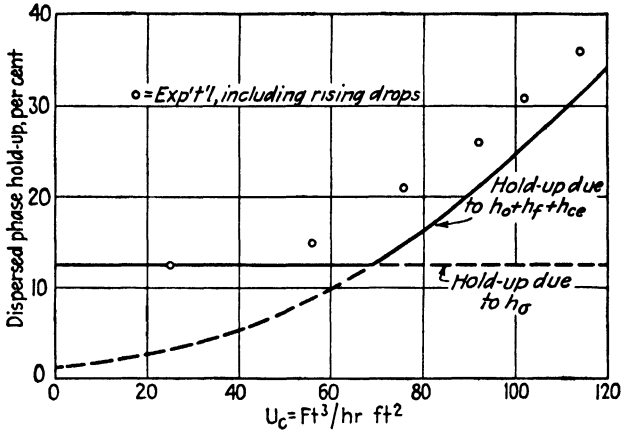



FIG. 10.18. Hold-up in a perforated-plate tower (2). Kerosene dispersed, $U_D = 80$; water continuous.

Figure 10.18 shows a comparison of the hold-up of dispersed phase in a small perforated-plate tower (2) with that calculated by the methods described. The measured data include the hold-up owing to dispersed phase droplets rising through the continuous phase and is consequently higher than the calculated hold-up, but the trend of the data is followed very well. The observations of several experimenters (2, 60, 70, 81) that the thickness of the layer of dispersed phase is apparently independent of dispersed phase flow rate can be shown to be due to the small numerical value of $h_0$ for these cases.

The few capacity data available, measured with laboratory columns, are shown in Fig. 10.19. Lack of complete data on physical properties of the liquids, which contained dissolved solutes, prevents attempts at correlation of these, but the great influence of downspout and perforation areas on limiting flows is evident. It would appear that downspout cross sections of 5 per cent and perforation areas of at least 10 per cent of the tower cross section will permit greatly improved flow rates and correspondingly smaller tower diameters.

**Spinner Columns.** The few flooding data reported for an 11.5-in.-diameter column of Scheibel's design (73), Fig. 10.11, obtained in the course of another study, cannot be systematized at this time. The limiting flow rates seem to be dependent upon the speed of the impeller as well as the properties of the liquids and are somewhat lower than the maximum reported for comparable systems in conventionally packed towers. Com-

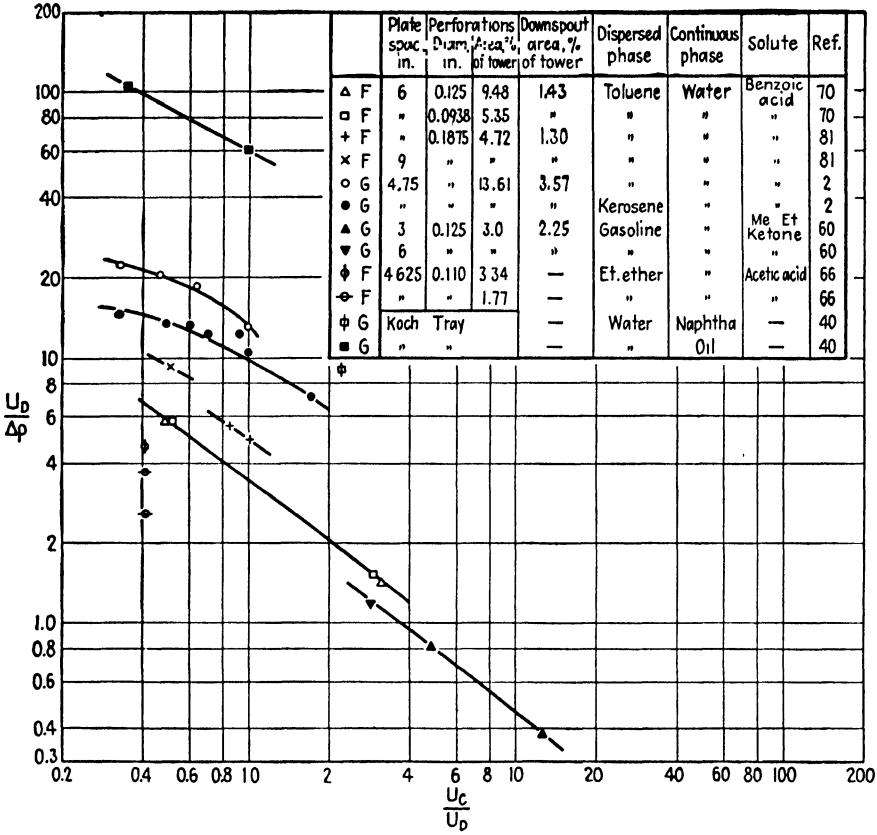



FIG. 10.19. Flow capacities of perforated-plate towers. $G$ = greatest reported, $F$ = flooded.

parison with data from a 1-in. column (72) indicates that the coarseness of the wire mesh used for the packed sections has a marked influence as well.

## EXTRACTION RATES

**Interpretation of Data.** Operating data may be interpreted in terms of either mass-transfer coefficients, *HTU*'s or H.E.T.S.'s, depending upon which of the methods of Chap. 8 it is planned to use later in design. The determination of the values of H.E.T.S. from such data requires no particular explanation. In the case of the others, under ordinary circumstances the experimental data lead to over-all values of coefficients or transfer units, and these should be expressed in terms of the phase where the principal resistance to diffusion lies, as explained in Chap. 5. Over-all *HTU*'s and *Ka*'s can be converted, one into the other, through Eqs. (8.12) and (8.14).

In most operations, one phase is dispersed into droplets or otherwise broken up while the other is continuous, and either one may be the raffinate

or the extract. Since the mass-transfer characteristics are more dependent upon the conditions of dispersion than the direction of extraction, these will be expressed as $K_Ca$, $K_Da$, $HTU_{OD}$, or $HTU_{OC}$, with the subscripts indicating the dispersed or continuous condition irrespective of direction of extraction. Thus, if the distribution coefficient $m$ is defined in terms of pound moles per cubic foot concentration units, Eq. (8.43) becomes

$$\frac{1}{K_Ca} = \frac{1}{k_Ca} + \frac{1}{mk_Da} \tag{10.7}$$

or, in terms of $K_Da$,

$$\frac{1}{K_Da} = \frac{1}{k_Da} + \frac{m}{k_Ca} \tag{10.8}$$

In the manner which has been so successful in the systematization of heat-transfer measurements, it is desirable to express the experimental data in terms of the individual-film transfer coefficients as functions of flow conditions and fluid properties.

On the assumption that the degree of turbulence of each phase is affected by the rate of flow of both, since the liquids are in direct contact, application of dimensional analysis leads to expressions of the following type:

$$\frac{dk_Da}{D_D} = \alpha(\mathrm{Re}_D)^\beta(\mathrm{Re}_C)^\gamma(\mathrm{Sc}_D)^\delta \tag{10.9}$$

where Re = Reynolds number = $dU\rho/\mu$
Sc = Schmidt number = $\mu/\rho D$
$D$ = diffusivity of solute
$d$ = some linear dimension characteristic of the equipment

The exponents on the various dimensionless groups are presumably constants, although the relationship between the groups need not necessarily be of the indicated form. Equation (10.7) then becomes

$$\frac{D_C}{K_Cad} = \frac{1}{\epsilon(\mathrm{Re}_D)^\eta(\mathrm{Re}_C)^\tau(\mathrm{Sc}_C)^\phi} + \frac{1}{m\alpha(\mathrm{Re}_D)^\beta(\mathrm{Re}_C)^\gamma(\mathrm{Sc}_D)^\delta} \tag{10.10}$$

But the Reynolds number cannot always be clearly defined in equipment of the type used in extraction, and furthermore it is not usually so clear an indication of the degree of turbulence as in simpler fluid systems. For a given apparatus and liquid system, where fluid properties vary little with operating conditions, Eq. (10.10) can be written

$$\frac{1}{K_Ca} = \frac{1}{\epsilon U_D^\tau U_C^\tau} + \frac{1}{m\alpha U_D^\beta U_C^\zeta} \tag{10.11}$$

where the expressions on the right-hand side each represent the individual-film resistances to mass transfer. A similar expression can be written for $K_Da$.

It is then necessary to establish the numerical value of the various constants from a study of the experimental data. This will ordinarily be successful only if one of the exponents equals zero. For example, if $\gamma$ were zero and the flow rate of the continuous phase had no influence on the mass transfer coefficient of the dispersed phase, then the various data could be grouped into series in each of which the value of $U_D$ is constant. Then, for each such series

$$\frac{1}{K_C a} = \frac{1}{\lambda U_C^{\tau}} + \psi \tag{10.12}$$

and $\tau$ could be obtained by various graphical treatments of the data (13, 82). The other constants could then be determined in a similar manner. None of the graphical treatments is very useful, since ordinarily the data are not nearly sufficiently precise to make them applicable. Sometimes the mass-transfer resistance of one of the phases can be eliminated or made very small by a rapid and irreversible chemical reaction, for example, so that $\psi$ becomes zero and a simple logarithmic plotting of $K_C a$ against $U_C$ will establish the value of $\tau$.

Alternately, Eqs. (8.7) and (8.9) indicate that $HTU$'s should be less sensitive to flow rates than the mass-transfer coefficients. Equations (8.46) and (8.47) have been therefore used as correlating devices, on the assumption that $HTU_C$ and $HTU_D$ are each substantially independent of flow rate. Thus,

$$HTU_{OC} = HTU_C + \frac{U_C}{mU_D} HTU_D \tag{10.13}$$

$$HTU_{OD} = HTU_D + \frac{mU_D}{U_C} HTU_C \tag{10.14}$$

and plotting $HTU_{OD}$ against $mU_D/U_C$ on arithmetic coordinates should give a straight line whose intercept is $HTU_D$ and whose slope is $HTU_C$. This is not always too successful, since on occasions negative intercepts result which cannot readily be interpreted. Nevertheless, these simple plots are useful for empirical correlation even if they cannot be interpreted in terms of $HTU_D$ and $HTU_C$.

**Wetted-wall Towers.** As indicated previously, these have been used in laboratory investigations where it was desired to exert some control over the interfacial area, but it is not likely that they will be useful in industrial work. The significant results will be summarized here only briefly.

Fallah, Hunter, Nash, and Strang (27, 77) studied the hydraulics of wetted-wall towers operated with stationary liquid cores composed of hydrocarbons and a moving wall-liquid of water. It was clearly shown that the interface and a portion of the core liquid immediately adjacent to the interface moved downward in the direction of the flow of wall-liquid.

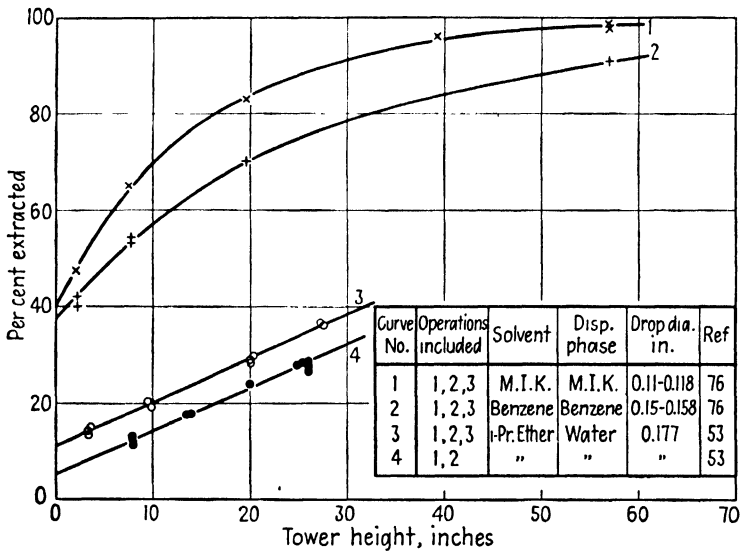
Later, Treybal and Work (82) made similar studies with a moving benzene core and water as a wall-liquid, establishing that the core velocity also influenced the interfacial velocity, although the interfacial velocity was always in the direction of flow of the wall-liquid. These studies have made it clear that each phase has an influence on the flow conditions of the other and that the core-liquid is never completely stationary even at zero net flow. Similar conclusions were drawn by Bergelin, Lockhart, and Brown (8), who used a nearly horizontal tube with water and tetrachloroethylene flowing countercurrently in the upper and lower halves.

Hunter, *et al.* (28, 78) studied the extraction of phenol from kerosene as a core-liquid, with water as a wall-liquid, both liquids in turbulent flow. The data were interpreted by an equation similar to Eq. (10.12), and it was concluded that, over the limited range studied, the wall-liquid did not influence the mass-transfer coefficient for the core. Working with the liquids benzene and water over a wide range of flow rates for each, with acetic acid as the diffusing solute, Treybal and Work (82) showed that an equation at least as complex as Eq. (10.11) was necessary to describe the results and were therefore unable to determine the value of the constants. These observations reinforced the conclusions respecting the influence of each rate of flow on the degree of turbulence in both liquids.

Comings and Briggs (20) studied the extraction of several solutes between benzene and water. For the extraction of benzoic acid, where the distribution favors the benzene, the major resistance to diffusion lay in the water phase. Addition of sodium hydroxide to the water reduced this resistance by causing a rapid chemical reaction, increased the mass-transfer coefficient, and made the effect of benzene rate on the over-all coefficient more pronounced, as would be expected. Similar experiences were obtained in the case of extraction of aniline, but in the case of acetic acid results were contrary to what was expected. The data apparently could be interpreted in terms of Eq. (10.11), with $\beta = 0.45 - 0.55$, $\gamma = 0 - 0.1$, $\eta = 0.40 - 0.55$, $\tau = 0.45 - 0.55$. Brinsmade and Bliss (13) extracted acetic acid from methyl isobutyl ketone (core) by water (wall). By making measurements at several temperatures, they were able to investigate the influence of Schmidt number on the rates and by graphical treatment of the data obtained values of the constants of Eq. (10.11) as follows: $\beta = 1$, $\eta = \gamma = 0$, $\tau = 0.67$, $\phi = \delta = 0.62$. Despite visual indication of violent wave motion in the experiments, neither flow rate apparently influenced the mass transfer coefficient of the other phase. On the other hand, Bergelin, *et al.* (8), in the horizontal apparatus mentioned above, did observe the mutual influence of flow rates on the coefficients which their flow studies would predict.

The observations from these investigations are curiously conflicting and cannot be reconciled at this time.

**Extraction from Single Drops.** Extraction from isolated liquid drops as they rise or fall through an immiscible liquid can provide an insight into the fundamental mechanism pertaining in spray, perforated-plate, and packed towers, since for the drops the interfacial surface can be estimated and treated separately from the mass-transfer coefficients. Sherwood, Evans, and Longcor (76) extracted acetic acid from methyl isobutyl ketone and benzene with water in this manner, with single drops issuing from nozzles and rising through various depths of quiet water. Some of their data are indicated in curves 1 and 2 of Fig. 10.20. Extrapolation of these curves to zero tower height indicates an appreciable residual amount of extraction. Licht and Conway (53) have postulated that the extraction in




| Curve No. | Operations included | Solvent | Disp. phase | Drop dia. in. | Ref |
|---|---|---|---|---|---|
| 1 | 1,2,3 | M.I.K. | M.I.K. | 0.11-0.118 | 76 |
| 2 | 1,2,3 | Benzene | Benzene | 0.15-0.158 | 76 |
| 3 | 1,2,3 | i-Pr. Ether | Water | 0.177 | 53 |
| 4 | 1,2 | " | " | " | 53 |

FIG. 10.20. Extraction of acetic acid from single drops.

such a tower can be divided into three portions, that which occurs (*a*) during drop formation at the nozzle, (*b*) during rise or fall of the drop, and (*c*) on coalescence of the drop into the interface at the other end of the tower. They extracted acetic acid from drops of water falling through three solvents in two devices, the first of which gave all three effects. Some of their data are indicated in curve 3 of the figure, and the intercept at zero height should show the extraction due to the first and third effects, as for curve 1. The second apparatus (curve 4) eliminated the coalescence effect, and the intercept should represent extraction during drop formation only. The vertical difference between the curves (3 to 4) should then represent the extraction occurring only during fall of the drops.

The over-all coefficients measured by Sherwood (76), plotted as a function of drop size in Fig. 10.21, indicate a strong effect of initial solute con-

centration in the case of benzene drops, which in part was accounted for by the effect on the fluid properties. The drops were not perfectly spherical and underwent a certain degree of deformation as they rose through the

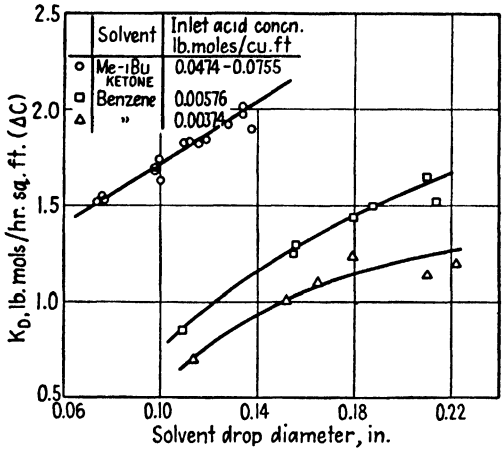



FIG. 10.21. Extraction of acetic acid from single drops, tower height 57.7 in. (76). (*With permission of American Chemical Society.*)

water, depending upon their size and interfacial tension. This was confirmed by a comparison of the molecular diffusivity of acetic acid in the solvents and the diffusivity which would have to be used in Eq. (5.27) to compute the extent of extraction assuming purely unsteady-state diffusion in the drops with no resistance in the continuous phase. The latter values were greater than the former by factors of 11 to 43, increasing with increased drop size and decreased interfacial tension, thus indicating the presence of eddy currents within the drop.

The extraction rates of Licht and Conway could be related to each portion of the process. Thus it was observed that the per cent of total extraction which occurred during drop coalescence was 6, 11, and 13 per cent for isopropyl ether, ethyl acetate, and methyl isobutyl ketone as solvents, respectively, irrespective of drop size over the limited range studied. Figure 10.22 shows the extraction coefficients during drop formation, and since the fractional extraction was constant in each system for each drop size, the variation of $K_D$ with drop size is due to the variation of interfacial area. The values of $K_D$ for the period while the drops were falling were reasonably independent of tower height, but

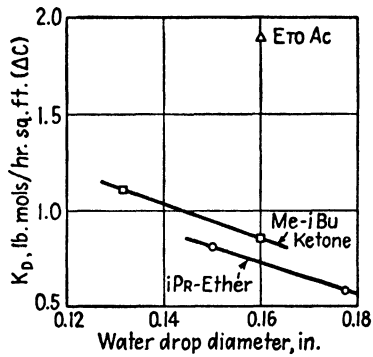



FIG. 10.22. Extraction of acetic acid from water during drop formation. Solvents are marked.

the ratio of effective diffusivity to molecular diffusivity cannot be computed for the drops in the manner described above, since evidently an appreciable portion of the diffusional resistance lies in the continuous phase leading to ratios considerably less than unity.

**End Effects.** While the available data do not yet permit quantitative calculation for all situations, the existence of very sizable end effects, as the phenomena described above are called, is nevertheless firmly established. Extraction coefficients for spray towers, consequently, might be expected to be smaller, and *HTU*'s larger, with increased height. This is confirmed by the data of Nandi and Viswanathan (61), Fig. 10.23, where the values of *HTU* and *Ka* tend to level off at increasing tower heights as the end effect becomes decreasingly important. The change in interfacial surface with acid concentration and different dispersed phase is probably largely responsible for the effect of these variables on the extraction rates. Johnson and Bliss (46) noted very small effects of tower height in extracting acetic acid from water by methyl isobutyl ketone. In the extraction of ferric chloride from aqueous solutions of hydrochloric acid by isopropyl ether in a spray column, Geankoplis and Hixson (30) used an ingenious internal sampling device to determine the end effects shown in Fig. 10.24. The end effect was apparently caused entirely by the coalescence of ether droplets at the interface and none by dispersion at the inlet ether nozzle, the absence of which is difficult to explain. Varying the rates of flow of the continuous phase and changing the position and cross section of the tower at the interface had no apparent influence. On the other hand, concentration of solute which through interfacial tension affects the ease of coalescence, and rate of flow of dispersed phase which changes the number of droplets are both important.

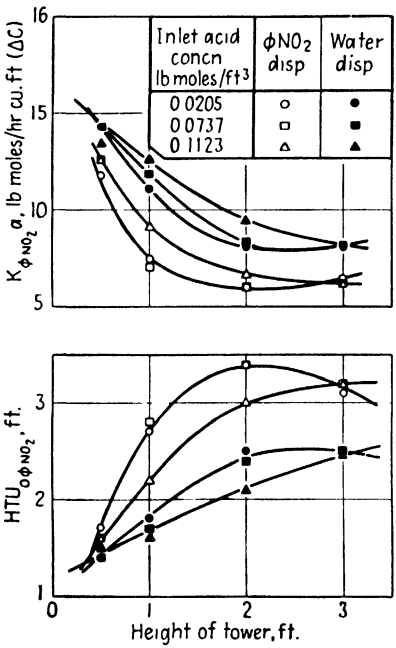



FIG. 10.23. End effect in extraction of acetic acid from water by nitrobenzene. Spray tower 1.36 in. diam., $U_{\phi NO_2} = 20.1$, $U_{H_2O} = 26.5$ ft./hr. (61).

**Spray Towers.** The performance of a spray tower will be a function of the variation of the individual mass-transfer coefficients $k$ of the two phases and the interfacial area $a$ with operating conditions. The value of $k$ for the dispersed phase can be expected to depend on drop size, diffusivity, and

such physical properties as viscosity, density, and interfacial tension which influence turbulence within the drop but should be relatively independent of continuous phase rate. The value of $k$ for the continuous phase can be expected to be influenced by the diffusivity and the viscosity, density, and rates of flow of both phases as these in turn influence turbulence. The variation of interfacial area, which will depend upon drop size and dispersed-phase hold-up, can be expected to be a most important factor and may entirely mask the influence of the variables on $k$. All the data representing

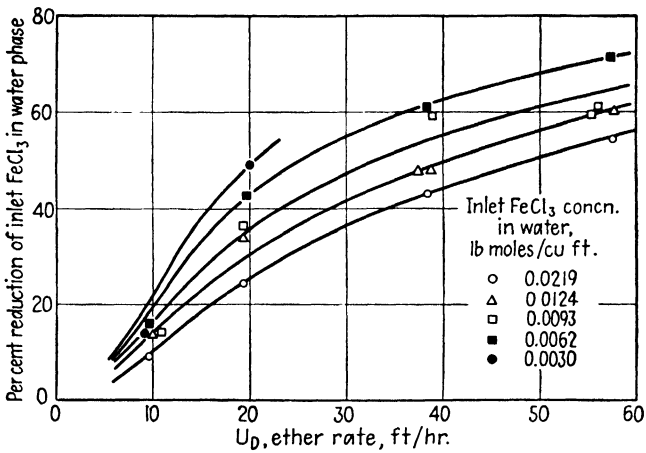



FIG. 10.24. End effect in extraction of $FeCl_3$ from aqueous HCl by isopropyl ether; spray tower, ether dispersed, 1.448 in. diam. (30). (*With permission of American Chemical Society.*)

systematic investigation of these effects were obtained on laboratory-sized equipment, usually a few inches in diameter at the most. This is perhaps not so serious, since the wall effect in the absence of packing is probably not very great.

The recent work of Laddha and Smith (51), who used a technique developed by Colburn and Welsh (19), is most illuminating since it presents data on the individual phase resistances. In this procedure two pure liquids of limited solubility are contacted in the absence of a third solute, and the approach to saturation of each phase can be calculated in terms of the individual resistances. The operation is analogous to contacting a pure gas with a pure liquid in [illegible] studies, whereby gas-film resistances alone are obtained. Laddha and Smith used isobutyraldehyde and 3-pentanol with water in a 2-in.-diameter tower and were able to obtain data for all but the pure aldehyde film. The dispersed-phase coefficients are shown in Fig. 10.25 as a function of dispersed-phase rate. In two of the cases, where the continuous-phase rate was relatively low, the coefficients appear to depend upon dispersed phase rate only. In the third, the influence of higher continuous-phase rates on dispersed-phase hold-up and interfacial

area is evident. Values of $k_Ca$, Fig. 10.26, are of the same order of magnitude as those of $k_Da$, as would be expected. They are again more dependent upon the rate of the dispersed than the continuous phase, and interfacial

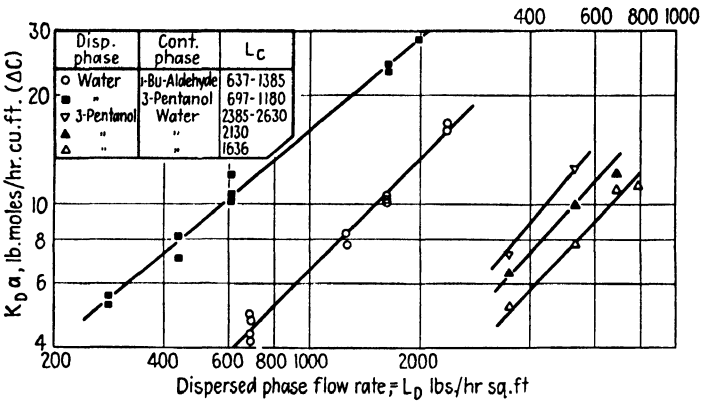



FIG. 10.25. Dispersed-phase mass-transfer coefficients; spray tower, 2-in. diam. (51).

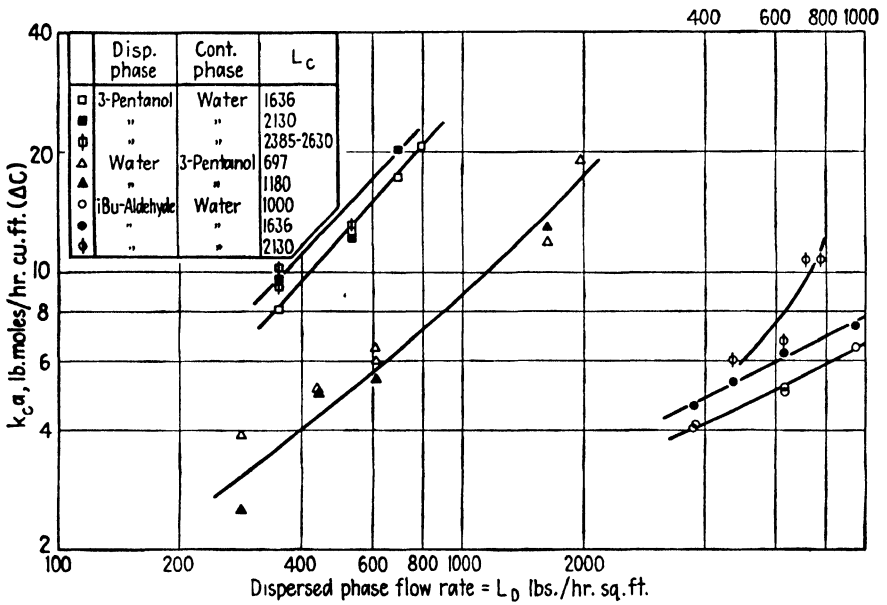



FIG. 10.26. Continuous-phase mass-transfer coefficients; spray tower, 2-in. diam. (51).

area probably plays the predominant role. The values of $HTU$ are shown in Fig. 10.27, where the ratio $L_D/L_C$ correlates all the data for a given operation very well. The slopes of these curves can be anticipated from the appearance of the figures and Eqs. (8.7) and (8.9), but the relative values of $HTU$ for the various situations cannot be clearly reconciled with

values of diffusivity or Schmidt number, probably again because the predominant factor is the interfacial area.

The remaining operating data on spray towers are limited to over-all coefficients or *HTU*'s, for which interpretation is frequently difficult. The very great influence of interfacial area on the extraction rate has been noted

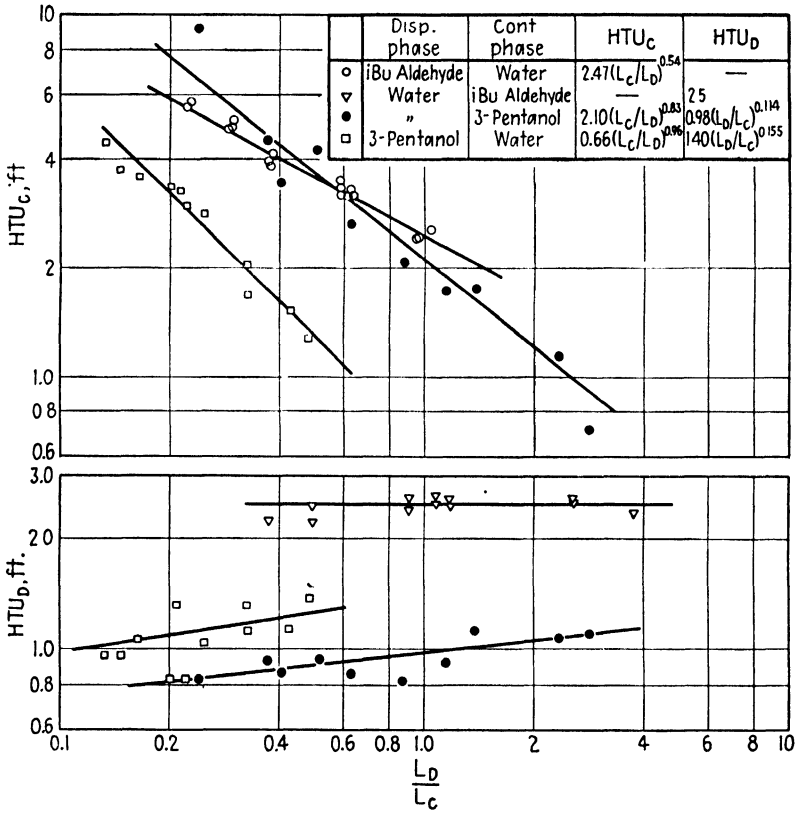



FIG. 10.27. Film *HTU*'s for a spray tower (51).

by several investigators and can readily be demonstrated. Figure 10.28 presents a portion of the data of Appel and Elgin (3) on the extraction of benzoic acid from a dispersed toluene solution by water. At constant rate for the continuous phase, the coefficients are plotted against dispersed phase rate for three different inlet nozzles which produced various drop sizes for the toluene. With each extraction curve is included another showing the dispersed phase hold-up, indicative to some extent of the interfacial area. In the case of the largest drops, for which the size and rate of rise were found to be constant, the coefficient is essentially independent of dispersed-phase rate and the curve parallels the corresponding hold-up data almost exactly. In the case of the smaller drops, the coefficients are larger

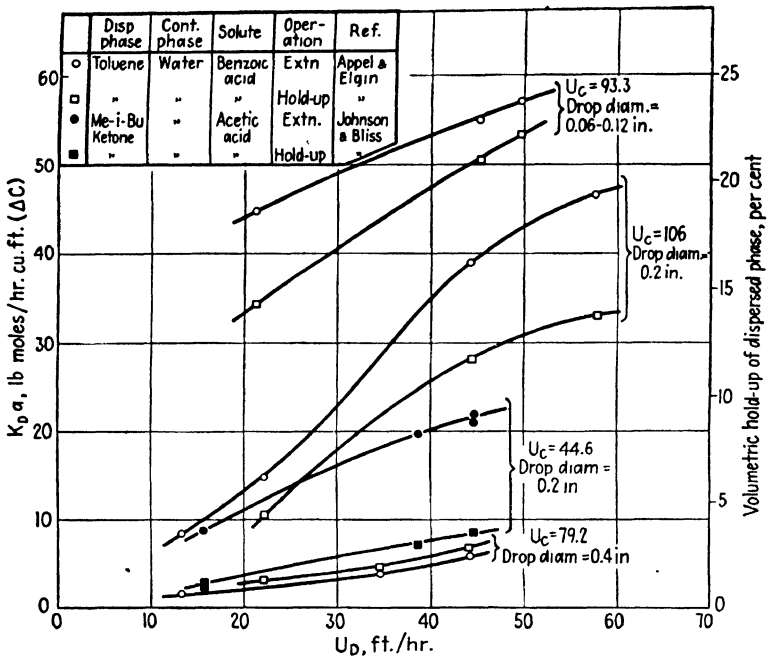



FIG. 10.28. Effect of dispersed-phase flow rate on $K_D a$ and hold-up for a spray tower.

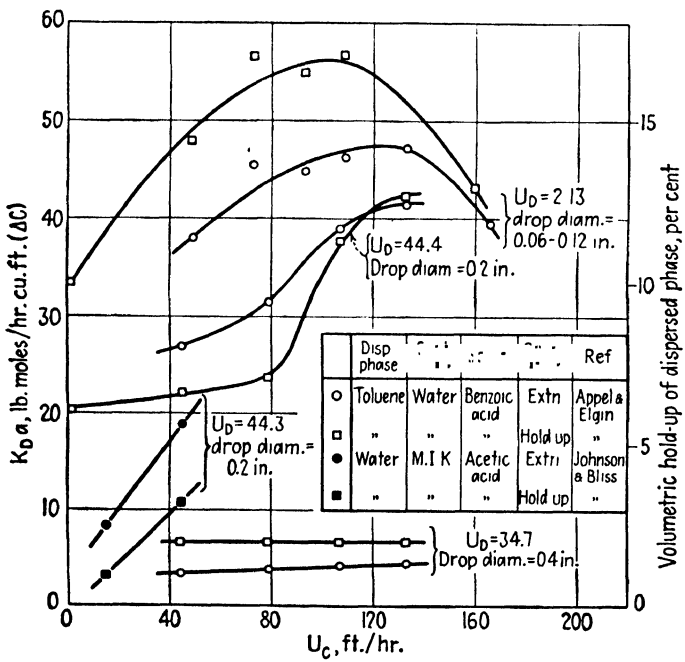



FIG. 10.29. Effect of continuous-phase flow rate on $K_D a$ and hold-up for a spray tower.

because of the larger drop surface, and the curves again parallel those for hold-up almost exactly. A few data for the extraction of acetic acid from water by methyl isobutyl ketone (46) are included to show the generality of these phenomena.

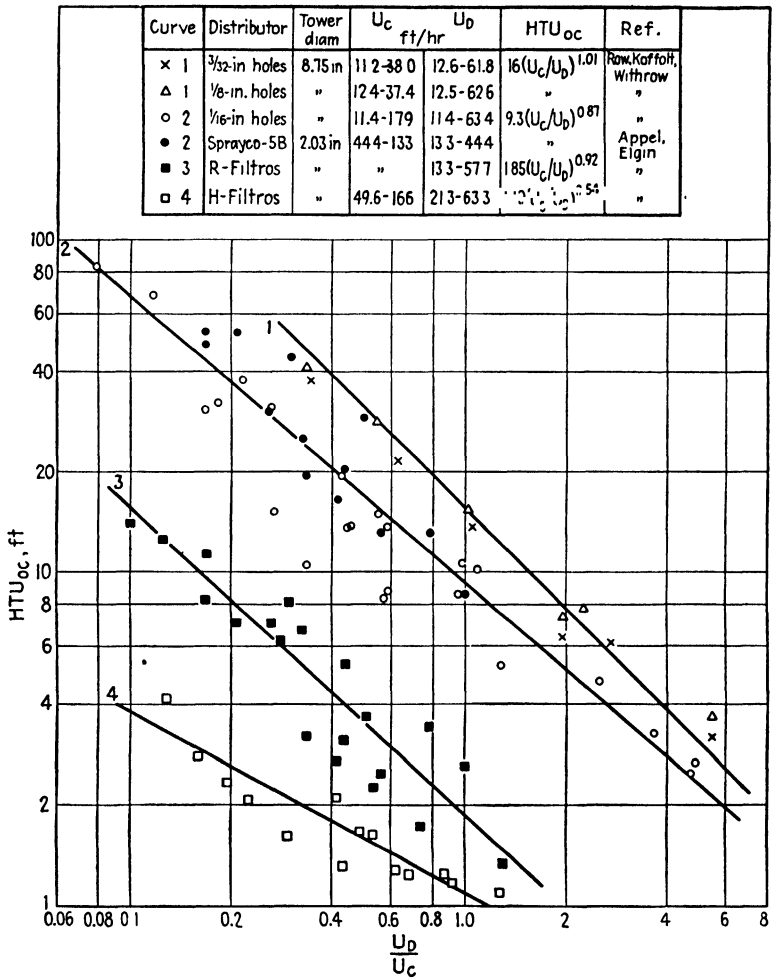



FIG. 10.30. Extraction of benzoic acid from toluene by water in spray towers, toluene dispersed.

Similarly in Fig. 10.29, where the data are plotted against rate of flow of continuous phase at constant dispersed-phase rate, the great influence of interfacial area is evident. For the large drops it was observed that their very rapid rate of rise was not influenced by the rate of the continuous phase; hold-up and coefficients therefore remain constant. For the smaller drops the rate of rise was markedly reduced by increased flow of the continuous phase, hold-up increased, and interfacial area and coefficients in-

creased. For the smallest toluene drops, considerable coalescence was observed at the higher water rates, which increases the rate of drop rise, decreases hold-up and interfacial surface, and lowers the coefficient. It is therefore evident that the rate of extraction for any system is very greatly dependent upon these factors, perhaps more so than on any others.

All the available data for the extraction of benzoic acid from toluene in a spray tower are shown in Fig. 10.30, grouped according to the size of the distributor nozzles for the dispersed phase and consequently accord-

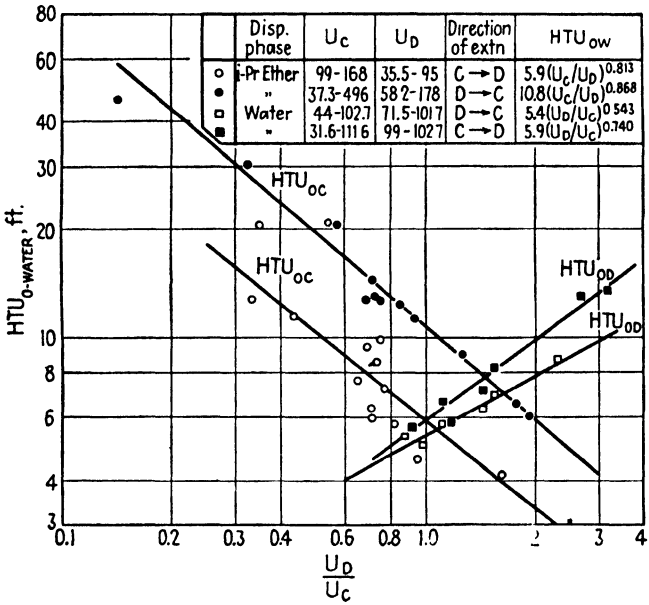



FIG. 10.31. Extraction of acetic acid between isopropyl ether and water in a spray tower, 2.03 in. diam., ⅛-in. diam. nozzle (25).

ing to drop size. The correlation is essentially empirical; the distribution coefficient might perhaps be included in the abscissa, but for the dilute solutions used it is essentially the same for all the data. Only in the case of four runs at the highest water rate for the 1/16-in. distributor is there any indication of segregation according to flow rate, and these give slightly lower values of *HTU*. The drop size for this distributor, while not recorded, can be estimated as roughly the same as that for the Sprayco nozzle of Appel and Elgin, and the coincidence of these data indicate the insignificant effect of tower diameter for the sizes used. The plot shows particularly the remarkable range of *HTU*'s obtainable for a given system and demonstrates the inadvisability of attempting to generalize the numerical value of this quantity. Values of H.E.T.S. computed from the original data are of the same order of magnitude as the *HTU*'s but cannot be so well correlated.

The data of Elgin and Browning (25) for the extraction of acetic acid between isopropyl ether and water are shown in Fig. 10.31. For approximately equal rates of flow of both phases, either phase may be dispersed with no very great effect on the *HTU*, but the *HTU*'s are invariably lower, or rate of extraction greater, at increased rates of the ether. Extraction

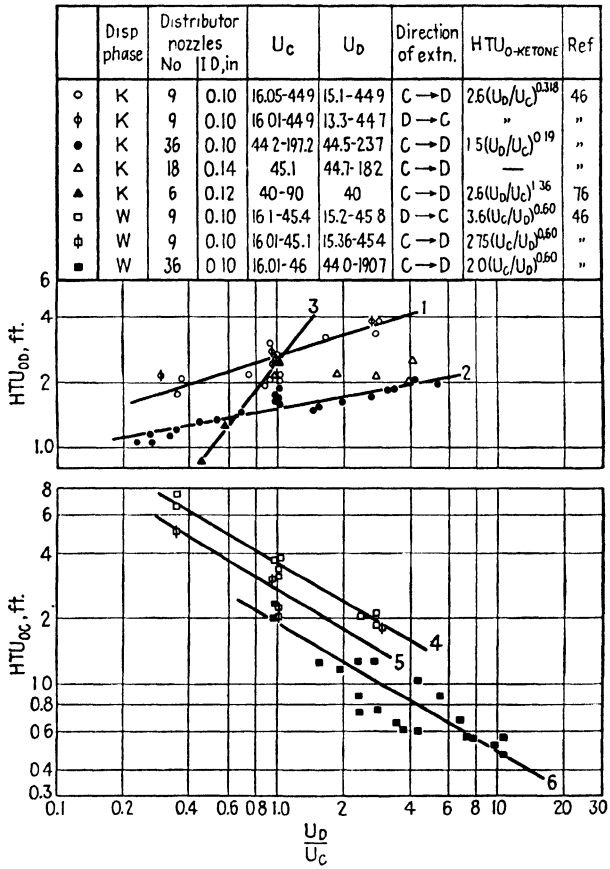



FIG. 10.32. Extraction of acetic acid between methyl isobutyl ketone and water in a spray tower.

in the direction water-to-ether always leads to lower *HTU*'s, probably because of a decreased drop size. Likewise, small increases in rate of extraction at increased acid concentration in the water phase were noted and could be ascribed to the decrease in drop size with decreased interfacial tension. A few data with larger nozzle diameters for the dispersed phase (not shown) indicated, as might be expected, lower rates of extraction.

Extraction of acetic acid between methyl isobutyl ketone and water provides the data of Fig. 10.32. For either phase dispersed, increasing the rate of water flow lowers the *HTU*. For ketone dispersed, the direction of ex-

traction seems unimportant, while for water dispersed slightly lower *HTU*'s result if the direction is ketone-to-water, although this is not well established. The major point brought out by Johnson and Bliss (46) in this work is the importance of proper distributor nozzles. Not only are the diameters of the nozzles important, but equally so is the use of a sufficient number to ensure reasonably uniform drop size. This results in less coalescence and lower *HTU*'s. The apparently anomalous results described by curve 3 can very probably be assigned to this factor. Hayworth and Treybal (36) found that uniform drop size can be expected from sharp-edged nozzles of diameters between 0.059 and 0.31 in. provided that the linear velocity of flow through the nozzle is not greater than approximately 0.3 ft./sec.

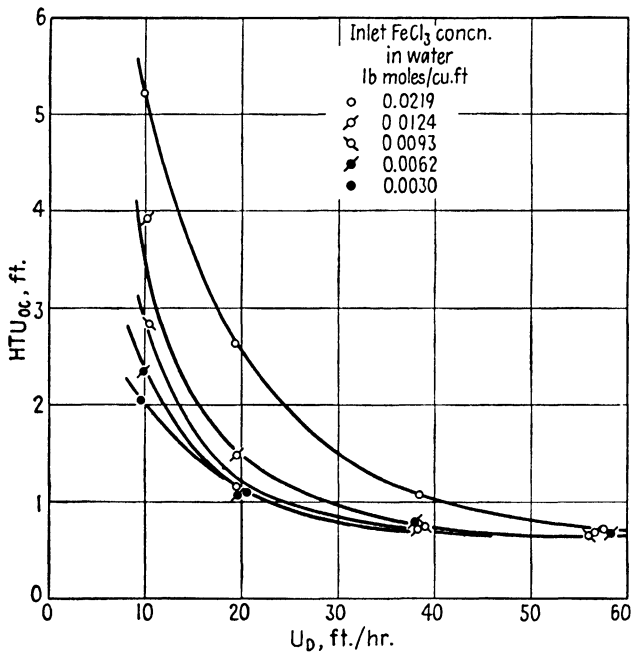



FIG. 10.33. $HTU_{OC}$ without end effects, extraction of $FeCl_3$ from aqueous HCl by isopropyl ether, ether dispersed; spray tower, 1.448 in. diam., $U_C$ = 55.8–58.3 (30). (*With permission of American Chemical Society.*)

Figure 10.33 presents the data of Geankoplis and Hixson (30) for the interesting case of extraction of an inorganic salt, corrected for the end effects shown in Fig. 10.24. The *HTU*'s so corrected are practically independent of position in the tower. The concentration effect is probably caused by the influence of interfacial tension on drop size, which becomes unimportant as the rate of the dispersed phase increases and in turn governs the interfacial area.

Several sets of data on a few isolated systems have been summarized in

TABLE 10.2. MISCELLANEOUS SPRAY-TOWER EXTRACTION DATA

| Dispersed phase | Continuous phase | Extracted solute | Direction of extraction | Tower diam., in. | Distributor nozzles | | $U_C$ | $U_D$ | Equation | Ref. |
|---|---|---|---|---|---|---|---|---|---|---|
| | | | | | No. | I.D. in. | Ft./hr. | | | |
| Water | Benzene | Acetic acid | $D \rightarrow C$ | 1.824 | 36 | 0.10 | 44.1–45.3 | 44–175 | $K_Ca = 0.158U_D$<br>$HTU_{OC} = 1.73$ to 6.34 | Johnson and Bliss, (46) |
| Benzene | Water | Acetic acid | $C \rightarrow D$ | 1.824 | 36 | 0.10 | 16–45.4 | 44.6–120 | $K_Da = 0.157U_D$<br>$HTU_{OD} = 5.4$ to 10.9 | Johnson and Bliss, (46) |
| Benzene | Water | Acetic acid | $C \rightarrow D$ | 3.55 | 6 | 0.12 | 10–60 | 30 | $HTU_{OD} = 3.5\left(\frac{U_D}{U_C}\right)^{0.132}$ | Sherwood, *et al.* (76) |
| Water | Methyl isobutyl ketone | Benzoic acid | $C \rightarrow D$ | 1.824 | 36 | 0.10 | 46–46.9 | 43.7–175 | $K_Ca = 0.00665U_D$<br>$HTU_{OC} = 37.5$ to 157 | Johnson and Bliss, (46) |
| Water | Methyl isobutyl ketone | Propionic acid | $C \rightarrow D$ | 1.824 | 36 | 0.10 | 43.9–46.0 | 15.9–132 | $K_Ca = 0.267U_D$<br>$HTU_{OC} = 1.18$ to 10.37 | Johnson and Bliss, (46) |
| Methyl isobutyl ketone | Water | Propionic acid | $C \rightarrow D$ | 1.824 | 36 | 0.10 | 44.2–45.0 | 49.6–132.0 | $K_Da = 0.281U_D$<br>$HTU_{OD} = 3.56$ | Johnson and Bliss, (46) |
| Methylethyl ketone | $CaCl_2$ brine | Water | $D \rightarrow C$ | 3.55 | 6 | 0.12 | 16.1–35.6 | 26.7–66.1 | $K_Da = 0.4U_D$<br>$HTU_{OD} = 2.5$ | Meissner, *et al.* (57) |

Table 10.2. The empirical equations indicated are of course applicable only over the range of conditions listed.

*Heat Transfer.* The use of an extraction tower to transfer heat between the dispersed and continuous liquids is an interesting variation of the operations under consideration. Rosenthal (69) and the author have found this a convenient means of comparing the tower performances for different conditions of operation. Typical spray-tower data are shown in Fig. 10.34,

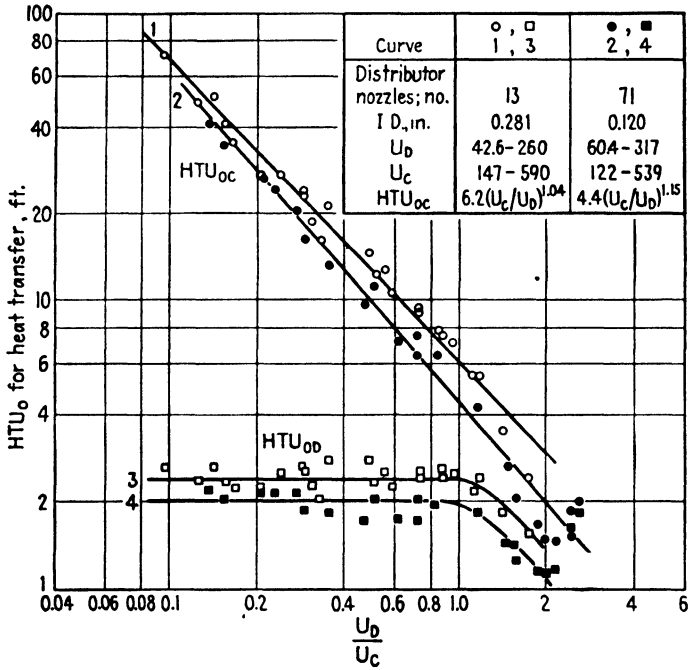



FIG. 10.34. Heat transfer in a spray tower, 5.38″ diam. × 10′9″; toluene dispersed, water continuous (69).

taken from a tower with end designs similar to those of Fig. 10.2.† The similarity between the performance curves for heat transfer and extraction is obvious, although the sudden drop in values of $HTU_{OD}$ at high values of $L_D$ has not been observed in extraction, and there appears to be a somewhat lesser dependency on distributor nozzle diameter. Over-all heat-transfer coefficients ($Ua$) calculated from the same data seem completely independent of continuous-phase rate over the range investigated, and values

† For heat transfer, heights of transfer units ($HTU$) and heat-transfer coefficients ($Ua$) are related by the expressions:

$$HTU_{OC} = \frac{h}{\int_{t_{C_1}}^{t_{C_2}} \frac{dt_C}{(t_C - t_D)}} = \frac{L_C C_C}{Ua}, \qquad HTU_{OD} = \frac{h}{\int_{t_{D_1}}^{t_{D_2}} \frac{dt_D}{(t_C - t_D)}} = \frac{L_D C_D}{Ua}$$

where $t$ = temp., $h$ = height of tower, $L$ = flow rates, and $C$ = heat capacity.

of H.E.T.S. vary from 2.0 to 8.6 ft. for the larger nozzles, from 1.3 to 5.6 ft. for the smaller. The utility of this type of heat transfer in continuous fat splitting is indicated by Allen, *et al.* (1), who report some heat-transfer data for the system fatty acids–water. Over a limited range of flow rates, ½-in.-ring packing gave over-all values of *HTU* calculated in the water phase of 3.2 to 3.6 ft., while the tray construction of Fig. 10.10 gave values of 0.7 to 1.3 ft.

**Packed Towers.** The introduction of packing into a tower may influence the rate of extraction in several ways. The packing particles hinder the rising droplets; consequently the hold-up of dispersed-phase and inter-

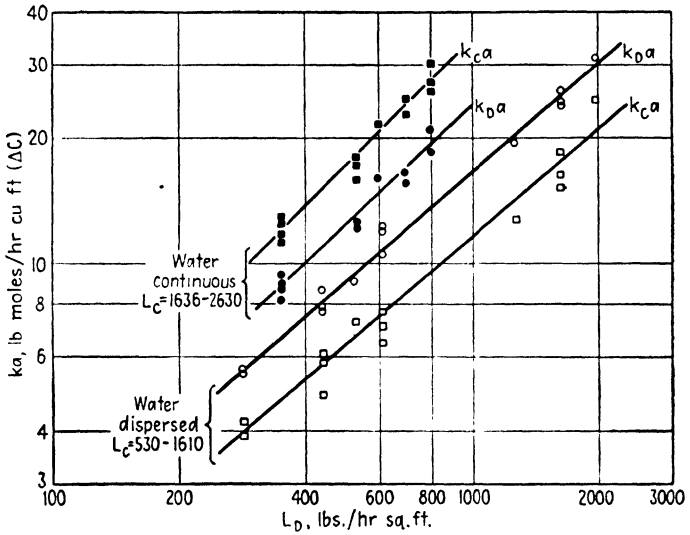



FIG. 10.35. Individual-film coefficients; water–3-pentanol, ¼-in. rings (51).

facial area is larger, and turbulence in the continuous phase will be increased. The coefficients are consequently larger for the packed tower than for a spray tower, for comparable operating conditions. The packing also regulates the size of the droplets of dispersed phase, to some extent, so that the influence of the distributor nozzle design is less important. In certain systems with high interfacial tension and a strong preferential wetting of the packing by the dispersed phase, there are no droplets. Instead the dispersed phase flows along the packing surface in rivulets whose surface area changes relatively little with flow rate. The operating characteristics in such cases can be very different from those first described, and an interchange of dispersion of the phases can have profound effects on the rate of extraction.

Individual-film coefficients and *HTU*'s in packed towers have been measured by Colburn and Welsh (19) and Laddha and Smith (51), using the technique previously described. Typical mass-transfer coefficients are shown in Fig. 10.35 for the system 3-pentanol–water, where the rate of the

continuous phase seems to have no influence. At higher flow rates, where the hold-up might be increased by increased values of $L_C$, an effect might be anticipated. Typical $HTU$'s are shown in Fig. 10.36, correlated in the manner used for spray towers, and a summary of all the single-film data is given in Table 10.3. In every case $HTU_D$ is practically constant, independent of flow rate of either phase, while $HTU_C$ is a strong function of flow rates. Variation in the value of $HTU$ from one system to another cannot be entirely reconciled on the basis of diffusivities, and the variation of interfacial area due to dispersion differences probably exerts the major influence. Comparison with the data for spray towers shows in most cases a 20 to 25 per cent lowering of the $HTU$'s by the packing.

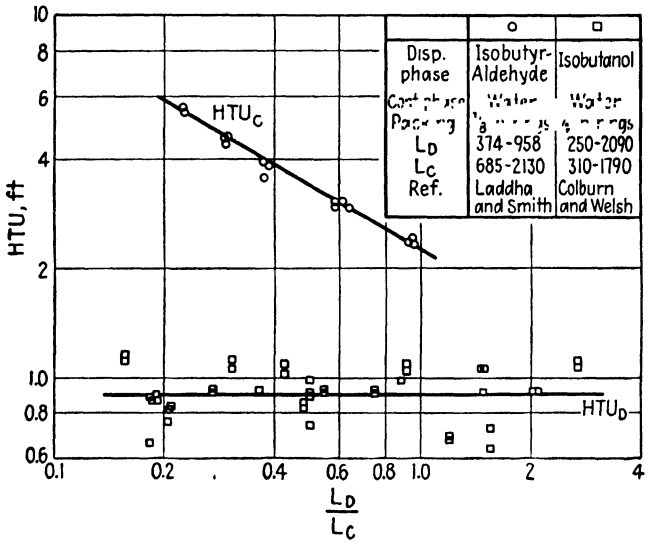



FIG. 10.36. Individual-film $HTU$'s for packed towers.

The remaining data representing the results of systematic tests are overall extraction coefficients and $HTU$'s. These were all taken from laboratory-sized equipment, and in many of these tests the tower diameter was too small to give a normal packing density. Numerical values of rates of extraction in such cases must be used with caution when applied to larger towers. The importance of this is corroborated by the observations of Gloyer (31), who reports on the extraction of vegetable oils with furfural in packed towers of 2, 22, and 66 in. in diameter. The effectiveness of unit height for the two large diameters was essentially the same but noticeably greater for the 2-in.-diameter tower.

The parallel in the variation of extraction rate and hold-up of dispersed phase with flow rate has been noted by several investigators. The data of Sherwood, *et al.* (76) on the extraction of acetic acid from water by benzene,

TABLE 10.3. INDIVIDUAL-FILM HTU'S FOR PACKED TOWERS

| Dispersed phase | Continuous phase | Packing | $HTU_C$ | $HTU_D$ | Ref. |
|---|---|---|---|---|---|
| Isobutanol | Water | ½-in. rings | $1.0\left(\frac{L_C}{L_D}\right)^{0.75}$ | 0.9 | Colburn and Welsh (19) |
| Water | Isobutanol | ½-in. rings | $2.0\left(\frac{L_C}{L_D}\right)^{0.75}$ | 0.6 | Colburn and Welsh (19) |
| Isobutyraldehyde | Water | ¼-in. rings | $1.95\left(\frac{L_C}{L_D}\right)^{0.58}$ | . ..... | Laddha and Smith (51) |
| Isobutyraldehyde | Water | ⅜-in. rings | $2.28\left(\frac{L_C}{L_D}\right)^{0.58}$ | . ... | Laddha and Smith (51) |
| Water | Isobutyraldehyde | ¼-in. rings | | $2.3\left(\frac{L_D}{L_C}\right)^{0.087}$ | Laddha and Smith (51) |
| Water | Isobutyraldehyde | ⅜-in. rings | . . . | 2.65 | Laddha and Smith (51) |
| 3-Pentanol | Water | ¼-in. rings | $0.50\left(\frac{L_C}{L_D}\right)^{0.98}$ | $0.9\left(\frac{L_D}{L_C}\right)^{0.04}$ | Laddha and Smith (51) |
| 3-Pentanol | Water | ⅜-in. rings | $0.51\left(\frac{L_C}{L_D}\right)^{0.94}$ | $0.9\left(\frac{L_D}{L_C}\right)^{0.04}$ | Laddha and Smith (51) |
| Water | 3-Pentanol | ¼-in. rings | $1.66\left(\frac{L_C}{L_D}\right)^{0.87}$ | $0.85\left(\frac{L_D}{L_C}\right)^{0.06}$ | Laddha and Smith (51) |
| Water | 3-Pentanol | ⅜-in. rings | $1.90\left(\frac{L_C}{L_D}\right)^{0.87}$ | $0.85\left(\frac{L_D}{L_C}\right)^{0.06}$ | Laddha and Smith (51) |

Fig. 10.37, is indicative. For three of the curves, with benzene as the dispersed phase, the coefficient increases with increased rate of continuous phase owing to increased hold-up of dispersed-phase droplets. At the higher rates of flow, considerable coalescence then reduced the interfacial area, and the coefficients fell rapidly. The strong influence of dispersed-phase rate is also evident. For the case where water was dispersed, it preferentially wet the carbon ring packing and flowed along the packing surface in rivulets as previously described. The hold-up and consequently

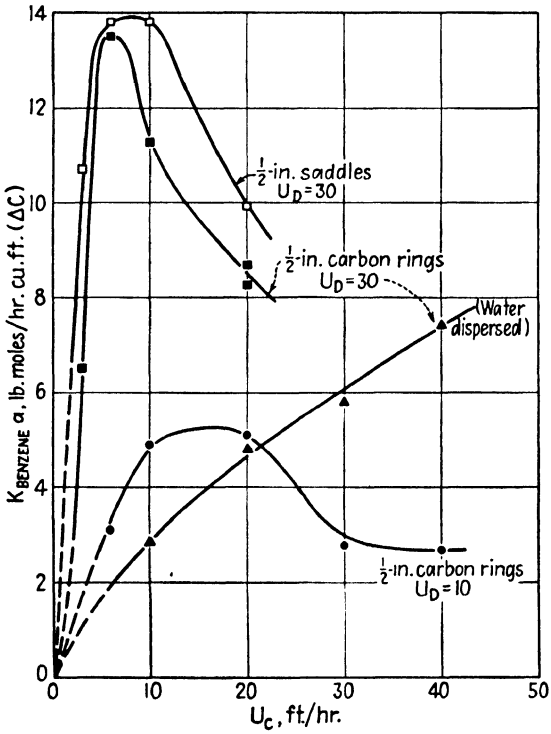



FIG. 10.37. Extraction of acetic acid from water by benzene in a packed tower, 3.55 in. diam., benzene dispersed (76).

the coefficient are much less influenced by rate of flow. The higher coefficients obtained when the dispersed phase does not wet the packing make this an important consideration in the choice of dispersed phase. Similar phenomena were observed by Meissner, *et al.* (57), whose data for the extraction of water from methyl ethyl ketone by calcium chloride brine are summarized in Table 10.4; the brine preferentially wet the ceramic packing, and when it was the dispersed phase not only were the coefficients lower but they were much less dependent upon the continuous-phase flow rate.†

† On the other hand, Berg, *et al.* (7), in extracting methyl ethyl ketone from naphtha by water, found that regardless of the preferential wetting lower values of H.E.T.S. resulted with water dispersed.

The extraction of benzoic acid from toluene by water provided the data for Fig. 10.38, representing tests on a variety of packings. These data are correlated in the empirical fashion previously used, which seems to be able to handle large variations in flow rates for either phase. The standard packings (rings and saddles) give better *HTU*'s than the knit copper cloth,

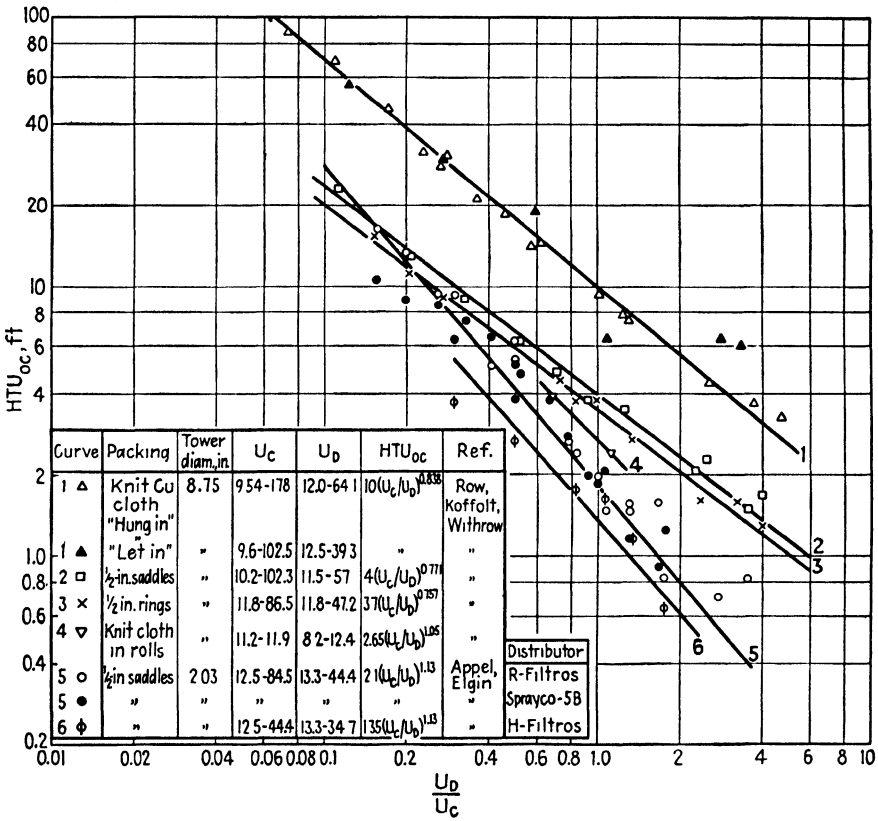



FIG. 10.38. Extraction of benzoic acid from toluene by water in packed towers, toluene dispersed.

except when the cloth is tightly rolled (curve 4). The inferior flooding characteristics make this packing impractical, however. The lesser influence of the design of the dispersed-phase distributor, in comparison to its importance in spray towers, is evident, and the variation in *HTU*'s for ring and saddle packing for the two investigators is more likely due to the different packing densities obtained in the two cases, as observed by Gloyer (31). Although the variation in *HTU* with flow rates is quite as large as for spray towers, the variation with type of packing is relatively small for the standard packings. A few data of Appel and Elgin (3) for water as the dispersed phase are summarized in Table 10.4.

TABLE 10.4. MISCELLANEOUS PACKED-TOWER EXTRACTION DATA

| Dispersed phase | Continuous phase | Extracted solute | Direction of extraction | Phase which wets packing | Packing | Tower diam., in. | Distributor nozzles | Temp., °C. | $U_C$, Ft/hr | $U_D$, Ft/hr | Equation | Ref |
|---|---|---|---|---|---|---|---|---|---|---|---|---|
| Water | Toluene | Benzoic acid | $C \rightarrow D$ | $D$ | ½-in. saddles | 2.03 | Sprayco-5B | 15–18 | 22.2 | 13.3–44.4 | $K_{Da} = 6 + 0.18U_D$ | Appel and Elgin (3) |
| | | | | | | | | | 44.4 | 13.3–44.4 | $K_{Da} = 7.5 + 0.18U_D$ | |
| Water | Benzene | Benzoic acid | $C \rightarrow D$ | $D$ | ½-in. saddles | 1.89 | | 30 | 7.4–96 | 19.2–77.5 | $K_{Da} = 4.42$ to 12.7 | Comings and Briggs (20) |
| Toluene | Water | Furfural | $C \rightarrow D$ | | ½-in. saddles | 4.0 | .. | 25 | 14.7–58.0 | 8.30–28.5 | $HTU_{OC} = 3.3\left(\frac{U_C}{U_D}\right)^{0.95}$ | Knight (49) |
| Toluene | Water | Diethyl amine | $C \rightarrow D$ | | 4-mm. glass beads | 1.312 | 2-mm diam.-tubes | 26.8 | 1.33–8.91 | 0.17–5.20 | $HTU_{OC} = 1.73\frac{U_C}{mU}$ | Morello and Beckmann (58) |
| | | | | | | | | 38.5 | 1.68–14.12 | 0.08–8.03 | $HTU_{OC} = 1.55\frac{U_C}{mU_D}$ | |
| | | | | | | | | 48.5 | 2.50–19.20 | 0.28–9.28 | $HTU_{OC} = 1.27\frac{U_C}{mU_D}$ | |
| | | | | | | | | 57.5 | 2.44–16.66 | 0.88–4.64 | $HTU_{OC} = 0.79\frac{U_C}{mU_D}$ | |
| Methyl isobutyl ketone | Water | Acetic acid | $C \rightarrow D$ | $C$ | ½-in. $C$ rings | 3.55 | Six 0.12 in. I.D. nozzles | 23–27 | 10–80 | 30–70 | $HTU_{OD} = 0.77\left(\frac{U_D}{U_C}\right)^{0.648}$ | Sherwood, *et al.* (76) |
| | | | | | | | | | 10–60 | 10 | $K_{Da} = 7.8 + 0.169U_C$ | |
| Methyl isobutyl ketone | Water | Acetic acid | $C \rightarrow D$ | $C$ | ½-in. saddles | 3.55 | Six 0.12 in. I.D nozzles | 23–27 | 10–40 | 40 | $K_{Da} = 2.13U_C$ | Sherwood, *et al.* (76) |
| Methyl isobutyl ketone | Water | Acetic acid | $C \rightarrow D$ | $C$ | 1-in $C$ rings | 3.55 | Six 0.12 in. I.D nozzles | 23–27 | 10–40 | 40 | $K_{Da} = 15 + 0.64U_C$ | Sherwood, *et al.* (76) |
| Methyl ethyl ketone | $CaCl_2$ brine | Water | $D \rightarrow C$ | $C$ | ½-in. saddles, ½-in. ceramic rings | 3.55 | Six 0.12 in I.D. nozzles | 25–28 | 16.1–34.1 | 26.1–69.5 | $K_{Da} = 0.74U_D$ | Meissner, *et al.* (57) |
| $CaCl_2$ brine | Methyl ethyl ketone | Water | $C \rightarrow D$ | $D$ | ½-in saddles | 3.55 | Six 0.12 in. I.D nozzles | 25–28 | 28.0–65.7 | 17.0–17.3 | $K_Ca = 3.8U_C^{0.42}$ | Meissner, *et al.* (57) |

The very large values of $HTU_{OC}$ indicated in Fig. 10.38, together with the previous observation that $HTU_D$ is relatively small and independent of flow rate (Table 10.3) indicates that the great majority of the diffusional resistance probably lies in the continuous phase for this system. This is corroborated by the data of Fig. 10.39, where the extractions of benzoic acid from dispersed kerosene, toluene, and benzene are all nearly brought together by the inclusion of the distribution coefficient in the abscissa, as

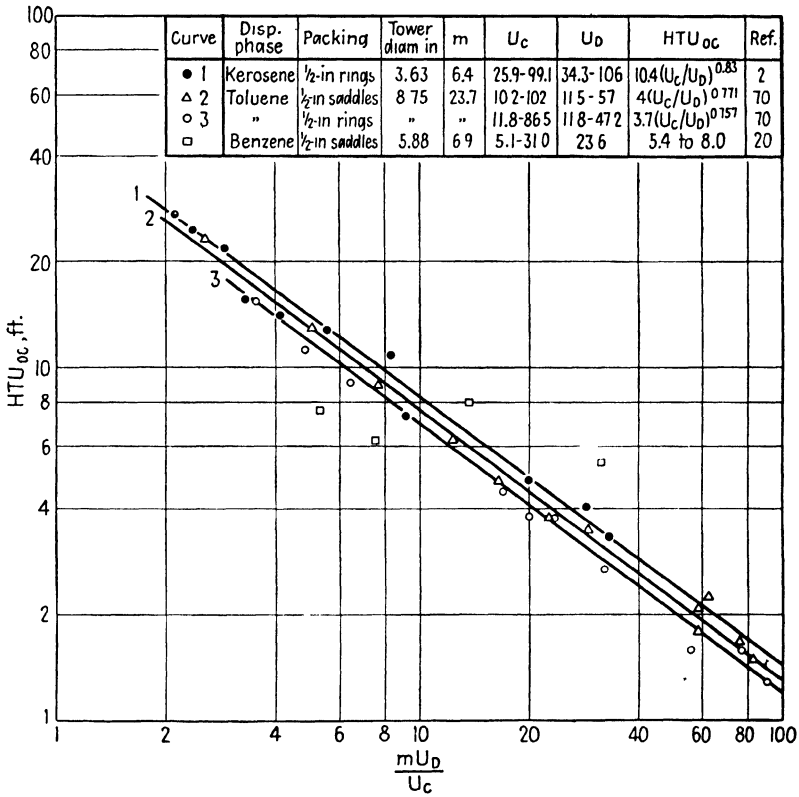



FIG. 10.39. Extraction of benzoic acid from hydrocarbons by water in packed towers, hydrocarbons dispersed.

suggested by Eq. (10.13). Exclusion of this term spreads the data considerably, as indicated by the empirical equations for each system. The interfacial tensions for these systems are all nearly alike, and consequently the interfacial areas are all roughly the same.

A comprehensive set of data on the contacting of water and vinyl acetate was obtained by Pratt and Glover (65), with acetone and acetaldehyde as distributed solutes, Fig. 10.40. The water preferentially wet the packing, and when dispersed formed the rivulets on the packing previously described. In addition to the empirical correlations of the figure, Pratt and Glover

showed that the data could be expressed by the following equations, in the form of Eq. (10.11):

Acetone extracted, vinyl acetate dispersed:

$$\frac{1}{K_{OD}a} = \frac{2.82}{U_D} + \frac{1.20}{U_C^{0.75}} \tag{10.15}$$

Acetaldehyde extracted, vinyl acetate dispersed:

$$\frac{1}{K_{OD}a} = \frac{3.10}{U_D} + \frac{0.92}{U_C^{0.75}} \tag{10.16}$$

Acetone extracted, water dispersed:

$$\frac{1}{K_{OC}a} = \frac{26.0}{U_D^{2.0}} + \frac{0.50}{U_C^{0.32}} \tag{10.17}$$

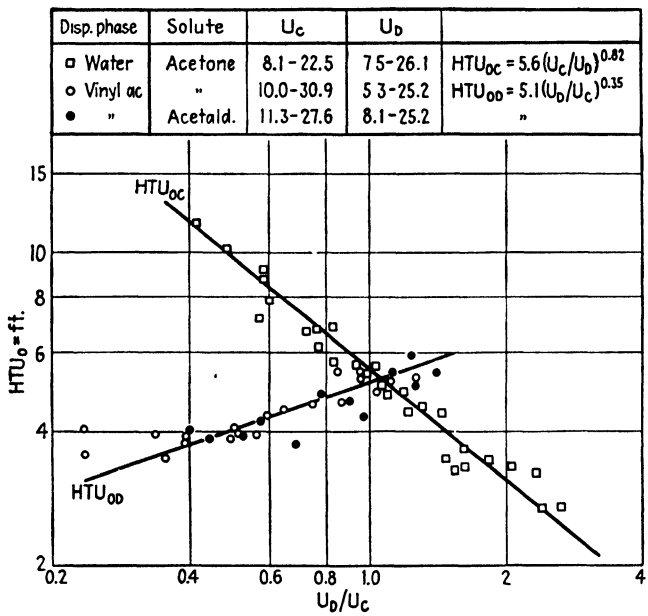



FIG. 10.40. Extraction of acetone and acetaldehyde from vinyl acetate with water in a packed tower, 1.78 in. diam., 10-mm. rings (65).

Values of H.E.T.S. for the case where vinyl acetate was dispersed varied from 4.5 to 5.5 ft. (acetone extracted) and from 5.5 to 6.3 ft. (acetaldehyde extracted). For water dispersed, H.E.T.S. varied from 4.1 to 7.1 ft.

The effect of temperature on extraction rates was investigated by Morello and Beckmann (58), whose data on the system diethylamine–toluene–water are summarized in Table 10.4. Most of the variation in temperature can be taken care of by inclusion of the distribution coefficient in the correlating

equations, as shown, but significant differences still remain which at this time can only be expressed in empirical fashion. The effect of addition of surface active agents to reduce the interfacial tension in the extraction of benzoic acid from benzene with water was investigated by Chu, Taylor, and Levy (16), who found a lowering of the over-all *HTU* with lowered interfacial tension in most instances. Increase of *HTU* in some cases was explained by the assumption of an increased interfacial diffusion resistance due to the adsorbed molecules of surface active agent at the interface. The data cannot be completely regularized.

Rushton (71), working with lubricating oil and nitrobenzene, studied extraction using a variety of packings in a 2.94-in.-diameter tower and obtained values of H.E.T.S. varying from 1.5 to 4.6 ft. over a wide range of operating conditions. With high viscosity oil, large packing was found most desirable, but as extraction proceeded and viscosity was reduced, smaller packing became more effective. Most of the data were therefore taken with a "graded" packing, using different sizes in various sections of the tower, and this arrangement gave the most effective extraction. Values of H.E.T.S. increased with ratio of solvent to oil and with raffinate rate. Slight improvement was noticed for a dispersed solvent phase.

Most of the remaining data are summarized in Table 10.4. The empirical equations are of course limited in applicability to the conditions pertaining in the various tests. Additional data on small packings suitable for laboratory extractions in towers of small diameter are available in the works of Varteressian and Fenske (84), Ney and Lochte (62), and Hou and Franke (39).

**Baffle Towers.** No systematic investigation of these has been reported. For designs of the type of Fig. 10.5, with baffle spacing of 4 to 6 in. in columns of 3 to 6 ft. in diameter, roughly 12 baffles are equivalent to a theoretical stage (33), dependent of course on the design and system. Hixson and Bockelmann (37) report that a baffle tower constructed of a 2.5-in. pipe, with baffles occupying 70 per cent of the cross section and placed 3 in. apart, gave values of H.E.T.S. of 2.1 to 4.7 ft. in the extraction of oleic acid from refined cottonseed oil by liquid propane at 175 to 200°F.

**Perforated-plate Towers.** The few systematic investigations that have been made with perforated-plate towers are summarized in Fig. 10.41 and Table 10.5. The distribution coefficient has been included in the abscissa of the figure in order to permit comparison particularly between the toluene and kerosene systems, and the data are compared with the results from ring-packed towers. It is noteworthy that, whereas both of these liquids gave approximately the same rate of extraction with carbon rings, the perforated plates gave better results with kerosene and slightly poorer results with toluene. Roughly equal flow capacities for both rings and plates are possible for the kerosene, while somewhat greater capacity for the toluene is

possible with the plates, although the flow capacities are greatly dependent on the plate design. The data for extraction of methyl ethyl ketone from gasoline by water and those for extraction of acetic acid by ethyl ether both involve systems of lower interfacial tension than the others. Dispersion into smaller drops and consequently improved extraction result. Unfortunately there are no data for these systems in other types of towers for comparison.

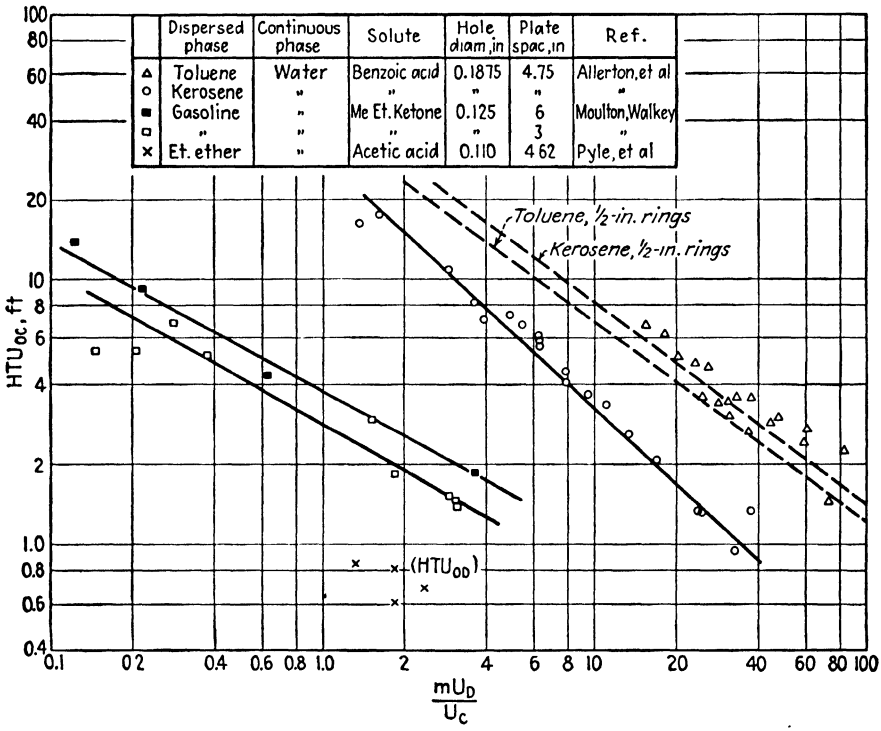



FIG. 10.41. Extraction in perforated-plate towers.

The effect of plate spacing has been studied for several systems. Moulton and Walkey (60) used 3- and 6-in. spacings, and as shown in Fig. 10.41, the 3-in. spacing which causes more frequent redispersion of the light liquid gives improved results. Treybal and Dumoulin (81) used 3-, 6-, and 9-in. spacings, and the summaries of their data in Table 10.5 show, by the coefficients in the empirical equations, that much greater improvement results from a change of 6 to 3 in. than 9 to 6. This is to be expected in the light of the studies that have been made of the end effects in spray towers. Similarly, Pyle, *et al.* (66) investigated spacings of 2.5 to 20 in. and found higher extraction efficiencies per plate at the greater spacings but lower separating effect per unit height of tower, with little change in plate efficiency at spacings greater than 8 in.

TABLE 10.5. EXTRACTION WITH PERFORATED-PLATE TOWERS

| Dispersed phase | Continuous phase | Extracted solute | Tower diam., in. | Plate spacing, in. | Holes diam., in. | Per cent of cross-section | Downspout, per cent of cross section | $U_D$ | $U_C$ | Equation | Ref. |
|---|---|---|---|---|---|---|---|---|---|---|---|
| | | | | | | | | Ft./hr. | | | |
| Toluene | Water | Benzoic acid | 3.56 | 3 | 0.1875 | 4.72 | 1.30 | 9.7–79.5 | 15.1–31.4 | $HTU_{OC} = 4.3\left(\frac{U_C}{U_D}\right)^{0.91}$ | Treybal and Dumoulin (81) |
| | | | | 6 | 0.1875 | 4.72 | 1.30 | 30.2–76.8 | 22.9–41.5 | $HTU_{OC} = 7.2\left(\frac{U_C}{U_D}\right)^{0.91}$ | |
| | | | | 9 | 0.1875 | 4.72 | 1.30 | 35.8–78.6 | 23.2–38.9 | $HTU_{OC} = 8.1\left(\frac{U_C}{U_D}\right)^{0.91}$ | |
| Toluene | Water | Benzoic acid | 8.75 | 6 | 0.1250 | 9.48 | 1.43 | 11.8–47.7 | 11.5–37.0 | $HTU_{OC} = 4.9\left(\frac{U_C}{U_D}\right)^{1.03}$ | Row, Koffolt, Withrow (70) |
| | | | | | 0.0938 | 5.35 | 1.43 | 12.5–47.7 | 11.8–37.1 | $HTU_{OC} = 4.3\left(\frac{U_C}{U_D}\right)^{1.32}$ | |
| Toluene | Water | Benzoic acid | 3.63 | 4.75 | 0.1875 | 13.61 | 3.57 | 38.6–144 | 36.4–77.6 | $HTU_{OC} = 5.4\left(\frac{U_C}{U_D}\right)^{0.94}$ | Allerton, *et al.* (2) |
| Kerosene | Water | Benzoic acid | 3.63 | 4.75 | 0.1875 | 13.61 | 3.57 | 33.8–162.2 | 24.7–136.0 | $HTU_{OC} = 5.4\left(\frac{U_C}{U_D}\right)^{0.94}$ | Allerton, *et al.* (2) |
| Gasoline | Water | Methyl ethyl ketone | 3.75 | 3 | 0.125 | 3.0 | 2.25 | 5.35–15.6 | 14.4–66.9 | $HTU_{OC} = 1.45\left(\frac{U_C}{U_D}\right)^{0.71}$ | Moulton and Walkey (60) |
| | | | | 6 | 0.125 | 3.0 | 2.25 | 2.34–16.8 | 14.0–49.4 | $HTU_{OC} = 1.95\left(\frac{U_C}{U_D}\right)^{0.72}$ | |
| Ether | Water | Acetic acid | 8.63 | 4.62 | 0.1100 | 3.34 | | 26.6–73.5 | 11.2–30.9 | $HTU_{OD} = 1.75\left(\frac{U_C}{U_D}\right)$ | Pyle, *et al.* (66) |

The effect of perforation size has been studied by Row, Koffolt, and Withrow (70) (Table 10.5) and Pyle, *et al.* (66), who also studied the effect of varying the percentage cross section devoted to the perforations (Fig. 10.42). The extraction rate is influenced relatively little by hole diameter but is increased by increased free area for flow. The latter factor also has a profound influence on the flow capacities, as discussed earlier.

Perforated plates of conical design were tried by Row, *et al.* (70) who found that they give essentially the same results as flat plates with the same perforation size. A few data on the relative efficiency of removal of phenol

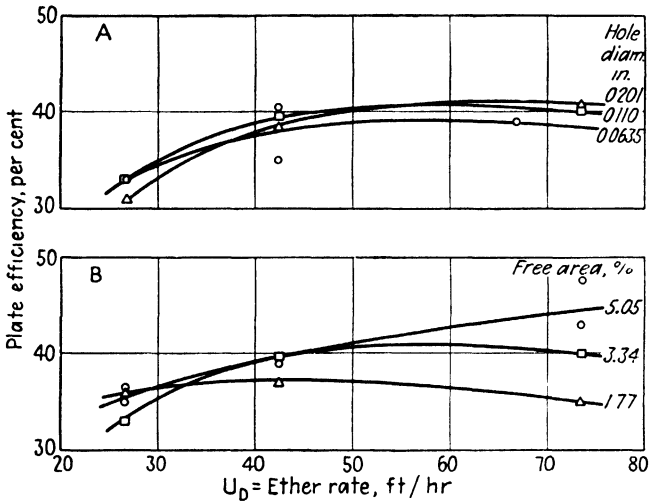
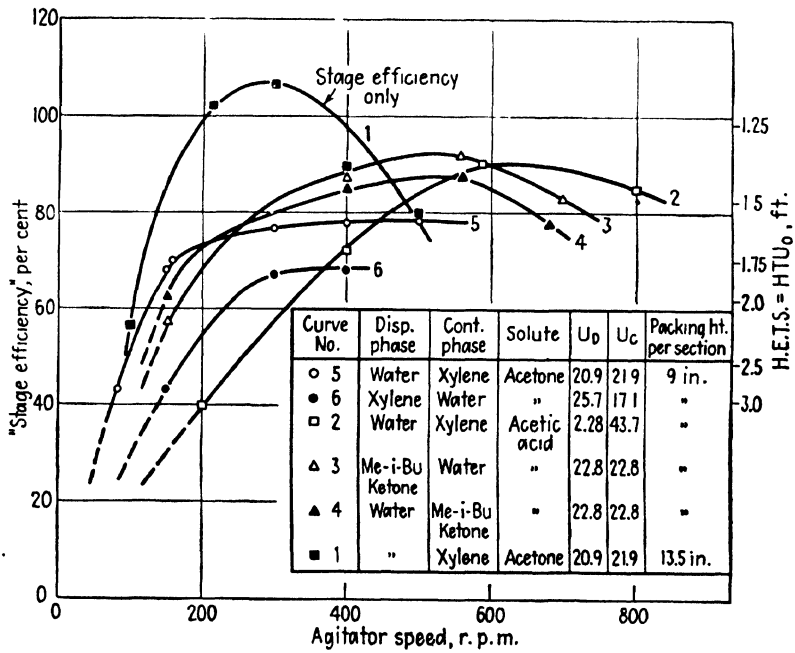



FIG. 10.42. Perforated-plate tower; (*A*) effect of hole diameter and (*B*) free area for flow: extraction of acetic acid from water by ethyl ether (dispersed); $U_D/U_C = 2.38$. [*Data of Pyle, Duffey, and Colburn* (66). *With permission of American Chemical Society.*]

from aqueous ammonia liquor by benzene are given by Hoening (38), who obtained a 73 per cent removal with perforated plates (water dispersed) and 25-mm. rings, 70 per cent with 60-mm. rings, and 55 per cent with a spray tower, 6 m. tall. Hunter and Nash (43) report a similar comparison between a spray and perforated-plate tower. A few data from an experimental Koch tower (Fig. 10.9) show tray efficiencies of 50 to 90 per cent in sweetening gasoline (29, 40).

**Spinner Column.** Recent tests on an 11.5-in.-diameter tower of Scheibel's design (Fig. 10.11) have been reported (73), and a few of the data are shown in Fig. 10.43. The data were all taken at such flow rates that the operating lines and equilibrium curves were essentially parallel, so that the values of over-all $HTU$ apply to concentration gradients in either phase and are numerically equal to values of H.E.T.S. A stage was considered to include one agitator together with one packed section for the purposes of computing stage efficiencies. While the data are too few for extensive

generalizations, it appears that the column performance is less dependent upon ratios of flow rates than are those of ordinary packed towers but greatly dependent upon speed of the agitator. For the 9-in. packed sections, little improvement in extraction is obtained beyond an agitator speed of 400 r.p.m., and increasing the speed too greatly causes emulsification and flooding Additional effects, such as those of liquid throughout, are discussed by Scheibel and Karr (73). In the case of the methyl isobutyl ketone–water–acetic acid system, a comparison of the performance of this




| Curve No. | Disp. phase | Cont. phase | Solute | $U_D$ | $U_C$ | Packing ht. per section |
|---|---|---|---|---|---|---|
| ○ 5 | Water | Xylene | Acetone | 20.9 | 21.9 | 9 in. |
| ● 6 | Xylene | Water | " | 25.7 | 17.1 | " |
| □ 2 | Water | Xylene | Acetic acid | 2.28 | 43.7 | " |
| △ 3 | Me-i-Bu Ketone | Water | " | 22.8 | 22.8 | " |
| ▲ 4 | Water | Me-i-Bu Ketone | " | 22.8 | 22.8 | " |
| ■ 1 | " | Xylene | Acetone | 20.9 | 21.9 | 13.5 in. |

FIG. 10.43. Extraction in a Scheibel column, 11.5 in. diam, 3-in. agitator sections; 4-in diam., four-bladed agitator. Extraction from dispersed phase (73).

novel device with that of the more conventional towers is shown in Fig. 10.44. The spray tower is much more susceptible to changes in dispersed phase than the agitated column and, as might be expected, gives a poorer performance. The system is one of low interfacial tension and is easily dispersed; apparently the conventional packings will do as well as the agitated column, at least at the flow rates for which comparison data are available. This may be due to failure of the mesh packing to break the emulsion formed by the agitator, resulting in some recirculation. Additional data for a laboratory-sized (1-in.-diameter) column, showing very low values of H.E.T.S., are also available (72).

**Centrifugal Extractor.** No systematic tests of the Podbielniak extractor have been reported. From 8 to 12 equivalent stages have been obtained

per machine in the extraction of *n*-butylamine between a naphtha and water (48), but these will vary at least with flow rate and system. Bartels and Kleiman (6) indicate 4 stages per machine in the extraction of streptomycin with amyl alcohol containing 15 per cent lauric acid from a buffered solution.

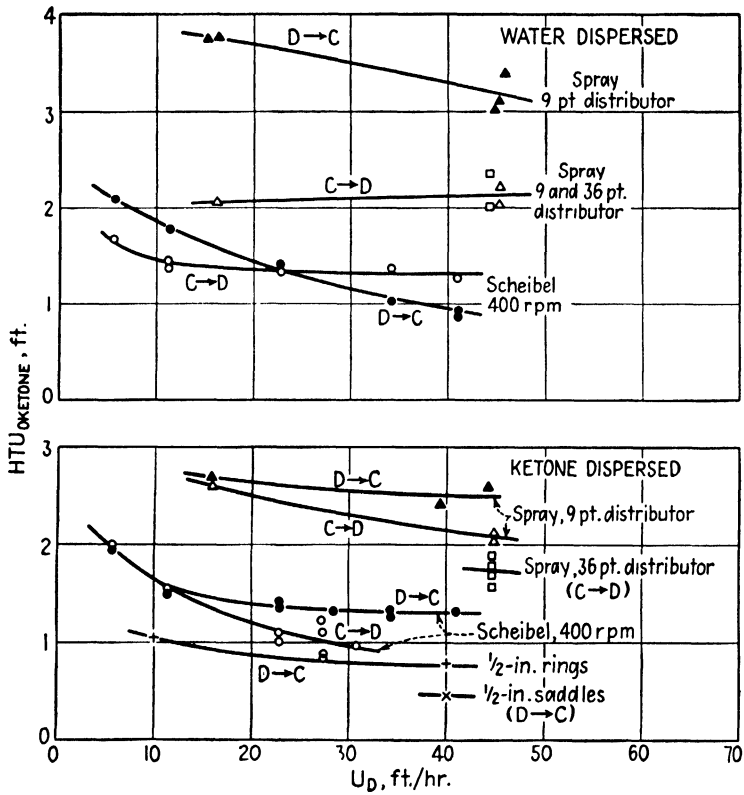



FIG. 10.44. Extraction of acetic acid between methyl isobutyl ketone and water. [*Data of Scheibel and Karr* (73). *Spray-tower data of Johnson and Bliss* (46). *Packed-tower data of Sherwood, et al.* (76).] Direction of extraction marked on the curves. $U_D/U_C = 1.0$.

**Miscellaneous.** Isolated data from a variety of industrial-sized towers have been reported by Morello and Poffenberger (59).

### Notation for Chapter 10

$a$ = interfacial surface (in flooding correlation, surface of packing), sq. ft./cu. ft.
$C$ = heat capacity, Btu/lb.°F.
$C_0$ = orifice constant.
$c$ = concentration, lb. moles/cu. ft.
$D$ = diffusivity, sq. ft./hr.
$d$ = a linear dimension, ft.

$d_0$ = internal diameter of nozzle, orifice, or perforation, ft.
$F$ = fractional free voids of a packing.
$g$ = gravitational constant = $4.17 \times 10^8$ ft./hr.$^2$.
$H$ = fractional volume hold-up of dispersed phase.
H.E.T.S. = height equivalent to a theoretical stage, ft.
$HTU$ = height of a transfer unit, ft.
$h$ = height of a tower, ft.
$h_{ce}$ = displacement of continuous phase due to contraction and expansion losses, ft.
$h_f$ = displacement of continuous phase due to friction, ft.
$h_0$ = displacement of continuous phase due to orifice, ft.
$h_\sigma$ = displacement of continuous phase to overcome interfacial tension, ft.
$K$ = over-all mass-transfer coefficient, lb. moles/hr. sq. ft. ($\Delta c$).
$Ka$ = over-all mass-transfer coefficient, lb. moles/hr. cu. ft. ($\Delta c$).
$k$ = individual-film mass-transfer coefficient, lb. moles/hr. sq. ft. ($\Delta c$).
$L$ = superficial mass velocity, lb./hr. sq. ft.
$m$ = distribution coefficient = $c_D/c_C$ at equilibrium.
Re = Reynolds number.
Sc = Schmidt number.
$S_0$ = cross-sectional area of perforations, sq. ft.
$S_t$ = cross-sectional area of tower, sq. ft.
$t$ = temperature, °F.
$U$ = superficial velocity, ft./hr. (volumetric flow rate, cu. ft./hr.)/(cross section of empty tower, sq. ft.)
$Ua$ = over-all heat-transfer coefficient, Btu/hr. cu. ft. °F.
$U_0$ = velocity through a perforation, ft./hr.
$U_p$ = Average velocity of a particle or drop relative to the wall of a tower, ft./hr.
$u$ = velocity through a nozzle, ft./sec. [Eq. (10.2)].
$v$ = volume of a drop, cu. ft.
$\mu$ = viscosity, lb./ft. hr. = 2.42 (centipoises).
$\mu'$ = viscosity, centipoises.
$\rho$ = density, lb./cu. ft.
$\Delta\rho$ = difference in density between phases, lb./cu. ft.
$\sigma$ = interfacial tension, lb./ft. = $6.89 \times 10^{-5}$ (dynes/cm.).
$\sigma'$ = interfacial tension, dynes/cm.
$\alpha, \beta, \delta, \epsilon, \eta, \lambda, \tau, \phi, \psi$ = constants.

Subscripts:
$C$ = continuous phase.
$D$ = dispersed phase.
$O$ = over-all.

## LITERATURE CITED

1. Allen, H. D., W. A. Kline, E. A. Lawrence, C. J. Arrowsmith, and C. Marsel: *Chem. Eng. Progress* **43**, 459 (1947).
2. Allerton, J., B. O. Strom, and R. E. Treybal: *Trans. Am. Inst. Chem. Engrs.* **39**, 361 (1943).
3. Appel, F. J., and J. C. Elgin: *Ind. Eng. Chem.* **29**, 451 (1937).
4. Atkins, G. T.: U.S. Pat. 2,274,030 (2/24/42).
5. Ballard, J. H., and E. L. Piret: *Ind. Eng. Chem.* **42**, 1088 (1950).
6. Bartels, C. R., and G. Kleiman: *Chem. Eng. Progress* **45**, 589 (1949).

7. Berg, C., M. Manders, and R. Switzer: Paper presented to *Am. Inst. Chem. Engrs.*, Los Angeles, Mar. 9, 1949.
8. Bergelin, O., F. J. Lockhart, and G. G. Brown: *Trans. Am. Inst. Chem. Engrs.* **39,** 173 (1943).
9. Blanding, F. H., and J. C. Elgin: *Trans. Am. Inst. Chem. Engrs.* **38,** 305 (1942).
10. Border, L. E.: *Chem. Met. Eng.* **47,** 776 (1940).
11. Borrmann, C. H.: *Z. angew. Chem.* **32,** I, 36 (1919).
12. Breckenfeld, R. R., and C. R. Wilke: *Chem. Eng. Progress* **46,** 187 (1950).
13. Brinsmade, D. S., and H. Bliss: *Trans. Am. Inst. Chem. Engrs.* **39,** 679 (1943).
14. Brown, J. W.: U.S. Pat. 2,161,405 (6/6/39).
15. Cattaneo, G., and P. Jodeck: U.S. Pat. 1,766,281 (6/24/30); Brit. Pat. 279,774 (11/1/26).
16. Chu, J. C., C. C. Taylor, and D. J. Levy: *Ind. Eng. Chem.* **42,** 1157 (1950).
17. Coahran, J. M.: U.S. Pat. 1,845,128 (2/16/32).
18. Colburn, A. P.: *Trans. Am. Inst. Chem. Engrs.* **38,** 335 (1942).
19. ——— and D. G. Welsh: *Trans. Am. Inst. Chem. Engrs.* **38,** 179 (1942).
20. Comings, E. W., and S. W. Briggs: *Trans. Am. Inst. Chem. Engrs.* **38,** 143 (1942).
21. Cornish, R. E., R. C. Archibald, E. A. Murphy, and H. M. Evans: *Ind. Eng. Chem.* **26,** 397 (1934).
22. Davis, H. R.: U.S. Pat. 2,468,044 (4/26/49).
23. Dons, E. M., O. G. Mauro, and D. B. Mapes: U.S. Pat. 2,144,797 (1/24/39).
24. Elgin, J. C.: U.S. Pat. 2,364,892 (12/12/44).
25. ——— and F. M. Browning: *Trans. Am. Inst. Chem. Engrs.* **31,** 639 (1935); **32,** 105 (1936).
26. ——— and H. C. Foust: *Ind. Eng. Chem.* **42,** 1127 (1950).
27. Fallah, R., T. G. Hunter, and A. W. Nash: *J. Soc. Chem. Ind.* **53,** 369T (1934).
28. ———, ———, and ———: *J. Soc. Chem. Ind.* **54,** 49T (1935).
29. Fuqua, F. D.: *Petroleum Processing* **3,** 1050 (1948).
30. Geankoplis, C. J., and A. N. Hixson: *Ind. Eng. Chem.* **42,** 1141 (1950).
31. Gloyer, S. W.: *Ind. Eng. Chem.* **40,** 228 (1948).
32. Gordon, J. J., and J. H. Zeigler: U.S. Pat. 2,258,982 (10/14/41).
33. Grad, M.: The Vulcan Copper and Supply Co., Personal communication (1949).
34. Harrington, P. J.: U.S. Pat 1,943,822 (1/16/34); Reissue 21,725 (2/25/41).
35. Hatch, B. F.: *Blast Furnace Steel Plant* **17,** 1797 (1929).
36. Hayworth, C. B., and R. E. Treybal: *Ind. Eng. Chem.* **42,** 1174 (1950).
37. Hixson, A. W., and J. B. Bockelmann: *Trans. Am. Inst. Chem. Engrs.* **38,** 891 (1942).
38. Hoening, P.: *Z. angew. Chem.* **42,** 325 (1929).
39. Hou, H. L., and N. W. Franke: *Chem. Eng. Progress* **45,** 65 (1949).
40. Hufnagel, J.: Koch Engineering Co., Personal communication (1949).
41. Humphrey, I. W.: *Ind. Eng. Chem.* **35,** 1062 (1943).
42. Hunter, T. G., and A. W. Nash: *Ind. Chemist* **9,** 245, 263, 313 (1933).
43. ——— and ———: *Trans. Chem. Eng. Congr. World Power Conf.* (London) **2,** 400 (1937).
44. Ittner, M. H.: U.S. Pat. 2,139,589 (12/6/38).
45. Jantzen, E.: "Das fraktionierte Destillieren und das fraktionierte Verteilen," Dechema Monograph Vol. 5, No. 48, Berlin, Verlag Chemie, 1932.
46. Johnson, H. F., and H. Bliss: *Trans. Am. Inst. Chem. Engrs.* **42,** 331 (1946).
47. Jones, H. E.: *Chem. Met. Eng.* **35,** 215 (1928).
48. Kaiser, H. R.: Podbielniak, Inc., Personal communication (1949).
49. Knight, O. S.: *Trans. Am. Inst. Chem. Engrs.* **39,** 439 (1943).

50. Koch, F. C.: U.S. Pat. 2,401,569 (6/4/46).
51. Laddha, G. S., and J. M. Smith: *Chem. Eng. Progress* **46,** 195 (1950).
52. Laird, W. G.: U.S. Pat. 1,320,396 (11/4/19).
53. Licht, W., and J. B. Conway: *Ind. Eng. Chem.* **42,** 1151 (1950).
54. Lister, D. A.: U.S. Pat. 2,054,432 (9/15/36).
55. Major, C. J.: Thesis, Cornell Univ., 1941.
56. Mann, M. D.: U.S. Pat. 2,153,507 (4/4/39).
57. Meissner, H. P., C. A. Stokes, C. M. Hunter, and G. M. Morrow: *Ind. Eng. Chem.* **36,** 917 (1944).
58. Morello, V. S., and R. B. Beckmann: *Ind. Eng. Chem.* **42,** 1078 (1950).
59. ——— and N. Poffenberger: *Ind. Eng. Chem.* **42,** 1021 (1950).
60. Moulton, R. W., and J. E. Walkey: *Trans. Am. Inst. Chem. Engrs.* **40,** 695 (1944).
61. Nandi, S. K., and T. R. Viswanathan: *Current Sci.* (India) **15,** 162 (1946).
62. Ney, W. O., and H. L. Lochte: *Ind. Eng. Chem.* **33,** 825 (1941).
63. Perry, J. H., Ed., "Chemical Engineers' Handbook," 3d ed., McGraw-Hill Book Company, Inc., New York, 1950.
64. Podbielniak, W.: U.S. Pat. 1,936,523 and others.
65. Pratt, H. R. C., and S. T. Glover: *Trans. Inst. Chem. Engrs.* (London) **24,** 54 (1946).
66. Pyle, C., A. P. Colburn, and H. R. Duffey: *Ind. Eng. Chem.* **42,** 1042 (1950).
67. Raschig, F.: *Z. angew. Chem.* **31,** 183 (1918).
68. Rogers, M. C., and E. W. Thiele: *Ind. Eng. Chem.* **29,** 529 (1937).
69. Rosenthal, H.: Thesis, New York Univ., 1949.
70. Row, S. B., J. H. Koffolt, and J. R. Withrow: *Trans. Am. Inst. Chem. Engrs.* **37,** 559 (1941).
71. Rushton, J. H.: *Ind. Eng. Chem.* **29,** 309 (1937).
72. Scheibel, E. G.: *Chem. Eng. Progress* **44,** 681, 771 (1948).
73. ——— and A. E. Karr: *Ind. Eng. Chem.* **42,** 1048 (1950).
74. Schutze, H. G., W. A. Quebedeaux, and H. L. Lochte: *Ind. Eng. Chem., Anal. Ed.* **10,** 675 (1938).
75. Sherwood, T. K.: *Trans. Am. Inst. Chem. Engrs.* **31,** 670 (1935).
76. ———, J. E. Evans, and J. V. A. Longcor: *Ind. Eng. Chem.* **31,** 1144 (1939); *Trans. Am. Inst. Chem. Engrs.* **35,** 597 (1939).
77. Strang, L. C., T. G. Hunter, and A. W. Nash: *Ind. Eng. Chem.* **29,** 278 (1937).
78. ———, ———, and ———: *J. Soc. Chem. Ind.* **56,** 50T (1937).
79. Swan, D. O., and S. M. Whitehall: *Natl. Petroleum News,* **37,** No. 27, R–529 (1945).
80. Thompson, R. F.: U.S. Pat. 2,400,962 (5/28/46).
81. Treybal, R. E., and F. E. Dumoulin: *Ind. Eng. Chem.* **34,** 709 (1942).
82. ——— and L. T. Work: *Trans. Am. Inst. Chem. Engrs.* **38,** 203 (1942).
83. Van Dijck, W. J. D.: U.S. Pat. 2,011,186 (8/13/35).
84. Varteressian, K. A , and M. R. Fenske: *Ind. Eng. Chem.* **28,** 928 (1936).
85. Wilhelm, R. H., and M. Kwauk: *Chem. Eng. Progress* **44,** 201 (1948).

# CHAPTER 11

# LIQUID-EXTRACTION PROCESSES

In this chapter no attempt will be made to treat all possible liquid-extraction processes nor even to discuss in an exhaustive manner those which are considered. The very rapid growth of the extraction applications would soon make any such treatment obsolete. Instead, typical industrial applications will be considered briefly for the purposes of indicating their frequently complex nature and the special usefulness of extraction as a separation technique.

## PETROLEUM REFINING

Petroleum is a mixture of literally thousands of compounds, principally hydrocarbons of various types, with small percentages of compounds of sulfur, nitrogen, and oxygen. These are initially separated by distillation into a variety of products on the basis of boiling point, which are then further refined and altered to provide various finished products such as gasoline and other fuels, lubricants, waxes, and asphalts. In the course of the initial separation and refining, the chemical nature of the original compounds is frequently changed.

Various compounds having different chemical properties and different physical properties such as density and viscosity occur in the same boiling ranges. Consequently the initial separation by distillation, with a few exceptions, makes substantially no segregation according to chemical type. Separation of these by action of various chemical reagents has long been used; for example, the action of sulfuric acid on unsaturated hydrocarbons. The reaction products formed with such reagents not only are frequently useless, thus representing a considerable loss of petroleum material, but also may introduce difficult problems of regenerating the chemical reagents and disposal of the reaction products. Separation by liquid extraction wherein solvents preferentially dissolve the various compounds according to chemical type without chemical reaction, thus permitting complete recovery of the solvents and the substance separated, obviously offers distinct advantages. This has long been recognized: successful industrial extraction of kerosenes in Rumania was established in 1909 with the process of Edeleanu (38), and as early as 1863 the use of fusel oil for kerosene extraction was suggested (165). Except for the various Edeleanu applications, however, most of the developments have been relatively recent.

The many refinery operations involving contact of the petroleum fractions with insoluble liquids which either bring about reversible or irreversible chemical action between reagent and parts of the oil, or which act purely by selective solution, are all generally carried out in conventional extraction equipment of the sort described in the previous chapter. Indeed, much of this equipment was first developed for these processes. Most of these operations are very adequately described in the many texts on petroleum technology (90, 93, 128), and discussion here will be limited to only a few.

## EXTRACTION OF NAPHTHAS

**Edeleanu Process.** The first commercially successful application of extraction of petroleum-refining processes was established by Edeleanu (38, 39), who extracted aromatic hydrocarbons from kerosenes with liquid sulfur dioxide to improve their burning qualities. The solvent is extremely selective for this purpose and acts without chemical reaction.

Kerosenes contain paraffinic, naphthenic, and aromatic hydrocarbons, which for the present purposes can be grouped as aromatics and nonaromatics. Defize (33) presents a large number of phase diagrams on this basis, showing the configurations of Type 1 systems, Fig. 2.8, where *A* represents the nonaromatic and *C* the aromatic hydrocarbons, with *B* the sulfur dioxide. For a typical kerosene, the binary critical solution temperature between nonaromatics and solvent is 45°C. (113°F.), but at −10°C. (14°F.) the solubility is small, and the binodal curve extends well into the triangular plot. Treatment of kerosene is customarily carried out between 10 and 20°F., somewhat higher temperatures being necessary for higher boiling distillates. No preferential selectivity for the various aromatic hydrocarbons in a given kerosene is apparent, and the nonaromatics are almost all equally insoluble (50). At the same time that the aromatics are preferentially extracted, sulfur compounds, particularly of the cyclic type such as thiophene, are also concentrated in the extract, and Brandt (19) indicates the extent of removal of these that can be expected. Nitrogen compounds are also removed (37*d*).

The early Edeleanu plants used two or three mixer-settler stages operated in countercurrent, but, in 1924, continuous contacting in tower extractors was introduced. Other parts of the process have also been modified and improved in the many years that it has been in use, and the simplified flowsheet of Fig. 11.1 indicates typical equipment arrangements. The charge to be treated is filtered and dried to remove water, which will otherwise form a solid hydrate with the solvent. The hydrate not only clogs distributors in the extraction towers but also leads to corrosion of the steel equipment when later it decomposes at higher process temperatures. After being chilled to extraction temperature, the charge is extracted in two towers with cold liquid sulfur dioxide. The extract and raffinate solutions, after heat

exchange with incoming charge and solvent, are sent to separate series of multiple evaporators operating at pressures of 150 lb/sq. in. to 25 mm. Hg abs. The relative volatility of the solvent is so high that excellent solvent removal is obtained. The sulfur dioxide from the evaporators is collected, dried, compressed, and liquefied for reuse. Finished extract and raffinate may then be treated with sulfuric acid for more complete desulfurization, or caustic-washed to remove traces of sulfur dioxide. Solvent/charge ratios vary between 1 and 2, depending upon the charge stock, and solvent losses are customarily less than 0.1 per cent of the charge.

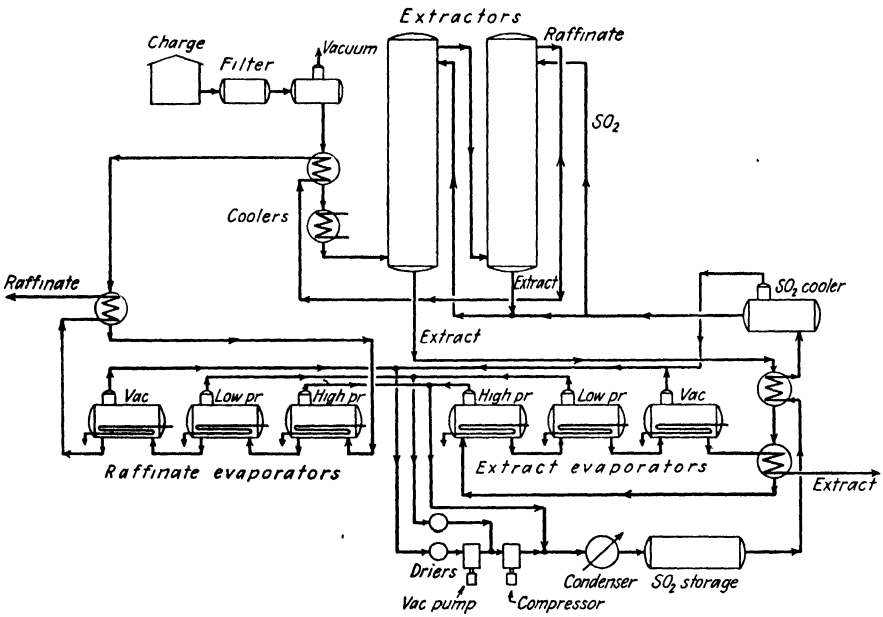



FIG. 11.1. Simplified flowsheet of Edeleanu process for kerosenes. [*Adapted from Defize* (33).]

By 1936, 40 plants of this general type were in operation, treating more than 180,000 bbl./day of kerosene (33). Diesel fuels may also be treated by this process to remove aromatic compounds which impair the ignition qualities of the fuel. A description of a recent installation is given by Dickey (34), and a thorough study of applications and a very complete bibliography is given by Defize (33). Furfural may also be used for this purpose (94).

**Recovery of Aromatics.** A most interesting adaptation of the Edeleanu process was used during the Second World War for production of toluene and other aromatic hydrocarbons for high-octane-number aviation fuels. A description of the process as used at the Abadan refinery of the Anglo-Persian Oil Co. is given by Moy (124). The ordinary Edeleanu process, since it operates with Type 1 phase diagrams, cannot produce a concentra-

tion of aromatics in the extract much higher than about 75 per cent without operating at excessively low temperatures. When the demand for an extract containing at least 95 per cent aromatics developed, operation at temperatures of −60 or −70°F. was discarded as requiring excessive refrigeration and involving other difficulties with common materials of construction. Further, the 25 per cent or so of paraffinic and naphthenic hydrocarbons in the extract cannot be separated by distillation from the aromatics because they have the same boiling range. Instead, the nonaromatics are replaced by others of a much lower volatility by contacting the $SO_2$-contain-

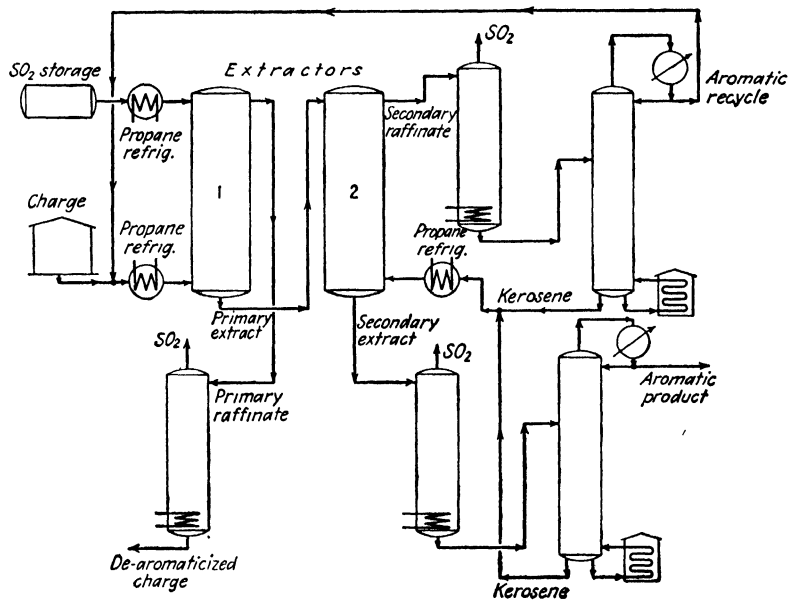



FIG. 11.2. Simplified flowsheet for production of high-purity aromatics. [*After Moy* (124).]

ing extract with a paraffinic kerosene of the necessary boiling range. Subsequent separation of the aromatics of the required purity is then possible. Although nonaromatics are lost to the second kerosene, these are entirely contained in the system by recycling. The principle of the process is similar to one described some years ago (166).

A much-simplified flowsheet is shown in Fig. 11.2. Feedstock containing the appropriate aromatics (roughly 17 per cent by weight, including toluene, ethylbenzene, the xylenes, and others containing 9 and 10 carbon atoms/molecule) is chilled by propane refrigeration and extracted with chilled liquid $SO_2$ at −20 to −24°F. in a 67-ft. tower. The raffinate is stripped of solvent and withdrawn. The primary extract is contacted in a 100-ft. tower with a paraffinic kerosene to remove the nonaromatics and replace them with high-boiling hydrocarbons. The secondary extract is

stripped of its $SO_2$ and distilled to remove the aromatic product, and the kerosene is then recycled. The raffinate from the second extraction is stripped of $SO_2$ and fractionated to produce the high-boiling kerosene as bottoms which is recycled to the second extractor, and the low-boiling aromatics as distillate. These are recycled to the first extractor. Sulfur dioxide is stripped from the various streams in multistage fractionators rather than the older type evaporators, is collected and reused.

By feeding the extraction plant with naphthas which are rich in particular aromatic hydrocarbons, those produced by hydroforming for example, high purity of the finished aromatic product is possible. At the Baytown refinery of the Humble Oil and Refining Co., nitration-grade toluene and other high-purity aromatic products are made by these methods, although the product from the extraction plant must be further treated with sulfuric acid and caustic to remove small amounts of olefins and diolefins (72).

Arnold and Coghlan (6) make the interesting proposal to use water as a solvent to separate toluene from hydroformed naphthas of high aromatic content (> 50 per cent toluene by volume), since the Type 2 systems involved then permit high-purity toluene to be obtained directly. Calculations show the equipment required to be reasonable in size if the process were operated at 576°F., although pressures of the order of 1,700 lb./sq. in. would be required to maintain the system in the liquid state. Smith and Funk (149) consider the suitability of a wide variety of solvents, including mixed solvents.

**Butadiene.** During the Second World War, the development of the synthetic-rubber program required the separation of relatively pure 1,3-butadiene from other $C_4$-hydrocarbons, produced for example by dehydrogenation of butane, when separation by ordinary distillation means was impossible. Extractive distillation (68), selective gas absorption, and liquid extraction (123) were used for this separation. In the case of the last, aqueous ammoniacal cuprous acetate solutions containing 3 to 3.5 gm. moles $Cu^+$/liter were used as solvents, which selectively extract diolefinic and acetylene-type hydrocarbons present in the concentrated hydrocarbon feed through a reversible chemical reaction with $Cu^+$. The process then involved the selective stripping of hydrocarbons other than butadiene from the copper solution by countercurrent contact with a butadiene-rich gas, followed by separate desorption of relatively pure butadiene. In the extraction step, towers packed with 1-in. Raschig rings were used, which gave the equivalent of an ideal stage for 10 to 12 ft. of height (about the same as for the same process operated with a gaseous hydrocarbon stream), or mixer-settler combinations with stage efficiencies of 75 to 100 per cent. Numerous details are given by Morrell, *et al.* (123), and equilibrium data for other solvents are discussed by Smith and Braun (148).

## DESULFURIZATION

The sulfur compounds in petroleum oils include hydrogen sulfide ($H_2S$), carbon disulfide ($CS_2$), mercaptans (RSH),† and thiophenols, thioethers (RSR'), polysulfides, thiophenes and thiophanes (heterocyclic compounds), and possibly others (93, 143). Elemental sulfur is sometimes found. These may be present in amounts ranging from a few tenths per cent (Pennsylvania and Mid-Continent sources), through 3 to 4 per cent (California and Mexico sources), to as high as 7 to 8 per cent (Iraq sources). The sulfur compounds are generally objectionable: hydrogen sulfide and mercaptans in the presence of sulfur, are corrosive; mercaptans are objectionably odoriferous; they adversely affect color and stability of the light distillates; they have an unfavorable influence on antiknock and oxidation characteristics of gasoline, particularly on the susceptibility to improvement of antiknock rating by tetraethyl lead; on combustion they yield corrosive oxidation products. For these reasons, they are generally removed, at least in part, or converted to the less objectionable forms.

**Hydrogen Sulfide.** Extraction of the petroleum fraction with an aqueous solution of NaOH (5 to 15 per cent concentration) is usually used to remove $H_2S$, frequently prior to other sulfur-removal operations. This will remove thiophenols as well. A line mixer (Chap. 9) followed by a settler in a one-stage contact, with recirculation of the caustic solution until its ability to remove $H_2S$ is spent, is usually the practice. The fouled extract, containing NaHS and $Na_2S$, cannot conveniently be regenerated by heating, since the acidity of $H_2S$ increases with increased temperature and the caustic thus retains the $H_2S$ more firmly. Oxidation by aeration is an unsatisfactory alternative, and usually the fouled solution is discarded.

Some of the standard processes used for removing $H_2S$ from industrial gases can also be adapted to extracting liquid hydrocarbons: the Girbotol process which uses an aqueous solution of ethanolamines (60), the Phosphate process which uses aqueous potassium phosphate (99), the Alkacid process which uses aqueous solutions of salts of a substituted alanine (8), and the Koppers process which uses aqueous sodium phenolate (26). These solutions, which hold the $H_2S$ less strongly than caustic, can be regenerated by steam stripping or oxidation of the $H_2S$ and reused but will require the equivalent of two- or three-stage countercurrent contact for extraction. The flowsheets for the processes are almost identical with those considered under sweetening, below.

**Sweetening.** Gasolines containing $H_2S$ and mercaptans are considered "sour," and the sweetening operation consists of removal of these substances or their conversion to less offensive compounds. The mercaptan

† R and R' represent alkyl groups.

TABLE 11.1. MERCAPTAN CONTENT OF GASOLINES FROM A MID-CONTINENT CRUDE (66)*

| Mercaptan | Per cent of total mercaptan sulfur | |
|---|---|---|
| | Typical straight-run gasoline | Typical cracked gasoline |
| Methyl | 4 | 19 |
| Ethyl | 6 | 34 |
| Propyl | 13 | 18 |
| Butyl | 19 | 15 |
| Amyl | 18 | 9 |
| Hexyl+ | 40 | 5 |
| Total | 100 | 100 |
| Total mercaptan S, % by wt. | 0.0265 | 0.0357 |

*With permission of *Oil and Gas Journal*

contents of a number of gasolines from various sources have been listed by Happel, Cauley, and Kelly (66), typical of which are the data of Table 11.1. Such mercaptan distribution data represent a certain amount of simplification, since no indication of the secondary or tertiary types is given. The straight-run gasolines are generally lower in mercaptan sulfur than those resulting from other refinery operations. In either case, mercaptans in appreciable concentrations cause disagreeable odor and together with disulfides lessen the response to addition of tetraethyl lead for antiknock improvement, and their concentrations must be reduced. In the past, the extent to which sweetening was carried out, usually by conversion of mercaptans to disulfides, was sufficient to provide a product giving a negative "doctor test," a chemical test which may be sensitive to roughly 0.0004 per cent mercaptan sulfur in the gasoline. The value of the test has been questioned, however, in view of the influence of disulfides on tetraethyl lead susceptibility (66, 107). The cost of such extensive sweetening is considerable, and in recent years there has been a tendency to consider the total cost of the mercaptan removal and tetraethyl lead dosage, together with considerations of odor, in arriving at the optimum mercaptan concentration in the product, which may then be in the neighborhood of 0.002 to 0.005 per cent mercaptan sulfur.

Following removal of $H_2S$, the common processes either (*a*) oxidize the mercaptans to disulfides as in "doctor-treating," (*b*) remove practically all sulfur compounds including mercaptans as in acid-, clay-, or catalytic-treating, or (*c*) extract all or a part of the mercaptans without substantially affecting other sulfur compounds. Processes of the first type involve liquid-liquid contacting and can be carried out in equipment similar to that

used for extraction. They are coming into disfavor since it is now realized that disulfides are almost as objectionable as mercaptans. Only extraction processes will be considered here.

*Caustic Washing.* A flowsheet of the type of Fig. 11.3 may be used, involving stagewise contacting. In the first extractor $H_2S$ is removed by a prewash of caustic, as outlined above. The next three stages are used for countercurrent extraction of the mercaptans from the gasoline with aqueous sodium hydroxide, and the treated gasoline is water-washed to remove

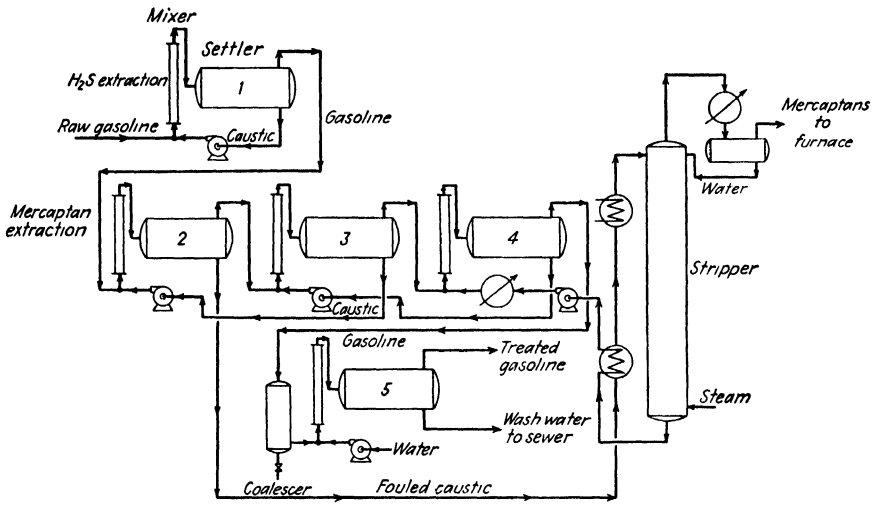



FIG. 11.3. Caustic sweetening of gasolines.

traces of caustic. The fouled caustic solution is steam-stripped for removal of mercaptans, the distillate decanted, and the mercaptans burned. The recovered caustic is recycled to the extraction stages, and the caustic entering the first mercaptan extractor is sometimes diluted with water to reduce gasoline losses in the extract from this stage. Packed towers are being increasingly used in place of the separate stages, since they are generally less costly.

The equilibrium relations existing during the distribution of a mercaptan between a gasoline and a solution of NaOH are indicated in Fig. 11.4. The various equilibria may be characterized as follows (114, 173):

(I) $$m_{\mathrm{I}} = \frac{(\mathrm{RSH}_{aq})}{(\mathrm{RSH}_{oil})} \tag{11.1}$$

(II) $$K_{\mathrm{II}} = \frac{(\mathrm{H^+})(\mathrm{RS^-})}{(\mathrm{RSH}_{aq})} \tag{11.2}$$

(III) $$K_w = \frac{(\mathrm{H^+})(\mathrm{OH^-})}{(\mathrm{H_2O})} \tag{11.3}$$

where the parentheses indicate molar concentrations of the substances enclosed within them. In addition, from a practical viewpoint, the distribution equilibrium between mercaptan in the oil phase and total mercaptan in the aqueous solution is important:

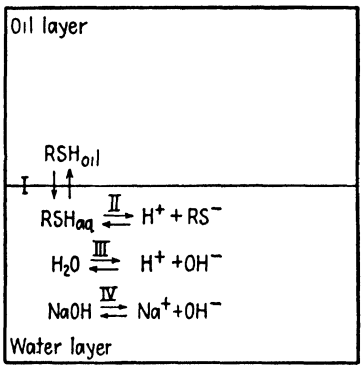



FIG. 11.4. Mercaptan equilibria.

$$m_T = \frac{(RS^-) + (RSH_{aq})}{(RSH_{oil})} \qquad (11.4)$$

The NaOH may be generally considered completely ionized, for relatively dilute solutions at least. Substitution of Eqs. (11.1) to (11.3) in Eq. (11.4) yields

$$m_T = \frac{K_{II} m_I (OH^-)}{K_w (H_2O)} + m_I \qquad (11.5)$$

and since $(RSH_{aq})$ is very small, Eq. (11.5) may be simplified to

$$m_T = \frac{K_{II} m_I (OH^-)}{K_w (H_2O)} \qquad (11.6)$$

Coefficients $m_T$, $m_I$, and $K_{II}$ are indicated in part in Fig. 11.5. The value of $m_T$ increases with increased caustic concentration, since $(OH^-)/(H_2O)$ is thereby increased. The increase in the latter in turn affects the ionization of the mercaptan, Eq. (11.2), and lowers $K_{II}$. In addition, the presence of higher concentrations of NaOH results in a salting out of the unionized mercaptan from the water phase, so that the increase in $m_T$ with caustic concentration is not so great as might at first be anticipated (173). For caustic concentrations up to about 1 normal, Eq. (11.6) can be used to estimate the approximate effect of concentration with the data of Fig. 11.5, on the assumption that $m_I$ and $K_w$ ($0.681 \times 10^{-4}$ at 20 °C.) remain constant and provided that the activity of water (partial pressure over the solution/vapor pressure) is used for $(H_2O)$. A few additional data at higher concentrations are available (29, 173). There is little variation with molecular weight of oil, at least for the naphthas customarily considered in these processes. Secondary and tertiary alkyl mercaptans give lower values of $m_T$ than the normal compounds, and a 20°F. drop in temperature increases $m_T$ by about 50 per cent. For dilute concentrations, the individual values of $m_T$ for the various mercaptans are independent and constant (67), but there is a considerable variation with mercaptan concentration at the higher values (29). For concentrated caustic solutions (*e.g.*, 25 to 30 per cent NaOH), the concentration of caustic during the extraction changes so little that $m_T$ for each mercaptan may be considered constant for a given process.

The caustic solution used in regenerative-type plants, Fig. 11.3, will extract organic acids of the aromatic and naphthenic series from the gaso-

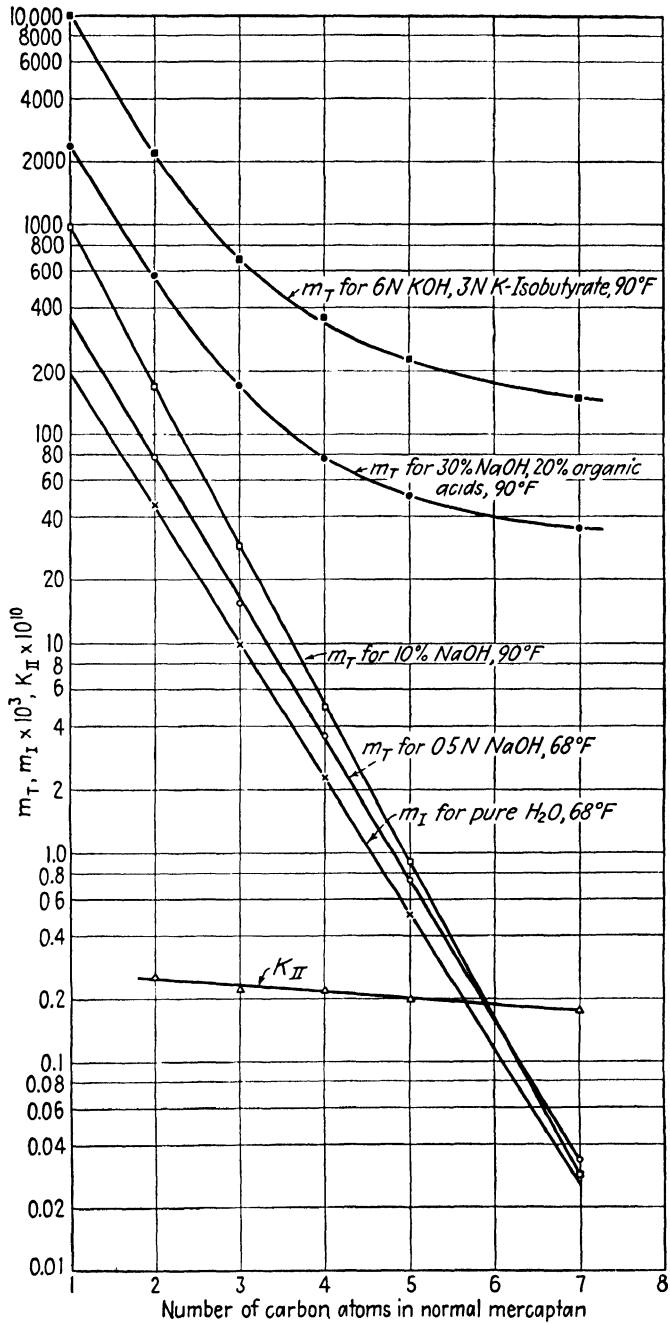



FIG. 11.5. Mercaptan equilibria. [*Data of Yabroff* (173) *and Happel, et al.* (66). *Courtesy, Oil and Gas Journal, and American Chemical Society.*]

line (66). These are not stripped in the caustic recovery system, and they consequently build up to equilibrium concentrations in the caustic. They increase the distribution coefficients $m_T$ for the mercaptans very considerably, particularly for the difficultly extracted mercaptans as indicated in Fig. 11.5. Behavior of this sort was described by Yabroff and White (175), who observed that the concentration of unionized mercaptan in the caustic increased considerably in the presence of a wide variety of organic substances in the caustic solution, and who present a large number of data on the corresponding distributions. The nature and concentration of the organic material naturally influence the distribution strongly.

The extent of extraction of mercaptans further depends upon the extent of their removal from the solvent in the stripper, but a general expression relating the extraction and stripping steps can be readily derived (65). Provided extracting solutions are sufficiently strong and mercaptan concentration sufficiently dilute that the value of $m_T$ can be considered constant, Eq. (6.134) can be written for the extraction operation for each mercaptan:

$$\frac{x_F - x_n}{x_F - \dfrac{y_s}{m_T}} = \frac{(m_T S/G)^{n+1} - (m_T S/G)}{(m_T S/G)^{n+1} - 1} = A \tag{11.7}$$

where $x_F$ = concentration of RSH in the raw gasoline feed
$x_n$ = concentration of RSH in the treated gasoline
$y_s$ = concentration of RSH in the recovered solvent
$S$ = quantity of solvent per unit time
$G$ = quantity of gasoline per unit time
$n$ = number of theoretical extraction stages

Equation (11.7) may be rearranged to read

$$y_s = \frac{m_T}{A}[x_n - (1 - A)x_F] \tag{11.8}$$

Similarly, an equation of the same sort applies to the stripping of the mercaptans in the regeneration step. For each mercaptan, and for open steam injection into the stripper,

$$\frac{y_1 - y_s}{y_1} = \frac{(K_s V/S)^{s+1} - (K_s V/S)}{(K_s V/S)^{s+1} - 1} = B \tag{11.9}$$

where $s$ = number of theoretical distillation trays in the stripper
$y_1$ = concentration of RSH in the fouled solvent leaving the extraction system and entering the stripper
$K_s$ = vaporization equilibrium constant for the mercaptan
$V$ = quantity of stripping steam per unit time

Rearranging Eq. (11.9),

$$y_1 = \frac{y_s}{(1 - B)} \tag{11.10}$$

A material balance for the extractor is

$$G(x_F - x_n) = S(y_1 - y_s) \tag{11.11}$$

Substituting Eqs. (11.8) and (11.10) in Eq. (11.11), and rearranging,

$$\frac{x_n}{x_F} = \frac{\left(\frac{1-B}{B}\right)\frac{G}{S} + m_T\left(\frac{1-A}{A}\right)}{\left(\frac{1-B}{B}\right)\frac{G}{S} + \frac{m_T}{A}} \tag{11.12}$$

$x_n/x_F$ is then the fraction of each mercaptan unextracted from the gasoline. Replacing the values of $A$ and $B$ and simplifying (66),

$$\frac{x_n}{x_F} = \frac{\left(1 - \frac{K_S V}{S}\right)\left[\left(\frac{m_T S}{G}\right)^{n+1} - \frac{m_T S}{G}\right]\frac{G}{S} + \left(\frac{m_T S}{G} - 1\right)\left[\frac{K_S V}{S} - \left(\frac{K_S V}{S}\right)^{s+1}\right]m_T}{\left(1 - \frac{K_S V}{S}\right)\left[\left(\frac{m_T S}{G}\right)^{n+1} - \frac{m_T S}{G}\right]\frac{G}{S} + \left[\left(\frac{m_T S}{G}\right)^{n+1} - 1\right]\left[\frac{K_S V}{S} - \left(\frac{K_S V}{S}\right)^{s+1}\right]m_T} \tag{11.13}$$

Consistent units should be used throughout. Values of $K_s$ are given for typical solutions in Fig. 11.6. Within the limitations inherent in the

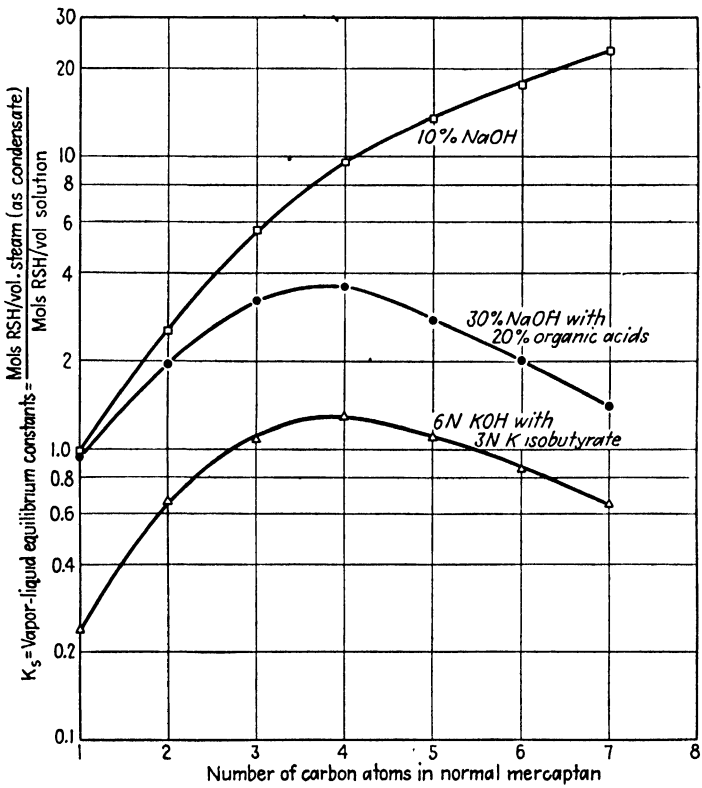



FIG. 11.6. Vaporization equilibrium constants for mercaptans at the boiling points of the solutions (66). (*Courtesy, Oil and Gas Journal.*)

equation and its derivation, it should be applicable to any extraction-stripping operation.

**Illustration 1.** The cracked gasoline of Table 11.1 is to be sweetened by extraction with a solution containing 30% NaOH, 20% organic acids, at 90°F. in a plant containing the equivalent of two theoretical extraction stages, with a solvent circulation rate of 15% of the volume of the gasoline. The stripper is to contain the equivalent of three theoretical trays and is to use 10 lb. stripping steam/bbl. (42 gal.) of gasoline treated (66). Compute the per cent of mercaptan sulfur in the finished gasoline.

*Solution.* $n = 2$, $s = 3$. $S/G = 0.15$ bbl. solution/bbl. gasoline. $V/S = 10/[8.33(42)0.15] = 0.191$ bbl. steam condensate/bbl. solution. For each mercaptan, values of $m_T$ and $K_S$ are read from Figs. 11.5 and 11.6, and the extraction and stripping factors, $m_TS/G$ and $K_SV/G$, calculated. Substitution in Eq. (11.13) permits computation of $x_n/x_F$. The fraction of each mercaptan unextracted multiplied by the fraction of the total mercaptan sulfur each mercaptan represents yields the fraction of the original mercaptan sulfur remaining. The tabulation summarizes the calculations.

| Mercaptan | $m_T$ | $K_S$ | $\frac{m_TS}{G}$ | $\frac{K_SV}{S}$ | $\frac{x_n}{x_F}$ | Fraction of total mercaptan S in raw gasoline | Fraction of mercaptan S remaining |
|---|---|---|---|---|---|---|---|
| Methyl | 2,380 | 0.94 | 357 | 0.1796 | 0.0127 | 0.19 | 0.00241 |
| Ethyl | 570 | 1.95 | 85.5 | 0.372 | 0.0205 | 0.34 | 0.00696 |
| Propyl | 170 | 3.25 | 25.5 | 0.620 | 0.0319 | 0.18 | 0.00575 |
| Butyl | 77 | 3.60 | 11.55 | 0.688 | 0.0611 | 0.15 | 0.00916 |
| Amyl | 51 | 2.75 | 7.65 | 0.525 | 0.1332 | 0.09 | 0.01200 |
| Hexyl$^+$ (assumed heptyl) | 36 | 1.40 | 5.40 | 0.267 | 0.354 | 0.05 | 0.01770 |
| Totals | | | | | | 1.00 | 0.0540 |

Weight per cent mercaptan sulfur remaining = 0.0540(0.0357) = 0.0019.

The results of other similar computations for different operating conditions are discussed by Happel, *et al.* (66). Methods of computation for the extraction only, allowing for variations in $m_T$, are considered by Happel and Robertson (67) and Crary and Holm (29).

The *Solutizer process* (18, 174, 175) uses as an extracting solution aqueous potassium hydroxide (6 normal) in which potassium isobutyrate (3 normal) has been dissolved. This solution gives enhanced extraction (Fig. 11.5) and is therefore particularly useful if the mercaptan content of the gasoline must be reduced to a very low value. A typical flowsheet is shown in Fig. 11.7 where a tower packed with 1-in. carbon rings is used for extraction. Border (18) gives a detailed description of a typical installation. The *Mercapsol process* (104) is similar and uses a sodium hydroxide solution with added naphthenic acids and cresols. The *Tannin process* (122) uses a solutizer solution with tannin, in which case the fouled solution is regenerated by air-blowing.

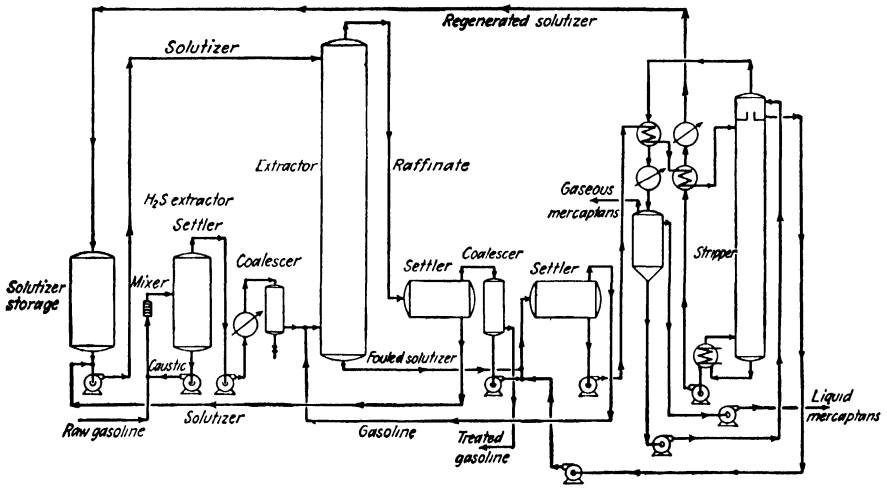



FIG. 11.7. Solutizer sweetening process (18). (*Courtesy, Chemical and Metallurgical Engineering.*)

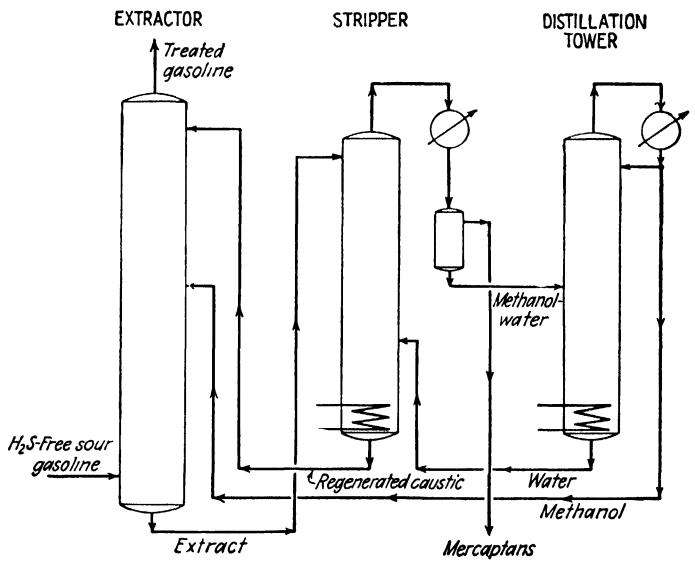



FIG. 11.8. Unisol sweetening process (107). Simplified flowsheet. (*Courtesy, Oil and Gas Journal.*)

The *Unisol process* (22, 47, 107, 122) uses methanol as the added agent to improve the caustic soda solution. Since it is soluble in gasoline, the flowsheet must be arranged to remove it, as in Fig. 11.8. $H_2S$-free gasoline is extracted with aqueous caustic-methanol in the lower part of the packed extraction tower, and the methanol is extracted from the treated gasoline by aqueous caustic in the upper part. The combined caustic-methanol

solution leaves the extractor fouled with mercaptans and is sent to a stripper which removes methanol, water, and mercaptans overhead. Recovered caustic is returned to the extractor, and the wet methanol-mercaptan mixture forms two liquid layers on condensation. The mercaptan layer is withdrawn, and the aqueous-methanol layer, substantially mercaptan-free, is distilled to give methanol and water which are recycled as shown. The extractor uses a very low rate of extracting solvent to gasoline ($\doteq$ 2-3 per cent) because of the high distribution coefficients of the mercaptans. Organic acids are extracted from the gasoline and build up to an equilibrium concentration in the caustic, as with the simpler processes.

## LUBRICATING OILS

The hydrocarbons present in the lubricating-oil fractions of various petroleum oils have not been entirely identified and will vary in the relative quantities of the different types depending upon the source of the crude. The major types encountered include (37*g*, 143):

1. Saturated straight-chain and branched paraffins, of general formula $C_nH_{2n+2}$. Dewaxed lubricants probably contain few pure paraffins.

2. Olefins, or unsaturated straight-chain and branched hydrocarbons, $C_nH_{2n}$ and $C_nH_{2n-2}$. These are not present in the original crudes but may be made in small amounts by cracking during distillation.

3. Naphthenes, which contain ring or cyclic structures with no double bonds, and with paraffinic side chains. The general formula is $C_nH_{2n-a}$, where $a$ is the number of closed rings.

4. Aromatics, which contain unsaturated ring structures such as those of benzene, naphthalene, and anthracene. Unrefined lubricating-oil fractions contain aromatics of the series $C_nH_{2n-2}$ and $C_nH_{2n-4}$ for the lighter grades, and $C_nH_{2n-8}$ for the heavier. The types represented by the series $C_nH_{2n-10}$ to $C_nH_{2n-18}$ may also be present.

5. Asphaltic and resinous compounds of undetermined structure. The hydrocarbon resins are volatile and are found in the distillate fractions, while the asphalts are nonvolatile.

The actual compounds in the oil ordinarily contain mixed nuclei of all the major types (93). The above list is given in the order of decreasing ratio of hydrogen to carbon content, which is generally the order of decreasing desirability in the finished lubricant for reasons of viscosity-temperature relationships and chemical stability.

The various organic solvents used or potentially useful in lubricant refining are classified as either extractive or precipitative, depending upon whether they dissolve or reject the undesirable components. For example, solvents such as aniline and furfural selectively extract aromatic and naphthenic hydrocarbons, with a selectivity for aromatics roughly six times as

great as that for naphthenes relative to paraffins, as measured by critical solution temperatures (50). Extraction with such solvents concentrates the predominantly paraffinic and naphthenic hydrocarbons in the raffinate and the predominantly aromatic in the extract (71). The loose terminology used in the industry which characterizes raffinates as paraffinic and extracts as naphthenic is thus basically incorrect. Precipitative solvents, such as propane and the lighter hydrocarbons and aliphatic alcohols, precipitate asphaltic compounds — these solvents are selective more according to molecular weight than chemical type. Both extractive and precipitative action to some extent is probably given by all such solvents. Concentrated sulfuric acid was used extensively for separations of this sort prior to the introduction of solvent refining and is still used to some extent, especially for production of white (colorless) oils from lubricating fractions. The action of the acid involves both chemical reaction and solution, but the extracted substances are not recoverable and introduce difficult disposal problems.

**Refining Indices.** Since it is impractical to analyze lubricants for the individual components, empirical expressions are used to indicate the degree of refining. The following are the most important for present purposes:

1. *Viscosity Index* (*V.I.*) (32). This is a measure of the change of viscosity with temperature. An oil of Pennsylvania origin (oil *L*) with a small viscosity-temperature coefficient was assigned a V.I. of 100, and one of Coastal origin (oil *H*) of large coefficient was assigned a value of 0. General relationships between the viscosities (Saybolt Universal) at 210 and 100°F. were determined for many fractions of each oil. To determine the V.I. of an unknown oil (oil *x*), its viscosity at 100 and 210°F. is determined and the following equation is used:

$$\text{V.I.} = \frac{\mu_L - \mu_x}{\mu_L - \mu_H}(100) \tag{11.14}$$

where $\mu_L$ = viscosity at 100°F. of the oil *L* fraction whose viscosity at 210°F. is the same as that of oil *x*

$\mu_H$ = viscosity at 100°F. of the oil *H* fraction whose viscosity at 210°F. is the same as that of oil *x*

$\mu_x$ = viscosity of oil *x* at 100°F.

All the above viscosities are to be expressed as Saybolt Universal seconds. The relationship was originally developed for viscosities at 210°F. between 45 and 160 Saybolt Universal sec. but has since been extended to include a wider range. V.I. is unfortunately not an additive property for mixtures. For lubricants required to work over a wide temperature range, high V.I is desirable.

2. *Viscosity-Gravity Constant* (V.G.C.) (74). The specific gravity of predominantly paraffinic oils is low, while that of aromatics is high, for a

given viscosity, and the V.G.C. which characterizes these properties for mixtures is computed from the relationship:

$$\text{V.G.C.} = \frac{10G - 1.0752 \log (\mu_{100} - 38)}{10 - \log (\mu_{100} - 38)} = \frac{G - 0.24 - 0.0222 \log (\mu_{210} - 35.5)}{0.755} \tag{11.15}$$

where $G$ = sp. gr. at 60°F.
$\mu_{100}$ = viscosity (Saybolt Universal) at 100°F.
$\mu_{210}$ = viscosity (Saybolt Universal) at 210°F.

The V.G.C. ranges from about 0.8 for highly paraffinic oils to about 0.95 for highly aromatic. Although originally developed for classifying crude oils, it is also used for refined products. It is an additive property for mixtures but shows no direct or simple relationship to V.I.

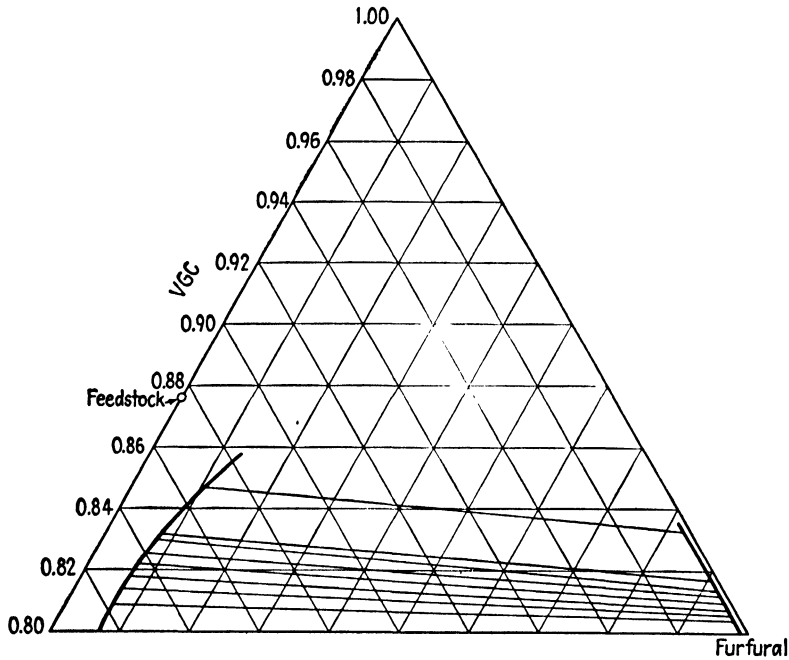



FIG. 11.9. Single-stage equilibria for furfural–Winkler County (Texas) distillate, 150°F. [*Data of Skogan and Rogers* (147).] (*Courtesy, Oil and Gas Journal.*)

3. *Aniline point* is the temperature at which complete miscibility occurs for a mixture of the oil and aniline containing 50 per cent by volume of each. It is nearly the critical solution temperature (50) and is a measure of the aromaticity of the oil.

Other indices such as carbon residue, color, oxidation stability, and pour and cloud points are described by Nelson (128).

The various compounds in the oil distribute between raffinate and extract

phases depending upon their degree of paraffinicity, naphthenicity, or aromaticity. V.G.C., since it is an additive property, has been used most often for extraction calculations (37*e*, *g*). Triangular coordinates are plotted as in Fig. 11.9, with the V.G.C. of the solvent-free oil substituting for per cent aromatics, from data obtained by making single-stage extractions. Solvent is plotted as volume per cent. Rectangular plotting has also been used, with per cent solvent and V.G.C. as coordinates (98) or, in the manner of Janecke (see Chap. 6), with solvent/oil ratio and specific volume of the solvent-free oil (135).

**Countercurrent Extraction.** Skogan and Rogers (147) carried out several series of countercurrent extractions using the oil and solvent of Fig. 11.9, and have reported the V.G.C.'s of the solvent-free products for three- and five-stage extractions at several solvent/oil ratios. In Fig. 11.10 there are plotted the number of stages required to produce their products as calculated by the methods of Chap. 6, and it is seen that too few stages are obtained by calculation. Ordinarily it would be assumed that in the experiments equilibrium had not been obtained and that the stage efficiency was low. Examination of their experimental procedure indicates that such low stage efficiencies would be highly unlikely, and indeed the same phenomena have been observed with other oil-solvent systems (82, 141, 147). The difficulty can be laid to the fact that the system is not composed of simply three components, and the distribution of a particular component will depend upon the amount and kind of others that are in the extract (90). The equilibria therefore change with the extent of extraction, and data based on single-stage batches cannot directly be applied to multistage extraction.

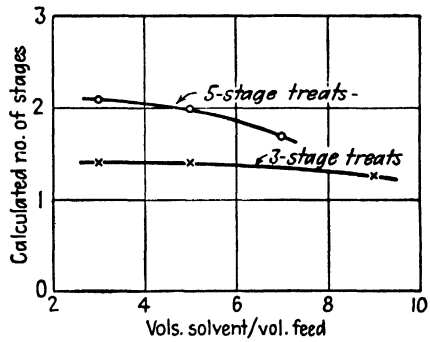



FIG. 11.10. Comparison of number of stages, calculated and measured, for countercurrent operation.

Skogan and Rogers (146, 147) have found, in the case of the few data which can be tested, that the operating point for stage construction on the diagram can be relocated, as in Fig. 11.11, to give calculated results which coincide with the observed extractions. Point $O$ is determined from the specifications for feed $F$, solvent $S$, and products $R$ and $E$ in the manner described in Chap. 6 for true three-component systems. The operating point $O'$, from which stage-lines are then constructed, is located so that $OO'$ is perpendicular to $RO$. The actual position must be determined for a given number of stages from actual experimental data, but the quantity $[(\overline{EO}/\overline{OO'}) + \overline{FE}]$ apparently remains constant for a fixed number of

stages irrespective of solvent ratio. Too few data are available to test this empirical correction fully.

A different approach to this problem has been considered by Kalichevsky (91, 92) and Reeves (136), who find that the following empirical equations

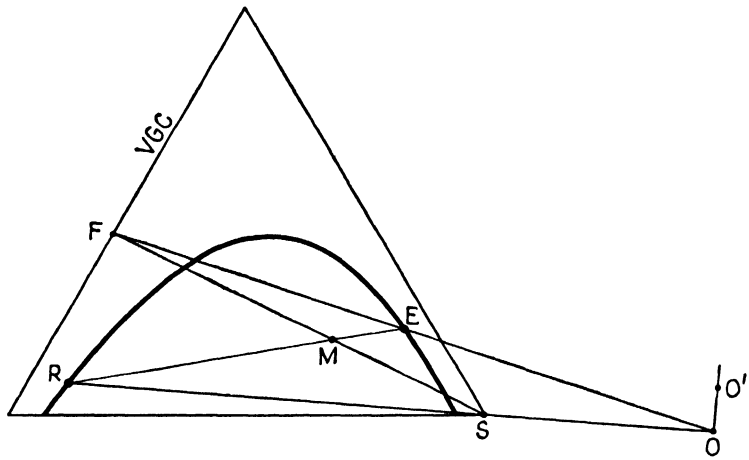



FIG. 11.11. Empirical location of operating point (147).

describe the amount of oil extracted and the amount of solvent entering the raffinate quite exactly for single solvent processes:

$$\log E' = (a + bT) \log S + c + dT \tag{11.16}$$

$$\log S_R = (e + fT) \log R' + g + hT \tag{11.17}$$

for a fixed number of stages, and

$$\log E' = (j + k \log T) \log n + l + m \log T \tag{11.18}$$

for a fixed solvent/feed ratio

where $E'$ = fraction of feed oil entering the extract
$T$ = temp.
$S$ = vol. of solvent per unit vol. of feed oil
$S_R$ = fraction of solvent entering the raffinate
$R'$ = vol. of oil per unit vol. of solvent in the raffinate
$n$ = no. of stages
$a, b, \ldots m$ = const.

The empirical constants must be determined by an appropriate number of laboratory experiments, and additional equations have been developed for mixed- and double-solvent processes. These equations may be manipulated to determine effects of solvent quantity, stages, and temperature on the yield of raffinate and extract but do not indicate the quality of the products which also depends upon these variables. In addition, Berg, *et al.* (14) have extended the "overlap coefficient" concept devised for multi-

component distillation (115) to oil extractions in such a manner as to permit correlation of raffinate yield and quality (V.I.) for a given oil and solvent.

**Yield.** To a large extent, the properties of a raffinate of fixed V.I. extracted from a given oil are essentially the same irrespective of the extraction processes (number of stages, solvent/oil ratio, solvent) used to obtain it (37*g*). For example, the oil for which equilibrium data are given in Fig. 11.9 gave raffinate products whose gravity and viscosity are shown as a

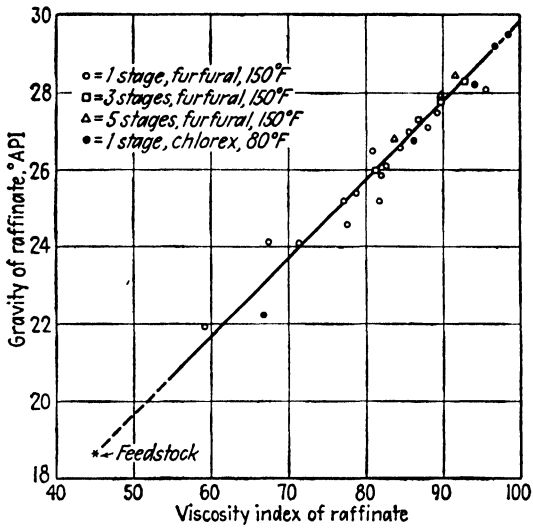



FIG. 11.12. Raffinate gravity in the countercurrent extraction of Winkler County (Texas) distillate. [*Data of Skogan and Rogers* (147).]

function of V.I. in Figs. 11.12 and 11.13. Various solvent/oil ratios, numbers of stages, and two different solvents were used; yet it is seen that there is relatively little segregation of the data. On the other hand, such qualities as carbon residue or color, for which the various solvents have diverse selectivities, may on occasion vary considerably from one product to another despite constancy of V.I. (90). The yield of raffinate of given quality (V.I.), on the other hand, varies appreciably with processing conditions. Figure 11.14 shows the yields for the oil of the previous figures, and the differences for single-stage operations for the different solvents are clear. For the furfural, multistage operation gives an improvement in yield, and the same could be expected for the Chlorex. Indeed, for multistage operation involving a considerable number of stages all solvents can be expected to give the same yield of a given quality raffinate. Additional data of this sort are presented by Kalichevsky (90). The choice of solvent then revolves about considerations of solvent quantity, cost, and other factors as discussed in Chap. 4. In any case, the quantity of solvent used

to produce a given quality raffinate will be much reduced by multistage countercurrent operation, as for the simpler case of three-component systems.

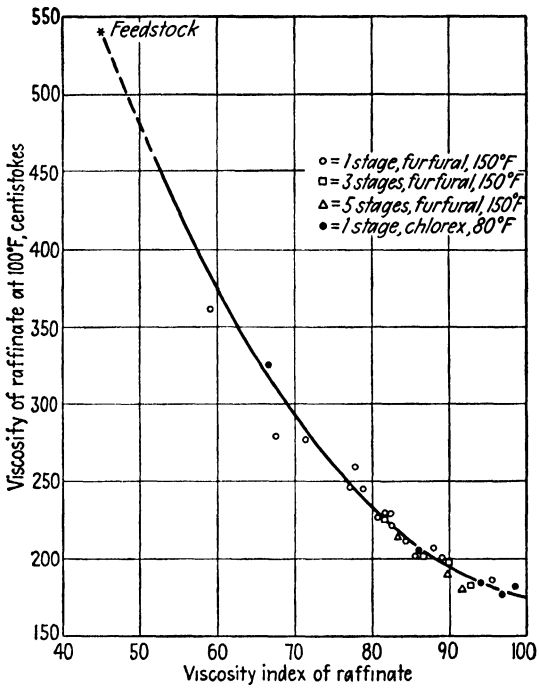



FIG. 11.13. Raffinate viscosity in the countercurrent extraction of Winkler County (Texas) distillate. [*Data of Skogan and Rogers* (147).]

**Reflux.** It is frequently the practice to operate extraction processes with reflux to improve the quality and yield of the product. As with three-component systems, this is most effective in the case of solvents of poorer selectivity, and the principles established in Chap. 6 can be used as a guide for such operation. Reflux is often provided by maintaining a temperature gradient throughout the extraction towers, with lowest temperatures at the extract end in the case of extractive solvents. This precipitates oil from the solvent-rich solutions by reducing solvent-oil solubilities, and the precipitated oil then enters the raffinate phase. As with three-component systems, more effective fractionation is obtained if the reflux is provided throughout the entire extraction.

**Relation to Other Processes.** The relative sequence of extraction and other refinery operations is largely a matter of choice to be made on the basis of economic considerations, since usually the same ultimate product can be recovered by several methods. In the case of distillates which contain paraffin wax, dewaxing may be done before or after the solvent refining

(37*b*). Paraffin wax concentrates in the raffinate during extraction, and consequently the pour point of the refined oil will be higher than that of the feedstock. If dewaxing is carried out first, the pour point of the feedstock to the extraction process must be lower than that desired in the finished product, and the wax is more difficult to finish. If dewaxing follows

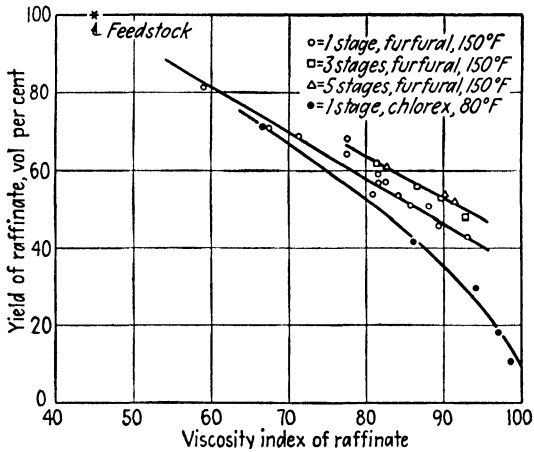



FIG. 11.14. Raffinate yield in the countercurrent extraction of Winkler County (Texas) distillate. [*Data of Skogan and Rogers* (147).]

extraction, any oil lost with the wax is the more valuable refined oil, and extraction may be hindered by precipitation of solid wax at refining temperatures. The refiner must also decide where to choose between distillation of the crude to produce lighter lubricant and deasphalting the heavier products. Frequently the sequence of operations can be chosen so that the same solvents can be used in connection with several. Thus, propane is useful in both deasphalting and dewaxing. The mixed solvent, sulfur dioxide-benzene, is useful for refining and dewaxing. The Duo-Sol process both refines and deasphalts. In any case, the solvent-refined, dewaxed, deasphalted lubricant is usually finished by percolation through activated clay, occasionally by light sulfuric acid treatment as well.

**Solvents.** The number of solvents that have been investigated and patented for lubricating-oil refining must number in the thousands. See Kalichevsky's review (90), for example. For a variety of reasons including cost and toxicity, those which are presently used industrially are limited to the following:

1. *Single-solvent Processes.* Extraction solvents: $\beta,\beta'$-dichloroethyl ether (Chlorex), furfural, nitrobenzene, phenol. Precipitative solvent: propane.
2. *Mixed-solvent Processes:* Benzene + sulfur dioxide (extractive mixture).
3. *Double-solvent Processes:* Propane-cresylic acid + phenol (Duo-Sol) (extractive and precipitative refining).

With the exception that the process of the third category is a fractional extraction, they are all basically the same. They differ only in details of processing temperatures, solvent/oil ratio, use of reflux and methods of obtaining it, and solvent recovery. Indeed, the majority of the equipment is devoted to the solvent-recovery problems.

**Chlorex Process** (9, 13, 37*a*, 70, 133). Chlorex ($\beta,\beta'$-dichloroethyl ether) is especially suited for refining Pennsylvania oils since oil solubility in the solvent is fairly high, although it is used successfully on Mid-Continent residua provided that these have been deasphalted prior to solvent treatment. Relatively low temperatures ($< 100°$F.) are customarily used which may then require that dewaxing be carried out prior to refining, although in at least one instance refining is done in the presence of wax in

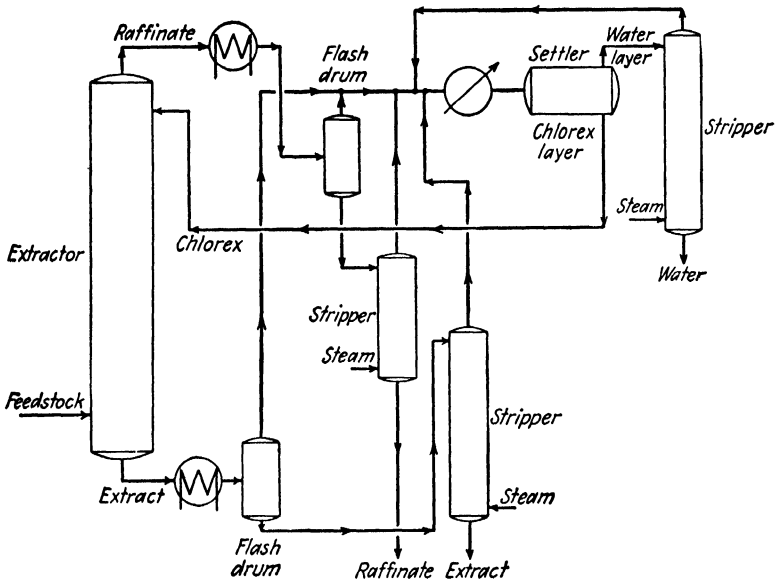



FIG. 11.15. Simplified flowsheet, Chlorex process.

stagewise equipment (90). Solvent/oil ratios as low as 0.75 to 1.5 are sufficient. Stagewise contact utilizing five to eight stages has been used, or towers packed with 1-in. Raschig rings as in the simplified flowsheet of Fig. 11.15. The solvent, which boils at 352°F. at atmospheric pressure, is readily vacuum-stripped from the extract and raffinate with steam, and the condensed vapors from the strippers form two liquid layers of saturated Chlorex-water solutions. The aqueous layer (1.01 per cent solvent at 68°F.) is stripped of its Chlorex, while the Chlorex layer ($\doteq$ 3 per cent water) is reused without drying. Some hydrolysis releases HCl, which should be neutralized with $NH_3$ to prevent corrosion.

In 1949, six plants using this process were treating 5,700 bbl./day, but no new plants have been installed since 1935.

**Furfural Process** (23, 37*f*, 41, 94, 103). Furfural as a selective solvent is used at relatively high temperatures, usually in the range from 150 to 250°F. The higher permissible temperatures allow for extraction of oils of high viscosity and waxy fractions even in packed towers without danger of clogging the packing.

In modern plants, the extraction is carried out in towers packed with approximately 20 ft. of 1-in. Raschig rings with provision for redistribution of the liquids, as in the flowsheet of Fig. 11.16. The solvent is the more dense and is introduced at the top, where the temperature is the highest in the extractor ($\doteq$ 200°F.). The feedstock is introduced in the central portion of the tower; extract is withdrawn at the bottom, raffinate at the top. Extract reflux, consisting of a portion of the extract stream from which most of the solvent has been removed, is returned at the bottom of the extractor. Additional internal extract reflux is induced by cooling the withdrawn oil layer at intervals, which decreases the solvent-oil solubility and increases the raffinate/extract ratio when the cooled mixture is returned to the tower. A temperature gradient of 20 to 50°F. is customarily maintained over the length of the tower.

The raffinate layer, containing roughly 10 per cent solvent, is heated in a direct-fired heater, stripped of its solvent in the presence of steam at atmospheric pressure, and sent to storage. The extract layer, containing in the neighborhood of 90 to 95 per cent solvent, is similarly heated, flash-evaporated at about 30 lb./sq. in. and again at atmospheric pressure, and split to provide extract reflux for the extractor. The remainder of the extract stream is steam-stripped at atmospheric pressure and sent to storage. The wet furfural vapor from the steam strippers is condensed, whereupon two liquid layers form. The water-rich layer is steam-stripped of its furfural, and the water is discarded. The wet furfural-rich layer is distilled, together with the vapors from the extract evaporator, to give dry furfural as bottoms which is reused for extraction, and the water-furfural azeotrope as distillate which is recycled.

By 1949, over 20 installations of this process were treating approximately 60,000 bbl./day of feedstock. A recent installation, the largest of its kind, includes deaeration of the feed and vacuum stripping of the raffinate and extract products, with flue-gas blanketing of the solvent storage tanks to minimize deterioration of the furfural (101).

**Nitrobenzene Process** (37*c*, 45, 46, 127). Nitrobenzene is both highly selective and fairly soluble with lubricating-oil fractions, and consequently is used at relatively low temperatures (50°F.) and in small amounts (50 to 200 per cent of the feed). The presence of precipitated paraffin wax does

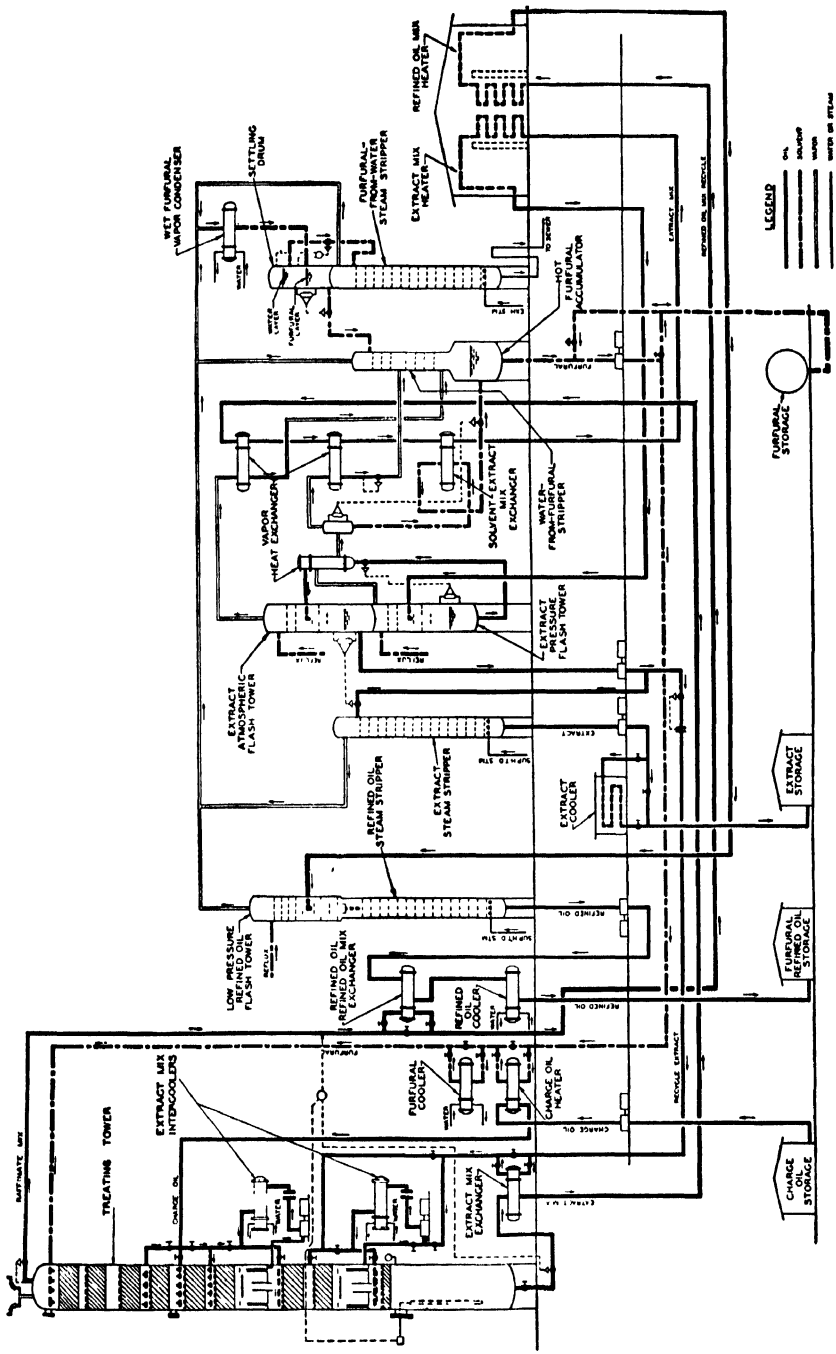



FIG. 11.16. The furfural process. *(Courtesy, Texaco Development Corp.)*

not interfere with the extraction, except that stagewise contacting is necessary. Five countercurrent stages are sufficient. The nitrobenzene is evaporated from the extract and raffinate solutions at 30 and 10 mm. Hg, 325°F., and vacuum steam-stripped at 65 mm. Hg. The wet nitrobenzene vapors are condensed, decanted, and distilled as in the case of furfural.

One plant has been constructed, which treats 2,350 bbl./day of feedstock. The poisonous nature of the solvent and the low temperature of operation have probably contributed largely to the lack of adoption of this solvent. Simultaneous extraction with nitrobenzene and sulfuric acid has been tried commercially but is apparently not successful.

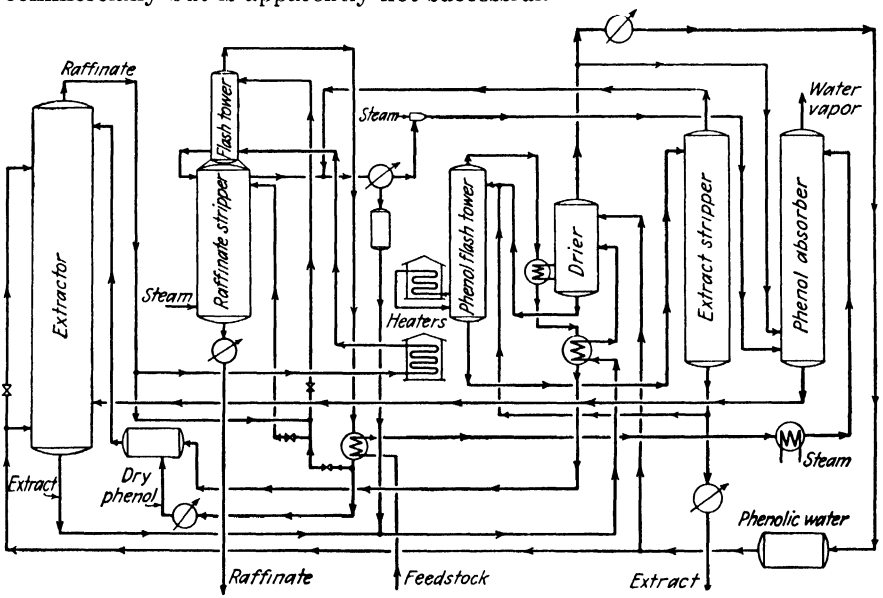



FIG. 11.17. The phenol process. (*Courtesy, Oil and Gas Journal.*)

**Phenol Process** (4, 37*h*, 154, 155, 156). Phenol is used at a sufficiently high temperature (≐ 200°F.) to permit treatment of oils of high viscosity and wax content. Early installations used separate stage contactors, but modern plants have packed or perforated-plate countercurrent towers. The solvent is used either substantially dry or with water injection into the extract end of the extractor to reduce oil solubility and induce extract reflux. The latter is used in the newer plants, according to the flowsheet of Fig. 11.17.

The feed is heated, absorbs phenol from stripping steam in the phenol absorber, and enters the extractor. Dry phenol enters at the top, and water containing 11 per cent phenol is introduced near the base, thus reducing the temperature and oil solubility to induce extract reflux. Raffinate containing about 20 per cent solvent is stripped of its phenol by flash vaporization

and steam stripping, and is sent to storage. Extract, which contains water and phenol to the extent of about 85 per cent, is dried by distillation of the phenol-water azeotrope, heated, stripped of its remaining phenol, and sent to storage. Dry phenol for the extractor is collected from the raffinate evaporator and extract stripper, while phenolic water from the drier is recirculated to the extractor for reflux. Phenol circulation amounts to 1 to

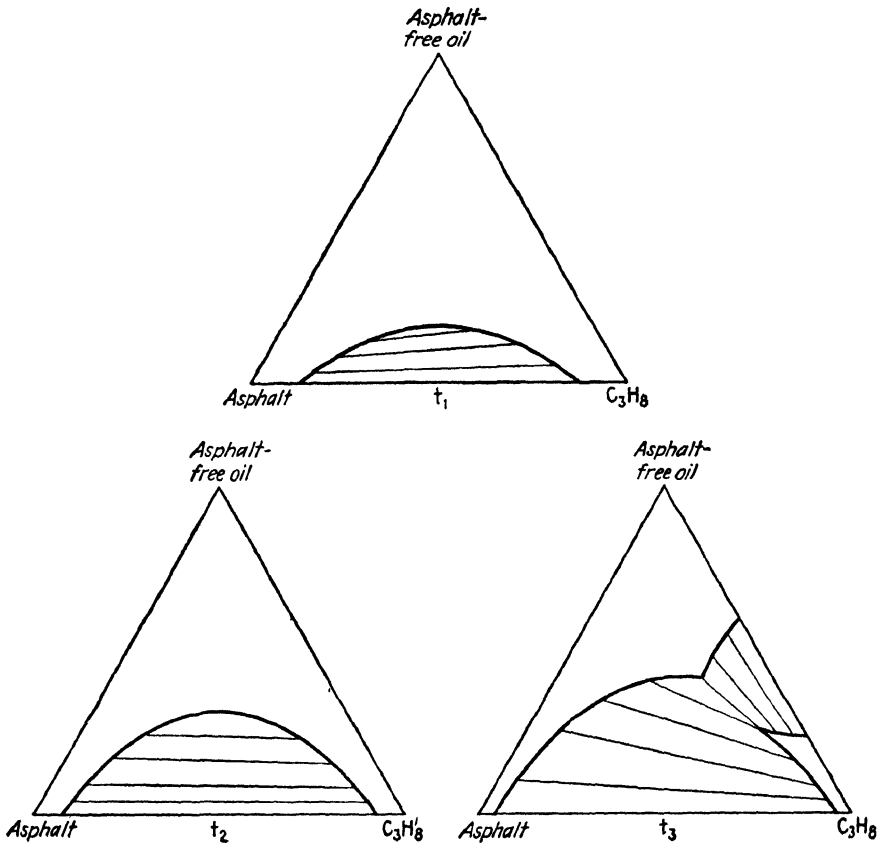



FIG. 11.18. Idealized phase diagrams for oil–propane systems (169).

2.5 times the volume of oil, depending upon the source of the crude. Although the melting point of pure phenol is high (105.6°F.), the presence of water and even small traces of extracted material reduces the melting point sufficiently to cause no problem with clogging of equipment.

In 1950, 19 plants (world-wide) were treating 73,800 bbl./day of oil by this process. The largest plant treats 7,500 bbl./day.

**Propane Deasphalting** (90, 135, 169). Propane is a most useful solvent for various refinery operations, since it is so readily and cheaply available at all refineries and because of its unusual solvent properties. If the com-

ponents of a typical residual oil can be generalized to include only asphalt and nonasphaltic oil, Fig. 11.18 explains the behavior encountered in typical propane treating (169). Propane exhibits lower critical solution temperatures with both asphalt and nonasphaltic oil. Actual phase diagrams and temperatures naturally depend upon the nature of the oil, but in the figure, $t_1$ can be taken as approximately 100°F. (somewhat above the critical solution temperature with asphalt), $t_2$ as 140°F., and $t_3$ as 180°F. (above the critical solution temperature with nonasphaltic oil). At temperatures near $t_3$, it should be possible to deasphalt the oil to any extent desired.

Modern deasphalting operates at temperatures somewhat below 250°F., with countercurrent extraction as in Fig. 11.19. Propane/oil ratios as high

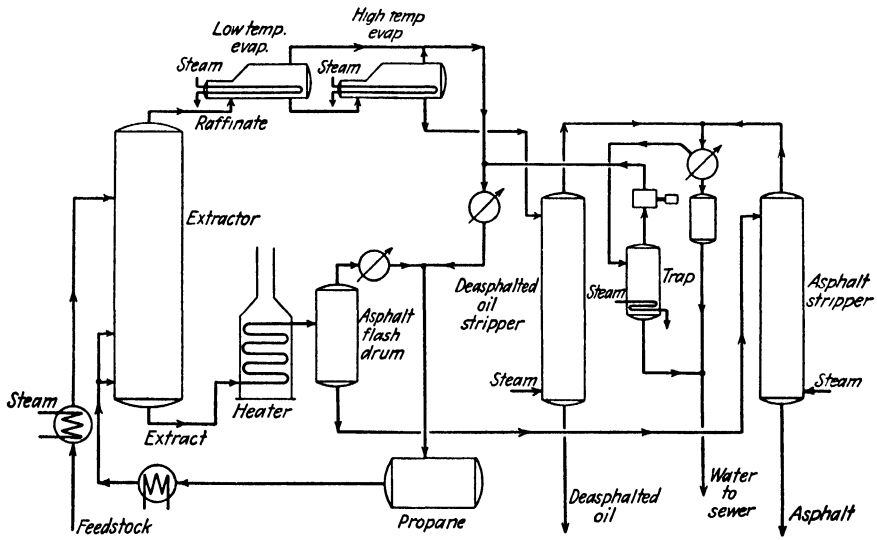



FIG. 11.19. Propane deasphalting. (*Courtesy, Oil and Gas Journal.*)

as 9 are sometimes used since, as indicated in Fig. 11.18, the oil is more thoroughly extracted from the asphalt the larger the solvent ratio. The high vapor pressure of propane permits its easy removal from both extract and raffinate. Alternatively, the raffinate solution can be cooled by propane evaporation and be dewaxed before complete propane removal is carried out.

**Sulfur Dioxide–Benzene Process** (16, 28, 33, 40, 54, 87). Sulfur dioxide alone is too highly selective for aromatic hydrocarbons to produce a raffinate of high V.I. from lubricating-oil fractions, since it rejects naphthenic compounds almost entirely. With a mixed solvent containing both sulfur dioxide and benzene, raffinate yield decreases and V.I. increases as percentage of benzene and solvent/oil ratio increase. The quantity of benzene used varies with the feedstock but may be in the neighborhood of 15 to 25

per cent. The flowsheet resembles that for treating light distillates with sulfur dioxide alone with the exception that the two solvents are separated from the oil separately, and consequently a more elaborate solvent-recovery scheme is required. Separate recovery permits ready adjustment of benzene concentrations, however. The process has not been widely adopted, and, in 1947, world-wide installations sufficient to refine 10,300 bbl./day of oil were in operation (151).

**Duo-Sol Process** (1, 116, 117, 163, 164). This is the only commercially established lubricating-oil process which utilizes fractional extraction (double-solvent) methods. The insoluble liquids are propane as the paraffinic-naphthenic solvent and a mixture of 40 per cent phenol and 60 per cent cresylic acid ("Selecto") as the aromatic-asphalt solvent. Cresylic acid has been proposed as a single solvent for lubricant refining with characteristics somewhat similar to nitrobenzene but has not been exploited industrially. The use of propane permits the double-solvent process to deasphalt and refine simultaneously, and consequently Mid-Continent residua are fairly readily handled without prior treatment. At the customary temperature of operation ($\doteq$ 100°F.), paraffin waxes are soluble in the propane and do not interfere. The process enjoys the advantage of being able to vary the ratio of the two solvents to oil separately in establishing the best operating conditions. Generally, increased Selecto/propane ratio results in high V.I., low carbon residue, low viscosity, and low yield of raffinate. Increased quantities of propane improve the raffinate color. While actual ratios vary considerably with different conditions of operation, a typical installation (1) uses propane/Selecto/oil = 5.8:3.7:1.0.

A typical flowsheet is indicated in Fig. 11.20. Countercurrent stagewise extraction with seven stages is customary, and it is found that, except for the initial introduction of the feed, causing the extract and raffinate streams to flow simultaneously through 10 or 15 ft. of piping at velocities of 10 to 16 ft./sec. provides adequate mixing. The feed is mixed with the countercurrently flowing streams by means of the device shown in Fig. 9.9. Settlers of the design shown in Fig. 9.18 are used. The propane-rich raffinate phase is stripped of propane and Selecto in that order and sent to storage, and the Selecto-rich extract is treated similarly. Propane is compressed and condensed for reuse. The Selecto vapor, which contains both propane and stripping steam, is condensed, stripped of its water and propane, and the Selecto sent to storage for reuse. The water, containing some dissolved Selecto, is sent to the propane storage tank where propane extracts most of the Selecto, and the remaining water is reused for stripping steam.

In 1950, 18 Duo-Sol plants (world-wide) were treating 65,000 bbl./day of oil (117), and detailed descriptions of very large recent installations are available (1, 101).

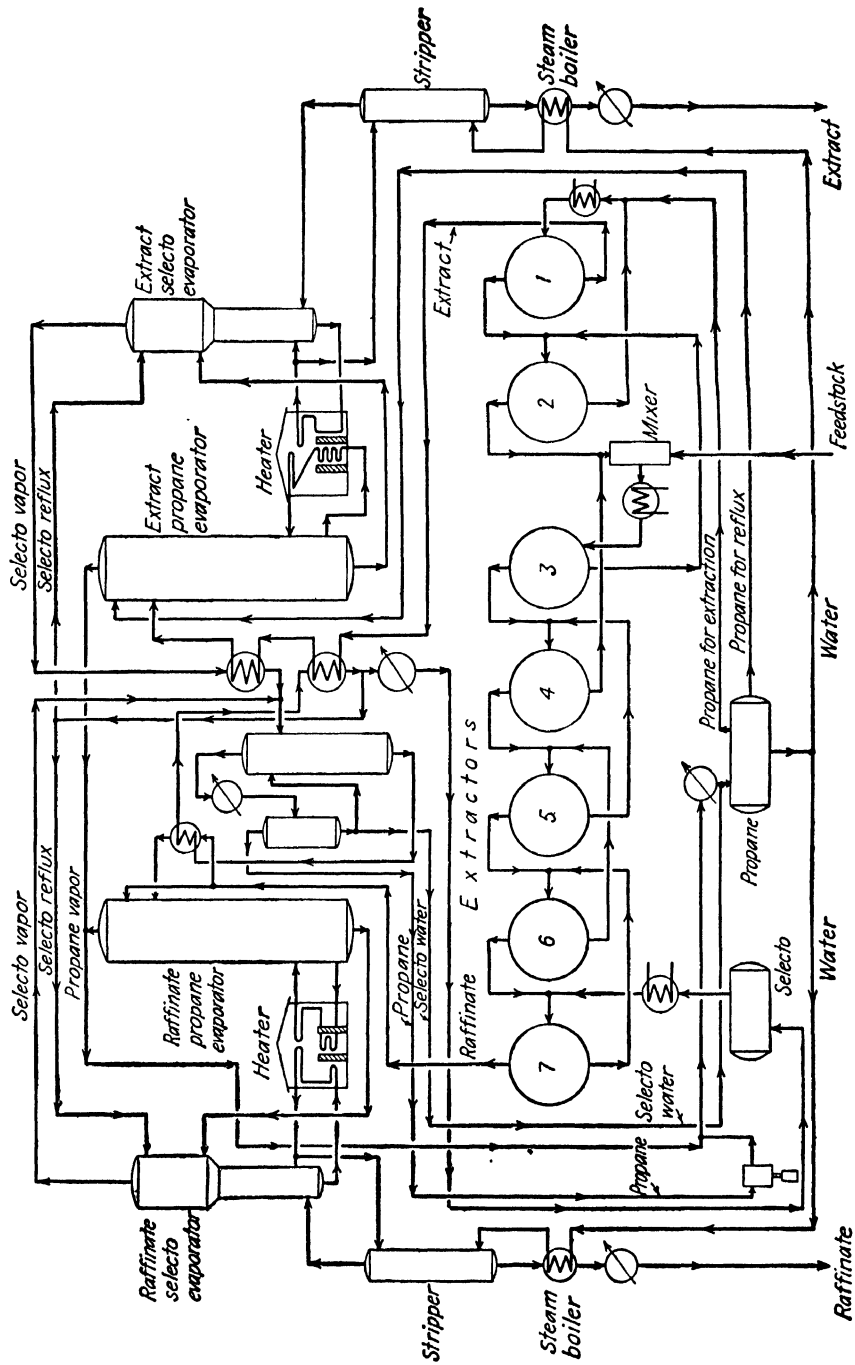



FIG. 11.20. The Duo-Sol process. (*Courtesy, Max B. Miller Co.*)

## FAT, OIL, AND RELATED PROCESSES

Fats and oils, substances of animal and plant origin, are principally triglyceryl esters of the fatty acids, or triglycerides, of general formulas $H_2C(OOR')—HC(OOR'')—H_2C(OOR''')$. R′, R″, and R‴ represent long, even-numbered, carbon-chain radicals, saturated and unsaturated, mostly of 8 to 22 carbon atoms each, all of which may be different for a given glyceride molecule. Any one fat or oil will contain many fatty acids, and these with some exceptions are relatively evenly distributed among the glyceride molecules, especially in the case of the vegetable seed oils. The various fats and oils then differ largely in the type, number, and distribution of the various fatty acids contained in the glycerides. In addition, at least in the unrefined products, there are small percentages of free fatty acids formed by partial hydrolysis of the triglycerides, phosphatides (triglycerides with one fatty acid replaced by a phosphoric acid ester, such as lecithin and cephalin), sterols, vitamins, carbohydrates, carotenoid pigments, proteins, tocopherols, and other substances of unknown structure (10). After various treatments and processes, the fats and oils enter into a wide variety of products such as foods, paints, soap, printing inks, fatty-acid derivatives, lubricants, cosmetics, and medicinal products. Extraction processes of interest here have been developed in connection with the separation of the constituents of the oils, the fatty acids or related substances, and in the hydrolysis of the oils.

**Propane Refining.** The equilibrium relationships existing between a large number of high-molecular-weight compounds related to the fat and oil industries in binary mixture with liquid propane have been studied in detail by Hixson, *et al.* (17, 35, 75, 76). Many of these compounds, as in the case of petroleum oils, show lower critical solution temperatures and solubility curves of the type of Fig. 2.2, where the decreased solubility at higher temperatures is attributed to the decreased density of the propane as its vapor-liquid critical point is approached. In the case of the esters and long-chain fatty acids, a correlation between the lower critical solution temperature and effective molecular weight has been developed as presented in Fig. 11.21 (17). In this correlation, the ordinary formula weights of the esters are used, but twice the ordinary values are required for the fatty acids in accordance with the proposal that the acids are associated as dimers in the hydrocarbon solution. It can be predicted from the correlation that esters and acids of effective molecular weight below about 460 will not exhibit a lower critical solution temperature with propane since the curve indicates that such temperatures should be above 214°F. The critical temperature (vapor-liquid) of propane is 212.2°F., that of the propane solutions will be only a few degrees at the most above this, and at higher temperatures the propane is no longer in the liquid state. This has been

confirmed in observations with ethyl stearate (mol. wt. = 312.5), lauric acid (effective mol. wt. = 400.6), and myristic acid (effective mol. wt. = 456.7); in the case of the last, the vapor-liquid and liquid-liquid critical temperatures seemed almost to coincide (17). Measurements have also been made with other types of compounds and with other hydrocarbons.

Ternary liquid equilibria of systems including acids and esters with propane have also been studied (35, 75, 76), and phase diagrams of the type of Fig. 2.14 result. The data indicate that for any fatty acid-ester combination, a difference in the binary critical solution temperature with propane of less than 9.9°F. does not lead to selectivities sufficiently great to permit

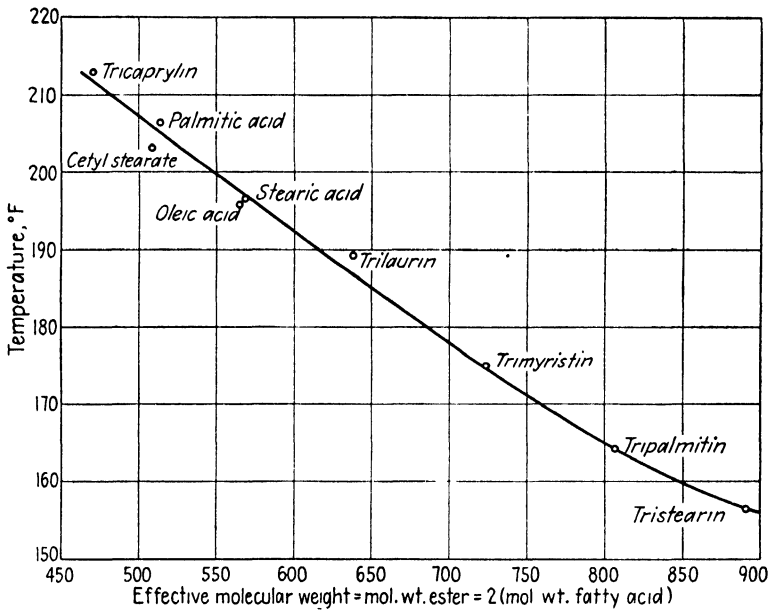
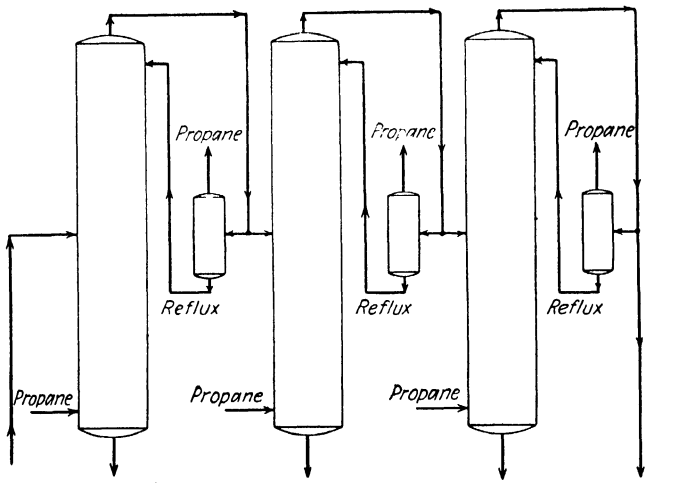



FIG. 11.21. Lower critical solution temperatures with liquid propane (17). (*Courtesy, American Institute of Chemical Engineers.*)

separation by extraction with propane, whereas differences of the order of 45°F. permit ready separation (see Chap. 3). In the case of a refined cottonseed oil, for example, a critical solution temperature with propane of 151.2°F. was found (75), and an excellent separation is possible between the glyceride and free oleic acid, as indicated in Fig. 4.5. Mixtures of stearic and palmitic acids, or of stearic and oleic acids, on the other hand, cannot be separated. Separation of compounds of different chemical type is possible despite relatively small differences in molecular weight. Thus, abietic acid (mol. wt. = 322) and oleic acid (mol. wt. = 282) are readily separated with propane (76).

The industrial refining of fats and oils with propane is known as the

*Solexol process* (3, 77, 134). The critical solution temperatures with propane of the various constituents of the oils and their solubilities at higher temperatures are sufficiently different to permit their separation in part. By increasing the temperature of a propane-oil solution in stepwise fashion, the solubilities of the various oil constituents in groups are exceeded one by one, and they can be removed in the order of their molecular complexity or molecular weight. Thus, for example, a scheme for fractionating a sardine oil is outlined in Fig. 11.22 (134), whereby the oil is decolorized and separated into fractions of different degrees of unsaturation and a vitamin




| Solvent-free properties | Crude sardine oil | Color bodies | High iodine-No fraction | Intermediate iodine-No. fraction | Vitamin concentrate |
|---|---|---|---|---|---|
| Yield, wt % | – | 3.0 | 35.0 | 47.0 | 15.0 |
| Color, Gardiner | 11 | Black | 8 | 4 | 5 |
| Vitamin A potency | 350 | – | – | – | 2100 |
| Free fatty acids, % | 1.0 | 0.5 | 0.4 | 0.3 | 6.0 |
| Saponification No | 192 | 184 | 188 | 192 | 194 |
| Iodine No. | 185 | 250 | 240 | 160 | 110 |

FIG. 11.22. Solexol process refining of sardine oil (134). (*Courtesy, American Chemical Society.*)

concentrate by maintenance of a suitable temperature gradient from one tower to the next. In similar fashion, crude soybean oil can either be merely decolorized and separated from its free fatty acids, or separated as well into a high iodine-number fraction and an edible fraction. Linseed oil, tallow, and other similar products can be similarly decolorized and fractionated. Conventional refining of products such as these involves such operations as caustic treatment and bleaching by adsorption or chemical means (10), but a better quality of final product at better yield is obtained by solvent refining, and the solvent process is clearly more versatile. In a manner similar to the propane dewaxing of deasphalted

lubricating oils, high melting-point constituents of the fats such as stearin can be crystallized from the extracted product by evaporation of the propane to produce chilling (134).

A description of a recent large installation provides typical details of the process (121). In a plant for the decolorization of 200,000 lb. of tallow/day, the extraction tower is 39.5 ft. high, 5.5 ft. in diameter, and contains 16 baffles. In a typical operation, crude tallow is preheated to 159°F. and enters the tower at approximately the midpoint, while liquid propane at 158°F. enters at the bottom in a 10–17:1 ratio to the tallow. Above the tallow inlet, three groups of steam coils adjust the temperature and consequently regulate the amount of reflux which flows down the tower, and the temperature at the top is kept at 162°F. with close temperature control. The pressure is kept at 465 lb./sq. in., roughly 85 lb./sq. in. greater than that required for complete liquefaction of the propane. The bottom extract product contains color bodies, dirt, and some glycerides in a 50 per cent solution with propane. The raffinate contains 98 per cent of the crude tallow in refined form. Both products are freed of propane by flash evaporation and steam stripping, and the propane is returned to the process. The temperature and solvent-to-fat ratio can of course be varied to suit the feed material and the product desired. Higher temperatures at the top of the tower, for example, increase the extract yield and improve the raffinate color.

**Furfural Refining.** The separation of the saturated from the unsaturated glycerides of vegetable oils has become increasingly desirable in recent years, as the paint and varnish industries have encountered interruptions of the flow of drying oils from foreign supply sources. If the unsaturated portions of oils such as corn oil (iodine number† $\doteq$ 125), cottonseed oil (iodine number $\doteq$ 106), or soybean oil (iodine number $\doteq$ 130) could be separated, these could augment the supplies of drying oils for paint manufacture considerably. In like fashion, exceptionally effective drying fractions could be separated from drying oils such as linseed oil (iodine number $\doteq$ 175). Unfortunately, the glycerides of such oils are mixed, so that it is impossible by direct extraction to make a complete separation of the saturated and unsaturated esters, regardless of the selectivity of the solvent used. For example, although some 14 per cent of the soybean oil fatty acids are saturated, there are apparently no completely saturated glycerides in the oil (96). A large number of solvents have been investigated (51, 142, 153), and in general polar solvents such as the nitroparaffins, sulfur dioxide, the sulfolanes, and furfural are most effective. Of these, only furfural has been used industrially.

Furfural selectively extracts the more unsaturated glycerides from the

† Iodine number = the number of grams of iodine absorbed per 100 gm. of oil; it is a measure of the degree of unsaturation.

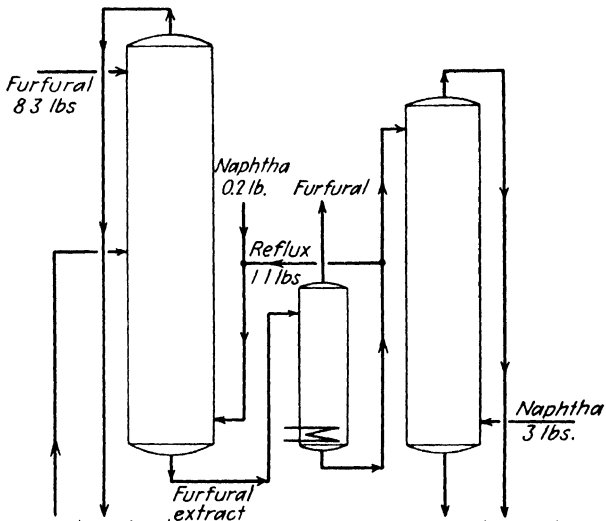
oils, as well as the free fatty acids and the more complex substances such as phosphatides and tocopherols. Equilibria for the glycerides can be expressed in terms of iodine number and can be treated graphically on triangular coordinates as in Fig. 2.34 or on Janecke coordinates (142). Presumably the same difficulties in translating equilibrium data obtained from single-stage batchwise experiments to multistage countercurrent extractions should arise for such complex mixtures as do for petroleum products, but too few data are available to evaluate this.

In the refining of soybean oil, either of two procedures may be used, depending upon whether the feed is a crude oil or has been alkali-refined prior to extraction (58). For refined oil, the oil feed is introduced into approximately the center of a packed tower, and furfural at a ratio of 8–14:1 of oil is introduced at the top. The raffinate leaving the top of the tower then consists of approximately 30 to 40 per cent of the feed oil (solvent-free basis) with an iodine number in the range 95 to 110. At the lower end of the tower, extract reflux may be returned at the rate of 110 to 120 per cent of the feed-oil rate, and the withdrawn extract product may consist of 60 to 70 per cent of the feed oil (solvent-free basis) of iodine number in the range 152 to 154. For unrefined oil, the furfural extract contains the free fatty acids, unsaponifiable matter, and antioxidants from both oil and furfural which delay the drying of the oil when it is used in paints (142). Consequently a scheme such as that indicated in Fig. 11.23 is used (58, 142). Here the furfural extract is contacted with a petroleum naphtha in a second extractor, which removes the desirable glycerides from the furfural solution but leaves behind the free fatty acids, antioxidants, and other undesirable portions. A small amount of naphtha is used with the extract reflux in the first column. The raffinate from such a fractionation is suitable for the preparation of hydrogenated fats, the extract is of varnish-grade quality, and the by-product fraction is a source of sterols, tocopherols, and free fatty acids. Linseed oil may be similarly fractionated for a high iodine-number fraction and marine oils for vitamin fractions (58). Furfural may also be used to separate the free fatty acids from each other, although since they are completely soluble in furfural, they must be selectively extracted from a naphtha solution.

A commercial plant for these processes follows the general scheme of Fig. 11.23 (95). For 200,000 lb./day of degummed soybean oil and a solvent ratio of 8.3:1, two extraction columns each 5.5 ft. in diameter, 87 ft. tall (75 ft. of packing), operate in parallel for the furfural extraction at 120°F. The interface is held between the oil and solvent inlets, so that both phases are dispersed in one section of the tower or the other. The naphtha extraction is carried out in a single packed tower 4.5 ft. in diameter, containing a 50-ft. depth of ½-in. Raschig rings, at 70°F. Furfural and naphtha are removed from the products by a series of multiple-effect

vacuum evaporators and strippers. Many details are provided by Kenyon, *et al.* (95).

For more complete separation of the saturated and unsaturated constituents of the oils than the direct extraction processes are capable of, it would seem necessary first to hydrolyze, or "split," the oil and fractionate the resulting fatty acids. The free acids can be separated with furfural if they are first dissolved in naphtha (12, 52, 85) or with propane (77). Alternatively, the glycerides may be converted by alcoholysis to monoesters, such




| Solvent-free property | Degummed soy bean oil | Raffinate | By-product fraction | Extract |
|---|---|---|---|---|
| Weight, lbs | 1.0 | 0.39 | 0.01 | 0.6 |
| Iodine no | 135 | 109 | 139 6 | 152.3 |
| Free fatty acids, % | - | 0.05 | 17.2 | 0.15 |
| Unsaponifiable, % | - | - | 7.8 | - |

FIG. 11.23. Typical fractionation of degummed soybean oil (58). (*Courtesy, American Chemical Society.*)

as ethyl esters, which after solvent fractionation can be reconstituted as glycerides (61).

**Fat Splitting.** Fat splitting is the hydrolysis of a fat or oil with water to produce glycerol and fatty acids. The fatty acids may then be either neutralized with caustic to produce soap or otherwise processed. While the splitting process is concerned only partly with extraction, the equipment and procedures follow typical extraction techniques. The mechanism of the reaction has been fairly well worked out (100, 119). Initially, while water is in contact with unsplit oil, the two are fairly insoluble and reaction

is heterogeneous and slow. As fatty acids are released, the solubility of water in the acid-oil solution increases, the reaction becomes largely homogeneous in the oil-phase and proceeds much more rapidly, increasingly so at higher temperatures. As glycerol is released it is extracted into the aqueous phase, and a reaction equilibrium is established which is independent of temperature, thus indicating the absence of any heat of reaction. The ultimate percentage of split of the oil in a batch process is then dependent upon the relative proportions of oil and water used and will be greater with increased amounts of water since the glycerol concentration is thereby reduced. Evidently the fatty acids are hydrolyzed from the triglycerides in stepwise fashion, so that the partially split fat contains a high proportion of mono- and diglycerides.

Catalysts such as zinc oxide or Twitchell reagent (alkylaryl sulfonic acids) may be used which increase the rate of reaction but not the extent of hydrolysis. Operations may be carried out batchwise at atmospheric pressure and 212°F. with the Twitchell catalyst, or in autoclaves at high pressures up to 450°F. with or without catalyst. Complete miscibility with water may occur at temperatures about 550 to 650°F., depending upon the fat. Continuous countercurrent contact of the water and oil at temperatures below complete miscibility increases the percentage splitting possible, to an extent depending merely upon the time of contacting.

The countercurrent process is of particular interest here. The advantages of such operation have been recognized since at least 1860 (161), although it is only in recent years that commercial exploitation has been practiced under more modern patents (84, 118, 126, 171). In typical operations (2, 105, 106) the oil, deaerated to lessen darkening of the finished fatty acids, is introduced into the bottom of a 78-ft. unpacked tower operating at 700 to 800 lb./sq. in. The oil-water interface is maintained at about 10 ft. from the bottom of the tower, and in the zone below the interface the dispersed oil phase is heated and saturated with water by direct contact with the aqueous phase. Additional heat is supplied at the top of the exchanger section by direct injection of deaerated steam to bring the oil to the operating temperature, 450 to 550°F. The 60-ft. height above the interface is the principal reaction-extraction zone, with the oil as the continuous phase having a hold-up of 2 to 3 hr. Injection of steam at intervals maintains the temperature at the desired value.

Deaerated soft water enters at the top and flows through 8 ft. of trays of the type shown in Fig. 10.10, where direct contact with the rising fatty acids provides heat exchange for heating the water and cooling the acids. The water is then dispersed by means of a perforated plate provided with a riser for the fatty acids entering from below. Cooling of the fatty acids in this manner to temperatures in the neighborhood of 200°F. precipitates practically all the dissolved water, and the acids are led to further process-

ing. With a total water/oil ratio of 0.5–0.8:1, 97 to 99 per cent hydrolysis of the oil can be expected. From the bottom of the tower the glycerol solution (sweet water), which may contain 10 to 25 per cent glycerol, is led to storage. This solution requires only a small application of lime for coagulation of impurities before concentration. Allen, *et al.* (2) report data respecting rates of heat transfer and extent of hydrolysis for various operating conditions.

The fat-splitting tower is lined with a special alloy, type 316 stainless steel or Inconel, since the hot fatty acids are highly corrosive, and the equipment is expensive in first cost. The high percentage of hydrolysis without catalyst, the purity and light color of the acids, and the high concentration of the sweet water nevertheless make the process attractive, and several installations have been made in the last several years.

Several interesting processes for solvent extraction of the glycerol from the sweet waters produced by either the continuous or other hydrolysis operations have recently been proposed (42).

**Rosin and Tall Oil.** Unrefined wood rosin, obtained by the steam distillation or naphtha leaching of pine-tree stumps, differs from the gum rosin obtained from the living tree in that it is dark in color and discolors badly when incorporated into soaps, paper sizing, and other products. In both cases, the unrefined products contain some 80 to 90 per cent abietic acid and isomers, $C_{19}H_{29}COOH$, in addition to more highly aromatic and oxygenated resinous materials. Wood rosin may be refined by treatment with sulfuric acid, by adsorption of undesirable materials on fuller's earth, or by solvent refining. In solvent refining, the crude rosin is dissolved in a petroleum naphtha approximating gasoline to give about 15 per cent solution, which is then contacted with furfural for the extraction of the objectionable substances (81, 88). Extraction is carried out countercurrently in a type of perforated-plate tower using a woven wire screen for the perforated plates (102), and these are customarily some 40 ft. tall, 3 ft. in diameter, with 8-in. spacing between plates. The naphtha raffinate is evaporated and steam-stripped to yield a light-colored rosin which is an acceptable substitute for the more expensive gum rosin for practically all purposes. Various grades, defined in terms of color, can be made depending upon the extent of extraction. The furfural extract, after removal of the solvent, has special uses in certain plastics, as an emulsifying agent, in core oils, and in other products. Alternatively, propane can be used as a solvent, in the manner of the Solexol process, for refining rosin (78), although apparently at this time there have been no industrial applications of this method.

Tall oil is a mixture of some 38 to 58 per cent rosin acids (principally abietic), 54 to 36 per cent of unsaturated fatty acids of 18 carbon atoms/molecule, and some 5 to 10 per cent of more complex material such as the sterols.

It is produced as a low-priced by-product of the sulfate process for papermaking. After refining by treatment with sulfuric acid or by vacuum distillation, it enters into a large number of diversified industrial products. Its value would be increased considerably if the rosin acids could be separated from the fatty acids, and to this end much research has been and is presently being carried on. Although many patents have been issued, the most promising processes so far proposed have been propane refining of the tall oil directly (76, 77, 134) and furfural refining of methylated tall oil (53, 58), which separates the methyl esters of the fatty acids from the unesterified rosin acids. Neither of these have had commercial exploitation as yet.

## DEPHENOLIZATION OF GAS LIQUOR

In the operation of by-product coke ovens, the gas evolved during coking is sprayed with water and cooled, thus depositing an aqueous solution, "gas liquor." The gas liquor contains in solution such materials as ammonium salts of a variety of ions ($CO_3^=$, $SCN^-$, and $SO_4^=$, etc.), and organic compounds such as mono- and polyhydric phenols, pyridine bases, organic acids, and neutral oils (unsaturated hydrocarbons and other organic substances). The actual composition varies widely, depending upon the coal used for coking and the details of the manufacturing procedure. In the past, the liquor was distilled for recovery of ammonia and the residue discarded to the sewer. The phenols particularly introduced into rivers in this way are very objectionable, since they are harmful to fish and affect the taste of the water when present in only the smallest amounts (0.1 p.p.m.). Chlorination of the water to make it potable produces chlorophenols whose taste is objectionable at 0.02-p.p.m. concentration. If unloaded upon sewage disposal plants, the residue may seriously overburden such facilities. The phenols are therefore removed from the gas liquor prior to distillation by any of several processes, one of which involves extraction with light oil (essentially benzene) or other solvents.

The various phenols in the untreated gas liquor may total anything from 0.5 to 1.5 gm./l. for coke-oven operation to as high as 12 gm./l. for low-temperature carbonization, with phenol itself usually accounting for the majority of the total. Phenol has the poorest distribution coefficient (2 to 2.5 for light oil as solvent) and is the most difficult to extract. Removal of total phenols is usually carried out to the extent of 95 to 99 per cent for coke-oven gas liquors.

A typical flowsheet is shown in Fig. 11.24 (86). In this installation, 1,500 gal./hr. of gas liquor is washed countercurrently with 1,800 gal./hr. of light oil in two extractors each 6 ft. in diameter, 36 and 34 ft. tall, respectively, arranged for gravity flow of the gas liquor from one to the other. Each extractor contains three 36-in. beds of egg-sized coke sup-

ported on wire screens at suitable intervals. The dephenolized gas liquor contains dissolved light oil which, in American practice, is largely recovered since it is evolved upon subsequent distillation of the liquor. The vapors are then returned to the main gas stream which is subsequently scrubbed to recover the light oil. The light oil extracts phenols, cresols, and higher phenols as well as small amounts of pyridine, naphthalene, and other tar oils. It is washed with a sodium hydroxide solution to extract the phenols as sodium phenolates by dispersing the light oil into the caustic in two 5-ft. by 14-ft. towers. The caustic is not circulated, but after it accumulates

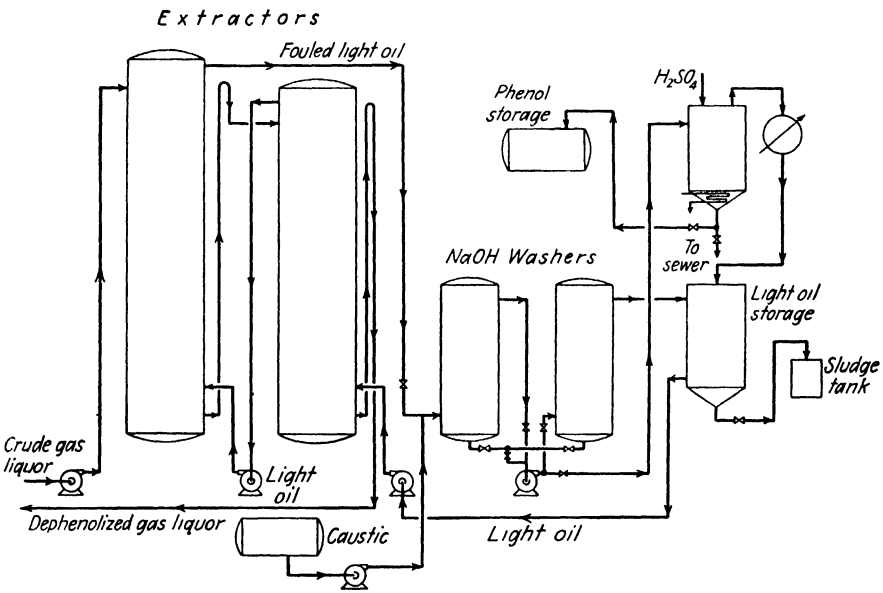



FIG. 11.24. Dephenolization of gas liquor (86). (*Courtesy, Chemical and Metallurgical Engineering.*)

phenols, it is pumped batchwise to the neutralizing tank where it is steam-distilled to remove dissolved benzene and acidified with sulfuric acid to release or "spring" the phenols. The latter are blown by air pressure to storage, and the sodium sulfate produced is discarded. The recovered light oil flows through a settling tank from which settled emulsions and sludge are periodically removed and returns to the extractors. It must be cleaned by distillation after 6 months' service. The recovered phenols can be worked up into USP grade phenol and highly refined cresol.

While flowsheets are generally the same in principle in other plants, they frequently differ in details. For example, Crawford (30) describes a plant in which the extractors are spray towers, where the pyridine is continuously removed from a portion of the extracting solvent by an acid wash, and where $CO_2$ or $NaHCO_3$ is used instead of $H_2SO_4$ to release the phenols from

the caustic solution, the resulting $Na_2CO_3$ being useful in removal of $H_2S$ from the gas. Hatch (69) describes extractors packed with a spiral arrangement of wooden grids. The caustic washing towers may be incorporated structurally in the same shell as the gas liquor extractors (170). Variants of these flowsheets are used extensively in Europe as well as in the United States (79, 97, 138, 167).

Stagewise extraction is also practiced in this country, with 3-stage plants using centrifugal pumps for mixers and with the settlers arranged in a single tower, one above the other (59). Particular care must be taken against the formation of unsettleable emulsions in these plants. An extensive description of a 10-stage Holley-Mott installation (Chap. 9) in Great Britain is available (125), where 1 stage is used for detarring of the gas liquor, 5 stages for dephenolizing with light creosote oil, 1 stage for water-washing of the light oil extract to remove $NH_3$ and $H_2S$, and 3 stages for caustic washing of the light oil to remove phenols.

Tricresyl phosphate has been used in Germany as a dephenolization solvent (56, 162) and offers the advantages of very favorable distribution coefficients for phenols and lower solubility in the gas liquor. Phenols are recovered by vacuum distillation. The solvent is relatively expensive and deteriorates with use, however. Butyl acetate ("phenosalvan") has also been used abroad. Bristow (21) provides a most complete description of the auxiliary processes in a low-temperature carbonization plant, including dephenolization and other extraction processes such as removal of tar acids from light and middle oils and chemical treating of light oils. A very complete review is also provided by Wilson and Wells (170).

## RECOVERY OF PENICILLIN

Penicillin, a minor product of the growth of the mold *Penicillium notatum* on suitable mediums, includes several acid substances which are antibiotic toward many disease-producing bacteria. Discovered in 1928 by Sir Alexander Fleming, it was not until 1939 that extensive studies regarding its qualities were undertaken; yet large-scale production methods were worked out sufficiently rapidly so that it was available in large quantities during the later half of the Second World War.

The concentration of the active principle formed in the original fermentation broth to the final packaged product presents many serious difficulties (137). The penicillins are biologically inactivated by acids and bases, moisture, heavy metal ions, oxidizing agents, high temperature, and certain bacterially produced enzymes such as penicillinase. In the broth before recovery, the potency may be reduced by as much as two-thirds in 24 hr. During certain concentration procedures, where it may be present in water solution at pH 2, 0°C., its half-life may be as low as 2.5 hr. It is more stable in dry neutral solutions, but in any case processing must be carried

out rapidly and under carefully controlled conditions throughout, both chemically and biologically. Concentration of the product is rapidly becoming a simpler process because of the tremendous advances being made in growing more concentrated solutions during the fermentation. In 1941, a broth potency of 2 Oxford units (O.U.)†/cu. cm., or roughly 1.2 p.p.m., was produced, but this was increased to 50 O.U./cu. cm. in 1943 and to 500 O.U./cu. cm. by 1949. The process flowsheets have been frequently altered to accommodate the improved raw materials.

Until recently, the concentration procedure generally involved the following steps (110, 140, 150, 158, 172). After growth of the mold in a culture medium of corn-steep liquor, the broth was filtered free of mold and the penicillin concentrated by adsorption on activated carbon. The carbon was filtered and the penicillin eluted from the solid by an 80 per cent acetone solution in water. This in turn was concentrated either by vacuum evaporation of the acetone at 65°F. or extraction of the acetone into a water-immiscible solvent. The aqueous penicillin was then chilled to 0°C., acidified to pH 2 with phosphoric acid, and extracted into chloroform or amyl acetate. This solution in turn was extracted with a dilute solution of sodium bicarbonate to pH 7, to give an aqueous solution of the sodium salt of penicillin. The solution was filtered and packaged into small vials, the water removed by freezing and sublimation at very low pressure, and the vials sealed. The most crucial stage in this procedure is the acidification of the concentrated activated carbon eluate and extraction into the organic solvent: efficient extraction requires low pH, yet the half-life of the penicillin is thereby rapidly lowered. For this reason, line mixers of the type of Fig. 9.14 and centrifugal phase separators were early introduced for this step, since the time of contact and hold-up was thereby kept small. Podbielniak centrifugal extractors (Fig. 10.12) proved to be especially useful because of their exceedingly low hold-up. Ethyl acetate, ethyl ether, cyclohexanone, dioxane, ethylene dichloride, furfuryl acetate, and methyl isobutyl ketone are all efficient penicillin solvents, but chloroform and amyl acetate are more selective although they offer somewhat lower distribution coefficients.

With the development in the fermentation broth of concentrations of the order of 500 O.U./cu. cm. total penicillin (80 per cent penicillin-*G*), the concentration procedures have not required adsorption on activated carbon (158). A presently recommended flowsheet (89) involves continuous, countercurrent, multistage extraction of the filtered and acidified (pH 2 to 2.15) broth with a one-fifth volume of amyl acetate in the centrifugal extractor at room temperature; similar extraction into a $\frac{1}{6}$ volume of cold buffer solution (pH 6.8 to 7.0); acidification to pH 2 and reextraction into a $\frac{1}{5}$

† The four principal pure penicillins are rated at 1,550 (penicillin-*F*), 1,667 (-*G*), 900 (-*X*), and 2,300 (-*K*) O.U./mg., respectively.

volume of amyl acetate. This solution contains 60,000 O.U./cu. cm. and may be extracted into a neutral buffer solution to give a product of high purity with an over-all loss of penicillin broth to crystalline product not exceeding 20 per cent. It can be expected that further improvement in broth concentrations and commercial development of synthetic penicillin will in time change these procedures, too.

Processes somewhat similar to these are probably also used in the concentration of other more recently developed antibiotic substances, such as streptomycin, chloromycetin, bacitracin, and aureomycin, although the technical details of these processes have not been made available.

## MISCELLANEOUS ORGANIC PROCESSES

There are so many organic chemical manufacturing processes using liquid extraction as a step in the procedure that no attempt will be made to describe or even list them all. They are all basically similar but differ in details, particularly with regard to the recovery of the solvent from the extract and raffinate solutions. They may be carried out either in batchwise or continuous fashion depending on the size of the manufacturing process. The following list includes a representative portion of these, which will serve to indicate the wide applicability of the extraction technique.

1. Acetic acid is extracted from the demethanolized pyroligneous liquors resulting from the destructive distillation of wood (20, 63, 130) and from solutions of the cellulose acetate industries (27), with ethyl ether, isopropyl ether, ethyl acetate, or a mixture of the last two as solvents, in continuous processes.

2. In the manufacture of phenol by the vapor-phase regenerative process (Raschig process) involving the indirect oxidation of benzene to phenol with chlorobenzene as an intermediate, liquid extraction is used in the washing of the crude chlorobenzene with caustic solution to remove HCl, and phenol is extracted from recovered HCl solution and from the principal aqueous stream by benzene in large extractors packed with Raschig rings (113, 129).

3. In the manufacture of phenol by the caustic hydrolysis of chlorobenzene in the liquid phase, the sodium phenolate solution is extracted continuously with chlorobenzene to remove diphenyl ether and phenyl xenyl ether prior to acidification to release the phenol. Alternatively, these can be allowed to build up in the mixture to an equilibrium concentration (64).

4. In the manufacture of nitroglycerine, the nitrated material is extracted with water and dilute sodium carbonate solution to remove excess acid either batchwise, or in Europe continuously (144).

5. In the manufacture of synthetic glycerol from propylene, the concentrated aqueous glycerol is extracted with xylene or isooctane to remove objectionable coloring matter in a continuous process (43, 168).

6. Aniline is recovered from dilute aqueous solution by batch extraction with nitrobenzene, in the manufacture of aniline from benzene (62).

7. In the manufacture of DDT, the product is extracted from the acid-reaction mixture by hexane (62) or by chlorobenzene (25), and the extract washed with water and dilute aqueous sodium carbonate in continuous processing.

8. Aluminum chloride catalyst is extracted from products of various Friedel-Krafts syntheses by water or caustic solution, as in the manufacture of ethylbenzene (120), and in the synthesis of phenylethyl alcohol or of chloracetophenone (62).

9. Batch extractions are used in the many intricate processes of drug preparation either by synthesis or by concentration from natural products, such as

*a*. The extraction by ethyl ether of *l*-phenylacetylcarbinol produced by the yeast fermentation of benzaldehyde in the manufacture of ephedrine (73).

*b*. The extraction of quinine by dilute acid from the naphtha solution obtained by leaching cinchona bark (44).

*c*. The extraction of ergonovine from liquid ammonia by ethyl ether, and the repeated extraction of the alkaloid between ether and water (157).

*d*. The extraction of ethyl malonate from the esterification mixture by benzene and the repeated washing of the benzene extract with caustic and water, in the manufacture of barbiturate drugs (139).

10. Continuous and batch operations are used in the manufacture of various esters, such as

*a*. The extraction of glycerol with water from the reaction mixture after the alcoholysis of glycerides (62).

*b*. The extraction of ethanol from ethyl acetate, or of butanol from butyl acetate by water (11).

11. Extraction is used in the manufacture of various emulsifying agents, for example, the extraction of unsulfated material with trichloroethylene in the sulfation of ricinoleic acid (15).

12. The washing of various synthetic organic chemicals to free them of by-products are extraction processes, such as the washing of spent nitric acid from nitroparaffins with water, or the washing of sodium sulfite from crude β-naphthol (62).

**Recovery of Organic Solvents.** In connection with the recovery of volatile organic substances from aqueous solution, as in the separation of acetone or ethanol from aqueous solutions containing less than 5 per cent solute, Othmer, *et al.* (131, 132) have shown that considerable savings can be expected in heat requirements if extraction by an appropriate *high-boiling* solvent followed by distillation of the extracted solute is used, as compared with direct rectification.

The simplified flowsheet of such an extraction and solvent-recovery plant for cases where the solvent is substantially immiscible is shown in Fig. 11.25, on the assumption that the extracting solvent has the lower density. Raffinate, substantially exhausted of solute and saturated with solvent, leaves the bottom of the extractor and may be discarded if the solvent concentration is very low. Ordinarily, however, it can be stripped of its solvent by a very simple distillation. Extract containing solvent and extracted solute, together with a small amount of water, is distilled, and provided

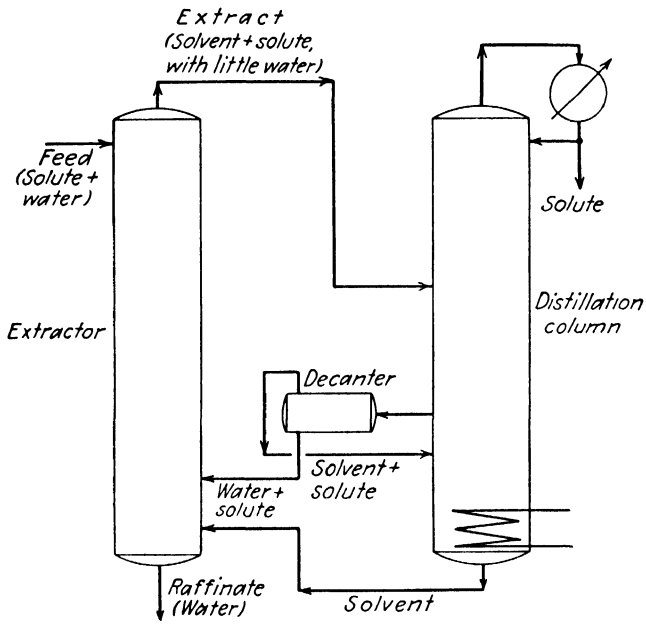



FIG. 11.25. Extraction and solvent recovery for a high-boiling immiscible solvent (132). (*Courtesy, American Institute of Chemical Engineers.*)

that the solute has the lowest boiling point in the system, it will distill overhead. The high-boiling solvent and water separate into two equilibrium liquid layers in the lower parts of the distillation column after removal of most of the solute, and these insoluble liquids can be withdrawn and decanted. The solvent-rich layer is returned to the distillation column to be further exhausted of solute and is ultimately returned to the extractor for reuse. The water-rich layer, saturated with solvent and solute, is introduced into the extraction column at a point appropriate to its solute concentration (see Chap. 6 for methods of designing extractors with multiple feed).

Should the solvent show substantial miscibility with water (or have a lower selectivity in the extraction of the dissolved solute), the raffinate stripping must be carefully done, as in the raffinate stripper of Fig. 11.26. The solvent-water azeotrope leaves the top of the stripper and is distilled

along with the extract solution in the extract distillation column. For good heat economy, it is essential that the azeotrope composition be poor in water, else too much heat is required for vaporization of the water. The remainder of the flowsheet is essentially the same as that previously considered. The necessary coolers, pumps, etc., are not shown.

Othmer and Ratcliffe (131) have presented experimental confirmation of these flowsheets and have obtained measurements of the heat requirements.

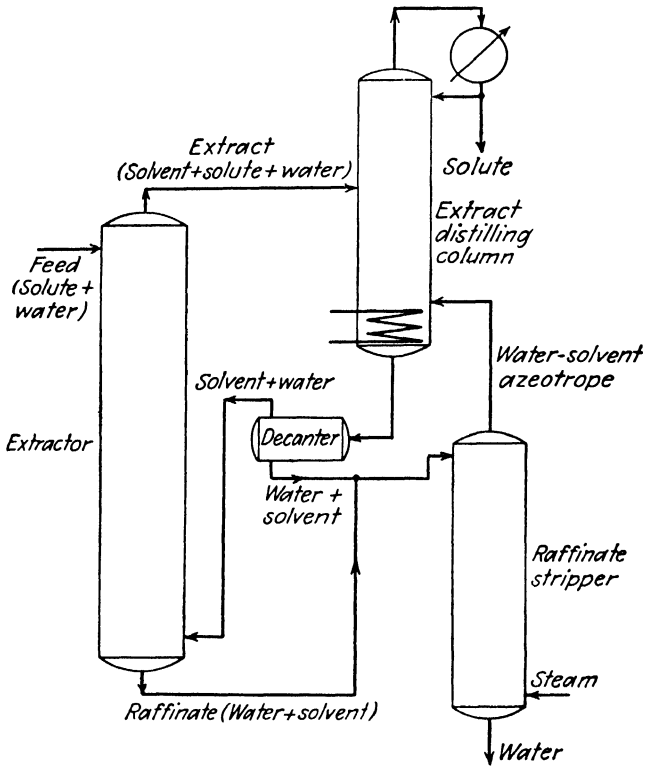



FIG. 11.26. Extraction and solvent recovery for a high-boiling, partially miscible solvent (132). (*Courtesy, American Institute of Chemical Engineers.*)

Heat economies by combined extraction-distillation processes, in comparison to direct distillation, will result depending upon the respective vapor-liquid equilibria involved. Meissner, *et al.* (111, 112) in turn have proposed the dehydration of concentrated aqueous solutions of certain organic liquids by extraction of the water by means of strong solutions of [illegible] salts.

## INORGANIC EXTRACTION PROCESSES

There have been relatively few applications of extraction in the inorganic chemical industries, but those that have been made are very effective. There should be ample opportunity for others.

**Purification of Sodium Hydroxide.** Sodium hydroxide produced in the electrolytic diaphragm cell contains several impurities which make it unfit for direct use in the manufacture of rayon, certain cold-process soaps, and in other processes. Successful extraction of certain of these impurities with liquid ammonia is now used successfully on a large scale (164). Fifty per cent caustic solution containing 0.9 to 1.1 per cent NaCl and 0.05 to 0.10 per cent $NaClO_3$ is customarily extracted to reduce the concentrations of these salts to 0.08 and 0.0002 per cent, respectively, in a continuous countercurrent operation. The ammonia used contains 70 to 95 per cent $NH_3$, and its strength governs the extent of extraction. A yield of 95 per cent of the feed caustic is obtained in the raffinate, the remainder leaving with the extract. Extract solution is distilled to recover anhydrous ammonia, and the ammonia in the raffinate is evaporated and recovered by absorption in water. The anhydrous and aqueous ammonia are then combined to give a solution of controlled strength which is then used in the extraction. Plants handling 150 tons/day of caustic are being operated.

**Metallurgical Applications.** In the atomic-energy program initiated during the Second World War, it was necessary to obtain uranium metal for conversion to plutonium which contained concentrations of elements such as boron, cadmium, indium, and others, of less than $10^{-4}$ per cent (83). Uranium metal that had previously been available was not nearly so pure, especially that produced on a relatively large scale. It has been known for some time, however, that uranyl nitrate $UO_2(NO_3)_2$ is quite soluble in ethyl ether, and the distribution characteristics of this salt between water and the ether are available (145). A metallurgical procedure involving leaching of the ore, precipitation of most of the undesirable metals, acidification with nitric acid to convert uranium to $UO_2(NO_3)_2$, and extraction with ethyl ether then gives a uranium which is purer than most of that available for laboratory purposes prior to the war. Although the details of the extraction are not available, Smyth (152) indicates that, by 1942, 30 tons/month of uranium dioxide of extreme purity were made by this method, with increased production later in the atomic-energy program.

Although it is not publicly known to what extent extraction operations have been applied in other parts of the atomic-energy program, there are many opportunities for application (83). For example, the metal slugs issuing from the piles contain plutonium, uranium, and a large number of other elements produced as fission by-products. The recovery of uranium from solutions of the slugs by ether extraction is a possibility, as is the simultaneous extraction of plutonium and uranium for the purpose of separating them from the fission by-products. The possibility of separating the various by-products by extraction is also good. The separation of thorium and uranium is necessary if thorium is to be irradiated to produce high concentrations of $U^{233}$. Both thorium nitrate and uranyl nitrate can be

extracted from water solution by ether (145), and since their distribution coefficients are different they can be separated by this means.

Other metal extractions have been made, but so far as is known, only on a laboratory scale. The extraction of ferric chloride from aqueous solution by isopropyl ether has been discussed previously (Figs. 10.24 and 10.33). In these studies (57), the distribution coefficient was found to be increased to as high as 6,000 in favor of the organic phase by addition of HCl to the system. Such an extraction has been suggested as a means of separating iron from the nickel and chromium in stainless-steel scrap (108). Similarly, the separation of nickel and cobalt chlorides by extraction of the aqueous solution with capryl alcohol in the presence of HCl has been studied (55). In addition to influencing the equilibrium by addition of a common ion, as in the above examples and in the extraction of uranyl nitrate in the presence of nitric acid, the addition of an organic compound to the solvent phase so as to form a coordination compound with the metal and thus increase the distribution coefficient can be profitable. Thus, zirconium ions form complexes with thenoyltrifluoroacetone in benzene and can be separated from hafnium by extraction (80). Another technique which may prove useful in cases where the aqueous solubilities are low is the addition of hydrotropic substances such as sodium xylenesulfonate, which can increase solubilities of inorganic substances a thousandfold (109).

The separation of the rare earth metals by liquid extraction is a most useful application, since by this method the tedious recrystallizations usually necessary are avoided. The work of Asselin and Comings (7) on the separation of neodymium and thorium, and the extensive work of Templeton (159, 160) and Fischer (48, 49) on separations of lanthanum and neodymium, zirconium and hafnium, and scandium from its accompanying elements has confirmed the success of this technique.

### Notation for Chapter 11

$A$ = defined by Eq. (11.7).
$a, b, \ldots m$ = constants.
$B$ = defined by Eq. (11.9).
$E'$ = fraction of feed oil entering extract.
$G$ = quantity of gasoline.
$K_S$ = vaporization equilibrium constant of mercaptan, concentration in vapor/concentration in liquid.
$K_w$ = ionization constant for water.
$K_{II}$ = ionization constant for mercaptan in aqueous solution.
$m_T$ = distribution coefficient for total mercaptan content between alkaline solutions and naphtha.
$m_I$ = distribution coefficient of unionized mercaptan between alkaline solution and naphtha.
$n$ = number of theoretical extraction stages.
p.p.m. = parts per million.

$R'$ = volume of oil per unit volume of solvent in the raffinate.
$S$ = quantity of solvent.
$S_R$ = fraction of solvent entering the raffinate.
$s$ = number of theoretical distillation trays.
$T$ = temperature.
$V$ = quantity of stripping steam.
V.G.C. = viscosity-gravity constant.
V.I. = viscosity index.
$x$ = concentration of mercaptan in gasoline.
$y$ = concentration of mercaptan in alkaline solution.
$\mu$ = viscosity.

Subscripts:
$F$ = feed.
$n$ = leaving extractor.
$s$ = leaving stripper.
1 = entering stripper.
100 = 100°F.
210 = 210°F.

## LITERATURE CITED


1. Albright, J. C.: *Petroleum Engr.* **22,** No. 2, C-11 (1950).
2. Allen, H. D., W. A. Kline, E. A. Lawrence, C. J. Arrowsmith, and C. J. Marsel: *Chem. Eng. Progress* **43,** 459 (1947).
3. Anon.: *Chemistry & Industry* **59,** 1016 (1946).
4. ———: *Oil Gas J.* **45,** No. 11, 173 (1947).
5. ———: *Oil Gas J.* **45,** No. 11, 175 (1947).
6. Arnold, G. B., and C. A. Coghlan: *Ind. Eng. Chem.* **42,** 177 (1950).
7. Asselin, G. F., and E. W. Comings: *Ind. Eng. Chem.* **42,** 1198 (1950).
8. Baehr, H.: *Refiner Natural Gasoline Mfr.* **17,** 237 (1938).
9. Bahlke, W. H., A. B. Brown, and F. F. Diworky: *Oil Gas J.* **32,** No. 23, 60, 72 (1933).
10. Bailey, A. E.: "Industrial Oil and Fat Products," Interscience Publishers, Inc., New York, 1945.
11. Bannister, W. J., and I. J. Krehma: U.S. Pat. 1,980,711 (11/13/34).
12. Beach, R. M., and E. A. Robinson: U.S. Pat. 2,265,020 (12/2/41).
13. Bennett, H. T.: U.S. Pats. 2,003,233-9 (5/28/35).
14. Berg, C., M. Manders, and R. Switzer: Paper presented to American Institute of Chemical Engineers, Los Angeles, Mar. 9, 1949.
15. Bertsch, H.: U.S. Pat. 1,906,924 (5/2/33).
16. Birchel, J. A., and R. N. J. Saal: U.S. Pat. 1,945,516 (2/6/34).
17. Bogash, R., and A. N. Hixson: *Chem. Eng. Progress* **45,** 597 (1949).
18. Border, L. E.: *Chem. Met. Eng.* **47,** 776 (1940).
19. Brandt, R. L.: *Ind. Eng. Chem.* **22,** 218 (1930).
20. Brewster, T. J.: Can. Pat. 247,385 (3/3/25).
21. Bristow, W. A.: *J. Inst. Fuel* **20,** 109 (1947).
22. Brown, K. M.: *World Petroleum* **18,** No. 8, 72 (1947).
23. Bryant, G. R., R. E. Manley, B. Y. McCarty: *Refiner Natural Gasoline Mfr.* **14,** 299 (1935).
24. Butchelder, A. H.: U.S. Pat. 2,285,795 (6/9/42).
25. Callahan, J. R.: *Chem. Met. Eng.* **51,** No. 10, 109 (1944).
26. Carvlin, G. M.: *Refiner Natural Gasoline Mfr.* **17,** No. 6, 275 (1938).
27. Clotworthy, H. R. S.: *Ind. Chemist* **7,** 111 (1931).

28. Cottrell, O. P.: *Refiner Natural Gasoline Mfr.* **12,** 432 (1933).
29. Crary, R. W., and M. M. Holm: *Ind. Eng. Chem.* **29,** 1389 (1937).
30. Crawford, R. M.: *Ind. Eng. Chem.* **18,** 313 (1926); **19,** 168 (1927).
31. Davis, G. H. B., M. Lapeyrouse, and E. W. Dean: *Oil Gas J.* **30,** No. 46, 92 (1932).
32. Dean, E. W., and G. H. B. Davis: *Chem. Met. Eng.* **36,** 618 (1929).
33. Defize, J. C. L.: "On the Edeleanu Process for the Selective Extraction of Mineral Oils" (in English), D. B. Centen's Uitgevers-Maatschappij, N. V., Amsterdam, 1938.
34. Dickey, S. W.: *Petroleum Processing* **3,** 538 (1948).
35. Drew, D. A., and A. N. Hixson: *Trans. Am. Inst. Chem. Engrs.* **40,** 675 (1944).
36. Dulton, J., C. P. Lancaster, and O. L. Brekke: *J. Am. Oil Chemists' Assoc.* **27,** 25 (1950).
37. Dunstan, A. E., Ed.: "Science of Petroleum," Vol. 3, Oxford University Press, New York, 1938.
    *a.* Bahlke, W. H.: p. 1915.
    *b.* Ferris, S. W.: p. 1875.
    *c.* Ferris, S. W.: p. 1904.
    *d.* Hall, F. C.: p. 1888.
    *e.* Hunter, T. G.: p. 1818.
    *f.* Manley, R. E., and McCarty, B. Y.: p. 1918.
    *g.* Thompson, F. E. A.: p. 1759, 1829.
    *h.* Stratford, R. K.: p. 1910.
38. Edeleanu, L.: Brit. Pat. 11,140 (5/22/08), and many others.
39. ———: *Z. angew. Chem.* **26,** 177 (1913).
40. Edeleanu G. m. b. H.: Ger. 571,712 (4/8/33).
41. Eichwald, E.: U.S. Pat. 1,550,523 (8/18/25).
42. Elgin, J. C.: U.S. Pat. 2,479,041 (8/16/49).
43. Evans, T. W.: U.S. Pat. 2,154,930 (1/18/39).
44. Evers, N.: "The Chemistry of Drugs," D. Van Nostrand Company, Inc., New York, 1926.
45. Ferris, S. W.: U.S. Pat. 1,788,562 (1/13/31).
46. ——— and W. F. Houghton: *Refiner Natural Gasoline Mfr.* **11,** 560, 581 (1932).
47. Field, H. W.: *Oil Gas J.* **40,** No. 20, 40 (1941).
48. Fischer, W., and R. Bock: *Z. anorg. u. allgem. Chem.* **249,** 146 (1942).
49. ——— and W. Chalybaeus: *Z. anorg. Chem.* **255,** 79, 277 (1947).
50. Francis, A. W.: *Ind. Eng. Chem.* **36,** 764, 1096 (1944).
51. Freeman, S. E.: U.S. Pats. 2,200,390–1 (5/14/40); 2,313,636 (3/9/43); 2,316,512 (4/13/43), and many others.
52. ———: U.S. Pat. 2,278,309 (3/31/42).
53. ——— and S. W. Gloyer: U.S. Pat. 2,423,232 (7/1/47).
54. Gard, E. W., and E. G. Ragatz: *Oil Gas J.* **39,** No. 4, 49 (1940).
55. Garwin, L., and A. N. Hixson: *Ind. Eng. Chem.* **41,** 2298, 2303 (1949).
56. Gasmeier-Kres, E.: *Brennstoff Chem.* **17,** 466 (1936).
57. Geankoplis, C. J., and A. N. Hixson: *Ind. Eng. Chem.* **42,** 1141 (1950).
58. Gloyer, S. W.: *Ind. Eng. Chem.* **40,** 228 (1948).
59. Gollmar, H. A.: *Ind. Eng. Chem.* **39,** 596 (1947).
60. Gordon, J. D.: *Oil Gas J.* **42,** No. 49, 202 (1944).
61. Goss, W. H., and H. F. Johnstone: U.S. Pat. 2,290,609 (7/21/42).
62. Groggins, P. H.: "Unit Processes in Organic Synthesis," 3d ed., McGraw-Hill Book Company, Inc., New York, 1947.
63. Guinot, H.: *Chimie & industrie* **25,** 1354 (1931).

64. Hale, W. J., and E. C. Britton: *Ind. Eng. Chem.* **20,** 114 (1928).
65. Happel, J.: Personal communication, 1950.
66. ———, S. P. Cauley, and H. S. Kelly: *Oil Gas J.* **41,** No. 27, 136 (1942).
67. ——— and D. W. Robertson: *Ind. Eng. Chem.* **27,** 941 (1935).
68. ——— *et al.*: *Trans. Am. Inst. Chem. Engrs.* **42,** 189 (1946).
69. Hatch, B. F.: *Blast Furnace Steel Plant* **17,** 1797 (1929).
70. Heath, B. L., and D. B. Williams: *Nat'l Petroleum News* **30,** R-318, 320 (1938).
71. Hibshman, H. J.: *Ind. Eng. Chem.* **41,** 1366, 1369 (1949).
72. Hightower, J. V.: *Chem. Eng.* **56,** No. 5, 139 (1949).
73. Hildebrandt, G., and W. Klavehn: U.S. Pat. 1,956,950 (5/1/34).
74. Hill, J. B., and J. B. Coats: *Ind. Eng. Chem.* **20,** 641 (1928).
75. Hixson, A. W., and J. B. Bockelmann: *Trans. Am. Inst. Chem. Engrs.* **38,** 891 (1942).
76. ——— and A. N. Hixson: *Trans. Am. Inst. Chem. Engrs.* **37,** 927 (1941).
77. ——— and R. Miller: U.S. Pats. 2,219,652 (10/29/40), 2,344,089 (3/14/44), 2,388,412 (11/6/45).
78. ——— and R. Miller: U.S. Pat. 2,439,807 (4/20/48).
79. Hoening, P.: *Z. angew. Chem.* **42,** 325 (1929).
80. Huffman, E. H., and L. J. Beaufait: *J. Am. Chem. Soc.* **71,** 3179 (1949).
81. Humphrey, I. W.: *Ind. Eng. Chem.* **35,** 1062 (1943).
82. Hunter, T. G., and A. W. Nash: *Ind. Eng. Chem.* **27,** 836 (1935).
83. Irvine, J. W.: In "The Science and Engineering of Nuclear Power," C. Goodman, Ed., Vol. 1, Addison-Wesley Press, Inc., Cambridge (Mass.), 1947.
84. Ittner, M. H.: U.S. Pats. 2,139,589 (12/6/38), Reissue 22,006 (1/13/42); 2,221,799 (11/19/40).
85. Jenkins, J. D.: U.S. Pat. 2,352,546 (6/27/44).
86. Jones, H. E.: *Chem. Met. Eng.* **35,** 215 (1928).
87. Kain, W.: *Refiner Natural Gasoline Mfr.* **11,** 553 (1932).
88. Kaiser, H. E., and R. S. Hancock: U.S. Pats. 1,715,085-8 (5/28/29).
89. Kaiser, H. R., Podbielniak, Inc.: Personal communication, 1949.
90. Kalichevsky, V. A.: "Modern Methods of Refining Lubricating Oil," Reinhold Publishing Corporation, New York, 1938.
91. ———: *Ind. Eng. Chem.* **38,** 1009 (1946).
92. ———: *Natl. Petroleum News* **38,** R-613 (1946).
93. ——— and B. A. Stagner: "Chemical Refining of Petroleum," 2d ed., Reinhold Publishing Corporation, New York, 1942.
94. Kemp, L. C., G. B. Hamilton, and H. H. Gross: *Ind. Eng. Chem.* **40,** 220 (1948).
95. Kenyon, R. L., S. W. Gloyer, and C. C. Georgian: *Ind. Eng. Chem.* **40,** 1162 (1948).
96. Kleinsmith, A. W., and Kraybill, H. R.: *Ind. Eng. Chem.* **35,** 674 (1943).
97. Krebs, O.: *Chem.-Ztg.* **57,** 721, 743 (1933).
98. Kurtz, S. S.: *Ind. Eng. Chem.* **27,** 845 (1935).
99. La Croix, H. N., and L. J. Coulthurst: *Refiner Natural Gasoline Mfr.* **18,** 337 (1938).
100. Lascary, L.: *Ind. Eng. Chem.* **41,** 786 (1949).
101. Lee, J. A.: *Chem. Eng.* **57,** No. 3, 94 (1950).
102. Lister, D. A.: U.S. Pat. 2,054,432 (9/15/36).
103. Livingstone, M. J., and J. T. Dickinson: *Natl. Petroleum News,* **27,** No. 27, 25 (1935).
104. MacKusick, B. L., and H. A. Alvers: *Oil Gas J.* **42,** No. 49, 126 (1944).
105. Marsel, C. J.: Personal communication (1950).
106. ——— and H. D. Allen: *Chem. Eng.* **54,** No. 6, 104 (1947).
107. Mason, C. F., R. D. Bent, and J. H. McCullough: *Oil Gas J.* **40,** No. 26, 114 (1941).
108. McCormack, R., and F. C. Vilbrandt: *Bull. Virginia Polytech. Inst. Engr. Station,* No. 64 (1946).

109. McKee, R. H.: *Ind. Eng. Chem.* **38,** 382 (1946).
110. McKeen, J. E.: *Trans. Am. Inst. Chem. Engrs.* **40,** 747 (1944).
111. Meissner, H. P., and C. A. Stokes: *Ind. Eng. Chem.* **36,** 816 (1944).
112. ———, C. A. Stokes, C. M. Hunter, and G. M. Morrow: *Ind. Eng. Chem.* **36,** 917 (1944).
113. Messing, R. F., and W. V. Keary: *Chem. Ind.* **63,** 234 (1948).
114. Meyer, P.: *J. Inst. Pet. Technol.* **17,** 621 (1931).
115. ———: *J. Inst. Pet. Technol.* **19,** 819 (1933).
116. Miller, Max B. Company: French Pat. 756,248 (12/6/33).
117. Miller, Max B., Jr.: Personal communications (1950).
118. Mills, V.: U.S. Pats. 2,156,863 (5/2/39); 2,233,845 (3/4/41).
119. ——— and H. K. McClain: *Ind. Eng. Chem.* **41,** 1982 (1949).
120. Mitchell, J. E.: *Trans. Am. Inst. Chem. Engrs.* **42,** 293 (1946).
121. Moore, E. B.: *J. Am. Oil Chemists' Assoc.* **27,** 75 (1950).
122. Moriarty, F. C.: *Petroleum World* **41,** No. 6, 53 (1944).
123. Morrell, C. E., W. J. Paltz, J. W. Packie, W. C. Asbury, and L. C. Brown: *Trans. Am. Inst. Chem. Engrs.* **42,** 473 (1946).
124. Moy, J. A. E.: *Ind. Chemist* **24,** 433, 505 (1948).
125. Murdock, D. G., and M. Cuckney: *Trans. Inst. Chem. Engrs.* (London) **24,** 90 (1946).
126. Murphy, J. F.: U.S. Pat. 2,310,986 (2/16/43).
127. Myers, W. A.: *Oil Gas J.* **34,** No. 44, 81 (1936).
128. Nelson, W. L.: "Petroleum Refinery Engineering," 3d ed., McGraw-Hill Book Company, Inc., New York, 1949.
129. Olive, T. R.: *Chem. Met. Eng.* **47,** 770 (1940).
130. Othmer, D. F.: *Trans. Am. Inst. Chem. Engrs.* **30,** 299 (1933).
131. ——— and R. L. Ratcliffe: *Ind. Eng. Chem.* **35,** 798 (1943).
132. ——— and E. Treuger: *Trans. Am. Inst. Chem. Engrs.* **37,** 597 (1941).
133. Page, J. M., C. C. Buckler, and S. H. Diggs: *Ind. Eng. Chem.* **25,** 418 (1933).
134. Passino, H. J.: *Ind. Eng. Chem.* **41,** 280 (1949).
135. Poettmann, F. H., and M. R. Dean: *Chem. Eng. Progress* **45,** 636 (1949).
136. Reeves, E. J.: *Ind. Eng. Chem.* **41,** 1490 (1949).
137. Regna, P. P.: *Trans. Am. Inst. Chem. Engrs.* **40,** 759 (1944).
138. Rosendahl, F.: *Teer u. Bitumen* **39,** 21 (1941).
139. Ross, A. A., and F. E. Bibbins: *Ind. Eng. Chem.* **29,** 1341 (1937).
140. Rowley, D., H. Steiner, and E. Zimkin: *J. Soc. Chem. Ind.* **65,** 237T (1946).
141. Rushton, J. H.: *Ind. Eng. Chem.* **29,** 309 (1937).
142. Ruthruff, R. F., and D. F. Wilcock: *Trans. Am. Inst. Chem. Engrs.* **37,** 649 (1941); U.S. Pat. 2,355,605 (8/15/44).
143. Sachanen, A. N.: "The Chemical Constituents of Petroleum," Reinhold Publishing Corporation, New York, 1945.
144. Schmid, A.: U.S. Pat. 1,901,003 (3/14/33); 1,946,414 (2/6/34).
145. Siedell, A.: "Solubilities of Inorganic and Metal Organic Compounds," Vol. 1, 3d ed., D. Van Nostrand Company, Inc., New York, 1940.
146. Skogan, V. G.: Personal communication (1950).
147. ——— and M. C. Rogers: *Oil Gas J.* **45,** No. 13, 70 (1947).
148. Smith, A. S., and T. B. Braun: *Ind. Eng. Chem.* **37,** 1047 (1945).
149. ——— and J. E. Funk: *Trans. Am. Inst. Chem. Engrs.* **40,** 211 (1944).
150. Smith, E. L.: *J. Soc. Chem. Ind.* **65,** 308T (1946).
151. Smoley, E. R., and D. Fulton: *World Petroleum* **18,** No. 8, 62 (1947).
152. Smyth, H. D.: "Atomic Energy for Military Purposes," Princeton University Press, Princeton, N.J., 1946.

153. Staatermas, H. G., R. C. Morris, R. M. Stager, and G. J. Pierotti: *Chem. Eng. Progress* **43,** 148 (1947).
154. Stiner, D. E.: *Oil Gas J.* **34,** No. 44, 75 (1936).
155. Stratford, R. K.: U.S. Pat. 1,860,823 (5/31/32).
156. ——— and J. L. Huggett: *Oil Gas J.* **33,** No. 32, 44 (1934).
157. Stuart, E. H.: U.S. Pat. 2,067,866 (1/12/37).
158. Taylor, T. H. M.: *Chem. Eng. Progress* **43,** 155 (1947).
159. Templeton, C. C.: *J. Am. Chem. Soc.* **71,** 2187 (1949).
160. ——— and J. A. Peterson: *J. Am. Chem. Soc.* **70,** 3967 (1948).
161. Tilghman, R. A.: U.S. Pat. 28,315 (5/15/1860).
162. Tupholme, C. H. S.: *Ind. Eng. Chem.* **25,** 303 (1933).
163. Tuttle, M. H.: U.S. Pats. 1,912,318-9 (5/30/33).
164. ——— and M. B. Miller: *Refiner Natural Gasoline Mfr.* **12,** 453 (1933); **14,** 289 (1935).
165. Tyler, C. N.: U.S. Pat. 38,015 (3/24/1863).
166. Van Dijck, W. J. D., and J. S. Oriel: *World Petroleum* **8,** No. 11, 164 (1937).
167. Wiegman, D. H.: *Gluckauf* **75,** 965 (1939).
168. Williams, E. C.: *Trans. Am. Inst. Chem. Engrs.* **37,** 157 (1941).
169. Wilson, R. E., P. C. Keith, and R. C. Haylett: *Ind. Eng. Chem.* **28,** 1065 (1936); *Trans. Am. Inst. Chem. Engrs.* **32,** 364 (1936).
170. Wilson, P. J., and J. H. Wells: "Chemistry of Coal Utilization," H. H. Lowry, Ed., John Wiley & Sons, Inc., New York, 1945.
171. Winer, B.: U.S. Pat. 2,313,692 (3/9/43).
172. Whitmore, F. C., *et al.: Ind. Eng. Chem.* **38,** 942 (1946).
173. Yabroff, D. L.: *Ind. Eng. Chem.* **32,** 257 (1940).
174. ——— and L. E. Border: *Refiner Natural Gasoline Mfr.* **18,** No. 5, 171, 203 (1939).
175. ——— and E. R. White: *Ind. Eng. Chem.* **32,** 950 (1940).

# PROBLEMS

## Chapter 2

The following are the data of Briggs and Comings [*Ind. Eng. Chem.* **35**, 411 (1943)], for the system water (*A*)–benzene (*B*)–acetone (*C*) at 15 and 45°C. Problems **1** through **9** refer to the system below, for both temperatures.

BINODAL CURVE

| 15°C. Weight per cent | | 45°C. Weight per cent | |
|---|---|---|---|
| Benzene | Acetone | Benzene | Acetone |
| 0 1 | 0.0 | 0.1 | 0.0 |
| 0.1 | 10.0 | 0.2 | 10.0 |
| 0.3 | 20.0 | 0.5 | 20.0 |
| 0.7 | 30.0 | 1.1 | 30.0 |
| 1.4 | 40.0 | 2.3 | 40.0 |
| 3.2 | 50.0 | 5.3 | 50 0 |
| 9.0 | 60.0 | 13.6 | 60.0 |
| 24.1 | 65 3 | 23.3 | 62.8 |
| 99.9 | 0.0 | 99.9 | 0.0 |
| 89.8 | 10.0 | 89.7 | 10.0 |
| 79.6 | 20 0 | 79.3 | 20.0 |
| 69.3 | 30 0 | 68 7 | 30.0 |
| 58.5 | 40.0 | 57.5 | 40.0 |
| 47.1 | 50.0 | 45.5 | 50.0 |
| 34.2 | 60.0 | 30.9 | 60.0 |

TIE LINES

| Benzene-rich phase | | Water-rich phase | |
|---|---|---|---|
| Weight per cent | | | |
| Benzene | Acetone | Benzene | Acetone |
| 15°C. | | | |
| 95.2 | 4.7 | 0.1 | 5.0 |
| 89.0 | 10.8 | 0.1 | 10.0 |
| 73.4 | 26.1 | 0.3 | 20.0 |
| 55.2 | 43.0 | 0.7 | 30.0 |
| 39.1 | 56.5 | 1.4 | 40.0 |
| 27.6 | 63.9 | 3.2 | 50.0 |
| 45°C. | | | |
| 92.9 | 6.9 | 0.2 | 5.0 |
| 84.0 | 15.6 | 0.2 | 10.0 |
| 63.6 | 34.6 | 0.5 | 20.0 |
| 44.0 | 51.2 | 1.1 | 30.0 |
| 29.7 | 60.6 | 2.3 | 40.0 |

**1.** Plot the binodal curve and tie lines and (*a*) triangular coordinates and (*b*) rectangular coordinates of Janecke.

**2.** Plot tie-line correlation curves according to Sherwood's method.

**3.** Plot simple distribution curves for the acetone between benzene and water.

**4.** Plot tie-line correlation curves of the Hand type. On the same set of coordinates, plot the binodal-solubility curves, as shown in Fig. 2.28. Determine the constants of Eq. (2.11).

**5.** Calculate the distribution coefficients [Eq. (2.7)], and plot against acetone concentration in the water-rich phase.

**6.** Devise a tie-line correlation curve for the rectangular coordinates of Problem **1** (*b*).

**7.** With the help of the plots of Problems **2, 3, 4,** and **6,** determine the equilibrium concentrations of all three components, in both phases, corresponding to an acetone concentration in the water-rich phase of 25%. Compare the results by the various methods.

**8.** Estimate the concentration of acetone at the plait point.

**9.** One hundred pounds of a mixture of the following composition are prepared: 30% acetone, 30% benzene, 40% water. Determine the weights and composition of both layers after equilibrium is established.

**10.** Repeat Problems **1** through **9** for the system water (*A*)–toluene (*B*)–isopropanol (*C*) at 25°C., data for which are given by Washburn and Beguin [*J. Am. Chem. Soc.* **62,** 579 (1940)].

**11.** Hunter and Brown [*Ind. Eng. Chem.* **39,** 1343 (1947)] have determined the equilibrium in the Type 2 system *n*-heptane (*A*)–aniline (*B*)–cyclohexane (*C*) at 25°C. For each of the equilibrium-data points reported, calculate $\beta$, the constant of Eq. (2.15), and average for the entire system. Plot the data in the manner of Fig. 2.30, together with the Eq. (2.15), using the average value of $\beta$. Comment on the ability of the equation to describe the data.

## Chapter 3

**1.** Dodge and Dunbar [*J. Am. Chem. Soc.* **49,** 591 (1927)] report the following vapor-liquid equilibrium between oxygen and nitrogen: temperature = 110.03°K; pressure = 10.734 atm.; mole per cent $O_2$ = 41.92 in the liquid, 25.64 in the vapor. Calculate the activity coefficients for the oxygen and nitrogen.

**2.** Calculate activity coefficients for the system chloroform–acetone at 35.17°C. from vapor-liquid data reported in "International Critical Tables" (Vol. III, p. 286). Fit one of the integrated Gibbs-Duhem equations to the data. With the help of heat of solution data, *ibid.*, Vol. V, pp. 151, 155, 158, estimate the values of the equation constants for 55.1°C., and calculate the activity coefficients for this temperature. Compare with those computed from vapor-liquid data at this temperature, *ibid.*, Vol. III, p. 286.

**3.** Calculate the activity coefficients from azeotropic data for the following systems using one of the integrated Gibbs-Duhem equations, obtaining the necessary data from the compilation of Horsley [*Ind. Eng. Chem., Anal. Ed.* **19,** 508 (1947)]. Compare with those calculated from the complete vapor-liquid data, as reported in "Chemical Engineers' Handbook."

**4.** Calculate the activity coefficients for the system isopropyl ether–isopropyl acetate from the data of Miller and Bliss [*Ind. Eng. Chem.* **32,** 123 (1940)]. Determine the best values of the constants of the van Laar, Margules, and Scatchard-Hamer equations for these data, and compare the ability of these equations to describe this system.

**5.** The total vapor pressures of benzene–ethyl acetate solutions at 20°C. are ("International Critical Tables," Vol. III, p. 288):

| Mole per cent ester..... | 0 | 10 | 20 | 30 | 40 | 50 | 60 | 70 | 80 | 90 | 100 |
|---|---|---|---|---|---|---|---|---|---|---|---|
| Vapor pressure, mm. Hg..... | 76.9 | 86.3 | 95.8 | 103.4 | 106.5 | 107.3 | 104.6 | 101.3 | 94.3 | 83.4 | 73.8 |

Determine the van Laar constants for this system.

**6.** Repeat Problem **5** for the system bromobenzene–toluene at 40°C.

**7.** The atmospheric-pressure boiling points of the system nitrobenzene–*n*-hexane are ("International Critical Tables," Vol. III, p. 314):

| Mole per cent nitrobenzene | 0 | 10 | 20 | 30 | 40 | 50 | 60 | 70 | 80 | 90 | 100 |
|---|---|---|---|---|---|---|---|---|---|---|---|
| Boiling point, °C. | 69.0 | 71.7 | 72.9 | 73.8 | 74.6 | 75.4 | 77.7 | 85.0 | 103.4 | 143.4 | 210 |

Determine the van Laar constants for this system.

**8.** Repeat Problem **7** for the system chloroform–toluene.

**9.** Saturated equilibrium solutions of aniline and water at 100°C. contain 0.0148 and 0.628 mole fraction aniline. From these data calculate the van Laar constants, and compare with the values used in Fig. 3.4*c*. Calculate the values of activity coefficients for the system using the constants so determined, and compare with the observed data, Fig. 3.4*c*.

**10.** Derive equations for the Margules constants in terms of the critical solution composition for a system with an upper C.S.T.

**11.** The upper critical solution point for furfural–water lies at 122.7°C., 51 wt. per cent furfural. Calculate the van Laar and Margules constants from this datum, and compare with the values of activity coefficient at $x = 0$ and 1.0 obtained from vapor-liquid data, "Chemical Engineers' Handbook." Explain the results in terms of the applicability of the van Laar and Margules equations to this system.

**12.** Repeat Problem **11** for the more symmetrical system methanol–cyclohexane, which has a critical solution point at 49.1°C., 71 wt. per cent cyclohexane. Vapor-liquid data are available in the form of an azeotrope: 61 wt. per cent methanol, 54.2°C., 760 mm. Hg.

**13.** In the case of the following systems, predict the distribution of substance *C*, and the selectivity of solvent *B* for *C*, using the data indicated and the appropriate ternary integrated Gibbs-Duhem equation. Compare with the observed data reported in the indicated reference.

*a.* Water (*A*)–benzene (*B*)–acetone (*C*), 45°C.

Binary *B*–*C*: vapor-liquid data, 1 atm., Othmer [*Ind. Eng. Chem.* **35**, 614 (1943)].

Binary *A*–*C*: vapor-liquid data, 1 atm., Brunjes and Bogart [*Ind. Eng. Chem.* **35**, 255 (1943)].

Binary *A*–*B*: Mutual-solubility data, "International Critical Tables," Vol. III, p. 389.

Ternary-liquid equilibrium: Briggs and Comings [*Ind. Eng. Chem.* **35**, 411 (1943)].

*b.* Trichloroethylene (*A*)–water (*B*)–allyl alcohol (*C*), 25°C.

Binaries *A*–*C* and *B*–*C*: vapor-liquid data, 1 atm. [Hands and Norman, *Trans. Inst. Chem. Engrs.* (London) **23**, 76 (1945)].

Binary *A*–*B*: Mutual-solubility data, McGovern [*Ind. Eng. Chem.* **35**, 1230 (1943)].

Ternary-liquid equilibria: Hands and Norman, *loc. cit.*

*c.* Water (*A*)–1,1,2,2-tetrachloroethylene (*B*)–acetone (*C*) 25°C.

Ternary-liquid data: Othmer, White, and Treuger [*Ind. Eng. Chem.* **33**, 1240 (1941)], and Fritzsche and Stockton [*ibid.* **38**, 737 (1946)].

Obtain binary data from the best sources.

*d.* Aniline (*A*)–*n*-hexane (*B*)–methylcyclopentane (*C*), 25°C. Mutual solubilities for the *A*–*B* and *A*–*C* binaries, and liquid equilibria, Darwent and Winkler [*J. Phys. Chem.* **47**, 442 (1943)]. Boiling points of *A*–*B* mixtures in "International Critical Tables" (Vol. III, p. 314). Assume the *B*–*C* binary to be ideal.

*e.* Aniline (*A*)–*n*-heptane (*B*)–methylcyclohexane (*C*), 25°C.

Ternary liquid equilibria: Varteressian and Fenske [*Ind. Eng. Chem.* **29**, 270 (1937)]. Obtain binary data from best sources available.

**14.** In the case of the following systems, predict the distribution of substance *C* and selectivity of *B* using the data indicated, neglecting the effect of solubility of solvents *A* and *B*. Compare with the observed data.

*a.* Water (*A*)–ethyl acetate (*B*)–*tertiary* butanol (*C*), 20°C. For binaries *A*–*C* and *B*–*C*, use azeotrope data, "Chemical Engineers' Handbook." Liquid equilibria: Beech and Glasstone (*J. Chem. Soc.* **1938**, 67).

*b.* Water (*A*)–Carbon tetrachloride (*B*)–ethanol (*C*), 0°C. Constant temperature vapor-liquid data for *A*–*C*, azeotropic data for *B*–*C*, and ternary liquid data in "International Critical Tables" (Vol. III).

*c.* Water (*A*)–*n*-butanol (*B*)–ethanol (*C*), 20°C.

Binary *A*–*C*: constant temperature vapor-liquid data, "International Critical Tables" (Vol. III). Binary *B*–*C*: vapor-liquid data, Brunjes and Bogart [*Ind. Eng. Chem.* **35**, 255 (1943)]. Ternary-liquid data, Drouillon [*J. chim. phys.* **22**, 149 (1925)].

*d.* Water (*A*)–monochlorbenzene (*B*)–acetone (*C*), 25°C.

Binary *B*–*C*: vapor-liquid data, Othmer [*Ind. Eng. Chem.* **35**, 616 (1943)]. Binary *A*–*C*: vapor-liquid data, Brunjes and Bogart [*Ind. Eng. Chem.* **35**, 255 (1943)]. Ternary-liquid data: Othmer, White, and Treuger [*Ind. Eng. Chem.* **33**, 1240 (1941)].

**15.** In the case of the following systems, predict the distribution of substance *C* by the best means available, and compare with the observed data reported in the accompanying reference.

*a.* Water (*A*)–trichloroethylene (*B*)–ethanol (*C*), 25°C. Colburn and Phillips [*Trans. Am. Inst. Chem. Engrs.* **40**, 333 (1944)].

*b.* Water (*A*)–cyclohexane (*B*)–ethanol (*C*), 25°C. Vold and Washburn [*J. Am. Chem. Soc.* **54**, 4217 (1932)].

*c.* Benzene (*A*)–glycerol (*B*)–ethanol (*C*), 25°C. McDonald [*J. Am. Chem. Soc.* **62**, 3183 (1940)].

*d.* Water (*A*)–xylene (*B*)–acetone (*C*), 25°C. Othmer, White, and Treuger [*Ind. Eng. Chem.* **33**, 1240 (1939)].

**16.** On the basis of the hydrogen-bonding classification, specify a solvent which will be selective for the organic substance in the following mixtures. Substantiate the choice by calculating selectivities from observed ternary data.

*a.* Water–acetaldehyde.

*b.* Water–ethanol.

**17.** On the basis of C.S.T. data, predict the selectivity of *B* for *C* in the following systems, and compare with observed data.

*a.* Aniline (*A*)–water (*B*)–phenol (*C*).

*b.* Water (*A*)–ethyl acetate (*B*)–*n*-butanol (*C*).

*c.* Ethyl acetate (*A*)–water (*B*)–furfural (*C*).

## Chapter 4

**1.** On the basis of the considerations discussed in this chapter, determine the relative desirability of the following solvents for selectively extracting acetone from dilute water solutions at ordinary temperatures.

*a.* Chloroform

*b.* Monochlorobenzene
*c.* 1,1,2-Trichloroethane
*d.* Benzene
*e.* Methyl isobutyl ketone
*f.* Xylene

**2.** Repeat Problem **1**, using the following solvents for separating ethanol from water solutions:

*a.* Carbon tetrachloride
*b.* Chloroform
*c.* *n*-Butanol
*d.* *n*-Amyl alcohol
*e.* Benzene
*f.* Cyclohexane

## Chapter 5

**1.** Estimate the following diffusivities and compare with the observed data tabulated in the "International Critical Table" (Vol. V).

*a.* *n*-Butanol in dilute aqueous solution, 15°C.
*b.* Glycerol in dilute aqueous solution, 10, 15, and 20°C.
*c.* Furfural in dilute methanol solution, 15°C.
*d.* Bromoform in dilute ethanol solution, 20°C.
*e.* Propanol in dilute benzene solution, 15°C.
*f.* Acetone in dilute bromoform solution, 20°C.
*g.* Nitric acid in dilute aqueous solution, 20°C.
*h.* Potassium sulfate in dilute aqueous solution, 20°C.

**2.** The diffusivity of 1,1,2,2-tetrachloroethane in 1,1,2,2-tetrabromoethane at very dilute concentrations is $0.45 \times 10^{-5}$ sq. cm./sec. at 10°C. With the help of viscosity or latent heat of vaporization data, predict the diffusivity at 25, 35, and 50°C. Compare with observed results as listed in the "International Critical Tables" (Vol. V).

**3.** The diffusivity of sodium chloride in water at 5.0°C. and a concentration of 0.05 gm. equivalents/liter is $0.89 \times 10^{-5}$ sq. cm./sec. Predict the diffusivity at 10, 15, 20, 25, and 30°C. at this concentration, and compare with observed results ("International Critical Tables," Vol. V).

**4.** Predict the diffusivity of sodium hydroxide in water at 15°C. as a function of concentrations up to 2 normal, and compare with observed results ("International Critical Tables," Vol. V).

**5.** A small drop of benzene initially containing ethanol at a uniform concentration of 5% by weight is allowed to rise through pure water at a temperature of 20°C. The diameter of the drop is 1.0 mm., and it may be assumed to be spherical. On the assumption that the liquid within the drop is stagnant and that the water offers negligible resistance to the diffusion, calculate the theoretical fractional extraction of ethanol after a time of contact between the drop and the water of 20 sec.

## Chapter 6

**1.** One hundred pounds of a solution containing 20% acetic acid, 80% water are to be extracted with methyl isobutyl ketone as solvent, at 25°C. Equilibrium data of Sherwood, Evans, and Longcor are available in [*Ind. Eng. Chem.* **31**, 1144 (1939)].

*a.* For single-contact extraction,
   1. What are the minimum and maximum amounts of solvent?
   2. What is the maximum concentration of acetic acid (solvent-free basis) attainable in the extract, and what amount of solvent should be used to obtain it?

3. Plot a curve of the percentage extraction of acetic acid from the feed solution and the concentration of acid in the extract against amount of solvent used, within the limits established above.

*b.* For cocurrent multiple contact, and a saturated raffinate containing 1% acetic acid, plot a curve of amount of solvent required against number of stages, assuming equal distribution of solvent to the stages.

**2.** Compare the effectiveness of an extraction with favorable and unfavorable distribution coefficients by repeating the calculations of Illustrations 3 and 5, substituting the system water (*A*)-*n*-heptane (*B*)-acetone (*C*), equilibrium data for which are available in *Ind. Eng. Chem.* **41**, 1761 (1949).

**3.** The distribution of 1,4-dioxane (*C*) between benzene (*B*) and water (*A*) at 25°C. [Berndt and Lynch, *J. Am. Chem. Soc.* **66**, 282 (1944)] is

| $X_{CA}$ | 0.051 | 0.189 | 0.252 |
|---|---|---|---|
| $X_{CB}$ | 0.052 | 0.225 | 0.32 |

Below 25% dioxane, the benzene and water are practically immiscible. One hundred pounds per hour of a 20% solution of dioxane in water are to be extracted with benzene, to remove 98% of the dioxane. For countercurrent multiple contact,

*a.* Calculate the minimum amount of solvent required.

*b.* Calculate the number of stages required for 1.2 times the minimum solvent.

*c.* Calculate the amount of solvent required to carry out the extraction in five stages. For cocurrent multiple contact,

*d.* Calculate the amount of solvent required to carry out the extraction in five stages, with equal subdivision of solvent among the stages.

**4.** Derive the necessary equations and explain their use for the solution of problems involving differential extraction on the Janecke type of coordinates.

**5.** One hundred pounds per hour of a solution containing 50% pyridine (*C*), 50% water (*A*) are to be reduced to a saturated raffinate containing 1% pyridine with benzene as solvent in a countercurrent multiple contact system. Equilibrium data are available at 25°C. (Woodman, *J. Chem. Soc.* **1925**, 2461). Calculate

*a.* The minimum solvent rate.

*b.* The number of ideal stages for 1.5 times the minimum solvent rate and the weights and concentrations of all extracts and raffinates.

**6.** One hundred pounds per hour of a solution containing 35% isopropanol, 65% water are to be reduced to 2% isopropanol with toluene as a solvent. Equilibrium data at 25°C. are available [Washburn and Beguin, *J. Am. Chem. Soc.* **62**, 579 (1940)].

*a.* Determine the number of stages for a countercurrent multiple-contact system with twice the minimum amount of solvent. Calculate the weight and concentration of final extract.

*b.* Determine the number of stages for a cocurrent multiple-contact system at the same total solvent as used in *a*, equally subdivided among the stages. Determine the weight and concentration of the composite extract.

*c.* Determine the amount of solvent, weight, and composition of composite extract, for differential extraction.

*d.* Determine the number of stages, weight, and composition of the extract, and solvent rate required for a countercurrent extraction with raffinate reflux only, at twice the minimum reflux ratio. Reflux and product streams are to be saturated.

**7.** A feed of 200 lb./hr. containing 50% acetone (*C*), 50% water (*B*), is to be extracted in a countercurrent multiple-contact plant with 50 lb./hr. of 1,1,2-trichloroethane (*B*) as solvent. The final saturated raffinate is to contain 2% acetone, and an intermediate saturated raffinate containing as nearly 25% acetone as possible is to be withdrawn from

the appropriate stage at the rate of 100 lb./hr. Calculate the number of theoretical stages required and the stage from which the intermediate raffinate is to be withdrawn.

**8.** A mixture containing 10% oleic acid (*C*), 90% cottonseed oil (*A*) is to be separated into a raffinate containing 0.1% oleic acid and an extract containing 95% acid, with liquid propane as the solvent in a countercurrent extraction with reflux, at 98.5°C. Equilibrium data of Hixson and Bockelmann will be found in *Trans. Am. Inst. Chem. Engrs.* **38,** 923 (1942). Feed and final products are to be solvent-free, reflux streams saturated with solvent. Per 100 lb. of feed, calculate the number of theoretical stages, position of feed stage, and weights and concentrations of all streams for an extract reflux ratio of 1.5 times the minimum.

**9.** A mixture of 50% oleic acid, 50% abietic acid is to be separated with the help of liquid propane as solvent in a countercurrent extraction with reflux. Equilibrium data are available at 81, 91, and 96.7°C. (Hixson and Hixson, *Trans. Am. Inst. Chem. Engrs.* **37,** 927 (1941).

*a.* What are the maximum purities possible for extract and raffinate at the three different temperatures?

*b.* For temperatures of 91 and 96.7°C., compare the solvent requirements and number of stages for products containing 95% and 5% oleic acid at a 3:1 extract reflux ratio, per 100 lb. of feed. Feed and final products are to be solvent-free, reflux saturated with solvent.

**10.** Equilibrium data for the Type 2 system *n*-heptane (*A*)–aniline (*B*)–methylcyclohexane (*C*) at 25°C. (23) show $\beta$ to be substantially constant, 1.90. Using this value, calculate the minimum number of enriching and stripping stages, and the minimum external raffinate and extract reflux ratios, for the separation of a mixture containing 50% *A*, 50% *C*, with *B* as solvent, into products containing 2% *A* and 98% *A*, all on a solvent-free basis. Feed, products, and refluxes are to be saturated with solvent.

## Chapter 7

**1.** Calculate the compositions of raffinate and extract for a single-contact, mixed-solvent extraction of 100 lb. of a solution containing 62.8% acetone (*A*), 37.2% chloroform (*B*), with 71.25 lb. of a mixed-solvent containing 61.5% water (*C*), 38.5% acetic acid (*D*). Compare the results with the experimental data of Brancker, Hunter, and Nash [*J. Phys. Chem.* **44,** 683 (1940)], who show the equilibrium concentrations for such an extraction to be 24.4% *A*, 6.9% *B*, 44.5% *C*, 24.2% *D*; 44.3% *A*, 30.8% *B*, 13.7% *C*, 11.2% *D*.

**2.** Calculate the compositions of solvent-free products for a single-contact double-solvent extraction of 100 lb. of a solution containing 69.9% acetone (*B*), 30.1% acetic acid (*C*), with the double-solvent 106.3 lb. chloroform (*A*)–117.7 lb. water (*D*). Compare the results with the experimental data of Brancker, Hunter, and Nash, who show the results to be 42.25% *B*, 57.75% *C*; 90.55% *B*, 9.45% *C*.

**3.** The distribution coefficients of formic and acetic acids between mutually saturated solutions of ethyl ether and water at 18°C. are ("International Critical Tables," Vol. III, pp. 422, 425):

| Concn. in ether, gm. moles/l. | | 0.02 | 0.05 | 0.10 | 0.20 | 0.40 | 0.60 |
|---|---|---|---|---|---|---|---|
| Concn. in water | m formic | 2.68 | 2.61 | 2.54 | 2.46 | 2.34 | 2.24 |
| Concn. in ether | m acetic | 2.07 | 2.03 | 1.93 | 1.89 | 1.77 | 1.68 |

A mixture consisting of 1 gm. mole each of formic and acetic acids is distributed simultaneously between 1 liter each of the mutually saturated solvents.

*a.* Calculate the separation obtained, assuming the distribution coefficients are completely independent of each other.

*b.* Recalculate the separation, taking into consideration the effect on the distribution of the common hydrogen ion on the aqueous phase. Assume no dissociation in the ether layer. The dissociation constants are $1.76 \times 10^{-4}$ and $1.75 \times 10^{-5}$ for formic and acetic acids, respectively.

**4.** A mixture of 40% *o*(*B*)–nitroaniline, 60% *m*(*C*)–nitroaniline is to be separated using the double-solvent benzene (*A*)–water (*D*) in a countercurrent continuous multistage system. Distribution coefficients at 25°C. for dilute solutions are $\mathbf{m}_B = 64.0$, $\mathbf{m}_C = 25.0$ ("International Critical Tables," Vol. III, p. 428), and may be assumed constant and independent.

*a.* Calculate the solvent ratio, number of stages, and solvent-free analysis of the products for a symmetrical separation with 90% recovery of *B* in the benzene solution, with $n' = n + 1$.

*b.* Compare the degree of separation obtained in *a* with those obtained with the same solvent ratio and total number of stages, with different ratios of $n' : (n + 1)$.

**5.** A mixture of 30% *o*-nitroaniline, 30% *m*-, 40% *p*-nitroaniline is to be fractionated with the double-solvent benzene-water. Distribution coefficients for dilute solutions are 64.0, 25.0, and 9.3, resp.

*a.* For a symmetrical separation of the ortho and meta isomers, calculate the solvent-free analysis of the composited benzene and water solutions from a batch extraction with 16 stages, arranged as in Fig. 7.13.

*b.* For a symmetrical separation of the ortho and meta isomers, 90% recovery of the ortho, and for $n' = n + 1$, calculate the number of stages and solvent-free analysis of the products for a continuous countercurrent extraction.

**6.** The distribution coefficients for *p*(*B*)-methoxyphenol and *o*(*C*)-methoxyphenol between the double-solvent 60% aqueous ethanol (*A*)-hydrocarbon (50% gasoline, 50% benzene) (*D*) are $\mathbf{m}_B = 2.4$, $\mathbf{m}_C = 1.6$ for 20 gm. solute distributed between 100 cu. cm. of each solvent (Van Dijck and Schaafsma, U.S. Pat. 2,245,945). Assume the distribution coefficients are constant. It is desired to obtain a 90% recovery of *B*, at 98% purity, from a mixture containing 50% each of *B* and *C*.

*a.* For a batch process following the diamond arrangement of Fig. 7.13, plot a curve of solvent ratio required vs. number of stages.

*b.* Repeat for a continuous countercurrent process.

**7.** Propane-1,1-dicarbonic acid (*B*) and propane-1,3-dicarbonic acid (*C*) distribute between ethyl acetate (*A*) and water (*D*) with $\mathbf{m}_B = 2.48$, $\mathbf{m}_C = 0.75$ (Van Dijck and Schaafsma, *loc. cit.*).

*a.* Calculate the number of stages required, and the position of the feed stage for separating 100 lb./hr. of a mixture of 50% each of the acids into two products, each 90% pure, with 200 lb./hr. of each solvent.

*b.* What purity of products would result for a system of eight stages, with the feed entering the third stage from the end where the ethyl acetate is introduced?

## Chapter 8

**1.** Calculate the height of a tower packed with 10 mm. Raschig rings required to reduce the acetaldehyde concentration of vinyl acetate from 6 to 0.01%, using water as solvent. A feed rate of 25 cu. ft./hr. sq. ft. is required, and a water rate of 1.5 times the minimum will be used. Equilibrium data and mass-transfer rates are given by Pratt and Glover [*Trans. Inst. Chem. Engrs.* (London) **24**, 54 (1946)]. See Chap. 10.

**2.** Calculate the concentration of acetic acid in the final raffinate that can be expected for the extraction of Illustration 2, if a tower of 20 ft. height is used, all other quantities remaining unchanged.

**3.** Trimble and Dunlop [*Ind. Eng. Chem., Anal. Ed.* **12,** 721 (1940)], report equilibrium data for the system ethyl acetate–water–furfural. They state further that when an aqueous solution of furfural containing 7% furfural was extracted countercurrently by an equal weight of ester in an 8-ft. packed tower, 99.9% of the furfural was removed. Compute the values of $HTU_{OR}$, $K_Ra$, and H.E.T.S.

## Chapter 11

**1.** Examine the effect of separately varying (*a*) the caustic-circulation rate from 10 to 20% of the gasoline volume, and (*b*) the stripping-steam rate from 10 to 20 lb./bbl. gasoline, on the mercaptan removal from the cracked gasoline of Table 11.1. Use 30% NaOH containing 20% "organic acids."

**2.** Explain the selectivity of liquid sulfur dioxide for aromatic with respect to paraffin hydrocarbons in terms of internal pressure. Use toluene and *n*-heptane as examples.

**3.** The following are extraction data for mixtures of Chlorex with the Winkler County (Texas) distillate of Fig. 11 9 at 80°F. [Skogan and Rogers, *Oil and Gas J.* **45,** No. 13, 70 (1947)].

| No. of stages | Vol. solvent / Vol. oil | Raffinate | | Extract | |
|---|---|---|---|---|---|
| | | V.G.C. (solvent-free) | Per cent solvent | V.G.C. (solvent-free) | Per cent solvent |
| 1 | 1.88 | 0 837 | 18.8 | 0.941 | 82.3 |
| 1 | 2.82 | 0.830 | 17.4 | 0.936 | 86.1 |
| 1 | 3.78 | 0.825 | 16.2 | 0.932 | 88.3 |
| 1 | 4.73 | | 15.8 | 0.927 | 89.8 |
| 1 | 1 | 0.850 | 21.0 | 0.945 | 75.0 |
| 1 | 5 | 0.818 | | | 89.7 |
| 1 | 9 | 0.808 | 18.5 | 0.907 | 93.3 |
| 1 | 15 | 0.801 | 24.6 | 0.895 | 94.8 |
| 1 | 20 | 0.797 | 25.2 | 0.888 | 95.8 |
| 2 | 1.90 | 0.823 | | 0.939 | |
| 3 | 1.92 | 0.815 | | 0.937 | |

The feedstock has a V.G.C. = 0.876. Calculate the number of stages and yield as a function of solvent/oil ratio required to produce a raffinate V.G.C. = 0.805.

**4.** Griswold, Chu, and Winsauer [*Ind. Eng. Chem.* **41,** 2352 (1949)] provide very complete data on the liquid-liquid and vapor-liquid equilibria in the system ethanol–ethyl acetate–water. Design a plant and solvent-recovery system for the recovery of 99.8% ethanol from 50,000 gal./day of a 5% solution in water, using ethyl acetate as extracting solvent. Solvent concentration in the raffinate phase is to be no greater than 0.001%.

# NAME INDEX


A

Albright, J. C., 374
Aldridge, B. B., 281
Allen, H. D., 301, 329, 382, 383
Allerton, J., 307, 309, 311, 312, 335, 338, 339
Alvers, H. A., 358
Andres, D., 45
Anglo-Persian Oil Company, Ltd., 283
Appel, F. J., 307, 309, 321–323, 333, 334
Archibald, R. C., 221, 301
Arnett, E. F., 45
Arnold, G. B., 350
Arnold, J. H., 98, 100, 102–105, 110
Arrowsmith, C. J., 301, 329, 382, 383
Asbury, W. C., 284, 350
Asquith, J. P., 288
Asselin, G. F., 238, 286, 393
Atkins, G. T., 300
Ayres, E. E., 280

B

Bachman, I., 26, 28, 29, 31
Baehr, H., 351
Bahlke, W. A., 368
Bailey, A. E., 376, 378
Ballard, J. H., 305–308
Bancroft, W. D., 27
Bannister, W. J., 389
Bartels, C. R., 220, 228, 236, 342
Bartels, W. E., 269
Beach, R. M., 381
Beare, W. G., 44
Beaufait, L. J., 393
Beckmann, R. B., 334, 336
Beech, D. G., 14, 67–69, 71, 74, 75, 87, 88, 90
Benedict, M., 43, 53, 62
Benenati, R. F., 61
Bennett, H. T., 368
Bent, R. D., 352, 359
Berg, C., 53, 332, 364
Berg, L., 80, 81
Bergelin, O., 315
Bergman, D. J., 271, 273, 277
Berkman, S., 275, 283
Berndt, R. J., 28–30
Bertsch, H., 389
Bibbins, F. E., 389
Bikerman, J. J., 275, 280
Birchel, J. A., 373
Bissell, E. S., 258–261
Blanding, F. H., 292, 303–305
Bliss, H., 314, 315, 318, 322, 323, 325–327, 342
Bock, R., 393
Bockelman, J. B., 18, 77, 78, 89, 90, 337, 376, 377
Bogart, M. J. P., 74
Bogash, R., 376, 377
Bogin, C. D., 21
Bohm, E., 273
Bond, W. N., 274
Border, L. E., 281, 294, 358, 359
Borrmann, C. H., 293
Brancker, A. V., 25, 26, 32, 33, 211
Brandt, R. L., 347
Braun, T. B., 33, 350
Breckenfeld, R. R., 305
Brewster, T. J., 388
Briggs, S. W., 15, 83, 315, 334, 335
Brinsmade, D. S., 314, 315
Bristow, W. A., 386
Britton, E. C., 388
Broderson, H. J., 269
Brown, A. B., 368
Brown, C. L., 284, 350
Brown, G. G., 174, 315
Brown, J. W., 300
Brown, K. M., 359
Brown, T. F., 31, 68, 70, 78, 90, 200
Browning, F. M., 308, 324, 325
Bruins, H. R., 101
Brunjes, A. S., 74
Bryant, G. R., 369
Buckler, C. C., 368
Burkhard, M. J., 271, 277

Burtis, T. A., 278, 281
Bush, M. T., 219, 222, 227

C

Cady, L. C., 101
Callahan, J. R., 389
Campbell, A. N., 5
Campbell, J. A., 25
Carlson, G. J., 262
Carlson, H. C., 47, 48, 50–53, 57, 59, 61
Carvlin, G. M., 351
Cattaneo, G., 293
Cauley, S. P., 352, 355–358
Chalybaeus, W., 393
Chang, K. C., 98, 99
Chase, W. O., 273
Chertow, B., 275, 280
Chu, J. C., 337
Clotworthy, H. R. S., 388
Coahran, J. M., 296
Coats, J. B., 361
Coghlan, C. A., 350
Cohen, E., 101
Colburn, A. P., 43, 47, 48, 50–54, 57, 59–61, 64, 245–247, 265, 298, 303, 305, 309, 310, 312, 319, 329–331, 338–340
Comings, E. W., 15, 83, 238, 286, 315, 334, 335, 393
Conway, J. B., 316, 317
Cornell, P. W., 350
Cornish, R. E., 221, 301
Cottrell, O. R., 373
Coulthurst, L. J., 351
Cox, E. R., 26
Craig, L. C., 219, 221, 222
Crary, R. W., 354, 358
Crawford, R. M., 385
Cuckney, M., 283, 284, 386

D

Daley, J. F., 27–30, 92, 93, 144, 153, 162, 169
Darwent, D. DeB., 18, 31, 78, 190
Davis, G. H. B., 361
Davis, H. R., 294
Dean, E. W., 361
Dean, M. R., 363, 372
Defize, J. C. L., 347, 348, 373
Densen, P. M., 219, 222, 227
Dickey, S. W., 348
Dickinson, J. T., 369
Diggs, S. H., 368
Diworky, F. F., 368
Dodge, B. F., 40, 41, 47, 48
Dons, E. M., 295
Drew, D. A., 77, 78, 376, 377
Drouillon, F., 28–30
Dryden, C. E., 31
Dryden, H. L., 116, 117
Duffey, H. R., 298, 310, 312, 338–340
Dumoulin, F. E., 311, 312, 338, 339
Dunstan, A. E., 360, 363, 365, 367–369, 371
Duriron Co., Inc., 269, 271

E

Eastman, D., 350
Edeleanu, G. m. b. H., 373
Edeleanu, L., 277, 346, 347
Edwards, W. K., 277
Egloff, G., 275, 283
Eichwald, E., 369
Einstein, A., 106, 107
Elgin, J. C., 77, 246, 251, 292, 293, 295, 303–305, 307–309, 321–325, 333, 334, 383
Evans, H. M., 221, 301
Evans, J. E., 253, 254, 309, 316, 317, 325, 327, 330, 332, 334, 342
Evans, T. W., 143, 151, 153, 156, 172, 388
Everett, H. J., 258–261
Evers, N., 389
Ewell, R. H., 80, 81
Eyring, H., 104–106, 108

F

Fallah, R., 314, 315
Fenske, M. R., 16, 31, 70, 78, 89, 90, 129, 130, 143, 159, 165, 177, 179, 183, 199, 337
Ferguson, J. B., 44
Ferris, S. W., 367, 369
Fick, A., 97, 98, 101
Field, H. W., 359
Findlay, A., 5
Fischer, W., 393
Folsom, R. G., 271
Foust, H. C., 303, 304
Fowle, M. J., 350
Francis, A. W., 77, 347, 361, 362
Franke, N. W., 337
Freeman, S. E., 379, 381, 384
Friedland, D., 64
Fritzsche, R. H., 20, 34

Fulton, D., 374
Funk, J. E., 350
Furnas, C. C., 57, 66
Fuqua, F. D., 340

G

Gard, E. W., 373
Gard, S. W., 281
Garland, F. M., 45
Garwin, L., 219, 393
Gasmeier-Kres, E., 386
Geankoplis, C. J., 318, 319, 326, 393
Georgian, C. C., 380, 381
Gibbs, J. W., 5, 12
Gibby, C. W., 20
Gilliland, E. R., 87, 88
Glasstone, S., 5, 14, 67–69, 71, 74, 75, 87, 88, 90, 104, 114
Glover, S. T., 309, 335, 336
Gloyer, S. W., 330, 333, 380, 381, 384
Gollmar, H. A., 273, 283, 284, 386
Golumbic, C., 219, 222
Goodman, C., 392
Gordon, A. R., 114
Gordon, J. D., 351
Gordon, J. J., 302
Goss, W. H., 381
Grad, M., 297, 308, 309, 337
Gress, K., 277
Griffin, C. W., 153
Griswold, J., 45
Groggins, P. H., 389
Gross, H. H., 348, 369
Guinot, H., 388

H

Hale, W. J., 388
Hall, F. C., 347
Hamer, W. J., 49, 51, 59
Hamilton, G. B., 348, 369
Hampton, A. C., 270
Hancock, R. S., 383
Hand, D. B., 21, 23, 27, 30, 31, 33, 72–74, 83
Happel, J., 350, 352, 354-358
Harned, H. S., 114
Harrington, P. J., 297
Harrison, J. M., 80, 81
Hatch, B. F., 293, 386
Hayes, J. G., 272, 281
Haylett, R. C., 372, 373
Hays, L. A., 272, 281
Hayworth, C. B., 16, 93, 304, 326
Heath, B. L., 368
Hendrixson, W. S., 25
Herschel, W. A., 275
Hesse, H. C., 258–261
Hibshman, H. J., 286, 361
Higbie, L., 118
Hightower, J. V., 350
Hildebrand, J. H., 60, 72, 81
Hildebrandt, G., 389
Hill, A. E., 16, 21
Hill, J. B., 361
Hixson, A. N., 77, 78, 219, 318, 319, 326, 376, 377, 384, 393
Hixson, A. W., 18, 77, 78, 89, 90, 265, 266, 337, 376–378, 381, 383, 384
Hnizda, V., 87, 88, 90
Hoening, P., 293, 340, 386
Holley, A. E., 283, 286
Holm, M. M., 354, 358
Hooker, T., 262
Horsley, L. H., 56, 91
Hou, H. L., 337
Hougen, O. A., 41, 43, 47, 53, 82
Houghton, W. F., 369
Huffman, E H., 393
Hufnagel, J., 312, 340
Huggett, J. L., 371
Humphrey, I. W., 298, 383
Hunter, C. M., 309, 327, 332, 334, 391
Hunter, T. G., 25, 26, 32, 33, 68, 70, 78, 132, 156, 158, 172, 176, 196, 200, 204, 207, 211, 222, 250, 262, 269, 273, 275, 297, 314, 315, 340, 363

I

Irvine, J. W., 392
Ittner, M. H., 295, 296, 301, 382

J

Janecke, E., 22
Jantzen, E., 176, 222, 301
Jenkins, J. D., 381
Jodeck, P., 277, 293
Johnson, C. A., 43, 53, 62
Johnson, H. F., 318, 322, 323, 325–327, 342
Johnstone, H. F., 381
Jones, C. A., 54
Jones, H. E., 293, 384, 385

K

Kain, W., 373
Kaiser, H. E., 383

Kaiser, H. R., 286, 342, 387
Kalichevsky, V. A., 347, 351, 360, 363–365, 367, 368, 372
Kalinske, A. A., 116, 117
Karr, A. E., 301, 311, 340–342
Keary, W. V., 388
Keith, P. C., 372, 373
Kellogg, M. W., Co., 299
Kelly, H. S., 352, 355–358
Kemp, L. C., 348, 369
Kenyon, R. L., 380, 381
Kincaid, J. F., 104
Kirkbride, C. G., 278, 281
Kister, A. T., 51
Klavehn, W., 389
Kleiman, G , 220, 228, 236, 342
Kleinschmidt, R. V., 281
Kleinsmith, A. W., 379
Kline, W. A., 301, 329, 382, 383
Knight, O. S., 334
Knox, W. T., 286
Koch Engineering Co., Inc., 300
Koch, F. C., 300
Koffolt, J. H., 307, 309, 311, 312, 323, 333, 335, 339, 340
Kraybill, H. R., 379
Krchma, I. J., 389
Krebs, O., 386
Kremser, A., 174
Kroll, A. E., 259
Kurtz, S. S., 363
Kwauk, M., 304

L

La Croix, H. N., 351
Laddha, G. S., 13, 25, 309, 319–321, 329–331
Laidler, K. J., 104
Laird, W. G., 298
Lascary, L., 381
Lawrence, E. A., 301, 329, 382, 383
Leaver, C., 272
Lee, J. A., 369, 374
Leighton, W. B., 57, 66
Levy, D. J., 337
Lewis, G. N., 40, 115
Lewis, W. K., 87, 88, 98, 99, 118, 121
Licht, W., 316, 317
Linnman, W., 277
Lister, D. A., 298, 383
Liu, T. H., 101
Livingstone, M. J., 369
Lochte, H. L., 301, 337
Lockhart, F. J., 315
Longcor, J. V. A., 253, 254, 309, 316, 317, 325, 327, 330, 332, 334, 342
Longtin, B., 125, 129, 160
Lowry, H. H., 386
Lynch, C. C., 28–30
Lyons, E. J., 259, 260

M

McAdams, W. H., 87, 88
McAteer, J. H., 286
McBain, J. W., 20, 101
McCarty, B Y., 369
McClain, H. K., 381
McCormack, R., 393
McCullough, J. H., 352, 359
McDonald, H. J., 21
McElvain, S. M., 80
Mack, D. E., 259
McKee, R. H., 219, 393
McKeen, J. E., 387
McKinnis, A. C., 53
MacKusick, B. L., 358
MacLean, G., 270
Macmullin, R. B., 265, 266
McPherson, R. H., 14
McVicar, G. A., 44
Mahoney, L. H., 262
Major, C. J., 310
Maloney, J. O., 185
Manders, M., 332, 364
Manley, R. E., 369
Mann, C. A., 262
Mann, M. D., 298
Mapes, D. B., 295
Marsel, C. J., 301, 329, 382, 383
Martin, A. J. P., 221, 286
Mason, C. F., 352, 359
Mauro, O. G., 295
Maxwell, J. C., 98
Meissner, H. P., 20, 275, 280, 309, 327, 332, 334, 391
Mensing, C. E., 271
Mertes, T. S., 43, 53
Messing, R. F., 388
Meyer, P., 353, 365
Mighton, H., 219, 222
Miller, F., 16
Miller, M. B., Jr., 270, 271, 285, 374
Miller, Max B., Company, Inc., 270, 278, 374, 375

Miller, R., 378, 381, 383, 384
Miller, S. A., 262
Miller, W. L., 14
Mills, V., 381, 382
Mitchell, J. E., 389
Moore, E. B., 379
Moore, W. C., 275
Morello, V. S., 283, 285, 293, 296, 302, 334, 336, 342
Moriarty, F. C., 358, 359
Morrell, C. E., 284, 350
Morrell, J. C., 271, 273, 277
Morris, R. C., 379
Morrow, G. M., 309, 327, 332, 334, 391
Mott, O. E., 283, 286
Moulton, R. W., 311, 312, 338, 339
Moy, J. A. E., 348, 349
Multer, H. J., 281
Murdock, D. G., 283, 284, 386
Murphree, E. V., 117
Murphy, E. A., 221, 301
Murphy, J. F., 382
Myers, W. A., 369

N

Nandi, S. K., 318
Nash, A. W., 25, 26, 32, 33, 132, 156, 158, 172, 176, 196, 211, 222, 250, 269, 275, 297, 314, 315, 340, 363
Nelson, W. L., 347, 362
Nernst, W., 24, 26, 112
New England Tank and Tower Co., 273
Newman, A. B., 101
Newman, M., 16, 93
Newton, D. A., 274
Ney, W. O., 301, 337
Nord, M., 153

O

Olive, T. R., 388
Olney, R. B., 262
Olsen, A. L., 28–30, 165
Oriel, J. S., 349
Othmer, D. F., 21, 26, 29, 31, 61, 138, 139, 155, 248, 249, 388–391
Owen, B. O., 114

P

Packie, W. J., 284, 350
Page, J. M., 368
Palit, S. R., 20
Paltz, W. J., 284, 350
Partington, J. R., 113
Passino, H. J., 378, 379, 384
Paulsen, I. A., 24
Peake, A. W., 271
Perry, J. H., 82, 153, 293, 310
Peterson, J. A., 393
Pfeiffer, K., 277
Pien, C. L., 116, 117
Pierotti, G. J., 379
Piret, E. L., 305–308
Podbielniak, Inc., 302
Podbielniak, W., 302
Poettmann, F. H., 363, 372
Poffenberger, N., 283, 285, 293, 296, 302, 342
Porter, C. A., 350
Post, O., 221
Powell, R. E., 104, 108
Pratt, H. R. C., 309, 335, 336
Prentiss, S. S., 51
Pyle, C., 298, 310, 312, 338–340

Q

Quebedeaux, W. A., 301

R

Ragatz, E. G., 373
Randall, M., 40, 115, 125, 129, 160
Raschig, F., 293
Ratcliffe, R. L., 389, 391
Raymond, C. L., 46
Redlich, O., 51
Reed, C. E., 12
Reeves, E. J., 364
Regna, P. P., 386
Robertson, D. W., 354, 358
Robinson, E. A., 381
Rogers, M. C., 300, 362–367
Rosendahl, F., 386
Rosenthal, H., 304, 328
Roseveare, W. E., 104, 108
Ross, A. A., 389
Row, S. B., 307, 309, 311, 312, 323, 333, 335, 339, 340
Rowley, D., 387
Rubin, L. C., 43, 53, 62
Rushton, J. H., 258–261, 265, 275, 337, 353
Ruthruff, R. R., 35, 379, 380

S

Saal, R. N. J., 24, 125, 176, 196, 373
Sachanen, A. N., 351, 360
Scatchard, G., 46, 49, 51, 52, 59, 60, 64, 81
Schaafsma, A., 219, 237
Scheibel, E. G., 64, 220, 228, 231, 232, 248, 249, 301, 311, 312, 340–342
Schmid, A., 388
Schoenborn, E. M., 54, 59–61
Schreinemakers, F. A. H., 15, 16, 19, 20
Schubert, A. E., 185
Schutte, A. H., 350
Schutze, H. G., 301
Selas Corporation of America, 282
Sharefkin, J. G., 153
Sheldon, H. W., 271
Sherwood, T. K., 12, 23, 98, 99, 116–118, 174, 175, 250, 253, 254, 300, 309, 316, 317, 325, 327, 330, 332, 334, 342
Shilling, D., 61
Siedell, A., 392, 393
Skogan, V. G., 362–367
Smith, A. S., 22, 33, 350
Smith, E. L., 387
Smith, J. C., 33, 211
Smith, J. M., 13, 25, 309, 319–321, 329–331
Smith, K., 77
Smith, M. I., 265, 266
Smoley, E. R., 374
Smyth, H. D., 392
Solomon, E., 43, 53, 62
Souders, M., 174
Soule, R. P., 277
Staaterman, H. G., 379
Stager, R. M., 379
Stagner, B. A., 347, 351, 360
Standard Oil Development Co., 298
Stearn, A. E., 104
Stefan, J., 98
Steiner, H., 387
Stiner, D. E., 371
Stockton, D. L., 20, 34
Stokes, C. A., 20, 309, 327, 332, 334, 391
Strang, L. C., 314, 315
Stratford, C. W., 273
Stratford Engineering Corp., 279
Stratford, R. K., 371
Strom, B. O., 307, 309, 311, 312, 335, 338, 339
Stuart, E. H., 389
Swan, D. O., 298
Switzer, R., 332, 364
Synge, R. L. M., 221, 286

T

Tarasenkov, D. N., 24
Taylor, C. C., 337
Taylor, G. I., 116
Taylor, H. S., 5, 104
Taylor, T. H. M., 387
Templeton, C. C., 393
Tetervsky, H., 77
Texaco Development Corp., 370
Thiele, E. W., 176, 196, 300
Thompson, F. E. A., 360, 363, 365
Thompson, R. F., 295
Thornton, E., 283
Tilghman, R. A., 382
Tiller, F. M., 173, 174
Timmermans, J., 19
Titus, E., 219, 222
Tobias, P. E., 21, 26, 29, 31, 155
Towle, W. L., 117
Treuger, E., 138, 139, 389–391
Treybal, R. E., 16, 27–31, 72, 74, 92, 93, 144, 153, 162, 169, 304, 307, 309–315, 326, 328, 335, 338, 339
Tupholme, C. H. S., 386
Tuttle, M. H., 374
Tyler, C. N., 346

U

Underwood, A. J. V., 152, 153

V

Valentine, K. S., 270
Van Dijck, W. J. D., 24, 125, 176, 196, 219, 237, 298, 349
Van Laar, J. J., 51
Varteressian, K. A., 16, 31, 70, 78, 89, 90, 129, 130, 143, 159, 165, 177, 179, 183, 199, 337
Vilbrandt, F. C., 393
Viswanathan, T. R., 318
Vold, R., 87, 88, 90
Vulcan Copper and Supply Co., 296

W

Walker, W. H., 87, 88
Walkey, J. E., 311, 312, 338, 339
Washburn, E. R., 28–30, 87, 88, 90, 165
Watson, H. E., 265

Watson, K. M., 41, 43, 47, 53, 82
Weber, L. D., 27–30, 92, 93, 144, 153, 162, 169
Weber, M., 265, 266
Weeks, R. L., 286
Wells, J. H., 386
Welsh, D. G., 309, 319, 329–331
White, E. R., 356, 358
White, R. E., 138, 139
Whitehall, S. M., 298
Whitman, W. G., 118, 121
Whitmore, F. C., 387
Wiegand, J. H., 211, 245
Wiegman, D. H., 386
Wilcock, D. F., 35, 379, 380
Wilhelm, R. H., 304
Wilke, C. R., 107–110, 112, 305
Williams, D. B., 368
Williams, E. C., 388
Williams, J. W., 101
Williamson, B., 222
Wilson, P. J., 386
Wilson, R. E., 372, 373
Winer, B., 382
Winkler, C. A., 18, 31, 78, 190
Withrow, J. R., 307, 309, 311, 312, 323, 333, 335, 339, 340
Woertz, B. B., 116, 117
Wohl, K., 49, 51, 52, 62-64
Wolfe, J. M., 153
Wood, H. S., 272, 281
Woodburn, H. M., 77
Work, L. T., 314, 315

Y

Yabroff, D. L., 353–356, 358
Yates, P. B., 265
York, Otto H., Co., Inc., 301
Young, H. W., 271

Z

Zawidzki, J. V., 45, 46
Zeigler, J. H., 302
Zimkin, E., 387

# SUBJECT INDEX


A

Abietic acid, 383
Absolute-rate theory, 104–112
Acetic acid recovery, 296, 297, 388
Activity, 41, 42, 44–47
  in diffusivity determination, 109–111
  in prediction of equilibrium, 65–72
Activity coefficient, 42–76
  calculation of, from mutual solubility, 59–62
    from vapor-liquid data, 56–58
  in diffusivity determination, 109–111, 114–115
Adsorption, 2, 92, 387
Agitation, effectiveness of, 262, 263
  power for, 261, 262
Alkacid process, 351
Ammonia, liquid, 392
Aniline, recovery of, 389
Aniline point, 77, 362
Association, 25, 26
Atomic-energy processes, 392
Azeotropes, 44–46, 56

B

Baffle towers, 295–297
  extraction rates of, 337
  flow capacity of, 309
Baffles, 258, 259, 273, 277, 278
Bubble-cap towers, 300
Butadiene, 285, 300

C

Caffeine extraction, 297
Centrifugal extractor (*see* Podbielniak extractor)
Chemical reaction, 94, 315
Chlorex process, 300, 365–369
Coalescers, 281, 282, 298, 301
Coordinates, Janecke, 22, 128
  rectangular, 22, 128, 129
  tetrahedral, 31–34, 204–217
  triangular, 12, 127, 128, 362
Corrosion, 94
Cost of solvent, 95
Cottonseed-oil processing, 379
Craig extractor, 221
Critical solution temperature, binary, 7–9
    effect on, of impurities, 11
      of pressure, 10
    lower, 8, 9, 18, 53, 377
    prediction of distribution from, 76–78, 377
    upper, 7–9, 14, 15, 347
  ternary, 14, 15
Crystallization, 2, 92, 393

D

DDT, 389
Deasphalting, 367, 372, 373
Density of solvent, 92, 93
Desulfurization, 348, 351–360
$\beta$, $\beta'$-Dichloroethyl ether (*see* Chlorex process)
Diffusion, eddy, 116, 317
  Fick's law of, 98
  Maxwell-Stefan concept of, 98, 99
  molecular, 97–116
  in spheres, 101
  unsteady-state, 100, 317
Diffusivity, eddy, 117
  molecular, 98
    absolute-rate theory and, 104–112
    of concentrated solutions, 108–111, 114, 115
    effect of temperature on, 103, 107, 111, 113
    empirical estimation of, electrolytes, 112–116
      nonelectrolytes, 102–112
    experimental determination of, 101
    Stokes-Einstein equation, 106
Dispersions (*see* Emulsions)
Dissociation, 25, 26
Distillation, azeotropic, 1, 3
  extraction analogy and, 125, 126
  extractive, 1, 3, 350

Distillation, fractional, 1, 3
Distribution coefficients, 19, 353–355
prediction of, 64–83
from activity coefficients, 64–76
from critical solution temperatures, 76–78
from hydrogen bonding, 79–81
from internal pressures, 81–83
Distribution law, 5, 24–30, 152, 153, 173–176, 218–229, 232, 235–237, 246–249, 353–357
Drops, extraction from, 101, 316–318
rate of rise (fall), 274, 303
size of, from nozzles, 304, 326
Drugs, 303, 342, 386–388
Duo-Sol process, 270, 271, 278, 285, 367, 374, 375

E

Edeleanu process, 347–348
for aromatic hydrocarbons, 348–350
for lubricants, 373–374
Elgin tower, 293
Emulsions, 273–283
coalescence of, 275, 280–282
stable, 282
stability of, 274, 275
unstable, 275, 276
End effects, spray towers, 318, 319
Equilibria, binary liquid-liquid, 5–10
effect of pressure on, 10
experimental determination of, 11
complex liquid-liquid, 34, 35, 362
quaternary liquid-liquid, 31–34
prediction of, 75, 76
ternary liquid-liquid, 12–31
experimental determination of, 20–22
prediction of, 64–74, 76–83
solid-phase, 19, 20
type one (one pair immiscible binaries), 13–15
type two (two pairs immiscible binaries), 16–18
vapor-liquid, 10, 39, 40–46, 56–59
Equipment, continuous countercurrent, 290–303
performance characteristics of, 303–342
stagewise contact, 257–289
agitated vessels, 257–262
in butadiene recovery, 350
Equipment, stagewise contact, in desulfurization, 351, 353
in Edeleanu process, 347
in lubricant refining, 368, 374, 375
in pharmaceutical manufacture, 387, 388
in phenol recovery, 386
Escaping tendency, 40, 42
Evaporation, 2
Extract, definition of, 126
Extraction, advantages of, 3
continuous, countercurrent contact, 241–256
degree of separation in, 220, 225
and distillation analogy, 125, 126
double solvents, 214–239
multiple-stage, batch, 221–228
continuous countercurrent, 228–238
selectivity in, 218
single-stage, 214–221
efficiency of, 174
fractional (*see* double solvents, above)
mixed solvents, 204–213
single-solvent, 125–201
cocurrent-multiple-contact, 129, 146–155, 165
countercurrent-multiple-contact, 129, 156–200
with constant selectivity, 199, 200
with extract reflux only, 194, 195, 366
with lubricating-oil systems, 363, 367
with multiple feed, 167–171
with raffinate reflux only, 196, 197
with reflux, 129, 176–200
differential, 129, 141–146, 165
single-contact, 129, 130–141, 165
Extraction factor, 174, 219, 235–237, 247, 251, 252, 314, 356, 357
Extraction rates, of batch agitators, 263–265
of continuous agitators, 265, 266
of continuous countercurrent equipment, 312–342
(*See also* Mass-transfer coefficients; Height of transfer unit)

F

Fat splitting, 381–383
Fick's law, 98
Flooding, of baffle towers, 309
of packed towers, 294, 305–308

Flooding, of perforated-plate towers, 298, 309–312
of spinner towers, 311
of spray towers, 292, 303, 304
Free energy, 47, 48
excess, 49
Freezing point, 95
Fugacity, of pure substances, 40
of solutions, 41
Furfural, in petroleum refining, 348, 362, 365–367, 369, 370
in rosin refining, 383
in vegetable-oil refining, 379–381

G

Gibbs-Duhem equation, 47
integrations of, 48–52, 56–64
Girbotol process, 351
Glycerol, recovery of, 383, 388, 389

H

Hafnium, 393
Heat of solution, 53–55
Heat transfer in extraction towers, 328, 329, 382
Height equivalent to theoretical stage (H.E.T.S.), 241
for baffle towers, 337
for packed towers, 336, 337
for spinner towers, 340, 341
for spray towers, 324, 329
Height of transfer unit (*HTU*), 251, 252, 255
for packed towers, 329–337, 342
for perforated-plate towers, 337–340
for spinner towers, 340–342
for spray towers, 318–329, 342
Holley-Mott apparatus, 283, 284, 286, 386
Hydrocarbons (*see* Petroleum refining)
Hydrogen bonding, 79–81
Hydrogen sulfide, 295, 351
(*See also* Sweetening processes)

I

Impellers, mixing, 259–261
Inflammability, 95
Injectors, 270, 271
Interfacial tension, 93
effect of, on capacity, perforated plates, 310, 311
on coalescence, 275, 282
Interfacial tension, effect of, on mixing, 262
on rate of extraction, 337
Internal pressure, 81–83
Iodine number, 34, 35, 378–381
Ionic mobilities, 112, 113

J

Jet mixers, 268–270

K

Kerosenes, Edeleanu treatment for, 347, 348
Koch tower, 300
extraction rates of, 340
flow capacity of, 312
Kopp's law, 103

L

Lanthanum, 393
Linseed oil, 379
Lubricating-oil treating, 360–375

M

Margules equations, binary, 50, 52, 59
ternary, 64
Mass-transfer coefficients, 117–122
calculation of, 249–251
data interpretation of, 312–314
over-all, 120–122
in packed towers, 329–337
in perforated-plate towers, 337–340
for single drops, 316–318
in spray towers, 318–329
in wetted-wall towers, 314–315
Maxwell-Stefan concept, 98, 99
Mercapsol process, 358
Mercaptans (*see* Sweetening processes)
Metal separations, 392, 393
Minimum solvent requirement, 131, 136, 157, 158, 174
Mixers, agitated vessels, 257–262
flow (line), 268–273, 351, 387

N

Naphtha treating, 347–360
Neodymium, 393
Nitrobenzene process, 337, 369, 370
Nitroglycerine, 388
Nozzle mixers, 271

O

Orifice mixers, 271, 272

P

Packed towers, 293–295
in butadiene recovery, 350
extraction rates of, 329–337, 342, 350
flow capacity of, 305–308
laboratory-size, 337
in lubricating-oil refining, 368–371
in phenol manufacture, 388
in sweetening processes, 353, 358
Penicillin, 303, 386–388
Perforated-plate towers, 297–300
flow capacities of, 309–312
extraction rates of, 337–340
in lubricating-oil refining, 371
in rosin refining, 383
Petroleum refining, 346–375
lubricants, 360–375
naphthas, 347–360
sweetening, 351–360
Pharmaceutical products, 303, 342, 386–389
Phase rule, 5–7, 14
Phenol, extraction of, from gas-works liquor, 273, 283, 284, 295, 297, 340, 384–386
manufacture of, 388
Phenol process, 371, 372
Phenosalvan process, 386
Phosphate process, 351
Plait point, 14, 21, 23, 27
Plutonium, 392
Podbielniak extractor, 302, 303, 387, 388
stage efficiency of, 341, 342
Propane, in deasphalting, 367, 372, 373
in vegetable-oil refining, 376–379, 381, 383, 384
(*See also* Duo-Sol process; Solexol process)
Propeller mixers, 260
Pumps, 272
Pyridine, 385

R

Raffinate, definition of, 126
Raoult's law, 39–41
deviations from, 42–46
Rare earth metals, 393
Raschig process, 388
Reflux ratio, 179, 180, 185–187, 238, 239
infinite, 183, 189, 199
minimum, 182, 188, 200
optimum, 183
Reynolds number, 313
Rosin, 383, 384

S

Salting-out, 2
Sardine oil, 378
Scandium, 393
Scatchard-Hamer equations, binary, 51, 52, 60
ternary, 64
Scheibel tower, 301
extraction rates of, 340–342
flow capacity of, 311–312
Schmidt number, 313
Selectivity, in countercurrent extraction with reflux, 199, 200
in double-solvent extraction, 218
importance of, 86–90
prediction of, 70, 71, 73, 74, 76
Settlers, 276–280
Sieve-plate towers (*see* Perforated-plate towers)
Sodium hydroxide, purification of, 392
(*See also* Sweetening processes)
Solexol process, 378, 379, 383
Solubility, in calculation of activity coefficients, 59–61
in choice of solvent, 94
Solutions, ideal, 39–41
nonideal, 41–83
regular, 53
Solutizer process, 358, 359
Solvent recovery, 3, 91, 92, 132–134, 137–138, 147, 148, 158, 181, 183, 206, 215, 389–391
Soybean oil, 379–381
Spinner tower (*see* Scheibel tower)
Spray towers, 290–293
end effect of, 318, 319
extraction rates of, 318–329, 342
in fat splitting, 382, 383
flow capacity of, 303, 304
heat transfer in, 328, 329
hold-up of dispersed phase in, 304, 321–324
in phenol recovery, 385
Stage, ideal, 126
Stage efficiency, 131, 150, 264, 266, 284–286, 350
Standard state, 41
Stokes-Einstein equation, 106
Stokes' law, 274, 275

Stripping, 2, 356, 357
Sulfur dioxide (*see* Edeleanu process)
Sweetening processes, 295, 300, 340, 351–360
System, binary, acetic acid–cyclohexane, 11
acetone–carbon disulfide, 45
–chloroform, 46, 72
aniline–cyclohexane, 68
–*n*-heptane, 68
cetyl stearate–propane, 377
chloroform–ethanol, 46
cyclohexane–*n*-heptane, 68
–sulfur dioxide, 9
ethanol–ethyl acetate, 42, 56, 57
–toluene, 58
*n*-hexane–*n*-pentane, 40
methanol–toluene, 43
oleic acid–propane, 377
palmitic acid–propane, 377
propane–stearic acid, 377
–tricaprylin, 377
–trilaurin, 377
–trimyristin, 377
–tripalmitin, 377
–tristearin, 377
water–acetaldehyde, 47
–acetic acid, 47
–acetone, 44, 72
–aniline, 9, 45
–*n*-butanol, 9
–carbon tetrachloride, 308
–diethylamine, 9
–2,6-dimethylpyridine, 9
–ethanol, 54, 55, 66, 100, 110, 111
–ethyl acetate, 66
–ethylene glycol mono-isobutyl ether, 9
–ethylene glycol mono-*n*-butyl ether, 9
–furfural, 9
–isobutanol, 309, 330, 331
–isobutyraldehyde, 309, 319–321, 330, 331
–kerosene, 311
–mannitol, 111
–methyl acetate, 9
–methyl ethyl ketone, 9, 61, 62
–methyl isobutyl ketone, 304, 305
–1-methyl piperidine, 9
–4-methyl piperidine, 9
–naphtha, 312
System, binary, water–nicotine, 9
–3-pentanol, 319–321, 329, 331
–petroleum ether, 308
–phenol, 7, 9, 15
–1,2-propylene glycol-2-propyl ether, 9
–sodium chloride, 47, 114, 115
–tetrachloroethylene, 315
–toluene, 304, 308, 328
–triethylamine, 9
–vinyl acetate, 309
–xylene, 304, 305
complex, asphalt–petroleum–propane, 372
chlorex–petroleum, 365–367
*o*- and *p*-chloronitrobenzene–heptane–methanol–water, 220, 221, 232–235
ethanol–*o*- and *p*-ethoxy aniline–hydrocarbon–water, 237, 238
furfural–petroleum, 362–367
hydrocarbon–mercaptan–sodium hydroxide–water, 353–355
quaternary, acetic acid–acetone–chloroform–water, 32, 211–213, 216, 217
acetone–isobutanol–tetrachloroethane–water, 34
butadiene–isobutene–furfural–naphtha, 33
chloroform–*o*- and *p*-nitrobenzoic acid–water, 226–228
ferric chloride–hydrogen chloride–isopropyl ether–water, 318, 319, 326
ternary, aniline–cyclohexane–*n*-heptane, 31, 70, 78, 200, 201
–*n*-heptane–methylcyclohexane, 16, 78, 89, 90
–*n*-hexane–methylcyclopentane, 78, 189–194
benzene–propylene glycol–sodium oleate, 20
cottonseed oil–oleic acid–propane, 18, 78, 89, 90, 337
1,6-diphenylhexane–docosane–furfural, 15, 83
iron–lead–zinc, 19
palmitic acid–propane–stearic acid, 78
water–acetaldehyde–toluene, 154, 155, 174–176
–vinyl acetate, 335, 336

System, ternary, water–acetic acid–benzene, 82, 309, 315–317, 327, 332
–ethyl acetate, 317
–ethyl ether, 312, 338, 339
–isopropyl ether, 308, 316, 317, 324, 325
–methyl isobutyl ketone, 253–255, 309, 315–318, 322, 325, 334, 341, 342
–nitrobenzene, 318
–toluene, 25
–xylene, 341
–acetone–chloroform, 72
–methyl isobutyl ketone, 138–141
–phenol, 15
–sodium hydroxide, 20
–1,1,2-trichloroethane, 28–30, 92, 144–146, 153, 154, 162–165, 169–171, 252, 253
–trichloroethylene, 93
–vinyl acetate, 335, 336
–xylene, 341
–amyl alcohol–ethylene glycol, 13
–aniline–benzene, 315
–phenol, 16
–benzene–benzoic acid, 300, 309, 315, 335, 337
–1,4–dioxane, 28–30
–ethanol, 83, 90
–isopropanol, 28–30, 165
–silver perchlorate, 16
–benzoic acid–kerosene, 309, 312, 335, 338, 339
–methyl isobutyl ketone, 327
–toluene, 309, 312, 321–323, 333–335, 338, 339
–*n*-butanol–ethanol, 28–30
–*n*-butylamine–naphtha, 342
–calcium chloride–methyl ethyl ketone, 309, 327, 332, 334
–carbon tetrachloride–iodine, 226–228
–chlorobenzene–methyl ethyl ketone, 16
–diethylamine–toluene, 334, 336
–ethanol–ethyl acetate, 14, 66–69, 71, 88, 90
–ethyl ether, 14, 197, 198
–potassium fluoride, 19, 20
–ethyl acetate–isopropanol, 74, 75
–ethyl ether–succinic nitrile, 19
System, ternary, water–furfural–toluene, 334
–gasoline–methyl ethyl ketone, 312, 338, 339
–isobutanol–sodium hydroxide, 20
–kerosene–phenol, 315
–methyl isobutyl ketone–propionic acid, 327
–methyl ethyl ketone–naphtha, 332
–silver perchlorate–toluene, 16

T

Tall oil, 383, 384
Tallow, 379
Tannin process, 358
Thorium, 392, 393
Tie-line correlations, 22–31
quaternary, 33
Toxicity, 95
Transfer units, number of, 242–249, 252–255
Transition flow, 306, 307
Tricresyl phosphate, 386
Turbine mixers, 261, 301
Two-film theory, 118–122

U

Unisol process, 359, 360
Uranium, 392

V

Van Laar equations, binary, 51, 52, 56, 58, 60, 61, 66
ternary, 63, 64, 67, 68, 71
Vapor pressure of solvent, 95
Vegetable oils, 34, 35, 295, 376–384
Viscosity, in choice of solvent, 95
eddy, 117
effect of, on diffusivity, 106–112, 114, 115
Viscosity-gravity constant, 361–363
Viscosity index, 361, 365–367
Vitamins, 378

W

Wetted-wall towers, 301–303
extraction rates of, 314, 315

Z

Zirconium, 393